B CELL ACTIVATION AND DIFFERENTIATION: NEW PERSPECTIVES ON AN ENDURING TOPIC

EDITED BY: Zhenming Xu, Mark Robin Boothby and Jayanta Chaudhuri
PUBLISHED IN: Frontiers in Immunology

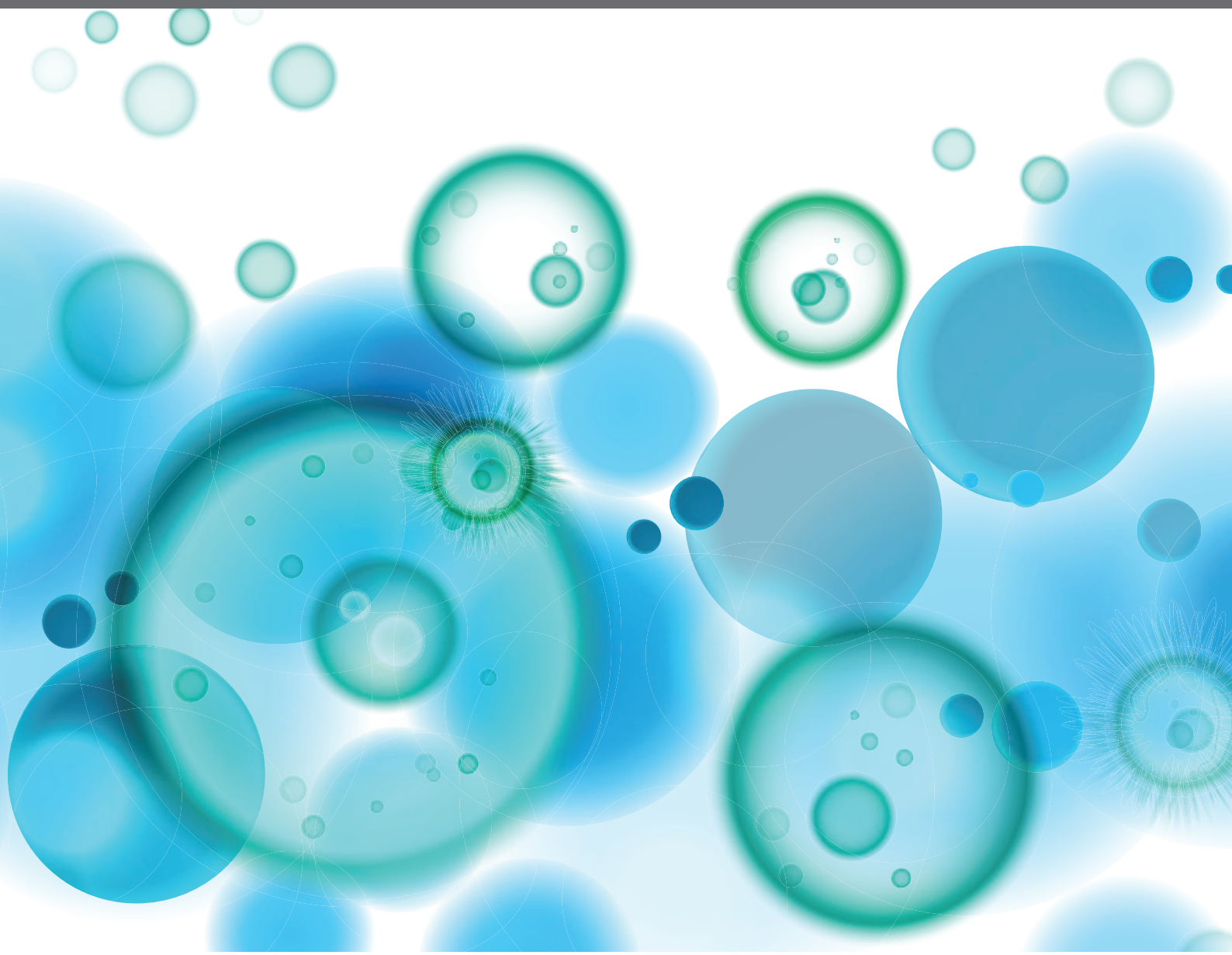

frontiers Research Topics

ISSN 1664-8714
ISBN 978-2-88971-958-7
DOI 10.3389/978-2-88971-958-7

About Frontiers

Frontiers is more than just an open-access publisher of scholarly articles: it is a pioneering approach to the world of academia, radically improving the way scholarly research is managed. The grand vision of Frontiers is a world where all people have an equal opportunity to seek, share and generate knowledge. Frontiers provides immediate and permanent online open access to all its publications, but this alone is not enough to realize our grand goals.

Frontiers Journal Series

The Frontiers Journal Series is a multi-tier and interdisciplinary set of open-access, online journals, promising a paradigm shift from the current review, selection and dissemination processes in academic publishing. All Frontiers journals are driven by researchers for researchers; therefore, they constitute a service to the scholarly community. At the same time, the Frontiers Journal Series operates on a revolutionary invention, the tiered publishing system, initially addressing specific communities of scholars, and gradually climbing up to broader public understanding, thus serving the interests of the lay society, too.

Dedication to Quality

Each Frontiers article is a landmark of the highest quality, thanks to genuinely collaborative interactions between authors and review editors, who include some of the world's best academicians. Research must be certified by peers before entering a stream of knowledge that may eventually reach the public - and shape society; therefore, Frontiers only applies the most rigorous and unbiased reviews.
Frontiers revolutionizes research publishing by freely delivering the most outstanding research, evaluated with no bias from both the academic and social point of view. By applying the most advanced information technologies, Frontiers is catapulting scholarly publishing into a new generation.

What are Frontiers Research Topics?

Frontiers Research Topics are very popular trademarks of the Frontiers Journals Series: they are collections of at least ten articles, all centered on a particular subject. With their unique mix of varied contributions from Original Research to Review Articles, Frontiers Research Topics unify the most influential researchers, the latest key findings and historical advances in a hot research area! Find out more on how to host your own Frontiers Research Topic or contribute to one as an author by contacting the Frontiers Editorial Office: frontiersin.org/about/contact

B CELL ACTIVATION AND DIFFERENTIATION: NEW PERSPECTIVES ON AN ENDURING TOPIC

Topic Editors:
Zhenming Xu, The University of Texas Health Science Center at San Antonio, United States
Mark Robin Boothby, Vanderbilt University Medical Center, United States
Jayanta Chaudhuri, Memorial Sloan Kettering Cancer Center, United States

Citation: Xu, Z., Boothby, M. R., Chaudhuri, J., eds. (2021). B Cell Activation and Differentiation: New Perspectives on an Enduring Topic.
Lausanne: Frontiers Media SA. doi: 10.3389/978-2-88971-958-7

Table of Contents

frontiers in Immunology

EDITORIAL
published: 09 November 2021
doi: 10.3389/fimmu.2021.797548

Editorial: B Cell Activation and Differentiation: New Perspectives on an Enduring Topic

Zhenming Xu[1]*, *Mark R. Boothby*[2]* and *Jayanta Chaudhuri*[3]*

[1] Department of Microbiology, Immunology and Molecular Genetics, The Joe R. and Teresa Lozano Long School of Medicine, University of Texas Health Science Center San Antonio, San Antonio, TX, United States, [2] Department of Pathology, Microbiology & Immunology, Department of Medicine, Vanderbilt University School of Medicine, Nashville, TN, United States, [3] Immunology Program, Memorial Sloan Kettering Cancer Center, New York, NY, United States

Keywords: B cell, germinal center, antibody response, autoimmunity, infection and vaccine

Editorial on the Research Topic

B Cell Activation and Differentiation: New Perspectives on an Enduring Topic

OPEN ACCESS

Edited and reviewed by:
Harry W. Schroeder, University of Alabama at Birmingham, United States

***Correspondence:**
Zhenming Xu
xuz3@uthscsa.edu
Mark R. Boothby
mark.boothby@vumc.org
Jayanta Chaudhuri
chaudhuj@mskcc.org

Specialty section:
This article was submitted to B Cell Biology, a section of the journal Frontiers in Immunology

Received: *18 October 2021*
Accepted: *25 October 2021*
Published: *09 November 2021*

Citation:
Xu Z, Boothby MR and Chaudhuri J (2021) Editorial: B Cell Activation and Differentiation: New Perspectives on an Enduring Topic. Front. Immunol. 12:797548. doi: 10.3389/fimmu.2021.797548

B lymphocytes, identified more than half a century ago, are crucial for sustained host immune responses to pathogens through differentiation into long-lived plasma cells and memory B cells, particularly those producing specific antibodies of switched immunoglobulin (Ig) isotypes (IgG, IgA, and IgE). Reflecting the diversity of microorganisms that they need to counter, B cells function as both innate and adaptive immune cells, with their activation driven or fine-tuned by signals from a multitude of immune receptors as well as conventional proteins such as integrins and nuclear receptors. Consequently, B cells significantly alter the network of signal transducers as well as transcription factors, thereby re-shaping their epigenome and transcriptome to instruct their activation, migration, proliferation, differentiation, and survival, particularly in the germinal center (GC) microenvironment. New insights have also been generated to understand how dysregulation of B cell responses leads to autoimmunity.

During the antibody response, B cells extensively interact with $CD4^+$ pre-T follicular helper (pre-Tfh) cells at the T-B border and with fully developed Tfh cells in follicles. In this Research Topic issue, Wishnie et al. focus on recent studies showing how such interactions are exquisitely regulated by the affinity of B cell receptor (BCR) to the cognate antigen, leading to the selection of locations of B cell responses, i.e., either in extrafollicular areas or within GCs. They also describe the propensity of B cells to differentiate into antibody-secreting cells (ASCs) and memory B cells if expressing high- and low-affinity BCRs, respectively, likely influenced by the location of B cell activation. In addition to dictating the duration and quality of interactions with Tfh cells, BCRs, upon crosslinking, trigger signaling pathways, such as those activating MAPK and NF-κB. These can also be activated by signals from CD40, as engaged by Tfh cell-expressed CD154, B-cell activating factor receptor (BAFF-R), also a TNF family receptor, and toll-like receptors (TLRs), which are innate receptors recognizing molecular patterns. By focusing on recent advances on the crosstalk between BCR signaling with CD40, BAFF-R, and TLR signaling, Chen and Wang discuss how such crosstalk imposes a checkpoint in class switch recombination (CSR) at the immunoglobulin heavy chain (*Igh*) gene locus and antibody responses as well as in breaking the B cell tolerance. Besides the well-studied BCR, CD40 and TLR signaling, other receptors and intracellular signaling pathways have been shown by

new studies to influence B cell development and differentiation. For example, Garis and Garrett-Sinha cover how the Notch signaling, an evolutionarily conserved pathway known to play a key role in hematopoietic stem cell maintenance and in specification of T lineage cells, also regulates B cells, including B lymphocyte lineage commitment, specification of marginal zone type B cells, and mature B cell activation and differentiation during immune responses. Sun et al. describe the impact of the Wnt signaling, a fundamental pathway involved in many aspects of biological systems, on B cell differentiation. They also contend that such impact is modulated by single-stranded oligonucleotides that target sclerostin, a Wnt antagonist.

The movement of B cells along the T:B border precedes the full-blown GC reaction. Ishihara et al. investigate the role of Rap1 small GTPase in this process by generating mice with B cell-specific knockout in both Rap1 isoforms, Rap1a and Rap1b. B cells from such double knockout mice are impaired in moving along a gradient of chemoattractants known to be critical for their localization in the follicles, leading to the defective GC formation, and antibody responses to immunization – B1a cell development is also defective in such mice. In addition to interacting with Tfh cells through CD40:CD154 engagement for their activation, B cells are heavily dependent on IL-21, the hallmark cytokine of Tfh cells, to sustain their GC reaction and differentiate into ASCs. In a research article, Wang et al. show that GC B cells, paradoxically, are sensitized by IL-21 to activate caspase 9 in the mitochondria-dependent intrinsic apoptosis pathway. Such caspase 9 activation would be contained if caspase 8 of the extrinsic apoptosis pathway remains inhibited by cFLIP to prevent amplification of the entire caspase network and irreversible cell death. Lack of linear ubiquitin assembly complex (LUBAC) results in cFLIP degradation and IL-21-induced apoptosis in CD40-activated B cells *in vitro* as well as GC B cell death *in vivo*, leading to defective antibody affinity maturation and the T-dependent antibody response. In an independent study, Wright et al. discover that BIM, a pro-apoptotic BCL2 family member, mediates IL-21-induced B cell apoptosis. Also, B cell-specific deficiency in BIM leads to uncontrolled expansion of B cells, production of a wide array of autoantibodies and tissue infiltration of lymphocytes, indicating that GC B cell apoptosis is checkpoint of autoimmunity, including lupus. Interestingly, the defective apoptosis of BIM-lacking B cells can be ameliorated by knockout of the BTK tyrosine kinase, suggesting a new signal transduction pathway operating in B cells, including those that have broken the tolerance. This adds to the role of PI3K signaling, which coordinates various signaling molecules involved in B cell development and activation, and IFNγ signaling, which is known to be elevated in both systemic lupus erythematosus (SLE) patients and mouse models of lupus, as reviewed by Bacalao and Satterthwaite. These authors also summarize recent data on how IFNγR signaling mediates the development of autoreactive GCs and autoantibody responses in murine lupus, particularly the enhancement of chromatin accessibility at potential transcription factor-targeting sites, alterations in DNA methylation, and acquisition of new histone acetylation that can be regulated by histone deacetylase inhibitors, as potential lupus therapeutics. The epigenetic regulation of B cell in immunity and SLE is further extended to microRNAs (miRNAs), which mediate genetic regulation at the post-transcriptional level. Given the relatively extensive literature on miRNAs in B cells, Schell and Rahman highlight miRNAs with confirmed functions in mouse models and provide a perspective on the areas of future studies and the potential of miRNA-centric therapeutics in SLE. Built on the observation that the frequency of memory B cells is increased in lupus mouse models and their previous seminal findings that autophagy specifically and critically maintains memory B cells, Jang et al. explore the role of memory B cell responses in lupus pathogenesis triggered by pristane injection. B cell-specific deletion of Atg7, which is essential for autophagy, leads to loss of autoreactive memory B cells, much reduced autoantibody production in pristane-treated mice, and attenuated development of glomerulonephritis and pulmonary inflammation. Importantly, autoantibody production in such knockout mice can be rescued by memory B cells isolated from pristane-injected wild-type mice, showing that autophagy is a new therapeutic target for lupus.

In work directed towards translating laboratory investigations into the understanding of human B cell immunology, Joosse et al. report the development of a new throughput screening pipeline to analyze the repertoire of autoreactive B cells in autoimmune patients. This pipeline entails phenotypical identification of different B cell subsets, expansion of such B cells *in vitro* and their differentiation into ASCs, and identification of autoantigen-specific B cells through autoantibody-specific ELISA. This robust tool allows the investigators to use a small amount of cryo-preserved peripheral blood mononuclear cells (PBMCs) to detect insulin-binding memory B cells in pre-symptomatic type 1 diabetes donors. Using naïve B cells, GC centroblasts, GC centrocytes, memory B cells, and plasma cells purified from human tonsils and a label-free LC-MS/MS approach, Díez et al. profile, for the first time, the proteome of human B cells at distinct differentiation stages and show that, despite the considerable overlap of their proteome, these B cells express factors associated with regulation of metabolic programming to instruct the transition between differentiation stages. These tools will likely be adapted by other investigators in the field to advance their own research on human B cells in different pathophysiological contexts. For example, Upasani et al. address the susceptibility of B cells, in addition to widely studied dendritic cells and macrophages, to acute infection by dengue virus (DENV) in a cohort of 60 Cambodian children, likely by using CD300a, a phosphatidylserine receptor, as the entry receptor. These findings are consistent with the observation that human B cells can support the replication of lab-adapted and patient-derived DENV strains *in vitro*, leading to the release of live viruses into the supernatant, but no apparent antibody-dependent enhancement effects. Direct DENV infection causes human B cells to proliferate *in vivo* and differentiate into plasma cells *in vitro*. Like DENV, malaria is a global burden of infectious disease and in urgent need of an effective vaccine against the *Plasmodium* parasite. As natural infection elicits a robust immune response against the blood stage of the parasite to provide protection against malaria, Gonzales et al. reason that a full understanding of the

mechanisms, acquisition and maintenance of naturally acquired immunity would pave the way for the development of a potential vaccine against the blood stage of *Plasmodium falciparum*. This topic is especially timely in light of the recent field-work success with the RTS,S vaccine and its protection of children from lethal *falciparum* malaria. Like all FDA-approved vaccines, new malaria vaccine candidates would elicit highly specific/neutralizing IgG, and possibly IgM, antibodies.

Altogether, these primary research and review articles have made this Research Topic a collection of new insights and perspectives on B cell biology. We are grateful to all the authors for their efforts and wish them success in continually pushing their respective fields forward.

AUTHOR CONTRIBUTIONS

All authors listed have made a substantial, direct, and intellectual contribution to the work and approved it for publication.

FUNDING

This work is supported by NIH/NIAID AI 153506 (to ZX) and Departmental funds of Pathology-Microbiology-Immunology Department, Vanderbilt University Medical Center (to MB).

Conflict of Interest: The authors declare that the research was conducted in the absence of any commercial or financial relationships that could be construed as a potential conflict of interest.

Publisher's Note: All claims expressed in this article are solely those of the authors and do not necessarily represent those of their affiliated organizations, or those of the publisher, the editors and the reviewers. Any product that may be evaluated in this article, or claim that may be made by its manufacturer, is not guaranteed or endorsed by the publisher.

frontiers in Immunology

REVIEW
published: 29 October 2020
doi: 10.3389/fimmu.2020.594653

Naturally Acquired Humoral Immunity Against *Plasmodium falciparum* Malaria

S. Jake Gonzales[†], *Raphael A. Reyes*[†], *Ashley E. Braddom*, *Gayani Batugedara*, *Sebastiaan Bol and Evelien M. Bunnik*[*]

Department of Microbiology, Immunology and Molecular Genetics, Long School of Medicine, The University of Texas Health Science Center at San Antonio, San Antonio, TX, United States

Malaria remains a significant contributor to the global burden of disease, with around 40% of the world's population at risk of *Plasmodium* infections. The development of an effective vaccine against the malaria parasite would mark a breakthrough in the fight to eradicate the disease. Over time, natural infection elicits a robust immune response against the blood stage of the parasite, providing protection against malaria. In recent years, we have gained valuable insight into the mechanisms by which IgG acts to prevent pathology and inhibit parasite replication, as well as the potential role of immunoglobulin M (IgM) in these processes. Here, we discuss recent advances in our understanding of the mechanisms, acquisition, and maintenance of naturally acquired immunity, and the relevance of these discoveries for the development of a potential vaccine against the blood stage of *Plasmodium falciparum*.

Keywords: antibody, protection, variant surface antigens, PfEMP1, merozoite, vaccine

OPEN ACCESS

Edited by:
Mark Robin Boothby, Vanderbilt University Medical Center, United States

Reviewed by:
Christopher Sundling, Karolinska Institutet (KI), Sweden
Julius Lautenbach, in collaboration with reviewer CS
Wanli Liu, Tsinghua University, China

***Correspondence:**
Evelien M. Bunnik
bunnik@uthscsa.edu

[†]*These authors have contributed equally to this work*

Specialty section:
This article was submitted to B Cell Biology, a section of the journal Frontiers in Immunology

Received: *14 August 2020*
Accepted: *07 October 2020*
Published: *29 October 2020*

Citation:
Gonzales SJ, Reyes RA, Braddom AE, Batugedara G, Bol S and Bunnik EM (2020) Naturally Acquired Humoral Immunity Against Plasmodium falciparum Malaria. Front. Immunol. 11:594653. doi: 10.3389/fimmu.2020.594653

INTRODUCTION

Malaria is a deadly disease caused predominantly by the parasite *Plasmodium falciparum*. In 2018, an estimated 228 million cases occurred globally, resulting in 405,000 deaths, of which most were children (1). With the distribution of long-lasting insecticide-treated bed nets, increased insecticide spraying, and earlier diagnosis and treatment, major progress has been made in reducing morbidity and mortality since 2010. However, malaria continues to be a major global public health challenge and have devastating socioeconomical impact, mainly in Sub-Saharan Africa. Because of the spread of drug-resistant parasites and insecticide-resistant mosquitoes, as well as lack of access to treatment, vaccine development remains the most promising avenue for the eradication of malaria.

Vaccine development efforts have focused on multiple stages of the parasite life cycle, including the pre-erythrocytic stages and the asexual blood stage (**Figure 1**). While the development of sporozoite vaccines is in a more advanced stage than blood stage vaccines [reviewed in (2, 3)], strategies against both stages still face multiple hurdles. Therefore, the ultimate malaria vaccine may need to target both life cycle stages to reach sufficient vaccine efficacy. The *Plasmodium* asexual blood stage is responsible for symptomatic disease and can elicit a robust immune response [reviewed in (4)]. Over the course of multiple infections, antibody responses against blood stage parasites broaden and reach a level that protects against malaria (5–7). However, eliciting a long-lasting, protective antibody response by vaccination has proven a difficult task. Among the many

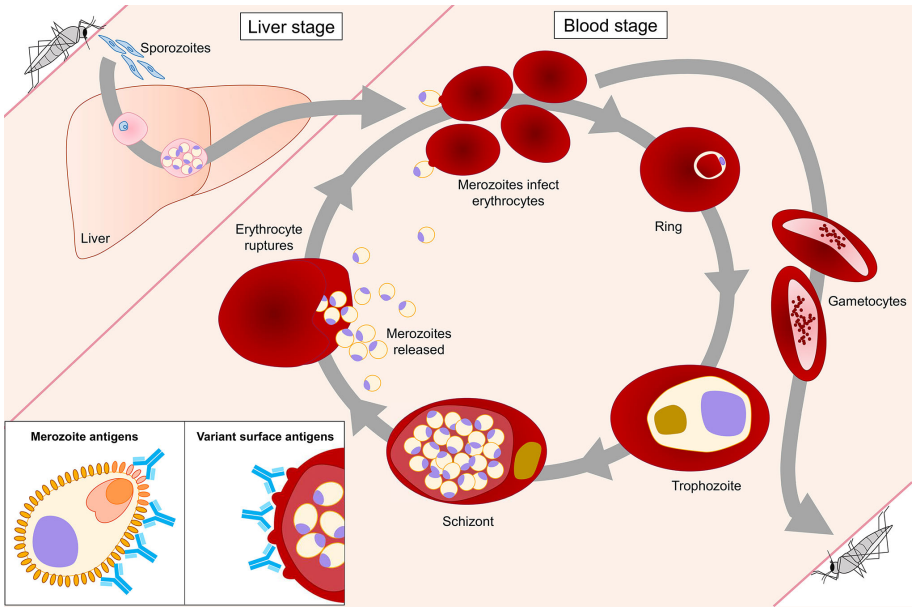

FIGURE 1 | *Plasmodium falciparum* life cycle stages in the human host. The blood stage of *P. falciparum* is the only life cycle stage responsible for disease in the human host. During the intraerythrocytic developmental cycle (IDC), merozoites invade erythrocytes, followed by development and replication of the parasite through ring, trophozoite, and schizont stages, until new merozoites egress and the cycle repeats. Antibody responses that protect against malaria are directed against two classes of antigens expressed during the IDC. Merozoite antigens, such as MSP1 and AMA1, are common targets of antibodies generated during natural *P. falciparum* infection. Antibodies against these antigens prevent merozoite invasion of erythrocytes *via* various effector mechanisms, including neutralization, opsonic phagocytosis, and complement activation. Variant surface antigens (VSAs) are expressed on the surface of infected erythrocytes. Antibodies against VSAs, including PfEMP1, RIFINs, and STEVORs, prevent cytoadherence of infected erythrocytes to vascular endothelium and rosetting, thereby promoting clearance of parasite-infected erythrocytes by the spleen.

reasons for the failures of historical blood stage vaccine candidates are i) sequence variation in vaccine targets that resulted in parasite strain-specific responses (8, 9), ii) inability of the vaccine to elicit sufficiently high antibody titers necessary for protection (10, 11), and iii) quick waning of elicited immune responses (6, 12–15). In parallel to these obstacles for vaccine development, many questions about the nature of naturally acquired immunity remain. For example, it is not fully understood why immunity against malaria develops relatively slowly, how long naturally acquired antibody responses are maintained in the absence of re-exposure, whether antibody responses are strain-transcending or a combination of strain-specific responses, and which (combinations of) antigen(s) should be prioritized for vaccine development.

The main antigenic targets of blood stage parasites can be divided into two categories: i) parasite variant surface antigens on the cell membrane of infected erythrocytes and ii) proteins that are located on the merozoite surface or secreted by merozoites during erythrocyte invasion (**Figure 1**). Recent studies examining naturally acquired immunity have revealed important insights into antibody responses against these two groups of *P. falciparum* antigens, including their development and maintenance, key molecular and immunological mechanisms of parasite inhibition, and a potential role for immunoglobulin M (IgM) in the protective response. This review provides an overview of these discoveries and highlights their relevance for vaccine development.

PLASMODIUM FALCIPARUM VARIANT SURFACE ANTIGENS

During the mature stages of the asexual blood stage, *P. falciparum* expresses variant surface antigens (VSAs) on the cell membrane of the infected erythrocyte. These proteins play crucial roles in both malaria pathogenesis and immune evasion. VSAs belong to multigenic families, most notably *P. falciparum* erythrocyte membrane protein 1 (PfEMP1), repetitive interspersed repeats (RIFIN), and subtelomeric variant open reading frame (STEVOR). PfEMP1 can bind to specific host receptors lining the vascular endothelium, resulting in sequestration of infected erythrocytes in capillaries, thereby preventing parasite clearance by the spleen (16–18) (**Figure 2**). In addition, members of all three VSA families mediate rosetting, the formation of a cluster of uninfected erythrocytes around an infected erythrocyte, which enhances microvascular obstruction (19–22). Rosetting and sequestration of infected erythrocytes can contribute to disease by reducing capillary perfusion and promoting parasite survival by preventing splenic clearance [reviewed in (23)]. Antibodies against VSAs may function by

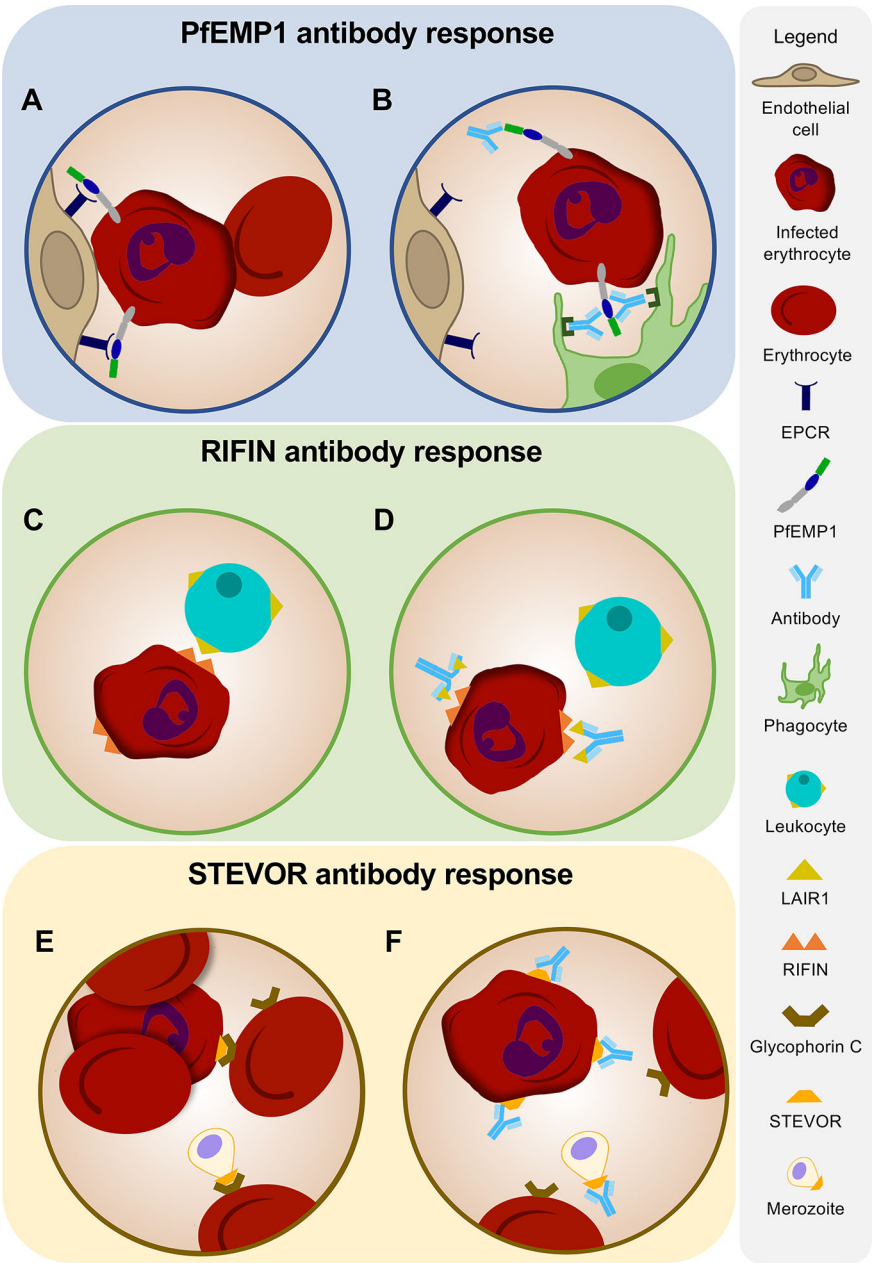

FIGURE 2 | Antibodies against variant surface antigens. **(A)** PfEMP1 on the surface of an infected erythrocyte facilitates binding to receptors on human vascular endothelium. **(B)** Humoral immune responses against PfEMP1 inhibit attachment of infected erythrocytes to host endothelium and induce opsonic phagocytosis of infected erythrocytes. **(C)** Immune evasion of infected erythrocytes is mediated by RIFINs expressed on the surface of the erythrocyte. Binding of RIFINs to LAIR1 on B cells and natural killer (NK) cells results in suppression of immune responses. **(D)** Antibodies against RIFINs may function in preventing the binding of infected erythrocytes to LAIR1 on leukocytes. Broadly reactive antibodies to RIFINs were found to contain an insertion of a fragment of LAIR1 in the arm of the antibody heavy chain. **(E)** STEVORs mediate rosette formation and may play a role in merozoite invasion by adhering to glycophorin C on the erythrocyte surface. **(F)** Antibodies targeting STEVORs can prevent rosetting and inhibit attachment of merozoites to erythrocytes, thereby potentially limiting parasite replication and survival.

countering these immune evasion strategies of the parasite (24–26). In addition, anti-VSA antibodies may contribute to directly killing infected erythrocytes through the induction of opsonic phagocytosis (27) or antibody-dependent cellular cytotoxicity by natural killer (NK) cells (28).

Antibody Responses Against PfEMP1

Each *P. falciparum* parasite encodes a diverse set of approximately 60 PfEMP1 proteins, but only one of these antigens will be expressed in a single parasite [reviewed in (29)]. PfEMP1 proteins display a high degree of sequence variation, both

among the different variants encoded within a single parasite and among those expressed by different parasite strains. Switching PfEMP1 variant expression therefore contributes to quick and efficient evasion of host humoral immune responses by the parasite (18). Unfortunately, the extreme sequence diversity among PfEMP1 variants has hampered our ability to study naturally acquired immunity against these antigens, as well as the development of a PfEMP1-based vaccine.

PfEMP1 proteins are composed of two to ten cysteine-rich interdomain regions (CIDRα, β, γ, and δ) and Duffy binding-like domains (DBLα, β, γ, δ, ϵ, ζ, and x) that can be further divided into 147 subtypes (30–32). These different domains can bind to different host receptors, including endothelial protein C receptor (EPCR), intercellular adhesion molecule 1 (ICAM1), and CD36. These host endothelial receptors are not expressed at similar levels in all organs (33, 34). For example, CD36 expression is low in brain vascular endothelium, while expression of EPCR is high and expression of ICAM1 is upregulated under conditions of inflammation (33, 34). Pathogenesis, disease symptoms, and the development of severe malaria are therefore partially dependent on which PfEMP1 variant is expressed by the parasite.

Severe malaria is mainly seen in children under 5 years of age and includes life-threatening complications such as cerebral malaria and severe anemia. These severe disease manifestations have been associated with the expression of specific subtypes of CIDR and DBL domains, including CIDRα1, DBLα1, DBLα2, and DBLβ (35, 36). Protection from severe malaria is acquired early in life after only a limited number of infections (37). In the past few years, multiple independent cohort studies have revealed the role of PfEMP1 IgG antibodies in this protective response and have shed light on which PfEMP1 domains are the main targets of protective antibodies. Although all PfEMP1 domains appear to be immunogenic (38), subjects with uncomplicated malaria showed higher anti-PfEMP1 IgG titers and harbored IgGs that target PfEMP1 variants associated with severe malaria (27, 39–42). In a cohort of 448 young children (29–56 months old) in Papua New Guinea, children with uncomplicated malaria had higher levels of anti-PfEMP1 IgGs than children with severe malaria (27). The ability of these antibodies to induce opsonic phagocytosis suggests that direct killing of infected erythrocytes may contribute to protection. However, it remains to be definitively established whether cellular immune mechanisms or the prevention of cytoadherence is the main mechanism of action of these antibodies. Similar to these results, a protein microarray analysis of serum reactivity against 170 PfEMP1 fragments showed that children in Mali with severe malaria had lower PfEMP1 antibody levels and these antibodies recognized fewer PfEMP1 variants than antibodies in control subjects (41). In this study, participants were age and residence matched to minimize differences in parasite exposure between groups. This similarity in exposure levels was experimentally confirmed by the observation that children with cerebral malaria and healthy controls showed only minor differences in immune responses against intracellular PfEMP1 domains and merozoite antigens. However, a limitation of this study is that only PfEMP1 domains from the reference *P. falciparum* strain 3D7 were used, which does not include several known PfEMP1 domains that are associated with severe malaria and does not necessarily match the parasite strains that these children have been exposed to. An extensive study of antibody responses against 456 DBLα domain variants from local parasite isolates among 232 children (0.9–3.2 years old) in Papua New Guinea showed that IgGs against 85 DBLα1 and DBLα2 variants were associated with 70–100% reduction in severe malaria (40). In this study, protection against severe malaria could be further narrowed down to antibody responses against 17 DBLα variants, many of which were physically linked to EPCR-binding CIDRα1 domains (see below). These results suggest that immunity against severe malaria is the result of antibodies targeting a relatively small panel of conserved PfEMP1 domains (less than 5% of the full PfEMP1 repertoire), providing support for developing a vaccine based on these pathogenic PfEMP1 domains. Similarly, Tuju et al. reported that children in Kenya with mild or severe disease (n = 36) showed distinct serological IgG profiles against DBLα domain variants and a similar, but weaker, qualitative difference for IgM (42). The underlying mechanisms that give rise to these different serological outcomes remain to be further investigated and will be informative for vaccine development.

CIDRα1 is a PfEMP1 domain type that may play a dominant role in the development of protection against severe malaria. CIDRα1 domains have been shown to bind to EPCR, and results from several studies suggest that this interaction plays an important role in the development of severe malaria, in particular cerebral malaria (43–45). In cross-sectional studies in two independent cohorts, IgG responses against EPCR-binding CIDRα1 domains were found to develop earlier in life than antibodies against other PfEMP1 CIDR domains (46, 47), highlighting their potential role in protection against clinical disease. In addition, a longitudinal analysis in the Malian cohort showed an ordered acquisition of IgGs against different CIDRα1 domains, starting with IgGs against CIDRα1.7 and CIDRα1.8 (46). This could signify the ordered expression of PfEMP1 variants by *P. falciparum*, potentially in response to the immune status of the host. Alternatively, it could reflect differences in parasite fitness and transmissibility, resulting in early infections preferentially caused by parasites circulating at higher prevalence (46).

Given the high degree of sequence variation among PfEMP1 variants, one would expect that many PfEMP1 antibodies are strain-specific. However, CIDRα1 domains were shown to have conserved structural features that allow many different PfEMP1 variants to bind to the same host receptor (48). This structural conservation of the EPCR binding site may allow the immune system to produce antibodies that are cross-reactive against many different CIDRα1 domains. Indeed, IgGs isolated from serum by affinity purification using a peptide comprising the EPCR binding site of one CIDRα1 domain were able to bind to other CIDRα1 domains and prevented interaction of the domain with EPCR (48). These results suggest that the structural conservation of CIDRα1 domains may provide an opportunity for the development of a vaccine that elicits protection against severe malaria.

Antibody Responses Against RIFINs

RIFINs are encoded by a set of 150 to 200 genes and are highly antigenically varied (49). Following the pattern of the PfEMP1 family in *P. falciparum*, a single RIFIN is expressed by each parasite (19). Members of the RIFIN family preferably bind to blood group A erythrocytes to form large rosettes and induce cytoadherence, thereby potentially contributing to severe disease (19). In addition, it has recently been shown that RIFINs can bind to inhibitory receptors expressed on B cells, T cells, and NK cells, including leukocyte immunoglobulin-like receptor B1 (LILRB1) and leukocyte-associated immunoglobulin-like receptor 1 (LAIR1) (50) (**Figure 2**). Binding of these receptors to their natural ligands results in the suppression of immune responses (51–53). RIFINs bind the same region of LILRB1 as MHC-I, its natural ligand, and mimic the function of MHC-I by co-localizing with LILRB1 in the immunological synapse and inhibiting NK cell activation (54). In addition, it has been demonstrated that binding of RIFIN to LILRB1 inhibited IgM production in primary human B cells and reduced NK-mediated killing of target cells (55). A direct effect of RIFIN-binding to LAIR1-expressing mouse T cell hybridoma reporter cells has not been observed, but the effect of the interaction between RIFIN and LAIR1 has yet to be tested under more relevant experimental conditions, such as using primary human leukocytes (55). Based on these observations, it has been hypothesized that one of the functions of RIFINs is to down-modulate immune responses against *P. falciparum* through the binding to these inhibitory receptors.

Interestingly, it has been discovered that the human immune system exploits the ability of RIFINs to bind LAIR1 to generate broadly reactive IgM and IgG antibodies to RIFINs (56, 57). These antibodies have highly unusual structures, caused by an insertion of a human LAIR1 exon into the antibody heavy chain variable region CDR3 or into the switch region (**Figure 2**). Gene insertions in switch regions showed higher prevalence in class-switched memory B cells as compared to naive B cells, suggesting a role for activation-induced cytidine deaminase in facilitating such insertions (56, 57). Through somatic hypermutation, these LAIR1 domains lost the ability to bind to their natural ligand, collagen, thereby preventing the generation of auto-antibodies, but retained high affinity for RIFINs. These LAIR1 antibodies were found in 5–10% of malaria-experienced individuals, whereas only 0.3% of European donors had LAIR1-containing IgG (56, 57). However, the presence of LAIR1 antibodies did not correlate with protection against malaria. Thus, while LAIR1 antibodies are testament to the exceptionally strong selection pressure of *P. falciparum* on the immune response of infected individuals, the question remains whether antibodies against RIFINs contribute to protection.

IgG antibodies against RIFINs (irrespective of a LAIR1 insert) were detected in children in Tanzania as early as 1 year after birth, but levels did not increase with age (19). No difference was observed in serum IgG reactivity against three RIFINs on a protein microarray between children (1–6 years old) and adults (18–55 years old) in Mali (58). IgGs in the sera from the adults in this cohort bound to more RIFIN peptides in both semi-conserved and hypervariable domains than did the antibodies in the sera from the children (58). However, there was no difference in seroreactivity between A-type RIFINs, expressed on the surface of the infected erythrocyte, and B-type RIFINs, localized inside the parasite, suggesting that the increased antibody reactivity in adults reflects the higher cumulative exposure to the malaria parasite as compared to the children, but not protection (58, 59). In line with this observation, in children in Kenya, IgGs against PfEMP1 were associated with protection from malaria, while antibodies against other VSAs were not (60), suggesting that PfEMP1 proteins are the main target of protective immune responses against parasite proteins expressed on the erythrocyte surface.

Antibody Responses Against STEVORs

Of the VSA families discussed in this review, STEVORs were the last to be identified and remain the least characterized. STEVORs represent a family of approximately 40 polymorphic proteins encoded by genes found in subtelomeric regions of the *P. falciparum* genome (61). RNA-sequencing analysis of the *P. falciparum* 3D7 strain revealed a biphasic expression profile of STEVORs within the intraerythrocytic cycle, peaking in early trophozoites and late schizonts/merozoites (62). Additionally, STEVOR expression has been identified in the sporozoite and gametocyte stage of the parasite (63). Localization of STEVORs in all three stages is distinct, suggesting different functions based on the life cycle stage. In both trophozoites and gametocytes, STEVORs can be found on the infected erythrocyte membrane (63), where they likely play a role in parasite sequestration [reviewed in (64, 65)]. In addition, STEVORs have been detected on the apical surface of merozoites (66). STEVORs can bind to glycophorin C on the erythrocyte surface, leading to rosette formation of erythrocytes infected with mature parasites (67) and attachment of merozoite to the erythrocyte membrane (20). Given the widespread distribution of STEVORs throughout the *P. falciparum* life cycle, antibody responses against these targets may inhibit parasite replication at various stages. Indeed, STEVOR-targeting monoclonal antibodies showed a reduction in rosetting (67) and inhibition of merozoite invasion (20).

Although it is clear that STEVORs are involved in host-pathogen interactions, their role in disease pathogenesis is incompletely understood. Several cohort studies have attempted to unravel this role by analyzing serum antibody responses against STEVORs. In a cohort of Ugandan individuals aged 6–22 years old, seroprevalence of antibodies against STEVORs was lower as compared to anti-RIFIN antibodies (68). Grouping of participants based on risk of febrile malaria revealed only a single STEVOR commonly targeted by the humoral immune system of protected individuals (68). In this study, seroreactivity was tested using a library of 30 unique STEVOR recombinant proteins, each expressed as 1 or 2 truncated fragments (68). As a result, it is possible that antibody reactivity was missed because of misfolding of these protein fragments. Future studies will therefore need to evaluate host immune responses to full length STEVOR proteins. A similar study took a closer look at seroreactivity in children versus adults in a Malian cohort using a

peptide array (58). Child and adult sera were able to bind all three RIFINs tested in this panel. While adult antibodies also reacted with all six STEVORs, children only showed reactivity to four of the six (58). A peptide array of these six STEVORs revealed that IgG from adults bound significantly more peptides and had more reactivity to semi-conserved and hypervariable regions as compared to IgG from children (58). When comparing sera obtained from children before and 90 days after a single clinical malaria episode, double the amount of STEVOR peptides were recognized by antibodies in the sera at the post-malaria time point, which more closely resembled the epitope profile targeted by adults (58). This study is limited in the repertoire of STEVOR proteins tested and only measured antibody responses against linear epitopes, but it does highlight how quickly antibodies to a single protein can develop over the course of a single infection. These findings are in line with the rapid acquisition of antibodies contributing to protection against severe disease after only a few clinical episodes.

Additional analyses will be required to distinguish if anti-STEVOR antibodies contribute to protection or merely correlate with antigen exposure. Future studies will require a more extensive analysis of STEVOR expression in clinical isolates, similar to what has been accomplished for PfEMP1. The use of 3D7-based antigens to measure anti-STEVOR antibody responses is a limiting factor when trying to understand the contribution of antibody response to protection, since analyses of clinical isolates have revealed regions within STEVORs with high sequence variation (69) and variability in STEVOR expression between fresh isolates and laboratory-adapted strains (66). Using STEVOR sequences from clinical isolates along with cohorts of individuals who are at risk of or clinically protected from malaria will provide a deeper understanding of variants involved in disease pathogenesis, anti-STEVOR antibody responses that are associated with protection, and potential targets for vaccine design.

PLASMODIUM FALCIPARUM MEROZOITE ANTIGENS

Erythrocyte invasion by merozoites is an essential step in the asexual replication cycle of *Plasmodium* parasites, a process that can be blocked by antibodies [reviewed in (70)]. As a result, merozoite antigens have been the subject of intensive research over the past decades, which unfortunately has not (yet) translated into a successful blood stage vaccine [reviewed in (71)]. Merozoites express a large repertoire of proteins on their surface and in specialized secretory organelles, micronemes, and rhoptries, that are released during the invasion process [reviewed in (70)]. Titers of antibodies against members of the merozoite surface protein (MSP) family are typically among the highest detected in malaria-experienced individuals (72, 73), most likely because of their abundance and exposed nature. However, associations between antibody specificities in serum and protection against malaria are generally weaker for merozoite surface proteins than for microneme or rhoptry proteins (74, 75). Because of genetic polymorphisms and functional redundancies among merozoite proteins, it is still unclear which antigens are the best candidates for vaccine development (8, 9). Delineating the key merozoite antigens and the mechanisms by which antibodies against these antigens confer protection therefore remain important areas of research for the development of a blood stage vaccine.

Dissecting Protective Antibody Responses to Merozoite Antigens

The prioritization of antigens for vaccine development has been hampered by multiple issues, including our lack of understanding which immunological measures correlate with protection and which mechanisms of antibody-mediated parasite inhibition are most relevant for immunity. Large-scale efforts will therefore be needed to systematically compare antibody responses across different cohorts using multiple readouts. One of the most high-throughput approaches has been to compare antibody specificities between protected and susceptible people using protein microarrays. These analyses have shown that a large proportion of the *P. falciparum* proteome is immunogenic and that the breadth and durability of IgG responses increases with cumulative exposure (5–7). In addition, protected individuals have higher levels of IgG against a broad range of antigens, with unique serological profiles for each individual (5–7). The difference between protection from and susceptibility to malaria cannot simply be explained by the presence or absence of one or a small number of antibody specificities. To better understand the high complexity of such data sets and move beyond analyzing IgG responses to individual antigens, recent studies have used machine learning approaches that are able to assess combinations of responses and their association with protection (76, 77). An analysis of protein microarray data comprising antibody reactivity against more than 1,000 antigens in children (2–10 years old) and young adults (18–25 years old) showed that protection was associated with a qualitative shift in antibody responses, with an increase in antibody titers against VSAs and a decrease in antibody titers against antigens enriched for conserved proteins with unknown function (77). Proietti et al. identified an immune signature of IgG responses against 15 antigens that predicted protection from malaria across two cohorts (76). Interestingly, most of these proteins were localized intracellularly and were expressed at different stages of the *P. falciparum* life cycle, making them unlikely direct targets of parasite-inhibitory antibodies. However, these results may highlight the importance of other components of the adaptive immune system, such as T cell responses, in driving protective B cell immunity. In addition, this immune signature can be used to predict disease susceptibility, monitor the acquisition of naturally acquired immunity over time, and assess the impact of malaria interventions.

One shortcoming of these large-scale protein microarray studies is that they only assess antibody binding, not antibody effector functions such as opsonization or complement fixation. Antibodies that bind to merozoite antigens do not necessarily inhibit erythrocyte invasion. For example, it has been shown that

the activity of inhibitory anti-MSP1 IgG can be blocked by non-inhibitory antibodies that compete for binding to overlapping epitopes or bind to more distal regions and presumably prevent binding of inhibitory antibodies through steric hindrance (78). Assays that assess different antibody effector functions are therefore essential to measure the ability of antibodies to inhibit parasite replication or induce parasite killing by immune cells. In recent years, the importance of antibody effector functions in parasite inhibition has been demonstrated and several studies have started to delineate the contribution of antibodies to individual antigens in this process. In the following sections, we summarize recent advances in our understanding of the nature, and mechanisms of acquired antibody-mediated protection against *P. falciparum* merozoite invasion.

Antibody Responses Against Combinations of Merozoite Antigens

Recent studies on naturally acquired immunity have provided the important insight that the breadth of antigen recognition is more predictive of immunity than antibody reactivity against any single antigen (74, 75, 79–82). This would suggest that a vaccine based on a single antigen may not be successful in eliciting a fully protective antibody response. To better understand how many different antigens should be targeted to achieve protection and whether antibody responses against certain combinations of antigens perform better than others, the cumulative protective effect of individual antibody specificities has been analyzed. In both Sub-Saharan African and Indian populations, combinations of IgGs against four or five antigens provided nearly full protection against malaria, with only limited contributions from antibodies against additional antigens (80, 82). The most effective combinations were reported to target antigens presented during distinct stages of the invasion process, thereby working synergistically to inhibit invasion (79). In some of these combinatorial analyses, IgG responses against several uncharacterized proteins that do not have a functional annotation but are referred to by their gene identifiers (for example, PF3D7_1136200 and PF3D7_0606800) were associated with the highest levels of protection. These findings support the approach to develop a multi-antigen vaccine and encourage further evaluation of several novel protective antigens as potential vaccine candidates.

Strain-Transcending Immunity

Circulating *P. falciparum* strains are genetically diverse (8, 9). One of the challenges for vaccine development is to elicit immunity against these genetically distinct parasite strains. Passive immunization studies in the 1960s and 1990s showed that the transfer of IgG from immune individuals living in West Africa to malaria patients in East Africa or Thailand resulted in almost complete clearance of parasitemia in the absence of other treatment (83, 84). These results suggest that IgG from immune individuals can inhibit the replication of different *P. falciparum* strains from diverse geographical regions. However, the question remained whether this protective effect was the result of a combination of strain-specific antibodies targeting multiple genetically diverse antigens, or if this was due to one or more antibodies targeting conserved epitopes and thereby conferring strain-transcending immunity. A recent study by Hill et al. sought to answer this question by measuring opsonic phagocytosis of merozoites from 15 different parasite strains induced by serum antibodies from semi-immune children (5–14 years old) living in Papua New Guinea (85). Children with serum IgGs that promoted phagocytosis of merozoites from all strains tested showed an 85% decrease in the risk of developing malaria during 6 months of follow-up as compared to children with narrow opsonic phagocytosis activity in serum. Depletion of serum antibodies that bound to one merozoite strain drastically reduced opsonization of merozoites from other *P. falciparum* strains. These results suggest that opsonic phagocytosis activity against merozoites from different strains is mediated by the same antibodies. However, it is important to mention that *P. falciparum* exposure levels were not matched between groups and it can therefore not be ruled out that differences in opsonic phagocytosis activity between these groups were driven by differences in antibody titers. More research will be required to fully understand the dynamics of strain-transcending immunity and to identify the conserved epitopes targeted by this response.

Antibody Effector Functions Associated With Protection

One of the priorities for malaria vaccine development is the establishment of correlates of protection and the standardization of *in vitro* assays to measure these immunological parameters. It is therefore important to better understand the molecular and immunological mechanisms by which antibodies inhibit merozoite invasion. In general, antibodies can act by blocking interactions between molecules (i.e., neutralization), or by promoting Fc-mediated effector functions, including complement activation, opsonic phagocytosis, and antibody-dependent cellular cytotoxicity.

Antibodies against several merozoite antigens have been shown to act by neutralization. For example, IgG binding to EBA-175 prevented attachment of this protein to glycophorin A on the erythrocyte surface, thereby inhibiting invasion (86). Similarly, anti-PfRH5 IgG engineered to not engage in any Fc-mediated effector functions was able to protect against *P. falciparum* challenge, demonstrating that neutralization is likely to be the primary mechanism of action (87). Although the growth inhibition assay has traditionally been the gold standard *in vitro* assessment of antibody neutralization, it generally does not correlate well with naturally acquired protection against malaria and may therefore be considered less valuable for assessing naturally acquired immune responses than other, more recently developed, assays (74). However, the growth inhibition assay seems well suited to measure the activity of antibodies that are known to mediate their effect through neutralization. We speculate that these antibodies most likely target antigens that are less abundant on the merozoite surface and are involved in essential interactions with ligands on the erythrocyte (**Figure 3**). The growth inhibition assay may therefore be the assay of choice to

evaluate vaccine-elicited antibody responses against EBA-175, PfRH5, and potentially other antigens.

The implementation of novel functional assays has revealed the role of opsonic phagocytosis and complement fixation in antibody-mediated inhibition and has uncovered these effector functions as correlates of naturally acquired protection. As mentioned, opsonic phagocytosis by naturally acquired antibodies, mainly IgG1 and IgG3, has been reported to be strain-transcending (85) and correlates well with protection from disease (81, 88). Opsonic phagocytosis of whole merozoites increased with greater breadth of antibody responses (81, 88), confirming that targeting multiple antigens is beneficial for anti-merozoite immunity. Various antigens have been identified as targets for these opsonizing antibodies, including MSP1, MSP2, and MSP3 (86, 88, 89). To further delineate the role of individual antigen specificities, Kana et al. used beads coated with recombinant proteins to measure the ability of IgG antibodies against single merozoite antigens to induce opsonic phagocytosis (90). Antibody-induced phagocytosis in this assay showed an association with protection against malaria in a longitudinal cohort of 134 children in Ghana for MSP1-19, MSP2 (3D7 allele), MSP3 (N-terminal region of K1 allele), GLURP (region 2), and PfRH2-2030 (the fragment of PfRH2 covering amino acid residues 2030–2528), but not against 21 other antigens that have been implicated as targets of the protective immune response (90). Combinations of antibody responses against six antigens correlated better with protection than responses to any individual antigen, suggesting that antibodies against multiple antigens may be necessary to induce optimal merozoite phagocytosis.

Complement fixation and subsequent activation of the classical complement pathway is also strongly associated with protection for various merozoite antigens (74, 91). This complement cascade culminates in the formation of the membrane attack complex, which mediates merozoite lysis. Reiling et al. determined that fixation of C1q, the first step in the complement cascade, correlated strongly with membrane attack complex formation and therefore measured the ability of serum IgM and IgG antibodies against various merozoite antigens to bind C1q as a proxy of complement-activating potential (74). The prevalence of C1q-fixing antibodies was high for the majority of merozoite antigens studied and correlated strongly with protection against malaria. The strongest protective associations were observed for C1q-fixing antibodies against EBA-140 (region III–V), MSP7, rhoptry-associated leucine zipper-like protein 1 (RALP1), GPI-anchored micronemal antigen (GAMA), and PfRH2-2030 (74). Again, combinations of antibodies against three different antigens showed an increased protective effect over single antigens or combinations of two antigens, with RALP1 and MSP7 among the antigens most frequently found in protective combinations.

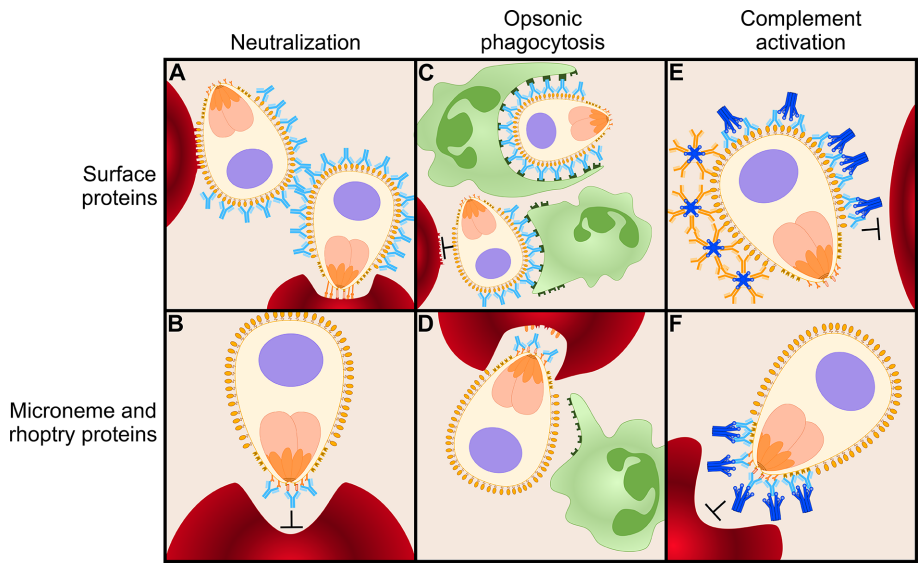

FIGURE 3 | Antibody-mediated inhibition of merozoites. Antibodies can function in several ways to mediate inhibition of merozoite invasion into erythrocytes. Here, we present a model of various antibody effector mechanisms for two different classes of antigens: highly abundant merozoite surface proteins and relatively scarce microneme and rhoptry proteins. **(A)** Immunoglobulins G (IgGs; shown in light blue) targeting surface proteins are not effective mediators of inhibition *via* neutralization, possibly because extremely high antibody concentrations are necessary to completely block the coat of proteins on the merozoite surface. **(B)** IgGs can effectively neutralize merozoites when targeting relatively scarce microneme and rhoptry proteins on the apical surface, such as PfRH5 and EBA-175. **(C)** When targeting abundant surface proteins, opsonic phagocytosis is effectively mediated *via* IgG1 and IgG3 by binding of phagocytic cells (green) to their Fc domain. **(D)** Many microneme and rhoptry proteins are only released to the surface of the merozoite once it has attached to an erythrocyte and is ready to commence the invasion process. At this moment, the erythrocyte will (partially) shield IgGs bound to microneme and rhoptry proteins from the Fc receptors of phagocytes. Thus, opsonic phagocytosis may not be an efficient effector function for antibodies against this class of proteins. **(E)** Both IgGs and IgMs (orange) efficiently initiate the classical complement cascade *via* C1q (dark blue) when targeting surface proteins to prevent merozoite invasion. **(F)** IgG is an effective mediator of the complement cascade when targeting microneme and rhoptry proteins. IgM may be less efficient against this class of proteins because large, pentameric IgM may not be able to reach between the erythrocyte and merozoite surfaces.

Interestingly, strong opsonic phagocytosis activity was mainly observed for antibodies targeting antigens expressed on the merozoite surface, while the strong complement-fixing activity was predominantly observed for antibodies directed against rhoptry and microneme proteins (74, 90). Of the antigens that were tested in both assays, antibodies that displayed strong opsonic phagocytosis activity against three out of four antigens in the bead-based assay performed by Kana et al. showed relatively weak or no complement-fixing activity and the reverse was true for IgG antibodies against EBA140RIII-V and RALP1 (74, 90). It is likely that multiple antibody effector mechanisms act in concert to provide immunity (92). Both complement fixation and opsonic phagocytosis are induced by the cytophilic IgG1 and IgG3 antibodies, underlining that a vaccine-induced response against merozoite antigens should be directed toward these isotypes. The results from Reiling et al. and Kana et al. suggest that cytophilic antibodies against different antigens preferentially act through one particular effector function, and it will be interesting to understand which antigenic properties influence this response. One explanation for the preferential opsonic phagocytosis activity of antibodies against merozoite surface proteins could be that many antigens located in rhoptries and micronemes only become exposed when the merozoite is in direct contact with an erythrocyte (93) [reviewed in (70, 94)] and may therefore be poorly accessible to phagocytes (**Figure 3**). However, the differences between results from Reiling et al. and Kana et al. could also be influenced by variation in antibody titers between individuals, the studied antigens, characteristics of the cohort, inclusion criteria for participants selected for the study, as well as other variables. To further evaluate the contribution of antibody specificities and effector mechanisms to inhibition of merozoite invasion, samples from the same individuals should be compared side-by-side in assays that measure these different effector functions against the same panel of merozoite antigens. Epitope mapping of antibodies with different levels of inhibitory activity against merozoites will also provide important insights into immune mechanisms. For example, binding of monoclonal IgGs to a non-neutralizing epitope of merozoite protein PfRH5 resulted in slower erythrocyte invasion, thereby increasing exposure times of other epitopes on PfRH5 to neutralizing antibodies (95). This resulted in a synergistic effect between the non-neutralizing and neutralizing antibodies (95). For MSP1, epitope mapping of non-inhibitory and inhibitory antibodies revealed MSP1 cleavage sites as the most vulnerable sites of this antigen (96). It would be highly informative to also perform such studies for other antigens to better understand how antibodies function and which epitopes should be targeted by vaccination to achieve an effective immune response.

Immunoglobulin M Responses Against Merozoite Proteins

Although the focus of studies on naturally acquired immunity has been on IgG, recent studies suggest that IgM may also play an important role in protection (97–99). IgM is an excellent mediator of complement activation and may function in this way to confer immunity (98). An interesting observation about the role of IgM in protection against malaria has come from a comparison between the Fulani and Dogon people, two genetically distinct ethnic groups living in West Africa with different susceptibility to malaria (100). The Fulani are more resistant to malaria but carry lower frequencies of classical malaria-resistance genes (101), which has prompted a search for immunological variables that can explain the observed differences in malaria susceptibility. Differences in the frequency of genetic variants in several immune-related genes have been identified between the Fulani and Dogon people, but the immunological consequences of these results are unclear (102). Transcriptional profiling showed that the Fulani have a strong inflammatory gene signature in the monocyte population during *P. falciparum* infection, leading to the hypothesis that monocytes in Fulani people exist in a "primed" state that will elicit a stronger immune response upon infection (103). The Fulani also had higher frequencies of activated memory B cells in the absence of infection and higher percentages of plasma cells during *P. falciparum* infection (104). These enhanced cellular immune responses most likely explain the increased IgM and IgG levels against many *P. falciparum* proteins in the Fulani as compared to the Dogon (97). Interestingly, the Fulani IgM responses recognized a broader repertoire of *P. falciparum* proteins than IgG responses, including a set of antigens to which antibody levels have been correlated with protection (97). These results suggest that IgM may play an underappreciated role in protection against malaria.

In a mouse model, IgM^+ memory B cells were shown to be the first responders in secondary *Plasmodium* infections, giving rise to both IgM and IgG antibody-secreting cells (99). IgM^+ memory B cells contained somatic hypermutations and recognized target antigens with high affinity, pointing to T-cell dependent affinity maturation within the germinal center. IgM^+ memory B cells with specificity for merozoite antigens were also detected in malaria-experienced humans (99). Finally, Boyle et al. recently showed that IgM against merozoite antigens appears rapidly upon *P. falciparum* infection and reaches high levels in individuals with life-long exposure (98). IgM levels were more stable under low transmission conditions than IgG levels and were associated with protection (98). However, children with high IgM levels also had high levels of IgG against merozoite antigens, which were also associated with protection. The independent contribution of these antibody classes to immunity therefore remains to be determined.

THE ACQUISITION AND MAINTENANCE OF HUMORAL IMMUNE RESPONSES AGAINST *PLASMODIUM FALCIPARUM*

Naturally acquired antibody responses against *P. falciparum* require repeated parasite exposure to attain protection, while probably never reaching sterilizing immunity. The rate of antibody acquisition against *P. falciparum* proteins is

influenced by various factors, including age of the human host, transmission intensity, and the type of antigen (72, 73, 105, 106). In general, antibody levels increase with both age and higher transmission intensity (72, 73, 105). Antibodies against different antigens accumulate at varying rates, with stronger responses typically seen for antibodies targeting extracellular or plasma membrane proteins and proteins that are highly abundant, highly polymorphic, or lack a human ortholog (106).

It has been shown that IgGs against PfEMP1 are acquired during the first years of life (47, 107), and their breadth increases with age and exposure (38, 60). In a cohort of children from Papua New Guinea, levels of PfEMP1 IgG antibodies positively correlated with protection in both younger children (1–4 years) and older children (5–14 years) (107). Interestingly, antibodies against merozoite antigens were only associated with protection in older children in this cohort (107). These results suggest that antibodies against PfEMP1 may provide a first line of defense against severe malaria pathogenesis early in life, while antibodies to other parasite antigens may contribute to protection against uncomplicated malaria in older children. This may seem counterintuitive given the extremely high diversity among PfEMP1 variants, at the level of both amino acid sequences and domain composition, while polymorphisms in merozoite antigens provide relatively modest sequence variation in comparison. However, as detailed in Section 2.1, only a small fraction of PfEMP1 domains are pathogenic, with particularly strong evidence for the role of CIDRα1 in severe malaria. Targeting one or a small panel of such pathogenic PfEMP1 domains may be sufficient to achieve protection against severe disease. In contrast, a broader antibody response with higher antibody titers may be necessary to effectively inhibit erythrocyte invasion by merozoites. Indeed, it has been reported that antibodies against merozoite antigens must reach a threshold level before associating with protection (10, 11). While such a functional threshold level is also likely to exist for antibodies against PfEMP1 and antigens on other pathogens, the requirement for recognition of multiple merozoite antigens at high antibody concentrations may be exceptionally high for *Plasmodium* infections. This may explain why relatively low antibody levels against merozoites in young children are not sufficient to provide protection to malaria in these individuals, while similar levels of anti-PfEMP1 antibodies confer protection against severe disease. The contribution of immune responses against these two main groups of antigens to immunity remains to be fully untangled.

An additional complication to the generation of a protective antibody response against *P. falciparum* is the ability of the parasite to modulate immune responses *via* several mechanisms. *Plasmodium* infections induce a pro-inflammatory immune response that drives differentiation of $CD4^+$ T cells into Th-1 polarized T follicular helper cells, resulting in impaired germinal center (GC) responses (108, 109). This pro-inflammatory environment also induces the expansion of a subset of B cells known as "atypical memory B cells" (110, 111) [reviewed in (112, 113)]. These cells express inhibitory receptors and have been described as functionally impaired (114, 115), although several studies have reported that these cells may in fact be functional and can contribute to anti-parasite immunity (116, 117). It has been postulated that naive B cells differentiate into atypical memory B cells in B cell follicles upon stimulation with interferon gamma produced by Th-1 polarized T follicular helper cells and Toll-like receptor agonists (118). In this process, atypical memory B cells may bypass the germinal center (GC) or exit the GC prematurely, thus limiting affinity maturation and the ability of these cells to produce high affinity antibodies. Finally, a recent study showed that in both human and mouse experimental *Plasmodium* infections, a large proportion of activated B cells differentiated into extrafollicular plasmablasts (119). The high demand of replicating plasmablasts for nutrients, in particular the amino acid L-glutamine, outcompeted that of GC B cells, thereby limiting the development of memory B cells and long-lived plasma cells. The disruption of GC formation during *Plasmodium* infections likely hampers the development of B cells with high affinity for parasite antigens. It is however conceivable that the chronic and repetitive nature of *P. falciparum* infections will ultimately allow for the acquisition of high levels of somatic hypermutations by consecutive rounds of memory B cell activation and affinity maturation, as observed in, for example, HIV-1-infected individuals (120–122). Alternatively, high affinity plasma cells could be derived from naive B cell precursors with intrinsic high binding affinity, which would limit the need for effective germinal center reactions (123). Longitudinal molecular studies of antibody evolution have not been performed in naturally *P. falciparum*-exposed individuals but would be useful to better understand how protective antibody responses develop over time.

Given the high levels of antibodies required for protection against malaria, protective antibody responses are generally not sustained over long periods of time without re-exposure. Antibody levels are maintained by long-lived antibody-secreting cells in the bone marrow. While these plasma cells are not easily accessible for study in humans, their half-life can be modeled based on serum antibody levels. Using this approach, Yman et al. found that antibody levels against merozoite antigens as well as the proportion of long-lived antibody-secreting cells after a malaria episode in individuals who were formerly exposed because of residency in an endemic area (a median of 14 years ago) were higher compared to previously malaria-naive travelers (12). These results suggest that repeated *P. falciparum* infections are necessary to drive the formation of long-lived antibody-secreting cells, providing an explanation for the observation that immunity requires prolonged exposure. In addition, the half-life of merozoite antigen-specific long-lived plasma cells was 2–4 years, which was shorter than that of long-lived antibody-secreting cells against tetanus toxoid (7 years) and explains why some degree of exposure is necessary to maintain immunity (12). However, this study also demonstrated that immunological memory is not completely lost after more than a decade of non-exposure. These results are in agreement with an earlier report that showed that in five Swedish residents who were previously treated for malaria following international travel,

P. falciparum merozoite antigen-specific memory B cells were detected up to 16 years later in the absence of re-exposure (124). Findings from a recent study in a low transmission region in Zambia suggest that the level of exposure necessary to maintain antibody levels is probably very low (73). In this setting, parasite prevalence in the population was approximately 2.5%, most infections were asymptomatic, and about half of all individuals with parasitemia had parasite levels that were undetectable with rapid diagnostic tests. In the absence of significant recent transmission, adults showed stable antibody levels over a period of 2 years, suggesting that infrequent infections with low-level parasitemia are sufficient to maintain humoral immune responses. Among targets of the strongest antibody responses were PfEMP1 variants and merozoite antigens. Neither of the studies discussed above included a functional assessment of antibody responses, and it is thus unclear whether the antibodies measured in these studies contribute to protection. However, assuming that long-lived antibody-secreting cells and antibodies targeting protective epitopes follow similar kinetics, these results suggest that long-term protection by vaccination may be possible with frequent boosting of the humoral immune response.

CONCLUDING REMARKS

The main targets of naturally acquired immune responses against *P. falciparum* are variant surface antigens on the plasma membrane of the infected erythrocytes and antigens expressed by merozoites. Antibody responses against PfEMP1 variants develop early in human life and seem to be the main driver of protection against severe malaria in young children. Protection against malaria in older children is achieved once antibodies against merozoite antigens reach sufficiently high levels. A vaccine based on a combination of these two classes of antigens may elicit antibodies that have an additive effect, or possibly even act synergistically, toward the prevention of all clinical manifestations of malaria.

The main obstacle for the development of a vaccine targeting PfEMP1 is the identification of conserved epitopes, given the enormous sequence variation among this protein family. The CIDRα1 domain has the most potential as a vaccine candidate against severe malaria, given its role in the pathogenesis of severe malaria through binding to EPCR, and because of structural conservation of the EPCR binding site.

Correlations with protection have been observed for antibody responses against many different merozoite antigens. Broader antibody responses provide better protection, with near full protection for responses against combinations of three to four antigens. What remains unclear is which of these (combinations of) antigens should be moved forward for vaccine development. Since many of these antigens are polymorphic, the identification of conserved epitopes has high priority. In addition, several candidates that have been identified have unknown functions and further characterization of these proteins will provide more insight into the merozoite invasion process.

Finally, recent studies have revealed mechanisms of antibody-mediated parasite inhibition. Understanding how antibodies function against different target antigens is important to be able to induce the most effective immune response by vaccination and to establish correlates of protection. Nature has provided us with proof-of-concept that protection against blood stage infection is achievable. Our increased understanding of naturally acquired immunity therefore provides hope for the development of a malaria blood stage vaccine.

AUTHOR CONTRIBUTIONS

The first draft of the manuscript was prepared by SG and RR, and revised by EB. AB, SB, and GB further edited the manuscript and provided intellectual contributions to the design of the figures. All authors contributed to the article and approved the submitted version.

FUNDING

This work was supported by the National Institutes of Health [grant numbers AI128466 and AI133274]. SG and AB are supported by Graduate Research in Immunology Program training grant NIH T32 AI138944. RR is supported by the National Center for Advancing Translational Sciences of the National Institutes of Health under Award Number TL1TR002647.

REFERENCES

1. World Health Organization. *World Malaria Report 2019*. Geneva: World Health Organization. (2019) Available at: https://www.who.int/publications/i/item/world-malaria-report-2019.
2. Draper SJ, Sack BK, King CR, Nielsen CM, Rayner JC, Higgins MK, et al. Malaria vaccines: recent advances and new horizons. *Cell Host Microbe* (2018) 24:43–56. doi: 10.1016/j.chom.2018.06.008
3. Cockburn IA, Seder RA. Malaria prevention: from immunological concepts to effective vaccines and protective antibodies. *Nat Immunol* (2018) 19:1199–211. doi: 10.1038/s41590-018-0228-6
4. Langhorne J, Ndungu FM, Sponaas AM, Marsh K. Immunity to malaria: more questions than answers. *Nat Immunol* (2008) 9:725–32. doi: 10.1038/ni.f.205
5. Camponovo F, Campo JJ, Le TQ, Oberai A, Hung C, Pablo JV, et al. Proteome-wide analysis of a malaria vaccine study reveals personalized humoral immune profiles in Tanzanian adults. *Elife* (2020) 9:e53080. doi: 10.7554/eLife.53080
6. Crompton PD, Kayala MA, Traore B, Kayentao K, Ongoiba A, Weiss GE, et al. A prospective analysis of the Ab response to *Plasmodium falciparum* before and after a malaria season by protein microarray. *Proc Natl Acad Sci USA* (2010) 107:6958–63. doi: 10.1073/pnas.1001323107

7. Dent AE, Nakajima R, Liang L, Baum E, Moormann AM, Sumba PO, et al. *Plasmodium falciparum* protein microarray antibody profiles correlate with protection from symptomatic malaria in Kenya. *J Infect Dis* (2015) 212:1429–38. doi: 10.1093/infdis/jiv224
8. Mu J, Awadalla P, Duan J, McGee KM, Keebler J, Seydel K, et al. Genome-wide variation and identification of vaccine targets in the *Plasmodium falciparum* genome. *Nat Genet* (2007) 39:126–30. doi: 10.1038/ng1924
9. Volkman SK, Sabeti PC, DeCaprio D, Neafsey DE, Schaffner SF, Milner DAJr., et al. A genome-wide map of diversity in *Plasmodium falciparum*. *Nat Genet* (2007) 39:113–9. doi: 10.1038/ng1930
10. Murungi LM, Kamuyu G, Lowe B, Bejon P, Theisen M, Kinyanjui SM, et al. A threshold concentration of anti-merozoite antibodies is required for protection from clinical episodes of malaria. *Vaccine* (2013) 31:3936–42. doi: 10.1016/j.vaccine.2013.06.042
11. Stanisic DI, Fowkes FJ, Koinari M, Javati S, Lin E, Kiniboro B, et al. Acquisition of antibodies against *Plasmodium falciparum* merozoites and malaria immunity in young children and the influence of age, force of infection, and magnitude of response. *Infect Immun* (2015) 83:646–60. doi: 10.1128/IAI.02398-14
12. Yman V, White MT, Asghar M, Sundling C, Sonden K, Draper SJ, et al. Antibody responses to merozoite antigens after natural *Plasmodium falciparum* infection: kinetics and longevity in absence of re-exposure. *BMC Med* (2019) 17:22. doi: 10.1186/s12916-019-1255-3
13. Kinyanjui SM, Conway DJ, Lanar DE, Marsh K. IgG antibody responses to *Plasmodium falciparum* merozoite antigens in Kenyan children have a short half-life. *Malar J* (2007) 6:82. doi: 10.1186/1475-2875-6-82
14. Fowkes FJ, McGready R, Cross NJ, Hommel M, Simpson JA, Elliott SR, et al. New insights into acquisition, boosting, and longevity of immunity to malaria in pregnant women. *J Infect Dis* (2012) 206:1612–21. doi: 10.1093/infdis/jis566
15. White MT, Griffin JT, Akpogheneta O, Conway DJ, Koram KA, Riley EM, et al. Dynamics of the antibody response to *Plasmodium falciparum* infection in African children. *J Infect Dis* (2014) 210:1115–22. doi: 10.1093/infdis/jiu219
16. Baruch DI, Pasloske BL, Singh HB, Bi X, Ma XC, Feldman M, et al. Cloning the *P. falciparum* gene encoding PfEMP1, a malarial variant antigen and adherence receptor on the surface of parasitized human erythrocytes. *Cell* (1995) 82:77–87. doi: 10.1016/0092-8674(95)90054-3
17. Su XZ, Heatwole VM, Wertheimer SP, Guinet F, Herrfeldt JA, Peterson DS, et al. The large diverse gene family var encodes proteins involved in cytoadherence and antigenic variation of *Plasmodium falciparum*-infected erythrocytes. *Cell* (1995) 82:89–100. doi: 10.1016/0092-8674(95)90055-1
18. Smith JD, Chitnis CE, Craig AG, Roberts DJ, Hudson-Taylor DE, Peterson DS, et al. Switches in expression of *Plasmodium falciparum var* genes correlate with changes in antigenic and cytoadherent phenotypes of infected erythrocytes. *Cell* (1995) 82:101–10. doi: 10.1016/0092-8674(95)90056-X
19. Goel S, Palmkvist M, Moll K, Joannin N, Lara P, Akhouri RR, et al. RIFINs are adhesins implicated in severe *Plasmodium falciparum* malaria. *Nat Med* (2015) 21:314–7. doi: 10.1038/nm.3812
20. Niang M, Bei AK, Madnani KG, Pelly S, Dankwa S, Kanjee U, et al. STEVOR is a *Plasmodium falciparum* erythrocyte binding protein that mediates merozoite invasion and rosetting. *Cell Host Microbe* (2014) 16:81–93. doi: 10.1016/j.chom.2014.06.004
21. Rowe JA, Moulds JM, Newbold CI, Miller LH. *P. falciparum* rosetting mediated by a parasite-variant erythrocyte membrane protein and complement-receptor 1. *Nature* (1997) 388:292–5. doi: 10.1038/40888
22. Semblat JP, Ghumra A, Czajkowsky DM, Wallis R, Mitchell DA, Raza A, et al. Identification of the minimal binding region of a *Plasmodium falciparum* IgM binding PfEMP1 domain. *Mol Biochem Parasitol* (2015) 201:76–82. doi: 10.1016/j.molbiopara.2015.06.001
23. Wahlgren M, Goel S, Akhouri RR. Variant surface antigens of *Plasmodium falciparum* and their roles in severe malaria. *Nat Rev Microbiol* (2017) 15:479–91. doi: 10.1038/nrmicro.2017.47
24. David PH, Hommel M, Miller LH, Udeinya IJ, Oligino LD. Parasite sequestration in *Plasmodium falciparum* malaria: spleen and antibody modulation of cytoadherence of infected erythrocytes. *Proc Natl Acad Sci USA* (1983) 80:5075–9. doi: 10.1073/pnas.80.16.5075
25. Ghumra A, Khunrae P, Ataide R, Raza A, Rogerson SJ, Higgins MK, et al. Immunisation with recombinant PfEMP1 domains elicits functional rosette-inhibiting and phagocytosis-inducing antibodies to *Plasmodium falciparum*. *PloS One* (2011) 6:e16414. doi: 10.1371/journal.pone.0016414
26. Guillotte M, Nato F, Juillerat A, Hessel A, Marchand F, Lewit-Bentley A, et al. Functional analysis of monoclonal antibodies against the *Plasmodium falciparum* PfEMP1-VarO adhesin. *Malar J* (2016) 15:28. doi: 10.1186/s12936-015-1016-5
27. Chan JA, Boyle MJ, Moore KA, Reiling L, Lin Z, Hasang W, et al. Antibody targets on the surface of *Plasmodium falciparum*-infected erythrocytes that are associated with immunity to severe malaria in young children. *J Infect Dis* (2019) 219:819–28. doi: 10.1093/infdis/jiy580
28. Arora G, Hart GT, Manzella-Lapeira J, Doritchamou JY, Narum DL, Thomas LM, et al. NK cells inhibit *Plasmodium falciparum* growth in red blood cells via antibody-dependent cellular cytotoxicity. *Elife* (2018) 7: e53080. doi: 10.7554/eLife.36806
29. Deitsch KW, Dzikowski R. Variant gene expression and antigenic variation by malaria parasites. *Annu Rev Microbiol* (2017) 71:625–41. doi: 10.1146/annurev-micro-090816-093841
30. Larremore DB, Sundararaman SA, Liu W, Proto WR, Clauset A, Loy DE, et al. Ape parasite origins of human malaria virulence genes. *Nat Commun* (2015) 6:8368. doi: 10.1038/ncomms9368
31. Olsen RW, Ecklu-Mensah G, Bengtsson A, Ofori MF, Kusi KA, Koram KA, et al. Acquisition of IgG to ICAM-1-binding DBLbeta comains in the *Plasmodium falciparum* erythrocyte membrane protein 1 antigen family varies between groups A, B, and C. *Infect Immun* (2019) 87:e00224-19. doi: 10.1128/IAI.00224-19
32. Rask TS, Hansen DA, Theander TG, Gorm Pedersen A, Lavstsen T. *Plasmodium falciparum* erythrocyte membrane protein 1 diversity in seven genomes–divide and conquer. *PloS Comput Biol* (2010) 6:e1000933. doi: 10.1371/journal.pcbi.1000933
33. Avril M, Benjamin M, Dols MM, Smith JD. Interplay of *Plasmodium falciparum* and thrombin in brain endothelial barrier disruption. *Sci Rep* (2019) 9:13142. doi: 10.1038/s41598-019-49530-1
34. Turner GD, Morrison H, Jones M, Davis TM, Looareesuwan S, Buley ID, et al. An immunohistochemical study of the pathology of fatal malaria. Evidence for widespread endothelial activation and a potential role for intercellular adhesion molecule-1 in cerebral sequestration. *Am J Pathol* (1994) 145:1057–69.
35. Kessler A, Dankwa S, Bernabeu M, Harawa V, Danziger SA, Duffy F, et al. Linking EPCR-binding PfEMP1 to brain swelling in pediatric cerebral malaria. *Cell Host Microbe* (2017) 22:601–614 e5. doi: 10.1016/j.chom.2017.09.009
36. Lavstsen T, Turner L, Saguti F, Magistrado P, Rask TS, Jespersen JS, et al. *Plasmodium falciparum* erythrocyte membrane protein 1 domain cassettes 8 and 13 are associated with severe malaria in children. *Proc Natl Acad Sci USA* (2012) 109:E1791–800. doi: 10.1073/pnas.1120455109
37. Gupta S, Snow RW, Donnelly CA, Marsh K, Newbold C. Immunity to non-cerebral severe malaria is acquired after one or two infections. *Nat Med* (1999) 5:340–3. doi: 10.1038/6560
38. Kanoi BN, Nagaoka H, Morita M, White MT, Palacpac NMQ, Ntege EH, et al. Comprehensive analysis of antibody responses to *Plasmodium falciparum* erythrocyte membrane protein 1 domains. *Vaccine* (2018) 36:6826–33. doi: 10.1016/j.vaccine.2018.08.058
39. Duffy MF, Noviyanti R, Tsuboi T, Feng ZP, Trianty L, Sebayang BF, et al. Differences in PfEMP1s recognized by antibodies from patients with uncomplicated or severe malaria. *Malar J* (2016) 15:258. doi: 10.1186/s12936-016-1296-4
40. Tessema SK, Nakajima R, Jasinskas A, Monk SL, Lekieffre L, Lin E, et al. Protective immunity against severe malaria in children is associated with a limited repertoire of antibodies to conserved PfEMP1 variants. *Cell Host Microbe* (2019) 26:579–590 e5. doi: 10.1016/j.chom.2019.10.012
41. Travassos MA, Niangaly A, Bailey JA, Ouattara A, Coulibaly D, Lyke KE, et al. Children with cerebral malaria or severe malarial anaemia lack immunity to distinct variant surface antigen subsets. *Sci Rep* (2018) 8:6281. doi: 10.1038/s41598-018-24462-4
42. Tuju J, Mackinnon MJ, Abdi AI, Karanja H, Musyoki JN, Warimwe GM, et al. Antigenic cartography of immune responses to *Plasmodium falciparum*

erythrocyte membrane protein 1 (PfEMP1). *PloS Pathog* (2019) 15: e1007870. doi: 10.1371/journal.ppat.1007870
43. Jespersen JS, Wang CW, Mkumbaye SI, Minja DT, Petersen B, Turner L, et al. *Plasmodium falciparum var* genes expressed in children with severe malaria encode CIDRalpha1 domains. *EMBO Mol Med* (2016) 8:839–50. doi: 10.15252/emmm.201606188
44. Mkumbaye SI, Wang CW, Lyimo E, Jespersen JS, Manjurano A, Mosha J, et al. The severity of *Plasmodium falciparum* infection is associated with transcript levels of *var* genes encoding endothelial protein C receptor-binding *P. falciparum* erythrocyte membrane protein 1. *Infect Immun* (2017) 85:e00841-16. doi: 10.1128/IAI.00841-16
45. Rambhatla JS, Turner L, Manning L, Laman M, Davis TME, Beeson JG, et al. Acquisition of antibodies against endothelial protein C receptor-binding domains of *Plasmodium falciparum* erythrocyte membrane protein 1 in children with severe malaria. *J Infect Dis* (2019) 219:808–18. doi: 10.1093/infdis/jiy564
46. Obeng-Adjei N, Larremore DB, Turner L, Ongoiba A, Li S, Doumbo S, et al. Longitudinal analysis of naturally acquired PfEMP1 CIDR domain variant antibodies identifies associations with malaria protection. *JCI Insight* (2020) 5:e137262. doi: 10.1172/jci.insight.137262
47. Turner L, Lavstsen T, Mmbando BP, Wang CW, Magistrado PA, Vestergaard LS, et al. IgG antibodies to endothelial protein C receptor-binding cysteine-rich interdomain region domains of *Plasmodium falciparum* erythrocyte membrane protein 1 are acquired early in life in individuals exposed to malaria. *Infect Immun* (2015) 83:3096–103. doi: 10.1128/IAI.00271-15
48. Lau CK, Turner L, Jespersen JS, Lowe ED, Petersen B, Wang CW, et al. Structural conservation despite huge sequence diversity allows EPCR binding by the PfEMP1 family implicated in severe childhood malaria. *Cell Host Microbe* (2015) 17:118–29. doi: 10.1016/j.chom.2014.11.007
49. Fernandez V, Hommel M, Chen Q, Hagblom P, Wahlgren M. Small, clonally variant antigens expressed on the surface of the *Plasmodium falciparum*-infected erythrocyte are encoded by the rif gene family and are the target of human immune responses. *J Exp Med* (1999) 190:1393–404. doi: 10.1084/jem.190.10.1393
50. Saito F, Hirayasu K, Satoh T, Wang CW, Lusingu J, Arimori T, et al. Corrigendum: Immune evasion of *Plasmodium falciparum* by RIFIN via inhibitory receptors. *Nature* (2018) 554:554. doi: 10.1038/nature25498
51. Meyaard L, Adema GJ, Chang C, Woollatt E, Sutherland GR, Lanier LL, et al. LAIR-1, a novel inhibitory receptor expressed on human mononuclear leukocytes. *Immunity* (1997) 7:283–90. doi: 10.1016/S1074-7613(00)80530-0
52. Naji A, Menier C, Morandi F, Agaugue S, Maki G, Ferretti E, et al. Binding of HLA-G to ITIM-bearing Ig-like transcript 2 receptor suppresses B cell responses. *J Immunol* (2014) 192:1536–46. doi: 10.4049/jimmunol.1300438
53. van der Vuurst de Vries AR, Clevers H, Logtenberg T, Meyaard L. Leukocyte-associated immunoglobulin-like receptor-1 (LAIR-1) is differentially expressed during human B cell differentiation and inhibits B cell receptor-mediated signaling. *Eur J Immunol* (1999) 29:3160–7. doi: 10.1002/(SICI)1521-4141(199910)29:10<3160::AID-IMMU3160>3.0.CO;2-S
54. Harrison TE, Morch AM, Felce JH, Sakoguchi A, Reid AJ, Arase H, et al. Structural basis for RIFIN-mediated activation of LILRB1 in malaria. *Nature* (2020). doi: 10.1038/s41586-020-2530-3
55. Saito F, Hirayasu K, Satoh T, Wang CW, Lusingu J, Arimori T, et al. Immune evasion of *Plasmodium falciparum* by RIFIN via inhibitory receptors. *Nature* (2017) 552:101–5. doi: 10.1038/nature24994
56. Pieper K, Tan J, Piccoli L, Foglierini M, Barbieri S, Chen Y, et al. Public antibodies to malaria antigens generated by two LAIR1 insertion modalities. *Nature* (2017) 548:597–601. doi: 10.1038/nature23670
57. Tan J, Pieper K, Piccoli L, Abdi A, Perez MF, Geiger R, et al. A LAIR1 insertion generates broadly reactive antibodies against malaria variant antigens. *Nature* (2016) 529:105–9. doi: 10.1038/nature16450
58. Zhou AE, Berry AA, Bailey JA, Pike A, Dara A, Agrawal S, et al. Antibodies to peptides in semiconserved domains of RIFINs and STEVORs correlate with malaria exposure. *mSphere* (2019) 4:e00097-19. doi: 10.1128/mSphere.00097-19
59. Petter M, Haeggstrom M, Khattab A, Fernandez V, Klinkert MQ, Wahlgren M. Variant proteins of the *Plasmodium falciparum* RIFIN family show distinct subcellular localization and developmental expression patterns. *Mol Biochem Parasitol* (2007) 156:51–61. doi: 10.1016/j.molbiopara.2007.07.011
60. Chan JA, Howell KB, Reiling L, Ataide R, Mackintosh CL, Fowkes FJ, et al. Targets of antibodies against *Plasmodium falciparum*-infected erythrocytes in malaria immunity. *J Clin Invest* (2012) 122:3227–38. doi: 10.1172/JCI62182
61. Limpaiboon T, Shirley MW, Kemp DJ, Saul A. 7H8/6, a multicopy DNA probe for distinguishing isolates of *Plasmodium falciparum*. *Mol Biochem Parasitol* (1991) 47:197–206. doi: 10.1016/0166-6851(91)90179-A
62. Wichers JS, Scholz JAM, Strauss J, Witt S, Lill A, Ehnold LI, et al. Dissecting the gene expression, localization, membrane topology, and function of the *Plasmodium falciparum* STEVOR protein family. *mBio* (2019) 10:e01500-19. doi: 10.1128/mBio.01500-19
63. McRobert L, Preiser P, Sharp S, Jarra W, Kaviratne M, Taylor MC, et al. Distinct trafficking and localization of STEVOR proteins in three stages of the *Plasmodium falciparum* life cycle. *Infect Immun* (2004) 72:6597–602. doi: 10.1128/IAI.72.11.6597-6602.2004
64. Lee WC, Russell B, Renia L. Sticking for a cause: the *falciparum* malaria parasites cytoadherence paradigm. *Front Immunol* (2019) 10:1444. doi: 10.3389/fimmu.2019.01444
65. Nilsson SK, Childs LM, Buckee C, Marti M. Targeting human transmission biology for malaria elimination. *PloS Pathog* (2015) 11:e1004871. doi: 10.1371/journal.ppat.1004871
66. Blythe JE, Yam XY, Kuss C, Bozdech Z, Holder AA, Marsh K, et al. *Plasmodium falciparum* STEVOR proteins are highly expressed in patient isolates and located in the surface membranes of infected red blood cells and the apical tips of merozoites. *Infect Immun* (2008) 76:3329–36. doi: 10.1128/IAI.01460-07
67. Singh H, Madnani K, Lim YB, Cao J, Preiser PR, Lim CT. Expression dynamics and physiologically relevant functional study of STEVOR in asexual stages of *Plasmodium falciparum* infection. *Cell Microbiol* (2017) 19:e12715. doi: 10.1111/cmi.12715
68. Kanoi BN, Nagaoka H, White MT, Morita M, Palacpac NMQ, Ntege EH, et al. Global repertoire of human antibodies against *Plasmodium falciparum* RIFINs, SURFINs, and STEVORs in a malaria exposed population. *Front Immunol* (2020) 11:893. doi: 10.3389/fimmu.2020.00893
69. Lavazec C, Sanyal S, Templeton TJ. Hypervariability within the Rifin, Stevor and Pfmc-2TM superfamilies in *Plasmodium falciparum*. *Nucleic Acids Res* (2006) 34:6696–707. doi: 10.1093/nar/gkl942
70. Cowman AF, Tonkin CJ, Tham WH, Duraisingh MT. The molecular basis of erythrocyte invasion by malaria parasites. *Cell Host Microbe* (2017) 22:232–45. doi: 10.1016/j.chom.2017.07.003
71. Beeson JG, Kurtovic L, Dobano C, Opi DH, Chan JA, Feng G, et al. Challenges and strategies for developing efficacious and long-lasting malaria vaccines. *Sci Transl Med* (2019) 11:eaau1458. doi: 10.1126/scitranslmed.aau1458
72. King CL, Davies DH, Felgner P, Baum E, Jain A, Randall A, et al. Biosignatures of Exposure/Transmission and Immunity. *Am J Trop Med Hyg* (2015) 93:16–27. doi: 10.4269/ajtmh.15-0037
73. Kobayashi T, Jain A, Liang L, Obiero JM, Hamapumbu H, Stevenson JC, et al. Distinct antibody signatures associated with different malaria transmission intensities in Zambia and Zimbabwe. *mSphere* (2019) 4: e00061-19. doi: 10.1128/mSphereDirect.00061-19
74. Reiling L, Boyle MJ, White MT, Wilson DW, Feng G, Weaver R, et al. Targets of complement-fixing antibodies in protective immunity against malaria in children. *Nat Commun* (2019) 10:610. doi: 10.1038/s41467-019-08528-z
75. Richards JS, Arumugam TU, Reiling L, Healer J, Hodder AN, Fowkes FJ, et al. Identification and prioritization of merozoite antigens as targets of protective human immunity to *Plasmodium falciparum* malaria for vaccine and biomarker development. *J Immunol* (2013) 191:795–809. doi: 10.4049/jimmunol.1300778
76. Proietti C, Krause L, Trieu A, Dodoo D, Gyan B, Koram KA, et al. Immune signature against *Plasmodium falciparum* antigens predicts clinical immunity in distinct malaria endemic communities. *Mol Cell Proteomics* (2020) 19:101–13. doi: 10.1074/mcp.RA118.001256
77. Valletta JJ, Recker M. Identification of immune signatures predictive of clinical protection from malaria. *PloS Comput Biol* (2017) 13:e1005812. doi: 10.1371/journal.pcbi.1005812

78. Guevara Patino JA, Holder AA, McBride JS, Blackman MJ. Antibodies that inhibit malaria merozoite surface protein-1 processing and erythrocyte invasion are blocked by naturally acquired human antibodies. *J Exp Med* (1997) 186:1689–99. doi: 10.1084/jem.186.10.1689
79. Bustamante LY, Powell GT, Lin YC, Macklin MD, Cross N, Kemp A, et al. Synergistic malaria vaccine combinations identified by systematic antigen screening. *Proc Natl Acad Sci USA* (2017) 114:12045–50. doi: 10.1073/pnas.1702944114
80. Garcia-Senosiain A, Kana IH, Singh SK, Chourasia BK, Das MK, Dodoo D, et al. Peripheral merozoite surface proteins are targets of naturally acquired immunity against malaria in both India and Ghana. *Infect Immun* (2020) 88: e00778-19. doi: 10.1128/IAI.00778-19
81. Kana IH, Garcia-Senosiain A, Singh SK, Tiendrebeogo RW, Chourasia BK, Malhotra P, et al. Cytophilic antibodies against key *Plasmodium falciparum* blood stage antigens contribute to protection against clinical malaria in a high transmission region of eastern India. *J Infect Dis* (2018) 218:956–65. doi: 10.1093/infdis/jiy258
82. Osier FH, Mackinnon MJ, Crosnier C, Fegan G, Kamuyu G, Wanaguru M, et al. New antigens for a multicomponent blood-stage malaria vaccine. *Sci Transl Med* (2014) 6:247ra102. doi: 10.1126/scitranslmed.3008705
83. Cohen S, Mc GI, Carrington S. Gamma-globulin and acquired immunity to human malaria. *Nature* (1961) 192:733–7. doi: 10.1038/192733a0
84. Sabchareon A, Burnouf T, Ouattara D, Attanath P, Bouharoun-Tayoun H, Chantavanich P, et al. Parasitologic and clinical human response to immunoglobulin administration in *falciparum* malaria. *Am J Trop Med Hyg* (1991) 45:297–308. doi: 10.4269/ajtmh.1991.45.297
85. Hill DL, Wilson DW, Sampaio NG, Eriksson EM, Ryg-Cornejo V, Harrison GLA, et al. Merozoite antigens of *Plasmodium falciparum* elicit strain-transcending opsonizing immunity. *Infect Immun* (2016) 84:2175–84. doi: 10.1128/IAI.00145-16
86. Irani V, Ramsland PA, Guy AJ, Siba PM, Mueller I, Richards JS, et al. Acquisition of functional antibodies that block the binding of Erythrocyte-Binding Antigen 175 and protection against *Plasmodium falciparum* malaria in children. *Clin Infect Dis* (2015) 61:1244–52. doi: 10.1093/cid/civ525
87. Douglas AD, Baldeviano GC, Jin J, Miura K, Diouf A, Zenonos ZA, et al. A defined mechanistic correlate of protection against *Plasmodium falciparum* malaria in non-human primates. *Nat Commun* (2019) 10:1953. doi: 10.1038/s41467-019-09894-4
88. Osier FH, Feng G, Boyle MJ, Langer C, Zhou J, Richards JS, et al. Opsonic phagocytosis of *Plasmodium falciparum* merozoites: mechanism in human immunity and a correlate of protection against malaria. *BMC Med* (2014) 12:108. doi: 10.1186/1741-7015-12-108
89. Jaschke A, Coulibaly B, Remarque EJ, Bujard H, Epp C. Merozoite Surface Protein 1 from *Plasmodium falciparum* is a major target of opsonizing antibodies in individuals with acquired immunity against malaria. *Clin Vaccine Immunol* (2017) 24:e00155-17. doi: 10.1128/CVI.00155-17
90. Kana IH, Singh SK, Garcia-Senosiain A, Dodoo D, Singh S, Adu B, et al. Breadth of functional antibodies is associated with *Plasmodium falciparum* merozoite phagocytosis and protection against febrile malaria. *J Infect Dis* (2019) 220:275–84. doi: 10.1093/infdis/jiz088
91. Boyle MJ, Reiling L, Feng G, Langer C, Osier FH, Aspeling-Jones H, et al. Human antibodies fix complement to inhibit *Plasmodium falciparum* invasion of erythrocytes and are associated with protection against malaria. *Immunity* (2015) 42:580–90. doi: 10.1016/j.immuni.2015.02.012
92. Murungi LM, Sonden K, Llewellyn D, Rono J, Guleid F, Williams AR, et al. Targets and mechanisms associated with protection from severe *Plasmodium falciparum* malaria in Kenyan children. *Infect Immun* (2016) 84:950–63. doi: 10.1128/IAI.01120-15
93. Zuccala ES, Gout AM, Dekiwadia C, Marapana DS, Angrisano F, Turnbull L, et al. Subcompartmentalisation of proteins in the rhoptries correlates with ordered events of erythrocyte invasion by the blood stage malaria parasite. *PloS One* (2012) 7:e46160. doi: 10.1371/journal.pone.0046160
94. Kats LM, Black CG, Proellocks NI, Coppel RL. *Plasmodium* rhoptries: how things went pear-shaped. *Trends Parasitol* (2006) 22:269–76. doi: 10.1016/j.pt.2006.04.001
95. Alanine DGW, Quinkert D, Kumarasingha R, Mehmood S, Donnellan FR, Minkah NK, et al. Human antibodies that slow erythrocyte invasion potentiate malaria-neutralizing antibodies. *Cell* (2019) 178:216–228 e21. doi: 10.1016/j.cell.2019.05.025
96. Blank A, Furle K, Jaschke A, Mikus G, Lehmann M, Husing J, et al. Immunization with full-length *Plasmodium falciparum* merozoite surface protein 1 is safe and elicits functional cytophilic antibodies in a randomized first-in-human trial. *NPJ Vaccines* (2020) 5:10. doi: 10.1038/s41541-020-0160-2
97. Arama C, Skinner J, Doumtabe D, Portugal S, Tran TM, Jain A, et al. Genetic resistance to malaria is associated with greater enhancement of Immunoglobulin (Ig)M than IgG responses to a broad array of *Plasmodium falciparum* antigens. *Open Forum Infect Dis* (2015) 2:ofv118. doi: 10.1093/ofid/ofv118
98. Boyle MJ, Chan JA, Handayuni I, Reiling L, Feng G, Hilton A, et al. IgM in human immunity to *Plasmodium falciparum* malaria. *Sci Adv* (2019) 5: eaax4489. doi: 10.1126/sciadv.aax4489
99. Krishnamurty AT, Thouvenel CD, Portugal S, Keitany GJ, Kim KS, Holder A, et al. Somatically hypermutated *Plasmodium*-specific IgM(+) memory B cells are rapid, plastic, early responders upon malaria rechallenge. *Immunity* (2016) 45:402–14. doi: 10.1016/j.immuni.2016.06.014
100. Dolo A, Modiano D, Maiga B, Daou M, Dolo G, Guindo H, et al. Difference in susceptibility to malaria between two sympatric ethnic groups in Mali. *Am J Trop Med Hyg* (2005) 72:243–8. doi: 10.4269/ajtmh.2005.72.243
101. Modiano D, Luoni G, Sirima BS, Lanfrancotti A, Petrarca V, Cruciani F, et al. The lower susceptibility to *Plasmodium falciparum* malaria of Fulani of Burkina Faso (west Africa) is associated with low frequencies of classic malaria-resistance genes. *Trans R Soc Trop Med Hyg* (2001) 95:149–52. doi: 10.1016/S0035-9203(01)90141-5
102. Maiga B, Dolo A, Toure O, Dara V, Tapily A, Campino S, et al. Human candidate polymorphisms in sympatric ethnic groups differing in malaria susceptibility in Mali. *PloS One* (2013) 8:e75675. doi: 10.1371/journal.pone.0075675
103. Quin JE, Bujila I, Cherif M, Sanou GS, Qu Y, Vafa Homann M, et al. Major transcriptional changes observed in the Fulani, an ethnic group less susceptible to malaria. *Elife* (2017) 6:e29156. doi: 10.7554/eLife.29156
104. Portugal S, Doumtabe D, Traore B, Miller LH, Troye-Blomberg M, Doumbo OK, et al. B cell analysis of ethnic groups in Mali with differential susceptibility to malaria. *Malar J* (2012) 11:162. doi: 10.1186/1475-2875-11-162
105. McCallum FJ, Persson KE, Fowkes FJ, Reiling L, Mugyenyi CK, Richards JS, et al. Differing rates of antibody acquisition to merozoite antigens in malaria: implications for immunity and surveillance. *J Leukoc Biol* (2017) 101:913–25. doi: 10.1189/jlb.5MA0716-294R
106. Liu EW, Skinner J, Tran TM, Kumar K, Narum DL, Jain A, et al. Protein-specific features associated with variability in human antibody responses to *Plasmodium falciparum* malaria antigens. *Am J Trop Med Hyg* (2018) 98:57–66. doi: 10.4269/ajtmh.17-0437
107. Chan JA, Stanisic DI, Duffy MF, Robinson LJ, Lin E, Kazura JW, et al. Patterns of protective associations differ for antibodies to *P. falciparum*-infected erythrocytes and merozoites in immunity against malaria in children. *Eur J Immunol* (2017) 47:2124–36. doi: 10.1002/eji.201747032
108. Obeng-Adjei N, Portugal S, Tran TM, Yazew TB, Skinner J, Li S, et al. Circulating Th1-cell-type Tfh cells that exhibit impaired B cell help are preferentially activated during acute malaria in children. *Cell Rep* (2015) 13:425–39. doi: 10.1016/j.celrep.2015.09.004
109. Ryg-Cornejo V, Ioannidis LJ, Ly A, Chiu CY, Tellier J, Hill DL, et al. Severe malaria infections impair germinal center responses by inhibiting T follicular helper cell differentiation. *Cell Rep* (2016) 14:68–81. doi: 10.1016/j.celrep.2015.12.006
110. Weiss GE, Crompton PD, Li S, Walsh LA, Moir S, Traore B, et al. Atypical memory B cells are greatly expanded in individuals living in a malaria-endemic area. *J Immunol* (2009) 183:2176–82. doi: 10.4049/jimmunol.0901297
111. Obeng-Adjei N, Portugal S, Holla P, Li S, Sohn H, Ambegaonkar A, et al. Malaria-induced interferon-gamma drives the expansion of Tbethi atypical memory B cells. *PloS Pathog* (2017) 13:e1006576. doi: 10.1371/journal.ppat.1006576
112. Portugal S, Obeng-Adjei N, Moir S, Crompton PD, Pierce SK. Atypical memory B cells in human chronic infectious diseases: An interim report. *Cell Immunol* (2017) 321:18–25. doi: 10.1016/j.cellimm.2017.07.003

113. Braddom A, Batugedara G, Bol S, Bunnik E. Potential functions of atypical memory B cells in *Plasmodium*exposed individuals. *Int J Parasitol* (2020). (In press). doi: 10.1016/j.ijpara.2020.08.003
114. Portugal S, Tipton CM, Sohn H, Kone Y, Wang J, Li S, et al. Malaria-associated atypical memory B cells exhibit markedly reduced B cell receptor signaling and effector function. *Elife* (2015) 4:e07218. doi: 10.7554/eLife.07218
115. Sullivan RT, Kim CC, Fontana MF, Feeney ME, Jagannathan P, Boyle MJ, et al. FCRL5 delineates functionally impaired memory B cells associated with *Plasmodium falciparum* exposure. *PloS Pathog* (2015) 11:e1004894. doi: 10.1371/journal.ppat.1004894
116. Muellenbeck MF, Ueberheide B, Amulic B, Epp A, Fenyo D, Busse CE, et al. Atypical and classical memory B cells produce *Plasmodium falciparum* neutralizing antibodies. *J Exp Med* (2013) 210:389–99. doi: 10.1084/jem.20121970
117. Ambegaonkar AA, Kwak K, Sohn H, Manzella-Lapeira J, Brzostowski J, Pierce SK. Expression of inhibitory receptors by B cells in chronic human infectious diseases restricts responses to membrane-associated antigens. *Sci Adv* (2020) 6:eaba6493. doi: 10.1126/sciadv.aba6493
118. Holla P, Ambegaonkar A, Sohn H, Pierce SK. Exhaustion may not be in the human B cell vocabulary, at least not in malaria. *Immunol Rev* (2019) 292:139–48. doi: 10.1111/imr.12809
119. Vijay R, Guthmiller JJ, Sturtz AJ, Surette FA, Rogers KJ, Sompallae RR, et al. Infection-induced plasmablasts are a nutrient sink that impairs humoral immunity to malaria. *Nat Immunol* (2020) 21:790–801. doi: 10.1038/s41590-020-0678-5
120. Wu X, Zhou T, Zhu J, Zhang B, Georgiev I, Wang C, et al. Focused evolution of HIV-1 neutralizing antibodies revealed by structures and deep sequencing. *Science* (2011) 333:1593–602. doi: 10.1126/science.1207532
121. Klein F, Diskin R, Scheid JF, Gaebler C, Mouquet H, Georgiev IS, et al. Somatic mutations of the immunoglobulin framework are generally required for broad and potent HIV-1 neutralization. *Cell* (2013) 153:126–38. doi: 10.1016/j.cell.2013.03.018
122. Liao HX, Lynch R, Zhou T, Gao F, Alam SM, Boyd SD, et al. Co-evolution of a broadly neutralizing HIV-1 antibody and founder virus. *Nature* (2013) 496:469–76. doi: 10.1038/nature12053
123. Murugan R, Buchauer L, Triller G, Kreschel C, Costa G, Pidelaserra Marti G, et al. Clonal selection drives protective memory B cell responses in controlled human malaria infection. *Sci Immunol* (2018) 3:eaap8029. doi: 10.1126/sciimmunol.aap8029
124. Ndungu FM, Lundblom K, Rono J, Illingworth J, Eriksson S, Farnert A. Long-lived *Plasmodium falciparum* specific memory B cells in naturally exposed Swedish travelers. *Eur J Immunol* (2013) 43:2919–29. doi: 10.1002/eji.201343630

Conflict of Interest: The authors declare that the research was conducted in the absence of any commercial or financial relationships that could be construed as a potential conflict of interest.

frontiers in Immunology

REVIEW
published: 14 January 2021
doi: 10.3389/fimmu.2020.615673

Recent Advances in Lupus B Cell Biology: PI3K, IFNγ, and Chromatin

Maria A. Bacalao[1] *and Anne B. Satterthwaite*[1,2]*

[1] Department of Internal Medicine, University of Texas Southwestern Medical Center, Dallas, TX, United States, [2] Department of Immunology, University of Texas Southwestern Medical Center, Dallas, TX, United States

In the autoimmune disease Systemic Lupus Erythematosus (SLE), autoantibodies are formed that promote inflammation and tissue damage. There has been significant interest in understanding the B cell derangements involved in SLE pathogenesis. The past few years have been particularly fruitful in three domains: the role of PI3K signaling in loss of B cell tolerance, the role of IFNγ signaling in the development of autoimmunity, and the characterization of changes in chromatin accessibility in SLE B cells. The PI3K pathway coordinates various downstream signaling molecules involved in B cell development and activation. It is governed by the phosphatases PTEN and SHIP-1. Murine models lacking either of these phosphatases in B cells develop autoimmune disease and exhibit defects in B cell tolerance. Limited studies of human SLE B cells demonstrate reduced expression of PTEN or increased signaling events downstream of PI3K in some patients. IFNγ has long been known to be elevated in both SLE patients and mouse models of lupus. New data suggests that IFNγR expression on B cells is required to develop autoreactive germinal centers (GC) and autoantibodies in murine lupus. Furthermore, IFNγ promotes increased transcription of BCL6, IL-6 and T-bet in B cells, which also promote GC and autoantibody formation. IFNγ also induces epigenetic changes in human B cells. SLE B cells demonstrate significant epigenetic reprogramming, including enhanced chromatin accessibility at transcription factor motifs involved in B cell activation and plasma cell (PC) differentiation as well as alterations in DNA methylation and histone modifications. Histone deacetylase inhibitors limit disease development in murine lupus models, at least in part *via* their ability to prevent B cell class switching and differentiation into plasma cells. This review will discuss relevant discoveries of the past several years pertaining to these areas of SLE B cell biology.

Keywords: lupus, B cell, autoimmunity, tolerance, PI3K, IFNγ, chromatin

OPEN ACCESS

Edited by:
Zhenming Xu,
The University of Texas Health Science Center at San Antonio, United States

Reviewed by:
Robert A. Eisenberg,
University of Pennsylvania, United States
Chaim Putterman,
Albert Einstein College of Medicine, United States

***Correspondence:**
Anne B. Satterthwaite
anne.satterthwaite@utsouthwestern.edu

Specialty section:
This article was submitted to B Cell Biology, a section of the journal Frontiers in Immunology

Received: *09 October 2020*
Accepted: *26 November 2020*
Published: *14 January 2021*

Citation:
Bacalao MA and Satterthwaite AB (2021) Recent Advances in Lupus B Cell Biology: PI3K, IFNγ, and Chromatin. Front. Immunol. 11:615673. doi: 10.3389/fimmu.2020.615673

INTRODUCTION

Systemic Lupus Erythematosus (SLE) is a systemic autoimmune disease that can have manifestations in multiple organ systems, including skin, musculoskeletal, cardiac, pulmonary, hematologic, and renal. SLE has a prevalence of 1:1,000 and a 10:1 female: male ratio (1). It is most common in women aged 20–40 (2), predominantly in those of African and Latin American heritage (3). It is associated with a threefold risk of death (4). The production of antibodies reactive to a

variety of cellular antigens, particularly those containing nucleic acids, by autoreactive B cells is key to the development of SLE. These antibodies form immune complexes which subsequently promote inflammation and tissue damage (5). Understanding mechanisms of B cell dysregulation is therefore critical for understanding the pathophysiology of SLE as a whole and may reveal new therapeutic approaches.

B cells normally undergo both central and peripheral tolerance mechanisms which eliminate and inactivate autoreactive B cells (6–10). In the bone marrow, autoreactive immature B cells undergo receptor editing, rearranging their Ig light chains again to hopefully acquire a non-autoreactive specificity. Cells that remain autoreactive after this process are deleted by apoptosis or rendered anergic and thus unable to respond to activating stimuli. Anergy and clonal deletion also play a role in peripheral B cell tolerance. More uniquely, inactivation by inhibitory receptors and the elimination of autoreactive B cells that emerge as a result of somatic hypermutation in germinal centers (GCs) are also important. Many of these tolerance checkpoints are impaired in murine lupus models and SLE patients (6–10). As described below, excessive signaling through the PI3K pathway can result in a breach of B cell tolerance.

Abnormal B cell activation *via* signaling from both the B cell antigen receptor (BCR) and Toll-like receptors (TLR) is also crucial for SLE pathogenesis. These signals function together in the initial activation of autoreactive B cells, and also help in breaching tolerance to self-antigens (11). TLRs are expressed in B cells, where they can recognize microbial invaders. In SLE however, the endosomal TLRs 7, 8, and 9 that typically would recognize microbial DNA and RNA will also recognize and be activated by self-nucleic acids. B cells reactive with antigens that contain nucleic acids thus receive signals through both the BCR and TLRs (11, 12). While TLR9 is required for the production of antibodies against DNA, it is surprisingly protective in murine lupus models (11, 12). TLR7 plays an important pathogenic role; it is required in B cells for the formation of autoantibodies and GCs in murine lupus models, and its overexpression dramatically enhances the development of autoimmunity (11, 12).

Also important in dysregulated B cell activation in lupus are altered cytokine levels (13). BAFF (also known as BlyS) is a TNF-family ligand that promotes B cell survival and is elevated in SLE patients (5, 11, 13). SLE patients also demonstrate an "interferon signature" indicative of elevated signaling by type 1 interferons (IFNs), IFNα and IFNβ (13, 14). B cell responsiveness to TLR7 is enhanced by type 1 IFNs in both mouse and human (15, 16). IFNγ is also elevated in SLE (13, 17), and as reviewed below, also plays a crucial role in B cells for the production of autoantibodies.

The above mechanisms, among others, lead to differences in peripheral blood B cell subsets between SLE patients and healthy controls. CD19+CD27- naïve B cells are decreased, while CD19+CD27+ memory cells are relatively increased, in SLE patients (18). CD27hi plasma cells are elevated in SLE patients and correlate with disease activity (19). Lastly, CD27-IgD- (double negative, or DN cells) are also increased in SLE. DN1 cells (CXCR5+CD21+) are the more prominent DN population in healthy controls, but DN2 cells (CXCR5-CD21-CD11c+) are the more prominent compartment in SLE (20). DN2 cells are an important effector B cell subpopulation for extrafollicular plasma cell (PC) differentiation and are thought to contribute to the autoantibody pool in SLE (20–22). A similar CD11c+ population, age-associated B cells (ABC), accumulate in aging mice and are prematurely expanded in mice by autoimmune disease and chronic viral responses (23, 24).

The alterations in B cell tolerance, B cell activation and B cell subsets as well as the pathogenic role of autoantibodies suggests that targeting B cells should be an effective treatment for SLE. Indeed, Belimumab, a monoclonal antibody against BAFF, was the first drug approved for SLE since 1955 (25, 26). However, two other B cell targeted therapies - B cell depletion with the anti-CD20 antibody Rituximab and enhancement of the inhibitory activity of CD22 with Epratuzumab - were initially promising (27, 28) but each failed to meet primary endpoints in two randomized controlled trials (26, 29, 30). Several other B cell directed approaches targeting CD20, the BAFF pathway, or CD19 have either not met their primary endpoint, had mixed results, or were stopped due to adverse events (29, 31, 32). This suggests that a more nuanced understanding of B cell defects in lupus is required to develop more effective therapeutic approaches.

The past few years have provided new insights into molecular events that contribute to the initial loss of B cell tolerance and the subsequent inappropriate activation of autoreactive B cells in lupus. While space limitations preclude us from reviewing all of these novel findings, we focus here on areas of progress which have recently been studied in depth from multiple perspectives. These include the role of PI3K signaling in B cell tolerance, a requirement for B cell intrinsic interferon gamma (IFNγ) signaling for autoantibody production, and altered chromatin accessibility in lupus B cells.

PI3K SIGNALING IN THE LOSS OF B CELL TOLERANCE

PI3K signaling plays an important role in many aspects of B cell development and activation (33–37). During B cell development, tonic signaling through PI3K promotes the positive selection of B cells that have successfully assembled a functional, but non-autoreactive, BCR (38). In the periphery, the B cell activating receptors BCR, CD40, and TLRs all engage the PI3K pathway (35–37). The strength of PI3K signaling also shapes B cell responses, with stronger signals limiting class switching (39).

Phosphorylation of PI(4,5)P2 (PIP2) by PI3K forms the product PI(3,4,5)P3 (PIP3), creating docking sites for various signaling molecules at the plasma membrane (33, 34). This promotes their activation and facilitates access to downstream substrates and effectors. Two major pathways downstream of PI3K are mediated by the kinases Akt and Btk (**Figure 1**). It has long been known that Btk signaling promotes autoimmune disease in murine lupus models – this is reviewed extensively elsewhere (40–44). PI3K signaling is limited by two inositol phosphatases, SHIP-1 and PTEN. These dephosphorylate PIP3,

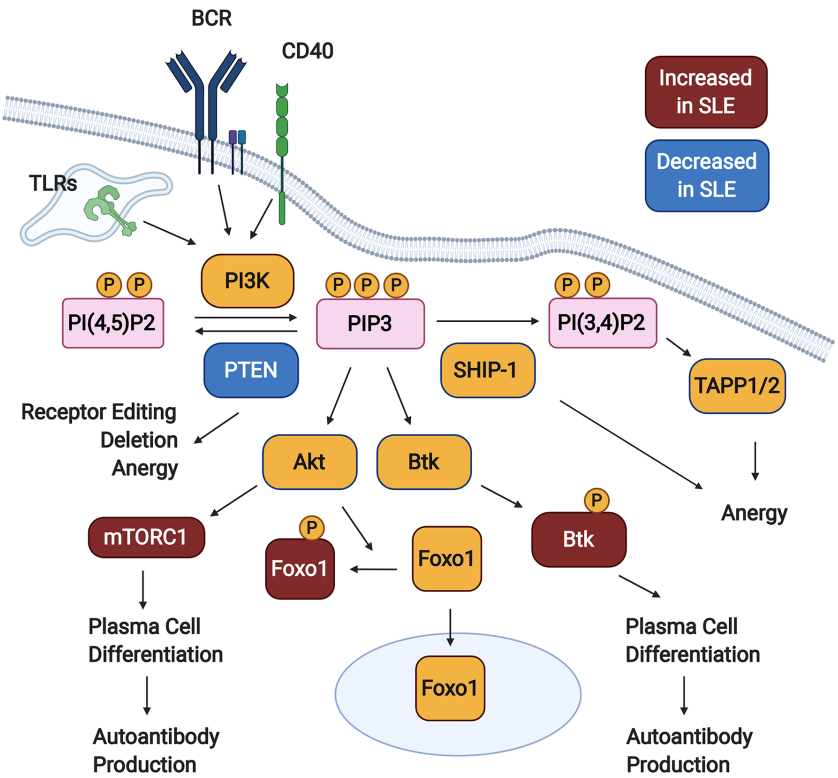

FIGURE 1 | PI3K signaling promotes loss of B cell tolerance. In response to activating signals, PI(4,5)P2 is phosphorylated by PI3K, generating PIP3. Downstream of PIP3, various signaling pathways are activated (not all shown), including those mediated by Akt and Btk. PI3K signaling is kept in check by the inositol phosphatases SHIP-1 and PTEN, which dephosphorylate PIP3 to form PI(3,4)P2 and PI(4,5)P2, respectively. Studies in animal models demonstrate that PTEN promotes both central and peripheral B cell tolerance checkpoints, while SHIP-1 plays a predominant role in maintaining anergy. B cells from Systemic Lupus Erythematosus (SLE) patients demonstrate some defects indicative of elevated PI3K signaling, including reduced PTEN expression, increased cytoplasmic Foxo1, increased mTORC1 activation, and increased phosphorylation of Btk. Created with BioRender.com.

with PTEN directly counteracting PI3K to form PI(4,5)P2 and SHIP-1 generating PI(3,4)P2. Over the last decade, we have learned that an appropriate balance of PI3K and SHIP-1 and/or PTEN activity is required to maintain both peripheral (anergy) and central (receptor editing and deletion) B cell tolerance (**Figure 1**). Inappropriately elevated PI3K activity in B cells promotes the production of autoantibodies in mice and is observed in B cells from SLE patients (**Figure 1**).

Studies in mouse models demonstrate an important contribution of SHIP-1 to peripheral B cell tolerance. Deletion of SHIP-1 throughout the B lineage results in a lupus-like autoimmune disease, with IgG autoantibodies focused toward nucleic acid containing antigens, Ig deposition in kidneys, and premature mortality (45). This is due primarily to the role of SHIP-1 in the maintenance of B cell anergy. Anergic B cells from two different mouse models –Ars/A1 Ig transgenic mice in which B cells recognize ssDNA, and the MD4 x ML5 model in which hen egg lysozyme (HEL) specific B cells recognize soluble HEL expressed as a self-antigen - demonstrate constitutive phosphorylation of SHIP-1 (45), indicative of increased inhibitory signaling (46, 47). Furthermore, B cell-specific SHIP-1-deficiency results in a loss of B cell anergy in both models (45, 48). Continuous SHIP-1 signaling is required to maintain tolerance, as acute deletion of SHIP-1 resulted in a rapid loss of anergy in the Ars/A1 system (49). Either induced loss of PTEN or induced expression of a constitutively active form of PI3K had the same effect, suggesting that SHIP-1 promotes anergy by limiting PI3K signaling (49). Indeed, a low dose of the PI3K inhibitor idelalisib restored anergy in Ars/A1 B cells heterozygous for both SHIP-1 and PTEN (50). In addition to limiting the levels of PIP3, SHIP-1 may also promote B cell anergy *via* its product, PI(3,4)P2. PI(3,4)P2 recruits the TAPP family of adaptor proteins to the plasma membrane. Mice expressing mutants of these adaptors that cannot bind to PI(3,4)P2 develop spontaneous germinal centers (GCs), ANAs and anti-DNA IgG, Ig deposition in the kidneys, and glomerulonephritis (51, 52). Two recent studies have suggested additional possible roles for SHIP-1 in limiting autoimmunity. When SHIP-1 is deleted in activated B cells using Aicda-cre, IL-10 expressing B cells are reduced. This may contribute to the observed autoantibody production in these animals (53). CD19-cre.SHIPf/f mice demonstrate an increase in CD11c+T-bet+ age associated B cells (ABCs), which are similar to the DN2 B cells that accumulate in SLE patients (54). These studies indicate that SHIP-1 is critical for maintaining peripheral B cell tolerance in mice.

PTEN can also promote B cell anergy in both mice and humans. Its expression is elevated in anergic B cells from healthy human subjects, and its inhibition restores normal responses to these cells (55). PTEN is also upregulated in anergic B cells in the MD4 x ML5 mouse model (45, 56), and its deficiency in B cells causes loss of tolerance in this system. Combined heterozygosity of both PTEN and SHIP-1 impairs anergy in Ars/A1 B cells (50), as does acute deletion of PTEN (49). 3-83ki mice, which carry a BCR transgene that recognizes the self-antigen MHC Class I H2-K^b, demonstrate that PTEN is not always necessary for the induction of anergy but reveal roles for PTEN in additional B cell tolerance mechanisms. Both receptor editing and deletion are impaired when B cells either lack PTEN or express a constitutively active PI3K alpha catalytic subunit in the 3-83ki system (57, 58). Autoreactive cells that escape receptor editing and deletion accumulate as anergic cells (57). Consistent with these observations, PTEN-deficient immature B cells are resistant to apoptosis induced by BCR crosslinking (59). Furthermore, loss of PTEN prevents B cell deletion in an IgM^b macroself model, in which mice express a superantigen that binds to IgM and induces apoptosis of immature B cells *in vivo* (60, 61). Overexpression of either of the miRNAs miR-19 or miR-148a, which target PTEN, also breaches tolerance in the IgM^b macroself model (60, 61). Thus, PTEN contributes to multiple mechanisms of B cell tolerance.

Taken together, these findings suggest that lupus B cells may demonstrate inappropriate activation of PI3K signaling. Indeed, increased phosphorylation of Akt, which occurs downstream of PI3K, is observed in B cells from Sle1.Sle3, BXSB, MRL.lpr, and Lyn-/- mice, all of which develop lupus (62, 63). Several recent observations suggest that PI3K signaling is also elevated in B cells from at least a subset of SLE patients. A study of treatment naïve SLE patients compared to healthy controls showed reduced levels of PTEN expression in most B cell subsets, except for memory cells (64). PTEN levels were inversely correlated with disease activity (64). Reduced PTEN levels in SLE B cells were due at least in part to increased expression of miRNAs, including miR-7, miR-21, and miR-22, that limit PTEN expression (64). Downstream of PI3K, the transcription factor Foxo1 is phosphorylated by Akt which results in its exclusion from the nucleus. Consistent with increased PI3K activity, cytoplasmic Foxo1 was shown to be elevated in SLE B cells (65). This is particularly pronounced in IgD- CD27- DN B cells and correlates with disease activity (65). Another function of PI3K signaling is activation of the mTORC1 pathway. This pathway was shown to be elevated in a CD11b+T-bet+ "atypical memory" population in SLE patients similar to DN2 cells that accumulate in correlation with disease activity and anti-dsDNA antibodies (66). This has functional consequences, as the mTORC1 inhibitor rapamycin prevents both the development of these cells *in vitro* and their differentiation into plasma cells (PCs) (66). Rapamycin also prevents the development of newly generated PCs and reduces autoantibody production in the NZB/W murine lupus model (67). Finally, phosphorylation of Btk, which is downstream of PI3K and promotes autoimmunity in mice (40–44), was found to be increased in SLE B cells relative to healthy controls (68).

The correlation between heightened PI3K signaling in SLE patients' B cells and disease activity suggests that this may be a consequence, rather than a cause, of increased B cell activation. The recent characterization of patients with activating mutations in the PI3K delta catalytic subunit allows an understanding of causal roles for PI3K signaling in human autoimmunity. These patients have a combined immunodeficiency which is associated with some form of autoimmunity in 28% of cases (69). Both IgM autoantibodies and B cells expressing VH4-34, which confers autoreactivity, are increased in these patients (70). Thus, hyperactive PI3K signaling can contribute to a loss of immune tolerance in humans. However, only a fraction of these patients with autoimmune involvement have SLE like or other rheumatic disease like symptoms (69), suggesting a general rather than disease specific role for PI3K in promoting human autoimmunity. Mice carrying an activating mutation of PI3K delta seen in these patients demonstrate a loss of B cell tolerance in the HEL system. The induction of anergy is impaired and mice accumulate autoreactive marginal zone B cells, PCs and GC B cells, although high affinity autoreactive GC B cells are selected against (70). An independently generated mouse strain with the same mutation developed autoimmunity in a manner dependent on the microbiota (71), suggesting that PI3K signaling may provide a link between gene/environment interactions in the development or amplification of autoimmune disease.

IFNγ SIGNALING IN B CELLS PROMOTES AUTOIMMUNITY

Much attention has been paid to the role of type 1 interferons in the pathogenesis of SLE (13, 14). However, of late there has been a resurgence in the study of interferon gamma (IFNγ) in lupus, particularly in the context of B cell responses. IFNγ has long been known to promote autoimmunity and nephritis in several murine lupus models, including NZB x NZW F1 mice, MRL.lpr mice, and pristane treated mice (17, 72). IFNγ is also elevated in the serum of SLE patients (17). Recent studies using patient serum samples collected prior to the diagnosis of SLE have shown that this increase in IFNγ occurs coincident with the appearance of autoantibodies and prior to the development of clinical symptoms (73). ANA+ healthy individuals also demonstrate increased IFNγ levels, although lower than those in SLE patients (74). This suggests that IFNγ may be involved in the initial loss of B cell tolerance early in the development of lupus.

Two genetically distinct mouse lupus models have recently been used to demonstrate a B cell intrinsic requirement for IFNγ receptor (IFNγR) expression in order to develop autoreactive GCs, produce autoantibodies, and undergo kidney damage. The first is a bone marrow chimera model in which B cell deficiency of Wiskott-Aldrich syndrome protein leads to lupus-like autoimmunity (75). The second involves the Sle1b lupus susceptibility allele, either alone (76), which breaches B cell tolerance, or in the context of enhanced TLR7 signaling (77),

which leads to full blown autoimmune disease. Of potentially significant therapeutic importance, IFNγ was not required for B cells to respond to immunization with either model antigens (76) or virus like particles (VLPs) (75). Phosphorylation of Stat1 at S727 is similarly required in B cells for autoimmunity in the Sle1b + TLR7 model, but not for responses to foreign antigens (78). Stat1 S727 can be phosphorylated downstream of both IFNγ and TLR7, suggesting that these signals may converge on Stat1 to promote autoantibody production (78).

IFNγ has numerous effects on B cells that contribute to the production of autoantibodies (**Figure 2**). It enhances the expression of IL-6 (79) and the transcription factors Bcl-6 (75) and T-bet (75, 76, 80, 81) by B cells responding to stimulation through the BCR in conjunction with TLR7, with or without CD40 engagement. Bcl-6 is critical for GC formation (75), and B cell-derived IL-6 is required for autoimmunity in the WAS chimera model (79). T-bet contributes to GCs and autoantibody production in some (76, 82, 83), although not all (75), lupus models. It also promotes PC differentiation of B cells activated in the presence of IFNγ (84). T-bet is also expressed in ABCs and DN2 cells, populations of CD11c+ B cells that accumulate in murine lupus models and human SLE patients, respectively, and differentiate efficiently into autoantibody secreting cells (20–24). IFNγ promotes both the development and terminal differentiation of DN2 cells *in vitro* (20, 82). Stimulation of human naïve B cells with anti-IgM, R848 (a TLR7/8 ligand), and IFNγ induces a T-bet+ DN (IgD-CD27-) population in an IFNγ-dependent manner (82). IFNγ stimulation in this context sensitizes human B cells to R848 and also primes cells for responsiveness to IL-21 by increasing IL-21R expression (82). IL-21 and R848 subsequently promote differentiation of the T-bet+ DN cells into antibody secreting PCs (22, 82). *In vivo*, systemic IFNγ levels and T-bet+ DN2 cells are correlated in SLE patients (82). Taken together, these observations suggest that IFNγ signaling in B cells contributes to autoimmunity by promoting the development of spontaneous GCs as well as supporting the development and subsequent differentiation of ABCs and DN2 cells.

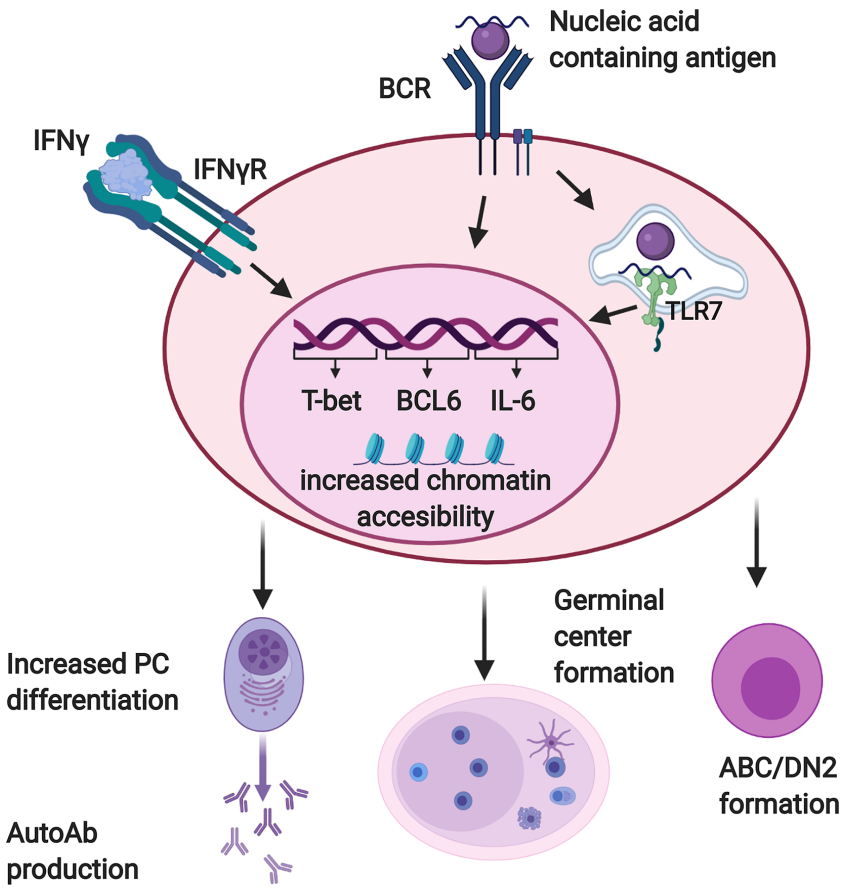

FIGURE 2 | Interferon γ (IFNγ) promotes autoreactive B cell activation and differentiation. B cells reactive with nucleic acid containing antigens receive dual activating signals *via* the BCR and endosomal, nucleic acid sensing Toll-like receptors (TLRs) including TLR7. Autoreactive B cells must also respond to IFNγ in order to produce autoantibodies and form germinal centers. When these three signals are received together, B cells upregulate factors which promote autoantibody production and germinal center formation, including T-bet, BCL-6, and IL-6. They also demonstrate increased chromatin accessibility at motifs for transcription factors that promote differentiation of DN2/ABC cells and plasma cells. Created with BioRender.com.

IFNγ likely exerts at least some of these effects by modulating B cell chromatin accessibility. In the context of stimulation through the BCR and TLR7, IFNγ and IL2 act synergistically to expand chromatin accessibility in human B cells *in vitro* (82). Accessibility was enhanced around T-bet, STAT5, NFkB, IRF4 and Blimp1 motifs, transcription factors needed for B cell differentiation into PCs. Chromatin accessibility was also enhanced around the IL-21 receptor locus. Stone et al. further evaluated the role that IFNγ-induced transcription factors had on PC development (84). Mouse B cells activated *in vitro* in the presence of Th1 cells, which secrete IFNγ, differentiated more efficiently into PCs than did those activated in the presence of Th2 cells, which do not express IFNγ. This depended on T-bet and B cell-intrinsic expression of the IFNγR, and was associated with increased chromatin accessibility at T-bet, IRF1, and Blimp-1 motifs. IFNγR signaling in B cells increased expression of both Blimp1 and T-bet, which promote PC differentiation in this context *via* distinct mechanisms. Blimp1 does so directly, while T-bet acts indirectly by limiting the transcription of pro-inflammatory genes that would otherwise reduce PC differentiation if unchecked. These studies suggest that IFNγ promotes changes in chromatin accessibility that prime B cells for subsequent differentiation into PCs, and may explain why ABCs and DN2 cells differentiate so efficiently.

Several factors have been found to facilitate the ability of B cells to respond to IFNγ in lupus. TLR7 stimulation increases B cell expression of IFNγR (77). Furthermore, IFNγ production by CD4+ T cells is enhanced by several lupus associated stimuli. B cell intrinsic defects that induce autoimmunity such as WAS-deficiency (75), constitutive activation of Btk (85), or galectin-3 deficiency (86) can drive IFNγ production by T cells in a manner dependent on B/T interaction. Topical treatment with the TLR7 ligand imiquimod leads to increased IFNγ expression by Tfh cells *in vivo* (77). BAFF can also act directly on T cells to increase IFNγ expression in the Lyn-/- model of lupus (87). Thus, in the lupus prone environment B cells can have both increased access and responsiveness to IFNγ.

Given the known association between type I IFNs and lupus, several recent studies compared the effects of IFNα and IFNγ. In both the WAS chimera (75) and the Sle1b + imiquimod mouse models (77), IFNα deficiency reduced, but did not completely abrogate, the development of autoimmunity. In contrast, IFNγ was absolutely required (75, 77). In humans, IFNγ was elevated earlier in the development of SLE than IFNα (73). The former preceded or was coincident with the appearance of autoantibodies, while the latter occurred after the acquisition of autoantibodies but prior to disease diagnosis (73). In ANA+ healthy individuals, IFNγ, but not IFNα, is increased relative to ANA- healthy controls (74). While autoimmune side effects have not been a major complication of therapeutic use of recombinant IFNγ (88, 89), there are reports of this treatment resulting in increased autoantibodies (90–94), suggestive of a role for IFNγ in promoting a loss of B cell tolerance in susceptible individuals. Taken together, these observations suggest a scenario in which B cell exposure to IFNγ contributes to the initial loss of B cell tolerance, while IFNα serves to amplify the subsequent inflammation that drives clinical disease.

ALTERED CHROMATIN ACCESSIBILITY IN SLE B CELLS

IFNγ drives both dramatic changes in chromatin accessibility and the production of pathogenic autoantibodies, highlighting the potential importance of epigenetic control of autoimmunity. Several recent studies have revealed alterations in chromatin accessibility in B cells from SLE patients and elucidated mechanisms by which histone modifiers affect B cell responses in autoimmune disease.

Recent studies of chromatin accessibility in SLE B cells have focused primarily on two measures: DNA methylation and ATAC-Seq. DNA methylation between paired CG groups leads to DNA compaction and decreased transcription (95). Perturbation in methylation increases apoptosis, leading to a release of apoptotic DNA that can trigger autoimmunity. DNA hypomethylation has been noted to trigger lupus-like conditions in mice. SLE patients have been noted to have altered DNA methylation as well (95). Hypomethylation is observed in the vicinity of type 1 IFN-regulated genes in lupus, consistent with the characteristic IFN signature (96–99). A recent study (100) found that ethnicity influences these DNA methylation patterns. They were most pronounced in African American SLE patients compared to healthy women and were apparent as early as the transitional B cell stage in African American patients. A large number of other genes demonstrate increased methylation in all subpopulations of SLE B cells tested compared to healthy controls (96, 98). Thus, complex global changes in DNA methylation are observed in lupus B cells and may contribute to aberrant B cell responses.

Scharer et al. have recently used ATAC-seq to elucidate changes in chromatin accessibility in SLE B cell subsets (96, 101). In naïve B cells from healthy volunteers, chromatin accessibility was enhanced at NRF1, CTCF and STAT5 binding sites (101). In naïve B cells from the SLE cohort, chromatin accessibility was instead enhanced at motifs for transcription factors involved in B cell activation and differentiation, namely NFκB, AP-1, BATF, IRF4, and PRDM1 (101). The epigenetic changes in resting naïve B cells in SLE were also present in other B cell subsets (96). As resting naïve B cells represent the earliest B cells available for an immune response, this data suggests that epigenetic dysregulation in SLE may occur early in B cell development. This study also demonstrated that DN2 cells have enhanced chromatin accessibility in genes involved in BCR and TLR signaling as well as costimulatory molecules in both healthy and SLE volunteers (96). DN2 cells were found to have greater accessibility at T-bet, EGR, and AP-1 motifs in comparison to other B cell subsets, while NFκB sites are less accessible in DN2 cells compared to naïve B cells (96). Similarly, the accessible chromatin structure in ABCs from lupus prone mice is enriched in AP-1, IRF and T-bet motifs (102). The increased accessibility at T-bet binding sites in DN2 cells and ABCs is consistent with a role for IFNγ in the development of these subpopulations. EGR family members, AP-1 family members, and the AP-1 superfamily member Atf3 are upregulated in SLE B cells. EGR family members and Atf3 are predicted to regulate many of the genes that are differentially expressed between SLE patients

and healthy control B cells (96). These observations suggest that AP-1 and EGR work in conjunction with T-bet to shape the unique epigenome of SLE B cells.

Consistent with altered chromatin structure in lupus B cells, histone modifiers affect the development of autoimmune disease in murine lupus models. The modification of histones on amino acid tails is one of the most important mechanisms that influence chromatin structure and accessibility. A variety of post-translational modifications on histones can regulate gene transcription, both positively and negatively. Key among these is histone acetylation. Acetylation of lysine residues within histones relaxes chromatin structure by neutralizing its positive charge, increasing the accessibility of the regulated gene for transcription factors (103). Acetylation is governed by various histone acetyltransferase (HAT) enzymes. Consequently, histone deacetylation, mediated by various histone deacetylase (HDAC) enzymes, leads to chromatin compaction, reduced chromatin accessibility and decreased gene transcription. Early studies demonstrated that HDAC inhibitors suberoylanilide hydroxamic acid and Trochostain A decrease renal disease and inflammatory cytokine production in the MRL/*lpr* and NZB/NZW F1 murine lupus models (104). More recent reports have revealed pathogenic roles for HDAC6 and HDAC9 in NZB/W and MRL.lpr mice, respectively (105–109). Here we review new advances in our understanding of how histone modifiers alter B cell responses in autoimmune disease.

Several recent reports define a role for HDACs in promoting B cell differentiation and class switching. Treating MRL/*lpr* mice with the HDAC inhibitor parabinostat reduced autoreactive PC and autoantibody production, leading to a reduction in nephritis (110). Parabinostat reduced the proliferation, survival, and PC differentiation of purified murine B cells *in vitro* in response to both T-independent and T-dependent stimuli (110). The short chain fatty acids (SFCAs) valproic acid (VPA), butyrate and proprionate act as classical HDAC inhibitors. They have potential for clinical use as VPA is an FDA approved drug and butyrate and proprionate are derived from the processing of dietary fiber by the microbiota. Treatment of MRL.lpr mice with either VPA or butyrate plus proprionate reduced autoantibodies, prevented kidney damage and skin lesions, and increased survival (111, 112). Importantly, VPA was effective in both prevention and treatment studies (112). SFCA were shown to decrease class switch recombination (CSR), somatic hypermutation (SHM) and PC differentiation in mice *in vivo*, and CSR and PC differentiation of both murine and human B cells *in vitro* (111, 112). This effect was more specific than that of parabinostat (110), as it was observed under conditions that did not impair B cell proliferation or survival (112). SFCAs reduce expression of both Blimp-1 (encoded by Prdm1), which is required for PC differentiation, and activation-induced cytidine deaminase (AID, encoded by Aicda), which is necessary for CSR and SHM (111, 112). SFCAs do not target these genes directly, but rather promote the upregulation of several miRNAs that subsequently downregulate Prdm1 (miR-23b, miR-30a, and miR-125b) and Aicda (miR-155, mir-181b, and miR-361) (112). SCFAs were shown to exert their effect on B cells by inhibiting HDACs rather than by acting as energy substrates or acting through G-protein coupled receptors (111).

Estrogen may also play a role in the epigenetic dysregulations occurring in SLE, which may partially explain the strong female predominance of the disease. Estrogen boosts the production of mature antibodies by promoting the expression of AID (113). A recent study by Casali et al. demonstrated that estrogen counteracts the activity of HDAC inhibitors on the class switching of mouse B cells and the production of autoantibodies (114). Mechanistically, estrogen reversed the HDAC inhibitor-mediated upregulation of miR26-A, which targets Aicda, the gene that encodes AID (114).

Inhibition of classical HDACs thus leads to amelioration of autoimmune disease in lupus models, at least in part due to a reduction of PC differentiation and class switching by B cells. These HDACs thus play a pathogenic role in lupus. Intriguingly, the non-classical HDAC Sirtuin1 (Sirt1) was recently demonstrated to have the opposite effect (115). Sirt1 was expressed in resting murine and human B cells. Its levels were decreased in response to stimuli that induce AID expression *in vitro* and in B cells that had elevated AID expression in both female MRL/Fas$^{lpr/lpr}$ mice and SLE patients. Deletion of Sirt1 specifically in activated murine B cells led to an increase in class-switched autoantibodies against dsDNA, histones, ribonucleoprotein (RNP), and RNA. In contrast, activation of Sirt1 reduced autoantibody levels in MRL.lpr mice. *In vitro*, Sirt1-deficient B cells demonstrated enhanced class switching and increased AID expression, while PC differentiation and Blimp-1 expression were unaffected. Sirt1 was shown to deacetylate histones, Dnmt1, and NFκB at the Aicda promoter. Thus, AID expression is tightly controlled by complex epigenetic mechanisms, an appropriate balance of which is required to limit autoantibody production.

In addition to affecting B cell differentiation and class switching, epigenetic modifiers have been shown to control B/T cognate interactions during autoimmunity. Tet2 and Tet3 can both demethylate DNA and recruit HDACs (116). B cell specific deletion of both Tet2 and Tet3 results in increased activation of B and T cells, autoantibody production, and a mild autoimmune disease (117). This depends on B/T interactions and results from enhanced expression of the costimulatory molecule CD86 on B cells. Tet2 and Tet3 are required for the binding of HDAC1 and HDAC2 to a CD86 enhancer. HDAC inhibitors result in increased CD86 expression on anergic cells, similar to the effect of Tet2/Tet3 deficiency.

Recent reports have also implicated enzymes involved in histone methylation in the development of lupus as well as the control of B cell activation. Histone methylation can either promote or repress transcription, depending on the position methylated. More specifically, the histone lysine methylations H3K4, H3K36, and H3K79 promote transcription while H3K9, H3K27, and H4K40 have a repressive effect (118). EZH2, a histone methyltransferase that produces H3K27me3, was found to be upregulated in CD4+ T cells, B cells, monocytes, and neutrophils in SLE patients (119, 120). Inhibiting EZH2 in MRL/lpr mice improved survival and decreased anti-dsDNA antibodies, inflammatory cytokine and chemokine levels, renal

disease, and lymphoproliferation (120). The pathogenic role of EZH2 in lupus may be in part due to its promotion of PC differentiation and antibody secretion. EZH2-deficient mice demonstrate a B cell intrinsic defect in PC formation *in vivo* in response to LPS (121). EZH2-deficient B cells failed to downregulate genes involved in inflammation and the B cell (as opposed to PC) fate. Furthermore, metabolic genes required for PC fitness and antibody secretion were not upregulated in the absence of EZH2. EZH2 also promotes PC differentiation in activated human B cells. In these cells it has been shown to bind to the promoter of Bach2, a repressor of PC differentiation, and inhibit its expression *via* methylation (122). In contrast, chemical inhibition of EZH2 promoted murine PC differentiation *in vitro*, although antibody secretion was not enhanced (123). This suggests possible context dependent roles for EZH2 in these processes.

The histone demethylases KDM4A and KDM4C, which promote demethylation of H3K9 (124), limit B cell activation and proliferation in response to stimulation with Tfh-derived signals. They are upregulated upon activation and subsequently promote the expression of *Wdr5*, which then upregulates the cell cycle inhibitors *Cdkn2c* and *Cdkn3.* The levels of KDM4A and KDM4C mRNA were upregulated in B cells from healthy human donors upon activation by IL21, BAFF, and anti IgM. However, these levels were reduced in both unstimulated and stimulated B cells from SLE patients compared to the healthy controls. The mRNA levels of *WDR5* and various cell cycle inhibitors were likewise reduced in SLE B cells, suggesting that impaired upregulation of KDM4A and KDM4C may result in enhanced proliferation of SLE B cells upon activation.

CONCLUSION

Recent studies have highlighted new pathways important for driving autoreactive B cell responses in lupus. These observations, which are discussed in this review and summarized in **Table 1**, highlight new mechanisms of B cell dysregulation and suggest potential new therapeutic approaches. Recent insights into PI3K signaling have elucidated its role in B cell tolerance and suggest a possible contribution to SLE pathogenesis. Studies in BCR transgenic mouse models have shown that either loss of negative regulators of the PI3K pathway or constitutive activation of PI3K can result in impaired central and peripheral B cell tolerance checkpoints. PI3K signaling is increased in SLE B cells. Aberrant PI3K signaling is correlated with disease activity. However, the degree to which PI3K signaling plays a causative role in loss of tolerance in humans is unclear, and not all humans with PI3K derangements have autoimmune disease. Subsequently, there are still unanswered questions regarding the role PI3K signaling plays in early autoimmunity and the influence it may have in tolerance checkpoints or inappropriate B cell activation in SLE patients. The therapeutic potential of the PI3K pathway also remains to be explored. Treatment of Ars/A1 mice heterozygous for both SHIP-1 and PTEN with idelalisib restored anergy in their B cells (50). Given that the PI3K pathway causes activation of the

TABLE 1 | Differences between healthy and lupus B cells discussed in this review.

1.1.1 Domain	1.1.2 Healthy B Cells	1.1.3 Lupus B Cells
1.1.4 B cell subsets	Human: Increased CD19+CD27- naïve B cells, decreased CD19+CD27+ memory cells, decreased CD27hi plasma cells, and decreased CD27-IgD-CD11c+T-bet+ DN2 cells compared to SLE B cells Mouse: Reduced germinal center B cells, plasma cells, and ABCs (murine equivalent of DN2 cells) compared to lupus B cells	Human: Decreased CD19+CD27- naïve B cells, increased CD19+CD27+ memory cells, increased CD27hi plasma cells, and increased CD27-IgD-CD11c+T-bet+ DN2 cells compared to healthy control B cells Mouse: Increased germinal center B cells, plasma cells, and ABCs (murine equivalent of DN2 cells) compared to wild type B cells
1.1.5 PI3K signaling	Appropriate balance of PI3K and SHIP-1 and/or PTEN PTEN and SHIP promote B cell tolerance in mice PTEN is elevated in healthy human anergic B cells and its inhibition impairs anergy	Elevated PI3K signaling or deletion of SHIP-1 or PTEN promote autoimmune disease in mice PTEN is reduced and signaling events downstream of PI3K (pBtk, cytoplasmic Foxo1, mTORC1 activation) are enhanced in B cells from SLE patients compared to healthy controls
1.1.6 IFNγ	Elevated in ANA+ healthy individuals, but less so than in SLE patients Not required to signal in B cells for response to model foreign antigens	Elevated in SLE patients prior to the development of clinical disease Must signal in B cells for autoimmunity in lupus mouse models. Induces expression of T-bet and promotes ABC, DN2, and PC differentiation in conjunction with TLR7 signaling Enhances chromatin accessibility in both human and mouse B cells
1.1.7 Epigenetic Changes	Increased methylation around type 1 IFN-regulated genes In healthy naïve B cells, chromatin accessibility is enhanced at NRF1, CTCF, and STAT5 binding sites	Hypomethylation around type 1 IFN-regulated genes In naïve SLE B cells, chromatin accessibility is enhanced around NFkB, AP-1, BATF, IRF4, and PRDM1 binding sites, promoting B cell activation and differentiation. DN2 cells have increased chromatin accessibility at T-bet, EGR, and AP-1 motifs. ABCs have increased chromatin accessibility at T-bet, IRF, and AP-1 motifs. HDACs generally promote B cell class switching, PC differentiation, and autoimmunity in mouse lupus models.

mTORC1 pathway, the mTORC1 inhibitor rapamycin may have therapeutic benefit. It has been shown to prevent the development of newly generated PCs and reduce autoantibody production in the NZB/W murine lupus model (67). Indeed, a recent open label phase 1/2 trial of sirolimus (rapamycin) demonstrated a reduction in disease activity in SLE, although B cell responses were not measured in this study (125). Another downstream component of PI3K signaling pathways in B cells, Btk, promotes the development of lupus in mouse models (40–44) and is being targeted in several clinical trials in SLE (www.clinicaltrials.gov).

Although type I interferons have long been implicated in SLE pathogenesis and have recently been successfully explored as therapeutic targets (126), IFNγ signaling has recently garnered renewed interest. IFNγ signaling to B cells is required for autoantibody production in mice and promotes the development of ABCs and DN2 cells *in vitro*. Tbet+ DN2 cells and IFNγ levels are correlated in SLE patients. IFNγ has also been implicated in early autoimmunity as its levels are elevated concurrently with autoantibody production in ANA+ healthy individuals. These observations suggest that IFNγ could prove a useful target for development of disease modifying therapeutics. However, a phase 1b clinical trial of an anti-IFNγ antibody did not demonstrate a clinical effect and did not reduce anti-dsDNA antibodies in SLE (127). This could reflect a difference in the relative importance of type 1 IFNs and IFNγ in mice vs. humans. It may also be that only subsets of SLE patients have IFNγ driven disease. Alternatively, IFNγ may play its unique and critical role during the initial loss of tolerance in the preclinical phase of SLE. If so, targeting it when patients have come to clinical attention might no longer be effective since type I IFN mediated amplification of inflammation would be dominant at that point. Therefore, strategies such as blocking IFNγ in particular subsets of patients (82), in combination with other targets (77), or at a different stage in the disease course may be more efficacious.

Lastly, chromatin accessibility has also been a fruitful area of research over the past several years. Alterations in chromatin structure have been noted in SLE B cells, with increased accessibility at motifs for transcription factors that promote B cell differentiation, autoantibody production, and the development of DN2/ABC cells. These factors include T-bet, IRF4, and Blimp1/PRDM1, among others. IFNγ signaling is one potential contributing factor. HDAC inhibitors and other modulators of chromatin accessibility block PC differentiation and CSR and subsequently reduce autoantibody production and disease activity in murine lupus models. The clinical applications of these observations are still unfolding. Some HDAC inhibitors, notably parabinostat which has powerful inhibitory effects on PC differentiation *in vitro* as well as in mouse models, may have a similar effect on human autoreactive B cells (110). Dietary fiber derived SCFAs with HDAC inhibitory activity likewise may have potential for clinical use in SLE, but their effectiveness is influenced by changes in gut microbiota (111). Further studies identifying the signals that drive lupus-associated changes in chromatin accessibility *in vivo* and defining those epigenetic changes that correlate with a robust response to treatment may illuminate more targeted therapeutic approaches for SLE.

AUTHOR CONTRIBUTIONS

MB wrote portions of the manuscript and designed the figures. AS wrote portions of the manuscript, modified the figures, and approved the final manuscript. All authors contributed to the article and approved the submitted version.

FUNDING

This work was supported by NIH grants AI122720 and AI137746 to AS.

REFERENCES

1. Manson JJ, Rahman A. Systemic Lupus Erythematosus. *Orphanet J Rare Dis* (2006) 1:6. doi: 10.1186/1750-1172-1-6
2. Klippel J. Systemic lupus erythematosus: demographics, prognosis, and outcome. *J Rheumatol Suppl* (1997) 48:67–71.
3. Johnson AE GC, Palmer RG, Bacon PA. The prevalence and incidence of systemic lupus erythematosus in Birmingham, England. Relationship to ethnicity and country of birth. *Arthritis Rheumatol* (1995) 38):551–8. doi: 10.1002/art.1780380415
4. Yurkovich M, Vostretsova K, Chen W, Avina-Zubieta JA. Overall and cause-specific mortality in patients with systemic lupus erythematosus: a meta-analysis of observational studies. *Arthritis Care Res (Hoboken)* (2014) 66(4):608–16. doi: 10.1002/acr.22173
5. Mamula MJ. Chapter 8 - B-Lymphocyte Biology in SLE. In: RG Lahita, editor. *Systemic Lupus Erythematosus*, *Fifth*. San Diego: Academic Press (2011). p. 143–61. doi: 10.1016/B978-0-12-374994-9.10008-7
6. Han S, Zhuang H, Shumyak S, Yang L, Reeves WH. Mechanisms of autoantibody production in systemic lupus erythematosus. *Front Immunol* (2015) 6:228. doi: 10.3389/fimmu.2015.00228
7. Nemazee D. Mechanisms of central tolerance for B cells. *Nat Rev Immunol* (2017) 17(5):281–94. doi: 10.1038/nri.2017.19
8. Tsubata T. B-cell tolerance and autoimmunity. *F1000Res* (2017) 6:391. doi: 10.12688/f1000research.10583.1
9. Woods M, Zou YR, Davidson A. Defects in Germinal Center Selection in SLE. *Front Immunol* (2015) 6:425. doi: 10.3389/fimmu.2015.00425
10. Tan C, Noviski M, Huizar J, Zikherman J. Self-reactivity on a spectrum: A sliding scale of peripheral B cell tolerance. *Immunol Rev* (2019) 292(1):37–60. doi: 10.1111/imr.12818
11. Rawlings DJ, Metzler G, Wray-Dutra M, Jackson SW. Altered B cell signalling in autoimmunity. *Nat Rev Immunol* (2017) 17(7):421–36. doi: 10.1038/nri.2017.24
12. Celhar T, Magalhaes R, Fairhurst AM. TLR7 and TLR9 in SLE: when sensing self goes wrong. *Immunol Res* (2012) 53(1-3):58–77. doi: 10.1007/s12026-012-8270-1
13. Ronnblom L, Elkon KB. Cytokines as therapeutic targets in SLE. *Nat Rev Rheumatol* (2010) 6(6):339–47. doi: 10.1038/nrrheum.2010.64
14. Obermoser G, Pascual V. The interferon-alpha signature of systemic lupus erythematosus. *Lupus* (2010) 19(9):1012–9. doi: 10.1177/0961203310371161
15. Bekeredjian-Ding IB, Wagner M, Hornung V, Giese T, Schnurr M, Endres S, et al. Plasmacytoid dendritic cells control TLR sensitivity of naive B cells via

type I IFN. *J Immunol* (2005) 174(7):4043–50. doi: 10.4049/jimmunol.174.7.4043
16. Thibault DL, Graham KL, Lee LY, Balboni I, Hertzog PJ, Utz PJ. Type I interferon receptor controls B-cell expression of nucleic acid-sensing Toll-like receptors and autoantibody production in a murine model of lupus. *Arthritis Res Ther* (2009) 11(4):R112. doi: 10.1186/ar2771
17. Pollard KM, Cauvi DM, Toomey CB, Morris KV, Kono DH. Interferon-gamma and systemic autoimmunity. *Discovery Med* (2013) 16(87):123–31.
18. Odendahl M, Jacobi A, Hansen A, Feist E, Hiepe F, Burmester GR, et al. Disturbed peripheral B lymphocyte homeostasis in systemic lupus erythematosus. *J Immunol* (2000) 165(10):5970–9. doi: 10.4049/jimmunol.165.10.5970
19. Jacobi AM, Odendahl M, Reiter K, Bruns A, Burmester GR, Radbruch A, et al. Correlation between circulating CD27high plasma cells and disease activity in patients with systemic lupus erythematosus. *Arthritis Rheum* (2003) 48(5):1332–42. doi: 10.1002/art.10949
20. Jenks SA, Cashman KS, Zumaquero E, Marigorta UM, Patel AV, Wang X, et al. Distinct Effector B Cells Induced by Unregulated Toll-like Receptor 7 Contribute to Pathogenic Responses in Systemic Lupus Erythematosus. *Immunity* (2018) 49(4):725–39. doi: 10.1016/j.immuni.2018.08.015
21. Jenks SA, Cashman KS, Woodruff MC, Lee FE-H, Sanz I. Extrafollicular responses in humans and SLE. *Immunol Rev* (2019) 288(1):136–48. doi: 10.1111/imr.12741
22. Wang S, Wang J, Kumar V, Karnell JL, Naiman B, Gross PS, et al. IL-21 drives expansion and plasma cell differentiation of autoreactive CD11c(hi)T-bet(+) B cells in SLE. *Nat Commun* (2018) 9(1):1758. doi: 10.1038/s41467-018-03750-7
23. Rubtsova K, Rubtsov AV, Cancro MP, Marrack P. Age-Associated B Cells: A T-bet-Dependent Effector with Roles in Protective and Pathogenic Immunity. *J Immunol* (2015) 195(5):1933–7. doi: 10.4049/jimmunol.1501209
24. Naradikian MS, Hao Y, Cancro MP. Age-associated B cells: key mediators of both protective and autoreactive humoral responses. *Immunol Rev* (2016) 269(1):118–29. doi: 10.1111/imr.12380
25. Dubey AK, Handu SS, Dubey S, Sharma P, Sharma KK, Ahmed QM. Belimumab: First targeted biological treatment for systemic lupus erythematosus. *J Pharmacol Pharmacother* (2011) 2(4):317–9. doi: 10.4103/0976-500X.85930
26. Samotij D, Reich A. Biologics in the Treatment of Lupus Erythematosus: A Critical Literature Review. *BioMed Res Int* (2019) 2019:8142368. doi: 10.1155/2019/8142368
27. Ramos-Casals M, Soto MJ, Cuadrado MJ, Khamashta MA. Rituximab in systemic lupus erythematosus: A systematic review of off-label use in 188 cases. *Lupus* (2009) 18(9):767–76. doi: 10.1177/0961203309106174
28. Wallace DJ, Gordon C, Strand V, Hobbs K, Petri M, Kalunian K, et al. Efficacy and safety of epratuzumab in patients with moderate/severe flaring systemic lupus erythematosus: results from two randomized, double-blind, placebo-controlled, multicentre studies (ALLEVIATE) and follow-up. *Rheumatology* (2013) 52(7):1313–22. doi: 10.1093/rheumatology/ket129
29. Lee WS, Amengual O. B cells targeting therapy in the management of systemic lupus erythematosus. *Immunol Med* (2020) 43(1):16–35. doi: 10.1080/25785826.2019.1698929
30. Clowse MEB, Wallace DJ, Furie RA, Petri MA, Pike MC, Leszczyński P, et al. Efficacy and Safety of Epratuzumab in Moderately to Severely Active Systemic Lupus Erythematosus: Results From Two Phase III Randomized, Double-Blind, Placebo-Controlled Trials. *Arthritis Rheumatol* (2017) 69 (2):362–75. doi: 10.1002/art.39856
31. Murphy G, Isenberg DA. New therapies for systemic lupus erythematosus - past imperfect, future tense. *Nat Rev Rheumatol* (2019) 15(7):403–12. doi: 10.1038/s41584-019-0235-5
32. Parodis I, Stockfelt M, Sjowall C. B Cell Therapy in Systemic Lupus Erythematosus: From Rationale to Clinical Practice. *Front Med (Lausanne)* (2020) 7:316. doi: 10.3389/fmed.2020.00316
33. Baracho GV, Miletic AV, Omori SA, Cato MH, Rickert RC. Emergence of the PI3-kinase pathway as a central modulator of normal and aberrant B cell differentiation. *Curr Opin Immunol* (2011) 23(2):178–83. doi: 10.1016/j.coi.2011.01.001
34. Pauls SD, Lafarge ST, Landego I, Zhang T, Marshall AJ. The phosphoinositide 3-kinase signaling pathway in normal and malignant B cells: activation mechanisms, regulation and impact on cellular functions. *Front Immunol* (2012) 3:224. doi: 10.3389/fimmu.2012.00224
35. Donahue AC, Fruman DA. PI3K signaling controls cell fate at many points in B lymphocyte development and activation. *Semin Cell Dev Biol* (2004) 15 (2):183–97. doi: 10.1016/j.semcdb.2003.12.024
36. Hodson DJ, Turner M. The role of PI3K signalling in the B cell response to antigen. *Adv Exp Med Biol* (2009) 633:43–53. doi: 10.1007/978-0-387-79311-5_5
37. Okkenhaug K, Vanhaesebroeck B. PI3K in lymphocyte development, differentiation and activation. *Nat Rev Immunol* (2003) 3(4):317–30. doi: 10.1038/nri1056
38. Verkoczy L, Duong B, Skog P, Ait-Azzouzene D, Puri K, Vela JL, et al. Basal B cell receptor-directed phosphatidylinositol 3-kinase signaling turns off RAGs and promotes B cell-positive selection. *J Immunol* (2007) 178 (10):6332–41. doi: 10.4049/jimmunol.178.10.6332
39. Omori SA, Cato MH, Anzelon-Mills A, Puri KD, Shapiro-Shelef M, Calame K, et al. Regulation of class-switch recombination and plasma cell differentiation by phosphatidylinositol 3-kinase signaling. *Immunity* (2006) 25(4):545–57. doi: 10.1016/j.immuni.2006.08.015
40. Satterthwaite AB. Bruton's Tyrosine Kinase, a Component of B Cell Signaling Pathways, Has Multiple Roles in the Pathogenesis of Lupus. *Front Immunol* (2017) 8:1986. doi: 10.3389/fimmu.2017.01986
41. Corneth OBJ, Klein Wolterink RGJ, Hendriks RW. BTK Signaling in B Cell Differentiation and Autoimmunity. *Curr Top Microbiol Immunol* (2016) 393:67–105. doi: 10.1007/82_2015_478
42. Lorenzo-Vizcaya A, Fasano S, Isenberg DA. Bruton's Tyrosine Kinase Inhibitors: A New Therapeutic Target for the Treatment of SLE? *Immunotargets Ther* (2020) 9:105–10. doi: 10.2147/ITT.S240874
43. Rip J, Van Der Ploeg EK, Hendriks RW, Corneth OBJ. The Role of Bruton's Tyrosine Kinase in Immune Cell Signaling and Systemic Autoimmunity. *Crit Rev Immunol* (2018) 38(1):17–62. doi: 10.1615/CritRevImmunol.2018025184
44. Crofford LJ, Nyhoff LE, Sheehan JH, Kendall PL. The role of Bruton's tyrosine kinase in autoimmunity and implications for therapy. *Expert Rev Clin Immunol* (2016) 12(7):763–73. doi: 10.1586/1744666X.2016.1152888
45. O'Neill SK, Getahun A, Gauld SB, Merrell KT, Tamir I, Smith MJ, et al. Monophosphorylation of CD79a and CD79b ITAM motifs initiates a SHIP-1 phosphatase-mediated inhibitory signaling cascade required for B cell anergy. *Immunity* (2011) 35(5):746–56. doi: 10.1016/j.immuni.2011.10.011
46. Chacko GW, Tridandapani S, Damen JE, Liu L, Krystal G, Coggeshall KM. Negative signaling in B lymphocytes induces tyrosine phosphorylation of the 145-kDa inositol polyphosphate 5-phosphatase, SHIP. *J Immunol* (1996) 157 (6):2234–8.
47. D'Ambrosio D, Fong DC, Cambier JC. The SHIP phosphatase becomes associated with Fc gammaRIIB1 and is tyrosine phosphorylated during 'negative' signaling. *Immunol Lett* (1996) 54(2-3):77–82. doi: 10.1016/S0165-2478(96)02653-3
48. Akerlund J, Getahun A, Cambier JC. B cell expression of the SH2-containing inositol 5-phosphatase (SHIP-1) is required to establish anergy to high affinity, proteinacious autoantigens. *J Autoimmun* (2015) 62:45–54. doi: 10.1016/j.jaut.2015.06.007
49. Getahun A, Beavers NA, Larson SR, Shlomchik MJ, Cambier JC. Continuous inhibitory signaling by both SHP-1 and SHIP-1 pathways is required to maintain unresponsiveness of anergic B cells. *J Exp Med* (2016) 213(5):751–69. doi: 10.1084/jem.20150537
50. Franks SE, Getahun A, Cambier JC. A Precision B Cell-Targeted Therapeutic Approach to Autoimmunity Caused by Phosphatidylinositol 3-Kinase Pathway Dysregulation. *J Immunol* (2019) 202(12):3381–93. doi: 10.4049/jimmunol.1801394
51. Jayachandran N, Landego I, Hou S, Alessi DR, Marshall AJ. B-cell-intrinsic function of TAPP adaptors in controlling germinal center responses and autoantibody production in mice. *Eur J Immunol* (2017) 47(2):280–90. doi: 10.1002/eji.201646596
52. Landego I, Jayachandran N, Wullschleger S, Zhang TT, Gibson IW, Miller A, et al. Interaction of TAPP adapter proteins with phosphatidylinositol (3,4)-bisphosphate regulates B-cell activation and autoantibody production. *Eur J Immunol* (2012) 42(10):2760–70. doi: 10.1002/eji.201242371

53. Chen Y, Hu F, Dong X, Zhao M, Wang J, Sun X, et al. SHIP-1 Deficiency in AID(+) B Cells Leads to the Impaired Function of B10 Cells with Spontaneous Autoimmunity. *J Immunol* (2017) 199(9):3063–73. doi: 10.4049/jimmunol.1700138
54. Zhang W, Zhang H, Liu S, Xia F, Kang Z, Zhang Y, et al. Excessive CD11c(+) Tbet(+) B cells promote aberrant TFH differentiation and affinity-based germinal center selection in lupus. *Proc Natl Acad Sci USA* (2019) 116 (37):18550–60. doi: 10.1073/pnas.1901340116
55. Smith MJ, Ford BR, Rihanek M, Coleman BM, Getahun A, Sarapura VD, et al. Elevated PTEN expression maintains anergy in human B cells and reveals unexpectedly high repertoire autoreactivity. *JCI Insight* (2019) 4(3): e123384. doi: 10.1172/jci.insight.123384
56. Browne CD, Del Nagro CJ, Cato MH, Dengler HS, Rickert RC. Suppression of phosphatidylinositol 3,4,5-trisphosphate production is a key determinant of B cell anergy. *Immunity* (2009) 31(5):749–60. doi: 10.1016/j.immuni.2009.08.026
57. Setz CS, Khadour A, Renna V, Iype J, Gentner E, He X, et al. Pten controls B-cell responsiveness and germinal center reaction by regulating the expression of IgD BCR. *EMBO J* (2019) 38(11):e100249. doi: 10.15252/embj.2018100249
58. Greaves SA, Peterson JN, Strauch P, Torres RM, Pelanda R. Active PI3K abrogates central tolerance in high-avidity autoreactive B cells. *J Exp Med* (2019) 216(5):1135–53. doi: 10.1084/jem.20181652
59. Cheng S, Hsia CY, Feng B, Liou ML, Fang X, Pandolfi PP, et al. BCR-mediated apoptosis associated with negative selection of immature B cells is selectively dependent on Pten. *Cell Res* (2009) 19(2):196–207. doi: 10.1038/cr.2008.284
60. Gonzalez-Martin A, Adams BD, Lai M, Shepherd J, Salvador-Bernaldez M, Salvador JM, et al. The microRNA miR-148a functions as a critical regulator of B cell tolerance and autoimmunity. *Nat Immunol* (2016) 17(4):433–40. doi: 10.1038/ni.3385
61. Lai M, Gonzalez-Martin A, Cooper AB, Oda H, Jin HY, Shepherd J, et al. Regulation of B-cell development and tolerance by different members of the miR-17 approximately 92 family microRNAs. *Nat Commun* (2016) 7:12207. doi: 10.1038/ncomms12207
62. Wu T, Qin X, Kurepa Z, Kumar KR, Liu K, Kanta H, et al. Shared signaling networks active in B cells isolated from genetically distinct mouse models of lupus. *J Clin Invest* (2007) 117(8):2186–96. doi: 10.1172/JCI30398
63. Maxwell MJ, Tsantikos E, Kong AM, Vanhaesebroeck B, Tarlinton DM, Hibbs ML. Attenuation of phosphoinositide 3-kinase delta signaling restrains autoimmune disease. *J Autoimmun* (2012) 38(4):381–91. doi: 10.1016/j.jaut.2012.04.001
64. Wu XN, Ye YX, Niu JW, Li Y, Li X, You X, et al. Defective PTEN regulation contributes to B cell hyperresponsiveness in systemic lupus erythematosus. *Sci Transl Med* (2014) 6(246):246ra99. doi: 10.1126/scitranslmed.3009131
65. Hritzo Ahye MK, Golding A. Cytoplasmic FOXO1 identifies a novel disease-activity associated B cell phenotype in SLE. *Lupus Sci Med* (2018) 5(1): e000296. doi: 10.1136/lupus-2018-000296
66. Wu C, Fu Q, Guo Q, Chen S, Goswami S, Sun S, et al. Lupus-associated atypical memory B cells are mTORC1-hyperactivated and functionally dysregulated. *Ann Rheum Dis* (2019) 78(8):1090–100. doi: 10.1136/annrheumdis-2019-215039
67. Jones DD, Gaudette BT, Wilmore JR, Chernova I, Bortnick A, Weiss BM, et al. mTOR has distinct functions in generating versus sustaining humoral immunity. *J Clin Invest* (2016) 126(11):4250–61. doi: 10.1172/JCI86504
68. Iwata S, Yamaoka K, Niiro H, Jabbarzadeh-Tabrizi S, Wang SP, Kondo M, et al. Increased Syk phosphorylation leads to overexpression of TRAF6 in peripheral B cells of patients with systemic lupus erythematosus. *Lupus* (2015) 24(7):695–704. doi: 10.1177/0961203314560424
69. Jamee M, Moniri S, Zaki-Dizaji M, Olbrich P, Yazdani R, Jadidi-Niaragh F, et al. Clinical, Immunological, and Genetic Features in Patients with Activated PI3Kdelta Syndrome (APDS): a Systematic Review. *Clin Rev Allergy Immunol* (2020) 59(3):323–33. doi: 10.1007/s12016-019-08738-9
70. Lau A, Avery DT, Jackson K, Lenthall H, Volpi S, Brigden H, et al. Activated PI3Kdelta breaches multiple B cell tolerance checkpoints and causes autoantibody production. *J Exp Med* (2020) 217(2):e20191336. doi: 10.1084/jem.20191336
71. Preite S, Cannons JL, Radtke AJ, Vujkovic-Cvijin I, Gomez-Rodriguez J, Volpi S, et al. Hyperactivated PI3Kdelta promotes self and commensal reactivity at the expense of optimal humoral immunity. *Nat Immunol* (2018) 19(9):986–1000. doi: 10.1038/s41590-018-0182-3
72. Richards HB, Satoh M, Jennette JC, Croker BP, Yoshida H, Reeves WH. Interferon-gamma is required for lupus nephritis in mice treated with the hydrocarbon oil pristane. *Kidney Int* (2001) 60(6):2173–80. doi: 10.1046/j.1523-1755.2001.00045.x
73. Munroe ME, Lu R, Zhao YD, Fife DA, Robertson JM, Guthridge JM, et al. Altered type II interferon precedes autoantibody accrual and elevated type I interferon activity prior to systemic lupus erythematosus classification. *Ann Rheum Dis* (2016) 75(11):2014–21. doi: 10.1136/annrheumdis-2015-208140
74. Slight-Webb S, Lu R, Ritterhouse LL, Munroe ME, Maecker HT, Fathman CG, et al. Autoantibody-Positive Healthy Individuals Display Unique Immune Profiles That May Regulate Autoimmunity. *Arthritis Rheumatol* (2016) 68(10):2492–502. doi: 10.1002/art.39706
75. Jackson SW, Jacobs HM, Arkatkar T, Dam EM, Scharping NE, Kolhatkar NS, et al. B cell IFN-gamma receptor signaling promotes autoimmune germinal centers via cell-intrinsic induction of BCL-6. *J Exp Med* (2016) 213(5):733–50. doi: 10.1084/jem.20151724
76. Domeier PP, Chodisetti SB, Soni C, Schell SL, Elias MJ, Wong EB, et al. IFN-gamma receptor and STAT1 signaling in B cells are central to spontaneous germinal center formation and autoimmunity. *J Exp Med* (2016) 213(5):715–32. doi: 10.1084/jem.20151722
77. Chodisetti SB, Fike AJ, Domeier PP, Singh H, Choi NM, Corradetti C, et al. Type II but Not Type I IFN Signaling Is Indispensable for TLR7-Promoted Development of Autoreactive B Cells and Systemic Autoimmunity. *J Immunol* (2020) 204(4):796–809. doi: 10.4049/jimmunol.1901175
78. Chodisetti SB, Fike AJ, Domeier PP, Schell SL, Mockus TE, Choi NM, et al. Serine Phosphorylation of the STAT1 Transactivation Domain Promotes Autoreactive B Cell and Systemic Autoimmunity Development. *J Immunol* (2020) 204(10):2641–50. doi: 10.4049/jimmunol.2000170
79. Arkatkar T, Du SW, Jacobs HM, Dam EM, Hou B, Buckner JH, et al. B cell-derived IL-6 initiates spontaneous germinal center formation during systemic autoimmunity. *J Exp Med* (2017) 214(11):3207–17. doi: 10.1084/jem.20170580
80. Naradikian MS, Myles A, Beiting DP, Roberts KJ, Dawson L, Herati RS, et al. Cutting Edge: IL-4, IL-21, and IFN-gamma Interact To Govern T-bet and CD11c Expression in TLR-Activated B Cells. *J Immunol* (2016) 197(4):1023–8. doi: 10.4049/jimmunol.1600522
81. Rubtsova K, Rubtsov AV, van Dyk LF, Kappler JW, Marrack P. T-box transcription factor T-bet, a key player in a unique type of B-cell activation essential for effective viral clearance. *Proc Natl Acad Sci USA* (2013) 110(34): E3216–24. doi: 10.1073/pnas.1312348110
82. Zumaquero E, Stone SL, Scharer CD, Jenks SA, Nellore A, Mousseau B, et al. IFNgamma induces epigenetic programming of human T-bet(hi) B cells and promotes TLR7/8 and IL-21 induced differentiation. *Elife* (2019) 8:e41641. doi: 10.7554/eLife.41641
83. Rubtsova K, Rubtsov AV, Thurman JM, Mennona JM, Kappler JW, Marrack P. B cells expressing the transcription factor T-bet drive lupus-like autoimmunity. *J Clin Invest* (2017) 127(4):1392–404. doi: 10.1172/JCI91250
84. Stone SL, Peel JN, Scharer CD, Risley CA, Chisolm DA, Schultz MD, et al. T-bet Transcription Factor Promotes Antibody-Secreting Cell Differentiation by Limiting the Inflammatory Effects of IFN-γ on B Cells. *Immunity* (2019) 50(5):1172–87.e7. doi: 10.1016/j.immuni.2019.04.004
85. Corneth OB, de Bruijn MJ, Rip J, Asmawidjaja PS, Kil LP, Hendriks RW. Enhanced Expression of Bruton's Tyrosine Kinase in B Cells Drives Systemic Autoimmunity by Disrupting T Cell Homeostasis. *J Immunol* (2016) 197 (1):58–67. doi: 10.4049/jimmunol.1600208
86. Beccaria CG, Amezcua Vesely MC, Fiocca Vernengo F, Gehrau RC, Ramello MC, Tosello Boari J, et al. Galectin-3 deficiency drives lupus-like disease by promoting spontaneous germinal centers formation via IFN-gamma. *Nat Commun* (2018) 9(1):1628. doi: 10.1038/s41467-018-04063-5
87. Scapini P, Hu Y, Chu CL, Migone TS, Defranco AL, Cassatella MA, et al. Myeloid cells, BAFF, and IFN-gamma establish an inflammatory loop that exacerbates autoimmunity in Lyn-deficient mice. *J Exp Med* (2010) 207 (8):1757–73. doi: 10.1084/jem.20100086

88. Baldo BA. Side effects of cytokines approved for therapy. *Drug Saf* (2014) 37 (11):921–43. doi: 10.1007/s40264-014-0226-z
89. Borg FA, Isenberg DA. Syndromes and complications of interferon therapy. *Curr Opin Rheumatol* (2007) 19(1):61–6. doi: 10.1097/BOR.0b013e328010c547
90. Aihara Y, Mori M, Katakura S, Yokota S. Recombinant IFN-gamma treatment of a patient with hyperimmunoglobulin E syndrome triggered autoimmune thrombocytopenia. *J Interferon Cytokine Res* (1998) 18(8):561–3. doi: 10.1089/jir.1998.18.561
91. Graninger WB, Hassfeld W, Pesau BB, Machold KP, Zielinski CC, Smolen JS. Induction of systemic lupus erythematosus by interferon-gamma in a patient with rheumatoid arthritis. *J Rheumatol* (1991) 18(10):1621–2.
92. Kung AW, Jones BM, Lai CL. Effects of interferon-gamma therapy on thyroid function, T-lymphocyte subpopulations and induction of autoantibodies. *J Clin Endocrinol Metab* (1990) 71(5):1230–4. doi: 10.1210/jcem-71-5-1230
93. Seitz M, Franke M, Kirchner H. Induction of antinuclear antibodies in patients with rheumatoid arthritis receiving treatment with human recombinant interferon gamma. *Ann Rheum Dis* (1988) 47(8):642–4. doi: 10.1136/ard.47.8.642
94. Weber P, Wiedmann KH, Klein R, Walter E, Blum HE, Berg PA. Induction of autoimmune phenomena in patients with chronic hepatitis B treated with gamma-interferon. *J Hepatol* (1994) 20(3):321–8. doi: 10.1016/S0168-8278(94)80002-2
95. Ren J, Panther E, Liao X, Grammer AC, Lipsky PE, Reilly CM. The Impact of Protein Acetylation/Deacetylation on Systemic Lupus Erythematosus. *Int J Mol Sci* (2018) 19(12):4007. doi: 10.3390/ijms19124007
96. Scharer CD, Blalock EL, Mi T, Barwick BG, Jenks SA, Deguchi T, et al. Epigenetic programming underpins B cell dysfunction in human SLE. *Nat Immunol* (2019) 20(8):1071–82. doi: 10.1038/s41590-019-0419-9
97. Chen S, Pu W, Guo S, Jin L, He D, Wang J. Genome-Wide DNA Methylation Profiles Reveal Common Epigenetic Patterns of Interferon-Related Genes in Multiple Autoimmune Diseases. *Front Genet* (2019) 10:223. doi: 10.3389/fgene.2019.00223
98. Ulff-Moller CJ, Asmar F, Liu Y, Svendsen AJ, Busato F, Gronbaek K, et al. Twin DNA Methylation Profiling Reveals Flare-Dependent Interferon Signature and B Cell Promoter Hypermethylation in Systemic Lupus Erythematosus. *Arthritis Rheumatol* (2018) 70(6):878–90. doi: 10.1002/art.40422
99. Zhu H, Mi W, Luo H, Chen T, Liu S, Raman I, et al. Whole-genome transcription and DNA methylation analysis of peripheral blood mononuclear cells identified aberrant gene regulation pathways in systemic lupus erythematosus. *Arthritis Res Ther* (2016) 18:162. doi: 10.1186/s13075-016-1050-x
100. Breitbach ME, Ramaker RC, Roberts K, Kimberly RP, Absher D. Population-Specific Patterns of Epigenetic Defects in the B Cell Lineage in Patients With Systemic Lupus Erythematosus. *Arthritis Rheumatol* (2020) 72(2):282–91. doi: 10.1002/art.41083
101. Scharer CD, Blalock EL, Barwick BG, Haines RR, Wei C, Sanz I, et al. ATAC-seq on biobanked specimens defines a unique chromatin accessibility structure in naïve SLE B cells. *Sci Rep* (2016) 6:27030. doi: 10.1038/srep27030
102. Manni M, Gupta S, Ricker E, Chinenov Y, Park SH, Shi M, et al. Regulation of age-associated B cells by IRF5 in systemic autoimmunity. *Nat Immunol* (2018) 19(4):407–19. doi: 10.1038/s41590-018-0056-8
103. Haberland M, Montgomery RL, Olson EN. The many roles of histone deacetylases in development and physiology: implications for disease and therapy. *Nat Rev Genet* (2009) 10(1):32–42. doi: 10.1038/nrg2485
104. Reilly CM, Regna N, Mishra N. HDAC inhibition in lupus models. *Mol Med* (2011) 17(5-6):417–25. doi: 10.2119/molmed.2011.00055
105. Regna NL, Vieson MD, Gojmerac AM, Luo XM, Caudell DL, Reilly CM. HDAC expression and activity is upregulated in diseased lupus-prone mice. *Int Immunopharmacol* (2015) 29(2):494–503. doi: 10.1016/j.intimp.2015.10.006
106. Regna NL, Vieson MD, Luo XM, Chafin CB, Puthiyaveetil AG, Hammond SE, et al. Specific HDAC6 inhibition by ACY-738 reduces SLE pathogenesis in NZB/W mice. *Clin Immunol* (2016) 162:58–73. doi: 10.1016/j.clim.2015.11.007
107. Ren J, Catalina MD, Eden K, Liao X, Read KA, Luo X, et al. Selective Histone Deacetylase 6 Inhibition Normalizes B Cell Activation and Germinal Center Formation in a Model of Systemic Lupus Erythematosus. *Front Immunol* (2019) 10:2512. doi: 10.3389/fimmu.2019.02512
108. Choi EW, Song JW, Ha N, Choi YI, Kim S. CKD-506, a novel HDAC6-selective inhibitor, improves renal outcomes and survival in a mouse model of systemic lupus erythematosus. *Sci Rep* (2018) 8(1):17297. doi: 10.1038/s41598-018-35602-1
109. Yan K, Cao Q, Reilly CM, Young NL, Garcia BA, Mishra N. Histone deacetylase 9 deficiency protects against effector T cell-mediated systemic autoimmunity. *J Biol Chem* (2011) 286(33):28833–43. doi: 10.1074/jbc.M111.233932
110. Waibel M, Christiansen AJ, Hibbs ML, Shortt J, Jones SA, Simpson I, et al. Manipulation of B-cell responses with histone deacetylase inhibitors. *Nat Commun* (2015) 6:6838. doi: 10.1038/ncomms7838
111. Sanchez HN, Moroney JB, Gan H, Shen T, Im JL, Li T, et al. B cell-intrinsic epigenetic modulation of antibody responses by dietary fiber-derived short-chain fatty acids. *Nat Commun* (2020) 11(1):60. doi: 10.1038/s41467-019-13603-6
112. White CA, Pone EJ, Lam T, Tat C, Hayama KL, Li G, et al. Histone deacetylase inhibitors upregulate B cell microRNAs that silence AID and Blimp-1 expression for epigenetic modulation of antibody and autoantibody responses. *J Immunol* (2014) 193(12):5933–50. doi: 10.4049/jimmunol.1401702
113. Mai T, Zan H, Zhang J, Hawkins JS, Xu Z, Casali P. Estrogen receptors bind to and activate the HOXC4/HoxC4 promoter to potentiate HoxC4-mediated activation-induced cytosine deaminase induction, immunoglobulin class switch DNA recombination, and somatic hypermutation. *J Biol Chem* (2010) 285(48):37797–810. doi: 10.1074/jbc.M110.169086
114. Casali P, Shen T, Xu Y, Qiu Z, Chupp DP, Im J, et al. Estrogen Reverses HDAC Inhibitor-Mediated Repression of Aicda and Class-Switching in Antibody and Autoantibody Responses by Downregulation of miR-26a. *Front Immunol* (2020) 11:491. doi: 10.3389/fimmu.2020.00491
115. Gan H, Shen T, Chupp DP, Taylor JR, Sanchez HN, Li X, et al. B cell Sirt1 deacetylates histone and non-histone proteins for epigenetic modulation of AID expression and the antibody response. *Sci Adv* (2020) 6(14):eaay2793–eaay. doi: 10.1126/sciadv.aay2793
116. Lio C-W, Zhang J, González-Avalos E, Hogan PG, Chang X, Rao A. Tet2 and Tet3 cooperate with B-lineage transcription factors to regulate DNA modification and chromatin accessibility. *eLife* (2016) 5:e18290. doi: 10.7554/eLife.18290
117. Tanaka S, Ise W, Inoue T, Ito A, Ono C, Shima Y, et al. Tet2 and Tet3 in B cells are required to repress CD86 and prevent autoimmunity. *Nat Immunol* (2020) 21(8):950–61. doi: 10.1038/s41590-020-0700-y
118. Hyun K, Jeon J, Park K, Kim J. Writing, erasing and reading histone lysine methylations. *Exp Mol Med* (2017) 49(4):e324–e. doi: 10.1038/emm.2017.11
119. Tsou P-S, Coit P, Kilian NC, Sawalha AH. EZH2 Modulates the DNA Methylome and Controls T Cell Adhesion Through Junctional Adhesion Molecule A in Lupus Patients. *Arthritis Rheumatol (Hoboken NJ)* (2018) 70 (1):98–108. doi: 10.1002/art.40338
120. Rohraff DM, He Y, Farkash EA, Schonfeld M, Tsou PS, Sawalha AH. Inhibition of EZH2 Ameliorates Lupus-Like Disease in MRL/lpr Mice. *Arthritis Rheumatol* (2019) 71(10):1681–90. doi: 10.1002/art.40931
121. Guo M, Price MJ, Patterson DG, Barwick BG, Haines RR, Kania AK, et al. EZH2 Represses the B Cell Transcriptional Program and Regulates Antibody-Secreting Cell Metabolism and Antibody Production. *J Immunol* (2018) 200(3):1039–52. doi: 10.4049/jimmunol.1701470
122. Zhang M, Iwata S, Hajime M, Ohkubo N, Todoroki Y, Miyata H, et al. Methionine Commits Cells to Differentiate Into Plasmablasts Through Epigenetic Regulation of BTB and CNC Homolog 2 by the Methyltransferase EZH2. *Arthritis Rheumatol* (2020) 72(7):1143–53. doi: 10.1002/art.41208
123. Scharer CD, Barwick BG, Guo M, Bally APR, Boss JM. Plasma cell differentiation is controlled by multiple cell division-coupled epigenetic programs. *Nat Commun* (2018) 9(1):1698. doi: 10.1038/s41467-018-04125-8
124. Hung K-H, Woo YH, Lin IY, Liu C-H, Wang L-C, Chen H-Y, et al. The KDM4A/KDM4C/NF-κB and WDR5 epigenetic cascade regulates the activation of B cells. *Nucleic Acids Res* (2018) 46(11):5547–60. doi: 10.1093/nar/gky281

125. Lai ZW, Kelly R, Winans T, Marchena I, Shadakshari A, Yu J, et al. Sirolimus in patients with clinically active systemic lupus erythematosus resistant to, or intolerant of, conventional medications: a single-arm, open-label, phase 1/2 trial. *Lancet* (2018) 391(10126):1186–96. doi: 10.1016/S0140-6736(18)30485-9
126. Morand EF, Furie R, Tanaka Y, Bruce IN, Askanase AD, Richez C, et al. Trial of Anifrolumab in Active Systemic Lupus Erythematosus. *N Engl J Med* (2020) 382(3):211–21. doi: 10.1056/NEJMoa1912196
127. Boedigheimer MJ, Martin DA, Amoura Z, Sanchez-Guerrero J, Romero-Diaz J, Kivitz A, et al. Safety, pharmacokinetics and pharmacodynamics of AMG 811, an anti-interferon-gamma monoclonal antibody, in SLE subjects without or with lupus nephritis. *Lupus Sci Med* (2017) 4(1):e000226. doi: 10.1136/lupus-2017-000226

Conflict of Interest: MB is a subinvestigator on clinical trials sponsored by Hoffman LaRoche, Eli Lilly, and UCB. AS holds stock in Amgen, is a Southwestern Medical Foundation Scholar in Biomedical Research and holds the Peggy Chavellier Professorship in Arthritis Research and Treatment.

frontiers in Immunology

REVIEW
published: 05 February 2021
doi: 10.3389/fimmu.2020.609324

Notch Signaling in B Cell Immune Responses

*Matthew Garis and Lee Ann Garrett-Sinha**

Department of Biochemistry, State University of New York at Buffalo, Buffalo, NY, United States

The Notch signaling pathway is highly evolutionarily conserved, dictating cell fate decisions and influencing the survival and growth of progenitor cells that give rise to the cells of the immune system. The roles of Notch signaling in hematopoietic stem cell maintenance and in specification of T lineage cells have been well-described. Notch signaling also plays important roles in B cells. In particular, it is required for specification of marginal zone type B cells, but Notch signaling is also important in other stages of B cell development and activation. This review will focus on established and new roles of Notch signaling during B lymphocyte lineage commitment and describe the function of Notch within mature B cells involved in immune responses.

Keywords: B cell, notch, jagged, delta-like ligand, differentiation

OPEN ACCESS

Edited by:
Zhenming Xu,
The University of Texas Health Science Center at San Antonio, United States

Reviewed by:
Rachel Maurie Gerstein,
University of Massachusetts Medical School, United States
Kay L. Medina,
Mayo Clinic, United States
Silvia Deaglio,
University of Turin, Italy
Xiao-Hong Sun,
Oklahoma Medical Research Foundation, United States

***Correspondence:**
Lee Ann Garrett-Sinha
leesinha@buffalo.edu

Specialty section:
This article was submitted to B Cell Biology, a section of the journal Frontiers in Immunology

Received: *23 September 2020*
Accepted: *23 December 2020*
Published: *05 February 2021*

Citation:
Garis M and Garrett-Sinha LA (2021) Notch Signaling in B Cell Immune Responses. Front. Immunol. 11:609324. doi: 10.3389/fimmu.2020.609324

THE CANONICAL NOTCH SIGNALING PATHWAY

Notch signaling is initiated by the interaction of cell-surface-bound Notch ligands (members of the Jagged and Delta-like families of proteins) to Notch receptors on adjacent cells. The Notch family of receptors and their ligands are highly evolutionarily conserved proteins, found in all metazoan animals tested (1). In mammals, there are 4 Notch receptors (Notch1, Notch2, Notch3, and Notch4) and 5 Notch ligands (Jagged1 (Jg1), Jagged2 (Jg2), Delta-like ligand1 (Dll1), Delta-like ligand 3 (Dll3) and Delta-like ligand 4 (Dll4) (2). The Notch pathways are involved in developmental decisions and cell fate choices in a wide variety of tissues in mammals and other organisms.

The Notch receptors are synthesized as precursor proteins and are first cleaved in the Golgi at a site referred to as Site 1 (**S1**), resulting in two fragments of the protein that non-covalently associate with one another (**Figure 1**) (3). The N-terminal portion contains the majority of the extracellular region of the protein, while the C-terminal portion contains a small region of the extracellular domain, the transmembrane and intracellular domains of the protein. The extracellular domain of Notch receptors contain numerous EGF repeats that function in ligand binding. NMR studies have shown the extracellular region of Notch receptors to be an elongated structure that sticks out into the extracellular space awaiting ligand binding at EGF domains in a calcium-dependent manner (4, 5). The EGF repeats are followed by a negative regulatory region (NRR) which prevents premature ligand-independent activation of Notch receptors by occluding a proteolytic cleavage site. The NRR domain also mediates the non-covalent interaction of the two fragments of the Notch receptor generated by cleavage at S1 (6). The intracellular region of Notch receptors is comprised of a RBP-Jκ association module (RAM) domain, seven ankyrin (ANK) repeats flanked by two nuclear localization signals, a transactivation domain (TAD), and a proline/glutamic acid/serine/

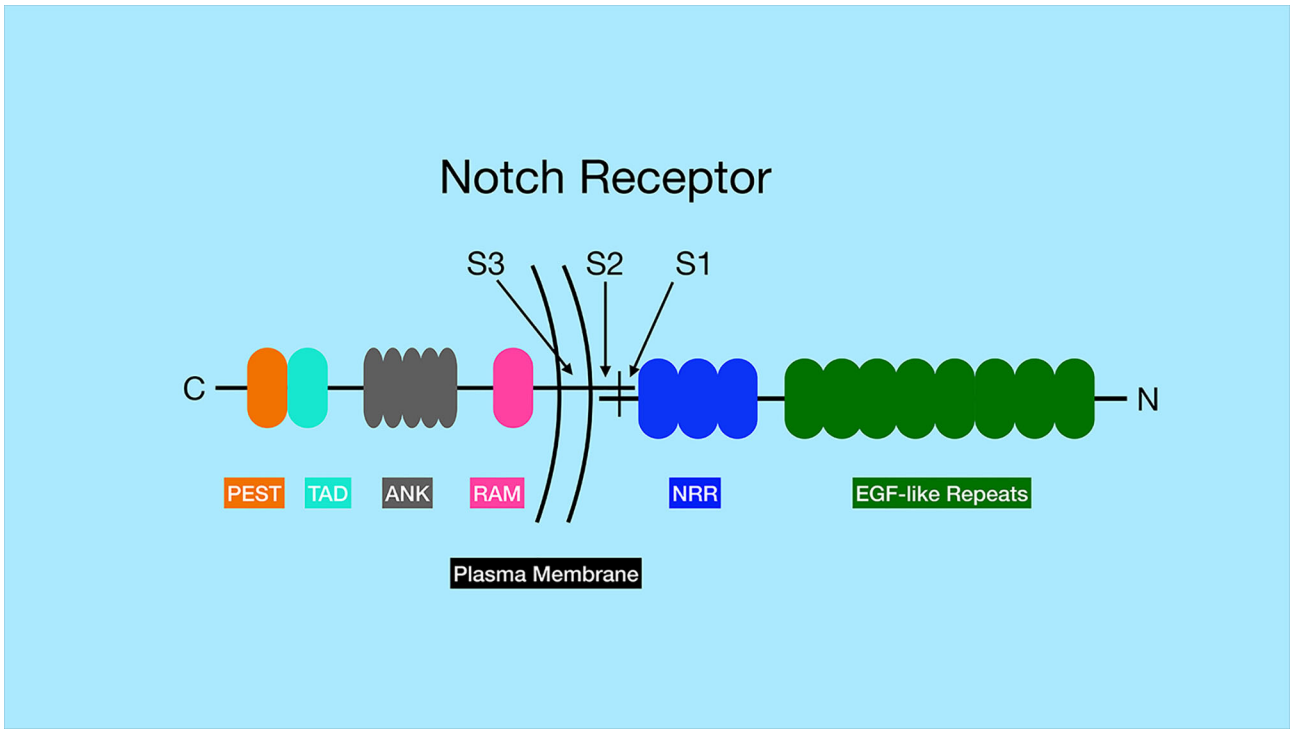

FIGURE 1 | General structure of Notch family of receptors. Notch receptors are proteolytically processed into two separate sub-parts that remain non-covalently associated. The N-terminus of the protein, located outside the cell, contains a series of EGF-like repeats (dark green) involved in ligand binding. The numbers of EGF-like repeats differ between different Notch family members. The extracellular portion of the Notch receptors also contains the negative regulatory region (NRR, blue), which prevents Notch signaling until ligand binds. The site of ADAM protease cleavage (Site 2 or S2) is located close to transmembrane domain. The transmembrane domain contains the site of γ-secretase cleavage (Site 3 or S3). The intracellular region of the Notch receptors contains an RBP-J associated molecular domain (RAM, pink), a series of ankyrin repeats (ANK, gray), a transactivation domain (TAD, aqua) and a proline-serine-threonine rich domain (PEST, orange). Note, that Notch3 and Notch4 lack the TAD domain, but contain the other domains indicated in the figure.

threonine-rich motifs (PEST) domain that promotes degradation (**Figure 1**). Once Notch receptor and Notch ligand bind, a force is generated which is thought to unfold the NRR domain and allow cleavage at a proteolytic site referred to as Site 2 (**S2**) by ADAM (a disintegrin and metalloproteinase domain) family metalloproteases (7, 8) (**Figure 2**). The pulling force is mediated by internalization of the Notch ligand by endocytosis while interacting with Notch receptors on adjacent cells. The endocytosis process internalizes Notch ligands while tugging on the Notch receptor and unraveling the NRR domain. Measurements of the force necessary to unravel Notch receptors showed that it takes roughly 4 to 9pN to activate the receptor (9, 10).

The ADAM family contains metalloproteases that function as sheddases as they cleave and "shed" extracellular portions of transmembrane proteins. While the ADAM family has approximately 30 identified members in mice and humans, ADAM10 and ADAM17 have been shown to be particularly important in Notch activation. ADAM17 was the first family member shown to be able to cleave Notch1 at the S2 site (7). However, ADAM17 knockout mice lack embryonic defects associated with impaired Notch signaling. Later studies in mouse embryonic fibroblasts (MEFs) showed that ADAM10 was the predominant ADAM family member that cleaves Notch in response to ligand binding (11). Furthermore, ADAM10 knockout mice have defects in Notch signaling pathways, consistent with an important role for ADAM10 in Notch activation (8, 12, 13). In fact, while many proteases can cleave Notch in a ligand-independent manner, ADAM10 is required for Notch1 cleavage in a ligand-dependent manner, while both ADAM10 and ADAM17 can cleave Notch1 in a ligand-independent manner (14). Exposure of the negatively charged phospholipid phosphatidylserine (PS) on the outer leaflet of the membrane is required to induce ADAM10 activity (**Figure 3**) (15). The ability of externalized PS to induce ADAM10 activation depends on interaction of positively charged amino acid residues in the ADAM10 stalk domain (the CANDIS domain), which interact with negatively charged phosphatidyl serine headgroups. These interactions are thought to bring the catalytic center of the ADAM10 close to the plasma membrane and to move an inhibitory loop out of the catalytic site, thereby activating ADAM10 protease activity (15). Patients with the bleeding disorder Scott syndrome have a mutation in the calcium-dependent phospholipid scramblase Anoctamin-6 (ANO6, also called TMEM16F), which flips phosphatidyl serine from the inner to outer leaflet of the

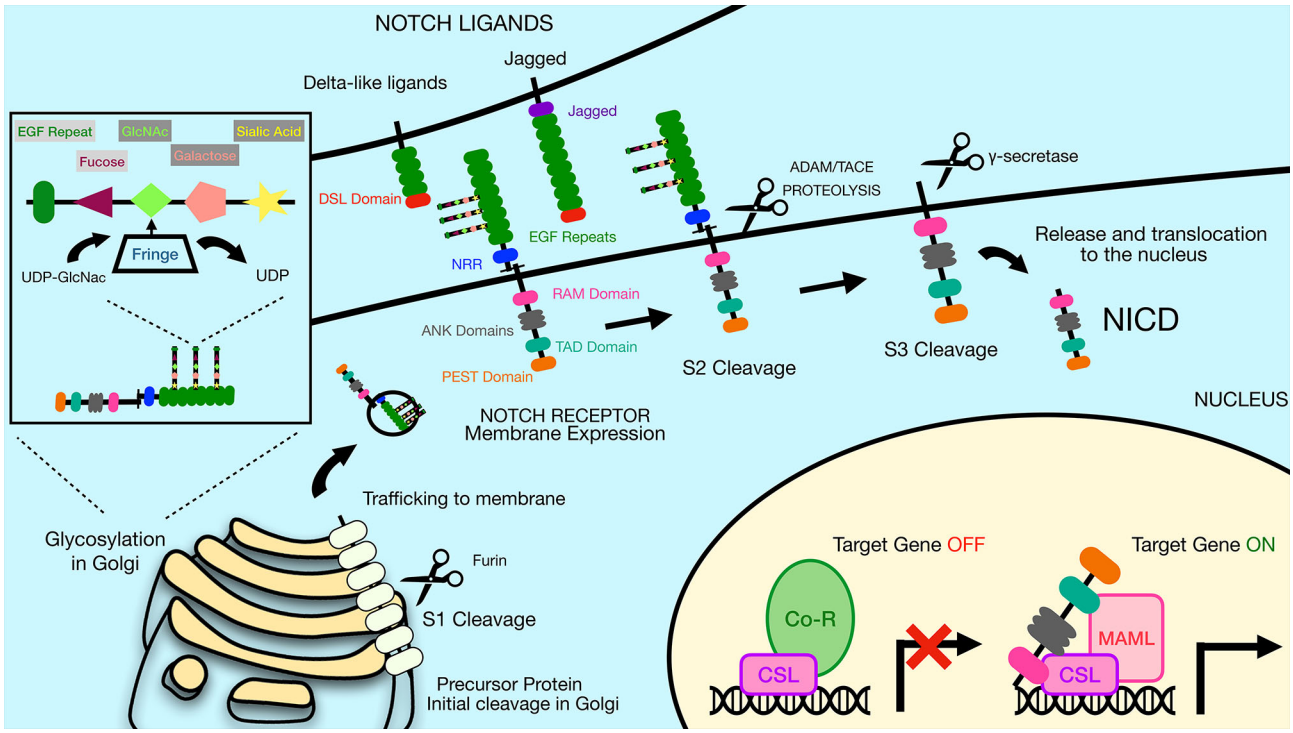

FIGURE 2 | The Notch signaling pathway is mediated by a series of proteolytic events. Notch receptors are generated by ribosomes bound to the endoplasmic reticulum (ER) and trafficked through the Golgi to the plasma membrane. During the time in the Golgi, Notch receptors are cleaved at Site 1 (S1) by furin-like proteases to generate two sub-parts that remain non-covalently associated. The N-terminal subunit can be O-glycosylated *via* the activity of a series of glycosyltransferase enzymes, including members of the Fringe family that catalyze addition of N-acetylglucosamine residues residues to the glycan chain. Once at the plasma membrane, Notch receptors are inactive unless bound by ligand on adjacent cells. Notch ligands constitute two families, the Delta-like ligands and the Jagged family ligands. Both types of ligands contain a conserved Delta-Serrate ligand (DSL) domain that mediates binding to Notch receptors. Upon ligand binding, Notch receptors undergo cleavage by ADAM family proteins at Site 2 (S2). This allows subsequent cleavage by γ-secretase at Site 3 (S3), releasing the Notch intracellular domain (NICD). The liberated NICD is translocated into the nucleus to bind to RBP-Jκ along with the coactivator Maml, leading to activation of target gene expression. Prior to binding of NICD and Maml, RBP-Jκ is associated with co-repressor proteins that prevent transcription of target genes. DSL, Delta/Serrate/Lag2; UDP, Uridine diphosphate; GlcNAc, N-acetylglucosamine; NICD, Notch intracellular domain; Maml, mastermind-like protein; Co-R, corepressor protein complexes.

membrane. B cells from Scott syndrome patients lack ADAM10 sheddase activity due to a failure to expose PS (15). Interestingly, in normal B cells BCR ligation leads to transient PS exposure (16, 17), suggesting that B cell activation through antigen receptors may lead to an enhanced ability for Notch signaling. The BCR-dependent exposure of PS may rely on ANO6 activity, since treatment of B cells with a calcium ionophore resulted in ANO6-dependent PS exposure (18).

Following ADAM cleavage at the S2 site, a membrane-tethered intermediate known as Notch extracellular truncation (NEXT) is formed, which in turn is a substrate for the multi-subunit protease complex γ-secretase (2). γ-secretase cleaves Notch receptors at Site 3 (**S3**), which frees the intracellular domain of the Notch receptors (NICD) to allow them to translocate to the nucleus (**Figures 1** and **2**) (2). NICD can then interact with DNA binding protein RBP-Jκ (also called CSL or CBF1) *via* the RAM domain found in the NICD (2). The intracellular domains of Notch1 and Notch2 contain transcription activation domains that directly play a role in their ability to effect gene expression and cellular processes, while Notch3 and Notch4 lack similar transactivation domains (19).

Interaction of Notch receptors with Notch ligands can be modulated by O-linked glycosylation of the Notch receptors (2). These particular modifications are initiated by the enzyme POFUT1, which attaches fucose to specific serine/threonine residues in the EGF repeats of the extracellular portion of the Notch receptor. Additional sugar residues can be added to the fucose moiety by the action of glycosyltransferases, including members of the Fringe family proteins (**Figure 2**). In mammals, there are three Fringe enzymes referred to as Lunatic (Lfng), Manic (Mfng), and Radical Fringe (2). These Fringe proteins catalyze addition of N-acetylglucosamine residues to the glycan chain. Notch receptor glycosylation by Lfng and Mfng leads to enhanced activation by Delta-like ligands and reduced activation by Jagged ligands, while glycosylation by Radical Fringe enhances activation by all Notch ligands (20).

There is some evidence that different lymphoid cell types may differentially regulate Notch activity. For instance, lysates from human B cell lines and primary human B cells contain the NICD

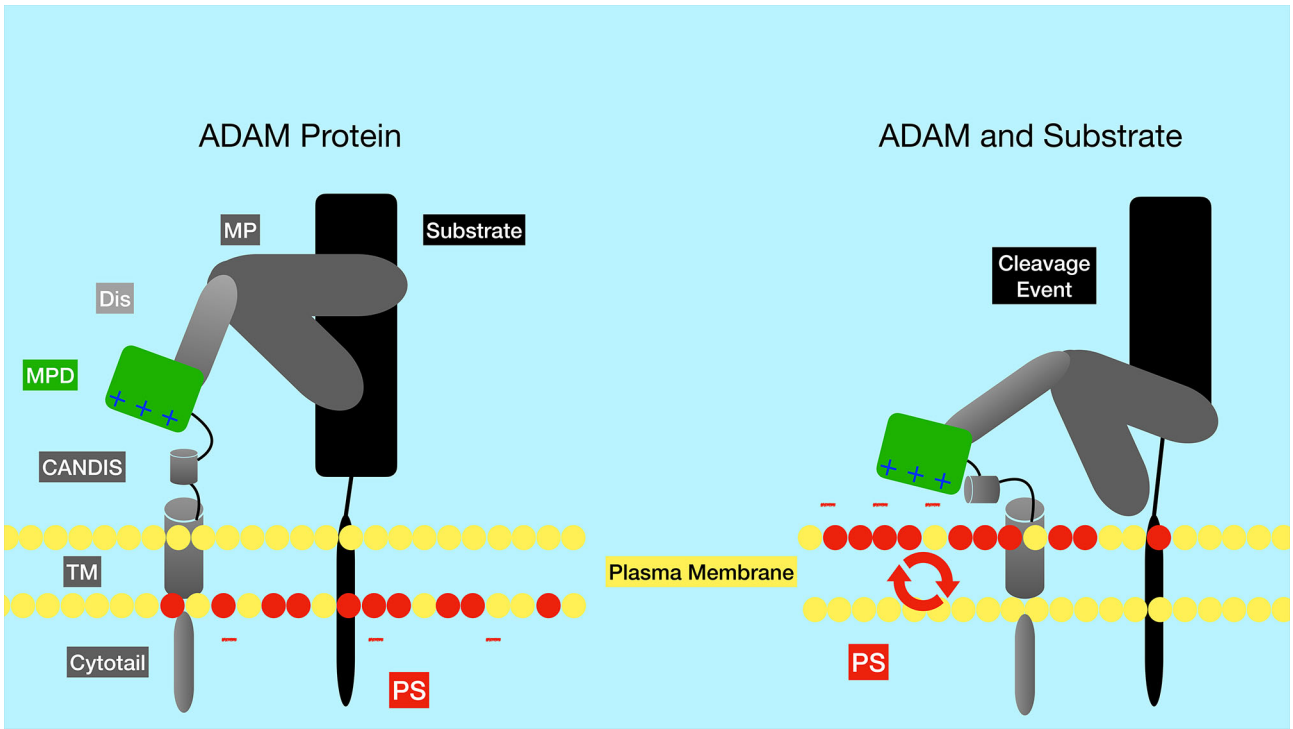

FIGURE 3 | Regulation of the ADAM metalloproteinases by phosphatidyl serine of the plasma membrane. The negatively charged membrane phospholipid phosphatidyl serine (red circles) is typically found in the inner leaflet of the membrane, but can be flipped to the outer leaflet by the action of phospholipid scramblase enzymes such as ANO6. Positively charged amino acid residues in the ADAM10 stalk domain (CANDIS) interact with negatively charged phosphatidyl serine, altering the conformation of ADAM10. These alterations are thought to bring the catalytic center of the enzyme closer to the plasma membrane and to move an inhibitory loop out of the catalytic site, thereby activating ADAM10 protease activity. PS, phosphatidyl serine; TM, transmembrane domain; CANDIS, Conserved ADAM Dynamic Interaction Sequence; MPD, membrane proximal domain; Dis, disintegrin domain; MP, metalloproteinase domain.

(p120 fragment) at levels similar to that found in T cell lysates, suggesting that Notch receptors are properly activated and cleaved in both cell types (21). But coimmunoprecipitation assays failed to find an association of NICD with RBP-Jκ in B cells, while this association was present in T cells. Interestingly, the EBNA2 protein of the EBV virus can associate with RBP-Jκ and result in transcriptional activation in the absence of NICD association (21). Although EBNA2 can compete with NICD for binding to RBP-Jκ, even B cells without EBV infection still failed to show an association of NICD with RBP-Jκ, suggesting that some aspect of the B cell intracellular environment prevents this association. As described in more detail below, Notch signaling also regulates various aspects of B cell maturation and function. Some of these processes have been shown to be dependent on RBP-Jκ, suggesting that the NICD-RBP-Jκ complex must form in B cells under certain conditions.

Mutations in the ANK repeats of Notch receptors abrogates Notch signaling (22). The ANK domains associate with cofactors such as Mastermind (Maml) forming a trimeric complex (RBP-Jκ, NICD and Maml) that is active for transcriptional stimulation (**Figure 2**). This complex was shown by crystal structure to bind directly to DNA (23). There are three mammalian Maml proteins, Maml1, Maml2 and Maml3. Both Maml1 and Maml2 are potent co-activators for all Notch family members, while Maml3 is a weaker activator and works most efficiently with Notch4 (24). Notch signaling induces expression of various target genes including those in the Hairy/Enhancer of Split (HES) family, such as Hes1, Hes5, Hey1, Hey2 and HeyL (25). These HES family proteins are basic helix-loop-helix proteins that repress the expression of other genes and thereby control differentiation processes in the cell. A summary of the major components of the canonical Notch signaling pathway described above are displayed in **Figure 2**. In addition to this canonical pathway of Notch signaling, Notch receptors can also transduce non-canonical signals as reviewed in Heitzler 2010 (26).

EXPRESSION OF NOTCH RECEPTORS IN B AND T CELL SUBSETS

Notch receptors are expressed by both B cells and T cells in the spleen. Early studies using qPCR showed expression of Notch1 and Notch3 in mouse B cells at all stages tested, with the highest levels detected in pro- and pre-B cells in the bone marrow (27) (**Table 1**). However, this level of expression of Notch1 and

TABLE 1 | Notch receptor expression in murine B cell subsets.

	Bone Marrow B cells		Splenic B cells			
	ProB	PreB	T1	T2	FoB	MZB
Notch1	+	+	+	+	+	+
Notch2	++	+	++	++	++	+++
Notch3	+	+	–	+	–	–
Notch4	–	–	–	–	–	–

(+) Weak expression, (++) moderate expression and (+++) high expression. (–) Little to no expression.

Notch3 in B cells was 10-20x lower than the levels found in double negative thymocytes. The high expression of Notch1 and Notch3 in thymocytes is consistent with an important role development. Notch1 is required for specifying T cell fate (28), while Notch3 is is required for normal numbers of thymocytes (29). By qPCR, Notch2 is expressed at high levels in mouse B cells, particularly on mature B cell subsets in the spleen (27). Flow cytometry analysis with antibodies specific to Notch receptors showed that Notch1 and Notch2 proteins were both easily detectable in B220+ B cells from the mouse spleen (30). On the other hand, Notch3 was expressed at low levels in mouse B cells, while Notch4 was undetectable (**Table 1**). Further analysis showed that Notch2 was expressed at the highest levels in marginal zone B cells and marginal zone precursors (30), in keeping with its role in specifying this subset (see details below). Using a lacZ reporter knockin to the mouse *Notch2* locus, expression of the reporter gene was found to be low in transitional type I (T1) B cells in the spleen and in mature follicular B cells, but higher in follicular B cell precursors, transitional type II (T2) B cells and marginal zone B cell precursors and mature marginal zone B cells (31). Both BCR stimulation and stimulation with LPS have been shown to upregulate Notch1 expression in mouse B cells (32–34).

Notch receptor expression in human B cell subsets shows some differences from that seen in mice (**Table 2**). During development in the bone marrow, Notch1 is expressed at all stages tested, while Notch2 is preferentially expressed in late pre-B cells (35, 36). To our knowledge, expression of Notch3 and Notch4 in human bone marrow B cell subsets has not been examined. In human CD20+ B cells in peripheral blood and tonsil, both Notch1 and Notch2 are expressed, while expression of Notch3 is low and Notch4 is not expressed (37, 38). In tonsillar B cells, naïve and memory subsets express Notch1 and Notch2, but germinal center cells do not (39, 40). Expression on Notch receptors in human B cell subsets is summarized in **Table 2**.

Various cell types in the mouse spleen and lymph node have been reported to express Notch ligands (**Table 3**). Recently, Zhu et al. reported that that Notch ligands Dll1 and Jg1 were expressed in purified B cells themselves (33). However, other studies have failed to identify Notch ligand expression in B cells and instead detected expression in a variety of other splenic cells. One study found that Notch ligands Dll1 and Jg2 are expressed on red pulp macrophages and more weakly on $CD11c^+$ dendritic cells of the mouse spleen using flow cytometry (30). Dll1 expression was also detected on erythroblasts in the same study. However, radiation bone marrow chimeras have shown that Dll1 expression on radiation-resistant stromal cells is required for formation of mouse marginal zone B cells (41). This result indicates that Notch ligand expression on hematopoietic-derived cell types such as macrophages and DC is not required at least for some Notch-dependent steps.

Another study making use of lacZ knockin mouse strains that express the lacZ enzyme under the control of the regulatory elements of the Dll1, Dll4, or Jg1 genes showed that these genes are expressed partially overlapping patterns in endothelial cells of blood vessels and/or the marginal sinus (31). Dll1 in particular

TABLE 2 | Notch receptor expression in human B cell subsets.

	Bone Marrow B cells					Peripheral B cells		
	Early B progenitor (CLP)	ProB	Early Pre-B	Late Pre-B	Immature B	Naïve B cells	Germinal Center B cells	Memory B cells
Notch1	+++	+++	+	++	+	++	+/–	++
Notch2	ND	–	–	++	–	++	+/–	ND
Notch3	ND	–	–	–	ND	–	–	ND
Notch4	ND	ND	ND	ND	ND	–	–	ND

(+) Weak expression, (++) moderate expression and (+++) high expression, (–) little to no expression, (+/–) expression seen in some studies and not in others.

TABLE 3 | Notch Ligand protein expression in murine cells.

	Conventional Dendritic cells	Follicular dendritic cells (FDC)	Macrophages	Endothelial cells	Erythroblasts
Dll1	+	+ *	+	+	+
Dll2	+	ND	ND	ND	ND
Dll4	+	ND	+	+	ND
Jg1	+	+ *	+	+	+
Jg2	+	ND	+	ND	ND

(+) expressed, (–) nor expressed. ND, not determined.

** Human FDC also express these Notch ligands.*

was found in blood vessels within the marginal zone of the spleen. Bone marrow chimeras confirmed that the lacZ-expressing cells were non-hematopoietic in origin (31). Stromal fibroblastic reticular cell (FRC) subsets also express Notch ligands and can contribute to Notch signaling in B cells. FRC can be subdivided into several subsets based on localization, marker gene expression and function. One type of FRC are follicular dendritic cells (FDC), which are known to be crucial in organizing B cell follicles, capturing surface-bound antigen and stimulating germinal center reactions (42). In keeping with this, immunostaining of mouse spleen detected Dll1 expression in FDC of germinal centers as well as the splenic marginal zone, while Jg1 was found only in the MZ (34). Interestingly, this study also suggests that different cells in the MZ express Jg1 versus Dll1, because co-staining with antibodies to both proteins failed to detect many co-expressing cells. The importance of FRC in presenting Notch ligands for MZ B cell development was shown by a study in which Dll1 was deleted in FRC or in CD11c+ DC or endothelial cells (43). Deletion of Dll1 in FRC, but not in DC or endothelial cells led to the complete loss of marginal zone B cells. Therefore, Notch ligand-expressing FRC are crucial for mouse MZ B cell development and may also play a role in other B cell differentiation steps in secondary lymphoid organs. But it remains possible that non-FRC cells that express Notch ligands (such as endothelial cells, macrophages or DC) could be involved in other B cell responses.

Notch ligand expression has also been studied in human lymphoid tissues. Yoon et al. demonstrated that Dll1 and Jg1 are expressed in human tonsil tissue (38). Expression of these ligands was found on follicular dendritic cells, similar to the expression of Dll1 on mouse FDCs. In the human spleen, non-lymphoid cells located in the marginal zone region have been shown to express Dll1 (44). Therefore, in both mice and humans, non-hematopoietic cells seem particularly important expressors of Notch ligands.

NOTCH SIGNALING REPRESSES B LINEAGE COMMITMENT

Hematopoietic stem cells (HSC) in the bone marrow undergo a series of differentiation steps that lead to formation of various progenitor cell populations including lymphoid-primed multi-potent progenitors (LMPP), early lymphoid progenitors (ELP) and common lymphoid progenitors (CLP). Some of these progenitor cells leave the bone marrow and travel to the thymus, where they encounter Notch ligands that trigger activation of the Notch1 receptor. Activation of Notch1 signaling in these progenitor cells is crucial for development of T cells (28, 45, 46). Ectopic Notch signaling driven by retroviral expression of the Notch1 intracellular domain in bone marrow progenitors inhibits hematopoietic progenitors from developing into B lineage committed cells in mice (47). Similarly, exposure of cultured human hematopoietic progenitors to Notch ligands Dll1 or Dll4 inhibits their differentiation to the B cell lineage, although exposure to Notch ligand Jg1 does not inhibit B cell differentiation (48, 49). Together, these results suggest that Notch signaling in the bone marrow environment has the potential to block B cell development from precursor cells (**Figure 4**). However, further study is needed to determine whether endogenous Notch signaling plays a role in this process, since the studies to date have only examined situations where Notch signaling was aberrantly activated in these progenitor populations. Constitutive expression of Notch1 intracellular domain (NICD) causes ectopic differentiation of T cells in the bone marrow (47). On the other hand, enforced expression of Deltex1, an inhibitor of Notch signaling, in hematopoietic progenitors results in B cell development at the expense of T cell development (50).

One proposed mechanism by which it does this is by promoting degradation of the transcription factor E2A, which is required for B cell differentiation (51). This process is mediated through ubiquitination and proteosomal degradation, following E2A phosphorylation by MAP kinases (52). E2A is also important in T cells. Interestingly, Notch signaling does not promote E2A degradation in T cell progenitors due to their inherent low basal levels of MAP kinase activity. In this way, Notch signals have an inhibitory effect on B cell lineage commitment, while allowing T cell fate decisions to be unaltered. Another proposed mechanism for Notch-mediated inhibition of B cell differentiation is its ability to interfere with binding of the transcription factor EBF to target genes (53). Like E2A, EBF is also required for B cell differentiation (54, 55). Notch signaling also controls expression of transcription factor LRF, another factor required for B cell differentiation (56). Transcription factor Pax5, also known as the B cell lineage specific activator protein (BSAP), is another fundamental regulator of B cell development. Pax5 expression in hematopoietic stem cells and early progenitors by knockin into the endogenous Ikaros locus promotes B-cell development at the expense of T-cell development (57). One mechanism by which it may do so is by Pax5-mediated repression of Notch1 expression. A summary of the expression pattern of Notch receptors and their roles in bone marrow B cell development are shown in **Figure 4**.

NOTCH REGULATION OF MZ B CELL DIFFERENTIATION

B cells can be subdivided into two main categories, B-1 B cells and B-2 B cells. B-1 B cells have been best studied in mice, where it was shown that they are produced mainly during fetal and early postnatal life, self-renew and are localized largely in body cavities such as the peritoneal cavity (58). B-2 B cells are derived from bone marrow hematopoietic progenitors and do not self-renew being instead replenished constantly by newly-generated immature B cells from the bone marrow. B-2 cells are localized in secondary lymphoid organs, such as spleen and lymph node and can be further subdivided into marginal zone and follicular

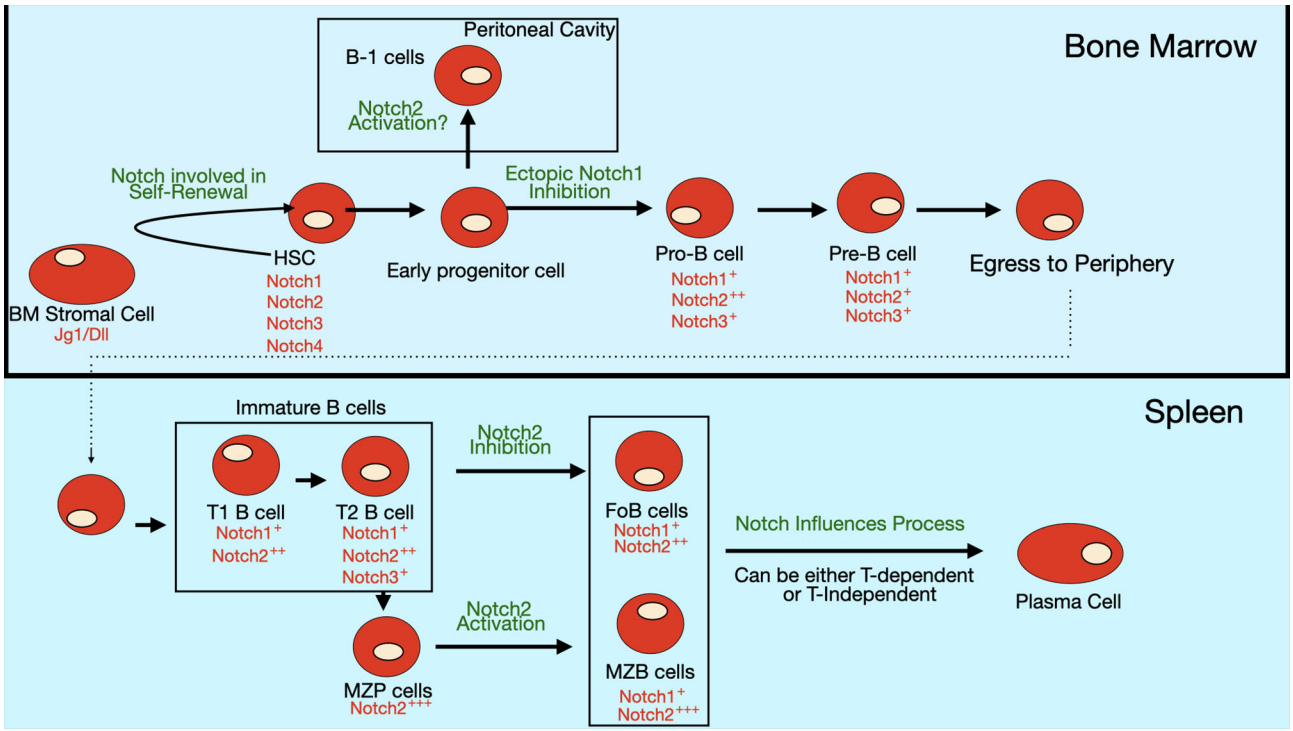

FIGURE 4 | Notch expression and role in B cell differentiation. Expression of Notch receptors and ligands (red text) on bone marrow B cell progenitors and peripheral B cell subsets. Notch signaling is thought to be involved in self-renewal of hematopoietic stem cells (HSCs). The differentiation of early progenitor cells to pro-B cells is inhibited by ectopic Notch signaling, though evidence is still lacking that endogenous Notch signaling controls this step. Some evidence suggests that Notch2 activation may regulate commitment to the B-1 subset, but this pathway is still controversial since there are contradictory findings in different studies. In the periphery, Notch2 signaling is required for specification of marginal zone (MZ) B cells, while it inhibits formation of follicular (FO) B cells. Notch signaling also stimulates the differentiation of mature B cells into antibody-secreting cells (ASCs).

subtypes (59). Follicular B cells recirculate *via* the bloodstream and lymphatics moving between spleen and lymph nodes and can also enter other tissues in response to inflammatory stimuli. When in the spleen and lymph node, follicular B cells are localized in B cell follicles, as their name implies. Marginal zone B cells do not circulate, but rather remain in the spleen localized outside of the B cell follicle in the marginal zone area. Marginal zone B cells are specialized for responding to blood borne antigens, since they are in close contact with blood flowing through the marginal sinus of the spleen (60).

Development of marginal zone, but not follicular B cells, requires Notch signaling (**Figure 4**). The first data supporting the role of Notch signaling in MZ B cells was deletion of a floxed allele of RBJ-Jκ in B cells using CD19-Cre (61). These mice showed a dramatic reduction in MZ B cell numbers, while follicular B cells and B-1 B cells were normal. This was accompanied by reduced numbers of B cells expressing high levels of CD1d and CD9, which are markers expressed on cells committed to become MZ B cells (61). As shown in **Table 1**, Notch2 levels are highest in splenic B cells. This is consistent with the fact that Notch2 is the important Notch receptor regulating MZ B cell development, because deletion of Notch2 in B cells results in absence of MZ B cells (27). The level of Notch2 on the surface of the cell is important, because even heterozygous mice that carry one functional copy of Notch2 show a diminished number of MZ B cells (27, 62). Notch2+/- mice have also been reported to show a reduction in B-1 B cells (62), while mice with a floxed allele of Notch2 crossed to CD19-Cre mice show normal B-1 numbers (27). The reason for this difference in B-1 phenotype between the two strains remains unknown. Constitutive expression of either the Notch1 intracellular domain or the Notch2 intracellular domain is capable of driving B cell differentiation towards the marginal zone fate, although the Notch2 intracellular domain seems to do so more strongly (63, 64). Knockout of Mint, an inhibitor of Notch signaling, leads to enhanced Notch signaling and a reduction in follicular B cells and increase in marginal zone B cells (65).

Dll1 is the crucial Notch ligand for specification of the marginal zone B cell fate, as deletion of Dll1 abrogates MZ B cell formation (66). Even mice with heterozygous loss of Dll1 demonstrated reduced MZ B cells. Interestingly though, development of MZ B cells in lupus-prone NZB/W mice is less dependent on Dll1 (30). In another autoimmune model, the non-obese diabetic (NOD) mouse that develops type I diabetes, heterozygosity for Notch2 does not lead to as significant a reduction in MZ B cells as is typically seen in Notch2+/- mice

on a non-autoimmune prone C57BL/6 background (67). Together these studies imply that the autoimmune milieu may provide signals that can overcome the need for the Notch2/Dll1 pathway in MZ B cell development.

Humans have marginal zone B cells as well, though they exhibit some differences as compared to their mouse counterparts (68). Unlike mouse MZ B cells, human MZ B cells frequently have mutated variable (V) regions in their antibody genes. They also express CD27, suggesting that they are antigen-experienced (68). Human MZ B cells can arise also in patients with mutations in CD40 or CD40 ligand indicating that they are at least in part activated in a T cell-independent fashion (69). Human MZ B cells may participate in responses to blood-borne bacteria, similar to mouse MZ B cells (68). Human transitional B cells isolated from cord blood and stimulated for 4 days with TLR9 ligand (CpG ODN) differentiated into cells with characteristics of MZ B cells and expressed high levels of Notch2 (70). A precursor population for human MZ B cells has been identified and shown to be responsive to DLL1 (44). Patients with Alagille syndrome involving mutations in Notch2 have a variety of developmental defects and show reduced MZ B cells (44).

Several other components of the Notch signaling pathways have also been shown to regulate generation of MZ B cells in mice. Loss of Nicastrin (a subunit of γ-secretase) (71), Adam10 (12) or Maml1 (72, 73), block MZ B cell generation. Loss of nicastrin also impairs B-1 cell development. Combined loss of Lfng or Mfng or of all three Fringe family members reduces MZ B cell numbers (31, 74). Deletion of Notch pathway inhibitor MINT results in increased MZ B cell numbers (75). On the other hand, deletion of Hes1 does not affect MZ B cell formation, though it impacts Notch-dependent T cell development (76).

The kinase Taok3, which is required for normal expression of Adam10 on transitional B cells in the spleen, is necessary for MZ B cell development (77). Interestingly, Taok3-dependent Adam10 upregulation on transitional B cells marks their commitment to become marginal zone B cells. Another signaling pathway controlling Adam10 levels on transitional B cells is the Gαi pathway (78). Deletion of Gαi2 or both Gαi2 and Gαi3 (encoded by the genes Gnai2 and Gnai3) in B cells leads to loss of marginal zone B cells. This is accompanied by poor expression of Adam10 on the surface of transitional B cells. Gαi signaling is triggered downstream of G protein-coupled receptors including chemokine receptors such as CXCR4 and CXCR5. S1PR1 is another G-protein-coupled receptor that could potentially influence Gαi activation and Notch signaling in marginal zone precursors. S1PR1 is required for marginal zone B cell precursor migration into the marginal zone region of the spleen (79).

Notch signaling can regulate transcription factor activity in B cells. For instance, B cells constitutively-expressing the Notch1 intracellular domain have elevated expression of Id2, which inhibits the function of E proteins such as E2A (64). Furthermore, as described above, Notch signaling in hematopoietic progenitors results in degradation of E2A downstream triggered by MAP kinase phosphorylation (51, 52). Expressing a form of E2A that is resistant to MAP kinase phosphorylation and degradation reverses the pro-MZ differentiation effect of the constitutively-active Notch1 intracellular domain (64). These results imply that Notch-mediated suppression of E protein function is one mechanism by which it promotes development of MZ B cells. Notch signaling also induces expression of the transcription factor Fos (80). Notch2 deletion in B cells results in decreased Fos expression, while over-expression of the Notch2 intracellular domain induces Fos. In a cell culture model system, retroviral-driven expression of Fos in Notch2-deficient B cells or bone marrow was suggested to partially restore MZ development based on an increase in the percentage of $CD23^{lo}CD21^{hi}$ cells observed (80). However, it is not clear if Fos expression is a key determinant of Notch activity as B cells lacking Fos were not studied. Irf4 seems to function as a negative regulator of the Notch pathway, since Irf4-deficient B cells have elevated expression and activation of Notch2 and elevated numbers of MZ B cells (81, 82). Irf4 also suppresses induction of activation of Notch1 in BCR and CD40 stimulated B cells, as measured by Western blot for the Notch1 intracellular domain (82). Importantly, that study also shows that retention of wild-type B cells in the marginal zone is dependent on continued signaling *via* Notch2, because inhibition of Notch2 signaling results in loss of MZ B cells to the peripheral blood.

CD19 can also influence Notch pathway activity in B cells. Loss of CD19 impairs generation of MZ B cells (63, 83). This is associated with a decreased expression of cell surface Notch2 on CD19-deficient B cells and restoring Notch2 activation using a lentiviral vector results promotes MZ development of CD19-deficient cells (83). Adam family member Adam28 is expressed at high levels of the precursors on marginal zone B cells (83, 84). Loss of CD19 was associated with reduced Adam28 levels on these precursor cells. Lentiviral driven expression of Adam28 promotes Notch2 cleavage and differentiation of MZ precursors to MZ B cells, even in the absence of CD19 (83). These data implicate Adam28 in Notch2 cleavage, but as described above, other data implicate Adam10 as being the relevant Adam family member that cleaves Notch2 (12, 77). Further study is needed to clarify the roles of these two Adam proteins.

Marginal zone B cells often express BCRs that are polyreactive or autoreactive (85). Mice carrying a transgene encoding a BCR that recognizes the self-antigen keratin as well as foreign antigens present on *Candida albicans* (the TgVH3B4 transgene) have an increase in MZ B cells as compared to non-transgenic littermates (86). When these mice were crossed to mice with a B cell-specific deletion of RBP-Jκ, the resulting TgVH3B4 RBP-Jκ deficient progeny had MZ B cells, while non-transgenic RBP-Jκ mice virtually lacked MZ B cells (86). Therefore, self-reactive B cells may be able to overcome the need for Notch signaling in the differentiation pathway to MZ B cells. As described above, data obtained with lupus-prone NZB/W mice and diabetes-prone non-obese diabetic (NOD) mice also suggest that autoimmunity can partially overcome the need for Notch signaling in the development of MZ B cells (30, 67).

NOTCH INTERACTIONS CAUSING DIFFERENTIATION OF B CELLS TO ANTIBODY-SECRETING CELLS (ASCS)

Antibody-secreting cells can be formed from B cells during either T-dependent or T-independent immune responses. T-independent responses tend to generate short-lived antibody-secreting cells that remain proliferative (plasmablasts), while T-dependent germinal center reactions tend to produce longer-lived, non-proliferative and antibody-secreting cells (fully differentiated plasma cells). Long-lived plasma cells contribute in a significant way to immunological memory, since they can persist in bone marrow for decades and continue to secrete high affinity isotype-switched antibodies (87). Some data indicates a role for the Notch pathway in ASC differentiation. Several studies have examined the effects of co-culturing B cells with stromal cells expressing the Notch ligand Dll1. Santos et al. showed that CD23+ B cells (follicular B cells) activated with LPS in the presence of stromal cells expressing Dll1 gave rise to an increased number ASCs and higher titers of antibodies without an alteration in B cell proliferation (34). Similar results were obtained with anti-CD40 stimulated B cells, except that in this case Dll1 stimulated both B cell proliferation and B cell differentiation to ASCs (34, 72). Dll1 also stimulates the proliferation of BCR-stimulated B cells and BCR and CD40 co-stimulated B cells (72). These roles of Notch signaling on ASC generation are summarized in **Figure 4**. Dll1 increased isotype switching and changed the pattern of secreted antibody isotypes in stimulated B cell cultures. B cells stimulated only with anti-CD40 secreted IgM and IgG1, while B cells stimulated with anti-CD40 in the presence of Dll1 also secreted IgG2b (72). B cells stimulated with both anti-IgM and anti-CD40 proliferate, but don't secrete much antibody. However, anti-IgM and anti-CD40 in the presence of Dll1 resulted in significant secretion of IgG1 and IgG2b. B cells stimulated with anti-CD40 + IL-4 typically secrete a large amount of IgG1 as well as some IgM and IgE. Co-culture with Dll1 expressing cells resulted in production of IgG2b along with IgG1, IgM and IgE (72). The effects of Dll1 on antibody secretion were dependent on activity of the Notch co-activator Maml1, since a dominant-negative version of this protein blocked Dll1 effects in upregulating IgG1 secretion.

Unlike Dll1, another Notch ligand Jagged1 (Jg1) was not able to induce increased ASC differentiation (34), suggesting specificity in the Notch ligand required. The effect of the Notch pathway was at a late stage of B cell differentiation after the upregulation of the plasma cell marker CD138 and could be blocked by a dominant-negative form of the Maml cofactor of the Notch signaling pathway (34, 72). Deletion of Notch1 reduces B cell antibody secretion in response to LPS stimulation (33). In this latter study, no stromal cells expressing Dll1 were used and hence Notch ligands must have been expressed by the B cells themselves or small numbers of other spleen cells that contaminated the B cell cultures (33). Interestingly, deletion of Notch1 had no effect on B cell antibody secretion in response to LPS if the B cells were not purified, but rather cultured as part of a mixture of whole spleen cells (33). This implies that an unknown factor produced by non-B cells in the cultures can substitute for the effects of Notch on ASC generation.

In another study, B cells over-expressing the Notch1 intracellular domain (and thereby mimicking constitutive Notch signaling) were reported to generate more CD138+ cells when stimulated *in vitro* with anti-IgM and anti-CD40 antibodies (32). Stimulating with anti-IgM and anti-CD40 in the presence of Dll1-expressing stromal cells resulted in an increase in the amount of IgM, IgG2a, IgG2b, and IgG3 antibodies secreted and this effect is abrogated in the absence of Notch1 (32). Using a mouse multiple myeloma model involving over-expression of the Xbp1 transcription factor, Kellner et al. discovered a post germinal center but pre-plasma cell population of mouse B cells that has high levels of Notch1 expression (88). These cells could reconstitute antibody production in B cell-deficient mice more efficiently than a terminally-differentiated ASC cell population. Together the studies above suggest that follicular B cells can upregulate Notch1 upon activation and that expression of Notch1 can stimulate generation of ASCs, either in response to T-independent stimuli (LPS) or T-dependent stimuli (anti-CD40).

Despite the studies that indicate a role for Notch signaling in ASC generation, loss of RBP-Jκ in B cells did not result in any change in ASC numbers in *ex vivo* isolated spleen, lymph node, bone marrow or Peyer's Patch cells (61). This result suggests that Notch1 signaling in mature B cells may proceed through a non-canonical RBP-Jκ independent pathway. It is also possible that differences in purification or stimulation conditions between these various experiments may have influenced the role of the Notch pathway on ASC generation.

NOTCH EFFECTS ON T CELL-INDEPENDENT IMMUNE RESPONSES

Marginal zone and B1 cells are the main B cell types that respond to T cell-independent stimuli (89). Mice with alterations in Notch2 signaling have strong reductions in MZ B cells, suggesting they may have reduced T cell-independent responses. However, RBP-Jκ deficient mice, which lack MZ B cells, show no antibody-secretion defect in response to NP-Ficoll and even show 2-3 fold increased antigen-specific responses in response to NP-LPS (61). B-1 B cells probably account for the responses to T-independent antigens when MZ B cells are absent allowing normal T-independent responses.

Deletion of Notch1 does not impair MZ B cell development (28). However, as noted above, Notch1 deficient B cells have reduced differentiation to ASCs in response to *in vitro* stimulation with the T cell-independent stimulus LPS. This observation suggests that there might be reduced responses to T-cell independent antigens *in vivo* in mice lacking Notch1. Indeed, Notch1 deficient mice showed reduced antigen-specific IgM and IgG production when immunized with the T cell-independent type I antigen (NP-LPS) (32). There was also a reduction in antigen-specific IgG when Notch1 deficient mice

were immunized with the T cell-independent type II antigen (NP-Ficoll), although this reduction was not as striking as the reduction in response to NP-LPS (32). Therefore, *in vivo* Notch1 seems more important than Notch2 for regulation of T-independent immune responses.

NOTCH EFFECTS ON T CELL DEPENDENT IMMUNE RESPONSES AND GERMINAL CENTERS

Follicular B cells are the main B cell type that responds to T cell-dependent stimuli, although marginal zone B cells can also participate in these reactions. Unlike MZ B cells, specification of the follicular B cell lineage is not controlled by Notch signaling. However, Notch signaling can influence T-dependent germinal center (GC) responses in which follicular B cells play the most prominent role (**Figure 5**). As described above, stimuli that mimic signals found in GCs (anti-CD40 or anti-IgM and anti-CD40 antibodies) can stimulate B cell differentiation to ASCs (32, 34, 72). Notch ligands are expressed by FDCs and Notch1 and Notch2 receptors are expressed by GC B cells (34, 38). GC B cells cultured with an FDC cell line (HK cells) along with CD40 ligand, IL-2 and either IL-4 or IL-21 undergo proliferation, differentiation to plasmablasts and secretion of antibodies and the addition of an inhibitor of the γ-secretase (DAPT) inhibits these processes (38). As was seen with T cell-independent responses, loss of RBP-Jκ does not interfere with antigen-specific antibody production in response to the T cell-dependent antigen NP-CGG (61). This may indicate that Notch effects in GC B cells are *via* a non-canonical Notch pathway. On the other hand, immunizing mice that have B cell-specific expression of dominant-negative Maml1 with the T cell-dependent antigen NP-CGG resulted in production of fewer NP-specific plasma cells compared to controls (72). Dominant-negative Maml1 mice also had decreased frequencies and numbers of IgG1+ B220-low plasma cells (72).

Notch signaling in GC B cells may be influenced by the transcription factor BCL6, which is crucial for GC B cell formation. In *Xenopus laevis*, the Notch1 intracellular domain

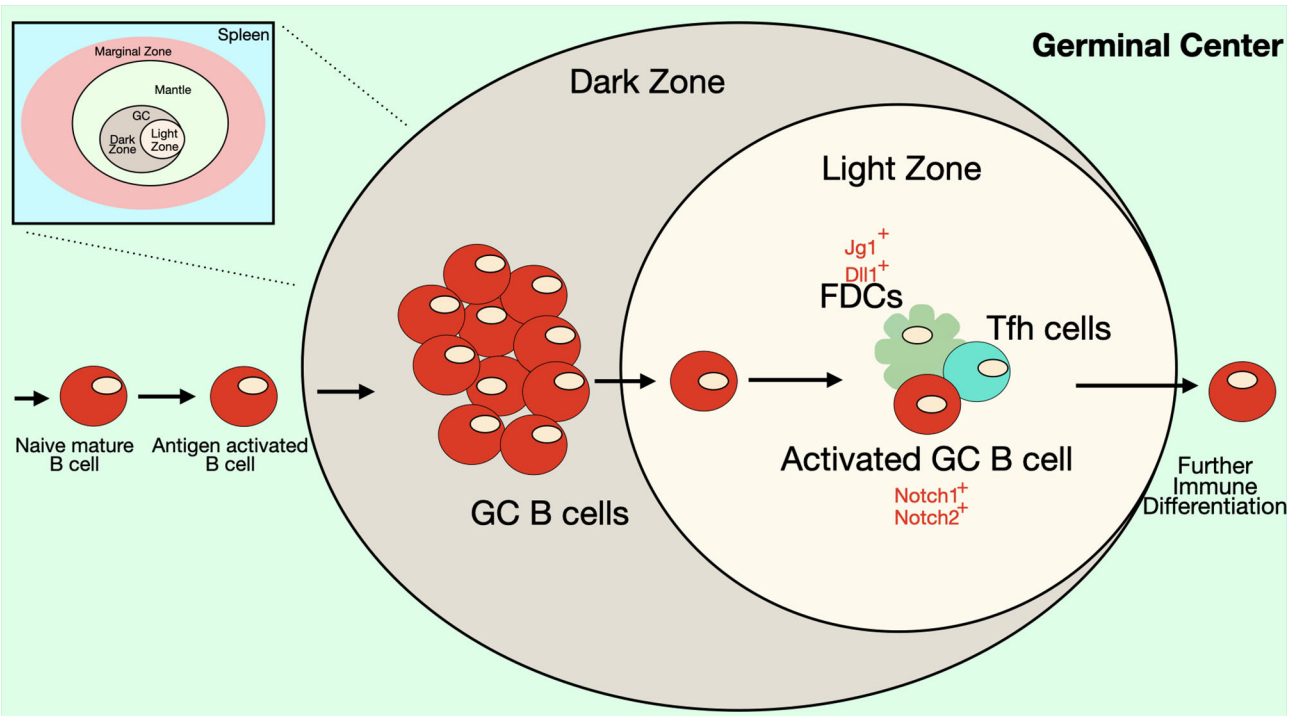

FIGURE 5 | Notch signaling in the Germinal Center. Some B cell follicles in the peripheral lymphoid organs contain germinal centers (GC), where B cells rapidly proliferate and undergo somatic hypermutation, affinity maturation and isotype-switching. The germinal center has two anatomical compartments. In the dark zone of the GC, B cell centroblasts rapidly proliferate while also undergoing somatic hypermutation. In the light zone of the GC, B cell centrocytes compete for binding antigen on follicular dendritic cells (FDCs) and receive signals from T follicular helper (Tfh) cells that promote survival and differentiation. Together these processes select for B cells with BCRs that recognize antigen with high affinity. FDCs express DSL ligands that may play a role in signaling during germinal center reactions. In mice, GC B cells express both Notch1 and Notch2 receptors, though in humans expression of these Notch receptors is low on GC B cells. Notch signaling in GC B cells has been shown to antagonize the effects of BCL6 and may play a role in differentiation of GC B cells into ASCs. Differentiation of Tfh cells also requires Notch signaling.

was shown to interact with BCL6 (90), displacing Maml proteins from the Notch intracellular domain. Because Maml proteins are co-activators of Notch-dependent transcription, their displacement results in weaker Notch-mediated transcriptional events. BCL6 also functions to recruit the co-repressor BCoR to the NICD, thus further suppressing Notch-dependent transcription (90). Another mechanism by which BCL6 could inhibit Notch signaling in GC B cells was described by Valls et al. in human follicular lymphomas, a tumor derived from GC B cells (40). In these cells, the BCL6 protein binds to regulatory elements of the Notch2 gene and other Notch pathway genes (Maml1, Maml2, RBP-Jκ and Hes1) to directly repress their expression. BCL6 and Notch pathway genes show an inverse correlation in expression patterns in primary human and murine GC B cells (40). BCL6-dependent repression of Notch2 seems to be crucial for GC maintenance, since tamoxifen-inducible expression of the Notch2 intracellular domain abrogates GC formation in mice (40). On the other hand, BCL6-targeting compounds or gene silencing leads to the induction of Notch2 activity. Together, these data indicate two possible mechanisms by which BCL6 may interfere with Notch signaling, either by binding to the NICD and displacing the co-activator Maml, while recruiting the co-repressor BCoR, or by directly binding to and repressing Notch pathway genes. Both mechanisms may take place in GC B cells. The ability of BCL6 to interfere with Notch signaling may be needed to prevent premature differentiation of GC B cells to ASCs, a process induced by Notch activity.

Notch signaling can also have B cell-extrinsic effects that influence GC formation. T follicular helper cells (Tfh) are a subset of CD4+ T cells that are specialized for helping B cells in germinal center reactions. Like GC B cells, Tfh cells express the transcription factor BCL6 and this transcription factor is crucial for the ability of Tfh cells to differentiate properly and provide B cell help (91). Combined deletion of both Notch1 and Notch2 using CD4-Cre results in impaired Tfh cell generation, while total CD4 cells, Tregs, memory CD4 T cells and naïve CD4 T cells are all normal (92). The decrease in Tfh cells results in impaired GC formation in response to immunization with T-dependent antigens or parasite infection. There was also impaired generation of high-affinity antigen-specific IgG antibodies. The few Tfh cells that develop in Notch1/Notch2-deficient mice express low levels of Tfh markers such as BCL6, IL-21, c-Maf and CXCR5 (92). Therefore, Notch signaling can have both B cell-intrinsic and B-cell extrinsic effects in the GC.

Germinal center-derived B cell lymphomas often have excessive and dysregulated Notch signaling caused by activating mutations (93). Many mutations in Notch receptors are localized in the PEST domain and result in premature truncation thereby blocking PEST-mediated degradation of NICD and causing prolonged Notch signaling. To test potential roles for this dysregulated Notch signaling, Arima et al. developed a mouse model in which the intracellular domain of Notch1 (NICD) was expressed in B cells under the control of the germinal center specific AICDA-Cre. This resulted in an increased percentage of GC cells, while other B cell subsets were normal (94). In this mouse model, B cells produced the cytokine IL-33, which led to secondary effects in the T cell compartment including an expansion of Treg and Th2 cell subsets and a decrease in cytokine production by Th1 and CD8+ T cells (94). Thus, increased Notch signaling in B cells can lead to B cell-extrinsic effects on the immune response.

CONCLUSIONS

In this review, we've summarized published studies implicating the evolutionarily-conserved Notch signaling pathway in regulating B cell differentiation and functional responses. These studies clearly show an important influence of the Notch pathway in guiding appropriate differentiation at many steps of B cell development from the hematopoietic progenitor cells in the bone marrow to terminally-differentiated B cells in immune responses. There are various compounds that can be used to target both the canonical and noncanonical pathways of Notch signaling and could potentially influence immune responses. However, the involvement of Notch signaling in crucial developmental decisions in a huge variety of cell types in the body makes it very difficult to specifically target B cell responses, unless methods can be developed to deliver Notch activators or inhibitors directly to B cells without affecting other nearby cell types. A number of interesting questions remain to define concerning Notch pathway activity in B cells. Notch2 is clearly required for the MZ fate specification, but Notch1 seems more important in ASC differentiation. However, Notch2 has not been inducibly-deleted in mature B cells to allow studies to test its function in generation of ASCs from already committed MZ and follicular B cells. Another interesting question is whether non-canonical Notch signaling plays an important role in B cell differentiation. Notch2 seems to trigger the canonical pathway to specify the MZ B cell fate, since loss of RBP-Jk interferes with this process. However, in T dependent and T-independent immune responses, B cells lacking Notch1 show a defect, while those lacking RBP-Jκ do not. This implies that a non-canonical pathway may be more important at this stage. Future studies will be important to address some of these interesting conundrums.

AUTHOR CONTRIBUTIONS

MG collected information, wrote the manuscript and prepared the figures. LG-S edited and approved the final version. All authors contributed to the article and approved the submitted version.

FUNDING

This work was supported by grants from the Lupus Research Alliance and the National Institute of Allergy and Infectious Disease (NIAID R01 AI122720).

REFERENCES

1. Gazave E, Lapebie P, Richards GS, Brunet F, Ereskovsky AV, Degnan BM, et al. Origin and evolution of the Notch signalling pathway: an overview from eukaryotic genomes. *BMC Evol Biol* (2009) 9:249. doi: 10.1186/1471-2148-9-249
2. Kopan R, Ilagan MX. The canonical Notch signaling pathway: unfolding the activation mechanism. *Cell* (2009) 137(2):216–33. doi: 10.1016/j.cell.2009.03.045
3. Logeat F, Bessia C, Brou C, Lebail O, Jarriault S, Seidah NG, et al. The Notch1 receptor is cleaved constitutively by a furin-like convertase. *Proc Natl Acad Sci USA* (1998) 95(14):8108–12. doi: 10.1073/pnas.95.14.8108
4. Cordle J, Johnson S, Tay JZ, Roversi P, Jarriault S, Wilkin MB, et al. A conserved face of the Jagged/Serrate DSL domain is involved in Notch trans-activation and cis-inhibition. *Nat Struct Mol Biol* (2008) 15(8):849–57. doi: 10.1038/nsmb.1457
5. Weisshuhn PC, Sheppard D, Taylor P, Whiteman P, Lea SM, Handford PA, et al. Non-Linear and Flexible Regions of the Human Notch1 Extracellular Domain Revealed by High-Resolution Structural Studies. *Structure* (2016) 24 (4):555–66. doi: 10.1016/j.str.2016.02.010
6. Sanchez-Irizarry C, Carpenter AC, Weng AP, Pear WS, Aster JC, Blacklow SC. Notch subunit heterodimerization and prevention of ligand-independent proteolytic activation depend, respectively, on a novel domain and the LNR repeats. *Mol Cell Biol* (2004) 24(21):9265–73. doi: 10.1128/MCB.24.21.9265-9273.2004
7. Brou C, Logeat F, Gupta N, Bessia C, Lebail O, Doedens JR, et al. A novel proteolytic cleavage involved in Notch signaling: the role of the disintegrin-metalloprotease TACE. *Mol Cell* (2000) 5(2):207–16. doi: 10.1016/S1097-2765(00)80417-7
8. Hartmann D, De Strooper B, Serneels L, Craessaerts K, Herreman A, Annaert W, et al. The disintegrin/metalloprotease ADAM 10 is essential for Notch signalling but not for alpha-secretase activity in fibroblasts. *Hum Mol Genet* (2002) 11(21):2615–24. doi: 10.1093/hmg/11.21.2615
9. Gordon WR, Zimmerman B, He L, Miles LJ, Huang J, Tiyanont K, et al. Mechanical Allostery: Evidence for a Force Requirement in the Proteolytic Activation of Notch. *Dev Cell* (2015) 33(6):729–36. doi: 10.1016/j.devcel.2015.05.004
10. Seo D, Southard KM, Kim JW, Lee HJ, Farlow J, Lee JU, et al. A Mechanogenetic Toolkit for Interrogating Cell Signaling in Space and Time. *Cell* (2016) 165(6):1507–18. doi: 10.1016/j.cell.2016.04.045
11. van Tetering G, Van Diest P, Verlaan I, Van Der Wall E, Kopan R, Vooijs M. Metalloprotease ADAM10 is required for Notch1 site 2 cleavage. *J Biol Chem* (2009) 284(45):31018–27. doi: 10.1074/jbc.M109.006775
12. Gibb DR, El Shikh M, Kang DJ, Rowe WJ, El Sayed R, Cichy J, et al. ADAM10 is essential for Notch2-dependent marginal zone B cell development and CD23 cleavage in vivo. *J Exp Med* (2010) 207(3):623–35. doi: 10.1084/jem.20091990
13. Weber S, Niessen MT, Prox J, Lullmann-Rauch R, Schmitz A, Schwanbeck R, et al. The disintegrin/metalloproteinase Adam10 is essential for epidermal integrity and Notch-mediated signaling. *Development* (2011) 138(3):495–505. doi: 10.1242/dev.055210
14. Bozkulak EC, Weinmaster G. Selective use of ADAM10 and ADAM17 in activation of Notch1 signaling. *Mol Cell Biol* (2009) 29(21):5679–95. doi: 10.1128/MCB.00406-09
15. Bleibaum F, Sommer A, Veit M, Rabe B, Andra J, Kunzelmann K, et al. ADAM10 sheddase activation is controlled by cell membrane asymmetry. *J Mol Cell Biol* (2019) 11(11):979–93. doi: 10.1093/jmcb/mjz008
16. Dillon SR, Constantinescu A, Schlissel MS. Annexin V binds to positively selected B cells. *J Immunol* (2001) 166(1):58–71. doi: 10.4049/jimmunol.166.1.58
17. Dillon SR, Mancini M, Rosen A, Schlissel MS. Annexin V binds to viable B cells and colocalizes with a marker of lipid rafts upon B cell receptor activation. *J Immunol* (2000) 164(3):1322–32. doi: 10.4049/jimmunol.164.3.1322
18. Suzuki J, Umeda M, Sims PJ, Nagata S. Calcium-dependent phospholipid scrambling by TMEM16F. *Nature* (2010) 468(7325):834–8. doi: 10.1038/nature09583
19. Chillakuri CR, Sheppard D, Lea SM, Handford PA. Notch receptor-ligand binding and activation: insights from molecular studies. *Semin Cell Dev Biol* (2012) 23(4):421–8. doi: 10.1016/j.semcdb.2012.01.009
20. Kakuda S, Haltiwanger RS. Deciphering the Fringe-Mediated Notch Code: Identification of Activating and Inhibiting Sites Allowing Discrimination between Ligands. *Dev Cell* (2017) 40(2):193–201. doi: 10.1016/j.devcel.2016.12.013
21. Callahan J, Aster J, Sklar J, Kieff E, Robertson ES. Intracellular forms of human NOTCH1 interact at distinctly different levels with RBP-jkappa in human B and T cells. *Leukemia* (2000) 14(1):84–92. doi: 10.1038/sj.leu.2401630
22. Jarriault S, Brou C, Logeat F, Schroeter EH, Kopan R, Israel A. Signalling downstream of activated mammalian Notch. *Nature* (1995) 377(6547):355–8. doi: 10.1038/377355a0
23. Nam Y, Sliz P, Song L, Aster JC, Blacklow SC. Structural basis for cooperativity in recruitment of MAML coactivators to Notch transcription complexes. *Cell* (2006) 124(5):973–83. doi: 10.1016/j.cell.2005.12.037
24. Wu L, Sun T, Kobayashi K, Gao P, Griffin JD. Identification of a family of mastermind-like transcriptional coactivators for mammalian notch receptors. *Mol Cell Biol* (2002) 22(21):7688–700. doi: 10.1128/MCB.22.21.7688-7700.2002
25. Borggrefe T, Oswald F. The Notch signaling pathway: transcriptional regulation at Notch target genes. *Cell Mol Life Sci* (2009) 66(10):1631–46. doi: 10.1007/s00018-009-8668-7
26. Heitzler P. Biodiversity and noncanonical Notch signaling. *Curr Top Dev Biol* (2010) 92:457–81. doi: 10.1016/S0070-2153(10)92014-0
27. Saito T, Chiba S, Ichikawa M, Kunisato A, Asai T, Shimizu K, et al. Notch2 is preferentially expressed in mature B cells and indispensable for marginal zone B lineage development. *Immunity* (2003) 18(5):675–85. doi: 10.1016/S1074-7613(03)00111-0
28. Radtke F, Wilson A, Stark G, Bauer M, Van Meerwijk J, Macdonald HR, et al. Deficient T cell fate specification in mice with an induced inactivation of Notch1. *Immunity* (1999) 10(5):547–58. doi: 10.1016/S1074-7613(00)80054-0
29. Kitamoto T, Takahashi K, Takimoto H, Tomizuka K, Hayasaka M, Tabira T, et al. Functional redundancy of the Notch gene family during mouse embryogenesis: analysis of Notch gene expression in Notch3-deficient mice. *Biochem Biophys Res Commun* (2005) 331(4):1154–62. doi: 10.1016/j.bbrc.2005.03.241
30. Moriyama Y, Sekine C, Koyanagi A, Koyama N, Ogata H, Chiba S, et al. Delta-like 1 is essential for the maintenance of marginal zone B cells in normal mice but not in autoimmune mice. *Int Immunol* (2008) 20(6):763–73. doi: 10.1093/intimm/dxn034
31. Tan JB, Xu K, Cretegny K, Visan I, Yuan JS, Egan SE, et al. Lunatic and manic fringe cooperatively enhance marginal zone B cell precursor competition for delta-like 1 in splenic endothelial niches. *Immunity* (2009) 30(2):254–63. doi: 10.1016/j.immuni.2008.12.016
32. Kang JA, Kim WS, Park SG. Notch1 is an important mediator for enhancing of B-cell activation and antibody secretion by Notch ligand. *Immunology* (2014) 143(4):550–9. doi: 10.1111/imm.12333
33. Zhu G, Wang X, Xiao H, Liu X, Fang Y, Zhai B, et al. Both Notch1 and its ligands in B cells promote antibody production. *Mol Immunol* (2017) 91:17–23. doi: 10.1016/j.molimm.2017.08.021
34. Santos MA, Sarmento LM, Rebelo M, Doce AA, Maillard I, Dumortier A, et al. Notch1 engagement by Delta-like-1 promotes differentiation of B lymphocytes to antibody-secreting cells. *Proc Natl Acad Sci USA* (2007) 104 (39):15454–9. doi: 10.1073/pnas.0702891104
35. Bertrand FE, Eckfeldt CE, Lysholm AS, Lebien TW. Notch-1 and Notch-2 exhibit unique patterns of expression in human B-lineage cells. *Leukemia* (2000) 14(12):2095–102. doi: 10.1038/sj.leu.2401942
36. Hystad ME, Myklebust JH, Bo TH, Sivertsen EA, Rian E, Forfang L, et al. Characterization of early stages of human B cell development by gene expression profiling. *J Immunol* (2007) 179(6):3662–71. doi: 10.4049/jimmunol.179.6.3662
37. Ohishi K, Varnum-Finney B, Flowers D, Anasetti C, Myerson D, Bernstein ID. Monocytes express high amounts of Notch and undergo cytokine specific apoptosis following interaction with the Notch ligand, Delta-1. *Blood* (2000) 95 (9):2847–54. doi: 10.1182/blood.V95.9.2847.009k19_2847_2854
38. Yoon SO, Zhang X, Berner P, Blom B, Choi YS. Notch ligands expressed by follicular dendritic cells protect germinal center B cells from apoptosis. *J Immunol* (2009) 183(1):352–8. doi: 10.4049/jimmunol.0803183
39. Fabbri G, Holmes AB, Viganotti M, Scuoppo C, Belver L, Herranz D, et al. Common nonmutational NOTCH1 activation in chronic lymphocytic

leukemia. *Proc Natl Acad Sci USA* (2017) 114(14):E2911–9. doi: 10.1073/pnas.1702564114
40. Valls E, Lobry AB, Geng H, Wang L, Cardenas M, Rivas M, et al. BCL6 Antagonizes NOTCH2 to Maintain Survival of Human Follicular Lymphoma Cells. *Cancer Discovery* (2017) 7(5):506–21. doi: 10.1158/2159-8290.CD-16-1189
41. Sheng Y, Yahata T, Negishi N, Nakano Y, Habu S, Hozumi K, et al. Expression of Delta-like 1 in the splenic non-hematopoietic cells is essential for marginal zone B cell development. *Immunol Lett* (2008) 121(1):33–7. doi: 10.1016/j.imlet.2008.08.001
42. Perez-Shibayama C, Gil-Cruz C, Ludewig B. Fibroblastic reticular cells at the nexus of innate and adaptive immune responses. *Immunol Rev* (2019) 289 (1):31–41. doi: 10.1111/imr.12748
43. Fasnacht N, Huang HY, Koch U, Favre S, Auderset F, Chai Q, et al. Specific fibroblastic niches in secondary lymphoid organs orchestrate distinct Notch-regulated immune responses. *J Exp Med* (2014) 211(11):2265–79. doi: 10.1084/jem.20132528
44. Descatoire M, Weller S, Irtan S, Sarnacki S, Feuillard J, Storck S, et al. Identification of a human splenic marginal zone B cell precursor with NOTCH2-dependent differentiation properties. *J Exp Med* (2014) 211 (5):987–1000. doi: 10.1084/jem.20132203
45. Han H, Tanigaki K, Yamamoto N, Kuroda K, Yoshimoto M, Nakahata T, et al. Inducible gene knockout of transcription factor recombination signal binding protein-J reveals its essential role in T versus B lineage decision. *Int Immunol* (2002) 14(6):637–45. doi: 10.1093/intimm/dxf030
46. Wilson A, MacDonald HR, Radtke F. Notch 1-deficient common lymphoid precursors adopt a B cell fate in the thymus. *J Exp Med* (2001) 194(7):1003–12. doi: 10.1084/jem.194.7.1003
47. Pui JC, Allman D, Xu L, Derocco S, Karnell FG, Bakkour S, et al. Notch1 expression in early lymphopoiesis influences B versus T lineage determination. *Immunity* (1999) 11(3):299–308. doi: 10.1016/S1074-7613(00)80105-3
48. Benne C, Lelievre JD, Balbo M, Henry A, Sakano S, Levy Y. Notch increases T/NK potential of human hematopoietic progenitors and inhibits B cell differentiation at a pro-B stage. *Stem Cells* (2009) 27(7):1676–85. doi: 10.1002/stem.94
49. Jaleco AC, Neves H, Hooijberg E, Gameiro P, Clode N, Haury M, et al. Differential effects of Notch ligands Delta-1 and Jagged-1 in human lymphoid differentiation. *J Exp Med* (2001) 194(7):991–1002. doi: 10.1084/jem.194.7.991
50. Izon DJ, Aster JC, He Y, Weng A, Karnell FG, Patriub V, et al. Deltex1 redirects lymphoid progenitors to the B cell lineage by antagonizing Notch1. *Immunity* (2002) 16(2):231–43. doi: 10.1016/S1074-7613(02)00271-6
51. Bain G, Maandag EC, Izon DJ, Amsen D, Kruisbeek AM, Weintraub BS, et al. E2A proteins are required for proper B cell development and initiation of immunoglobulin gene rearrangements. *Cell* (1994) 79(5):885–92. doi: 10.1016/0092-8674(94)90077-9
52. Nie L, Xu M, Vladimirova A, Sun XH. Notch-induced E2A ubiquitination and degradation are controlled by MAP kinase activities. *EMBO J* (2003) 22(21):5780–92. doi: 10.1093/emboj/cdg567
53. Smith EM, Akerblad P, Kadesch T, Axelson H, Sigvardsson M. Inhibition of EBF function by active Notch signaling reveals a novel regulatory pathway in early B-cell development. *Blood* (2005) 106(6):1995–2001. doi: 10.1182/blood-2004-12-4744
54. Gyory I, Boller S, Nechanitzky R, Mandel E, Pott S, Liu E, et al. Transcription factor Ebf1 regulates differentiation stage-specific signaling, proliferation, and survival of B cells. *Genes Dev* (2012) 26(7):668–82. doi: 10.1101/gad.187328.112
55. Lin H, Grosschedl R. Failure of B-cell differentiation in mice lacking the transcription factor EBF. *Nature* (1995) 376(6537):263–7. doi: 10.1038/376263a0
56. Maeda T, Merghoub T, Hobbs RM, Dong L, Maeda M, Zakrzewski J, et al. Regulation of B versus T lymphoid lineage fate decision by the proto-oncogene LRF. *Science* (2007) 316(5826):860–6. doi: 10.1126/science.1140881
57. Souabni A, Cobaleda C, Schebesta M, Busslinger M. Pax5 promotes B lymphopoiesis and blocks T cell development by repressing Notch1. *Immunity* (2002) 17(6):781–93. doi: 10.1016/S1074-7613(02)00472-7
58. Baumgarth N. A Hard(y) Look at B-1 Cell Development and Function. *J Immunol* (2017) 199(10):3387–94. doi: 10.4049/jimmunol.1700943
59. Allman D, Pillai S. Peripheral B cell subsets. *Curr Opin Immunol* (2008) 20 (2):149–57. doi: 10.1016/j.coi.2008.03.014
60. Martin F, Oliver AM, Kearney JF. Marginal zone and B1 B cells unite in the early response against T-independent blood-borne particulate antigens. *Immunity* (2001) 14(5):617–29. doi: 10.1016/S1074-7613(01)00129-7
61. Tanigaki K, Han H, Yamamoto N, Tashiro K, Ikegawa M, Kuroda K, et al. Notch-RBP-J signaling is involved in cell fate determination of marginal zone B cells. *Nat Immunol* (2002) 3(5):443–50. doi: 10.1038/ni793
62. Witt CM, Won WJ, Hurez V, Klug CA. Notch2 haploinsufficiency results in diminished B1 B cells and a severe reduction in marginal zone B cells. *J Immunol* (2003) 171(6):2783–8. doi: 10.4049/jimmunol.171.6.2783
63. Hampel F, Ehrenberg S, Hojer J, Draeseke A, Marschall-Schroter G, Kuhn R, et al. CD19-independent instruction of murine marginal zone B-cell development by constitutive Notch2 signaling. *Blood* (2011) 118(24):6321–31. doi: 10.1182/blood-2010-12-325944
64. Zhang P, Zhao Y, Sun XH. Notch-regulated periphery B cell differentiation involves suppression of E protein function. *J Immunol* (2013) 191(2):726–36. doi: 10.4049/jimmunol.1202134
65. Yabe D, Fukuda H, Aoki M, Yamada S, Takebayashi S, Shinkura R, et al. Generation of a conditional knockout allele for mammalian Spen protein Mint/SHARP. *Genesis* (2007) 45(5):300–6. doi: 10.1002/dvg.20296
66. Hozumi K, Negishi N, Suzuki D, Abe N, Sotomaru Y, Tamaoki N, et al. Delta-like 1 is necessary for the generation of marginal zone B cells but not T cells in vivo. *Nat Immunol* (2004) 5(6):638–44. doi: 10.1038/ni1075
67. Case JB, Bonami RH, Nyhoff LE, Steinberg HE, Sullivan AM, Kendall PL. Bruton's Tyrosine Kinase Synergizes with Notch2 To Govern Marginal Zone B Cells in Nonobese Diabetic Mice. *J Immunol* (2015) 195(1):61–70. doi: 10.4049/jimmunol.1400803
68. Bemark M. Translating transitions - how to decipher peripheral human B cell development. *J BioMed Res* (2015) 29(4):264–84. doi: 10.7555/JBR.29.20150035
69. Weller S, Faili A, Garcia C, Braun MC, Le Deist FF, De Saint Basile GG, et al. CD40-CD40L independent Ig gene hypermutation suggests a second B cell diversification pathway in humans. *Proc Natl Acad Sci USA* (2001) 98 (3):1166–70. doi: 10.1073/pnas.98.3.1166
70. Guerrier T, Youinou P, Pers JO, Jamin C. TLR9 drives the development of transitional B cells towards the marginal zone pathway and promotes autoimmunity. *J Autoimmun* (2012) 39(3):173–9. doi: 10.1016/j.jaut.2012.05.012
71. Choi JH, Han J, Theodoropoulos PC, Zhong X, Wang J, Medler D, et al. Essential requirement for nicastrin in marginal zone and B-1 B cell development. *Proc Natl Acad Sci USA* (2020) 117(9):4894–901. doi: 10.1073/pnas.1916645117
72. Thomas M, Calamito M, Srivastava B, Maillard I, Pear WS, Allman D. Notch activity synergizes with B-cell-receptor and CD40 signaling to enhance B-cell activation. *Blood* (2007) 109(8):3342–50. doi: 10.1182/blood-2006-09-046698
73. Wu L, Maillard I, Nakamura M, Pear WS, Griffin JD. The transcriptional coactivator Maml1 is required for Notch2-mediated marginal zone B-cell development. *Blood* (2007) 110(10):3618–23. doi: 10.1182/blood-2007-06-097030
74. Song Y, Kumar V, Wei HX, Qiu J, Stanley P. Lunatic, Manic, and Radical Fringe Each Promote T and B Cell Development. *J Immunol* (2016) 196(1):232–43. doi: 10.4049/jimmunol.1402421
75. Kuroda K, Han H, Tani S, Tanigaki K, Tun T, Furukawa T, et al. Regulation of marginal zone B cell development by MINT, a suppressor of Notch/RBP-J signaling pathway. *Immunity* (2003) 18(2):301–12. doi: 10.1016/S1074-7613(03)00029-3
76. Wendorff AA, Koch U, Wunderlich FT, Wirth S, Dubey C, Bruning JC, et al. Hes1 is a critical but context-dependent mediator of canonical Notch signaling in lymphocyte development and transformation. *Immunity* (2010) 33(5):671–84. doi: 10.1016/j.immuni.2010.11.014
77. Hammad H, Vanderkerken M, Pouliot P, Deswarte K, Toussaint W, Vergote K, et al. Transitional B cells commit to marginal zone B cell fate by Taok3-mediated surface expression of ADAM10. *Nat Immunol* (2017) 18(3):313–20. doi: 10.1038/ni.3657
78. Hwang IY, Boularan C, Harrison K, Kehrl JH. Galphai Signaling Promotes Marginal Zone B Cell Development by Enabling Transitional B Cell ADAM10 Expression. *Front Immunol* (2018) 9:687. doi: 10.3389/fimmu.2018.00687

79. Cinamon G, Matloubian M, Lesneski MJ, Xu Y, Low C, Lu T, et al. Sphingosine 1-phosphate receptor 1 promotes B cell localization in the splenic marginal zone. *Nat Immunol* (2004) 5(7):713–20. doi: 10.1038/ni1083
80. Iwahashi S, Maekawa Y, Nishida J, Ishifune C, Kitamura A, Arimochi H, et al. Notch2 regulates the development of marginal zone B cells through Fos. *Biochem Biophys Res Commun* (2012) 418(4):701–7. doi: 10.1016/j.bbrc.2012.01.082
81. Ochiai K, Maienschein-Cline M, Simonetti G, Chen J, Rosenthal R, Brink R, et al. Transcriptional regulation of germinal center B and plasma cell fates by dynamical control of IRF4. *Immunity* (2013) 38(5):918–29. doi: 10.1016/j.immuni.2013.04.009
82. Simonetti G, Carette A, Silva K, Wang H, De Silva NS, Heise N, et al. IRF4 controls the positioning of mature B cells in the lymphoid microenvironments by regulating NOTCH2 expression and activity. *J Exp Med* (2013) 210 (13):2887–902. doi: 10.1084/jem.20131026
83. Zhang Y, Zhu G, Xiao H, Liu X, Han G, Chen G, et al. CD19 regulates ADAM28-mediated Notch2 cleavage to control the differentiation of marginal zone precursors to MZ B cells. *J Cell Mol Med* (2017) 21(12):3658–69. doi: 10.1111/jcmm.13276
84. Mabbott NA, Gray D. Identification of co-expressed gene signatures in mouse B1, marginal zone and B2 B-cell populations. *Immunology* (2014) 141(1):79–95. doi: 10.1111/imm.12171
85. Martin F, Kearney JF. B-cell subsets and the mature preimmune repertoire. Marginal zone and B1 B cells as part of a "natural immune memory". *Immunol Rev* (2000) 175:70–9. doi: 10.1111/j.1600-065X.2000.imr017515.x
86. Zhang Z, Zhou L, Yang X, Wang Y, Zhang P, Hou L, et al. Notch-RBP-J-independent marginal zone B cell development in IgH transgenic mice with VH derived from a natural polyreactive antibody. *PloS One* (2012) 7(6):e38894. doi: 10.1371/journal.pone.0038894
87. Hammarlund E, Thomas A, Amanna IJ, Holden LA, Slayden OD, Park B, et al. Plasma cell survival in the absence of B cell memory. *Nat Commun* (2017) 8(1):1781. doi: 10.1038/s41467-017-01901-w
88. Kellner J, Wallace C, Liu B, Li Z. Definition of a multiple myeloma progenitor population in mice driven by enforced expression of XBP1s. *JCI Insight* (2019) 4(7). doi: 10.1172/jci.insight.124698
89. Cerutti A, Cols M, Puga I. Marginal zone B cells: virtues of innate-like antibody-producing lymphocytes. *Nat Rev Immunol* (2013) 13(2):118–32. doi: 10.1038/nri3383
90. Sakano D, Kato A, Parikh N, Mcknight K, Terry D, Stefanovic B, et al. BCL6 canalizes Notch-dependent transcription, excluding Mastermind-like1 from selected target genes during left-right patterning. *Dev Cell* (2010) 18(3):450–62. doi: 10.1016/j.devcel.2009.12.023
91. Crotty S. T Follicular Helper Cell Biology: A Decade of Discovery and Diseases. *Immunity* (2019) 50(5):1132–48. doi: 10.1016/j.immuni.2019.04.011
92. Auderset F, Schuster S, Fasnacht N, Coutaz M, Charmoy M, Koch U, et al. Notch signaling regulates follicular helper T cell differentiation. *J Immunol* (2013) 191(5):2344–50. doi: 10.4049/jimmunol.1300643
93. Arruga F, Vaisitti T, Deaglio S. The NOTCH Pathway and Its Mutations in Mature B Cell Malignancies. *Front Oncol* (2018) 8:550. doi: 10.3389/fonc.2018.00550
94. Arima H, Nishikori M, Otsuka Y, Kishimoto W, Izumi K, Yasuda K, et al. B cells with aberrant activation of Notch1 signaling promote Treg and Th2 cell-dominant T-cell responses via IL-33. *Blood Adv* (2018) 2(18):2282–95. doi: 10.1182/bloodadvances.2018019919

Conflict of Interest: The authors declare that the research was conducted in the absence of any commercial or financial relationships that could be construed as a potential conflict of interest.

frontiers in Immunology

ORIGINAL RESEARCH
published: 12 February 2021
doi: 10.3389/fimmu.2020.594813

Direct Infection of B Cells by Dengue Virus Modulates B Cell Responses in a Cambodian Pediatric Cohort

*Vinit Upasani[1,2], Hoa Thi My Vo[1], Heidi Auerswald[3], Denis Laurent[4], Sothy Heng[4], Veasna Duong[3], Izabela A. Rodenhuis-Zybert[2], Philippe Dussart[3] and Tineke Cantaert[1]**

[1] Immunology Unit, Institut Pasteur du Cambodge, Institut Pasteur International Network, Phnom Penh, Cambodia, [2] Department of Medical Microbiology and Infection Prevention, University of Groningen and University Medical Center Groningen, Groningen, Netherlands, [3] Virology Unit, Institut Pasteur du Cambodge, Institut Pasteur International Network, Phnom Penh, Cambodia, [4] Kantha Bopha Children Hospital, Phnom Penh, Cambodia

Dengue is an acute viral disease caused by dengue virus (DENV), which is transmitted by *Aedes* mosquitoes. Symptoms of DENV infection range from inapparent to severe and can be life-threatening. DENV replicates in primary immune cells such as dendritic cells and macrophages, which contribute to the dissemination of the virus. Susceptibility of other immune cells such as B cells to direct infection by DENV and their subsequent response to infection is not well defined. In a cohort of 60 Cambodian children, we showed that B cells are susceptible to DENV infection. Moreover, we show that B cells can support viral replication of laboratory adapted and patient-derived DENV strains. B cells were permissive to DENV infection albeit low titers of infectious virions were released in cell supernatants CD300a, a phosphatidylserine receptor, was identified as a potential attachment factor or receptor for entry of DENV into B cells. In spite of expressing Fcγ-receptors, antibody-mediated enhancement of DENV infection was not observed in B cells in an *in vitro* model. Direct infection by DENV induced proliferation of B cells in dengue patients *in vivo* and plasmablast/plasma cell formation *in vitro*. To summarize, our results show that B cells are susceptible to direct infection by DENV *via* CD300a and the subsequent B cell responses could contribute to dengue pathogenesis.

Keywords: infectious diseases, B cell response, dengue viral infection, plasma cell development, DENV entry mechanism

OPEN ACCESS

Edited by:
Jayanta Chaudhuri, Memorial Sloan Kettering Cancer Center, United States

Reviewed by:
Prasad Srikakulapu, University of Virginia, United States
*Shengli Xu, Bioprocessing Technology Institute (A*STAR), Singapore*

***Correspondence:**
Tineke Cantaert
tineke.cantaert@pasteur.fr

Specialty section:
This article was submitted to B Cell Biology, a section of the journal Frontiers in Immunology

Received: *14 August 2020*
Accepted: *24 December 2020*
Published: *12 February 2021*

Citation:
Upasani V, Vo HTM, Auerswald H, Laurent D, Heng S, Duong V, Rodenhuis-Zybert IA, Dussart P and Cantaert T (2021) Direct Infection of B Cells by Dengue Virus Modulates B Cell Responses in a Cambodian Pediatric Cohort. Front. Immunol. 11:594813. doi: 10.3389/fimmu.2020.594813

INTRODUCTION

Dengue is an arthropod-borne viral disease caused by dengue virus (DENV), a positive sense single-stranded RNA virus belonging to the *Flaviviridae* family and is transmitted by *Aedes* mosquitoes (1). DENV strains are classified into four antigenically distinct serotypes, DENV-1 to -4 (2). Dengue is a major threat to global health, estimated to infect around 390 million people annually affecting more than 100 countries. Around 25% of infections result in clinical disease (3). Dengue disease ranges from mild dengue fever (DF), which is self-limiting, to more severe forms of disease such as dengue hemorrhagic fever (DHF) and dengue shock syndrome (DSS) (4). Previous studies have shown that the more severe forms of dengue occur mainly after secondary infection with a different serotype,

leading to skewed and enhanced memory immune responses (5). In humans, cells belonging to the myeloid lineage such as immature and mature dendritic cells, monocytes and macrophages have been shown to be susceptible and permissive to direct DENV infection *in vitro* (6–10). Moreover, these cells can also be infected by a process termed as antibody dependent enhancement (ADE), whereby antibodies produced during previous DENV infection mediate the uptake of DENV *via* Fc receptors (11, 12).

Upon entering the cell, DENV RNA is translated into a single polyprotein which is then cleaved into individual proteins by NS2B3 protease, yielding three structural and seven non-structural (NS) proteins. NS3, one of the non-structural proteins, has helicase and triphosphatase activity which is important for viral replication and is present at the replication sites near the endoplasmic reticulum (13–15). Hence, NS3 protein is only detected in cells upon active infection by DENV and translation of viral proteins, and the detection of DENV NS3 intracellularly in infected cells is indicative of viral replication (8).

Infection with dengue virus has major impacts not only on the myeloid compartment in the blood but also on lymphoid cells (16). For example, it has been shown that circulating $CD19^+$ cells are increased in dengue patients (17, 18) and that their subset distribution is significantly altered during infection (19). For example, a massive increase in the frequencies of plasmablasts and plasma cells, reaching up to 50% of circulating B cells during the acute phase of infection has been reported (19, 20). Moreover, enhanced B cell activation and plasma cell development have been observed in hospitalized dengue patients compared to asymptomatic infected patients (21). In addition, we and others have also showed altered antibody-independent B cell responses in dengue patients, as measured by cytokine production and upregulation of activation markers after *in vitro* stimulation (19, 22).

However, it is not known whether these changes in subset distribution and altered functions observed during the acute phase of dengue infection are due to direct infection of B cells by DENV or due to bystander mechanisms as a consequence of viral infection. Indeed, B cells might be susceptible to DENV infection (23–28). Moreover, viral RNA and protein have been demonstrated in secondary lymphoid organs and within the germinal center suggesting that infected B cells can aid in the dissemination of the virus (29–32). B cells also express Fc receptors such as FcγRIIB and LILRB1 which are implicated in ADE and thus could be targets of enhanced viral infection.

Hence, in this study, we sought to investigate whether B cells were susceptible and permissive to DENV infection both *ex vivo* and *in vitro* and to determine if direct infection altered B cell responses and contributed to viral spread. We observed that B cells from dengue patients were found to support viral replication of laboratory adapted and patient-derived DENV strains both *ex vivo* and *in vitro*. Next, we identified CD300a, a phosphatidylserine receptor, as a potential attachment factor or receptor for entry of DENV into B cells. Infection with DENV induced proliferation of B cells in dengue patients *in vivo* as well as plasmablast and plasma cell formation *in vitro*. Overall, our results show that B cells are susceptible to direct infection by DENV of B cells through CD300a, and the responses of B cells to the infection could play a role in pathogenesis of dengue.

MATERIALS AND METHODS

Ethics Statement

Ethical approval for the study was obtained from the National Ethics Committee of Health Research of Cambodia. Written informed consent was obtained from all participants or the guardians of participants before inclusion in the study.

Healthy Donor and Patient Recruitment

Venous blood was collected from clinically healthy adult volunteers who presented at the International Vaccination Centre, Institut Pasteur Cambodia. Blood samples were obtained from hospitalized children (≥2 years) who presented with dengue-like symptoms at the Kanta Bopha Hospital in Phnom Penh, Cambodia. The time point for collection of blood samples was within 96 h of fever onset at hospital admittance. Dengue infection was confirmed by diagnostic testing as described below and dengue-negative patients were categorized as febrile controls. Dengue-positive patients were classified according to the WHO 1997 criteria upon hospital discharge into (dengue fever, DF) dengue hemorrhagic fever (DHF) or dengue shock syndrome (DSS). A total of 60 dengue-positive patients were included in the study. In addition, age- and sex-matched healthy donors were recruited from a cluster-based investigation in Kampong Cham province (n = 16) and included for the functional analysis (**Tables 1** and **2**).

Laboratory Diagnosis

Plasma specimens from patient samples were tested for the presence of DENV using nested RT-qPCR at the Institut Pasteur in Cambodia, the National Reference Center for arboviral diseases in Cambodia (33). Detection of DENV NS1 and anti-DENV IgM/IgG in patient plasma was done using rapid diagnostic tests (SD Bioline Dengue Duo kits, Standard Diagnostics, Abbott, USA). Additionally, anti-DENV IgM was measured with an in-house IgM-capture ELISA (MAC-ELISA), as previously described (34).

Virus Production

Infections with DENV were carried out using two laboratory/cell culture-adapted reference strains: DENV-1 Hawaii (GenBank: AF425619) and DENV-2 New Guinea C (GenBank: AF038403) and two DENV strains, DENV-1 isolate 91212506 and DENV-2

TABLE 1 | Demographic data of included healthy donors, DENV-negative febrile controls and dengue patients.

	Healthy donors	Febrile controls	dengue patients
Number of samples	16	16	60
M/F ratio	1.66	0.78	1.14
Age (mean ± SD)	9.06 ± 3.78	8.04 ± 4.23	8.6 ± 3.8

TABLE 2 | Demographic data and clinical parameters of included dengue patients.

	DF	DHF/DSS
Number of samples	48	12
M/F ratio	1.09	1.4
Age (mean ± SD)	8.3 ± 3.8	10.1 ± 3.9
Day of fever at inclusion (mean, range)	3.4 (1–4)	3.5 (1–4)
NS1 + RDT	34	10
DENV RT-qPCR +	47	11
Viral load (RNA copies/ml) (median, IQR)	3,480 (7.6–16,300,000)	21.30 (4.4–19,600)
DENV-1	26	3
DENV-2	19	6
DENV-3	0	0
DENV-4	2	1
Secondary infection (%)	77.1%	83.3%

Patients are characterized according to the WHO 1997 criteria. DENV serotype and viral load were determined by RT-qPCR using a standard curve. Viral load is expressed as RNA copies/ml. NS1 positivity was determined by rapid test. Primary or secondary infection was determined based on HIA results on acute and convalescent samples; IQR, interquartile range; NS1, non-structural protein 1; RDT, rapid diagnostic test; DF, dengue fever; DHF, dengue hemorrhagic fever; DSS, dengue shock syndrome.

isolate B0623518, both obtained from Cambodian patients by isolation and passaging two to three times in C6/36 cells. Briefly, *Aedes albopictus* C6/36 cells were infected with virus at an MOI of 0.1 and cultured at 28°C for 5–7 days in Leibovitz 15 medium (Sigma-Aldrich, MO, USA) supplemented with 2% FBS (Gibco, MT, USA), 1% L glutamine (Gibco), 10% tryptose-phosphate (Gibco) and 100 U/ml penicillin–streptomycin (Gibco). DENV was harvested from supernatants of infected C6/36 cells and concentrated using 40% polyethylene glycol (PEG)8000 (Sigma-Aldrich) as previously described (35). The concentrated virus was resuspended in RPMI supplemented with 10% FBS and stored at −80°C. Virus inactivation was done by incubation of virus aliquots under UVS-28 UV Lamp (Analytik Jena, Germany) for 30 min.

Focus-Forming Assay

Viral titer of produced viral stocks and the permissivity of B cells to DENV infection were determined by focus-forming assay to detect infectious DENV particles in supernatants from infected cells. Briefly, Vero cells (ATCC CCL-81) seeded in 96-well plates were incubated with serially-diluted supernatants from DENV infected B cells and monocytes for 1 h at 37°C and overlaid with Dulbecco's modified Eagle medium (DMEM; Sigma-Aldrich) supplemented with 3% FBS and 1.8% w/v carboxymethylcellulose (CMC) (Sigma-Aldrich). After 2–3 days, cells were fixed, permeabilized, and stained with DENV serotype-specific polyclonal mouse hyperimmune ascite fluids (Institut Pasteur in Cambodia) as described in Auerswald et al. (36). The number of foci was counted for each dilution, and viral titers were expressed as focus forming units (ffu)/ml.

Isolation and Infection of B Cells and Monocytes *In Vitro*

PBMCs were isolated from healthy donors using Ficoll-Histopaque density gradient centrifugation. Purified $CD19^+$ B cells were isolated from PBMCs by two rounds of separation using positive selection CD19 Microbeads (Miltenyi-Biotec, Germany) as per the manufacturer's protocol. The purity of B cells obtained was 90–95% as determined by flow cytometry. $CD14^+$ monocytes were isolated similarly using CD14 Microbeads (Miltenyi-Biotec, Germany).

For infection experiments, 8×10^4 B cells or monocytes were plated per well in a 96-well plate and infected with DENV-1 or -2 at an MOI of 20 for 90 min at 37°C, 5% CO_2. The virus inoculum was removed after centrifugation at 1,500pm for 10 min, and cells were washed twice with plain RPMI. The cells were then resuspended in RPMI supplemented with 10% FBS and incubated at 37°C and 5% CO_2 for 24 h.

Flow Cytometry

To detect DENV infection in B cells and monocytes from dengue patients and healthy donors infected *in vitro*, cells were stained first with Zombie Aqua Fixable Viability Kit (BioLegend, CA, USA) for live/dead cell gating followed by surface staining with CD19-APC/Cy7 (clone HIB19), CD20 PerCP-Cy5.5 (clone 2H7) or CD14-APC (clone 63D3) (all from BioLegend) for 30 min at 4°C followed by fixation and permeabilization with True-Nuclear Transcription Factor Buffer Kit (BioLegend, USA) as per manufacturer's protocol. Intracellular staining for detection of DENV infection was done using a rabbit polyclonal anti-DENV NS3 antibody or (GTX124252; GeneTex, CA, USA) or rabbit polyclonal isotype control followed by a goat anti-rabbit secondary antibody conjugated with AF488 (Molecular probes, OR, USA) or anti-DENV E protein (clone 4G2) labelled with AF488 (Molecular probes, OR, USA). Samples were run on BD FACS Canto II (BD Biosciences, NJ, USA) and analyzed by FlowJ0 v10 (BD Biosciences, USA). For the detection of the cytokine BAFF (B-cell activating factor) in the plasma of healthy donors and dengue patients, a LEGENDplex Human B cell Activator Panel immunoassay (BioLegend, USA) was used as per the manufacturer's instructions. Samples were acquired using BD FACS Canto II and analyzed using LEGENDplex v7.0 (Vigene Tech, MA, USA) software.

Real-Time PCR on Infected Cells and Cell-Free Supernatants

RNA was extracted from DENV-infected B cells and monocytes from healthy donors and dengue patients using RNeasy Micro Kit (QIAGEN, Germany) as per manufacturer's protocol. From the supernatants of infected B cells and monocytes, RNA isolation was done using QIAamp Viral RNA Mini kit (QIAGEN, Germany). cDNA was synthetized from extracted RNA with SuperScript II Reverse Transcriptase kit (ThermoFisher, MA, USA) and N6 random primers (Promega, WI, USA) respectively. Real-time PCR was done using primers and probes specific for DENV-1, DENV-2 and DENV-4 (**Table 3**). HPRT (Hypoxanthine-guanine phosphoribosyltransferase) was used as housekeeping gene and $2^{-\Delta\Delta Ct}$ values were calculated. The running conditions for DENV real-time RT-qPCR were as follows: 50°C for 2 min, 95°C for 10 min, 40 cycles of 95°C for 15 s and 60°C for 1 min.

TABLE 3 | List of primers and probes used for RT-qPCR.

Serotype	Primer/probe sequence (5′–3′)
DENV-1 fw	ATCCATGCCCAYCACCAAT
DENV-1 rev	TGTGGGTTTTGTCCTCCATC
DENV-1 Probe	FAM-TCAGTGTGGAATAGGGTTTGGATAGAGGAA-BHQ1
DENV-2 fw	TCCATACACGCCAAACATGAA
DENV-2 rev	GGGATTTCCTCCCATGATTCC
DENV-2 Probe	FAM-AGGGTGTGGATTCGAGAAAACCCATGG-BHQ1
DENV-4 fw	GYGTGGTGAAGCCYCTRGAT
DENV-4 rev	AGTGARCGGCCATCCTTCAT
DENV-4 Probe	Cyan500-ACTTCCCTCCTCTTYTTGAACGACATGGGA-BHQ1
HPRT fw	TGACACTGGCAAAACAATGCA
HPRT rev	GGTCCTTTTCACCAGCAAGCT
HPRT Probe	FAM-CTTGACCATCTTTGGATTATACTGCCTGACCA-BHQ1

Identification of Receptor on B Cells for Dengue Virus

$CD19^+$ B cells were incubated with different concentrations (1–10 ug/ml) of an IgG2a monoclonal antibody directed against CD300a (clone P192; LSBio, WA, USA) for 30 min, washed, and infected with DENV-2 at an MOI of 20 for 24 h. An isotype-matched monoclonal antibody was used as a negative control. Percentages of DENV-infected B cells were determined by flow cytometry using anti-DENV NS3 antibody as described above, and fold change in percentage of infected cells with respect to the control was calculated.

Antibody-Dependent Enhancement Assay

Human monoclonal antibody G10 (kind gift from Katja Fink, A*STAR, Singapore) is specific for the fusion loop of DENV E protein and has been shown to mediate the antibody-dependent enhancement of DENV infection *in vitro* (37). Human myelomonocyte cell line U937 (ATCC CRL-1593.2) was cultured in RPMI (Gibco) supplemented with 10% FBS (Gibco), 100 U/ml penicillin–streptomycin (Gibco), and 1% L glutamine (Gibco) (38). Serum was obtained from a pediatric patient with primary DENV-2 infection at day 8 after onset of symptoms (early convalescent phase). The G10 antibody and DENV-2 patient serum were serially diluted five-fold (1:100 to 1:1,562,500) in RPMI and incubated with DENV-1 virus corresponding to MOI of 1 for 1 h at 37°C, 5% CO_2. Immune complexes were then transferred to purified B cells from healthy donors and incubated for 90 min at 37°C, 5% CO_2. Direct infection with DENV in the absence of G10 antibody was used as control. After infection, cells were washed and incubated for 72 h at 37°C, 5% CO_2. Cells were surface stained with Zombie Aqua (AmCyan) viability dye (BioLegend) for live/dead cell gating and then fixed, permeabilized, and stained for the presence of DENV using anti-DENV E protein antibody (clone 4G2, ATCC HB-112) labeled with AF488 (Molecular probes). Fold change of infection was calculated for each serum dilution with respect to direct DENV infection to represent enhancement of DENV infection.

In Vitro Plasma Cell Differentiation

Purified $CD19^+$ B cells from healthy donors' PBMCs were infected with DENV-1 at MOI of 5 for 90 min, washed and cultured in the presence of CD40L (0.25 μg/ml; ITS Vietnam), IL-2 (1 ng/ml; Peprotech, NJ, USA), and IL-21 (50 ng/ml; Peprotech) for 6 days. The cells were harvested and stained with Zombie Aqua (AmCyan) viability dye (BioLegend) for live/dead cell gating followed by antibodies CD19 PE/Cy7 (clone HIB19), CD20 PerCp/Cy5.5 (clone 2H7), CD27 APC/Cy7 (clone O323), CD38 APC (clone HB7) and CD138 BV421 (clone MI15), and the percentages of $CD27^+CD38^+$ plasmablasts and $CD27^+CD138^+$ plasma cells were determined in uninfected and infected B cells with or without stimulation.

B Cell Proliferation Assay

B cells isolated from healthy donors were labeled with carboxyfluorescein diacetate succinimidyl ester (CFSE) (Biolegend) and either infected with DENV-2 at an MOI of 5 or remained uninfected. After 2 h of inoculation, cells were washed to remove the inoculum and stimulated with CpG oligodeoxynucleotides (1 μg/ml; Invivogen, San Diego, CA, USA) and $F(ab')_2$ anti-IgM antibody (4 μg/ml; Jackson ImmunoResearch, PA, USA) or remained unstimulated. Cells were cultured in RPMI supplemented with 10% FBS for 6 days. The cells were then harvested and stained with Zombie Aqua (AmCyan) viability dye (BioLegend) followed by CD19 PE/Cy7 (clone HIB19) and CD20 PerCp/Cy5.5 (clone 2H7) to identify live B cells and analyzed for the expression of CFSE in the FITC channel. Proliferation was measured as the percentage of B cells with decreased intensity of CFSE compared to unstimulated B cells.

Statistical Analysis

Statistical analyses were done using GraphPad Prism 7.00 software (GraphPad Software, Inc., La Jolla, CA, USA). Since the data did not pass the criteria for normality using D'Agostino & Pearson normality test, the non-parametric Mann–Whitney *U*-test was used to compare data between two groups or by non-parametric paired Wilcoxon matched pairs signed rank test for paired data. Statistical analysis of data with more than two groups was done using the Kruskal–Wallis test followed by Dunn's post-test for multiple comparisons. For comparing paired samples between three conditions, Friedman's test was used. Correlations were calculated by Spearman analysis. For all analyses, $p < 0.05$ was considered significant.

RESULTS

B Cells Are Susceptible to Dengue Virus Infection *In Vivo*

Previously published studies on susceptibility of immune cells to DENV infection have primarily used the 4G2 antibody, a pan-flaviviral antibody binding to the fusion loop of the Envelop (E) protein. However, the presence of E protein cannot distinguish between binding/internalization and productive infection. Therefore, we aimed to detect viral non-structural protein 3 (NS3). NS3 protein is only detected in cells upon active infection by DENV, and translation of viral proteins and the intracellular

detection of DENV NS3 is indicative of viral replication (16, 39). To validate the anti-NS3 antibody, we infected C6/36 cells, which are highly susceptible to DENV infection, with DENV-1 at MOI of 5 for 24 h and stained with anti-DENV NS3 antibody and its corresponding isotype control. Representative histogram of NS3 staining in C6/36 cells is shown in **Supplementary Figure 1A**. To further confirm the specificity of the anti-DENV NS3 antibody, C6/36 mosquito cell line and primary monocytes, well known targets of DENV infection, were infected with DENV and UV-inactivated DENV particles (UV-DENV). An increase in percentage of $NS3^+$ cells was observed in DENV infected cells compared to uninfected and UV-DENV infected cells (**Supplementary Figure 1B**).

In order to investigate whether B cells are susceptible to DENV infection *in vivo*, we obtained PBMCs from a cohort of 60 acute-infected Cambodian children with RT-qPCR confirmed DENV infection and stained with anti-DENV NS3 and E antibodies (**Figures 1A–D**, **Supplementary Figure 2**). Only a subset of patients was stained with anti-E, when sufficient PBMC could be purified due to the low amount of blood obtained from the pediatric cases.

The percentage of E^+ cells was significantly higher in $CD14^+$ monocytes compared to $CD19^+$ B cells (**Figures 1C, D**). We confirmed productive infection in both $CD14^+$ monocytes and $CD19^+$ B cells as we could detect DENV NS3 protein. In parallel, the percentage of $CD19^+NS3^+$ B cells in dengue patients was significantly lower compared to $CD14^+NS3^+$ monocytes (20.9 *vs* 56.5%; $p < 0.05$) (**Figures 1A, B**). When the patients were stratified according to disease severity, no difference was observed in the percentages of $CD19^+NS3^+$ B cells between patients with DF (n = 46) and those with DHF/DSS (n = 12) (**Figure 1E**). Since different subsets of B cells have different

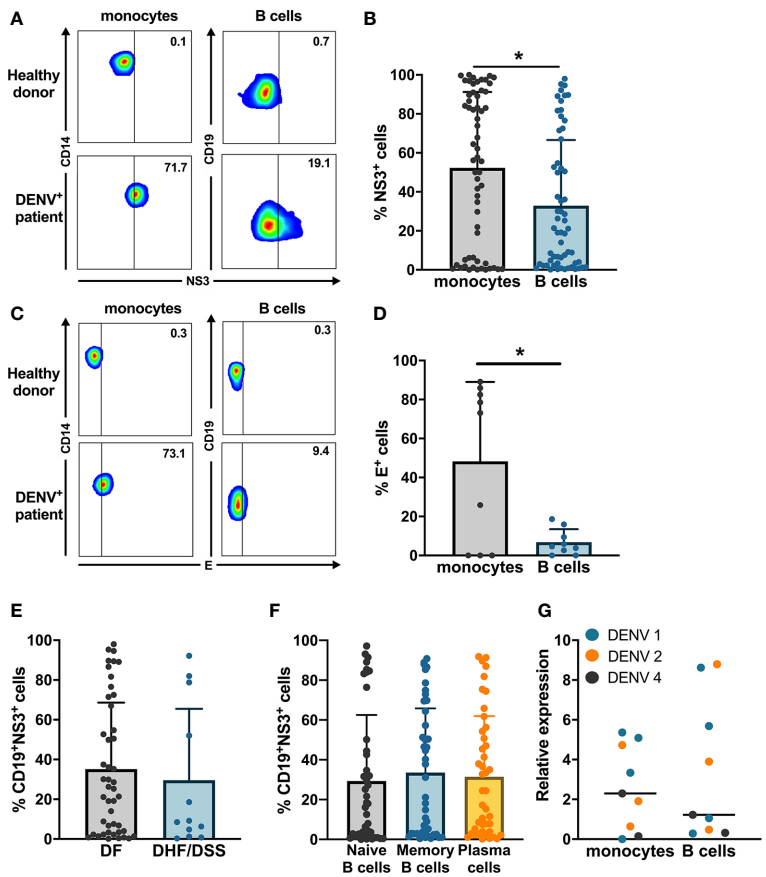

FIGURE 1 | *Ex vivo* detection of DENV in B cells from dengue patients. PBMCs from patients in the acute phase of DENV infection (n = 60) were stained on the surface with antibodies for immune cell markers and intracellularly with anti-DENV NS3 antibody or pan flaviviral fusion loop specific 4G2 antibody. **(A, B)** Representative plots for NS3 staining in $CD14^+$ monocytes and $CD19^+$ B cells. The percentage of $NS3^+$ cells were determined for $CD14^+$ monocytes and $CD19^+$ B cells. **(C, D)** Representative plot for anti-E staining in $CD14^+$ monocytes and $CD19^+$ B cells. Percentages of E^+ monocytes and B cells were determined in a subset of dengue patients (n = 9). **(E)** DENV patients were classified as DF (n = 46) and DHF/DSS (n = 12) as per WHO 1997 classification, and the percentage of $CD19^+NS3^+$ cells was determined. p-values were calculated using Mann–Whitney U test for comparing two groups. **(F)** B cells from dengue patients were gated for naive B cells ($CD19^+CD27^-$), memory B cells ($CD19^+CD27^+CD138^-$) and plasma cells ($CD19^+CD27^+CD138^+$), and the percentage of $NS3^+$ cells was determined. **(G)** $CD14^+$ monocytes and $CD19^+$ B cells were isolated from PBMCs from dengue patients by magnetic sorting. RT-qPCR was done for DENV by serotype-specific PCR and HPRT. Relative expression was calculated using $2^{-\Delta\Delta Ct}$ method. For all panels, P-values were calculated using Mann–Whitney U test for comparing two groups. Bars and lines represent mean and standard deviation (SD). (*$P < 0.05$).

functions, we wanted to determine which subset of B cells is particularly susceptible to DENV infection. Therefore, using flow cytometry we classified $CD19^+$ B cells as naïve B cells ($CD19^+CD27^-$), memory B cells ($CD19^+CD27^+CD138^-$) and plasma cells ($CD19^+$ $CD27^+CD138^+$) (**Supplementary Figure 3**). The percentage of DENV $NS3^+$ cells was similar between naïve, memory B cells, and plasma cells suggesting that all B cell subsets seem to be equally susceptible to DENV infection (**Figure 1F**). As we observed wide variability in the percentages of infected cells, we aimed to see if this correlated to biological parameters of disease severity. However, no correlations could be observed between percentages of $NS3^+$ infected B cell subsets and hematocrit or platelet counts (**Supplementary Figure 2**). To confirm the presence of DENV RNA, we performed RT-qPCR with DENV-serotype specific primers on purified $CD19^+$ B cells and $CD14^+$ monocyte fractions isolated from patients (n = 9) Relative expression of DENV ($2^{-\Delta\Delta Ct}$) was calculated using HPRT as a reference housekeeping gene. Hence, we measure presence of viral RNA which can originate both from surface bound and internalized viral particles. In parallel to the detection of DENV-NS3 protein, the relative expression of DENV was higher in $CD14^+$ monocytes compared to $CD19^+$ B cells even though the difference was not significant possibly due to the small sample size (**Figure 1G**).

B Cells Are Susceptible and Permissive to Dengue Virus Infection *In Vitro*

Next, we wanted to determine if B cells isolated from healthy donors were susceptible to DENV infection *in vitro*. $CD19^+$ B cells and $CD14^+$ monocytes isolated from healthy donors were infected with either of a laboratory reference strains DENV1 Hawaii, DENV2 New Guinea C or low passaged DENV-1 and -2 isolated from acute dengue patients. The percentages of DENV $NS3^+$ cells were similar between monocytes and B cells infected with the low-passaged DENV-1 or DENV-2. Of interest, no difference was observed between percentages of $NS3^+$ cells in B cells and monocytes infected with laboratory reference strains and low-passaged DENV-1 and -2 strains (**Figure 2A**).

As we observed that B cells are susceptible to DENV infection, we investigated whether B cells are permissive to DENV, *i.e.*, the

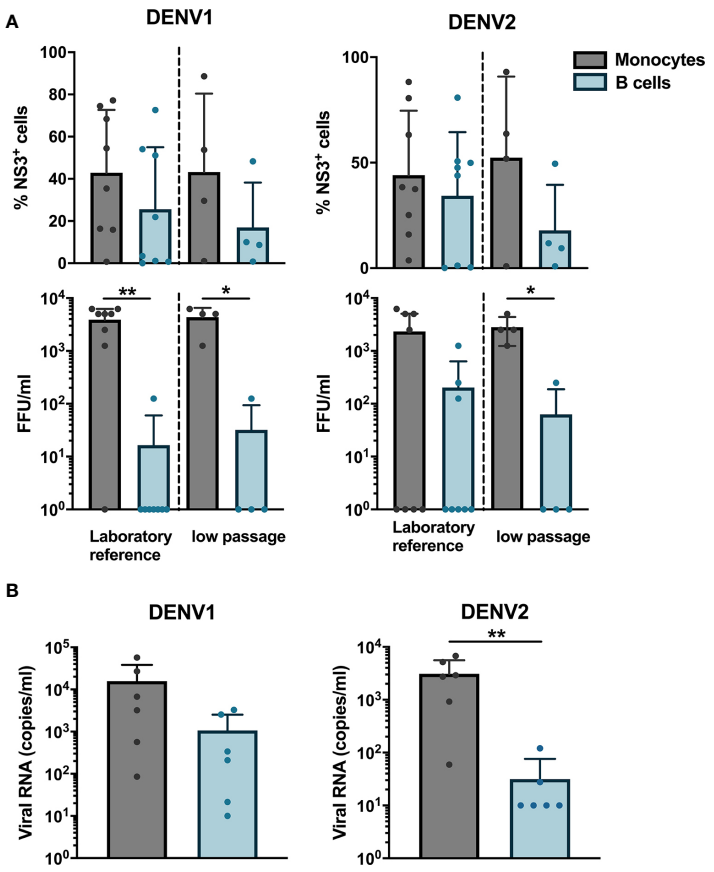

FIGURE 2 | Susceptibility and permissiveness of B cells to DENV infection *in vitro*. **(A)** $CD14^+$ monocytes and $CD19^+$ B cells were isolated from PBMCs from healthy donors by magnetic sorting and infected with reference or low-passaged DENV-1 and DENV-2 strains at MOI of 20. At 24 h post infection, the cells were stained intracellularly with anti-DENV NS3 antibody. Infectious viral progeny in supernatants from healthy donors (n = 6) infected with DENV-1 and -2 reference or low-passaged stains at MOI 20 for 24 h was determined by focus-forming assay. **(B)** Total DENV viral RNA copies in supernatants from healthy donors (n = 6) infected with DENV-1 and -2 reference stains at MOI 20 for 24 h was determined by RT-qPCR. For all panels, bars and lines represent mean and standard deviation (SD). (*P < 0.05; **P < 0.01).

ability of the virus to complete its replication cycle in B cells and release complete, mature virions which can infect new cells. To answer this question, a focus forming assay was performed on Vero cells using supernatants from B cells and monocytes infected *in vitro* with DENV. Monocytes produced higher titers of both DENV-1 and DENV-2, except for one donor where no foci were observed. A low virus titer could be observed in cells incubated with supernatants from DENV-infected B cells from one donor infected with DENV-1 reference strain and from three donors infected with DENV-2 reference strain (**Figure 2A**). A similar trend was observed for monocytes and B cells infected with low passaged DENV-1 and -2 (**Figure 2A**). Furthermore, to estimate the total amount of DENV particles, we measured RNA copies in the supernatants from monocytes and B cells from six healthy donors infected with laboratory reference DENV-1 and -2. Higher quantities of viral RNA copies were detected in supernatants from DENV-infected monocytes compared to B cells, especially for DENV-2 where the differences were significant ($p < 0.01$) (**Figure 2B**). Interestingly, detectable quantities of RNA copies were observed in B cells from five out of six donors infected with DENV-1 compared to 2 for DENV-2. Taken together, these results indicate that DENV can productively infect B cells; however, this seems to be donor-dependent and with low efficiency.

Identification of Entry Mechanism for Dengue Virus in B Cells

As we observed the presence of DENV antigen in B cells upon infection *in vitro*, we aimed to identify a potential attachment factor or receptor for entry of DENV into B cells. Based on published studies, we identified CD300a, belonging to the CD300 family of phospholipid receptors, as a potential receptor involved in binding or entry of DENV (40). CD300a is moderately expressed on all B cell subsets and has been shown to be downregulated during HIV infection (41, 42). Higher expression of CD300a is observed in memory B cells and plasmablasts compared to naïve B cells (42). To test whether CD300a could play a role in DENV infection in B cells, $CD19^+$ B cells were infected with DENV-1 in the presence of blocking antibody for CD300a or isotype control. Blocking of CD300a leads to a decrease in percentage of DENV-infected $CD19^+NS3^+$ cells in a concentration-dependent manner but had no effect on viability of $CD19^+$ B cells. A significant decrease in infection of more than 50% was observed between direct infection and 10 ug concentration of CD300a blocking antibody ($p < 0.05$) (**Figure 3A**). However, complete abrogation of DENV infection in B cells was not observed even at higher concentrations of CD300a blocking antibody suggesting possible involvement of other receptors or attachment factors in entry of DENV into B cells.

Since B cells express Fcγ receptor FcγRIIB, we wanted to test whether B cells are susceptible to antibody-mediated DENV infection. Therefore, DENV-1 at MOI of 1 was incubated with serial dilutions of a monoclonal antibody (clone G10) with antibody-dependent enhancement potential (37) or patient serum obtained 8 days after a primary DENV-2 infection and tested on B cells obtained from healthy donors (n = 3) and

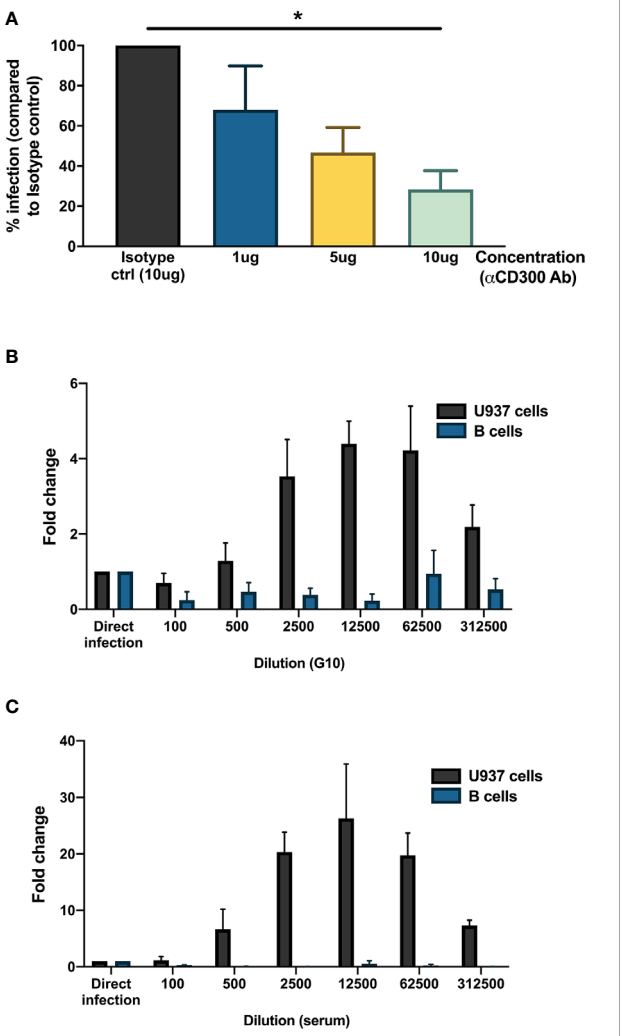

FIGURE 3 | Mechanisms for DENV entry into B cells. **(A)** $CD19^+$ B cells were isolated from PBMCs from healthy donors (n = 4) by magnetic sorting, incubated with different concentrations of blocking antibody against CD300a or isotype control antibody and infected with reference DENV-1 or DENV-2 strains at MOI 20. At 24 h post infection, cells were stained with anti-DENV NS3 antibody. Percentage of infection is represented with respect to isotype control. **(B, C)** Monoclonal antibody G10 or serum from patient with DENV-2 infection was serially diluted five-fold (1:100 to 1:1,562,500) in RPMI and incubated with DENV-1 virions corresponding to MOI of 1 for 1 h at 37°C, 5% CO_2. These immune complexes were then transferred to U937 cells and B cells and incubated for 90 min at 37°C, 5% CO_2. Direct infection with DENV in the absence of G10 antibody or patient serum was used as control. At 72 h post infection, cells were fixed, permeabilized, and stained with anti-E antibody (clone 4G2). Fold change is represented for each dilution with respect to direct infection. Bars represent mean and SEM, where the experiment was replicated with three different healthy donors. (*$P < 0.05$).

FcγRIIA bearing cells U937 as positive control. Here, whereas both the monoclonal antibody G10 and patient serum induced ADE in U937 cells, no enhancement of infection was observed with the primary B cells isolated from healthy donors. (**Figures 3B, C**). This indicates that antibody-dependent enhancement of DENV infection does not occur in B cells.

Infected B Cells Show a Higher Proliferation History

Regardless of the observed low permissiveness of B cells to DENV, direct infection could alter B cell responses, such as proliferation. Therefore, we looked at the expression of intracellular proliferation marker Ki-67 in total naïve CD19$^+$ B cells from dengue patients, healthy, and febrile controls. Increased expression of Ki-67 in naïve B cells was observed in dengue patients compared to healthy controls and dengue-negative febrile controls ($p < 0.05$) suggesting that B cells are proliferating more in dengue patients (**Figure 4A**). Hence, we analyzed the serum concentrations of B-cell activating factor (BAFF), a cytokine produced by cells of the myeloid lineage and is known to be a potent activator of B cells in plasma of DENV patients. Indeed, concentrations of BAFF were significantly higher in dengue-infected patients compared to healthy donors, which could contribute to the increased proliferation observed (**Figure 4B**). However, BAFF serum concentrations were even more increased in febrile controls.

Next, we questioned if direct infection of B cells by DENV alters the activation and proliferation of DENV-infected B cells. Therefore, B cells from dengue patients were stained with anti-Ki-67 and anti-CD69/anti-CD86, two activation markers, and with anti-NS3 to identify infected cells. Cells were classified as naïve (CD19$^+$CD27$^-$) and memory (CD19$^+$CD27$^+$) B cells and then separated as uninfected (NS3$^-$) and infected (NS3$^+$) cells (**Supplementary Figure 4**). The presence of DENV seemed to have no effect on the activation of naïve and memory B cells as the percentages of CD69$^+$CD86$^+$ cells were similar between NS3$^-$ and NS3$^+$ cells (**Figure 4C**). However, higher proliferation was seen in infected memory B cells compared to uninfected cells ($p < 0.05$) indicating that DENV-infected B cells show enhanced proliferation (**Figure 4D**). Here, no difference was observed for infected *versus* non-infected naïve B cells. These data suggest that the observed increase in naïve B cell proliferation compared to controls as observed in **Figure 4A** could be due to an indirect effect, rather than direct B cell infection, such as increased BAFF concentrations.

Therefore, we investigated whether infection of B cells by DENV *in vitro* induced their proliferation. For this, B cells from healthy donors (n = 4) were labeled with CFSE and stimulated with CpG and F(ab′)$_2$ anti-IgM antibody for 6 days. Proliferation was defined as percentage of B cells with lower CFSE signal (CFSE^{low}) upon stimulation compared to unstimulated cells (**Figure 4E**). We evaluated proliferation in B cells that were either infected with DENV-2 or were uninfected at the start of the culture. No difference was observed in the percentage of CFSE^{low} B cells between uninfected and infected B cells of the same individuals (median: 56.4 *vs* 43.8%) (**Figure 4F**). Altogether, these data suggest that the observed increase in

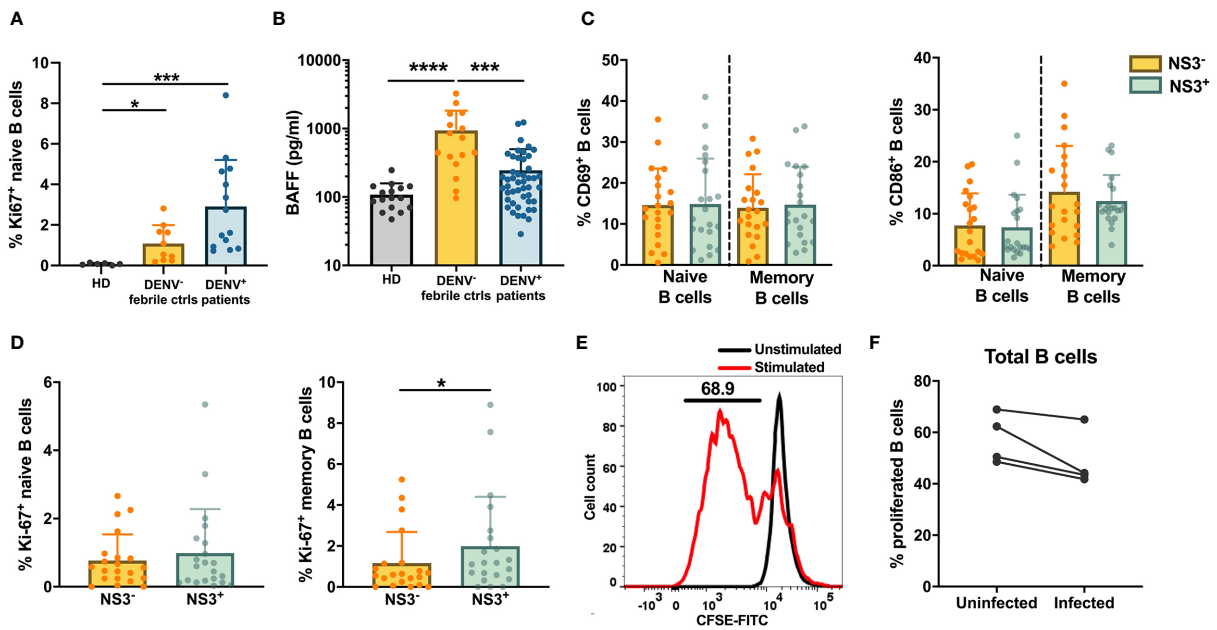

FIGURE 4 | Activation and proliferation of DENV-infected B cells *in vivo*. **(A)** Frequencies of Ki-67$^+$ naive (CD19$^+$CD27$^-$) B cells in healthy donors, DENV-negative febrile controls and dengue patients. **(B)** Concentrations of B-cell activating factor (BAFF) were analyzed in plasma of age-matched healthy donors, febrile controls and and patients with acute dengue infection. **(C, D)** CD19$^+$ B cells from dengue patients were stained with B cell subset markers and anti-DENV NS3 antibody. Frequencies of **(C)** activated CD69$^+$ and CD86$^+$ and **(D)** proliferating Ki-67$^+$ B cells within NS3$^-$ and NS3$^+$ populations of naive (CD19$^+$CD27$^-$) and memory B cells (CD19$^+$CD27$^+$CD138$^-$) from dengue patients. **(E)** Representative histogram to determining percentage of proliferated B cells upon stimulation with F(ab′)$_2$ anti-IgM antibody and CpG compared to unstimulated cells. **(F)** Frequencies of proliferated B cells isolated from healthy donors (n = 4) infected with or without DENV-2 reference strain *in vitro* followed by stimulation with F(ab′)$_2$ anti-IgM antibody and CpG for 6 days. For all panels, P-values were calculated using Mann–Whitney U test for comparing two groups. Bars and lines represent mean and standard deviation (SD). (*P < 0.05; ***P < 0.001; ****P < 0.0001).

proliferation in dengue patients *in vivo* can be attributed to direct DENV infection and bystander mechanisms such as increased serum BAFF concentrations.

Direct Infection of B Cells by Dengue Virus Increases the Differentiation to Plasmablasts

Previous studies have shown that the frequencies of plasmablasts are significantly increased during the early phase of DENV infection where plasmablasts can account for more than 50% of circulating $CD19^+$ B cells (19, 20). To check if DENV can induce differentiation of B cells into plasmablasts and plasma cells *in vitro*, purified $CD19^+$ B cells from healthy donors were infected with DENV-1 and cultured with or without stimulation with CD40L, IL-2 and IL-21 for 6 days, which mimics the conditions of the germinal center *in vitro*. From the $CD19^+$ purified cells, we gated for plasmablasts ($CD20^+CD27^+CD38^+CD138^-$) and plasma cells ($CD20^+/^{dim}CD27^+CD38^+CD138^+$) (**Supplementary Figure 5**), and their percentages were determined As expected, stimulation of B cells with cytokines induced differentiation into plasmablasts and plasma cells. Interestingly, higher frequencies of plasmablasts and plasma cells were observed when stimulation was done after infection compared to uninfected stimulated B cells (median: plamsablasts—16.1 *versus* 18.5% and plasma cells—2.6 *versus* 3.5%; $p < 0.05$) (**Figure 5**). These data suggest that DENV infection of B cells increases the differentiation to plasmablasts and plasma cells.

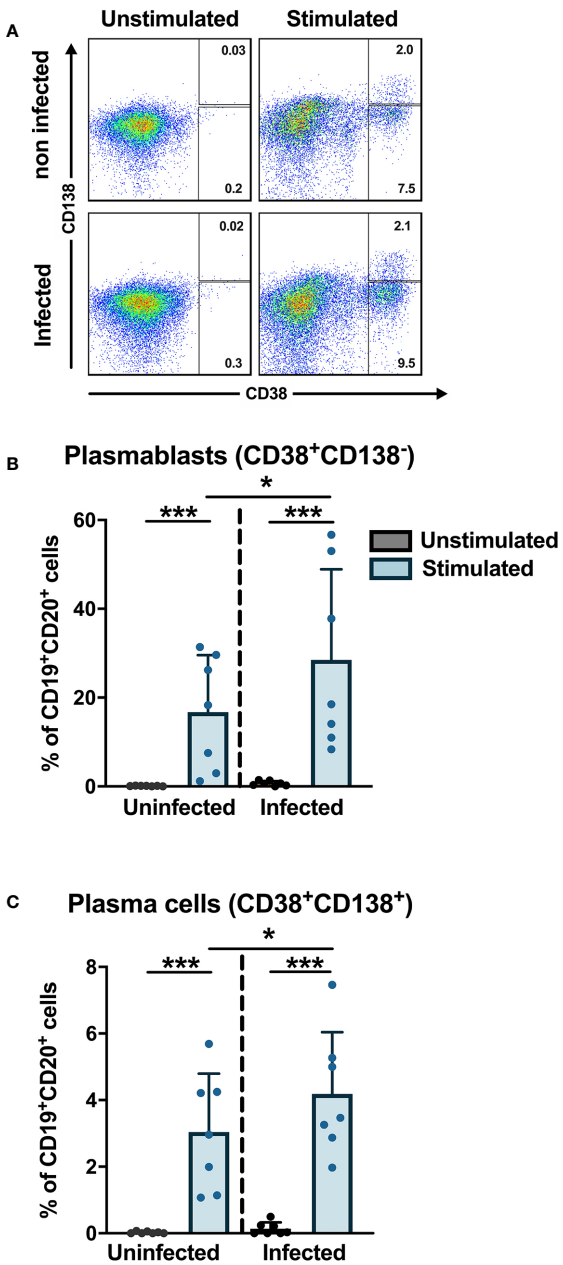

FIGURE 5 | *In vitro* plasmablast and plasma cell development after DENV infection in B cells. B cells isolated from healthy donors (n = 6) were infected with or without DENV-1 reference strain or uninfected and cultured in the presence of IL-2, IL-21, and CD40L for 6 days and stained for B cell subset markers. Percentages of $CD38^+CD138^-$ plasmablasts and $CD38^+CD138^+$ plasma cells were determined within the $CD19^+CD27^+$ B cell population. Bars and lines represent mean and standard deviation (SD). P-values were calculated with Wilcoxon match pairs signed ranked test and Mann–Whitney U test to compare conditions in different groups. (*$P < 0.05$; ***$P < 0.001$).

DISCUSSION

The aim of this study was to investigate the susceptibility and permissivity of B cells to infection with DENV and their response to direct infection with the virus. DENV has been shown to infect a variety of cell types such as monocytes, dendritic cells, and T lymphocytes (6, 8, 9, 43). Studies have shown that B cells can be infected by DENV and may contribute to the spread of the virus to the germinal center (23–32). Here, we showed that B cells are susceptible and permissive to DENV infection both *ex vivo*, in patients with acute DENV infection, and *in vitro*.

The presence of NS3 protein in infected cells indicates uncoating and translation of viral RNA which is a pre-requisite for initiating DENV replication (16, 39) Therefore, the detection of NS3 protein is indicative of viral replication. Indeed, we detected $NS3^+$ B cells in the blood of dengue patients, suggesting that B cells are susceptible to infection by DENV. Percentages of DENV $NS3^+$ and E^+ B cells were lower compared to monocytes. Moreover, B cells appeared less permissive to infection as infection of $CD19^+$ B cells did not always lead to the production of infectious virus. Infection could result in immature or functionally impaired virions that may not be capable of infecting other susceptible cells as seen by the low titer of infectious DENV in supernatants from B cells.

We identified CD300a as potential attachment/entry receptor for DENV in B cells. CD300a belongs to the CD300 family of phospholipid receptors and recognizes phosphatidylserine and phosphatidylethanolamine, which are exposed on the outer side of the plasma membrane of dead and activated cells. In addition, these molecules can be present in viral envelopes derived from the lipid bilayer of the host cell plasma membrane, as is the case

for DENV. Indeed, Carnec et al. have described that human and mouse CD300a bind the four DENV serotypes and enhance the infection through clathrin-mediated endocytosis (40). This was also demonstrated for Yellow fever, West Nile, and Chikungunya viruses (40). Furthermore, blocking of CD300a receptor in monocyte-derived macrophages naturally expressing CD300a leads to a decrease in DENV infection (40). In our study, we identified CD300a as an attachment/entry factor for DENV in B cells. We observed that when CD300a was blocked on $CD19^+$ B cells, a significant decrease in infection was observed in a concentration-dependent manner suggesting CD300a can be an attachment/entry factor or receptor for DENV in B cells. However, infection was not completely abrogated, probably due to the high MOI used in our experiments. It could also indicate a potential role for other attachment factors or receptors like TIM-1, which needs to be investigated further (44, 45). B cells express Fcγreceptor FcγRIIB and Fc-like receptor LILRB1, both of which are implicated in the mechanism of antibody-dependent enhancement and have shown to be upregulated after DENV infection (19, 46, 47). Hence, theoretically, B cells could be susceptible to antibody-mediated DENV infection. We tested this hypothesis and could not observe an enhancement of infection using a monoclonal anti-E antibody and patient serum, whereas ADE was readily observed with FcγR bearing U937 cells. Indeed, FcγRIIB receptor contains an immunoreceptor tyrosine-based inhibitory motif (ITIM) and has been shown to inhibit ADE of DENV infection (48).

We observed increased proliferation as measured by presence of proliferation marker Ki-67 in total B cells from dengue patients compared to febrile controls and in DENV-infected B cells compared to non-infected cells *ex vivo* suggesting that infection with DENV may induce the proliferation of B cells. However, after *in vitro* stimulation of purified B cells *via* BCR/TLR9 and DENV infection, we did not see an increase in proliferation indicating that perhaps contact with other (infected) PBMCs may be needed for proliferation. It remains to be investigated which stimuli account for the observed increased proliferation *in vivo*. One of the cytokines stimulating B cell proliferation is BAFF (B-cell activating factor). The protein exists as a soluble monomer in the serum or as a homotrimer on the surface of myeloid cells and binds to tumor-necrosis factor receptors BAFF-R, BCMA and TACI expressed on B cells, triggering the activation and proliferation of B cells (49). Indeed, we observed increased plasma concentrations of BAFF in dengue patients compared to healthy donors. The source of BAFF in our DENV patient cohort may be $CD14^{++}CD16^+$ intermediate monocytes as shown in a study by Kwissa et al. in which frequencies of $CD14^{++}CD16^+$ intermediate monocytes positively correlated with concentrations of BAFF in blood of dengue patients (50).

Here, we investigated the capacity of DENV to induce differentiation of B cells into antibody-secreting plasmablasts and plasma cells *in vitro*. Upon culturing with IL-2, IL-21, and CD40L, we observed increased differentiation of DENV-infected B cells into $CD27^+CD38^+$ plasmablasts and $CD138^+$ plasma cells compared to uninfected cells. These findings suggest that DENV infection of B cells increases the differentiation to plasmablasts and plasma cells, independent of the BCR specificity of these cells. This could play a role in disease pathogenesis through antibody-independent functions such as production of plasma cell-derived cytokines IL-35 and IL-10 (51). Alternatively, production of cross-reactive and autoreactive antibodies by plasmablasts could play a role in disease pathogenesis. During DENV infection, several autoantibodies against host factors such as endothelial cells, platelets, and components in coagulation pathways were observed (52–55). Moreover, direct infection could stimulate B cells with BCRs with weak affinity for DENV and/or cross-reactive BCRs to differentiate to plasmablasts and produce IgG with low affinity or little specificity that could contribute to antibody-dependent enhancement (56, 57). Finally, direct infection of B cells by DENV could trigger intracellular responses leading to changes in IgG Fc glycosylation pathways. Indeed, altered abundance of total and DENV-specific IgG afucosylated forms have been observed during acute DENV infection correlating with platelet count and haematocrit (58).

In summary, we have shown that B cells are susceptible to laboratory adapted and low-passaged DENV strains. Infectious virus can be detected after B cell infection, albeit the amount is low. We identified CD300a, a phosphatidylserine receptor, as a potential attachment factor/entry receptor of DENV into B cells. Infection with DENV induced proliferation of B cells in dengue patients *in vivo* and plasmablast/plasma cell formation *in vitro*. The responses of B cells to direct DENV infection could play a role in pathogenesis of DENV.

DATA AVAILABILITY STATEMENT

The original contributions presented in the study are included in the article/**Supplementary Material**; further inquiries can be directed to the corresponding author.

ETHICS STATEMENT

The studies involving human participants were reviewed and approved by the National Ethics Committee of Health Research of Cambodia. Written informed consent to participate in this study was provided by the participants' legal guardian/next of kin.

AUTHOR CONTRIBUTIONS

TC conceived the project, designed the study, analyzed and interpreted data, and wrote the manuscript. VU conducted the experiments, performed the data analysis, and prepared the manuscript. DL and SH coordinated the recruitment of dengue patients. HV and HA conducted the experiments and performed the data analysis. IR-Z interpreted the data. PD, VD, and TC

classified the dengue patients and selected the samples. HV, HA, IR-Z, and PD revised the manuscript. All authors contributed to the article and approved the submitted version.

FUNDING

TC was funded by the Institute Pasteur International Network and is an HHMI-Wellcome Trust International Research Scholar (208710/Z/17/Z). VU was funded by the Institute Pasteur International Network Calmette and Yersin Ph.D. scholarship.

ACKNOWLEDGMENTS

We thank Dr Katja Fink, (Agency for Science, Technology and Research, Singapore, A*STAR) for the generous donation of G10 monoclonal antibody. We would like to thank all patients and legal guardians who participated in the study. We would like to thank all the doctors at Kantha Bopha Children's Hospital and International Vaccination Centre, Institute Pasteur Cambodia who were involved in recruitment and inclusion of patients and healthy donors respectively.

SUPPLEMENTARY MATERIAL

The Supplementary Material for this article can be found online at: https://www.frontiersin.org/articles/10.3389/fimmu.2020.594813/full#supplementary-material

Supplementary Figure 1 | Optimization of anti-DENV NS3 antibody. **(A)** C6/36 cells were infected with DENV-1 at MOI of 20 for 24 h and stained with rabbit polyclonal anti-DENV NS3 antibody and secondary goat antibody conjugated with AF488. A non-specific rabbit polyclonal antibody was used as negative control. **(B)** C6/36 cells and $CD14^+$ monocytes isolated from healthy donors were infected *in vitro* with DENV1 or UV-inactivated DENV1 (UV-DENV1) at MOI 10 and stained at 24 h post infection with rabbit polyclonal anti-DENV NS3 antibody and secondary goat antibody conjugated with AF488.

Supplementary Figure 2 | No correlation between biological parameters and percentages of DENV-infected B cells. Correlations between platelet counts and hematocrit levels at hospital admittance and percentages of DENV-infected B cell subsets were determined by Spearman's correlation.

Supplementary Figure 3 | Representative gating strategy used to detect DENV infection in B cells and monocytes in PBMCs from dengue patients. PBMCs were gated for lymphocytes and monocytes followed by removal of doublets. Single $CD14^+$ monocytes and $CD19^+$ B cells were gated and DENV $NS3^+$ cells were selected.

Supplementary Figure 4 | Representative gating strategy used to detect DENV infection in B cell subsets in PBMCs from dengue patients. Lymphocytes from PBMCs were further gated for $CD19^+$ B cells. Based on expression of CD19 and CD27, total B cells were further gated as naïve B cells ($CD19^+CD27^-$). $CD27^+$ B cells were gated as memory B cells ($CD19^+CD27^+CD138^-$) and antibody secreting cells ($CD19^+CD27^+CD138^+$) based on CD138 expression. Positivity for DENV infection was determined for each B cell subset based on expression of viral protein NS3.

Supplementary Figure 5 | Representative gating strategy used to assess activation markers CD69, CD86 and proliferation marker Ki-67 in B cells isolated from dengue patients. B cells from dengue patients were stained for CD20 and CD27 to determine naive B cells ($CD20^+CD27^-$) and memory B cells ($CD20^+CD27^+$). Uninfected and DENV infected cells were defined as $NS3^-$ and $NS3^+$ based on expression of DENV NS3. $NS3^-$ and $NS3^+$ cells were further gated for CD69, CD86, and Ki-67 to assess activation and proliferation of B cells.

Supplementary Figure 6 | Representative gating strategy for *in vitro* plasmablast and plasma cell development after DENV infection in B cells. Total cells were gated followed by exclusion of doublets and dead cells. $CD20^+$ B cells were gated and further sub-gated based on expression of CD27. $CD20^+CD27^+$ B cells were defined as plasmablasts ($CD20^+CD27^+CD38^+CD138^-$) and plasma cells ($CD20^+CD27^+CD38^+CD138^+$).

REFERENCES

1. Guzman M. Dengue and dengue hemorrhagic fever in the Americas: lessons and challenges. *J Clin Virol* (2003) 27(1):1–13. doi: 10.1016/S1386-6532(03)00010-6
2. Rico-Hesse R. Microevolution and virulence of dengue viruses. *Adv Virus Res* (2003) 59:315–41. doi: 10.1016/s0065-3527(03)59009-1
3. Bhatt S, Gething PW, Brady OJ, Messina JP, Farlow AW, Moyes CL, et al. The global distribution and burden of dengue. *Nature* (2010) 496: (7446):504–7. doi: 10.1038/nature12060
4. Simmons CP, Farrar JJ, Nguyen VV, Wills B. Dengue. *N Engl J Med* (2012) 366(15):1423–32. doi: 10.1056/NEJMra1110265
5. St. John AL, Rathore APS. Adaptive immune responses to primary and secondary dengue virus infections. *Nat Rev Immunol* (2019) 19(4):218–30. doi: 10.1038/s41577-019-0123-x
6. Marovich M, Grouard-Vogel G, Louder M, Eller M, Sun W, Wu SJ, et al. Human dendritic cells as targets of dengue virus infection. *J Invest Dermatol Symp Proc* (2001) 6(3):219–24. doi: 10.1046/j.0022-202x.2001.00037.x
7. Miller JL, de Wet BJ, deWet BJ, Martinez-Pomares L, Radcliffe CM, Dwek RA, et al. The mannose receptor mediates dengue virus infection of macrophages. *PLoS Pathog* (2008) 4(2):e17. doi: 10.1371/journal.ppat.0040017. Erratum in: PLoS Pathog. 2008 Mar;4(3). doi: 10.1371/annotation/98b92fca-fa6e-4bf3-9b39-13b66b640476. deWet, Barend J M [corrected to de Wet, Barend J M].
8. Durbin AP, Vargas MJ, Wanionek K, Hammond SN, Gordon A, Rocha C, et al. Phenotyping of peripheral blood mononuclear cells during acute dengue illness demonstrates infection and increased activation of monocytes in severe cases compared to classic dengue fever. *Virology* (2008) 376(2):429–35. doi: 10.1016/j.virol.2008.03.028
9. Sun P, Fernandez S, Marovich MA, Palmer DR, Celluzzi CM, Boonnak K, et al. Functional characterization of ex vivo blood myeloid and plasmacytoid dendritic cells after infection with dengue virus. *Virology* (2009) 383(2):207–15. doi: 10.1016/j.virol.2008.10.022
10. Boonnak K, Slike BM, Burgess TH, Mason RM, Wu SJ, Sun P, et al. Role of dendritic cells in antibody-dependent enhancement of dengue virus infection. *J Virol* (2008) 82(8):3939–51. doi: 10.1128/JVI.02484-07
11. Flipse J, Diosa-Toro MA, Hoornweg TE, van de Pol DP, Urcuqui-Inchima S, Smit JM. Antibody-Dependent Enhancement of Dengue Virus Infection in Primary Human Macrophages; Balancing Higher Fusion against Antiviral Responses. *Sci Rep* (2016) 6:29201. doi: 10.1038/srep29201
12. Sun P, Bauza K, Pal S, Liang Z, Wu SJ, Beckett C, et al. Infection and activation of human peripheral blood monocytes by dengue viruses through the mechanism of antibody-dependent enhancement. *Virology* (2011) 421(2):245–52. doi: 10.1016/j.virol.2011.08.026
13. Chambers TJ, Hahn CS, Galler R, Rice CM. Flavivirus genome organization, expression, and replication. *Annu Rev Microbiol* (1990) 44:649–88. doi: 10.1146/annurev.mi.44.100190.003245
14. Wengler G, Wengler G. The NS 3 nonstructural protein of flaviviruses contains an RNA triphosphatase activity. *Virology* (1993) 197(1):265–73. doi: 10.1006/viro.1993.1587
15. Warrener P, Tamura JK, Collett MS. RNA-stimulated NTPase activity associated with yellow fever virus NS3 protein expressed in bacteria. *J Virol* (1993) 67(2):989–96. doi: 10.1128/JVI.67.2.989-996.1993

16. Aguilar-Briseño JA, Upasani V, Ellen BMT, Moser J, Pauzuolis M, Ruiz-Silva M, et al. TLR2 on blood monocytes senses dengue virus infection and its expression correlates with disease pathogenesis. *Nat Commun* (2020) 11(1):3177. doi: 10.1038/s41467-020-16849-7
17. Jampangern W, Vongthoung K, Jittmittraphap A, Worapongpaiboon S, Limkittikul K, Chuansumrit A, et al. Characterization of atypical lymphocytes and immunophenotypes of lymphocytes in patients with dengue virus infection. *Asian Pac J Allergy Immunol* (2007) 25(1):27–36.
18. Boonpucknavig S, Lohachitranond C, Nimmanitya S. The pattern and nature of the lymphocyte population response in dengue hemorrhagic fever. *Am J Trop Med Hyg* (1979) 28(5):885–9. doi: 10.4269/ajtmh.1979.28.885
19. Upasani V, Vo HTM, Ung S, Heng S, Laurent D, Choeung R, et al. Impaired Antibody-Independent Immune Response of B Cells in Patients With Acute Dengue Infection. *Front Immunol* (2019) 10:2500. doi: 10.3389/fimmu.2019.02500
20. Wrammert J, Onlamoon N, Akondy RS, Perng GC, Polsrila K, Chandele A, et al. Rapid and massive virus-specific plasmablast responses during acute dengue virus infection in humans. *J Virol* (2012) 86(6):2911–8. doi: 10.1128/JVI.06075-11
21. Simon-Lorière E, Duong V, Tawfik A, Ung S, Ly S, Casadémont I, et al. Increased adaptive immune responses and proper feedback regulation protect against clinical dengue. *Sci Transl Med* (2017) 9(405):eaal5088. doi: 10.1126/scitranslmed.aal5088
22. Perdomo-Celis F, Romero F, Salgado DM, Vega R, Rodríguez J, Angel J, et al. Identification and Characterization at the Single-Cell Level of Cytokine-Producing Circulating Cells in Children With Dengue. *J Infect Dis* (2018) 217(9):1472–80. doi: 10.1093/infdis/jiy053
23. Correa AR, Berbel AC, Papa MP, Morais AT, Peçanha LM, Arruda LB. Dengue Virus Directly Stimulates Polyclonal B Cell Activation. *PLoS One* (2015) 10(12):e0143391. doi: 10.1371/journal.pone.0143391
24. King AD, Nisalak A, Kalayanrooj S, Myint KS, Pattanapanyasat K, Nimmannitya S, et al. B cells are the principal circulating mononuclear cells infected by dengue virus. *Southeast Asian J Trop Med Public Health* (1999) 30(4):718–28.
25. Lin YW, Wang KJ, Lei HY, Lin YS, Yeh TM, Liu HS, et al. Virus replication and cytokine production in dengue virus-infected human B lymphocytes. *J Virol* (2002) 76(23):12242–9. doi: 10.1128/jvi.76.23.12242-12249.2002
26. Zanini F, Robinson ML, Croote D, Sahoo MK, Sanz AM, Ortiz-Lasso E, et al. Virus-inclusive single-cell RNA sequencing reveals the molecular signature of progression to severe dengue. *Proc Natl Acad Sci U S A* (2018) 115(52):E12363–9. doi: 10.1073/pnas.1813819115
27. Baclig MO, Gervacio LT, Suarez LA, Buerano CC, Matias RR, Kumatori A, et al. Flow cytometric analysis of dengue virus-infected cells in peripheral blood. *Southeast Asian J Trop Med Public Health* (2010) 41(6):1352–8.
28. Srikiatkhachorn A, Wichit S, Gibbons RV, Green S, Libraty DH, Endy TP, et al. Dengue viral RNA levels in peripheral blood mononuclear cells are associated with disease severity and preexisting dengue immune status. *PLoS One* (2012) 7(12):e51335. doi: 10.1371/journal.pone.0051335
29. Bhoopat L, Bhamarapravati N, Attasiri C, Yoksarn S, Chaiwun B, Khunamornpong S, et al. Immunohistochemical characterization of a new monoclonal antibody reactive with dengue virus-infected cells in frozen tissue using immunoperoxidase technique. *Asian Pac J Allergy Immunol* (1996) 14(2):107–13.
30. Jessie K, Fong MY, Devi S, Lam SK, Wong KT. Localization of dengue virus in naturally infected human tissues, by immunohistochemistry and in situ hybridization. *J Infect Dis* (2004) 189(8):1411–8. doi: 10.1086/383043
31. Aye KS, Charngkaew K, Win N, Wai KZ, Moe K, Punyadee N, et al. Pathologic highlights of dengue hemorrhagic fever in 13 autopsy cases from Myanmar. *Hum Pathol* (2014) 45(6):1221–33. doi: 10.1016/j.humpath.2014.01.022
32. Yam-Puc JC, García-Cordero J, Calderón-Amador J, Donis-Maturano L, Cedillo-Barrón L, Flores-Romo L. Germinal center reaction following cutaneous dengue virus infection in immune-competent mice. *Front Immunol* (2015) 6:188. doi: 10.3389/fimmu.2015.00188
33. Hue KD, Tuan TV, Thi HT, Bich CT, Anh HH, Wills BA, et al. Validation of an internally controlled one-step real-time multiplex RT-PCR assay for the detection and quantitation of dengue virus RNA in plasma. *J Virol Methods* (2011) 177(2):168–73. doi: 10.1016/j.jviromet.2011.08.002
34. Duong V, Ly S, Lorn Try P, Tuiskunen A, Ong S, Chroeung N, et al. Clinical and virological factors influencing the performance of a NS1 antigen-capture assay and potential use as a marker of dengue disease severity. *PLoS Negl Trop Dis* (2011) 5(7):e1244. doi: 10.1371/journal.pntd.0001244
35. Lewis GD, Metcalf TG. Polyethylene glycol precipitation for recovery of pathogenic viruses, including hepatitis A virus and human rotavirus, from oyster, water, and sediment samples. *Appl Environ Microbiol* (1988) 54(8):1983–8. doi: 10.1128/AEM.54.8.1983-1988.1988
36. Auerswald H, de Jesus A, Seixas G, Nazareth T, In S, Mao S, et al. First dengue virus seroprevalence study on Madeira Island after the 2012 outbreak indicates unreported dengue circulation. *Parasit Vectors* (2019) 12(1):103. doi: 10.1186/s13071-019-3357-3
37. Xu M, Zuest R, Velumani S, Tukijan F, Toh YX, Appanna R, et al. A potent neutralizing antibody with therapeutic potential against all four serotypes of dengue virus. *NPJ Vaccines* (2017) 2:2. doi: 10.1038/s41541-016-0003-3
38. Puerta-Guardo H, Mosso C, Medina F, Liprandi F, Ludert JE, del Angel RM. Antibody-dependent enhancement of dengue virus infection in U937 cells requires cholesterol-rich membrane microdomains. *J Gen Virol* (2010) 91(Pt 2):394–403. doi: 10.1099/vir.0.015420-0
39. Clyde K, Kyle JL, Harris E. Recent advances in deciphering viral and host determinants of dengue virus replication and pathogenesis. *J Virol* (2006) 80(23):11418–31. doi: 10.1128/JVI.01257-06
40. Carnec X, Meertens L, Dejarnac O, Perera-Lecoin M, Hafirassou ML, Kitaura J, et al. The Phosphatidylserine and Phosphatidylethanolamine Receptor CD300a Binds Dengue Virus and Enhances Infection. *J Virol* (2015) 90(1):92–102. doi: 10.1128/JVI.01849-15
41. Zenarruzabeitia O, Vitallé J, García-Obregón S, Astigarraga I, Eguizabal C, Santos S, et al. The expression and function of human CD300 receptors on blood circulating mononuclear cells are distinct in neonates and adults. *Sci Rep* (2016) 6:32693. doi: 10.1038/srep32693
42. Silva R, Moir S, Kardava L, Debell K, Simhadri VR, Ferrando-Martínez S, et al. CD300a is expressed on human B cells, modulates BCR-mediated signaling, and its expression is down-regulated in HIV infection. *Blood* (2011) 117(22):5870–80. doi: 10.1182/blood-2010-09-310318
43. Silveira GF, Wowk PF, Cataneo AHD, Dos Santos PF, Delgobo M, Stimamiglio MA, et al. Human T Lymphocytes Are Permissive for Dengue Virus Replication. *J Virol* (2018) 92(10):e02181–17. doi: 10.1128/JVI.02181-17
44. Meertens L, Carnec X, Lecoin MP, Ramdasi R, Guivel-Benhassine F, Lew E, et al. The TIM and TAM families of phosphatidylserine receptors mediate dengue virus entry. *Cell Host Microbe* (2012) 12(4):544–57. doi: 10.1016/j.chom.2012.08.009
45. Jemielity S, Wang JJ, Chan YK, Ahmed AA, Li W, Monahan S, et al. TIM-family proteins promote infection of multiple enveloped viruses through virion-associated phosphatidylserine. *PLoS Pathog* (2013) 9(3):e1003232. doi: 10.1371/journal.ppat.1003232
46. Chan KR, Zhang SL, Tan HC, Chan YK, Chow A, Lim AP, et al. Ligation of Fc gamma receptor IIB inhibits antibody-dependent enhancement of dengue virus infection. *Proc Natl Acad Sci U S A* (2011) 108(30):12479–84. doi: 10.1073/pnas.1106568108
47. Chan KR, Ong EZ, Tan HC, Zhang SL, Zhang Q, Tang KF, et al. Leukocyte immunoglobulin-like receptor B1 is critical for antibody-dependent dengue. *Proc Natl Acad Sci U S A* (2014) 111(7):2722–7. doi: 10.1073/pnas.1317454111
48. Boonnak K, Slike BM, Donofrio GC, Marovich MA. Human FcγRII cytoplasmic domains differentially influence antibody-mediated dengue virus infection. *J Immunol* (2013) 190(11):5659–65. doi: 10.4049/jimmunol.1203052
49. Sakai J, Akkoyunlu M. The Role of BAFF System Molecules in Host Response to Pathogens. *Clin Microbiol Rev* (2017) 30(4):991–1014. doi: 10.1128/CMR.00046-17
50. Kwissa M, Nakaya HI, Onlamoon N, Wrammert J, Villinger F, Perng GC, et al. Dengue virus infection induces expansion of a CD14(+)CD16(+) monocyte population that stimulates plasmablast differentiation. *Cell Host Microbe* (2014) 16(1):115–27. doi: 10.1016/j.chom.2014.06.001
51. Shen P, Fillatreau S. Antibody-independent functions of B cells: a focus on cytokines. *Nat Rev Immunol* (2015) 15(7):441–51. doi: 10.1038/nri3857

52. Lin CF, Lei HY, Shiau AL, Liu CC, Liu HS, Yeh TM, et al. Antibodies from dengue patient sera cross-react with endothelial cells and induce damage. *J Med Virol* (2003) 69(1):82–90. doi: 10.1002/jmv.10261
53. Chuang YC, Lei HY, Lin YS, Liu HS, Wu HL, Yeh TM. Dengue virus-induced autoantibodies bind to plasminogen and enhance its activation. *J Immunol* (2011) 187(12):6483–90. doi: 10.4049/jimmunol.1102218
54. Chuang YC, Lin YS, Liu HS, Wang JR, Yeh TM. Antibodies against thrombin in dengue patients contain both anti-thrombotic and pro-fibrinolytic activities. *Thromb Haemost* (2013) 110(2):358–65. doi: 10.1160/TH13-02-0149
55. Lin CF, Lei HY, Liu CC, Liu HS, Yeh TM, Wang ST, et al. Generation of IgM anti-platelet autoantibody in dengue patients. *J Med Virol* (2001) 63: (2):143–9. doi: 10.1002/1096-9071(20000201)63:2<143::AID-JMV1009>3.0.CO;2-LJMedVirol
56. Katzelnick LC, Gresh L, Halloran ME, Mercado JC, Kuan G, Gordon A, et al. Antibody-dependent enhancement of severe dengue disease in humans. *Science* (2017) 358(6365):929–32. doi: 10.1126/science.aan6836
57. Salje H, Cummings DAT, Rodriguez-Barraquer I, Katzelnick LC, Lessler J, Klungthong C, et al. Reconstruction of antibody dynamics and infection histories to evaluate dengue risk. *Nature* (2018) 557(7707):719–23. doi: 10.1038/s41586-018-0157-4
58. Wang TT, Sewatanon J, Memoli MJ, Wrammert J, Bournazos S, Bhaumik SK, et al. IgG antibodies to dengue enhanced for FcγRIIIA binding determine disease severity. *Science* (2017) 355(6323):395–8. doi: 10.1126/science.aai8128

Conflict of Interest: The authors declare that the research was conducted in the absence of any commercial or financial relationships that could be construed as a potential conflict of interest.

frontiers in Immunology

REVIEW
published: 25 February 2021
doi: 10.3389/fimmu.2021.602330

The Roles of Sclerostin in Immune System and the Applications of Aptamers in Immune-Related Research

Meiheng Sun [1,2,3†], Zihao Chen [4†], Xiaoqiu Wu [1,2,3†], Yuanyuan Yu [1,2,3], Luyao Wang [1,2,3], Aiping Lu [1,2,3,5,6], Ge Zhang [1,2,3*] and Fangfei Li [1,2,3*]*

[1] Law Sau Fai Institute for Advancing Translational Medicine in Bone and Joint Diseases, School of Chinese Medicine, Hong Kong Baptist University, Hong Kong, China, [2] Institute of Integrated Bioinfomedicine and Translational Science, School of Chinese Medicine, Hong Kong Baptist University, Hong Kong, China, [3] Institute of Precision Medicine and Innovative Drug Discovery, HKBU Institute for Research and Continuing Education, Shenzhen, China, [4] School of Chinese Medicine, Faculty of Medicine, The Chinese University of Hong Kong, Hong Kong, China, [5] Institute of Basic Research in Clinical Medicine, China Academy of Chinese Medical Sciences, Beijing, China, [6] Institute of Arthritis Research, Shanghai Academy of Chinese Medical Sciences, Shanghai, China

Wnt signaling is one of the fundamental pathways that play a major role in almost every aspect of biological systems. In addition to the well-known influence of Wnt signaling on bone formation, its essential role in the immune system also attracted increasing attention. Sclerostin, a confirmed Wnt antagonist, is also proven to modulate the development and differentiation of normal immune cells, particularly B cells. Aptamers, single-stranded (ss) oligonucleotides, are capable of specifically binding to a variety of target molecules by virtue of their unique three-dimensional structures. With in-depth study of those functional nucleic acids, they have been gradually applied to diagnostic and therapeutic area in immune diseases due to their various advantages over antibodies. In this review, we focus on several issues including the roles of Wnt signaling and Wnt antagonist sclerostin in the immune system. For the sake of understanding, current examples of aptamers applications for the immune diseases are also discussed. At the end of this review, we propose our ideas for the future research directions.

Keywords: sclerostin, Wnt signaling pathway, aptamers, immune system, B cell malignancies

OPEN ACCESS

Edited by:
Jayanta Chaudhuri, Memorial Sloan Kettering Cancer Center, United States

Reviewed by:
Masaki Hikida, Akita University, Japan
To-Ha Thai, Beth Israel Deaconess Medical Center and Harvard Medical School, United States

***Correspondence:**
Aiping Lu
aipinglu@hkbu.edu.hk
Ge Zhang
zhangge@hkbu.edu.hk
Fangfei Li
fangfeili@hkbu.edu.hk

†These authors have contributed equally to this work

Specialty section:
This article was submitted to B Cell Biology, a section of the journal Frontiers in Immunology

Received: *26 September 2020*
Accepted: *14 January 2021*
Published: *25 February 2021*

Citation:
Sun M, Chen Z, Wu X, Yu Y, Wang L, Lu A, Zhang G and Li F (2021) The Roles of Sclerostin in Immune System and the Applications of Aptamers in Immune-Related Research. Front. Immunol. 12:602330. doi: 10.3389/fimmu.2021.602330

INTRODUCTION

Wnt signaling is one of the fundamental pathways that play a major role in a range of biological systems, such as stem cell development, tissue homeostasis, and immune cell modulation, the dysregulation of which is responsible for various disorders (1–3). Therefore, as a strong Wnt antagonist, the roles of sclerostin in the immune system have gained increasing research attention. Mechanistically, sclerostin executes its tasks in Wnt signaling pathway based primarily on

competitively binding to Wnt co-receptors low-density lipoprotein receptor-related proteins 5 and 6 (LRP5/6) (4). Wnt-LRP5/6 dimers then form a trimer with seven-pass transmembrane Frizzled (Fz or Fzd) proteins to maintain the stability of β-catenin, a critical regulatory factor in the transcriptional function of Wnt signaling (5). Hence, a significant feature of sclerostin is its ability to mediate the developmental gene expression programs.

Regarding the roles of Wnt signaling pathway on B cells, divergent results were reported between mice and human. Wnt signaling cascade plays a central role in B cell development in murine fetal liver and bone marrow, while Wnt pathway acts as a negative regulator of proliferation potential of B cells in human bone marrow, which needs further investigation (6–8). However, when it comes to the roles of sclerostin on B cells, accumulating direct or indirect evidence suggests that sclerostin plays an indispensable role in normal B lymphocyte development. Absence of sclerostin resulted in enhanced B cell apoptosis and reduced CXCL12, a critical B cell growth-stimulating factor (9). Interestingly, loss of sclerostin in different osteolineage cells demonstrated differentially altered B lymphocyte development through an unknown mechanism that needs further in-depth research (10). In addition, the essential roles of sclerostin on B cell maturation were further confirmed indirectly by the study about von Hippel-Lindau (Vhl), which modulates sclerostin expression *via* hypoxia response signaling pathway, implying the link between sclerostin and B cell development (11).

Taking advantages of aptamers-based high affinity and strong inhibitory roles to the target proteins, aptamers that could rival antibodies but are superior, have been used as essential approaches for diagnostic and therapeutic strategies in immune diseases (12). In some cases, they act as inhibitors by selectively and efficiently binding to targets; in other cases, thanks to their excellent targeting and subsequent endocytosis-mediated internalization capacities, aptamers could also be used as ideal carriers to deliver therapeutic agents for targeted therapy. In the context of multiple myeloma (MM) activities, a modified RNA aptamer, apt69.T, was synthesized to target B cell maturation antigen (BCMA), a critical factor in promoting plasma cells (PCs) survival, to inhibit MM activities (13). In addition, B cell antigens including CD19 and CD20 that are overexpressed on various B cell malignancies, are also suitable markers for aptamer targeting (14–16). Further, due to the cell-binding and internalization properties, a framework combining aptamers and therapeutic agents could be used for the therapeutic strategy for immune diseases (17, 18). Aptamers could also act as biotherapeutic agents by regulating cell cycles to achieve synergistic effects with drugs; the potential molecular basis of the process needs more experiments to elucidate (19). Interestingly, aptamers could also be used as an excellent tool for quality control of biosimilars due to their ability of detecting subtle conformational variations of molecules (20, 21). For diagnostic purposes, aptamer-imaging molecules conjugation complex would be formulated for convenient *in vivo* visualization (22, 23). Therefore, it is clear that aptamers can facilitate the development of novel therapeutic and diagnostic strategies for immune diseases.

SCLEROSTIN: AN INHIBITOR OF WNT SIGNALING PATHWAY

Sclerostin is a glycoprotein containing 213 residues with approximately calculated molecular weight 40 kDa. It is a well-known negative regulatory factor for bone-forming osteoblast, secreted by several cell types, primarily mature osteocytes (24). In the past debate, due to the unique cysteine-knot motif, sclerostin was classified as a member of neuroblastoma (DAN) protein family, which has been shown to have the ability to antagonize bone morphogenetic proteins (BMP) (25). Therefore, it was presumed that sclerostin inhibits bone growth through serving as a BMPs antagonist (26, 27), just like other members of the DAN family. Still, more recent research indicated that the sequence similarity between sclerostin and other members of the DAN family is somewhat limited (28). In addition, although sclerostin could bind to BMPs *in vitro*, the binding affinities were weak (26, 29). In order to address the unclear mechanism by which sclerostin antagonizes BMPs, van Bezooijen et al. discovered that sclerostin exerted its function through blocking Wnt signaling pathway but not acting as a BMPs antagonist (30). Mechanically, sclerostin was proven to inhibit Wnt signaling pathway through binding competitively to Wnt co-receptors low-density lipoprotein receptor-related proteins 5 and 6 (LRP5/6) (4, 5).

The mechanism of sclerostin as a Wnt inhibitor/antagonist blocking the Wnt signaling cascade has been demonstrated in a number of studies (31–34). As a critical pathway in almost every aspect of the developmental process and self-renewal in a number of adult tissues, Wnt signaling plays pivotal roles in changing the expression patterns of specific target genes (35, 36). An essential and heavily studied pathway in the Wnt signaling is the β-catenin dependent Wnt signaling, also known as canonical Wnt signaling, which modulates the stabilization and transfer of transcriptional co-activator β-catenin to nucleus. In the nucleus, β-catenin forms a complex with DNA-bound T cell factor proteins/lymphoid enhancer factor (TCFs/LEF), which are the leading partners of β-catenin to participate in developmental gene expression programs (37). The activation of canonical Wnt signaling pathway occurs as Wnt ligands bind with its co-receptors LRP5/6, which then form a complex with seven-pass transmembrane Frizzled (Fz or Fzd) proteins. The Wnt-Fz-LRP5/6 complex could then elicit a cascade of molecular events that inhibit the phosphorylation of β-catenin through Axin-mediated destruction complex, which consists of scaffolding protein Axin, adenomatous polyposis coli (APC), casein kinase 1 (CK1), and glycogen synthase kinase 3 (GSK3). As soon as Wnt-Fz-LRP5/6 complex is formed, the Axin-mediated destruction complex would translocate to the plasma membrane *via* being phosphorylated by other proteins within the destruction complex, thereby inhibiting the phosphorylation of β-catenin (38, 39). Therefore, in the situation of the Wnt

signaling blocking, cytoplasmic β-catenin is degraded continuously under the influence of the destruction complex, since the phosphorylation of β-catenin creates a binding site that could be recognized by E3 ubiquitin ligase, which is responsible for the subsequent proteasomal degradation of β-catenin (40). Interestingly, TCF/LEF would combine with the repressor Groucho/TLE proteins when β-catenin is missing, which promotes histone deacetylation and chromatin compaction, thereby acting as a transcriptional repressor for the expression of target genes (41, 42). Therefore, when sclerostin competitively binds to LRP5/6 on the plasma membrane, it would result in significantly reduced β-catenin stability, thereby inhibiting the expression profiles of Wnt target genes (shown in **Figure 1**).

Numerous studies have supported the function of sclerostin in the canonical Wnt signaling pathway; several studies also showed that it could execute action in non-canonical Wnt signaling. For instance, sclerostin inhibits both the canonical Wnt signaling and the c-Jun N-terminal kinase (JNK) pathway, which is categorized into non-canonical Wnt signaling pathway, in osteoarthritis (43). In addition, similar with sclerostin, Dickkopf-1 (Dkk1), another inhibitor of the canonical Wnt signaling pathway, has also been proven to participate in the canonical Wnt signaling pathway, and to promote the β-catenin independent Wnt signaling in many types of cancers (44–46). But so far, the research about the roles of sclerostin in the non-canonical Wnt pathway in cancers are still lacking, which deserves more attention and effort of further exploration.

THE ROLES OF SCLEROSTIN IN MODULATING THE IMMUNE CELLS

Effects of Canonical Wnt Signaling on B Lymphocyte

B lymphocytes are capable of generating immunoglobulins (Igs) to develop an antibody response to specific antigens when combating an infection (47). Together with T lymphocytes, these cells comprise the adaptive immune system. In a tightly ordered process, B cells first originated from hematopoietic stem cells (HSCs), then mature in fetal liver and bone marrow and finally reach secondary lymphoid organs. B lymphopoiesis in bone marrow relies heavily on assembly of the functional B-cell antigen receptors on the surface through different combinations of gene segments, known as V(D)J recombination, which is a crucial part of proper lymphocyte development (48). The developmental process includes several stages beginning with pro-B cells, to pre-B cells, immature B cells, and finally to mature B cells (49).

Studies on mice and human suggest that canonical Wnt signaling cascade is involved in the B cell development although the exact roles of Wnt signaling are not consistent in different microenvironment, which are summarized in **Table 1**. The expression of lymphocyte enhancer factor -1 (LEF-1) in developing B cells, which is a member of the TCF/LEF-1 transcription factors in Wnt signaling cascade, indicates the possibility that Wnt signaling might participate in the proliferation and/or differentiation of lymphoid cells. To

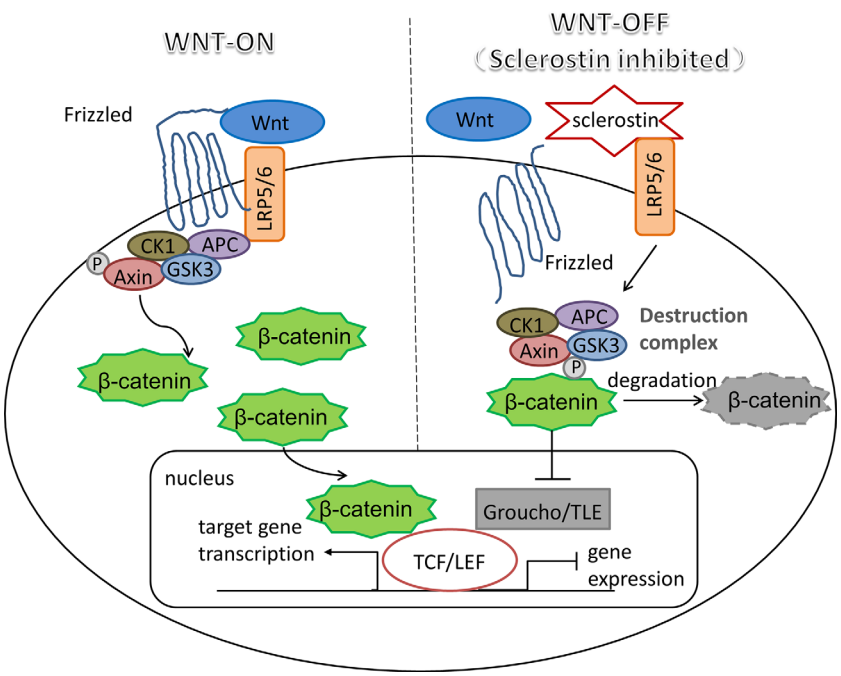

FIGURE 1 | Sclerostin: an inhibitor of canonical Wnt signaling pathway. Wnt-LRP5/6-Fz complex elicits a molecular cascade that transfer Axin-mediated destruction complex, which is essential to β-catenin degradation, to the plasma membrane. Increased β-catenin moves into the nucleus, where it represents the molecular mechanism that β-catenin binds to TCF/LEF, which are the main partners of β-catenin to serve the transcriptional function of canonical Wnt signaling pathway. Sclerostin inhibits Wnt signaling by binding competitively to LRP5/6, thereby promoting the degradation of β-catenin mediated by destruction complex, resulting in the interaction between TCF/LEF and repressor Groucho/TLE proteins to halt the expression of target genes.

TABLE 1 | Effects of Wnt signaling pathway on B cells.

Effects on B cells	Ref
LEF-1-deficient mice lead to defective pro-B cell proliferation and survival but not differentiation	(6)
FZD9−/− mice elicit defects in developing B cells in bone marrow, particularly pre-B cell	(7)
B lymphopoiesis is inhibited by activation of canonical Wnt signaling pathway in human bone marrow	(8)

address this question, Reya et al. examined proliferation, survival, and differentiation of B cells in LEF-1-deficient mice. They found that the absence of LEF-1 lead to defective pro-B cell proliferation and survival but not differentiation. Further, the potential molecular basis of this finding might be the increased apoptosis of B cells due to up-regulated *fas* and *c-myc* transcription, which could trigger cell death. Moreover, incubation of fetal liver pro-B cells with Wnt3A conditioned medium, which could activate canonical Wnt signaling cascade, lead to enhanced pro-B cell proliferation. Therefore, the results suggest a novel role of LEF-1-dependent Wnt signaling pathway in normal B cell proliferation (6). In addition, FZD9−/− mice, which also implicated the blockade of Wnt signaling, elicited pronounced defects in developing B cells in bone marrow, particularly pre-B cells. The above reports established that Wnt signaling cascade plays a central role in B cell development (7). However, in contrast to the findings made in murine pro-B cells from fetal liver, in the case of human bone marrow, it is found that B lymphopoiesis was inhibited by Wnt3A stimulation. In addition, this inhibitory effect was blocked by the Wnt antagonists sFRP1 or Dkk1. These results suggest that the canonical Wnt pathway acts as a negative regulator of proliferation potential of B cells in human bone marrow (8). The divergent results about positive and negative influence of Wnt signaling on murine and human B cells might be explained by the distinction in species and/or microenvironment between fetal liver and adult bone marrow, which needs further exploration.

Effects of Sclerostin on B Lymphocyte

In addition to the bone resorption and formation mediated by a variety of cytokines produced by T and B lymphocytes, osteoblast lineage cells also support hematopoietic cell survival and differentiated descendants such as B cells. Recently, the cross-talking between hematopoietic cells and bone cells has been an active area of investigation (50–52). Cain et al. were the first to explore the influence of sclerostin on the immune system. They found that sclerostin loss-of-function mice showed not only significantly elevated activity of osteoblast, but also altered normal B lymphocyte development through promoting B cell apoptosis. Absence of sclerostin expression in hematopoietic cells and any B cell population implied that the substantial B defects in sclerostin$^{-/-}$ mice results from a non-cell autonomous effect, a result which was confirmed by reciprocal sclerostin$^{-/-}$➡WT and WT➡ sclerostin$^{-/-}$ chimeras studies. The transplantation of WT bone marrow into sclerostin$^{-/-}$ recipients was followed by a decrease in B cells, whereas reciprocal sclerostin$^{-/-}$➡WT was not. The results supported the idea that B-cell defects are not results from the changes in B-cell themselves, but from the alterations in the bone microenvironment. Low levels of CXCL12, an essential B cell growth-stimulating factor, were also observed in sclerostin$^{-/-}$ mice, compatible with B defects. The results match with another study that illustrated the negative correlation between the activation of Wnt signaling and CXCL12 levels (53). Therefore, the results suggest that sclerostin belongs to a group of factors that play critical roles in both bone formation and immune system. Interestingly, that known Wnt target genes *Lef-1* and *Ccnd1* expression pattern remains unchanged implies sclerostin plays a novel part to support B cell development in bone marrow independent of direct influence of Wnt signaling pathway on B cells. It might be explained by the indirect role of sclerostin on the mesenchymal stem cells (MSCs), a kind of stromal cells, which have been found to express CXCL12. Therefore, whether a causative link exists between sclerostin, MSCs, CXCL12, and B development remains unknown that needs further investigation (9, 54, 55). Moreover, depletion of B cells was only occurs in bone marrow but not the spleen. Under normal conditions, a majority of B cells in bone marrow are plasma cells that play a critical role in fighting an infection through rapid release of antigen-specific antibodies. Recirculating B cells migrate back to the bone marrow after stimulation in secondary lymphoid organs. The clear reduction of recirculating B cells in bone marrow suggests that bone marrow environment is not conductive for maintenance of B cells even after the completion of activation of the B cells in the periphery. Therefore, immunodeficiency might occur in the patients receiving sclerostin antibodies treatment, which should deserve more attention.

However, whether sclerostin in different osteolineage cells contributes differently to the B lymphocytes development is still a significant knowledge gap. Subsequently, Yee et al. reported that conditional loss of sclerostin in different osteolineage cells induced differentially altered B lymphocyte development. The results showed that sclerostin in mesenchymal stem cells (MSCs) and osteoblasts is essential for B cell development, while sclerostin in mature osteocytes does not play a critical role in B cell survival. The findings are consistent with the previous hypothesis that sclerostin might mediate B cell development which depends on MSCs and CXCL12 that needs to be tested through further studies. Sclerostin-deficiency in MSCs (*Prx1-Cre)* mice displayed abnormal accumulation of cells lacking IgM and IgD. The presence of IgM and IgD is the feature of mature B cells, suggesting sclerostin in *Prx1*+ cells plays a role at the later stages of B cell progression. On the other hand, sclerostin-deficiency in mature osteoblasts (*Coll-Cre)* delayed the early phase of B cell maturation due to significantly high proportion of IgM^{-}IgD^{-} cells in B progenitors at B220^{+}CD43^{high} stage. However, whether CXCL12 expression is also changed in MSCs and osteoblasts and the underlying mechanism still remains poorly understood, which needs further experimental studies to elucidate (10).

Additionally, the critical role of sclerostin in B cell development was further examined indirectly by the study in which von Hippel-Lindau (Vhl) depletion contributes towards concomitant high bone mass and impaired B cell development through promoting Wnt signaling pathway and reducing the expression of sclerostin (11). According to the variation of oxygen levels, proline hydroxylated hypoxia-inducible factor (HIF) acts as a transcription factor *via* the interaction between HIF-β and one of HIF-α isoforms (HIF-1α, HIF-2α, and HIF-3α). Under normoxic conditions, HIF1α would be targeted by E3 ligase complex Vhl and ultimately degraded *via* the proteasome. In contrast, under hypoxic state, increased HIF1α accumulation is achieved by inhibiting prolyl hydroxylation. The HIF complex would then transfer into the nucleus acting as a transcription factor. Therefore, in Vhl-knockout mice, HIF1α is stabilized. In addition, reduction in sclerostin and concomitant increase in activated β-catenin was observed by immunocytochemistry, which indirectly further examines the link between sclerostin and B cell development (56). For example, absolute numbers of $CD45^+$ hematopoietic cells and $CD19^+$ B lymphocytes were significantly reduced. Additionally, B cell maturation was also disrupted in the spleen through reducing mature B cells ($CD19^{high}B220^{high}$) with abnormally immature phenotype (IgM^+IgD^{low}).

Although sclerostin has been proven to participate in normal B cell development and differentiation, in the case of immune diseases, the research on the applications of monoclonal sclerostin antibody is still mainly limited to its influence on bone formation. For example, elevated levels of sclerostin in serum and osteocytes were reported in multiple myeloma (MM), an aggressive lethal hematologic disease accompanied with detectable severe bone destruction (57, 58). As expected, combining anti-sclerostin antibody with chemotherapy could control MM growth and reverse osteolysis (59). Surprisingly, several *in vivo and vitro* studies reported that sclerostin inhibition alone did not affect tumor burden, an issue that needs further research through more experimental studies (60).

Taken together, the above research studies imply that people receiving any therapies directed at anti-sclerostin might suffer from B cell defects. Still, no data from clinical trials of the romosozumab, a monoclonal antibody that targets sclerostin, is available about its effects on the immune functions of patients (61, 62). Moreover, knowledge about the roles of sclerostin in immune diseases is still limited, which needs further in-depth research.

Effects of Sclerostin on T Lymphocyte

Although Cain et al. illustrated that the absence of sclerostin results in B cell-specific defects but not the difference of cell numbers in T lymphocytes, natural killer cells, monocytes, granulocytes, and erythroid cells, You et al. demonstrated that sclerostin is necessary for inducing T helper 17 (Th17) cell differentiation, which is responsible for bone resorption, through promoting the levels of IL-6 and TFG-β that are related to Th17 differentiation. In addition, sclerostin inhibits the differentiation of regulatory T (Treg) cells *via* reducing the expression of IL-10 and Foxp3, which play an essential role in Treg cell development (63). Given that Th17 and Treg cells plays vital roles in inflammatory bone diseases, the research provides valuable hints about the therapeutic strategy for this kind of disease involving the imbalance of Th17 and Treg cells development. Taken together, the exact roles of sclerostin in immune cells are summarized in **Table 2**.

APTAMERS-BASED RESEARCH ON IMMUNE DISEASES

Aptamers are single-stranded (ss) oligonucleotide sequences (DNA/RNA) with a length of approximate 25–80 bases that are capable of binding to a variety of specific target molecules by virtue of their unique three-dimensional structures. Considering their high binding affinity and specificity, ease in production, modification flexibility, minimal batch-to-batch variability, low immunogenicity, *etc*., in recent years, aptamers have gained extensive research attention as a potent alternative of antibodies (12). An aptamer's selection technology, known as Systematic Evolution of Ligands by Exponential Enrichment (SELEX), was first developed in 1990 by two laboratories (64, 65). The fundamental selection cycle requires three critical steps: 1) incubating a target with a chemically synthesized oligonucleotide library containing randomized sequences (DNA/RNA); 2) removing unbound sequences and splitting bound sequences from target; 3) amplifying the bound sequences by PCR. In the case of RNA aptamer selection, additional reverse transcription into DNA is necessary (66). A number of selection cycles are then performed until the sequence with desired affinity is obtained. Several critical modifications are introduced to achieve long-lasting action time through overcoming nuclease degradation (67). On the one hand, aptamers act as inhibitors that can interfere with the normal function of a target protein, mimicking the functional properties of monoclonal antibodies. On the other hand, some aptamers will internalize after binding to receptors on the cell membrane, so that they can act as vehicles to deliver drugs, imaging agents, microRNAs, small interfering RNAs (siRNA), *etc*. Therefore, since aptamers have both inhibitory and carrier capabilities, significant clinical applications have been developed to realize their diagnostic and therapeutic potentials (68–71).

TABLE 2 | Effects of sclerostin on immune cells.

Effects on immune cells	Affected immune cell	Ref
absence of sclerostin inhibits normal B lymphocyte development through promoting B cell apoptosis		(9)
conditional loss of sclerostin in different osteolineage cells indicated differentially altered B lymphocyte development	B cell	(10)
von Hippel-Lindau (Vhl) depletion showed the enhanced Wnt signaling activity through inhibiting sclerostin expression with subsequent impaired B cell development		(11)
sclerostin is necessary in inducing T helper 17 (Th17) cell differentiation, and inhibiting the differentiation of regulatory T (Treg) cells	T cell	(63)

Multiple myeloma (MM) is characterized by abnormal accumulation of malignant plasma cells (PCs) that produce immunoglobulins (72). B cell maturation antigen (BCMA) is exclusively expressed on the surface of terminally differentiated B cells and is highly expressed on malignant PCs (73). Mechanically, BCMA promotes long-survival of PCs through binding to their specific ligands, B cell activating factor (BAFF) and the proliferation-inducing ligand (APRIL), which could trigger the activation of downstream nuclear factor kB (NF-kB) pathway (74, 75). As a result, monoclonal antibodies (mAbs) targeting BCMA have been used as effective therapeutic tools for MM (76, 77). Considering the various advantages of aptamers over antibodies, Catuogno et al. selected a 2′Fluoro-Pyrimidine modified RNA aptamer, apt69.T, that could effectively bind to BCMA-enriched myeloma cells with excellent serum stability. Further, subsequent internalization of apt69.T into the cells makes it a suitable tool for direct targeting and delivery of therapeutics (13). Overexpression of BAFF receptor was also observed on the surface of numerous B cell malignancies (78). Therefore, Zhou et al. formulated a BAFF aptamer–siRNA conjugation complex through a "sticky bridge" for B-cell lymphoma therapy (17). In conclusion, aptamer-based targeted therapies and drug delivery system provide a framework for the future therapeutic strategy for immune diseases.

The B-lymphocyte antigen (CD20) is another suitable candidate for recognition of B cells, since it expresses on the surface of the almost all the precursor and mature B lymphocytes, even malignant B cells, except in normal plasma cells (79). CD20 acts as a voltage-independent Ca^{2+} channel that regulates the activation and proliferation of B-cells through mediating the concentration of Ca^{2+} and triggering tyrosine kinase signaling pathways (80, 81). The significant outcomes of rituximab, an anti-CD20 monoclonal antibody, have been achieved in various B cell malignancies, such as non-Hodgkin's lymphoma, Burkitt's mature B-cell lymphoma, and chronic lymphocytic leukemia (CLL) (82, 83). However, limitations of antibodies including their thermal instability and immunogenicity underscore the urgent need to develop appropriate aptamers that could be used as an alternative and effective tool for therapeutic practices. After 10 rounds of SELEX screening, a panel of candidate aptamers was generated. Further analysis of characterization demonstrated that the most thermodynamically stable aptamer AP-1 has the strongest binding affinities with CD20 (14). However, in order to accelerate the clinical translation of therapeutic aptamers, inherent physicochemical characteristics and safety should be evaluated through further in-depth investigation.

Interestingly, aptamers can also act as an efficient quality control tool for biosimilars (products with high similarity of reference biological medicines) due to their ability of detecting subtle conformational variations of biologics. Although the amino acid sequences of biosimilars are identical to that of the originators, the biosimilars might still be different from the reference products due to post-translational modifications, which could be induced by highly complex production process. Therefore, it is necessary to evaluate the detailed characterization, such as 3D shape, which is crucial to detecting the differences between biosimilars and originators. However, there are only a limited number of laborious methods, such as NMR, X-ray crystallography, or monoclonal antibodies that can specifically target biologics. In addition, difficulties and high cost of producing appropriate antibody panels greatly hinder the development and approval of biosimilars. In order to improve the quality assessment for properties of biosimilars, aptamers were generated to monitor conformational similarities of biosimilars and reference products. Wildner et al. screened a first panel of anti-CD20 antibody rituximab-specific aptamers that could detect conformational variations. In addition, the selected aptamers also demonstrated the changes in structure upon thermo or UV exposure of rituximab. In the study, the authors chose a 40 nucleotide random part instead of general oligonucleotide libraries with a length of 20–80 nucleotides to obtain stable structures with high affinity to the target protein (20). In addition to recognition of native state of rituximab, the same team further generated six high-affinity DNA aptamers capable of selectively recognizing the distinct structural determinants of heat-treated rituximab prior to precipitation. None of the reaction was observed with the antibody in its native state or when being exposed to other physical stresses (21). Hence, aptamers could be used as a suitable sensor for detecting structural variations of biologics, with the potential for stringent biopharmaceutical quality control. They can also serve as a useful tool for studying the unfolding process of proteins when stresses exposure occurs.

Following the success of CD20-targeted antibody rituximab, other attempts are also made to develop novel therapies for B cell malignancies. High and stable levels of CD19 were also detected on the surfaces of various B cell malignancies, such as acute lymphocytic leukemia, chronic lymphocytic leukemia, and Non-Hodgins lymphoma (84). Mechanically, CD19 enhances the chance of B cell survival by triggering B cell antigen receptor (BCR) signaling (85). Further, CD19-targeted chimeric antigen receptor (CAR)-modified T cell therapy achieved unprecedented success in clinical trials (86). Such evidence suggests that CD19 is of great significance as a diagnostic marker and therapeutic target for B cell malignancies. Hu et al. selected a first CD19 aptamer (LC1) to specifically target CD19-positive lymphoma cells but not CD19- negative cell lines. Furthermore, an aptamer–doxorubicin complex (Apt–Dox) was formulated and used to selectively deliver doxorubicin, a cytotoxic drug, to CD19-positive lymphoma cells *in vitro*. Free doxorubicin could diffuse into both the CD19-positive and negative cells. However, through targeted delivery of drug into CD19 positive cells *via* Apt–Dox, the problem of drug toxicity to negative cells can be solved, which has the potential for the development of targeted therapy. Additionally, although LC1 aptamer could be used as an important ligand with diagnostic or therapeutic potential through conjugating imaging contrasts or various drugs; however, the detailed mechanism of how Apt–Dox enter cells was not well known. In order to facilitate the development of other aptamer–drug conjugates, more in-depth research about such mechanism of internalization is needed (15). Since drug

resistance always occurs with chemotherapy treatment, the elevated levels of P-glycoprotein (P-gp) on the cell surface would result in drug resistance through limiting drug entry into cells (87). Another protein, B-cell lymphoma 2 (Bcl2), acting as an anti-apoptotic factor on the mitochondrial membrane, also contributes to the drug resistance through inhibiting cell death (88). Therefore, Pan et al. constructed a multifunctional DNA origami-based carrier, a promising candidate for tumor imaging, with both doxorubicin and two different antisense oligonucleotides (ASOs) that target P-gp and Bcl2, for enhancing efficacy of treatment (16). This strategy reveals the potential of combining chemotherapy and oligonucleotides in aptamer-based targeted therapy. In order to study the structural–affinity relationships between aptamers and the target proteins, Danquah et al. discovered an 'aptamer walking' mechanism through molecular dynamics (MD) simulation. They constructed a CD19–aptamer complex based on data available in the protein data bank. The results indicated that aptamer molecules could gradually adjust its configuration and shift to a favorable binding position, whilst CD19 remains relatively stable. The aptamers and their stable binding-poses relative to CD19 might be used as suitable templates in designing potential aptamer molecules. In addition, the structural approach adopted in this study provides a novel direction for searching various aptamer molecules for specific targets in future (89).

The cytotoxic effects of doxorubicin on lymphoma depend on Topoisomerase II alpha (TopIIA), a DNA repair enzyme complex. The complex plays a key role in repairing DNA damage due to its ability to relax supercoiled DNA (90). Although anthracyclines, including doxorubicin and etoposide, have shown great clinical significance in the treatment of large B-cell lymphoma (DLBCL), the response of the cancer cells to the therapy vary considerably across cases (91). Previous studies reported that elevated expression of nucleolin in B-cell lymphoma cell lines, involving DLBCL, compared to normal B cells (92). Although nucleolin was proven to be associated with several key DNA repair proteins, the functions of nucleolin in DNA damage response are unclear (93). Jain et al. found that nucleolin plays a novel modulatory role in DNA repair when binding to TopIIA. The results demonstrated that the nucleolin–TopIIA interaction prevents the killing effects of TopIIA targeting agents on DLBCL cells by facilitating DNA damage repair instead of cleavage. In other words, silencing of nucleolin could enhance the TopIIA targeting agent-induced DNA damage and apoptosis of DLBCL. Consequently, combining nucleolin inhibitor (aptamer AS1411) with doxorubicin greatly reduces the survival chance of DLBCL cells by compromising DNA repair capabilities provided by TopIIA. Thus, in order to improve the efficacy of TopIIA targeting agents, combination of agents and nucleolin-targeted aptamers might be a promising solution (18).

Protein tyrosine kinase 7 (PTK7) membrane receptor was reported to participate and up-regulate in the progression of various cancers, including hematological malignancies (94). Also, PTK7 expression promotes cultured leukemia cells resistance to anthracycline-induced apoptosis (95). Sgc8-c aptamer, the truncated form of original aptamer Sgc8, was used to target PTK7 as a therapeutic tool with similar binding affinities of Sgc8 (96, 97). To serve as the radiolabeled probe for theranostic purpose, Sgc8-c aptamer was labeled with ^{67}Ga and metal chelator NOTA conjugation with good biodistribution and molecular imaging both *in vivo* and *vitro* evaluation (23). In addition, other PTK7-targeting aptamer-fluorescent and -radiolabeled probes with fluorescent dye AlexaFluor647 and 6-hydrazinonicotinamide (HYNIC) chelator were also formulated for *in vivo* visualization (22). However, in order to further enhance tumor retention, additional chemical modifications have to be performed.

Interestingly, in addition to the cell-binding property, aptamers might also act as biotherapeutic agents by regulating cell cycles. Li et al. synthesized an ssDNA aptamer specifically targeting Maver-1 lymphoma cells with concomitant endocytosis-mediated internalization that triggered S-phase arrest. The induced arrest primed target cells for cytarabine chemotherapy, which primarily kills lymphoma cells at S-phase (19). Therefore, the synergistic killing effects achieved by the combination of aptamers and chemotherapeutic agents open a new avenue for precision therapy. However, although some efforts about the detection of expression of several key proteins in cellular signaling pathways have been made, the exact mechanism through which internalized aptamers regulate the intracellular signaling pathways remains unclear, which needs further investigation.

To sum up, the review in this section suggests that we could use aptamers as promising research tools to develop therapeutic and diagnostic strategies for immune diseases based on the inhibitory or carrier properties of the aptamers (shown in **Table 3**).

CONCLUSIONS AND FUTURE PERSPECTIVES

As a negative regulator of bone growth, sclerostin, a Wnt signaling antagonist based primarily on binding competitively

TABLE 3 | Aptamers-based research on immune diseases.

Functions of aptamers	Targets/modifications/therapeutic agents	Ref
Inhibitors	B cell maturation antigen (BCMA) 2′Fluoro-Pyrimidine modification	(13)
	CD20	(14)
Delivery carriers	B cell activating factor (BAFF) + siRNA	(17)
	CD19 +doxorubicin +doxorubicin+ASOs targeting P-gp and Bcl2	(15, 16)
	Nucleolin + doxorubicin	(18)
Diagnostic agents	PTK7 +67Ga+metal chelator NOTA +AlexaFluor647 +6-hydrazinonicotinamide (HYNIC)	(22, 23)
Others	anti-CD20 antibody rituximab Maver-1 lymphoma cells	(19–21)

to Wnt co-receptors LRP5/6, received not only extensive attention for its therapeutic effects in bone diseases, but also plays critical roles on development and differentiation of immune cells, especially B cells.

On the one hand, multiple studies have reported that sclerostin is indispensable for B cell survival and development. Sclerostin loss-of-function mice showed B cell defects through enhanced B cell apoptosis, concomitant with reduced levels of CXCL12, a critical B cell growth-stimulating mediator. Interestingly, unchanged Wnt target genes *Lef-1* and *Ccnd1* expression pattern implies a novel role of sclerostin in supporting B cell functions independent of Wnt signaling pathway, which needs further investigation. In addition, conditional loss of sclerostin in different osteolineage cells demonstrated differentially altered B lymphocyte development. The essential influence of sclerostin on B cell maturation was further confirmed indirectly by the study about von Hippel-Lindau (Vhl), which modulates sclerostin expression *via* hypoxia response signaling pathway, revealing the relationship between sclerostin and B cell development. In spite of the effects of sclerostin antibodies in immune diseases that mainly focus on bone formation, the roles of sclerostin in these immune diseases need further investigation to facilitate the development of sclerostin-based therapies for immune diseases.

Currently, a variety of aptamers have been generated and used in various studies of immune diseases. Thanks to their excellent targeting and subsequent endocytosis-mediated internalization capabilities, aptamers act as inhibitors or valuable carriers for targeted therapy. In order to accelerate the clinical translations of these therapeutic aptamers, aptamers should be made to improve factors including physicochemical characteristics, modifications, safety, *etc*.

In summary, although the underlying mechanism of sclerostin in immune diseases has not yet been fully elucidated, its roles in normal immune cell development, especially B cells, have become increasingly apparent. It is clear that aptamers are competent tools for subsequent progress in translational pharmacology based on the sclerostin functional study. The utilization of aptamers might facilitate the development of novel anti-immune diseases therapeutic and diagnostic strategies based on sclerostin.

AUTHOR CONTRIBUTIONS

MS wrote the manuscript. FL, XW, and YY helped in revising the manuscript. MS, ZC, and LW contributed in figure designing. FL, AL, and GZ supervised the preparation of the manuscript. All authors contributed to the article and approved the submitted version.

FUNDING

This study was supported by the National Key Research and Development Program of China (2018YFA0800804), the Interdisciplinary Research Matching Scheme Hong Kong Baptist University (RC-IRMS/15-16/01), the Hong Kong General Research Fund (12101018, 12102518, 12102120), Theme-based Research Scheme Hong Kong Research Grants Council (TRS/RGC T12-201-20-R), and the National Natural Science Foundation Council of China (81703049).

REFERENCES

1. Clevers H, Nusse R. Wnt/β-catenin signaling and disease. *Cell* (2012) 149 (6):1192–205. doi: 10.1016/j.cell.2012.05.012
2. Staal FJT, Luis TC, Tiemessen MM. WNT signalling in the immune system: WNT is spreading its wings. *Nat Rev Immunol* (2008) 8(8):581–93. doi: 10.1038/nri2360
3. Haseeb M, Pirzada RH, Ain QU, Choi S. Wnt Signaling in the Regulation of Immune Cell and Cancer Therapeutics. *Cells* (2019) 8(11):1380. doi: 10.3390/cells8111380
4. Li X, Zhang Y, Kang H, Liu W, Liu P, Zhang J, et al. Sclerostin binds to LRP5/6 and antagonizes canonical Wnt signaling. *J Biol Chem* (2005) 280 (20):19883–7 doi: 10.1074/jbc.M413274200
5. Semënov M, Tamai K, He X. SOST is a ligand for LRP5/LRP6 and a Wnt signaling inhibitor. *J Biol Chem* (2005) 280(29):26770–5 doi: 10.1074/jbc.M504308200
6. Reya T, O'Riordan M, Okamura R, Devaney E, Willert K, Nusse R, et al. Wnt signaling regulates B lymphocyte proliferation through a LEF-1 dependent mechanism. *Immunity* (2000) 13(1):15–24. doi: 10.1016/s1074-7613(00)00004-2
7. Ranheim EA, Kwan HC, Reya T, Wang YK, Weissman IL, Francke U. Frizzled 9 knock-out mice have abnormal B-cell development. *Blood* (2005) 105 (6):2487–94. doi: 10.1182/blood-2004-06-2334
8. Døsen G, Tenstad E, Nygren MK, Stubberud H, Funderud S, Rian E. Wnt expression and canonical Wnt signaling in human bone marrow B lymphopoiesis. *BMC Immunol* (2006) 7:13. doi: 10.1186/1471-2172-7-13
9. Cain CJ, Rueda R, McLelland B, Collette NM, Loots GG, Manilay JO. Absence of sclerostin adversely affects B-cell survival. *J Bone Miner Res* (2012) 27 (7):1451–61. doi: 10.1002/jbmr.1608
10. Yee CS, Manilay JO, Chang JC, Hum NR, Murugesh DK, Bajwa J, et al. Conditional Deletion of Sost in MSC-Derived Lineages Identifies Specific Cell-Type Contributions to Bone Mass and B-Cell Development. *J Bone Miner Res* (2018) 33(10):1748–59. doi: 10.1002/jbmr.3467
11. Loots GG, Robling AG, Chang JC, Murugesh DK, Bajwa J, Carlisle C, et al. Vhl deficiency in osteocytes produces high bone mass and hematopoietic defects. *Bone* (2018) 116:307–14. doi: 10.1016/j.bone.2018.08.022
12. Ni S, Zhuo Z, Pan Y, Yu Y, Li F, Liu J, et al. Recent Progress in Aptamer Discoveries and Modifications for Therapeutic Applications. *ACS Appl Mater Interfaces* (2020). doi: 10.1021/acsami.0c05750
13. Catuogno S, Di Martino MT, Nuzzo S, Esposito CL, Tassone P, de Franciscis V. An Anti-BCMA RNA Aptamer for miRNA Intracellular Delivery. *Mol Ther Nucleic Acids* (2019) 18:981–90. doi: 10.1016/j.omtn.2019.10.021
14. Haghighi M, Khanahmad H, Palizban A. Selection and Characterization of Single-Stranded DNA Aptamers Binding Human B-Cell Surface Protein CD20 by Cell-SELEX. *Molecules* (2018) 23(4):715. doi: 10.3390/molecules23040715
15. Hu Y, Li X, An Y, Duan J, Yang XD. Selection of a novel CD19 aptamer for targeted delivery of doxorubicin to lymphoma cells. *Oncotarget* (2018) 9 (42):26605–15. doi: 10.18632/oncotarget.24902
16. Pan Q, Nie C, Hu Y, Yi J, Liu C, Zhang J, et al. Aptamer-Functionalized DNA Origami for Targeted Codelivery of Antisense Oligonucleotides and Doxorubicin to Enhance Therapy in Drug-Resistant Cancer Cells. *ACS Appl Mater Interfaces* (2020) 12(1):400–9. doi: 10.1021/acsami.9b20707
17. Zhou J, Rossi JJ, Shum KT. Methods for assembling B-cell lymphoma specific and internalizing aptamer-siRNA nanoparticles via the sticky bridge. *Methods Mol Biol* (2015) 1297:169–85. doi: 10.1007/978-1-4939-2562-9_12
18. Jain N, Zhu H, Khashab T, Ye Q, George B, Mathur R, et al. Targeting nucleolin for better survival in diffuse large B-cell lymphoma. *Leukemia* (2018) 32(3):663–74. doi: 10.1038/leu.2017.215

19. Li H, Yang S, Yu G, Shen L, Fan J, Xu L, et al. Aptamer Internalization via Endocytosis Inducing S-Phase Arrest and Priming Maver-1 Lymphoma Cells for Cytarabine Chemotherapy. *Theranostics* (2017) 7(5):1204–13. doi: 10.7150/thno.17069
20. Wildner S, Huber S, Regl C, Huber CG, Lohrig U, Gadermaier G. Aptamers as quality control tool for production, storage and biosimilarity of the anti-CD20 biopharmaceutical rituximab. *Sci Rep* (2019) 9(1):1111. doi: 10.1038/s41598-018-37624-1
21. Kohlberger M, Wildner S, Regl C, Huber CG, Gadermaier G. Rituximab-specific DNA aptamers are able to selectively recognize heat-treated antibodies. *PLoS One* (2020) 15(11):e0241560. doi: 10.1371/journal.pone.0241560
22. Calzada V, Moreno M, Newton J, González J, Fernández M, Gambini JP, et al. Development of new PTK7-targeting aptamer-fluorescent and -radiolabelled probes for evaluation as molecular imaging agents: Lymphoma and melanoma in vivo proof of concept. *Bioorg Med Chem* (2017) 25(3):1163–71. doi: 10.1016/j.bmc.2016.12.026
23. Sicco E, Baez J, Ibarra M, Fernández M, Cabral P, Moreno M, et al. Sgc8-c Aptamer as a Potential Theranostic Agent for Hemato-Oncological Malignancies. *Cancer Biother Radiopharm* (2020) 35(4):262–70. doi: 10.1089/cbr.2019.3402
24. Hernandez P, Whitty C, John Wardale R, Henson FMD. New insights into the location and form of sclerostin. *Biochem Biophys Res Commun* (2014) 446 (4):1108–13. doi: 10.1016/j.bbrc.2014.03.079
25. Nolan K, Thompson TB. The DAN family: modulators of TGF-β signaling and beyond. *Protein Sci* (2014) 23(8):999–1012. doi: 10.1002/pro.2485
26. Winkler DG, Sutherland MK, Geoghegan JC, Yu C, Hayes T, Skonier JE, et al. Osteocyte control of bone formation via sclerostin, a novel BMP antagonist. *EMBO J* (2003) 22(23):6267–76. doi: 10.1093/emboj/cdg599
27. Brunkow ME, Gardner JC, Van Ness J, Paeper BW, Kovacevich BR, Proll S, et al. Bone dysplasia sclerosteosis results from loss of the SOST gene product, a novel cystine knot-containing protein. *Am J Hum Genet* (2001) 68(3):577–89. doi: 10.1086/318811
28. Avsian-Kretchmer O, Hsueh AJ. Comparative genomic analysis of the eight-membered ring cystine knot-containing bone morphogenetic protein antagonists. *Mol Endocrinol (Baltimore Md)* (2004) 18(1):1–12. doi: 10.1210/me.2003-0227
29. Kusu N, Laurikkala J, Imanishi M, Usui H, Konishi M, Miyake A, et al. Sclerostin is a novel secreted osteoclast-derived bone morphogenetic protein antagonist with unique ligand specificity. *J Biol Chem* (2003) 278(26):24113–7. doi: 10.1074/jbc.M301716200
30. van Bezooijen RL, Svensson JP, Eefting D, Visser A, van der Horst G, Karperien M, et al. Wnt but not BMP signaling is involved in the inhibitory action of sclerostin on BMP-stimulated bone formation. *J Bone Miner Res* (2007) 22(1):19–28. doi: 10.1359/jbmr.061002
31. van Dinther M, Zhang J, Weidauer SE, Boschert V, Muth EM, Knappik A, et al. Anti-Sclerostin antibody inhibits internalization of Sclerostin and Sclerostin-mediated antagonism of Wnt/LRP6 signaling. *PLoS One* (2013) 8 (4):e62295. doi: 10.1371/journal.pone.0062295
32. Krause C, Korchynskyi O, de Rooij K, Weidauer SE, de Gorter DJ, van Bezooijen RL, et al. Distinct modes of inhibition by sclerostin on bone morphogenetic protein and Wnt signaling pathways. *J Biol Chem* (2010) 285(53):41614–26. doi: 10.1074/jbc.M110.153890
33. Genetos DC, Toupadakis CA, Raheja LF, Wong A, Papanicolaou SE, Fyhrie DP, et al. Hypoxia decreases sclerostin expression and increases Wnt signaling in osteoblasts. *J Cell Biochem* (2010) 110(2):457–67. doi: 10.1002/jcb.22559
34. Krishna SM, Seto SW, Jose RJ, Li J, Morton SK, Biros E, et al. Wnt Signaling Pathway Inhibitor Sclerostin Inhibits Angiotensin II-Induced Aortic Aneurysm and Atherosclerosis. *Arterioscler Thromb Vasc Biol* (2017) 37 (3):553–66. doi: 10.1161/atvbaha.116.308723
35. Nusse R. Wnt signaling in disease and in development. *Cell Res* (2005) 15 (1):28–32. doi: 10.1038/sj.cr.7290260
36. Clevers H. Wnt/beta-catenin signaling in development and disease. *Cell* (2006) 127(3):469–80. doi: 10.1016/j.cell.2006.10.018
37. Arce L, Yokoyama NN, Waterman ML. Diversity of LEF/TCF action in development and disease. *Oncogene* (2006) 25(57):7492–504. doi: 10.1038/sj.onc.1210056
38. Kimelman D, Xu W. beta-catenin destruction complex: insights and questions from a structural perspective. *Oncogene* (2006) 25(57):7482–91. doi: 10.1038/sj.onc.1210055
39. Itoh K, Krupnik VE, Sokol SY. Axis determination in Xenopus involves biochemical interactions of axin, glycogen synthase kinase 3 and beta-catenin. *Curr Biol* (1998) 8(10):591–4. doi: 10.1016/s0960-9822(98)70229-5
40. Stamos JL, Weis WI. The β-catenin destruction complex. *Cold Spring Harb Perspect Biol* (2013) 5(1):a007898. doi: 10.1101/cshperspect.a007898
41. Behrens J, von Kries JP, Kühl M, Bruhn L, Wedlich D, Grosschedl R, et al. Functional interaction of beta-catenin with the transcription factor LEF-1. *Nature* (1996) 382(6592):638–42. doi: 10.1038/382638a0
42. Daniels DL, Weis WI. Beta-catenin directly displaces Groucho/TLE repressors from Tcf/Lef in Wnt-mediated transcription activation. *Nat Struct Mol Biol* (2005) 12(4):364–71. doi: 10.1038/nsmb912
43. Bouaziz W, Funck-Brentano T, Lin H, Marty C, Ea HK, Hay E, et al. Loss of sclerostin promotes osteoarthritis in mice via β-catenin-dependent and -independent Wnt pathways. *Arthritis Res Ther* (2015) 17(1):24. doi: 10.1186/s13075-015-0540-6
44. Krause U, Ryan DM, Clough BH, Gregory CA. An unexpected role for a Wnt-inhibitor: Dickkopf-1 triggers a novel cancer survival mechanism through modulation of aldehyde-dehydrogenase-1 activity. *Cell Death Dis* (2014) 5: e1093. doi: 10.1038/cddis.2014.67
45. Wang S, Zhang S. Dickkopf-1 is frequently overexpressed in ovarian serous carcinoma and involved in tumor invasion. *Clin Exp Metastasis* (2011) 28 (6):581–91. doi: 10.1007/s10585-011-9393-9
46. Tao Y-M, Liu Z, Liu H-L. Dickkopf-1 (DKK1) promotes invasion and metastasis of hepatocellular carcinoma. *Dig Liver Dis* (2013) 45(3):251–7. doi: 10.1016/j.dld.2012.10.020
47. Parra D, Reyes-Lopez FE, Tort L. Mucosal Immunity and B Cells in Teleosts: Effect of Vaccination and Stress. *Front Immunol* (2015) 6:354. doi: 10.3389/fimmu.2015.00354
48. Stengel KR, Barnett KR, Wang J, Liu Q, Hodges E, Hiebert SW, et al. Deacetylase activity of histone deacetylase 3 is required for productive VDJ recombination and B-cell development. *Proc Natl Acad Sci U S A* (2017) 114 (32):8608–13. doi: 10.1073/pnas.1701610114
49. Hardy RR, Kincade PW, Dorshkind K. The protean nature of cells in the B lymphocyte lineage. *Immunity* (2007) 26(6):703–14. doi: 10.1016/j.immuni.2007.05.013
50. Pacifici R. The immune system and bone. *Arch Biochem Biophys* (2010) 503 (1):41–53. doi: 10.1016/j.abb.2010.05.027
51. Horowitz MC, Fretz JA, Lorenzo JA. How B cells influence bone biology in health and disease. *Bone* (2010) 47(3):472–9. doi: 10.1016/j.bone.2010.06.011
52. Guder C, Gravius S, Burger C, Wirtz DC, Schildberg FA. Osteoimmunology: A Current Update of the Interplay Between Bone and the Immune System. *Front Immunol* (2020) 11:58. doi: 10.3389/fimmu.2020.00058
53. Tamura M, Sato MM, Nashimoto M. Regulation of CXCL12 expression by canonical Wnt signaling in bone marrow stromal cells. *Int J Biochem Cell Biol* (2011) 43(5):760–7. doi: 10.1016/j.biocel.2011.01.021
54. Sugiyama T, Kohara H, Noda M, Nagasawa T. Maintenance of the hematopoietic stem cell pool by CXCL12-CXCR4 chemokine signaling in bone marrow stromal cell niches. *Immunity* (2006) 25(6):977–88 doi: 10.1016/j.immuni.2006.10.016
55. Ding L, Morrison SJ. Haematopoietic stem cells and early lymphoid progenitors occupy distinct bone marrow niches. *Nature* (2013) 495 (7440):231–5. doi: 10.1038/nature11885
56. Donham C, Manilay JO. The Effects of Sclerostin on the Immune System. *Curr Osteoporos Rep* (2020) 18(1):32–7. doi: 10.1007/s11914-020-00563-w
57. Delgado-Calle J, Anderson J, Cregor MD, Hiasa M, Chirgwin JM, Carlesso N, et al. Bidirectional Notch Signaling and Osteocyte-Derived Factors in the Bone Marrow Microenvironment Promote Tumor Cell Proliferation and Bone Destruction in Multiple Myeloma. *Cancer Res* (2016) 76(5):1089–100. doi: 10.1158/0008-5472.Can-15-1703
58. Eda H, Santo L, Wein MN, Hu DZ, Cirstea DD, Nemani N, et al. Regulation of Sclerostin Expression in Multiple Myeloma by Dkk-1: A Potential Therapeutic Strategy for Myeloma Bone Disease. *J Bone Miner Res* (2016) 31(6):1225–34. doi: 10.1002/jbmr.2789
59. McDonald MM, Reagan MR, Youlten SE, Mohanty ST, Seckinger A, Terry RL, et al. Inhibiting the osteocyte-specific protein sclerostin increases bone mass

and fracture resistance in multiple myeloma. *Blood* (2017) 129(26):3452–64. doi: 10.1182/blood-2017-03-773341
60. Delgado-Calle J, Anderson J, Cregor MD, Condon KW, Kuhstoss SA, Plotkin LI, et al. Genetic deletion of Sost or pharmacological inhibition of sclerostin prevent multiple myeloma-induced bone disease without affecting tumor growth. *Leukemia* (2017) 31(12):2686–94. doi: 10.1038/leu.2017.152
61. McClung MR, Brown JP, Diez-Perez A, Resch H, Caminis J, Meisner P, et al. Effects of 24 Months of Treatment With Romosozumab Followed by 12 Months of Denosumab or Placebo in Postmenopausal Women With Low Bone Mineral Density: A Randomized, Double-Blind, Phase 2, Parallel Group Study. *J Bone Miner Res* (2018) 33(8):1397–406. doi: 10.1002/jbmr.3452
62. Horowitz MC, Fretz JA. Sclerostin: A new mediator of crosstalk between the skeletal and immune systems. *J Bone Miner Res* (2012) 27(7):1448–50. doi: 10.1002/jbmr.1672
63. You L, Chen L, Pan L, Peng Y, Chen J. SOST Gene Inhibits Osteogenesis from Adipose-Derived Mesenchymal Stem Cells by Inducing Th17 Cell Differentiation. *Cell Physiol Biochem* (2018) 48(3):1030–40. doi: 10.1159/000491971
64. Ellington AD, Szostak JW. In vitro selection of RNA molecules that bind specific ligands. *Nature* (1990) 346(6287):818–22. doi: 10.1038/346818a0
65. Tuerk C, Gold L. Systematic evolution of ligands by exponential enrichment: RNA ligands to bacteriophage T4 DNA polymerase. *Science* (1990) 249 (4968):505–10. doi: 10.1126/science.2200121
66. Darmostuk M, Rimpelova S, Gbelcova H, Ruml T. Current approaches in SELEX: An update to aptamer selection technology. *Biotechnol Adv* (2015) 33 (6 Pt 2):1141–61. doi: 10.1016/j.biotechadv.2015.02.008
67. Kovacevic KD, Gilbert JC, Jilma B. Pharmacokinetics, pharmacodynamics and safety of aptamers. *Adv Drug Deliv Rev* (2018) 134:36–50. doi: 10.1016/j.addr.2018.10.008
68. Wang H, Lam CH, Li X, West DL, Yang X. Selection of PD1/PD-L1 X-Aptamers. *Biochimie* (2018) 145:125–30. doi: 10.1016/j.biochi.2017.09.006
69. Nozari A, Berezovski MV. Aptamers for CD Antigens: From Cell Profiling to Activity Modulation. *Mol Ther Nucleic Acids* (2017) 6:29–44. doi: 10.1016/j.omtn.2016.12.002
70. Tan W, Donovan MJ, Jiang J. Aptamers from cell-based selection for bioanalytical applications. *Chem Rev* (2013) 113(4):2842–62. doi: 10.1021/cr300468w
71. He F, Wen N, Xiao D, Yan J, Xiong H, Cai S, et al. Aptamer-Based Targeted Drug Delivery Systems: Current Potential and Challenges. *Curr Med Chem* (2020) 27(13):2189–219. doi: 10.2174/0929867325666181008142831
72. Raab MS, Podar K, Breitkreutz I, Richardson PG, Anderson KC. Multiple myeloma. *Lancet* (2009) 374(9686):324–39. doi: 10.1016/s0140-6736(09)60221-x
73. Novak AJ, Darce JR, Arendt BK, Harder B, Henderson K, Kindsvogel W, et al. Expression of BCMA, TACI, and BAFF-R in multiple myeloma: a mechanism for growth and survival. *Blood* (2004) 103(2):689–94. doi: 10.1182/blood-2003-06-2043
74. Tai YT, Li XF, Breitkreutz I, Song W, Neri P, Catley L, et al. Role of B-cell-activating factor in adhesion and growth of human multiple myeloma cells in the bone marrow microenvironment. *Cancer Res* (2006) 66(13):6675–82. doi: 10.1158/0008-5472.Can-06-0190
75. Thompson JS, Bixler SA, Qian F, Vora K, Scott ML, Cachero TG, et al. BAFF-R, a newly identified TNF receptor that specifically interacts with BAFF. *Science* (2001) 293(5537):2108–11. doi: 10.1126/science.1061965
76. Oden F, Marino SF, Brand J, Scheu S, Kriegel C, Olal D, et al. Potent anti-tumor response by targeting B cell maturation antigen (BCMA) in a mouse model of multiple myeloma. *Mol Oncol* (2015) 9(7):1348–58. doi: 10.1016/j.molonc.2015.03.010
77. Ryan MC, Hering M, Peckham D, McDonagh CF, Brown L, Kim KM, et al. Antibody targeting of B-cell maturation antigen on malignant plasma cells. *Mol Cancer Ther* (2007) 6(11):3009–18. doi: 10.1158/1535-7163.Mct-07-0464
78. Ge XJ, Wang YL, Wu YP, Feng ZX, Liu L, Li MY, et al. Regulatory effect of Act1 on the BAFF pathway in B-cell malignancy. *Oncol Lett* (2019) 17 (4):3727–34. doi: 10.3892/ol.2019.10047
79. Cragg MS, Walshe CA, Ivanov AO, Glennie MJ. The biology of CD20 and its potential as a target for mAb therapy. *Curr Dir Autoimmun* (2005) 8:140–74. doi: 10.1159/000082102
80. Du J, Wang H, Zhong C, Peng B, Zhang M, Li B, et al. Structural basis for recognition of CD20 by therapeutic antibody Rituximab. *J Biol Chem* (2007) 282(20):15073–80. doi: 10.1074/jbc.M701654200
81. Perosa F, Favoino E, Caragnano MA, Prete M, Dammacco F. CD20: a target antigen for immunotherapy of autoimmune diseases. *Autoimmun Rev* (2005) 4(8):526–31. doi: 10.1016/j.autrev.2005.04.004
82. Hoelzer D, Walewski J, Döhner H, Viardot A, Hiddemann W, Spiekermann K, et al. Improved outcome of adult Burkitt lymphoma/leukemia with rituximab and chemotherapy: report of a large prospective multicenter trial. *Blood* (2014) 124(26):3870–9. doi: 10.1182/blood-2014-03-563627
83. Grillo-López AJ. Monoclonal antibody therapy for B-cell lymphoma. *Int J Hematol* (2002) 76(5):385–93. doi: 10.1007/bf02982803
84. Wang K, Wei G, Liu D. CD19: a biomarker for B cell development, lymphoma diagnosis and therapy. *Exp Hematol Oncol* (2012) 1(1):36. doi: 10.1186/2162-3619-1-36
85. Schweighoffer E, Tybulewicz VL. Signalling for B cell survival. *Curr Opin Cell Biol* (2018) 51:8–14. doi: 10.1016/j.ceb.2017.10.002
86. Hay KA, Turtle CJ. Chimeric Antigen Receptor (CAR) T Cells: Lessons Learned from Targeting of CD19 in B-Cell Malignancies. *Drugs* (2017) 77 (3):237–45. doi: 10.1007/s40265-017-0690-8
87. Löscher W, Potschka H. Drug resistance in brain diseases and the role of drug efflux transporters. *Nat Rev Neurosci* (2005) 6(8):591–602. doi: 10.1038/nrn1728
88. Cory S, Adams JM. The Bcl2 family: regulators of the cellular life-or-death switch. *Nat Rev Cancer* (2002) 2(9):647–56. doi: 10.1038/nrc883
89. Danquah MK, Guo HB, Tan KX, Bhakta M. Atomistic probing of aptameric binding of CD19 outer membrane domain reveals an "aptamer walking" mechanism. *Biotechnol Prog* (2020) 36(3):e2957. doi: 10.1002/btpr.2957
90. Nitiss JL, DNA topoisomerase II. and its growing repertoire of biological functions. *Nat Rev Cancer* (2009) 9(5):327–37. doi: 10.1038/nrc2608
91. Li S, Young KH, Medeiros LJ. Diffuse large B-cell lymphoma. *Pathology* (2018) 50(1):74–87. doi: 10.1016/j.pathol.2017.09.006
92. Wise JF, Berkova Z, Mathur R, Zhu H, Braun FK, Tao RH, et al. Nucleolin inhibits Fas ligand binding and suppresses Fas-mediated apoptosis in vivo via a surface nucleolin-Fas complex. *Blood* (2013) 121(23):4729–39. doi: 10.1182/blood-2012-12-471094
93. Goldstein M, Derheimer FA, Tait-Mulder J, Kastan MB. Nucleolin mediates nucleosome disruption critical for DNA double-strand break repair. *Proc Natl Acad Sci U S A* (2013) 110(42):16874–9. doi: 10.1073/pnas.1306160110
94. Gruszka AM, Valli D, Alcalay M. Wnt Signalling in Acute Myeloid Leukaemia. *Cells* (2019) 8(11):1403. doi: 10.3390/cells8111403
95. Prebet T, Lhoumeau AC, Arnoulet C, Aulas A, Marchetto S, Audebert S, et al. The cell polarity PTK7 receptor acts as a modulator of the chemotherapeutic response in acute myeloid leukemia and impairs clinical outcome. *Blood* (2010) 116(13):2315–23. doi: 10.1182/blood-2010-01-262352
96. Shangguan D, Cao ZC, Li Y, Tan W. Aptamers evolved from cultured cancer cells reveal molecular differences of cancer cells in patient samples. *Clin Chem* (2007) 53(6):1153–5. doi: 10.1373/clinchem.2006.083246
97. Shangguan D, Tang Z, Mallikaratchy P, Xiao Z, Tan W. Optimization and modifications of aptamers selected from live cancer cell lines. *Chembiochem* (2007) 8(6):603–6. doi: 10.1002/cbic.200600532

Conflict of Interest: The authors declare that the research was conducted in the absence of any commercial or financial relationships that could be construed as a potential conflict of interest.

frontiers in Immunology

MINI REVIEW
published: 25 March 2021
doi: 10.3389/fimmu.2021.663443

How the Signaling Crosstalk of B Cell Receptor (BCR) and Co-Receptors Regulates Antibody Class Switch Recombination: A New Perspective of Checkpoints of BCR Signaling

Zhangguo Chen[1]* *and Jing H. Wang*[2]*

[1] Department of Immunology and Microbiology, University of Colorado, Aurora, CO, United States, [2] Department of Medicine, Division of Hematology and Oncology, UPMC Hillman Cancer Center, University of Pittsburgh School of Medicine, Pittsburgh, PA, United States

OPEN ACCESS

Edited by:
Zhenming Xu,
The University of Texas Health Science Center at San Antonio, United States

Reviewed by:
Egest Pone,
University of California, Irvine, United States
Niklas Engels,
University Medical Center Göttingen, Germany

***Correspondence:**
Zhangguo Chen
zhangguo.chen@cuanschutz.edu
Jing H. Wang
wangj28@upmc.edu

Specialty section:
This article was submitted to B Cell Biology, a section of the journal Frontiers in Immunology

Received: *02 February 2021*
Accepted: *11 March 2021*
Published: *25 March 2021*

Citation:
Chen Z and Wang JH (2021) How the Signaling Crosstalk of B Cell Receptor (BCR) and Co-Receptors Regulates Antibody Class Switch Recombination: A New Perspective of Checkpoints of BCR Signaling. Front. Immunol. 12:663443. doi: 10.3389/fimmu.2021.663443

Mature B cells express B cell antigen receptor (BCR), toll-like receptors (TLR) and TNF family receptors including CD40 and B-cell activating factor receptor (BAFFR). These receptors transduce cellular signals to govern the physiological and pathological processes in B cells including B cell development and differentiation, survival, proliferation, and antibody-mediated immune responses as well as autoimmune diseases and B cell lymphomagenesis. Effective antibody-mediated immune responses require class switch recombination (CSR), a somatic DNA recombination event occurring at the immunoglobulin heavy chain (*Igh*) gene locus. Mature B cells initially express IgM as their BCR, and CSR enables the B cells to switch from expressing IgM to expressing different classes of antibodies including IgG, IgA or IgE that exhibit distinct effector functions. Here, we briefly review recent findings about how the signaling crosstalk of the BCR with TLRs, CD40 and BAFFR regulates CSR, antibody-mediate immune responses, and B cell anergy.

Keywords: B cell receptor, class switch recombination, activation-induced deaminase, tumor necrosis factor receptor-associated factor-3, B cell homeostasis

INTRODUCTION

Antibody is also known as immunoglobulin (Ig), consisting of a heavy (IgH) and a light (IgL) chain. Each IgH molecule is composed of an assembled variable (V) region and a constant (C) region. Antigen contact is mediated by the V region, while the C region of IgH mediates effector functions of antibodies. Productive V(D)J recombination at the *Igh* locus assembles the V region exon that is located upstream of the Cμ IgH constant region exons, allowing generation of μ heavy chain mRNA and μ heavy chain protein. The μ heavy chains pair with IgL chains that are produced from a productively rearranged *Igl* locus to form IgM, which lead to generation of surface IgM^+ B cells. IgM^+ B cells migrate to secondary lymphoid organs such as spleen or lymph nodes, where upon encounter with antigens they are activated to undergo class switch recombination (CSR), a somatic

DNA recombination/deletion process that replaces Cμ with a different set of IgH constant region exons (**Figure 1**).

In mice, there are 8 sets of C_H exons organized as 5'–VDJ–Cμ–Cδ–Cγ3–Cγ1–Cγ2b–Cγ2a–Cε–Cα–3'. CSR is a DNA rearrangement process that occurs to the 8 sets of C_H exons at the *Igh* locus (**Figure 1**). CSR allows the assembled V region to be expressed first with Cμ exons and then with one of the sets of downstream C_H exons (referred to as C_H genes), and enables production of different IgH classes (e.g., IgG, IgE, and IgA) encoded by corresponding C_H genes (e.g., Cγ, Cε, and Cα). The detailed molecular mechanisms of CSR have been extensively reviewed elsewhere (1–4). Briefly, to initiate CSR, B cells need to express a specific enzyme, activation-induced cytidine deaminase (AID) (5, 6). AID introduces DNA lesions to the evolutionarily conserved switch (S) regions preceding each set of C_H exons; subsequently, AID-induced DNA lesions are converted into double-stranded DNA breaks (DSBs) at the upstream donor Sμ region and one of the downstream acceptor S regions (7). DSBs at S regions are joined by non-homologous end-joining (NHEJ) pathway including classical and alternative NHEJ (8–11), which eventually leads to the switching of the C regions of antibody molecules. Of note, AID can potentially target all transcriptionally active genes and induces genome-wide instability that contributes to B cell lymphomagenesis (12, 13). Thus, AID poses a threat to the B cell genome and its expression has to be tightly regulated. Consequently, AID expression is only induced in activated B cells *via* integrated signals from the B cell antigen receptor (BCR) and other co-receptors (3).

Antibody CSR is essential for effective humoral immune responses. Mature naïve B cells express IgM as surface BCR or secrete IgM antibodies; however, effector functions of IgM are rather limited (3, 14, 15). CSR enables B cells to produce isotype-switched antibodies, such as IgG and IgA, that can combat infectious pathogens or neutralize toxins much more effectively than IgM. Consequently, more than 90% of current vaccines deliver protective effects *via* eliciting isotype-switched antibodies (16). On the other hand, defects in CSR lead to primary immunodeficiency diseases (PID) such as Hyper-IgM syndrome (HIGM) caused by genetic mutations in BCR or co-receptor signaling components (e.g., CD19 or CD40) (17, 18). In

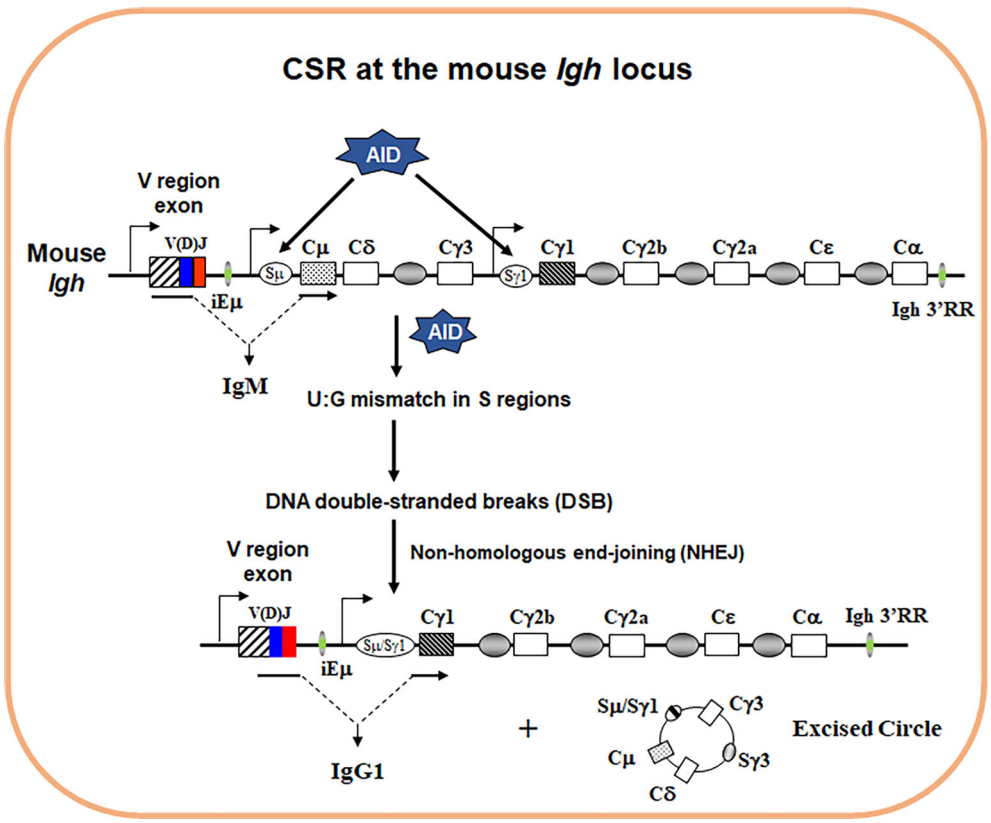

FIGURE 1 | Schematics of IgH CSR. The genomic configuration of the rearranged *Igh* locus in mouse. Variable (V) region exon is located upstream, and eight different sets of C_H exons are located downstream. AID introduces point mutations into V region exon during somatic hypermutation (SHM) (not depicted). To initiate CSR, AID introduces U:G mismatches in the donor Sμ and the downstream acceptor Sγ1 regions that are subsequently converted into DNA double-stranded breaks (DSBs) by basic excision and mismatch repair pathways. Broken S regions are joined by non-homologous end-joining (NHEJ), whereas the intervening DNA is excised as a circle. Active transcription is essential for both SHM/CSR with promoters depicted for V region, Sμ and Sγ1 region (arrows). When CSR is completed, originally expressed Cμ exons are replaced by Cγ1 exons that are juxtaposed to the same V region exon. Therefore, naïve IgM^+ B cells switch to activated $IgG1^+$ B cells.

addition, HIGM can be caused by mutations in AID or uracil glycosylase that are essential enzymes to catalyze CSR (17, 18). PID patients suffer from recurrent infections with a shorter life expectancy (19–21). Hence, it is critical to better understand how the signaling crosstalk of BCR and co-receptors regulates antibody CSR.

CAN THE BCR INDUCE CSR IN THE ABSENCE OF CO-STIMULATION?

Pathogen infection or antigen immunization activates multiple receptors on B cells including BCR, CD40, toll-like receptors (TLRs), B-cell activating factor receptor (BAFFR) and cytokine receptors (e.g., IL-4R) depending on different antigen characteristics. The prevailing view of CSR induction is that the BCR cannot induce CSR in the absence of co-stimulation, and the co-stimulatory signals are provided in the form of CD40 ligand (CD40L) expressed by activated T cells for T-cell dependent (TD) antigens, or TLR ligands directly expressed by pathogens or present in the adjuvants for T-cell independent (TI) antigens. Given that it is not practically feasible yet to pinpoint which and how individual receptor(s) induce CSR during *in vivo* immunization, *ex vivo* CSR models have been established and widely applied to study underlying mechanisms of CSR by culturing purified B cells in the presence of different stimuli and analyzing CSR level a few days after culture (2, 22).

It is well-known that engaging CD40 can induce CSR in the presence of proper cytokines such as IL-4 (2, 22). TLRs can also induce a low level of CSR in the presence of cytokines; moreover, TLRs synergize with the BCR to induce a robust level of CSR (23). In contrast, engaging the BCR cannot induce CSR in the presence of cytokines such as IL-4 (23, 24). The BCR recognizes antigen and activates multiple signaling pathways, including nuclear factor kappa B (NF-κB) and phosphatidylinositol 3-kinases (PI3K), to initiate antigen-specific humoral immune response. Hence, it is counterintuitive why the BCR cannot induce CSR in the presence of cytokines as CD40 does (3). Basically, why does the BCR need co-stimulation to induce CSR and what does co-stimulation do to enable the BCR to induce CSR?

Our recent study has shed light on this decade long puzzle by revealing that there are negative regulatory mechanisms restricting the BCR's ability to induce CSR (25). We identified two of such checkpoint molecules including TNF receptor associated factor 2/3 (TRAF2 and TRAF3) (**Figure 2**). When TRAF2 and/or TRAF3 are deleted in B cells, engaging the BCR can induce CSR in the absence of co-stimulation (25). These data demonstrate that the BCR has the ability to induce CSR; however, this ability is normally restrained by checkpoint molecules such as TRAF2 and TRAF3. Upon the deletion of these checkpoint molecules, the BCR's need for co-stimulation to induce CSR can now be bypassed. We found that the BCR-induced CSR in the absence of TRAF3 requires NF-κB2 in a B cell-intrinsic manner (25). Mechanistically, TRAF3 restricted BCR signaling by preventing the processing of BCR-induced NF-κB2 precursor (p100) into active NF-κB2 (p52); consequently, TRAF3 deletion resulted in more active NF-κB2 (p52) upon anti-IgM/IL-4 stimulation (25). Of note, NF-κB2 activation is specifically required for the BCR signaling to induce CSR but not for CD40 or TLR4 (25, 26), suggesting that TRAF3 restricts NF-κB2 activation to specifically limit the BCR's ability to induce CSR. Furthermore, we found that TRAF3 also inhibited BCR proximal signaling; as such, B-cell intrinsic deletion of TRAF3 led to elevated BCR proximal signaling strength, evidenced by increased phosphorylation of Bruton tyrosine kinase (BTK) and spleen tyrosine kinase (Syk) and enhanced calcium flux upon antigen or anti-IgM stimulation (25). While our recent study addressed how TRAF3 inhibits the BCR signaling, it remains unknown how TRAF2 regulates the BCR signaling intensity either singularly or cooperatively with TRAF3.

HOW DO TRAF2 AND TRAF3 DIFFERENTIALLY INFLUENCE CSR AND HOW DOES THE BCR COOPERATE WITH CO-RECEPTORS TO INDUCE CSR?

Both TRAF2 and TRAF3 are adaptor molecules of TNF receptors (TNFRs) including CD40 and BAFFR and function to transmit signaling downstream of TNFRs (27). In resting B cells, TRAF2, TRAF3 and cellular inhibitor of apoptosis protein1/2 (cIAP1/2) form a complex to suppress NF-κB inducing kinase (NIK) activity by mediating NIK degradation (**Figure 2**). In activated B cells upon CD40 or BAFFR stimulation, TRAF3 can be degraded (25, 28, 29), thereby allowing NIK accumulation that eventually activates NF-κB2 (**Figure 2**). Although TRAF2 and TRAF3 both serve as adaptors of TNFRs and their individual knockout (KO) mice exhibited similar phenotypes (30–32), TRAF2 and TRAF3 play distinct roles in mediating CSR and *in vivo* antibody responses against TD or TI antigens.

With regard to CD40-induced CSR, we found that TRAF2 is required for CD40-induced AID expression and IgG1 CSR because TRAF2 plays an essential role in CD40-induced NF-κB1 activation (33). Consistently, B-cell intrinsic deletion of TRAF2 significantly impaired *in vivo* IgG antibody responses against TD antigens (33), given that TD antigen-induced IgG antibody responses need CD40/CD40L interaction. Contrary to the essential role of TRAF2 in CD40-induced CSR, TRAF3 is completely dispensable for CD40-induced AID expression and CSR (33). As such, B-cell intrinsic TRAF3 deletion did not affect IgG antibody responses against TD antigens *in vivo* (32, 33).

However, in the context of BCR-induced CSR, both TRAF2 and TRAF3 function as checkpoint molecules to prevent the BCR from inducing AID expression and CSR (25). This conclusion is supported by several important observations: (1) B cell-intrinsic TRAF2 deletion promotes the BCR-induced CSR *ex vivo*; (2) B cell-intrinsic TRAF3 deletion also promotes the BCR-induced CSR *ex vivo*, which occurs completely independent of any potential developmental effects; and (3) double deletion of TRAF2 and TRAF3 leads to a higher level of BCR-induced CSR

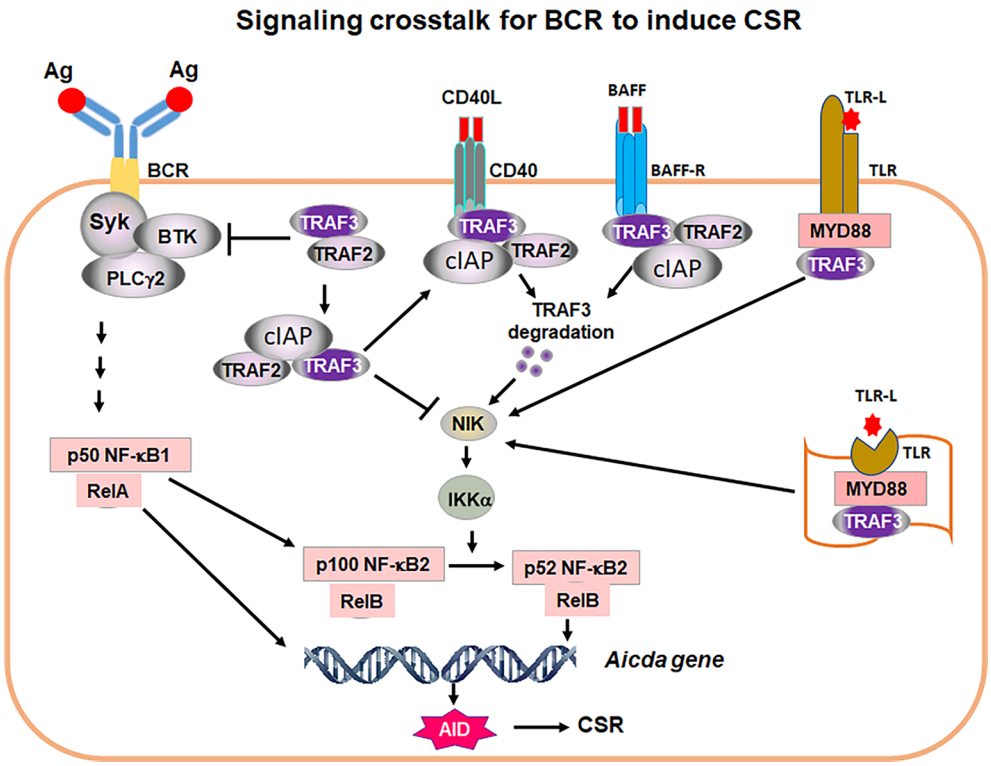

FIGURE 2 | A proposed model of signaling crosstalk for the BCR to induce CSR. Ag stimulation of BCR activates proximal signaling elements, Syk, BTK and PLCγ2, leading to transcription factor NF-kB1 activation. NF-κB1 p50/RelA complex is required for AID transcription. NF-κB1 p50/RelA also induces NF-kB2 p100 transcription. TRAF2/3 restrict BCR proximal signaling strength. TRAF2 and TRAF3 also block NIK activity. Thus, Syk/BTK/PLCγ2 complex cannot signal to generate transcription factor NF-κB2 p52 that is required for AID expression. Removal of TRAF3 and/or TRAF2 leads to NIK accumulation, which activates IKKα pathway, resulting in NF-κB2 p100 being processed into active NF-κB2 p52. NF-κB2 p52/RelB complex and NF-κB1 p50/RelA together with additional factors initiate AID transcription. AID protein initiates CSR by targeting *Igh* locus. During humoral immune responses, CD40, BAFF-R as well as cell surface and intracellular TLRs are activated by corresponding ligands, CD40L, BAFF or TLR ligand (TLR-L), respectively. TRAF3/TRAF2 are recruited to cell membrane where TRAF3 is degraded by CD40 and BAFF-R signaling or sequestrated by TLRs. As a consequence, NIK and NF-κB2 complex can be activated. NF-κB2 activation allows the BCR to induce CSR. Thus, the critical function of co-stimulatory signals is to degrade or sequestrate TRAF3 to permit NF-κB2-dependent BCR-induced CSR essential for *in vivo* antibody responses. It is worthy of note that TRAF3 restricts Syk, BTK and PLCγ2 hyper-activation upon Ag stimulation that may be especially important for maintaining autoreactive B-cell anergy.

than either single deletion does (25). In line with these observations, B-cell intrinsic deletion of TRAF2 or TRAF3 increased *in vivo* IgG antibody responses against TI antigens (33).

Of note, TI antigens can activate B cells in the absence of T cell help. Consistent with TRAF3's role in restricting the BCR's ability to induce CSR, we envision that increased IgG antibody responses against TI antigens are caused by elevated BCR signaling intensity *in vivo* upon TI antigen immunization in the absence of TRAF2 or TRAF3. However, this point remains to be determined; in addition, it remains unknown whether TRAF2/TRAF3 double KO mice will develop more robust IgG antibody responses against TI antigens. It is noteworthy that TRAF2 and TRAF3 play distinct roles in CD40-induced CSR and TD antigen-mediated responses, whereas they both function as checkpoints for BCR-induced CSR. Taken together, these studies highlight the complexity and fine-tuning potential of antibody-mediated immune responses that may have important implications for vaccine design of different types of antigens, such as TD vs. TI antigens.

If the BCR has the ability to induce CSR, why do B cells need co-stimulation and what does co-stimulation provide in the context of CSR induction? We suggest that CD40 aids BCR-induced CSR *in vivo* by inducing TRAF3 degradation (**Figure 2**), which is supported by our *ex vivo* studies showing that anti-CD40/IL-4 stimulation caused TRAF3 degradation in B cells (25). Subsequently, transient degradation of TRAF3 will allow NF-κB2 activation, AID expression and CSR induction. Once CD40 co-stimulation ceases, TRAF3 expression would resume and CSR would be terminated. However, this notion still needs to be tested in an *in vivo* setting. Regarding the role of BAFFR in CSR induction, our recent studies also suggest that BAFFR's function is to degrade TRAF3, thus permitting the BCR to induce CSR (25) (**Figure 2**), although this point still needs to be confirmed experimentally. Nevertheless, this idea is supported by the observations that BAFF/IL-4 cannot induce a robust level of CSR, whereas BAFF/IL-4/anti-IgM induced a much higher level of IgG1 CSR that is not significantly enhanced in TRAF3 conditional KO B cells (25).

TLRs have been shown to synergize with the BCR to induce CSR by enhancing NF-κB2 activation, and such synergistic effects depend on a regulatory subunit of PI3Ks, p85 (23). However, the catalytic subunits of PI3Ks inhibit AID expression and CSR induced by CD40 (34), TLR4 (24) and BCR. Thus, the precise mechanisms remain elusive about how TLRs and the BCR synergize to enhance NF-κB2 activation to promote CSR. TLRs can bind TRAF3 *via* their adaptors myeloid differentiation primary response protein (MYD88) and TIR-domain-containing adapter-inducing interferon-β (TRIF). In contrast, TLRs do not induce TRAF3 degradation like CD40 does, because TRAF3 is required for TLR-induced cytokine production (35). Hence, we suggest that TLRs may sequester TRAF3 *via* adaptors MYD88 and/or TRIF, thereby releasing NIK that eventually activates NF-κB2 (p52) to induce AID expression and CSR (**Figure 2**).

WHAT ARE THE CONSEQUENCES OF BCR CHECKPOINT REMOVAL?

When TRAF3 is deleted specifically in B cells *via* CD19Cre (B-TRAF3-KO), mice develop autoimmune manifestations including splenomegaly, lymphocyte infiltration in liver and immune-complex deposition in kidney at the age of 9-12 months (32). B-TRAF2-KO mice exhibit similar phenotypes to B-TRAF3-KO mice in B cell development and survival as well as lymph organ homeostasis (30–32). However, it remains incompletely understood how TRAF3 deficiency leads to autoimmune manifestations. Previous studies showed that B cell hyperplasia in B-TRAF3-KO mice was independent of BAFF-BAFFR signaling by using TACI-Ig, a soluble fusion protein that blocks both BAFF and APRIL from binding to their receptors (32). In addition, another study showed that the expansion of marginal zone (MZ) B cells in B-TRAF2-KO mice was independent of BAFF (30), suggesting that B-TRAF2-KO phenotypes were also independent of BAFF receptor signaling.

Based on our data (25), we suggest that the phenotypes of increased B cell number, splenomegaly, and autoimmune manifestations in B-TRAF3-KO mice depend on BCR signaling. We found that TRAF3-deficiency-mediated lymphoid organ disorders and autoimmune manifestations were rectified by attenuating BCR proximal signaling strength using a BTK inhibitor, Ibrutinib (25). Importantly, autoimmune phenotypes were completely rescued in B-TRAF3-KO mice by introducing an antigen-specific BCR recognizing hen egg lysozyme (HEL) (25). Given that B-TRAF3-KO mice do not express HEL antigens, these HEL-specific B cells cannot receive stimulatory signals from their BCR. We infer that introducing a non-autoreactive BCR abrogates the abnormal expansion of B cells and reduces the severity of autoimmunity. Furthermore, our data showed that NF-κB2 is required for the expansion of B cells, especially MZ B cells, and splenomegaly in B-TRAF3-KO mice (25). TRAF3 restricted BCR signaling by preventing the processing of BCR-induced NF-κB2 precursor (p100) into active NF-κB2 (p52) upon anti-IgM/IL-4 stimulation (25). Taken together, these data suggest that the phenotypes of B-TRAF3-KO mice largely attribute to dysregulated BCR signaling pathway.

Anergy is an important mechanism to maintain B cell tolerance *via* unresponsiveness of the BCR to antigen stimulation (36). Anergic autoreactive B cells express a low level of surface IgM that does not induce calcium flux when stimulated with specific antigens or agonist anti-IgM (37, 38). We employed a bone marrow chimera system to establish an anergic autoreactive model by transferring B cells with HEL-specific BCR into ML5 transgenic mice that constitutively express HEL antigens, and showed that B cell anergy was well maintained in this model (25), consistent with prior studies (37, 39, 40). In contrast, we found that autoreactive B cell anergy was broken by TRAF3-deficiency in HEL-specific B cells evidenced by enhanced calcium flux upon HEL antigen stimulation (25). If anergy is properly maintained, secreted anti-HEL IgM production should be reduced, and surface IgM expression downregulated, a classic anergy phenotype, upon HEL stimulation. However, TRAF3-deficiency enables HEL-specific B cells to produce a high level of anti-HEL IgM and fail to downregulate surface IgM expression (25). We think that TRAF3-deficiency breaks B cell anergy possibly *via* elevating BCR proximal signaling strength, which is supported by our findings that TRAF3 deletion enhances BCR-induced phosphorylation of Syk and BTK as well as phospholipase Cγ2-dependent calcium flux (25); however, it remains to be addressed how TRAF3 restricts BCR proximal signaling strength.

DISCUSSION

Our recent studies discover novel checkpoint molecules, including TRAF2 and TRAF3, that were not appreciated previously. We found that these checkpoint molecules function to restrict the ability of the BCR to induce AID expression and CSR. However, additional questions remain to be addressed. Deletion of TRAF2 or TRAF3 in B cells enhances BCR-induced calcium flux (25), an early functional output of the BCR signaling. What mechanisms are employed by TRAF2 and TRAF3 to restrict BCR signaling intensity? Are there other signaling components of the BCR and co-receptor pathways that can also function as checkpoints and similarly affect the ability of the BCR to induce aberrant AID expression? How do TRAF2 and TRAF3 cooperate to restrain BCR-induced CSR since double deficiency of TRAF2 and TRAF3 does not further increase AID expression but significantly enhances CSR level compared to either single deficiency? Does TRAF2 deficiency break autoreactive B cell anergy as TRAF3 does? Addressing these questions may allow us to develop new strategies to rescue defective antibody responses in CD40-deficient mouse model or human PID patients, and to better treat autoimmunity or B cell lymphoma by modulating BCR signaling pathways.

Our data show that B cells from B-TRAF3-KO mice proliferate more robustly than control B cells upon BCR engagement (25). One unique characteristics of germinal

center (GC) B cells is their hyperproliferative capacity in the dark zone of GCs where somatic hypermutation (SHM) is thought to occur (41). Prior studies also showed that B-TRAF3-KO mice developed spontaneous GC formation (32). Thus, we speculate that TRAF2 and TRAF3 may also play a critical role in regulating SHM and antibody affinity maturation, which is the outcome of GC reaction.

Taken together, our studies present a new concept that may better explain how signaling components of the BCR and co-receptor pathways assure robust humoral immune responses while simultaneously preserve B cell homeostasis and prevent malignancy by fine-tuning the BCR signaling intensity. We propose that when BCR signaling intensity is increased to a level sufficient to induce AID expression and CSR, it may disrupt autoreactive B cell tolerance and perturb B cell homeostasis. Moreover, AID can induce DSBs and mutations in Ig and non-Ig genes that may initiate B cell genomic instability and lymphomagenesis. Thus, it may be critical to restrain the BCR from inducing AID expression in the absence of co-stimulation because this could serve as a protective mechanism that prevents overstimulated self-reactive B cells from turning cancerous.

AUTHOR CONTRIBUTIONS

ZC and JW wrote the manuscript. All authors contributed to the article and approved the submitted version.

FUNDING

This work was supported by UPMC Hillman Cancer Center startup funds to JHW, R21-CA184707, R21-AI110777, R01-CA166325, R21-AI133110, R01-CA229174 and R01-CA249940 to JHW, and a fund from American Cancer Society (ACS IRG #16-184-56) to ZC. The sponsors or funders have no role in the preparation, review, or approval of the manuscript.

ACKNOWLEDGMENTS

We thank Rachel A. Woolaver for proofreading the manuscript. We apologize to those whose work was not cited due to length restrictions.

REFERENCES

1. Stavnezer J, Guikema JE, Schrader CE. Mechanism and regulation of class switch recombination. *Annu Rev Immunol* (2008) 26:261–92. doi: 10.1146/annurev.immunol.26.021607.090248
2. Stavnezer J, Schrader CE. IgH chain class switch recombination: mechanism and regulation. *J Immunol* (2014) 193(11):5370–8. doi: 10.4049/jimmunol.1401849
3. Chen Z, Wang JH. Signaling control of antibody isotype switching. *Adv Immunol* (2019) 141:105–64. doi: 10.1016/bs.ai.2019.01.001
4. Vaidyanathan B, Yen WF, Pucella JN, Chaudhuri J. AIDing Chromatin and Transcription-Coupled Orchestration of Immunoglobulin Class-Switch Recombination. *Front Immunol* (2014) 5:120. doi: 10.3389/fimmu.2014.00120
5. Muramatsu M, Kinoshita K, Fagarasan S, Yamada S, Shinkai Y, Honjo T. Class switch recombination and hypermutation require activation-induced cytidine deaminase (AID), a potential RNA editing enzyme. *Cell* (2000) 102 (5):553–63. doi: 10.1016/s0092-8674(00)00078-7
6. Muramatsu M, Sankaranand VS, Anant S, Sugai M, Kinoshita K, Davidson NO, et al. Specific expression of activation-induced cytidine deaminase (AID), a novel member of the RNA-editing deaminase family in germinal center B cells. *J Biol Chem* (1999) 274(26):18470–6. doi: 10.1074/jbc.274.26.18470
7. Chaudhuri J, Basu U, Zarrin A, Yan C, Franco S, Perlot T, et al. Evolution of the immunoglobulin heavy chain class switch recombination mechanism. *Adv Immunol* (2007) 94:157–214. doi: 10.1016/S0065-2776(06)94006-1
8. Yan CT, Boboila C, Souza EK, Franco S, Hickernell TR, Murphy M, et al. IgH class switching and translocations use a robust non-classical end-joining pathway. *Nature* (2007) 449(7161):478–82. doi: 10.1038/nature06020
9. Boboila C, Yan C, Wesemann DR, Jankovic M, Wang JH, Manis J, et al. Alternative end-joining catalyzes class switch recombination in the absence of both Ku70 and DNA ligase 4. *J Exp Med* (2010) 207(2):417–27. doi: 10.1084/jem.20092449
10. Boboila C, Alt FW, Schwer B. Classical and alternative end-joining pathways for repair of lymphocyte-specific and general DNA double-strand breaks. *Adv Immunol* (2012) 116:1–49. doi: 10.1016/B978-0-12-394300-2.00001-6
11. Boboila C, Oksenych V, Gostissa M, Wang JH, Zha S, Zhang Y, et al. Robust chromosomal DNA repair via alternative end-joining in the absence of X-ray repair cross-complementing protein 1 (XRCC1). *Proc Natl Acad Sci USA* (2012) 109(7):2473–8. doi: 10.1073/pnas.1121470109
12. Alt FW, Zhang Y, Meng FL, Guo C, Schwer B. Mechanisms of programmed DNA lesions and genomic instability in the immune system. *Cell* (2013) 152 (3):417–29. doi: 10.1016/j.cell.2013.01.007
13. Chen Z, Wang JH. Generation and repair of AID-initiated DNA lesions in B lymphocytes. *Front Med* (2014) 8(2):201–16. doi: 10.1007/s11684-014-0324-4
14. Matter MS, Ochsenbein AF. Natural antibodies target virus-antibody complexes to organized lymphoid tissue. *Autoimmun Rev* (2008) 7(6):480–6. doi: 10.1016/j.autrev.2008.03.018
15. Pone EJ, Xu Z, White CA, Zan H, Casali P. B cell TLRs and induction of immunoglobulin class-switch DNA recombination. *Front Biosci (Landmark Ed)* (2012) 17:2594–615. doi: 10.2741/4073
16. Plotkin SA. Correlates of protection induced by vaccination. *Clin Vaccine Immunol* (2010) 17(7):1055–65. doi: 10.1128/CVI.00131-10
17. International Union of Immunological Societies Expert Committee on Primary I, Notarangelo LD, Fischer A, Geha RS, Casanova JL, Chapel H, et al. Primary immunodeficiencies: 2009 update. *J Allergy Clin Immunol* (2009) 124(6):1161–78. doi: 10.1016/j.jaci.2009.10.013
18. Liadaki K, Sun J, Hammarstrom L, Pan-Hammarstrom Q. New facets of antibody deficiencies. *Curr Opin Immunol* (2013) 25(5):629–38. doi: 10.1016/j.coi.2013.06.003
19. Parvaneh N, Casanova JL, Notarangelo LD, Conley ME. Primary immunodeficiencies: a rapidly evolving story. *J Allergy Clin Immunol* (2013) 131(2):314–23. doi: 10.1016/j.jaci.2012.11.051
20. Platt C, Geha RS, Chou J. Gene hunting in the genomic era: approaches to diagnostic dilemmas in patients with primary immunodeficiencies. *J Allergy Clin Immunol* (2014) 134(2):262–8. doi: 10.1016/j.jaci.2013.08.021
21. IJ H, Wentink M, van Zessen D, Driessen GJ, Dalm VA, van Hagen MP, et al. Strategies for B-cell receptor repertoire analysis in primary immunodeficiencies: from severe combined immunodeficiency to common variable immunodeficiency. *Front Immunol* (2015) 6:157. doi: 10.3389/fimmu.2015.00157
22. Xu Z, Zan H, Pone EJ, Mai T, Casali P. Immunoglobulin class-switch DNA recombination: induction, targeting and beyond. *Nat Rev Immunol* (2012) 12 (7):517–31. doi: 10.1038/nri3216
23. Pone EJ, Zhang J, Mai T, White CA, Li G, Sakakura JK, et al. BCR-signalling synergizes with TLR-signalling for induction of AID and immunoglobulin class-switching through the non-canonical NF-kappaB pathway. *Nat Commun* (2012) 3:767. doi: 10.1038/ncomms1769
24. Heltemes-Harris LM, Gearhart PJ, Ghosh P, Longo DL. Activation-induced deaminase-mediated class switch recombination is blocked by anti-IgM signaling in a phosphatidylinositol 3-kinase-dependent fashion. *Mol Immunol* (2008) 45(6):1799–806. doi: 10.1016/j.molimm.2007.09.020
25. Chen Z, Krinsky A, Woolaver RA, Wang X, Chen SMY, Popolizio V, et al. TRAF3 Acts as a Checkpoint of B Cell Receptor Signaling to Control Antibody Class Switch Recombination and Anergy. *J Immunol* (2020) 205(3):830–41. doi: 10.4049/jimmunol.2000322

26. Caamano JH, Rizzo CA, Durham SK, Barton DS, Raventos-Suarez C, Snapper CM, et al. Nuclear factor (NF)-kappa B2 (p100/p52) is required for normal splenic microarchitecture and B cell-mediated immune responses. *J Exp Med* (1998) 187(2):185–96. doi: 10.1084/jem.187.2.185
27. Lin WW, Hostager BS, Bishop GA. TRAF3, ubiquitination, and B-lymphocyte regulation. *Immunol Rev* (2015) 266(1):46–55. doi: 10.1111/imr.12299
28. Hostager BS, Haxhinasto SA, Rowland SL, Bishop GA. Tumor necrosis factor receptor-associated factor 2 (TRAF2)-deficient B lymphocytes reveal novel roles for TRAF2 in CD40 signaling. *J Biol Chem* (2003) 278(46):45382–90. doi: 10.1074/jbc.M306708200
29. Liao G, Zhang M, Harhaj EW, Sun SC. Regulation of the NF-kappaB-inducing kinase by tumor necrosis factor receptor-associated factor 3-induced degradation. *J Biol Chem* (2004) 279(25):26243–50. doi: 10.1074/jbc.M403286200
30. Gardam S, Sierro F, Basten A, Mackay F, Brink R. TRAF2 and TRAF3 signal adapters act cooperatively to control the maturation and survival signals delivered to B cells by the BAFF receptor. *Immunity* (2008) 28(3):391–401. doi: 10.1016/j.immuni.2008.01.009
31. Grech AP, Amesbury M, Chan T, Gardam S, Basten A, Brink R. TRAF2 differentially regulates the canonical and noncanonical pathways of NF-kappaB activation in mature B cells. *Immunity* (2004) 21(5):629–42. doi: 10.1016/j.immuni.2004.09.011
32. Xie P, Stunz LL, Larison KD, Yang B, Bishop GA. Tumor necrosis factor receptor-associated factor 3 is a critical regulator of B cell homeostasis in secondary lymphoid organs. *Immunity* (2007) 27(2):253–67. doi: 10.1016/j.immuni.2007.07.012
33. Woolaver RA, Wang X, Dollin Y, Xie P, Wang JH, Chen Z. TRAF2 Deficiency in B Cells Impairs CD40-Induced Isotype Switching That Can Be Rescued by Restoring NF-kappaB1 Activation. *J Immunol* (2018) 201(11):3421–30. doi: 10.4049/jimmunol.1800337
34. Chen Z, Getahun A, Chen X, Dollin Y, Cambier JC, Wang JH, et al. Imbalanced PTEN and PI3K Signaling Impairs Class Switch Recombination. *J Immunol* (2015) 195(11):5461–71. doi: 10.4049/jimmunol.1501375
35. Hoebe K, Beutler B. TRAF3: a new component of the TLR-signaling apparatus. *Trends Mol Med* (2006) 12(5):187–9. doi: 10.1016/j.molmed.2006.03.008
36. Yarkoni Y, Getahun A, Cambier JC. Molecular underpinning of B-cell anergy. *Immunol Rev* (2010) 237(1):249–63. doi: 10.1111/j.1600-065X.2010.00936.x
37. Goodnow CC, Crosbie J, Adelstein S, Lavoie TB, Smithgill SJ, Brink RA, et al. Altered Immunoglobulin Expression and Functional Silencing of Self-Reactive Lymphocytes-B in Transgenic Mice. *Nature* (1988) 334(6184):676–82. doi: 10.1038/334676a0
38. Duty JA, Szodoray P, Zheng NY, Koelsch KA, Zhang Q, Swiatkowski M, et al. Functional anergy in a subpopulation of naive B cells from healthy humans that express autoreactive immunoglobulin receptors. *J Exp Med* (2009) 206(1):139–51. doi: 10.1084/jem.20080611
39. Phan TG, Amesbury M, Gardam S, Crosbie J, Hasbold J, Hodgkin PD, et al. B cell receptor-independent stimuli trigger immunoglobulin (Ig) class switch recombination and production of IgG autoantibodies by anergic self-reactive B cells. *J Exp Med* (2003) 197(7):845–60. doi: 10.1084/jem.20022144
40. Cambier JC, Gauld SB, Merrell KT, Vilen BJ. B-cell anergy: from transgenic models to naturally occurring anergic B cells? *Nat Rev Immunol* (2007) 7(8):633–43. doi: 10.1038/nri2133
41. De Silva NS, Klein U. Dynamics of B cells in germinal centres. *Nat Rev Immunol* (2015) 15(3):137–48. doi: 10.1038/nri3804

Conflict of Interest: The authors declare that the research was conducted in the absence of any commercial or financial relationships that could be construed as a potential conflict of interest.

frontiers in Immunology

ORIGINAL RESEARCH
published: 30 March 2021
doi: 10.3389/fimmu.2021.637832

OPEN ACCESS

Edited by:
Zhenming Xu,
The University of Texas Health Science Center at San Antonio, United States

Reviewed by:
Niklas Engels,
University Medical Center Göttingen, Germany
Paolo Casali,
University of Texas Health Science Center at San Antonio, United States

***Correspondence:**
Manuel Fuentes
mfuentes@usal.es

†Present address:
Department of Immunology, Leiden University Medical Center (LUMC), Leiden, Netherlands

Specialty section:
This article was submitted to B Cell Biology, a section of the journal Frontiers in Immunology

Received: *04 December 2020*
Accepted: *10 March 2021*
Published: *30 March 2021*

Citation:
Díez P, Pérez-Andrés M, Bøgsted M, Azkargorta M, García-Valiente R, Dégano RM, Blanco E, Mateos-Gomez S, Bárcena P, Santa Cruz S, Góngora R, Elortza F, Landeira-Viñuela A, Juanes-Velasco P, Segura V, Manzano-Román R, Almeida J, Dybkaer K, Orfao A and Fuentes M (2021) Dynamic Intracellular Metabolic Cell Signaling Profiles During Ag-Dependent B-Cell Differentiation. Front. Immunol. 12:637832. doi: 10.3389/fimmu.2021.637832

Dynamic Intracellular Metabolic Cell Signaling Profiles During Ag-Dependent B-Cell Differentiation

Paula Díez[1,2†], Martín Pérez-Andrés[1], Martin Bøgsted[3], Mikel Azkargorta[4], Rodrigo García-Valiente[2], Rosa M. Dégano[2], Elena Blanco[1], Sheila Mateos-Gomez[1], Paloma Bárcena[1], Santiago Santa Cruz[5], Rafael Góngora[1], Félix Elortza[4], Alicia Landeira-Viñuela[1], Pablo Juanes-Velasco[1], Victor Segura[6], Raúl Manzano-Román[2], Julia Almeida[1], Karen Dybkaer[3], Alberto Orfao[1] and Manuel Fuentes[1,2]*

[1] Department of Medicine and Cytometry General Service-Nucleus, CIBERONC, Cancer Research Centre (IBMCC/CSIC/USAL/IBSAL), Salamanca, Spain, [2] Proteomics Unit, Cancer Research Centre (IBMCC/CSIC/USAL/IBSAL), Salamanca, Spain, [3] Department of Haematology, Aalborg University Hospital, Aalborg, Denmark, [4] Proteomics Platform, CIC bioGUNE, CIBERehd, ProteoRed-ISCIII, Derio, Spain, [5] Service of Otolaryngology and Cervical Facial Pathology, University Hospital of Salamanca, Salamanca, Spain, [6] Division of Hepatology and Gene Therapy, Proteomics and BioInformatics Unit, Centre for Applied Medical Research (CIMA), University of Navarra, Pamplona, Spain

Human B-cell differentiation has been extensively investigated on genomic and transcriptomic grounds; however, no studies have accomplished so far detailed analysis of antigen-dependent maturation-associated human B-cell populations from a proteomic perspective. Here, we investigate for the first time the quantitative proteomic profiles of B-cells undergoing antigen-dependent maturation using a label-free LC-MS/MS approach applied on 5 purified B-cell subpopulations (naive, centroblasts, centrocytes, memory and plasma B-cells) from human tonsils (data are available *via* ProteomeXchange with identifier PXD006191). Our results revealed that the actual differences among these B-cell subpopulations are a combination of expression of a few maturation stage-specific proteins within each B-cell subset and maturation-associated changes in relative protein expression levels, which are related with metabolic regulation. The considerable overlap of the proteome of the 5 studied B-cell subsets strengthens the key role of the regulation of the stoichiometry of molecules associated with metabolic regulation and programming, among other signaling cascades (such as antigen recognition and presentation and cell survival) crucial for the transition between each B-cell maturation stage.

Keywords: B-cell differentiation, naive B cell, centroblast, centrocyte, memory B cell, quantitative proteomics, transcriptomics integration

INTRODUCTION

The final stages of antigen-dependent human B-cell differentiation leading to (oligo)clonal B-cell expansion and affinity maturation are associated with activation of naive B-cells to their terminal differentiation into antibody-secreting plasma cells (PC) and memory B-cells, in secondary lymphoid tissues (SLT) such as tonsils (1). To initiate this highly dynamic and strictly regulated process, immature B lymphocytes leave the bone marrow and migrate *via* the peripheral blood (PB) to the spleen for maturation into naive B cells, which can then travel to the germinal centers (GC) of SLTs (2, 3). The antigen-dependent maturation starts with the presentation of protein antigens to helper T cells and the production of cytokines. Then, a broad antibody repertoire can be generated in developing B cells by means of somatic recombination. In order to increase the affinity and avidity of antibodies, an affinity maturation process occurs as a result of somatic hypermutation of immunoglobulin (Ig) genes in B cells, giving rise to the selection of strongly binding B cell receptors (BCR) (**Supplementary Figure S1A**) (3, 4).

Within the GC, the dark zone—where proliferation and somatic hypermutation occur—hosts the centroblasts (CB), which further differentiate into smaller centrocytes (CC) that enter the light zone of the GC. Both GC B-cell populations display a considerable overlap in their gene expression profiles, despite showing a clearly distinct morphological appearance (4, 5).

The specific molecular pathway, leading to the generation of memory B-cells following the GC reaction still remain largely unclear (5, 6). Most likely, different factors, such as the affinity of the BCR and the CD40 and CD40L signaling are key elements involved in this process (6). Thus, Smith et al. (7) have proposed a model for memory selection in which memory B-cells and PC are formed from different GC driving pathways, and Scheeren et al. revealed the role of STAT5 in the regulation of memory B-cell differentiation (6). In addition, Kulis et al. (8) through the analysis of the DNA methylome of 5 maturation-associated subpopulations of B-cells (pre-BII cells, naive B- cells, GC B-cells, memory B-cells and PC) showed a dynamic CpG methylation pattern during B-cell maturation, where memory B-cells and bone marrow PC showed the lowest methylation levels.

In recent years, several studies have investigated the genomic, epigenetic and transcriptomic profiles along normal B-cell differentiation (9–15). In turn, most data generated so far about the proteomic profile of B-cells at distinct differentiation stages has been derived from the study of cell lines at different time points after *in vitro* stimulation (e.g. anti-sIgM, lipopolysaccharide) using classical (16, 17) and innovative (18, 19) proteomic strategies. To the best of our knowledge, only one proteomic study (20) analyzed SLT-derived primary GC cells to investigate the similarities between the proteome of mantle cell lymphoma (MCL) cells and normal GC cells. However, the quantitative proteome of SLT-derived non-tumoral human primary B-cells along antigen-dependent B-cell maturation (from naive B-cells to PC and memory B-cells) has not been described so far.

Identification of aberrant protein profiles (related to the splicesome, proteasome, phagosome, HLA molecules, protein synthesis and stability) associated with physiological and pathological conditions such as aging, cancer, auto-immunity, allergy or immunodeficiency is of key relevance for the understanding of the underlying mechanisms involved since proteins are the biochemical effectors in virtually all cellular processes (21). Therefore, the analysis of the proteome of the normal B-cell counterpart of e.g. tumoral B-cells becomes a critical step.

Here, the role of multiple metabolic pathways at different stages of antigen (Ag)-dependent maturation is revealed from the overall (quantitative) global proteome of non-tumoral B-cell populations at different stages of Ag-dependent maturation from naive B-cells to recently generated PCs and memory B-cells from primary non-tumoral tonsils. Furthermore, we integrated the proteomics data set with publicly available transcriptomic data sets to provide a better view and understanding of the normal B-cell maturation process triggered by recognition, and to create a reference map for the identification of altered B-cell-associated protein expression profiles during life and in specific disease conditions.

Abbreviations: Ag, Antigen; BCR, B-cell receptor; CB, Centroblasts; CC, Centrocytes; FDR, False discovery rate; GC, Germinal centers; Igs, Immunoglobulins; MCL, Mantle cell lymphoma; M, Memory B-cell; N, Naive B-cell; PC, Plasma cells; PCA, Principal component analysis; PB, Peripheral blood; RT, Room temperature; SLT, Secondary lymphoid tissues; SHM, Through somatic hypermutation.

MATERIALS AND METHODS

Sample Collection

Freshly collected human tonsils were obtained from 5 donors (see **Table 1**) after routine tonsillectomies. In cases A, B, C, and D, tonsils were removed due to more than seven documented throat infections in the year preceding the surgery. In case E, tonsillectomy was performed to improve obstructive sleep apnea. In all cases, informed consent was given by the donor according to the guidelines of the local ethics committee of the University Hospital of Salamanca, in accordance with the Helsinki Declaration of 1975, as revised in 2008.

Single tonsil cell suspensions were obtained (immediately after surgery) by using conventional mechanical disaggregation procedures (3) in PBS. A minimum of 150 x 10^6 tonsil cells were stained in parallel in several different tubes (15 min at room temperature (RT) in the darkness) with the following 8-color combination panel of monoclonal antibodies: CD45 conjugated with fluorescein isothiocyanate (CD45-FITC), CD184 conjugated with phycoerythrin (CD184-PE), CD38 conjugated with peridinin chlorophyll protein-Cy5.5 (CD38-PerCPCy5.5), CD10 conjugated with PE- Cy7 (CD10-PECy7), CD20 and CD19 conjugated with APC (CD20-APC, CD19-APC), CD3 conjugated with allophycocyanine-H7 (CD3-APCH7), and CD27 conjugated with Brilliant Violet™ 421 (CD27-BV421) (22). Then, B-cell populations were systematically sorted by FACSAria (BD) at 4° C (cell population gating strategy shown in **Supplementary Figure S2**, sorting purity values shown in **Table 1**) based on the

TABLE 1 | Tonsil sample characteristics.

Tonsil	Sex	Age[a] (years)	Diagnosis	Tonsil-purified cells[b] (x 10^6) [%purity]				
				N	CB	CC	M	PC
I	M	6	Sleep apnea	6.9 [95%]	10.4 [95%]	8.5 [95%]	10.5 [90%]	1.7 [75%]
II	F	4	Tonsillitis	15.0 [98%]	13.0 [95%]	16.8 [99.9%]	12.8 [95%]	1.1 [85%]
III	F	26	Tonsillitis	5.7 [98%]	2.1 [98%]	2.1 [99.5%]	4.4 [98%]	<0.1 [91%]
IV	F	20	Tonsillitis	5.2 [93%]	5.5 [96%]	4.5 [99%]	3.3 [93%]	<0.1 [70%]
V	F	17	Tonsillitis	8.0 [98%]	3.0 [93%]	8.9 [99%]	8.3 [97%]	<0.1 [82%]

[a]*Age at time of surgery.*

[b]*By FACS-Aria sorting (Becton/Dickinson Biosciences, San José, CA).*

M, male; F, female; N, naive B-cell; CB, centroblast; CC, centrocyte; M, memory B-cell; PC, plasma cell.

The sex and age of the patients, as well as the diagnosis for tonsil surgery, are indicated. Additionally, the number of total purified cells from each tonsil sample is depicted together with the purity percentage of the sorted cells.

following phenotypes: naive B-cells ($CD45^+$, $CD184^-$, $CD38^-$, $CD10^-$, $CD19/CD20^+$, $CD3^-$, $CD27^-$), centroblasts ($CD45^+$, $CD184^+$, $CD38^+$, $CD10^+$, $CD19/CD20^+$, $CD3^-$, $CD27^{het}$), centrocytes ($CD45^+$, $CD184^-$, $CD38^+$, $CD10^+$, $CD19/CD20^+$, $CD3^-$, $CD27^{het}$), memory B-cells ($CD45^+$, $CD184^-$, $CD38^-$, $CD10^-$, $CD19/CD20^+$, $CD3^-$, $CD27^+$), and plasma cells ($CD45^+$, $CD184^-$, $CD38^{++}$, $CD10^+$, $CD19/CD20^+$, $CD3^-$, $CD27^{++}$) (3). Purified cells were immediately processed for protein extraction.

Protein Extraction

Each cell population (naive B-cells, CB, CC, memory B-cells, and PC) was washed three times with PBS (5 min, 1500 g). After draining off the total PBS volume without disturbing the cell pellet, the lysis buffer (9 M urea, 1 mM activated sodium orthovanadate, 2.5 mM sodium pyrophosphate, 1 mM β-glycerol phosphate, 20 mM HEPES pH 8.0) was added to the cell pellet (15 µL per 1 x 10^6 cells), followed by sonication on ice (3 bursts of 15 seconds each). Then, samples were centrifuged at maximum speed for 15 min and the supernatant containing the proteins was collected at -80°C until further processing.

Protein Quantification and SDS-PAGE

Proteins were quantified using the DC™ Protein Assay Kit II, as recommended by the manufacturer. A total of 15 µg of proteins from naive B-cell, CB, CC and memory B-cell samples were separated on a 4-20% gradient SDS-PAGE gel. After electrophoresis, gels were stained in a solution of 0.5% (w/v) Coomassie Brilliant Blue and stored at 4°C in an aqueous solution containing 1% (v/v) acetic acid, until analysis. PC protein samples were processed in solution.

In-Gel and In-Solution Protein Digestion

Two protein digestion approaches were performed due to PC sample limitations. Proteins from naïve B-cells, CB, CC, and memory B-cells were digested in gel, whereas proteins from PC were digested in solution since the amount of sample was not enough (high difficulty in isolating PC from tonsils due to their low relative numbers) to be processed in the gel. For in-gel protein digestion, each gel lane was cut into five fragments and digested with trypsin following the method of Shevchenko et al. (23) with slight modifications. Briefly, gel pieces were destained with 50% acetonitrile (ACN) and 50 mM ammonium bicarbonate. Protein reduction and alkylation were performed with 10 mM dithiothreitol (DTT) at 56°C for 45 min, and with 55 mM iodoacetamide at RT for 30 min, respectively. Proteins were digested with trypsin (6.25 ng/mL) at 37°C for 18 h. The peptide solution was acidified with 0.1% trifluoroacetic acid and desalted by using C18-Stage-Tips columns (24). The samples were partially dried and stored at −20°C until analysis by LC-MS/MS. For in-solution protein digestion, a total of 4 µg of protein from PC were reduced with 10 mM DTT at RT for 45 min and alkylated as previously indicated. Proteins were then digested with trypsin (1:50 w/w) at 37°C for 18 h and the peptide solution was processed as done for in-gel protein digestion.

LC-MS/MS Analysis

A nanoUPLC system (nanoAcquity, Waters Corp., Milford, MA) coupled to a LTQ Orbitrap XL mass spectrometer (Thermo Fisher Scientific, San Jose, CA) *via* a nanoelectrospray ion source (Proxeon Biosystems) was used for reversed-phase LC-MS/MS analysis. Peptides were loaded onto a trapping column (Symmetry 300 C18 UPLC Trap Column, 180 µm × 20 mm, 5 µm, Waters Corp.). Peptides were separated on a BEH130 C18 column 75 µm × 200 mm, 1.7 µm (Waters Corp.) equilibrated in 3% ACN and 0.1% formic acid with a linear gradient of 3% to 50% ACN at a flow rate of 300 nL/min over 140 min for in-gel digested proteins (naive B-cell, CB, CC, memory B-cell samples), and 170 min for in-solution digested proteins (PC samples). The nUPLC- LTQ Orbitrap XL was operated in the positive ion mode by applying a data-dependent automatic switch between survey MS scan and tandem mass spectra (MS/MS) acquisition. Survey scans were acquired in the mass range of m/z 400 to 2000 with a 30 000 resolution at m/z 400. The 6 most intense ions with states of 2 and 3 were selected in the ion trap for fragmentation by collision-induced dissociation with normalized energy. Dynamic exclusion was enabled for 30 s.

Gene Expression Microarrays

Data from the expression profiling of FACS-sorted B-cell subsets from 6 human tonsils on Affymetrix Human Exon 1.0 ST arrays were downloaded from the NCBI's Gene Expression Omnibus dataset (accession code GSE69033). Raw data was processed as described below.

Proteomics Analyses

Full downstream analysis was done employing a homemade custom program, using R v.3.4 (25) in the RStudio suite (26) (**Supplementary File 1**).

Qualitative Protein Expression Profiles

A binary heatmap of absence-presence was generated in order to compare all populations and analyze which patterns were shared by the different replicates. For each population, functional and pathway analyses *via* over-representation tests were done using the clusterProfiler package (27).

Quantitative Protein Expression Levels

Due to protein retrieval constraints, only four populations (CB, CC, naive, and memory subsets) could be compared for quantitative protein expression levels. Using the Progenesis suite, an ANOVA test with a q-value cutoff of 0.05 followed up by individual T-tests was used to determinate which proteins discriminated among different cell populations. The corresponding heatmap was generated by normalizing each protein by its own z-score among them. Absent proteins in a sample were considered to have zero expression. Hierarchical dendrograms using Euclidean distances were employed for clustering both genes and cell populations.

Transcriptomics Analyses

To operate with the gene expression profiling and analysis of the different populations of B-cells, the gene expression results of the GSE69033 (13) data set, including six biological replicates of each population, were selected. The mRNA of these cells was hybridized on an Affymetrix Human Exon 1.0 ST Array high-density oligonucleotide microarray. For each gene, an ANOVA test was performed followed by a Bonferroni p-value correction, and those genes with a p-value lower than 0.05 were investigated by a Tukey HSD test with the same cutoff, to determinate which populations could be distinguished.

Integration of Proteomics and Transcriptomics Datasets

Our proteomics and transcriptomics datasets come from different samples and subjects. To address this issue, a proteomics set and a transcriptomics set for each population were generated including the mean value for each protein or transcript present in all replicates (**Supplementary File 1**). To determine the expression patterns using both data sets, three Circos track plots (28) were generated. Each Circos plot contained line tracks with the quantitative information of the four comparable cell populations; one Circos plot had information of the log10 of our proteomics data (only proteins present in all 5 replicates), the second one for the log10 of the transcriptomic data (only transcripts whose proteins were present in all 6 replicates), and the last one contained the information of the log10 of the direct ratio between the proteomics and transcriptomics datasets. The results of the earlier mentioned ANOVA tests and follow-up tests were represented in attribute plots (29). At the same time, protein/transcript ratios were represented as a heatmap, scaling each ID by its own z-score. Populations were clustered *via* hierarchical dendrograms, using Euclidean distance, while ratios were clustered in four groups using density based clustering of applications with noise clustering *via* the dbscan package (30). ID conversion and coordinate retrieval were done using the biomaRt package (31, 32).

Quantification Analysis Using Progenesis

Progenesis QI for proteomics v3.0 software (Nonlinear Dynamics, Quayside, Newcastle Upon Tyne, UK) was used for quantification of the multiplexed LC-MduriS data. We compared the B-cell populations by analyzing 5 biological replicates. Specifically, for in-gel digested samples, the Progenesis LC-MS fractionation workflow was performed analyzing 5 fractions from each sample (each fraction corresponded to each band gel sliced during the gel processing). For sample alignment, the sensitivity was set to 5 and MS spectra with intensities > 500 0000, and ions with charges 2-7 were considered for the filtering process. Normalization was applied automatically to all features. Peptide identification was performed using Mascot Search engine (Matrix Science, London, UK) on Proteome Discoverer 1.4. software (Thermo) by searching against the neXtProt database (release December 20, 2016), including the common contaminant sequences (e.g., human keratins, trypsin, BSA). Search parameters were set as follows: carbamidomethylation of cysteine as a fixed modification, oxidation of methionine and acetylation of the protein N-terminus as variable ones, precursor and fragment mass tolerances were set to 10 ppm and 0.6 Da, respectively, and fully tryptic digestion with up to two missed cleavages. False discovery rate (FDR) was set at 1%. Peptide results were imported into the Progenesis QI software, for quantitative analysis and statistical evaluation. Identified peptides were refined removing identifications with a score less than 30, sequence length less than 6 and not human proteins. Peptides assigned to more than one protein were considered conflicting and resolved according to Progenesis guidelines. For reporting peptides and proteins, ANOVA ($p \leq 0.05$) and max fold change (≥2) values were calculated.

RESULTS

Mapping Ag-Dependent B-Cell Differentiation *via* Characterization of the Global Proteome of Tonsillar B-Cells at Different Maturation Stages

Qualitative evaluation of the global proteome of human B-cells at different stages of maturation was performed on purified naive B-cells, CB, CC, memory B-cells, and PC from 5 primary human tonsils (**Table 1**) as described in the *"Materials and Methods"* section (**Supplementary Figure S1**).

Only those proteins that were identified in all B-cell subpopulation replicates of the 5 tonsil samples were considered for further analyses. Overall, similar numbers of distinct proteins were identified for all B-cell subsets analyzed (a total of 1,992 proteins were identified on naive B-cells, 2,472 on CB, 2,548 on CC, and 2,567 on memory B-cells) except for PC

(n=393), which is potentially due to the overall lower protein amount obtained from the purified PC samples vs the other 4 B-cell subpopulations (median of 4 vs 15 µg of protein, respectively), due to the very low frequency of PC in tonsils (**Supplementary Table S1**; **Figure 1**). A more detailed analysis of the distribution of these proteins revealed an overlap of 350 proteins among the 5 B-cell subpopulations, up to 1,547 proteins being shared by naive B-cells, CB, CC and memory B-cells (in-gel processed subsets) (**Supplementary Figure S1**).

The binary heatmap in **Supplementary Figure S3** illustrates the clustering of tonsil B-cell subsets based on the presence/absence of proteins (qualitative proteomics characterization). Thus, two main groups were observed; group 1 included only the PC while group 2 included naive B-cells, CB, CC, and memory B-cells. Since such clustering was mainly due to the limited amount of sample processed for PC as discussed above, we further investigated the differences in protein expression profiles of the cell populations included in the second group. Such analysis showed that, among the 4 B-cell populations in the second group, naive B-cells were those showing a clearly distinct proteome, with clearly lower numbers of proteins identified, and suggesting that the overall number of proteins expressed increases as B-cell differentiation progresses from naive to memory B-cells. Of note, proteins exclusively expressed in GC B-cells (33) (**Supplementary Table S2**), mostly included proteins involved in DNA and RNA synthesis (RNA polymerase, MED21; RNA helicase, DDX47; DNA replication complex, GINS3; transcription, GTF2A2; translation, EIF4G2; initiation factors; nuclear pore glycoprotein, NUP62; and histone, HIST2H2BC). In turn, the proteins expressed solely in GC B- cells (i.e. CB and CC) laid in the expression of 24 of 2,472 (1%) specific proteins (**Figure 1**; **Supplementary Table S2**) in CB (proteins affecting B-cell receptor signaling such as VAV1, VAV2, GTPase RAP1GDS1; proteins involved in transcription process and histone acetylation such as BRD2 and in cell apoptosis process such as FADD) and 50 of 2,548 (2%) in CC (**Figure 1**; **Supplementary Table S2**) (e.g. NR3C1, BCL7A, PEG10, RGS13). Likewise, the investigation of naive B-cells displayed 7 of 1,992 (0.4%) proteins uniquely identified in this cellular subset (RNASEH2C, MRPL21, PURB, NDUFA3, HBQ1, PCBD2, and C9orf64) (**Figure 1**; **Supplementary Table S2**). Interestingly, the expression of specific proteins may determine the fate of the B-cells from the GC to differentiate into memory B-cells or PC. The qualitative comparison of the protein profiles of both subpopulations (i.e. memory B-cells and PC) (**Supplementary Table S1**) displayed that 29 proteins of the PC proteome were not expressed by memory B-cells, 25 of 393 (6%) of them were exclusively expressed in PC. These 29 PC-specific proteins included specific Ig molecules (IGKV3-11, IGKV3-15, IGHD, IGLC3, and JCHAIN), cytochrome C oxidases (COX6B1, COX7C), regulatory and transcription factors (IRF4, GTF2A1, LZTFL1), and the Abl interactor (ABL1) among other proteins. In addition, two of the remaining proteins were detected in both cell subsets but in different isoforms - isoform 1 (memory B-cells) and isoforms 5 and 2 (PC) for ADAR and PRKCAB proteins, respectively-. In contrast, 48 of 2,567 (2%) proteins were exclusively expressed by memory B- cells and not detected in PC (**Supplementary Table S2**), including the EBF1, BCL2L13, LRBA, IRF9, ITGB1, NMI, MRPL55, and THEMIS2 proteins.

Quantitative Maturation-Associated Protein Profiles From Naive to GC and Memory B-Cells

For quantitative protein analyses, a restriction criterion was established when a protein presented a value=0 for ≥1 of the 5 sample replicates investigated within each B-cell subpopulation; in such case, a value=0 was also assigned to the other replicates for that subpopulation (i.e. following the criteria established above for the qualitative analysis). However, the protein was not removed from the analysis as 0 has a quantitative meaning

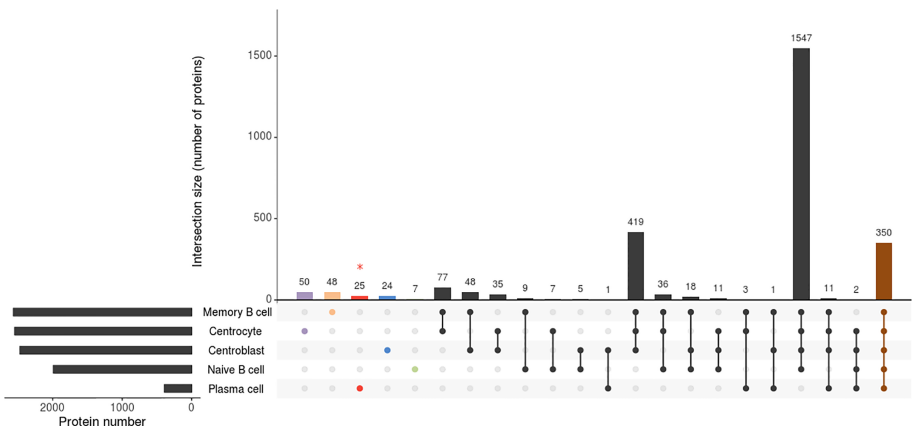

FIGURE 1 | Attribute plot displaying the qualitative proteomic analysis of the 5 B-cell subpopulations (naive B-cells, centroblasts, centrocytes, memory B-cells, and plasma cells). Each column indicates unique protein numbers and corresponds to either a unique population (violet-, orange-, red-, blue- and green-filled dots for centrocytes, memory B cells, plasma cells, centroblasts and naïve B cells, respectively) or a set of populations (black- and brown-filled intersected dots). The bar chart on the bottom left side plots the total number of proteins identified per B-cell population. * The proteomics processing of plasma cells was different due to sample limitations.

(absence of protein expression). In contrast, whenever a protein was "absent" across all B-cell populations analyzed, that protein was removed from further analyses. Thus, only differentially expressed proteins (ANOVA p-value<0.05) were included in the quantitative analysis for a total of 753 proteins expressed at significantly different levels (p-value<0.05) among the distinct B-cell subsets (**Supplementary Table S3**). Of note, due to the limited protein amount of PC protein samples, this B-cell subpopulation was not included in the quantitative proteome analyses that were thereby, exclusively performed on naive B-cells, CB, CC, and memory B-cells.

The quantitative proteomics data collected in **Supplementary Table S3** was the basis for the principal component analysis (PCA) shown in **Supplementary Figure S4**, which revealed grouping of the B-cell subpopulations according to the relative protein abundances with a clearly higher separation between naive B-cells and the other three B-cell populations. In turn, CB and CC clustered closely together, while memory B-cells appeared to be closer to naive B-cells.

The distribution of the 753 differentially expressed proteins across the distinct human chromosomes and the different B-cell subpopulations are depicted in **Supplementary Figure S5** (panels **A**, **B**, **C**). Of note, highly similar protein expression patterns were detected at the chromosome level for the GC and memory B-cells in contrast to naive B-cells, the latter showing lower expression levels for specific proteins encoded on chromosomes 1-4, 6, 8-9, 11, 14-15, 22 and X. Regarding the remaining chromosomes, protein expression profiles were similar among the four maturation-associated B-cell subsets analyzed, except for chromosome 11, for which naive B-cells and CB on one side, and CC and memory B-cells on the other side, were closer to each other.

Figure 2 depicts a hierarchical clustering analysis of the levels of these proteins differentially expressed among the distinct B-cell populations (naive B-cells, CB, CC, memory B-cells) (n=753) for each tonsil (1–5) sample analyzed. Overall, a high similarity was observed for all samples between CB and CC on one side, and to a less extent also, between naive and memory B-cells on the other side (except for two outliers, M5 and CB2). As discussed already above, this quantitative heatmap (together with that of **Supplementary Figure S3**) showed that the lowest protein expression values corresponded to the naive B-cells (coded as blue, Z-score values<0) whereas the highest ones corresponded to both CC and CB (coded as orange and red, respectively; Z-score values ≥2). Protein expression profiles of memory B-cells were more heterogeneous, including proteins presenting high expression levels and others being absent or expressed at low levels.

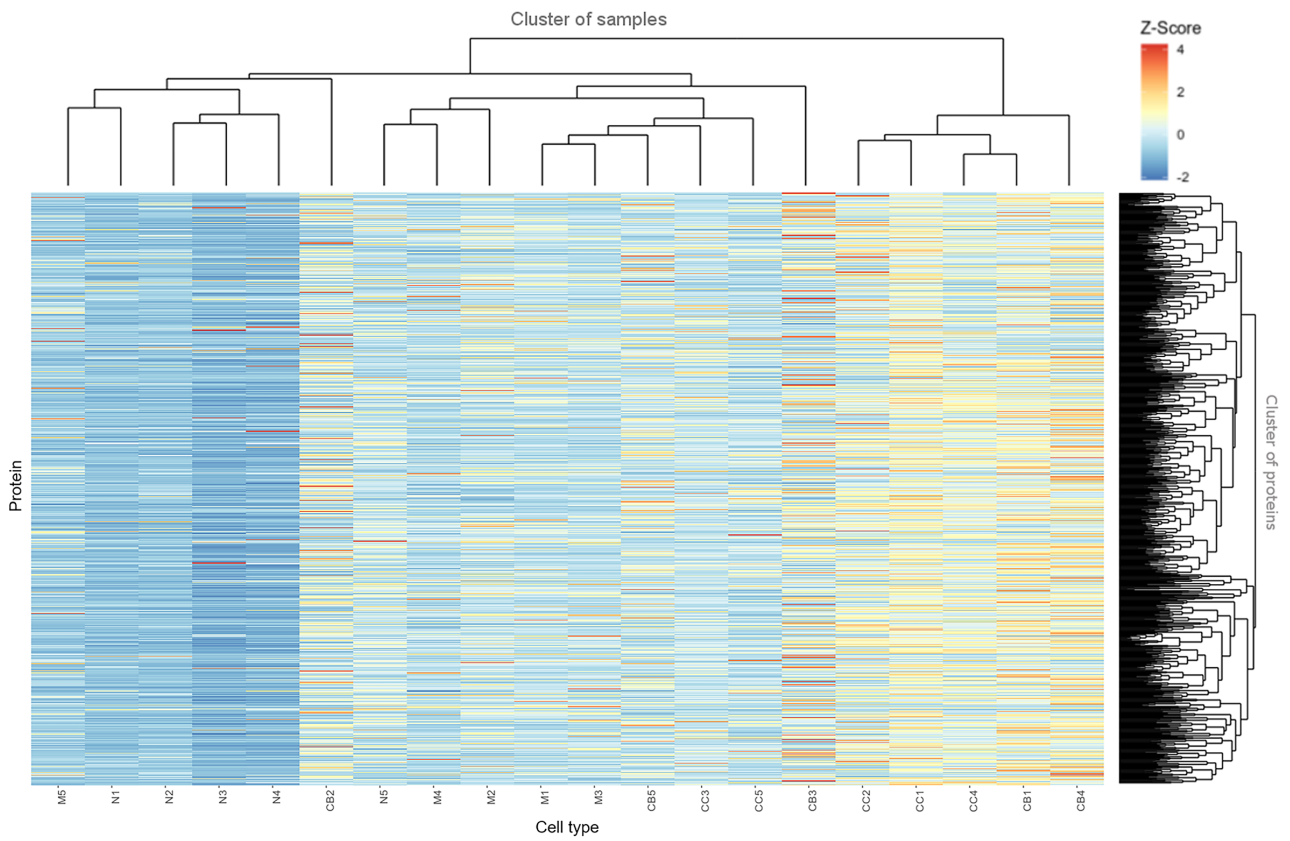

FIGURE 2 | Heatmap based on Z-score values for the proteins identified and quantitatively measured in naive B-cells (N), centroblasts (CB), centrocytes (CC) and memory B-cells (M). The color gradually changed from 4 (red) to 1 (yellow) and -2 (blue).

The distribution per cell population of the proteins showing the highest expression levels was as follows: 363 of 753 (48%) proteins were most strongly expressed in CB; 271 of 753 (36%) in CC; 97 of 753 (13%) in memory B-cells; and 22 of 753 (3%) were most strongly expressed in naive B-cells (as illustrated in **Supplementary Figure S6**). Conversely, the lowest expression levels for most proteins corresponded to the less differentiated cells (naive B-cells) - 608 of 753 (81%) proteins -, followed by memory B-cells – 92 of 753 (12%) -, and both CC and CB – 29 of 753 (4%) and 24 of 753 (3%) -, respectively (**Supplementary Table S3**).

Pairwise comparisons (1 vs 1) between the different B-cell subsets (**Supplementary Table S3**) showed (summarized results in **Supplementary Table S4** and **Supplementary Figure S7**) proteins with significantly different relative abundances between each pair of B-cell populations (p-value<0.05). Once again, naive B-cells were those with lower numbers of proteins being over-expressed (<10% of all differentially expressed proteins). Of note, CB and CC showed a homogeneous distribution (60-40%, respectively) indicating the great similarity between both B-cell populations. Additionally, proteins associated with memory B-cells were found to be under-expressed in all pair-wise comparisons, except vs naive B-cells.

Functional Evaluation of the Differential Protein Profiles Identified Across Different Maturation-Associated B-Cell Populations

Functional enrichment screening for those proteins differentially expressed across the distinct B-cell populations in the 5 tonsil samples analyzed (**Supplementary Table S5**) revealed that those 350 proteins which were systematically detected in all B-cell subsets (**Supplementary Table S1**) were annotated in 56 functional clusters highly enriched in general cell functions (e.g. actin and tubulin binding, biosynthesis, proteolysis, cell-cell adhesion, RNA processing and glucose metabolism).

Further analyses of the functional pathways associated with the individual B-cell subsets (**Supplementary Figure S8**; **Supplementary Table S5**) showed that proteins that were exclusively identified in naive B-cells participated in a few pathways (e.g. ribosome, metabolic pathways, and DNA replication) also common to the other B-cell subsets. In turn, memory B-cell proteins were related to a greater number of pathways, particularly the protein processing (i.e. synthesis, PTMs, stability, degradation), antigen processing and presentation, and JAK-STAT signaling pathways. Specific proteins expressed by CB and CC were related to Fc-gamma-R-mediated phagocytosis and chemokine signaling pathways. In turn, CB and memory subsets shared (specific) proteins belonging to the Toll-like receptor, TGF-beta, WNT, cAMP, IL17, Fc epsilon R, TNF and cell cycle signaling pathways. Likewise, the ERBB, PI3K-AKT, MAPK, and mTOR signaling pathways included proteins exclusively identified on CC and memory B-cells. Regarding PC-specific proteins, these were mostly involved in protein export, spliceosome, and metabolic pathways. Overall, the EGFR tyrosine kinase inhibitor resistance, DNA replication, MAPK signaling, antigen processing and presentation, ribosome, protein export, spliceosome and metabolic pathways were those most differentially represented across the naive, CB, CC, memory and PC proteomes.

Protein enrichment within these networks revealed the more significant modules (**Supplementary Figure S9A**, **Supplementary Table S6**) and pathways (**Supplementary Figure S9B**, **Supplementary Table S6**) involved. Thus, the module with a greater number of genes/proteins detected in all B-cell subpopulations related to ribosome/protein synthesis, also associated with the spliceosome network in the pathway analysis. Of note, the citrate cycle was the most significant pathway in PC.

Quantitative Protein Differences During B-Cell Differentiation

The variation in the (quantitative) levels of specific proteins throughout the four maturation-associated B-cell populations analyzed (i.e. naive B-cells, CB, CC, memory B-cells) provided interesting insights into the B-cell differentiation process. Relevant protein groups for B-cell development, functioning and survival are depicted in **Figure 3** and listed below. Findings are further explained in the *Discussion* section.

HLA proteins, responsible for the regulation of the immune system. In general, HLA-A proteins showed an increased expression in CB and memory B-cells with decreased values (even absent) in naive B-cells and CC. HLA-A-1 was significantly over-expressed in memory B-cells. Regarding HLA-B proteins, their expression progressively increased with higher B-cell differentiation from naive to memory B-cells, except for HLA-B-44. In turn, the HLA-DP, HLA-DQ and HLA-DR proteins showed a similar expression pattern, with a transient reduction in CB followed by a progressive recovery up to the memory B-cell subset; HLA-DOA displayed significantly higher expression levels in naive and memory B-cells.

Ig, serving as antigen receptors or neutralizing agents against specific antigens. Concerning Ig, no significant differences were observed for the IGHV as well as IGHM proteins. However, IGHA and IGHG1 displayed higher expression levels in GC B-cells (i.e. CB and CC). Regarding the Ig kappa/lambda light chains, the greatest differences among B-cell subsets were observed for the IGLL5 protein whose expression levels were decreased in CB and memory B-cells, while increased in naive B-cells and CC.

14-3-3 proteins, playing an isoform-specific role in class switch recombination. The expression profile of 14-3-3 proteins was constant across all 4 B-cell populations with higher levels in GC B-cells (CB and CC), and lower levels in naive and memory B-cells.

Caspases, for cell cycle regulation. Caspases and caspase-related proteins showed an unequal distribution along B-cell differentiation: some of these proteins showed low levels in CB and CC (CARD16, CASP14), another displayed increasing expression levels from naive to memory B-cells (CARD11), and another one had clear higher expression levels in the CB (CASP3).

B-cell associated proteins and adhesion molecules. The expression of these membrane proteins was characterized by

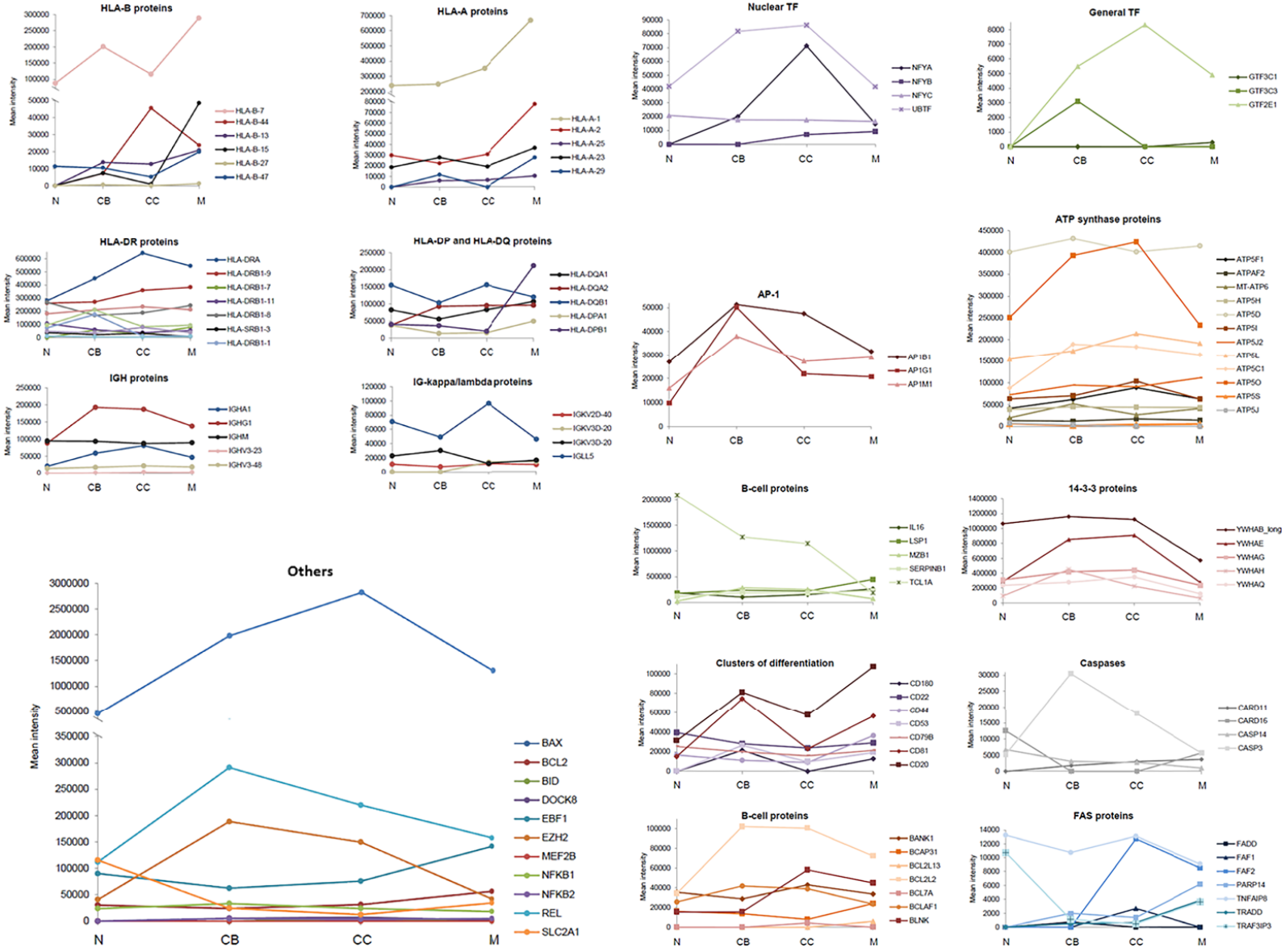

FIGURE 3 | Expression of specific groups of proteins across the different maturation-associated B-cell populations analyzed. The mean intensity obtained in the mass spectrometry analysis of the 5 replicates for each B-cell population was calculated and represented by family groups. *N*, naive B-cells; *CB*, centroblasts; *CC*, centrocytes; *M*, memory B-cells.

either high levels in CB and memory subsets (CD20, CD81, CD53, CD180) or uniform expression levels across all 4 B-cell subsets with a slight increase among naive B-cells (CD22, CD44, CD79B).

FAS-associated proteins, involved in apoptosis. Interestingly, Fas-associated proteins were absent in naive B-cells (FADD, FAF1, FAF2, PARP14, TRADD), except for TRAF3IP3 and TNFAIP8, which presented the highest levels in this B-cell subset. For the TRADD and PARP14 proteins, memory B-cells were those showing the highest expression values.

Transcription factors (TF). Expression of TF was increased in GC B-cells (CB and CC) compared to naive and memory B-cells, both as regards the nuclear and overall TFs identified to be positively expressed. The same distribution pattern was found for the AP-1 proteins.

ATP synthase proteins, to catalyze the cell energy production. No significant differences were observed for these proteins among naive, CB, CC and memory B-cells, except for ATP5O, which almost doubled its expression in CC (vs. naïve and memory B-cells).

"Missing Proteins" and their patterns across B-cell subpopulations. The Human Proteome Project (HPP) has identified a set of proteins called "missing proteins" in based the reported evidence of these proteins (34). These missing proteins are classified by HPP in 5 groups called PE1 (evidence at protein level), PE2 (evidence at transcript level), PE3 (inferred from homology), PE4 (predicted), PE5 (uncertain). Then, complementary study to quantitative protein expression levels was evidence of protein existence (PE) classification (way to classify the so-called "Missing Proteins"). Here, it is explored only from the protein datasets (mean protein expression value) which identified protein candidates on groups PE1, PE2, PE5. Thus, 606 proteins have been correlated with a transcriptomics counterpart in the expression microarray, where 599 are include in PE1, one in PE2 and 6 in PE5. In the case of PE2 protein, RGS13 (with evidence at transcript level) is involved in signal transduction; while the six proteins (NCF1B, HSP90AB3P, HIST2HBC, SNX29P2, RPL0P6, POTEKP) in group PE5 are involved in stress response, DNA-binding, phosphatidylinositol binding, ribosomal protein and ATP binding (**Supplementary Table S7**). Within this group of PE5 proteins, the proteins HSP90AB3P, HIST2HBC and RPLP0P6, related with DNA-binding, stress response and ribosomal functions, show a differential protein profile during B-cell differentiation, where low levels are observed in naive B-cells and memory B-cells and progressive level expression increase is depicted for CB, whereas for CC there is a progressive decrease. Regarding the proteins NCF1B and SNX29P2, which are phosphatidylinositol binding proteins, present a similar pattern a similar profile, with progressive increasing of its expression level from naive B-cells to CC, and low levels in memory B-cells. Finally, POTEKP presents a completely different pattern from the other ones, with low levels in naive B-cell, increasing pattern in CB and memory B-cell and decrease profile in CC (**Supplementary Figure S10**).

Other proteins. IL16, LSP1, MZB1, SERPINB1, BCAP31, and BCL2L13 showed higher expression levels on memory B-cells vs all other subsets. In contrast, the highest expression levels for TCL1A were found in naive B-cells, gradually decreasing down to the memory B-cells compartment. Also, BCL2L2 presented the lowest expression levels among naive B-cells whereas the highest ones were detected in CB, CC and, particularly memory B-cells. EBF1 was expressed at slightly higher levels in CC vs CB, with the highest levels being observed on memory B-cells. In turn, REL, EZH2, and BAX presented the lowest expression levels in naive B-cells and high expression levels in CB. Regarding the expression level of BCL2, the memory subset displayed the highest values of the quantitative expression.

Correlation Between the Transcriptome and the Proteome of Distinct Maturation-Associated B-Cell Populations

The results of previously reported transcriptomics analyses, performed on the same maturation-associated B-cell populations, following identical processing and purification strategies (13), were compared with our proteomics results. A total of 6 tonsils were analyzed for transcriptomics and the resulting values (after processing transcriptomics data) were averaged as performed also for the proteomics data of this study.

First, the global list of genes contained in the transcriptomics platform, together with the differentially expressed genes (**Supplementary Table S8**) and their correspondence to differentially expressed proteins (ANOVA p-value<0.05) detected by LC-MS/MS was integrated and evaluated. Results of such comparative analyses (**Supplementary Figure S7A**) revealed a greater number of molecules differentially expressed by transcriptomics than those detected in the proteomics analysis (**Supplementary Figure S7B**), which could have been expected due to the total genome coverage of the transcriptomics platform vs the quantitative proteomics dataset. Thus, only 6% (201 of 3,241) of those transcripts that were found to be differentially expressed were associated also with a significantly differentially expressed (translated) protein. Additionally, a greater number of differentially expressed genes between naive B-cells and GC B-cells was found (2,826 of 3,241 genes; 87%). By contrast, naive and memory B-cells were more similar at the transcriptomic level showing only 450 of 3,241 (14%) genes differentially expressed between them. As done for the proteomics dataset, a representative cluster plot was generated to evaluate the distribution of the genes expressed in the different B-cell populations per chromosome (**Supplementary Figure S5B**).

To evaluate the correlation between transcriptomics and proteomics datasets for the different B- cell populations analyzed (naive, CB, CC, and memory), an updated version of the R-script tool previously described by our group (35) for integrating both sets of data was used. After calculating the corresponding ratios between proteomics and transcriptomics expression values (**Supplementary Table S9**), the results revealed higher protein/transcript ratios for CB, CC and memory B-cells than for the naive B-cells (**Figure 4**). A total of 569 paired genes/proteins were present in both datasets and therefore compared (expressed genes not detected by the proteomics approach were not included in this correlation analysis, **Supplementary Table S8**). This hierarchical clustering analysis (**Figure 4**) revealed two main groups of cells: group 1 consisting of naive and memory B-cells;

and group 2, that included GC (CB and CC) B-cells. These data are also represented in **Supplementary Figure S5C** displaying the differences among the distinct B-cell subpopulations at the gene/protein levels per chromosome (i.e. protein-encoding genes in chromosomes 1, 4-6, 9, 15-16, 19, 22). Also, **Supplementary Table S10** and **Supplementary Figure S11** display five major protein clusters (obtained after self-organizing map (SOM) analysis from data collected in **Supplementary Table S3**) representing once more the protein expression dynamics across the distinct B-cell subpopulations. For example: SRSF2 and PDIA4 proteins from cluster 1 displayed higher gene/protein ratios at CC population, whereas proteins from cluster 5 (TRAF3IP3, CPOX, TPK1, S100A6, DCTD, LGMN) depicted lower ratio levels in the same population.

Evaluation of the Expression of Proteins Specific for One or More Maturation-Associated B-Cell Populations by Multi-color Flow Cytometry (FCM)

The expression patterns of a subset of 11 differentially expressed proteins across the 4 B-cell populations analyzed (i.e. naive B-cells, CB, CC, and memory B-cells) was also quantitatively evaluated by FCM on the B-cell surface membrane (CD20, CD22, CD44, CD45, CD54, CD71, CD74, CD79B, CD81, and CD98) or at the intracellular levels also TCL1A. Overall, highly similar expression patterns were found for around half of these proteins (511; 45%) (**Supplementary Figure S12**): CD44, CD54, CD71, CD74, and TCL1A. Of note, FCM analysis confirmed our previous results about the expression levels of the TCL1A

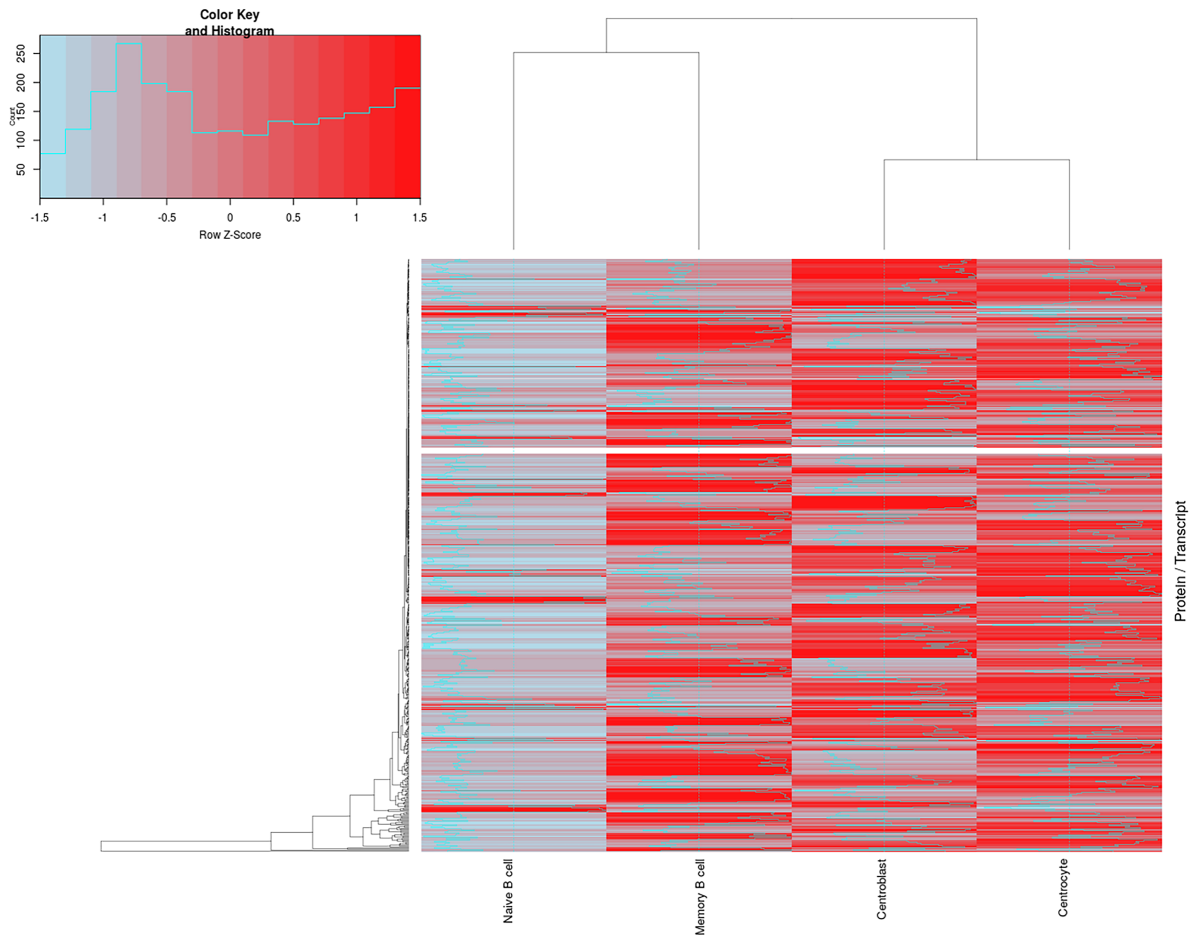

FIGURE 4 | Correlation between the proteomics and transcriptomics datasets for the distinct maturation-associated B-cell populations analyzed. The figure depicts a total of 569 genes/proteins detected by both approaches and the corresponding hierarchical clustering analysis for the 4 B-cell subpopulations (naive B-cells, centroblast, centrocyte and memory B-cells) investigated. Z-score values assuming the differences of proteomics/transcriptomics correlations are color-coded (blue for low P/T ratios and red for high P/T ratios). Lists of genes/proteins, as well as the ratio values, are shown in **Supplementary Table S9**.

protein, which decreased with increasing B-cell differentiation from naive to GC and memory B-cells.

DISCUSSION

Human B-cell differentiation has been extensively investigated on genomics and transcriptomics grounds (12, 15, 35), providing relevant data about those genes (and their modifications) and transcripts that regulate B-cell differentiation. Nevertheless, no studies have addressed so far, a detailed analysis of cells at different Ag-dependent human B-cell maturation stages from a quantitative and differential intracellular signaling proteomic perspective. Despite genomic information is highly relevant to understand the molecular basis of B-cell differentiation, the dynamics of this process can only be fully understood by also exploring and integrating the corresponding transcriptome and proteome information for each maturation stage (33, 34, 36, 37). Specifically, the main level of information required to understand the functioning of cells is the global analysis of proteins (i.e. key functional components of the cell) (38). However, the accomplishment of this examination is complex due to the amino acids features, the protein modifications and degradation, and the intricate and variable signaling networks in which proteins are involved (37).

Here, the quantitative proteomic profiles of human B-cells undergoing Ag-dependent maturation in tonsils have been described, depicting the intracellular pathways involved and the correlation with transcriptomics data. Thus, 5 different B-cell subpopulations at distinct stages of maturation (naive B-cells, CB, CC, memory B-cells, and PC) were highly purified from 5 human tonsils and proteomics-profiled by using a label-free quantitative LC-MS/MS approach. Qualitative analyses were performed on all 5 B-cell subsets, providing insights into their proteome maps that contributed to the understanding of how each B-cell subset gives rise to the next one. Quantitative proteomics comparisons shed further light on those differentially significantly expressed proteins, which may influence the switch among the studied B-cell maturation stages. Overall, our results showed a high overlap of the proteome of the 5 B-cell populations. Focusing on naive B-cells, CB, CC and memory B-cells, which were processed in a fully comparable way, this overlapping involved up to 1,897 proteins, which constituted 95% of proteins expressed by naive B-cells and ~75% of proteins detected in CB, CC, and memory B-cells. As might be expected, these proteins were typically involved in general cell functions such as actin and tubulin binding, biosynthesis, proteolysis, cell-cell adhesion, RNA processing and glucose metabolism. Despite the high intersection among the proteomes of B-cells at different maturation stages, specific proteins were also identified within each B-cell subset. Thus, GC-specific proteins included MED21, DDX47, GINS3, GTF2A2, EIF4G2, NUP62, and HIST2HBC, found in both the CB and CC proteomes, which are associated with FC-gamma-R-mediated phagocytosis and chemokine signaling pathways. In turn, while CB expressed VAV1, VAV2, RAP1GDS1, BRD2, and FADD among other proteins, CC exclusively expressed NR3C1, BCL7A, PEG10, and RGS13 within a total group of 50 unique proteins in the absence of the above listed CB-specific proteins. Of note, RGS13, whose expression was restricted to CC, has an important role in chemotaxis and the limitation of the expansion of GC cells (39). In turn, the expression of the VAV1/2 proteins restricted to CB is crucial for PC development and secretory Ig production (40), suggesting that PC might originate from a subset of CB-cells that up-regulate VAV1 and VAV2 expression leading to the induction of PC formation. In turn, naive B-cells presented only 7 exclusive proteins (i.e. RNASEH2C, MRPL21, PURB, NDUFA3, HBQ1, PCBD2 and C9orf64) involved in ribosome formation, metabolic pathways, and DNA replication.

At present, the precise proteins that are associated with differentiation of GC B-cells to memory B-cells vs PC still remain largely to be identified (41). Overall, our results showed 29 PC-specific proteins that were not identified in paired memory B-cells. These proteins were related to Ig (IGKV3-11, IGKV3-15, IGHD, IGLC3 and JCHAIN), cytochrome C oxidases (COX6B1, COX7C), regulatory and transcription factors (IRF4, GTF2A1, LZTFL1), and the Abl interactor ABL1. From these proteins, IRF4 has been claimed to define Ig-secreting PC by De Silva et al. (4, 42), being its expression associated with protein networks related to protein export, the spliceosome, and metabolic pathways among which the citric acid cycle network is the most significant. This, together with increased expression of cytochrome C oxidases in PC vs GC and memory B-cells might reflect the high energy consumption of PC, probably required because of their high Ig-secreting functionality. In parallel, high expression of multiple transcription factors discloses a unique increase in gene expression in these cells affecting previously silenced genes (i.e. a new transcriptional cell program). Finally, overexpression of ABL1 confirms previous observations by Li et al. (43) which revealed the role of this tyrosine kinase on PC survival.

In turn, the EBF1, BCL2L13, LRBA, IRF9, ITGB1, NMI, MRPL55 and THEMIS2 proteins were exclusively expressed in memory B-cells. Among others, these memory B-cells linked proteins involved in metabolic pathways, antigen processing and presentation, and the JAK-STAT signaling pathway. Thus, LRBA promotes proliferation, clonal expansion and cell survival of antibody-secreting cells and its deficiency has been demonstrated to reduce proliferation (44, 45). In turn, high levels of ITGB1 (also known as CD29) have been detected in memory B-cells (46). Of note, THEMIS2 was exclusively identified in the memory B-cell compartment, despite it seems to be not required for B-cell development (47).

Overall, naive B-cells emerged as the less differentiated cells of all B-cell subsets analyzed as for its protein expression profile strongly overlapped with that of the other B-cell populations, which showed greater proteomic diversity. However, qualitative differences existed for only a limited number of all expressed proteins. In contrast, more differentially expressed proteins were identified when the relative quantity of each protein across the distinct B-cell differentiation stages was considered. Additionally, quantitative analysis depicted 753 proteins to be differentially expressed in naïve B-cells, CB, CC, and memory B-cells.

Interestingly, for these proteins, similar amounts and expression patterns were found for CB and CC on one side, and for naive and memory B-cells on the other side, with the lowest protein expression values being detected in naive B-cells further supporting their less differentiated nature. In contrast, the highest levels of protein expression were found for GC B-cells depicting the high functionality and protein turnover characteristic of these cells (2). Subsequent pair-wise comparisons between each B-cell population and both the previous and/or subsequent maturation stages confirmed the highly similar and homogeneous (quantitative) proteomics profile of CB and CC (2). By contrast, proteins of naive B-cells were under-expressed vs all other maturation stages.

More detailed analysis of those specific protein groups differentially expressed across the different maturation-associated B-cell populations revealed new insights into their functional proteomics throughout B-cell maturation. Thus, for the HLA-associated proteins, significantly high expression levels of HLA-DO were found in naive and memory B-cells vs GC cells, confirming previous observations by others studies (2, 48). In contrast, expression of the HLA-DR and CD74 molecules was higher within GC cells compared with the other two B-cell populations. These results support those of Chalouni et al. suggesting that when a specific Ag encounters naive B-cells, synthesis of new HLA II molecules is initiated to favor CB selection (48). Within the HLA I, expression of HLA-A and HLA-B proteins progressively increased as the B-cell maturation process advanced, except for HLA-B44, which would support the greater endogenous Ag-peptide presenting capacity of long-lived PC and memory B-cells vs short-lived naive B-cells. Regarding Ig molecules, two main expression patterns were observed: i) no differences among the B-cell subsets were found for IGHM and IGHV, while ii) greater expression values were found for IGHA, IGHG, Igλ, Igκ in GC B-cells vs both naive and memory B lymphocytes. Whereas the production of the mu and variable heavy chains of the Ig starts in the bone marrow, production of IgG and IgA requires class switch recombination in the GC, which likely explains our observations (49). In line with these findings, the 14-3-3 proteins involved in class-switch recombination expressed also significantly higher levels in CB and CC B-cells as also previously demonstrated by Xu et al. (50).

Interestingly, a relatively high number of differentially expressed proteins play distinct roles in apoptosis and/or survival of B-cells. For instance the CARD11 scaffold protein showed increasing levels from naive B-cells (lacking CARD11 expression) to memory B-cells, this protein being altered in a spectrum of diffuse large B-cell lymphomas (DLBCL) (51), mainly those derived from GC (GCB-DLBCL) and activated B-cells (ABC-DLBCL) (52), where it plays a key role in activating the NF-kB pathway to induce the B-cell proliferation and the proliferation vs death checkpoint in activated B-cells (52). TRADD also activates this pathway (53) and it was found to be overexpressed in memory B-cells vs less differentiated mature B-cells; which may be very interesting from a pathogenic point of view. Conversely, CASP3, a key regulator of Fas-mediated cell death in mature peripheral B-cells (54), was highly expressed in GC cells, particularly in CB (55). Of note, most Fas-related proteins were missing in naive B-cells, which might be due to the need of these cells to expand for continuing their B-cell differentiation and ensuring antibody production.

Study of missing proteins patterns shows expression profiles in accordance with the processes that occur along the cellular differentiation of the B-lymphocyte. High levels of DNA binding protein in CB are related to mutation for function receptor generation and cell proliferation, and this type of proteins decreases its levels as B cells differentiate into CC and memory B-cells. A similar pattern was observed for stress response and ribosomal proteins, since CB presented high expression levels due to the changing environment in which they are found. Regarding phosphatidylinositol binding protein, high levels were observed in CC, correlating with the active cell signaling due to antigen presentation required at this differentiation stage. Finally, ATP-binding protein presented a higher relative expression in memory B-cells compared to others, which correlated with the vesicle transport processes occurring in the immune synapse for antigen presentation in MHC molecules to T lymphocyte (56–61). Regarding other B-cell related proteins, distinct differentiation-associated profiles were observed. Thus, while CD22, CD44, and CD79B showed similar expression values throughout the B-cell maturation, other markers such as TCL1A, CD20, CD53, CD81 and CD80 varied substantially. Accordingly, expression of TCL1A was detected at the highest levels in the first stages of maturation (e.g. naive B-cells), it was reduced upon GC development and silenced in long-lived memory B-cells, as previously shown also by others (62). In contrast, IL16 protein levels peaked in memory B-cells and the highest CD20, CD53, CD81, and CD180 protein amounts were observed in CB and memory B-cells. Of note, expression of CD20 correlated with the expression of both HLA-A and HLA–B molecules, and CD81, which could reflect the well-known role of CD20-HLA-I and CD20-CD81 interactions required for the regulation of cell cycle progression in B-cells (63). Similarly, NFKB1 and NFKB2, two proteins that play an important role in B-cell activation and GC formation, were both detected at higher levels in CB and CC vs naive and memory B-cells (4). In turn, BCL2 was highly expressed in memory B-cells, supporting its role in the development and survival of the long-lived B-cell subset. In line with these observations, the expression of the BAX and BID pro-apoptotic proteins was higher in CB vs both naive and memory B-cells, respectively (64). Finally, the expression of EZH2 was increased in both CB and CC GC B-cells, their levels decreasing thereafter when the cells leave the GC (4).

In summary, our results provide a first map of the proteome of Ag-dependent B-cell maturation in tonsils supporting the value of quantitative proteomics data, which provides more information than that of qualitative proteomics solely based on the presence vs absence of the proteins. In addition, we show that along the differentiation of mature B-cells, the naive B-cell compartment typically shows expression of fewer proteins usually at lower levels, most of which are shared by the immature GC and memory B-cells. Of note, a highly similar proteomics profile was found for CB and CC while memory B-cells more closely mimicked naive B-cells

despite both cell compartments are at the greatest distance B-cell maturation process.

DATA AVAILABILITY STATEMENT

The full mass spectrometry proteomics data reported in this paper has been deposited to ProteomeXchange Consortium via the PRIDE (65) partner repository with the dataset identifier PXD006191.

AUTHOR CONTRIBUTIONS

Conceptualization, AO, MF, and PD. Methodology, PD, MP-A, MB, MA, RMD, EB, SM-G, PB, FE, RM-R, VS, AL-V, PJ-V, and KD. Software, RG-V. Validation, PD and RG-V. Formal analysis, PD and RG-V. Investigation, PD. Resources, MF, AO, JA, RG, SSC, MP-A, KD, and FE. Writing—original draft, PD. Writing—review and editing. RM-R, MF, and AO. Visualization, PD, RG-V, VS, AL-V, and PJ-V. Supervision, MF and AO Funding acquisition, MF and AO. All authors contributed to the article and approved the submitted version.

FUNDING

We gratefully acknowledge financial support from the Spanish Health Institute Carlos III (ISCIII) for the grants: FIS PI14/01538, FIS PI17/01930 and CB16/12/00400. We also acknowledge Fondos FEDER (EU) and Junta Castilla-León (COVID19 grant COV20EDU/00187). Fundación Solórzano FS/38-2017.The Proteomics Unit belongs to ProteoRed, PRB3-ISCIII, supported by grant PT17/0019/0023, of the PE I + D + I 2017-2020, funded by ISCIII and FEDER. AL-V is supported by VIII Centenario-USAL PhD Program. PJ-V is supported by JCYL PhD Program and scholarship JCYL-EDU/601/2020. PD and EB are supported by a JCYL-EDU/346/2013 Ph.D. scholarship. The authors thank the Cell Sorting Service (NUCLEUS, University of Salamanca) for technical assistance.

SUPPLEMENTARY MATERIAL

The Supplementary Material for this article can be found online at: https://www.frontiersin.org/articles/10.3389/fimmu.2021.637832/full#supplementary-material

Supplementary Table 1 | Qualitative results. The lists of identified proteins are shown for each B-cell subpopulation (naive B-cells, N (sheet 1); centroblasts, CB (sheet 2); centrocytes, CC (sheet 3); memory B-cells, M (sheet 4); plasma cells, PC (sheet 5)) including the protein identifier (Uniprot ID), complete name of the protein (description), abundance values for each B-cell subpopulation and replicate (1-5), and mean value. The sheet 6 contains the lists of proteins in common among B-cell subpopulations and the unique proteins per group resulting from a Venn analysis.

Supplementary Table 2 | Unique proteins identified per B-cell subpopulation. Lists of proteins (gene name) exclusively identified in the indicated B-cell subpopulation are shown.

Supplementary Table 3 | Quantitative analysis. The lists of proteins of the quantitative analysis are depicted (sheet 1) together with the 1-to-1 comparisons (sheets 2-7). The UniProt ID (accession), the number of detected peptides per protein (peptide count), the number of unique peptides per protein (unique peptides), the confidence score, the ANOVA p-value (ANOVA (p)), the max fold change, the B-cell population with the highest mean for each protein (highest mean condition), the B-cell population with the lowest mean for each protein (lowest mean condition), the complete name of the protein (description), and the normalized abundance for each replicate within each B-cell population are indicated. The significant proteins (ANOVA p-value < 0.05) detected after pair-wise comparisons of B-cell subpopulations. 1 means "significant differences", 0 means "no significant differences" (sheet 8).

Supplementary Table 4 | Quantitative protein results after comparing B-cell subpopulations with each other. The total number of significantly expressed proteins within each comparison is depicted as well as the number and percentage of proteins highly expressed in one subpopulation compared to the other one.

Supplementary Table 5 | Functional enrichment analysis (FEA) of the proteins identified in the 5 B-cell subpopulations. The file contains 5 Tables with the annotated clusters (p-value<0.05): (I) Table "350 in common" shows the 56 annotated clusters identified for the proteins in common across the naïve (N), CB, CC, memory (M), and PC subsets. (II) Table "1547_N_CB_CC_M" includes the 129 annotated clusters identified for the proteins in common across N, CB, CC, and M subsets. (III) Table "419_CB_CC_M" displays the 63 annotated clusters for proteins in common in CB, CC, and M subsets. (IV) Table "77_CC_M" shows the two annotated clusters for proteins in common between CC and M subpopulations. (V) Table "25_PC" depicts the two annotated clusters identified for the 25 proteins exclusively detected in the PC subset. (VI) Lists of proteins identified within each B-cell subpopulation across the pathways represented in **Supplementary Figure S8**.

Supplementary Table 6 | Significantly enriched modules and pathways related to the 5 B-cell subpopulations. The file contains 2 Tables: (I) Table "Modules" shows the different modules per B-cell subpopulation and the corresponding p-value, q-value and adjusted p-value, as well as the GeneName and GeneSymbol of the genes included in the module. (II) Table "Pathways" shows the same information as stated above for the pathways.

Supplementary Table 7 | Data set missing proteins detected by MS/MS. Information on missing proteins detected after proteomic analyses in progress of B-lymphocyte differentiation during antigen-dependent phase.

Supplementary Table 8 | Transcriptomic data. The file contains: (I) the results of the expression profiling of B-cell subsets sorted from human tonsils on Affymetrix Human Exon 1.0 ST arrays (raw data deposited at NCBI's Gene Expression Omnibus database, GSE69033) after calculating the mean expression values (6 biological replicates) for each B-cell subset (naive B-cells, centroblasts, centrocytes, memory B-cells and plasma cells). The presence/absence of each gene displayed on the array in the proteomic analysis is also indicated. (II) The significant genes (ANOVA p-value < 0.05) detected after pair-wise comparisons of B-cell subpopulations. 1 means "significant differences", 0 means "no significant differences". (III) Lists of proteins, genes and their combination which have shown significant differences in the ANOVA test (p-value<0.05).

Supplementary Table 9 | Proteomics/transcriptomics ratios. The correlation between both strategies was calculated according to the mean values for each gene/protein within each B-cell subpopulation. (I) Proteomics mean values for the 606 proteins having a transcriptomic counterpart in the expression microarray. (II) Proteomics/transcriptomics ratios for the 569 genes/proteins presenting values in both datasets.

Supplementary Table 10 | Data set Proteomic clusters. Protein clusters were built by applying a hierarchical self-organizing map (SOM) algorithm and including Gene Ontology information. Each protein value was calculated as the mean protein expression in each B-cell population. Graphs showing these data are represented in **Supplementary Figure S11**.

Supplementary Figure 1 | Proteomic workflow performed on B-cells. Panel **(A)** shows the B-cell ontogeny from the hematopoietic stem cell (HSC) to the long-lived B-cell populations. Panel **(B)** depicts the procedure followed to process the proteins from naive B-cells (N), centroblasts (CB), centrocytes (CC), memory B-cells (M) and plasma cells (PC) for further mass spectrometric (MS) analysis after in-solution and in-gel protein digestions.

Supplementary Figure 2 | Gating strategy used for the classification of tonsilar B-cell populations. In a first step, total B-cells were subsequently gated as FSClow/SSClow, CD19+/CD20+/CD45+ and CD3- (pink dots) **(A)**. In a second step **(B)**, these gated B-cells were dissected into 5 subpopulations based on their staining profile for CD10, CD27, CD38, and CD184. CC: Centrocytes. CB: Centroblasts. MBC, Memory B-cells. PC, Plasma cells.

Supplementary Figure 3 | Binary heatmap based on the presence/absence of the proteins identified in the B-cell subpopulations. The blue color represents the absence of a protein whereas the red color means presence.

Supplementary Figure 4 | Principal component analysis (PCA) graphics of B-cell subpopulation comparisons after quantitative analysis of the identified proteins. The quantitative proteomics data used for this PCA is collected in **Supplementary Table S3**.

Supplementary Figure 5 | Circular graphical representation of differentially expressed proteins **(A)**, genes **(B)** and the corresponding proteomics/transcriptomics ratios **(C)**. Each graphic has four layers. From the outer layer to the inner one, data for memory B-cells (orange), centrocytes (purple), centroblasts (blue) and naive (green) B-cells are represented. Each layer depicts the quantitative values for each protein within each chromosome. Remarkable proteins within the dataset are indicated in the graphic. Since it is difficult to read such protein names in the graphics, they are also mentioned here (in clockwise direction, same proteins/genes for panels **A–C**): THEMIS2, CD53, RGS13, TRAF3IP3 (chromosome 1); REL, XPO1, SF3B1 (chromosome 2); NFKB1 (chromosome 4); MZB1, CD74 (chromosome 5); HLA-B(x6), NFKBIE (chromosome 6); EZH2 (chromosome 7); LYN (chromosome 8); VIM, GDI1 (chromosome 10); CD44, MS4A1, CASP1 (chromosome 11); GAPDH (chromosome 12); TCL1A, HSP90AA1 (chromosome 14); GINS3, PSMD7, IRF8 (chromosome 16); STAT3 (chromosome 17); VAV1, DNMT1, VASP (chromosome 19); BID, MYH9 (chromosome 22).

Supplementary Figure 6 | Diagram representation of stacked deviations of proteins identified and quantitatively measured in the B-cell subpopulations (naive B-cells, centroblasts, centrocytes, memory B-cells). The number of proteins that were differentially expressed, according to an outlier statistic, were calculated and represented in intervals of Z-distance from the mean.

Supplementary Figure 7 | Attribute plots of pair-wise comparisons of **(A)** proteins (data connected to **Supplementary Tables S3** and **S4**) and **(B)** genes (data connected to **Supplementary Table S8**) differentially expressed (ANOVA p-value < 0.05) across the B-cell subpopulations. Set size refers to the total number of proteins **(A)** or genes **(B)** present in each pair of populations (e.g. almost 600 proteins in common for CC and M). Intersection size depicts the number of proteins or genes in common for the paired populations only (orange, brown, pink, grey, black and yellow for CC-M, CB-M, N-CC, N-CB, CB-CC and N-M, respectively) or their combinations (bars in dark grey, combinations of paired-populations indicated by black dots connected by black lines in the bottom part of the graph). The bigger the intersection size, the more proteins/genes detected in those paired-populations or combinations of paired-populations. N, naive B-cells; M, memory B-cells; CB, centroblasts; CC, centrocytes.

Supplementary Figure 8 | Graphical visualization of the protein involvement in signaling pathways. Bars length represents the total number of proteins contained in the given pathways: in green (proteins of naive B-cells), blue (proteins of centroblasts), light purple (proteins of centrocytes), light orange (proteins of memory B-cells), red (proteins of plasma cells), and brown (proteins in common). The related lists of proteins are collected in **Supplementary Table S5**.

Supplementary Figure 9 | Significantly enriched modules and pathways. Panel **(A)** shows the modules detected as significantly enriched across the 5 B-cell subpopulations. Panel **(B)** displays the significantly enriched pathways. The size of the dots correlates with the number of genes identified in the corresponding B-cell population belonging to the referenced module. The adjusted p-value is color-coded from 0.01 and 0.004 (red) to 0.04 and 0.016 (blue) for modules (panel **A**) and pathways (panel **B**), respectively. s.p., signaling pathway.

Supplementary Figure 10 | Mean protein expression pattern of missing proteins detected for MS/MS in B-cell populations. The mean intensity of the 5 replicates for each B-cell population was represented by family groups. N, naive B-cells; CB, centroblasts; CC, centrocytes; M, memory B-cells.

Supplementary Figure 11 | Proteomic mean expression. The figure shows clusters of proteins built by applying a hierarchical self-organizing map (SOM) algorithm and including Gene Ontology information (molecular function and/or subcellular location). Each protein value in each cluster corresponds to the mean protein expression level (information collected in **Supplementary Table S10**, original data in **Supplementary Table S3**) across the five biological replicates analyzed per B-cell subpopulation. The figure shows how these proteins are differently expressed in naïve (N), centroblast (CB), centrocyte (CC) and memory B-cell (M) populations.

Supplementary Figure 12 | Comparative analysis of specific proteins investigated by flow cytometry (FCM) and mass spectrometry (MS/MS) approaches. The intensity values obtained with each strategy are represented in each graphic for each evaluated protein. The gray line represents the FCM data, whereas the orange one depicts the MS/MS results. N, naive B-cells; CB, centroblast; CC, centrocyte; M, memory B-cell.

Supplementary File 1 | R Script for the processing and analysis of proteomic MS/MS data and transcriptomic microarray results and their ulterior multi-omics integration for the study of the dynamics of B-cell populations.

REFERENCES

1. Pérez ME, Billordo LA, Baz P, Fainboim L, Arana E. Human memory B cells isolated from blood and tonsils are functionally distinctive. *Immunol Cell Biol* (2014) 92:882–7. doi: 10.1038/icb.2014.59
2. Allen CDC, Okada T, Cyster JG. Germinal-Center Organization and Cellular Dynamics. *Immunity* (2007) 27:190–202. doi: 10.1016/j.immuni.2007.07.009
3. Kjeldsen MK, Perez-Andres M, Schmitz A, Johansen P, Boegsted M, Nyegaard M, et al. Multiparametric flow cytometry for identification and fluorescence activated cell sorting of five distinct B-cell subpopulations in normal tonsil tissue. *Am J Clin Pathol* (2011) 136:960–9. doi: 10.1309/AJCPDQNP2U5DZHVV
4. De Silva NS, Klein U. Dynamics of B cells in germinal centres. *Nat Rev Immunol* (2015) 15:137–48. doi: 10.1038/nri3804
5. Shinnakasu R, Inoue T, Kometani K, Moriyama S, Adachi Y, Nakayama M, et al. Regulated selection of germinal-center cells into the memory B cell compartment. *Nat Immunol* (2016) 17:861–9. doi: 10.1038/ni.3460
6. Scheeren FA, Naspetti M, Diehl S, Schotte R, Nagasawa M, Wijnands E, et al. STAT5 regulates the self-renewal capacity and differentiation of human memory B cells and controls Bcl-6 expression. *Nat Immunol* (2005) 6:303–13. doi: 10.1038/ni1172
7. Smith KG, Light A, O'Reilly LA, Ang SM, Strasser A, Tarlinton D. bcl-2 transgene expression inhibits apoptosis in the germinal center and reveals differences in the selection of memory B cells and bone marrow antibody-forming cells. *J Exp Med* (2000) 191:475–84. doi: 10.1084/jem.191.3.475
8. Kulis M, Merkel A, Heath S, Queiros AC, Schuyler RP, Castellano G, et al. Whole-genome fingerprint of the DNA methylome during human B cell differentiation. *Nat Genet* (2015) 47:746–56. doi: 10.1038/ng.3291
9. Matthias P, Rolink AG. Transcriptional networks in developing and mature B cells. *Nat Rev Immunol* (2005) 5:497–508. doi: 10.1038/nri1633
10. Orkin SH, Zon LI. Hematopoiesis: An Evolving Paradigm for Stem Cell Biology. *Cell* (2008) 132:631–44. doi: 10.1016/j.cell.2008.01.025

11. Novershtern N, Subramanian A, Lawton LN, Mak RH, Haining WN, McConkey ME, et al. Densely interconnected transcriptional circuits control cell states in human hematopoiesis. *Cell* (2011) 144:296–309. doi: 10.1016/j.cell.2011.01.004
12. Puente XS, Pinyol M, Quesada V, Conde L, Ordóñez GR, Villamor N, et al. Whole-genome sequencing identifies recurrent mutations in chronic lymphocytic leukaemia. *Nature* (2011) 475:101–5. doi: 10.1038/nature10113
13. de Yébenes VG, Bartolomé-Izquierdo N, Ramiro AR. Regulation of B-cell development and function by microRNAs. *Immunol Rev* (2013) 253:25–39. doi: 10.1111/imr.12046
14. Andersson A, Nilsson K, Fagerberg L, Hallstrom BM, Sundstrom C, Danielsson A, et al. The transcriptomic and proteomic landscapes of bone marrow and secondary lymphoid tissues. *PloS One* (2014) 9:e115911. doi: 10.1371/journal.pone.0115911
15. Petri A, Dybkær K, Bøgsted M, Thrue CA, Hagedorn PH, Schmitz A, et al. Long noncoding RNA expression during human B-cell development. *PloS One* (2015) 10:e0138236. doi: 10.1371/journal.pone.0138236
16. Salonen J, Rönnholm G, Kalkkinen N, Vihinen M. Proteomic Changes during B Cell Maturation: 2D-DIGE Approach. *PloS One* (2013) 8:e77894. doi: 10.1371/journal.pone.0077894
17. Salonen JM, Valmu L, Ronnholm G, Kalkkinen N, Vihinen M. Proteome analysis of B-cell maturation. *Proteomics* (2006) 6:5152–68. doi: 10.1002/pmic.200600156
18. Romijn EP, Christis C, Wieffer M, Gouw JW, Fullaondo A, van der Sluijs P, et al. Expression clustering reveals detailed co-expression patterns of functionally related proteins during B cell differentiation: a proteomic study using a combination of one-dimensional gel electrophoresis, LC-MS/MS, and stable isotope labeling by amino acid. *Mol Cell Proteomics* (2005) 4:1297–310. doi: 10.1074/mcp.M500123-MCP200
19. Garcia-Manteiga JM, Mari S, Godejohann M, Spraul M, Napoli C, Cenci S, et al. Metabolomics of B to plasma cell differentiation. *J Proteome Res* (2011) 10:4165–76. doi: 10.1021/pr200328f
20. Stranneheim H, Orre LM, Lehtiö J, Flygare J. A comparison between protein profiles of B cell subpopulations and mantle cell lymphoma cells. *Proteome Sci* (2009) 7:43. doi: 10.1186/1477-5956-7-43
21. Mann M, Kulak NA, Nagaraj N, Cox J. The Coming Age of Complete, Accurate, and Ubiquitous Proteomes. *Mol Cell* (2013) 49:583–90. doi: 10.1016/j.molcel.2013.01.029
22. Nieto WG, Almeida J, Romero A, Teodosio C, Lo A, Henriques AF, et al. Increased frequency (12 %) of circulating chronic lymphocytic leukemia – like B-cell clones in healthy subjects using a highly sensitive multicolor flow cytometry approach. *Blood* (2009) 114:33–7. doi: 10.1182/blood-2009-01-197368.The
23. Shevchenko A, Tomas H, Havliš J, Olsen JV, Mann M. In-gel digestion for mass spectrometric characterization of proteins and proteomes. *Nat Protoc* (2007) 1:2856–60. doi: 10.1038/nprot.2006.468
24. Rappsilber J, Mann M, Ishihama Y. Protocol for micro-purification, enrichment, pre-fractionation and storage of peptides for proteomics using StageTips. *Nat Protoc* (2007) 2:1896–906. doi: 10.1038/nprot.2007.261
25. R Development Core Team R. *R: A Language and Environment for Statistical Computing*. (2011). doi: 10.1007/978-3-540-74686-7
26. RStudio Team. RStudio: Integrated Development for R. (2016). doi: 10.1007/978-81-322-2340-5 [Online] RStudio, Inc, Boston, MA.
27. Yu G, Wang L-G, Han Y, He Q-Y. clusterProfiler: an R Package for Comparing Biological Themes Among Gene Clusters. *OMICS* (2012) 16:284–7. doi: 10.1089/omi.2011.0118
28. Zhang H, Meltzer P, Davis S. RCircos: an R package for Circos 2D track plots. *BMC Bioinformatics* (2013) 14:244. doi: 10.1186/1471-2105-14-244
29. Lex A, Gehlenborg N, Strobelt H, Vuillemot R, Pfister H. {UpSet}: Visualization of Intersecting Sets. *IEEE Trans Vis Comput Graph ({InfoVis} '14)* (2014) 20:1983–92. doi: 10.1109/TVCG.2014.2346248
30. Khalil B, Ali C. Density-based spatial clustering of application with noise algorithm for the classification of solar radiation time series. In: *2016 8th Int Conf Model Identif Control*. (2016) pp. 279–83. doi: 10.1109/ICMIC.2016.7804123
31. Durinck S, Moreau Y, Kasprzyk A, Davis S, De Moor B, Brazma A, et al. BioMart and Bioconductor: A powerful link between biological databases and microarray data analysis. *Bioinformatics* (2005) 21:3439–40. doi: 10.1093/bioinformatics/bti525
32. Durinck S, Spellman PT, Birnez E, Huber W. Mapping identifiers for the integration of genomic datasets with the R/Bioconductor package biomaRt. *Nat Protoc* (2009) 4:1184–91. doi: 10.1038/nprot.2009.97
33. Frenkel-Morgenstern M, Lacroix V, Ezkurdia I, Levin Y, Gabashvili A, Prilusky J, et al. Chimeras taking shape: potential functions of proteins encoded by chimeric RNA transcripts. *Genome Res* (2012) 22:1231–42. doi: 10.1101/gr.130062.111
34. Baker M. Proteomics: The interaction map. *Nature* (2012) 484:271–5. doi: 10.1038/484271a
35. Diez P, Droste C, Degano RM, Gonzalez-Munoz M, Ibarrola N, Perez-Andres M, et al. Integration of Proteomics and Transcriptomics Data Sets for the Analysis of a Lymphoma B-Cell Line in the Context of the Chromosome-Centric Human Proteome Project. *J Proteome Res* (2015) 14:3530–40. doi: 10.1021/acs.jproteome.5b00474[doi
36. Vogel C, Marcotte EM. Insights into the regulation of protein abundance from proteomic and transcriptomic analyses. *Nat Rev Genet* (2012) 13:227–32. doi: 10.1038/nrg3185
37. Altelaar AFM, Munoz J, Heck AJR. Next-generation proteomics: towards an integrative view of proteome dynamics. *Nat Rev Genet* (2013) 14:35–48. doi: 10.1038/nrg3356
38. Cox J, Mann M. Is Proteomics the New Genomics? *Cell* (2007) 130:395–8. doi: 10.1016/j.cell.2007.07.032
39. Hwang IY, Hwang KS, Park C, Harrison KA, Kehrl JH. Rgs13 Constrains Early B Cell Responses and Limits Germinal Center Sizes. *PloS One* (2013) 8:e60139. doi: 10.1371/journal.pone.0060139
40. Stephenson LM, Miletic AV, Kloeppel T, Kusin S, Swat W. Vav proteins regulate the plasma cell program and secretory Ig production. *J Immunol* (2006) 177:8620–5. doi: 10.4049/jimmunol.177.12.8620
41. Suan D, Sundling C, Brink R. Plasma cell and memory B cell differentiation from the germinal center. *Curr Opin Immunol* (2017) 45:97–102. doi: 10.1016/j.coi.2017.03.006
42. Klein U, Casola S, Cattoretti G, Shen Q, Lia M, Mo T, et al. Transcription factor IRF4 controls plasma cell differentiation and class-switch recombination. *Nat Immunol* (2006) 7:773–82. doi: 10.1038/ni1357
43. Li Y-F, Xu S, Huang Y, Ou X, Lam K-P. Tyrosine kinase c-Abl regulates the survival of plasma cells. *Sci Rep* (2017) 7:40133. doi: 10.1038/srep40133
44. Lebien TW, Tedder TF. B lymphocytes: How they develop and function. *Blood* (2008) 112:1570–80. doi: 10.1182/blood-2008-02-078071
45. Lopez-Herrera G, Tampella G, Pan-Hammarström Q, Herholz P, Trujillo-Vargas CM, Phadwal K, et al. Deleterious mutations in LRBA are associated with a syndrome of immune deficiency and autoimmunity. *Am J Hum Genet* (2012) 90:986–1001. doi: 10.1016/j.ajhg.2012.04.015
46. Berkowska MA, Schickel JN, Grosserichter-Wagener C, de Ridder D, Ng YS, van Dongen JJ, et al. Circulating Human CD27-IgA+ Memory B Cells Recognize Bacteria with Polyreactive Igs. *J Immunol* (2015) 195:1417–26. doi: 10.4049/jimmunol.1402708
47. Hartweger H, Schweighoffer E, Davidson S, Peirce MJ, Wack A, Tybulewicz VLJ. Themis2 Is Not Required for B Cell Development, Activation, and Antibody Responses. *J Immunol* (2014) 193:700–7. doi: 10.4049/jimmunol.1400943
48. Chalouni C, Banchereau J, Vogt AB, Pascual V, Davoust J. Human germinal center B cells differ from naive and memory B cells by their aggregated MHC class II-rich compartments lacking HLA-DO. *Int Immunol* (2003) 15:457–66. doi: 10.1093/intimm/dxg037
49. Casola S, Cattoretti G, Uyttersprot N, Koralov SB, Seagal J, Segal J, et al. Tracking germinal center B cells expressing germ-line immunoglobulin gamma1 transcripts by conditional gene targeting. *Proc Natl Acad Sci USA* (2006) 103:7396–401. doi: 10.1073/pnas.0602353103
50. Xu Z, Fulop Z, Wu G, Pone EJ, Zhang J, Mai T, et al. 14-3-3 adaptor proteins recruit AID to 5′-AGCT-3′–rich switch regions for class switch recombination. *Nat Struct Mol Biol* (2010) 17:1124–35. doi: 10.1038/nsmb.1884
51. Lenz G, Davis RE, Ngo VN, Lam LT, George T, Wright GW, et al. CARD11 as an Oncogene in Diffuse Large B Cell Lymphoma. *Blood* (2015) 110:692 LP – 692. doi: 10.1182/blood.V110.11.692.692
52. Schneider C, Pasqualucci L, Dalla-Favera R. Molecular pathogenesis of diffuse large B-cell lymphoma. *Semin Diagn Pathol* (2011) 28:167–77. doi: 10.1053/j.semdp.2011.04.001
53. Pobezinskaya YL, Liu Z. The role of TRADD in death receptor signaling. *Cell Cycle* (2012) 11:871–6. doi: 10.4161/cc.11.5.19300
54. Woo M, Hakem R, Furlonger C, Hakem A, Duncan GS, Sasaki T, et al. Caspase-3 regulates cell cycle in B cells: a consequence of substrate specificity. *Nat Immunol* (2003) 4:1016–22. doi: 10.1038/ni976

55. Lebecque S, de Bouteiller O, Arpin C, Banchereau J, Liu YJ. Germinal center founder cells display propensity for apoptosis before onset of somatic mutation. *J Exp Med* (1997) 185:563–71. doi: 10.1084/jem.185.3.563
56. Müschen M, Lee S, Zhou G, Feldhahn N, Barath VS, Chen J, et al. Molecular portraits of B cell lineage commitment. *Proc Natl Acad Sci USA* (2002) 99:10014–9. doi: 10.1073/pnas.152327399
57. Burnstock G, Boeynaems JM. Purinergic signalling and immune cells. *Purinergic Signal* (2014) 10:529–64. doi: 10.1007/s11302-014-9427-2
58. Obino D, Diaz J, Sáez JJ, Ibañez-Vega J, Sáez PJ, Alamo M, et al. Vamp-7-dependent secretion at the immune synapse regulates antigen extraction and presentation in B-lymphocytes. *Mol Biol Cell* (2017) 28:890–7. doi: 10.1091/mbc.E16-10-0722
59. Przybyla T, Sakowicz-Burkiewicz M, Pawelczyk T. Purinergic signaling in B cells. *Acta Biochim Pol* (2018) 65:1–7. doi: 10.18388/abp.2017_1588
60. Ratajczak W, Niedźwiedzka-Rystwej P, Tokarz-Deptuła B, DeptuŁa W. Immunological memory cells. *Cent Eur J Immunol* (2018) 43:194–203. doi: 10.5114/ceji.2018.77390
61. Akkaya M, Kwak K, Pierce SK. B cell memory: building two walls of protection against pathogens. *Nat Rev Immunol* (2020) 20:229–38. doi: 10.1038/s41577-019-0244-2
62. Herling M, Patel KA, Weit N, Lilienthal N, Hallek M, Keating MJ, et al. High TCL1 levels are a marker of B-cell receptor pathway responsiveness and adverse outcome in chronic lymphocytic leukemia. *Blood* (2009) 114:4675–86. doi: 10.1182/blood-2009-03-208256
63. Vale AM, Schroeder HW. Clinical consequences of defects in B-cell development. *J Allergy Clin Immunol* (2010) 125:778–87. doi: 10.1016/j.jaci.2010.02.018
64. Peperzak V, Slinger E, Ter Burg J, Eldering E. Functional disparities among BCL-2 members in tonsillar and leukemic B-cell subsets assessed by BH3-mimetic profiling. *Cell Death Differ* (2017) 24:111–19. doi: 10.1038/cdd.2016.105
65. Vizcaíno JA, Csordas A, Del-Toro N, Dianes JA, Griss J, Lavidas I, et al. update of the PRIDE database and its related tools. *Nucleic Acids Res* (2016) 44:D447–56. doi: 10.1093/nar/gkv1145

Conflict of Interest: The authors declare that the research was conducted in the absence of any commercial or financial relationships that could be construed as a potential conflict of interest.

frontiers in Immunology

ORIGINAL RESEARCH
published: 19 April 2021
doi: 10.3389/fimmu.2021.658048

LUBAC Suppresses IL-21-Induced Apoptosis in CD40-Activated Murine B Cells and Promotes Germinal Center B Cell Survival and the T-Dependent Antibody Response

Jingwei Wang[1,2], *Tianbao Li*[3†], *Hong Zan*[1], *Carlos E. Rivera*[1], *Hui Yan*[1*] *and Zhenming Xu*[1*]

[1] Department of Microbiology, Immunology and Molecular Genetics, Joe R. and Teresa Lozano Long School of Medicine, University of Texas Health Science Center at San Antonio, San Antonio, TX, United States, [2] Division of Neonatology, Department of Pediatrics, The Second Xiangya Hospital, Central South University, Changsha, China, [3] Department of Molecular Medicine, Joe R. and Teresa Lozano Long School of Medicine, University of Texas Health Science Center at San Antonio, San Antonio, TX, United States

B cell activation by Tfh cells, i.e., through CD154 engagement of CD40 and IL-21, and survival within GCs are crucial for the T-dependent Ab response. LUBAC, composed of HOIP, SHARPIN, and HOIL-1, catalyzes linear ubiquitination (Linear M1-Ub) to mediate NF-κB activation and cell survival induced by TNF receptor superfamily members, which include CD40. As shown in this study, B cells expressing the *Sharpin* null mutation *cpdm* (*Sharpin*^{cpdm}) could undergo proliferation, CSR, and SHM in response to immunization by a T-dependent Ag, but were defective in survival within GCs, enrichment of a mutation enhancing the BCR affinity, and production of specific Abs. *Sharpin*^{cpdm} B cells stimulated *in vitro* with CD154 displayed normal proliferation and differentiation, marginally impaired NF-κB activation and survival, but markedly exacerbated death triggered by IL-21. While activating the mitochondria-dependent apoptosis pathway in both *Sharpin*$^{+/+}$ and *Sharpin*^{cpdm} B cells, IL-21 induced *Sharpin*^{cpdm} B cells to undergo sustained activation of caspase 9 and caspase 8 of the mitochondria-dependent and independent pathway, respectively, and ultimately caspase 3 in effecting apoptosis. These were associated with loss of the caspase 8 inhibitor cFLIP and reduction in cFLIP Linear M1-Ub, which interferes with cFLIP poly-ubiquitination at Lys48 and degradation. Finally, the viability of *Sharpin*^{cpdm} B cells was rescued by caspase inhibitors but virtually abrogated – together with Linear M1-Ub and cFLIP levels – by a small molecule HOIP inhibitor. Thus, LUBAC controls the cFLIP expression and inhibits the effects of caspase 8 and IL-21-activated caspase 9, thereby suppressing apoptosis of CD40 and IL-21-activated B cells and promoting GC B cell survival.

Keywords: affinity maturation, apoptosis, cFLIP, germinal center B cells, IL-21, linear ubiquitination, positive selection, SHARPIN

OPEN ACCESS

Edited by:
Hermann Eibel,
University of Freiburg Medical Center, Germany

Reviewed by:
Kazuhiro Iwai,
Kyoto University, Japan
Shengli Xu,
*Singapore Immunology Network (A*STAR), Singapore*

***Correspondence:**
Hui Yan
yanh3@uthscsa.edu
Zhenming Xu
xuz3@uthscsa.edu

†Present address:
Tianbao Li,
Geneis Diagnostics, Beijing, China

Specialty section:
This article was submitted to B Cell Biology, a section of the journal Frontiers in Immunology

Received: *25 January 2021*
Accepted: *22 March 2021*
Published: *19 April 2021*

Citation:
Wang J, Li T, Zan H, Rivera CE, Yan H and Xu Z (2021) LUBAC Suppresses IL-21-Induced Apoptosis in CD40-Activated Murine B Cells and Promotes Germinal Center B Cell Survival and the T-Dependent Antibody Response. Front. Immunol. 12:658048. doi: 10.3389/fimmu.2021.658048

INTRODUCTION

B lymphocytes are central to humoral immunity, as they differentiate into "effector" cells that secrete class-switched (IgG, IgA, and IgE) and high-affinity mature antibodies (Abs) or "helper" cells that produce regulatory cytokines (1–3). During the Ab response, B cells expressing antigen (Ag)-specific B cell receptors (BCRs) are engaged by activated T follicular helper cells (Tfh) in secondary lymphoid organs, leading to their robust proliferation and differentiation in germinal centers (GCs), from which plasma cells emerge as long-lived Ab secreting cells (ASCs) and memory B cells are also generated to establish recallable immunity (3–5). Among the Tfh cell-expressed factors, CD154 (CD40 ligand, CD40L) engages CD40, a member of the TNF receptor superfamily, on target B cells and functions as a "primary" stimulus by inducing epigenetic modulation, activating transcription factor (e.g., NF-κB) and expanding the transcriptome to drive B cell proliferation and differentiation (2, 6). The sustained GC reaction requires IL-21, the hallmark cytokine of Tfh cells (7, 8), to boost B cell proliferation and induce plasma cell differentiation by upregulating BLIMP-1, the master transcription factor of plasma cells (9–12). IL-21 also synergizes with CD154 to induce AID, an activated B cell-restricted cytidine deaminase that introduces DNA lesions in the immunoglobulin (Ig) genes to initiate class switch DNA recombination (CSR) and somatic hypermutation (SHM), which underpin Ab class-switching (e.g., from IgM to different IgG isotypes) and affinity maturation, respectively (2, 13). Other $CD4^+$ T helper cells, such as Th1 and Th2 cells, also participate in the GC reaction, e.g., through their hallmark cytokines. In particular, Th2 cytokine IL-4 synergizes with CD154 to activate NF-AT to enhance B cell proliferation as well as induce AID expression and IgH Iγ1-Cγ1 and Iε-Cε germline transcription to initiate CSR to IgG1 and IgE (2, 14).

CSR, most notably IL-4-dependent CSR to IgG1, is likely completed before the full development of IL-21^+ Tfh cells and GCs (15, 16). Within the GC dark zone, class-switched B cells (and some IgM^+ cells) acquire a high load of mutations in the V(D)J region DNA to alter the affinity of BCRs to the Ag. B cells bearing the BCRs of higher affinities are positively selected in the GC light zone and then shuttle back into the dark zone for new rounds of proliferation and SHM, an iterative process that eventually leads to affinity maturation (17). This can be manifested by the appearance – at the peak of the GC reaction – of several dominant BCR families whose members carry the signature mutation obtained by the founders. The positive selection of founder B cells and a subset of progenies in later rounds could be based on their superior survival in GCs, a notion consistent with that a high proportion of GC B cells are apoptotic and likely subclones outcompeted and failing to cross the survival threshold (18–20). Increasing evidence suggests that higher-affinity BCRs result in more efficient Ag uptake and MHC presentation to Tfh cells, which in turn endow GC B cells with a better survival capacity (21, 22). However, the stimuli that trigger the death of GC B cells and survival mechanisms employed by B cells are still poorly understood.

The linear ubiquitin chain assembly complex (LUBAC), which is composed of the HOIP catalytic subunit, SHARPIN structural subunit, and HOIL-1, is at the nexus of regulation of NF-κB activation and cell survival induced by TNF receptor superfamily members (23, 24). Prompted by this, we hypothesize that LUBAC plays an important role in CD40-mediated B cell proliferation, survival, and/or differentiation in response to immunization to T-dependent Ags. To test our hypothesis, we used a well-defined *in vitro* culture system to recapitulate the opposing impact of Tfh cell stimuli, i.e., induction of B-cell death by IL-21 and maintenance of survival by CD154, on B cells expressing the *cpdm* null mutation of *Sharpin* ($Sharpin^{cpdm}$) and/or treated with HOIPIN-8, a recently discovered small molecule inhibitor of HOIP (25, 26). We also explored the molecular mechanisms underpinning IL-21-induced B cell apoptosis and the role of SHARPIN and LUBAC in regulating this process. We further addressed the B cell-intrinsic role of SHARPIN in specifically mediating the GC B cell survival and Ab responses to a T-dependent Ag *in vivo* by generating mice with B cell-specific expression of $Sharpin^{cpdm}$ (B-$Sharpin^{cpdm}$) and mice in which $Sharpin^{cpdm}$ B cells directly competed against wildtype B cells within the same GC environment. Finally, we performed SHM analysis of over 20,000 BCR-encoding sequences to provide molecular evidence that B-cell SHARPIN promotes positive selection for high-affinity Abs.

Abbreviations: AID, Activation induced cytidine deaminase; Ab, antibody; Ag, antigen; ASCs, antibody secreting cells; mAb, monoclonal antibody; BCR, B cell receptor; CDR, complementarity determining region; FADD-like IL-1β-converting enzyme -inhibitory protein; cFLIP, cellular FLICE; CSR, class switch DNA recombination; $Sharpin^{cpdm}$, *Sharpin* chronic proliferative dermatitis mutation; FR, framework region; GC, germinal center; HOIL-1, Heme-Oxidized IRP2 Ubiquitin Ligase 1; HOIP, HOIL-1-interacting protein; HOIPIN-8, HOIP inhibitor 8; IgH, immunoglobulin heavy chain; LUBAC, linear ubiquitin chain assembly complex; NF-κB, nuclear factor κB; SHARPIN, SHANK-associated RH domain interacting protein; SHM, somatic hypermutation; Tfh cells, T follicular helper cells; XIAP, X-linked inhibitor of apoptosis.

MATERIALS AND METHODS

Mice and Immunization

C57BL/6 (also $CD45.2^+$, stock #000664), C57/$CD45.1^+$ (B6.SJL-$Ptprc^aPepc^b$/BoyJ, #002014), $Sharpin^{cpdm/cpdm}$ ($Sharpin^{cpdm}$, #007599, $CD45.2^+$) and μMT mice (#002288) were from the Jackson Laboratory. To generate mixed bone marrow chimera mice with B cell-specific $Sharpin^{cpdm}$ or $Sharpin^{+/+}$ genotype (B-$Sharpin^{cpdm}$ and B- $Sharpin^{+/+}$, respectively), bone marrow cells from μMT mice ($4x10^6$) and sex-matched $Sharpin^{cpdm}$ or $Sharpin^{+/+}$ littermate donor mice (10^6) were mixed at the 80:20 ratio after red blood cell lysis and T cell depletion using a biotinylated anti-CD3 Ab and streptavidin-conjugated beads. Bone marrow cells were transplanted through intravenous (i.v.) injection into 8-week old C57 mice that had been γ-irradiated with a lethal dose (10 Gy) using a ^{137}Cs source and recovered for 24 h in the presence of neomycin. Circulating leukocytes were monitored weekly by flow cytometry until full reconstitution of immune cells, typically after 8 weeks. To generate mixed bone

marrow chimera mice carrying both CD45.2$^+$ *Sharpin*^{cpdm} and CD45.1$^+$ *Sharpin*$^{+/+}$ hematopoietic lineage cells, 8-week old sex-matched CD45.2$^+$ *Sharpin*^{cpdm} and CD45.1$^+$ C57 donor mice were co-housed for one week before sacrificed to obtain bone marrow cells, which were mixed at the 50:50 ratio (2.5x10^6 each) and injected i.v. into irradiated C57 recipient mice, as above. The immune cell reconstitution was verified by FACS.

All mice were maintained in a pathogen-free vivarium at the University of Texas Health Science Center at San Antonio (UTHSCSA). For immunization, mice were injected intraperitoneally (i.p.) with 100 μg of NP-CGG (in average 16 molecules of NP, 4-hydroxy-3-nitrophenyl acetyl, conjugated to one molecule of CGG, chicken γ-globulin; Biosearch Technologies) in the presence of 100 μl of alum (Imject® Alum adjuvant, ThermoFisher) in the central-left abdomen area. Both male and female mice were used. All protocols were in accordance with the rules and regulations of the Institutional Animal Care and Use Committee (IACUC) of UTHSCSA.

B Cell Isolation, Culture, and Stimulation

Mouse immune cells were isolated from single cell suspensions prepared from the spleen. Spleen cells were resuspended in ACK Lysis Buffer (Lonza) to lyse red blood cells. After quenching with RPMI 1640 medium supplemented with 10% FBS, 50 μM β-mercaptoethanol and 1x antibiotic-antimycotic mixture (Invitrogen) (RPMI-FBS), cells were resuspended in PBS for flow cytometry analysis or further preparation. To isolate B cells, splenocytes were subjected to negative selection (against CD43, CD4, CD8, CD11b, CD49b, CD90.2, Gr-1 or Ter-119) using EasySep™ Mouse B cell Isolation Kit (StemCell™ Technologies) following the manufacturer's instructions, resulting in the preparation of more than 99% IgM$^+$IgD^{hi} B cells. After pelleting, B cells were directly used for genomic DNA extraction for genotyping, RNA extraction, or resuspended in RPMI-FBS for stimulation. In genotyping experiments, non-B cells, i.e., those that bound the Ab cocktail and magnetic beads, were also subjected to genomic DNA extraction.

B cells were cultured (3.5x10^5 cell/ml, 1 ml in a 48-well plate) in RPMI-FBS at 37°C and stimulated with CD154 (3 U/ml or as indicated), which was prepared as membrane fragments isolated from Sf21 insect cells infected by CD154-expressing baculovirus, to activate B cells for proliferation and differentiation, as described (6). The membrane fragments from non-infected Sf21 cells failed to activate B cells. IL-4 (5 ng/ml; R&D Systems) and IL-21 (50 ng/ml; R&D Systems) were added, as indicated. Other stimuli include an agonistic anti-CD40 Ab (clone FGK4.5; BioXcel; αCD40, 3 μg/ml or as indicated), TLR1/2 ligand Pam_3CSK_4 (100 ng/ml, Invivogen), TLR4 ligand lipid A (1 μg/ml, Invivogen), TLR7 ligand R-848 (30 ng/ml, Invivogen), TLR9 ligand ODN1826 (sequence 5'-TCCATGACGTTCCTGACGTT-3') with a phosphorothioate backbone (CpG, 1 μM; Eurofins), F(ab')2 of a goat anti-mouse μ chain Ab (anti-μ F(ab') 2, 1 μg/ml; αIgM; Southern Biotech), which crosslinks IgM BCR, or anti-Igδ mAb (clone 11-26c conjugated to dextran, αIgD/dex, 100 ng/ml; Fina Biosolutions), which crosslinks IgD BCR (6). B cells were collected 24h later for RNA extraction or protein lysate preparation, or 96h later for FACS analysis of viability, proliferation, and expression of surface markers.

Flow Cytometry and B Cell Proliferation Analysis

To analyze B cells and other immune cells *ex vivo*, spleen or blood cells (2x10^6) were first stained in Hank's Buffered Salt Solution plus 0.1% BSA (HBSS-BSA) for 20 m with fluorophore-labeled mAbs to surface markers (**Supplementary Table 1**) in the presence of mAb Clone 2.4G2, which blocks FcγIII and FcγII receptors, and fixable viability dye (FVD) or 7–AAD without permeabilization. After washing, cells were resuspended in HBSS for FACS analysis. FACS data were analyzed by the FlowJo® software (BD).

To analyze B cell proliferation *in vivo*, mice were injected twice i.p. with 2 mg of bromodeoxyuridine (BrdU) in 200 μl PBS, with the first and second injection at 24 h and 1 h prior to sacrificing, respectively. Splenocyte (2x10^6) were washed with BSA-HBSS and stained with Abs specific for surface markers in the presence of FVD. After washing, cells were resuspended in the BD Cytofix/Cytoperm™ buffer (250 μl) and incubated at 4°C for 20 m. After washing twice with the BD Perm/Wash™ buffer, cells were counted again and 10^6 cells were resuspended in 100 μl of BD Cytofix/Cytoperm™ buffer for staining with fluorochrome-conjugated anti-BrdU mAb and/or 7–AAD for 30 m. After washing with BD Perm/Wash™ buffer, cells were analyzed by FACS. All data were analyzed by FlowJo® (BD).

To analyze B cells stimulated *in vitro*, cells were harvested, stained with FVD or 7–AAD without permeabilization in HBSS-BSA for 20 m and analyzed by flow cytometry for expression of Igγ3, Igγ1 and Igγ2b expression (CSR to IgG3, IgG1, and IgG2b), CD138 (plasma cell marker) and other B cell surface molecules. To analyze B cell proliferation *in vitro*, CellTrace™ Yellow Cell Proliferation Kit (ThermoFisher) was used following the manufacturer's instructions with minor modifications. Briefly, 10x10^6 purified naïve B cell were stained with CellTrace™ Yellow (10 μM, diluted from the 5 mM stock solution in 1 ml DPBS) for 5 m at 37°C with protection from light. After incubation, cells were pelleted by centrifugation for 5 m at 800g, washed with 10 ml RPMI-FBS before cultured for stimulation. Up to 10 cell divisions could be traced after 96 h of stimulation by CD154. B cells were harvested and analyzed by flow cytometry (Ex532nm, Em555/580nm).

Cell Viability, Apoptosis, and Caspase Activity Analysis

For viability analysis, B cells were stained with 7–AAD, which enters the cell that had a compromised plasma membrane integrity, together with Abs specific surface marker in HBSS-BSA for 20 m, washed once, and resuspended in HBSS-BSA for FACS analysis. To analyze apoptosis and necrosis using 7–AAD and Annexin V, which binds to the phosphatidylserine that was located at the intracellular leaflet of the plasma membrane and exposed to Annexin V once "flipped" outside, B cells were stained with Abs specific for surface markers in HBSS-BSA on ice for 20 m. After washing, cells were resuspended in 100 μl Annexin V binding buffer (BioLegend) containing 7–AAD and

1:50 diluted FITC-conjugated Annexin V (BioLegend) at RT for 15 m. After staining, 400 µl of Annexin V binding buffer was added and cells were immediately analyzed by flow cytometry to analyze apoptotic (Annexin V^+7–AAD^{lo}) cells and necrotic (Annexin V^+7–AAD^{hi}) cells. The caspase activity in freshly harvested spleen B cells from immunized mice was detected using the CaspACE™ FITC-VAD-FMK (Promega), a FITC-conjugated analog of the pan caspase inhibitor Z-VAD-FMK that could diffuse into cells and irreversibly bind to all activated caspases. Splenocyte (10^6) were cultured with CaspACE™ FITC-VAD-FMK (10 µM) in RPMI-FBS at 37°C for 15 m and then harvested for staining with Abs specific for surface markers in HBSS-BSA on ice for 20 m. After washing once and resuspended in HBSS-BSA, cells were analyzed by FACS. To analyze cleaved caspase 3 in B cells by intracellular staining, splenocyte (10^6) were washed with BSA-HBSS and stained with Abs specific for surface markers in the presence of FVD. After washing, cells were fixed with the BD Cytofix/Cytoperm™ (200 µl) at 4°C for 20 m. After washing twice with BD Perm/Wash™ buffer, cells were stained in the same buffer with PE-conjugated Ab for cleaved caspase 3.

Mitochondrial Membrane Potential Assay

Mitochondrial membrane potential ($\Delta\psi m$) was measured by the JC-1 Mitochondrial Membrane Potential Assay Kit (Abcam) following the manufacturer's instructions. When the mitochondrial membrane potential is low, JC-1 (tetraethylbenzimidazolylcarbocyanine iodide, a cationic dye) becomes a monomer that yields green fluorescence (JC-1 green) detectable in the FITC channel (530 nm Em) in flow cytometry. When the mitochondrial membrane potential is high, the dye accumulates into high concentrations in mitochondria, thereby aggregating and yielding red fluorescence (JC-1 red) detectable in the PE channel (590 nm Em). Stimulated B cells were washed with 1x dilution buffer and then stained with 10 µM JC-1 in 1x dilution buffer for 15 m at 37°C. Cells were washed once with 1x dilution buffer and stained for surface markers before flow cytometry analysis.

ELISA and ELISPOT

Serum samples were collected at d 0, 7, and 14 after immunization. To analyze total serum IgM, IgG subclasses, and IgA tilter in homeostasis, samples collected at d 0 were diluted with PBS (pH 7.4) plus 0.05% (v/v) Tween-20 (PBST). Two-fold serially diluted samples and standards for each Ig isotypes were applied to 96-well plates coated with goat anti–IgM, anti–IgA or anti–IgG Abs (all 1 mg/ml, **Supplementary Table 1**) and incubated for 2h at 37 °C to capture IgM, IgA, and different IgG isotypes (IgG1, IgG2a, IgG2b, and IgG3) Abs. After washing with PBST, captured Igs were detected with biotinylated anti–IgM, –IgA, –IgG1, –IgG2a, –IgG2b and –IgG3 Abs (**Supplementary Table 1**) followed by reaction with horseradish peroxidase (HRP)-labeled streptavidin (Sigma-Aldrich), development with o-phenylenediamine and measurement of absorbance at 492 nm. Ig concentrations were determined using Prism® (GraphPad). To analyze titers of high-affinity and total NP-specific Abs, plates were coated with NP_7-BSA (7 NP molecules on one BSA molecule) and NP_{34}-BSA, respectively. Captured Igs were detected with anti–IgM, –IgG1, –IgG2b, –IgG3, and –IgA Abs. Data are relative values based on end-point dilution factors.

For ELISPOT analysis of NP_7-binding and total IgM^+ and $IgG1^+$ ASCs, Multi-Screen® filter plates (Millipore) were activated with 35% ethanol, washed with PBS, and coated with anti–IgM, anti–IgG or NP_7-BSA (all 5 µg/ml) in PBS. Single spleen or bone marrow cell suspensions were cultured at 250,000 cells/ml (in plates coated with NP_7-BSA) or 125,000 cells/ml (in plates coated with anti–IgM or anti–IgG) in RPMI-FBS at 37°C for 16 h. After supernatants were removed, plates were incubated with biotinylated goat anti-mouse IgM or –IgG1 Ab, as indicated, for 2 h and, after washing, incubated with HRP-conjugated streptavidin. Plates were developed using the Vectastain AEC peroxidase substrate kit (Vector Laboratories). The stained area in each well was quantified using the CTL Immunospot software (Cellular Technology) and depicted as the number of spots for quantification.

RNA Isolation, qRT-PCR and RNA-Seq

Total RNA was extracted from 5 x 10^6 B cells using the RNeasy Mini Kit (Qiagen). First-strand complementary DNA (cDNA) was synthesized from equal amounts of total RNA (4 µg) using the SuperScript III System (Invitrogen) and an oligo-dT primer. cDNA was analyzed by qPCR using SYBR Green (Bio-Rad) and appropriate primers (**Supplementary Table 2**). PCR was performed in a CFX96™ Real-Time PCR System (Bio-Rad Laboratories) according to the following protocol: 95°C for 30 s, 40 cycles of 95°C for 10 s, 55°C for 30 s, 72°C for 30 s. Melting curve analysis was performed at 72°C–95°C. The ΔΔCt method was used to analyze transcript levels and data were normalized to the expression of *Cd79b*, which encodes BCR Igβ, as constitutively expressed in B cells.

For RNA-Seq, after RNA integrity was verified using an Agilent Bioanalyzer 2100™ (Agilent), RNA was processed using an Illumina TruSeq RNA sample prep kit v2 (Illumina). Clusters were generated using TruSeq Single-Read Cluster Gen. Kit v3-cBot-HS on an Illumina cBot Cluster Generation Station. After quality control procedures, individual RNA-Seq libraries were pooled based on their respective 6-bp index portion of the TruSeq adapters and sequenced at 50 bp/sequence using an Illumina HiSeq 3000 sequencer. The resulting reads, typically 16 million reads per sample, were checked by assurance (QA) pipeline and initial genome alignment (Alignment). De-multiplexing with CASAVA was employed to generate a Fastq file for each sample. After removing the adaptor and poor-quality reads using Trim Galore, all sequencing reads were aligned with the (GRCm38/mm10) reference genome by using HISAT2 with default settings, yielding Bam files, which were further processed using HTSeq-count to obtain counts for each gene. RNA expression levels were determined using GENCODE annotation. Differential expression analysis was performed using the Deseq2 package in R post-normalization based on a Benjamini-Hochberg false discovery rate (FDR)-corrected threshold for statistical significance of p value <0.01 and $\log_2$FC >1 The count of differentially expressed genes was used

to generate heatmaps using Clustvis software. For gene set enrichment analysis, the 112 RelA target genes identified by Ngo et al (27) were used for GSEA analysis of the enrichment of the Deseq2 package normalized RNA-Seq data.

High-Throughput Repertoire and SHM Analysis

To analyze the repertoire usage and SHM in the $V_{186.2}$ region DNA, RNA was extracted from splenic B cells for cDNA synthesis, as described above. Rearranged $V_{186.2}DJ_H$-Cμ and $V_{186.2}DJ_H$-Cγ1 cDNA was amplified using Phusion™ high-fidelity DNA polymerase (New England BioLabs) and a $V_{186.2}$ leader-specific forward primer and a reverse primer specific for the Cμ or Cγ1 exon (**Supplementary Table 2**), followed by the second round of PCR using the same forward primer and a nest reverse primer tagged with an Illumina clustering adapter (**Supplementary Table 2**), using the following protocol: 98°C for 10 s, 60°C for 45 s and 72°C for 1 m for 30 cycles. The amplified library was tagged with barcodes for sample multiplexing and analyzed by 300-bp pair ended sequencing (the Illumina Mi-Seq system).

The BCR repertoire usage and mutations in $V_{186.2}$ (V1-72) segments were analyzed using the web-interfaced International ImmunoGeneTics Information System® IMGT/HighV-QUEST (http://www.imgt.org). The mutation collection process is described in our previous study (28). Briefly, IgBLAST v1.15.0 (http://www.ncbi.nlm.nih.gov/igblast/) was applied for the alignment of the datasets of SHM sequencing (29). Change-O v1.0.0 (https://changeo.readthedocs.io/en/stable/) python package was applied for processing the output of V(D)J sequencing data (30). For mutation counting, Fasta.fmt7 files were generated by MakeDb.py with reference of imgt_mouse_ig_v.fasta, imgt_mouse_ig_d.fasta, imgt_mouse_ig_j.fasta and ParseDb.py was applied with –if SEQUENCE_ID –sf SEQUENCE_IMGT –mf V_CALL DUPCOUNT. Mutations in the $V_{186.2}$ (IMGT V1-72) segment were filtered and aligned based on a single nucleotide with uncertain or missing bases replaced by "N" or "NA". The final step was applied by metric summary. Only unique sequences were further analyzed. The R pipeline was used to count point-mutations.

Mitochondria-Free Cytosolic Fractionation, Immunoblotting, and Immunoprecipitation (IP)

To prepare whole-cell lysates, B cells (10^7) were harvested by centrifugation at 500 g for 5 m, resuspended in 0.5 ml of lysis buffer (20 mM Tris-Cl, pH 7.5, 150 mM NaCl, 0.5 mM EDTA, 1% (v/v) NP-40) supplemented with Halt™ Protease & Phosphatase Inhibitors Cocktail (ThermoScientific). To prepare mitochondria-free cytosolic fractions, B cells (10^7) were centrifuged at 500 g for 5 m. Cell pellets were processed to obtain the mitochondria-free cytosolic fraction using the Mitochondrial Isolation Kit (ThermoFisher, Cat# 89874) following the manufacturer's instructions. The whole cell lysates and the mitochondria-free cytosolic fraction were subjected to SDS–PAGE, and immunoblotting involving specific Abs (**Supplementary Table 1**). Membranes were then stripped with Restore™ PLUS Western Blot Stripping Buffer (ThermoScientific) for re-immunoblotting. Signals were quantified by ImageJ® (NIH).

For IP, spleen B cells (10^7) were resuspended in lysis buffer (20 mM Tris-Cl, pH 7.5, 100 mM NaCl, 1 mM EDTA, 0.5% (v/v) NP-40) supplemented with Halt™ Protease and Phosphatase Inhibitors Cocktail. After sonication and centrifugation, protein lysates were precleared with equilibrated Protein A/G-conjugated Sepharose™ 4B beads (ThermoFisher, 50 μl) and incubated with anti–cFLIP mouse Ab in 500 μl of lysis buffer at 4°C for 4 h in the presence of Protein A/G Sepharose™ 4B beads. After washing with lysis buffer 3 times, immunoprecipitated proteins were eluted in SDS sample buffer for immunoblotting.

HOIPIN-8 Synthesis and Drug Treatment

HOIPIN-8 (sodium (E)-2-(3-(2,6-difluoro-4-(1H-pyrazol-4-yl) phenyl)-3-oxoprop-1-en-1-yl)-4-(1-methyl-1H-pyrazol-4-yl) benzoate) was synthesized using a two-step process. First, 1-(4-bromo-2,6-difluorophenyl)ethan-1-one (**Compound 1**; 1g, 4.26 mmol) was dissolved in the dioxane-H_2O mixture (47 and 6 ml, respectively) in a 150-ml pressure vessel flask together with 4-(4,4,5,5-tetramethyl-1,3,2-dioxaborolan-2-yl)-1H-pyrazole (1g, 5.19 mmol), K_2CO_3 (1.76g, 12.77 mmol) and [1,1'-Bis (diphenylphosphino)ferrocene]dichloropalladium (II) complexed with dichloromethane (348 mg, 0.426 mmol). After the atmosphere in the flask was displaced with argon gas five times, the mixture was stirred and heated at 100°C for 16 h. The reaction was cooled to RT, quenched with HCl (12 ml, 2M), diluted with ethyl acetate (EtOAc), and filtered through celite. The organic layer of the filtrate was further separated and dried over Na_2SO_4. After filtration and concentration, the residue was purified by flash chromatography using Hexanes:EtOAc mixture (v/v=2/1 to 1/1), yielding 1-(2,6-difluoro-4-(1H-pyrazol-4-yl) phenyl)ethan-1-one (**Compound 2**; 945 mg, quantitative yield) with the following profile: ^{1}H NMR (400 MHz, cdcl$_3$) δ 7.88 (s, 2H), 7.06 (d, J = 9.5 Hz, 2H), 2.55 (s, 3H); ESI-MS: m/z 223.2 [M+H]+.

In a separate reaction, 3-Hydroxy-5-(1-methyl-1H-pyrazol-4-yl) isobenzofuran-1(3H)-one (**Compound 5**) was synthesized, starting from 5-bromoisobenzofuran-1(3H)-one (**Compound 3**) and involving the intermediate 5-bromo-3-hydroxyisobenzofuran-1 (3H)-one (**Compound 4**), following a published protocol (25).

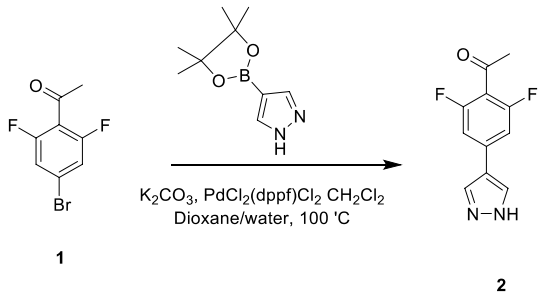

1 2

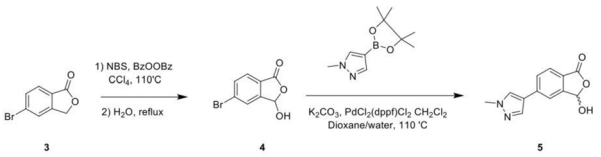

In the second step, Compound 2 (483 mg, 2.17 mmol) and Compound 5 (500 mg, 2.17 mmol) were dissolved in EtOH (12 mL) in a 100-ml glass round-shaped flask. The suspension was cooled to 0°C and, with NaOH (2.9 ml, 6M, 17.34 mmol in total) added, allowed to warm to RT. The mixture was stirred for 16 h until the reaction was quenched with HCl (12 ml, 2M), transferred to a separator funnel, and extracted with chloroform:isopropanol (3:1) three times. The organic layers were collected and dried over Na_2SO_4. After filtration and concentration, the residue was purified by C18 reversed phase flash chromatography using a 0-55% acetonitrile:water gradient to give the HOIPIN-8 base. Finally, the (HOIPIN-8) freebase (80 mg, 0.184 mmol) was dissolved in EtOH (1.5 ml) in a 100-ml glass round-shaped flask, added NaOH (0.2 mL, 1M, 0.184 mmol) at 0°C and stirred for 1 h, warmed to RT and stirred for 2 h. The suspension was then lyophilized to obtain HOIPIN-8 a yellow powder (25% yield) with the following profile: ^{1}H NMR (400 MHz, dmso) δ 8.78 (d, J = 16.3 Hz, 1H), 8.32 – 8.19 (m, J = 8.9 Hz, 3H), 7.92 (d, J = 21.3 Hz, 2H), 7.57 (d, J = 8.0 Hz, 1H), 7.54 – 7.47 (m, 3H), 7.13 (d, J = 16.2 Hz, 1H), 3.86 (s, 3H); ESI-MS: m/z 435.4 [M+H]+.

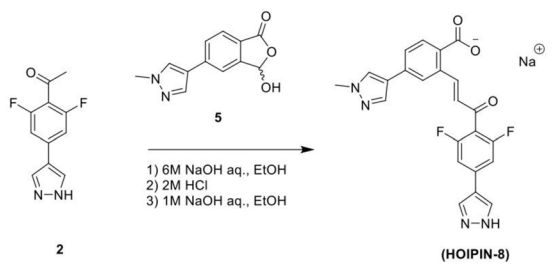

To treat B cells with HOIPIN-8, lyophilized HOIPIN-8 was dissolved in DMSO to yield a stock solution of 40 mM, which was further diluted in RPMI-FBS and added to the cell culture medium, with a final concentration of 20 μM or as indicated. To treat B cells with Z-VAD-FMK, Z-LEHD-FMK, or Z-IETD-FMK, these compounds, as dissolved in DMSO, were added to B cell cultures at indicated concentrations.

Immunofluorescence Imaging

Spleens were embedded in OCT (Tissue-Tek) and snap-frozen on dry ice. Cryostat sections (5 μm) were fixed in pre-chilled acetone for 10 m, air dried at 25°C, washed with PBS, and blocked with 5% FBS in DPBS for 1 h. Sections were stained with FITC-conjugated anti-B220 mAb (1:500) and PerCP-Cy5.5-conjugated anti-GL-7 mAb (1:100) in a humidified chamber overnight at 4°C. Slides were mounted using ProLong® Gold with DAPI for analysis under a Zeiss LM710 confocal microscope. All images are pseudocolored.

Statistical Analysis

Statistical analysis was performed by either GraphPad (Prism®) or Excel (Microsoft) software to determine p values by Student t-test. p values less than 0.05 were considered significant. Correlation analyses were performed using Prism®.

RESULTS

B-Cell SHARPIN Promotes T-Dependent Ab Responses and a BCR Affinity-Enhancing Mutation

Like B cell-specific ablation of HOIP in *mb1*$^{+/cre}$*Hoip*$^{fl/fl}$ mice (31), B cell-specific deficiency in SHAPRIN in B-*Sharpin*^{cpdm} mice did not affect the maturation of follicular or marginal zone B cells or other immune cells, including T cells, dendritic cells (DCs), macrophages and neutrophils (**Supplementary Figure 1A** and **Figures 1A, B**). Upon injection with alum-mixed NP-CGG, which elicits a T-dependent Ab response, B-*Sharpin*^{cpdm} mice showed severe impairment in the GC development in the spleen and the output of FAS^{hi}GL-7^{hi} GC B cells and CD138$^+$ plasma cells despite normal GC and total B cell proliferation (**Figures 1C, D** and **Supplementary Figure 1B**), culminating in decreased formation of ASCs that produced NP-binding IgM and IgG1 Abs as well as much reduced titers of NP-specific IgM and high-affinity (NP_7-binding) IgG1, IgG2b, IgG3 and IgA (**Figures 1E, F**) – total NP-specific (NP_{34}-binding) IgG1 titers were also reduced to similar extents (**Figure 1G**). ASCs secreting non-specific IgM and IgG1 were reduced too, resulting in decreased titers of circulating IgM and IgG1 – also decreased were IgG2a and IgA, as elicited by both T-dependent and T-independent antigens, as well as IgG3 and IgG2b, as elicited mainly by T-independent antigens (**Figures 1H, I**). Residual B-*Sharpin*^{cpdm} GC B cells, however, expressed IgG1 at high levels, indicating their normal CSR (**Figure 1J**).

Upon NP-CGG immunization, B cells with a recombined IgH $V_{186.2}$ region, which encodes NP-binding BCRs, enter GCs and accumulate $V_{186.2}$ DNA mutations to generate BCR mutants for selection (32–34). As shown by analysis of IgM-encoding $V_{186.2}DJ_H$-Cμ and IgG1-encoding $V_{186.2}DJ_H$-Cγ1 transcript, NP-CGG-immunized B-*Sharpin*^{cpdm} mice had similar BCR repertoires in IgG1$^+$ B cells as B-*Sharpin*$^{+/+}$ mice, but more diverse ones in IgM$^+$ B cells (**Figure 2A** and **Supplementary Figure 1C**). $V_{186.2}$ DNA mutations occurred at high levels in $V_{186.2}DJ_H$-Cγ1 of both B-*Sharpin*$^{+/+}$ and B-*Sharpin*^{cpdm} mice, averaging $1.0x10^{-2}$ and $0.6x10^{-2}$ change per base, respectively (**Figure 2B** and **Supplementary Figure 1D**). They also frequently occurred in $V_{186.2}$ DJ_H-Cμ and featured G→A and C→T transitions as major substitutions (**Figure 2B**), likely due to the "replication over" of uracils generated after AID deamination of cytidines (pairing "A" with "U" instead of "G" with the original C). Such transitions were also dominant, albeit not as much, in $V_{186.2}DJ_H$-Cγ1, likely reflecting mutation spreading by error-prone DNA synthesis.

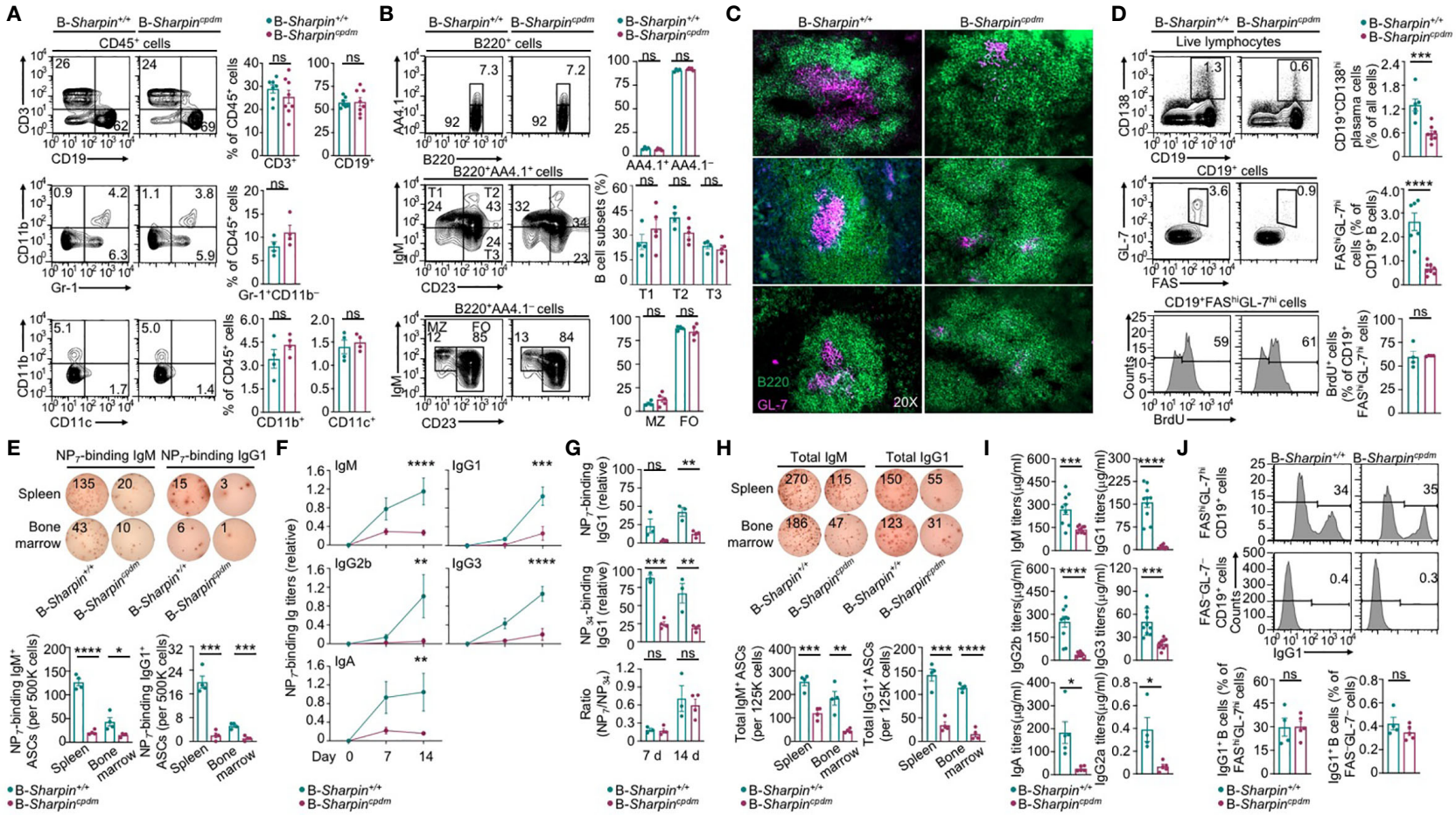

FIGURE 1 | B cell-intrinsic role of SHARPIN in the GC development and Ab responses. **(A, B)** Flow cytometry analysis of different immune cell populations, as indicated, in the spleen of B-*Sharpin*$^{+/+}$ or B-*Sharpin*^{cpdm} mice immunized with NP-CGG/alum for 14 d. **(C)** Fluorescence imaging analysis of GCs in the spleen in mice, as in **(A, B)**. **(D)** Flow cytometry analysis of plasma cells, GC B cells, and GC B cell proliferation (by BrdU incorporation) in immunized mice. **(E–G)** ELISPOT analyses of ASCs producing NP-specific IgM or IgG1 in the spleen and the bone marrow in mice 14 d after immunization **(E)** and ELISA of circulating NP_7-binding and NP_{34}-binding Ig Abs 7 and 14 d after immunization **(F, G)**. **(H, I)** ELISPOT analyses of ASCs producing total IgM or IgG **(H)** and ELISA of circulating total Ig Abs **(I)** in mice, as in **(E, F)**. Data are pooled from 2 independent experiments. **(J)** Flow cytometry analysis of surface IgG1 expression in GC and non-GC B cells. *p<0.05; **p<0.01; ***p<0.001; ****p<0.0001; ns, not significant; t-test.

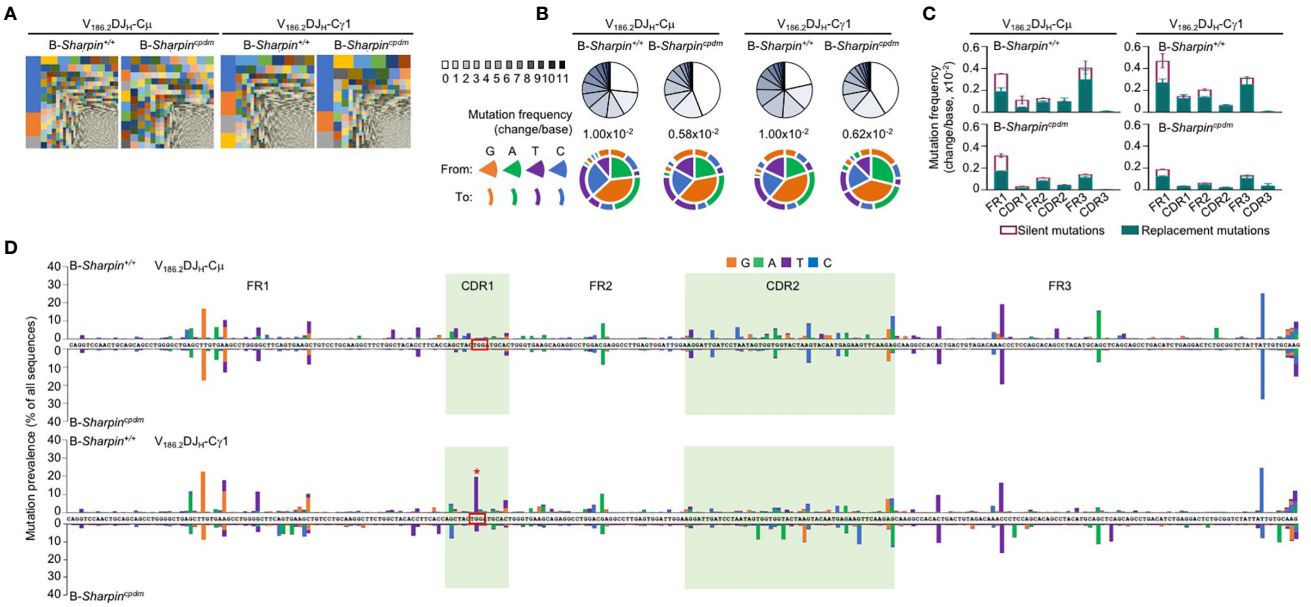

FIGURE 2 | SHARPIN mediates the generation of high-affinity BCR mutants. **(A)** Treemap charts depicting B cell clones identified by unique CDR3 sequences in the V_H region of $V_{186.2}DJ_H$-Cμ and $V_{186.2}DJ_H$-Cγ1 in B-*Sharpin*$^{+/+}$ and B-*Sharpin*^{cpdm} mice 14 d after NP-CGG/alum immunization. Each rectangle represents a unique clone and the size of each rectangle depicts the relative abundance of the clone within the total population. **(B)** Proportions of $V_{186.2}DJ_H$-Cμ and $V_{186.2}DJ_H$-Cγ1 clones carrying given numbers of point-mutations in $V_{186.2}$ region in mice, as in **(A)**, as depicted by pie chart slices (top row; sequences with over 12 point-mutations were excluded from analysis), the overall mutation frequencies (middle), and the nature of such point-mutations, as depicted by concentric pie chart slices and rings (bottom row). **(C,D)** Histograms depict the silent and replacement mutations in different CDRs and FRs as well as in the entire $V_{186.2}DJ_H$-Cμ and $V_{186.2}DJ_H$-Cγ1 regions **(C)** and the spectrum and distribution of point-mutations (**D**, "*" denotes the G98->T98 mutation) in mice, as in **(A,B)**. Data are pooled from three mice in each group.

In both B-*Sharpin*$^{+/+}$ and B-*Sharpin*^{cpdm} mice, base changes in CDR1 and CDR2 of $V_{186.2}$ DJ_H-Cγ1 DNA were dominated by replacement mutations (**Figure 2C**), consistent with the notion that amino acid residues in CDRs are altered to serve as the substrates for selection. In particular, a G→T transversion substitution (G_{98}→T_{98}) changes the CDR1 Trp_{33} residue (TGG) to Leu (TTG) to raise the BCR/Ab affinity to NP by 10-fold (34, 35). It was the most frequent mutation within the CDR regions of $V_{186.2}$ DJ_H-Cγ1 in B-*Sharpin*$^{+/+}$ mice, occurring in 19.7% of B cells in these mice, much higher than the 4.18% frequency in B-*Sharpin*^{cpdm} B cells – all other CDR mutations showed smaller differences (**Figure 2D** and **Table 1**). Furthermore, among the ten most frequent mutations in the entire $V_{186.2}$ DJ_H-Cγ1 DNA, all but G_{98}→T_{98} were in the FR regions (five in FR1, one in FR2, and three in FR3) and showed less difference between B-*Sharpin*$^{+/+}$ and B-*Sharpin*^{cpdm} mice (**Figure 2D** and **Table 1**). In addition, G_{98}→T_{98} was unique to $V_{186.2}$ DJ_H-Cγ1 DNA, in contrast to the frequent occurrence of all other dominant mutations also in $V_{186.2}$ DJ_H-Cμ DNA (**Figure 2D**). Finally, while the CDR1 in $V_{186.2}$ DJ_H-Cμ did not show overall enrichment of replacement mutations (**Figure 2C**), the CDR1 G_{92}→A_{92} and CDR2 G_{197}→A_{197} or T_{197} replacement mutations occurred much less frequently in B-*Sharpin*^{cpdm} mice (**Figure 2D** and **Table 1**).

Thus, SHARPIN plays a B cell-autonomous role in promoting the GC reaction, accumulation of the affinity-augmenting G_{98}→T_{98} substitution and maturation of the T-dependent Ab response.

B Cell-Intrinsic Role of SHARPIN in Promoting GC B Cell Survival

B cell clones with higher-affinity BCRs need to survive in GCs towards maturation of the Ab responses. In association with much-decreased high-affinity NP-specific IgG Abs and enrichment of the affinity-enhancing G_{98}→T_{98} mutation in B-*Sharpin*^{cpdm} mice, $FAS^{hi}GL\text{-}7^{hi}$ GC B cells in these mice had increased death, including more apoptosis and necrosis (**Figure 3A**). Among live B-*Sharpin*^{cpdm} GC B cells, more than half showed caspase activation (Z-VAD-FMK^+), a hallmark of pre-apoptotic and apoptotic cells (**Figure 3B**). The proportions of apoptotic, necrotic, and Z-VAD-FMK^+ cells in non-GC ($FAS^-GL\text{-}7^-$) B cells were all much lower than those in GC B cells in both B-*Sharpin*$^{+/+}$ and B-*Sharpin*^{cpdm} mice. They were comparable in these mice, showing that SHARPIN deficiency selectively affects GC B cell survival.

Tfh cells, which are thought to mediate the GC B cell survival (37), were normal in B-*Sharpin*^{cpdm} mice (**Figure 3C**), suggesting that B-*Sharpin*^{cpdm} GC B cells had intrinsic defects to survive in an otherwise normal microenvironment. This was addressed in *Cd45.1*$^+$-*Sharpin*$^{+/+}$/*Cd45.2*$^+$-*Sharpin*^{cpdm} chimera mice, as generated by γ-irradiated C57 mice engrafted with an equal number of *Cd45.1*$^+$-*Sharpin*$^{+/+}$ and *Cd45.2*$^+$-*Sharpin*^{cpdm} bone marrow cells, which had comparable numbers of hematopoietic

TABLE 1 | Distribution and frequencies of dominant $V_{186.2}$ mutations in B-*Sharpin*$^{+/+}$ and B-*Sharpin*^{cpdm} mice immunized with NP-CGG and the ratio of mutation frequencies in B-*Sharpin*$^{+/+}$ mice to those in B- *Sharpin*^{cpdm} mice.

$V_{186.2}DJ_H$-Cμ, CDRs Mutation	Frequency (x10^{-2} change/base)		Ratio	Mutation	$V_{186.2}DJ_H$-Cμ, FRs Frequency (x10^{-2} change/base)		Ratio
/region	B-*Sharpin*$^{+/+}$	B-*Sharpin*^{cpdm}		/region	B-*Sharpin*$^{+/+}$	B-*Sharpin*^{cpdm}	
AG$_{92}$C/CDR1†	4.04	0.29	14.1	CTT$_{33}$/FR1	16.8	17.4	0.97
AGC$_{93}$/CDR1†*	6.00	1.89	3.17	GTG$_{36}$/FR1	6.55	5.86	1.12
CAC$_{105}$/CDR1	3.39	3.73	0.91	AA$_{38}$G/FR1	10.6	13.0	0.82
AG$_{149}$G/CDR2	5.24	5.03	1.04	G$_{46}$CT/FR1	6.41	6.76	0.95
G$_{154}$AT/CDR2	4.85	4.57	1.06	C$_{58}$TG/FR1	9.87	8.53	1.16
A$_{160}$AT/CDR2	6.67	0.90	7.45	CG$_{128}$A/FR2	8.72	8.72	1.00
G$_{169}$GT/CDR2	5.94	5.24	1.13	C$_{208}$TG/FR3	7.00	8.41	0.83
AAG$_{177}$/CDR2	8.70	7.70	1.13	C$_{223}$CC/FR3	19.3	19.5	0.99
A$_{196}$GC/CDR2	5.36	6.70	0.80	CAG$_{246}$/FR3	15.8	7.32	2.16
AG$_{197}$C/CDR2	12.7	2.26	5.62	TAT$_{285}$/FR3	25.4	27.8	0.91
$V_{186.2}DJ_H$-Cγ1, CDRs#					$V_{186.2}DJ_H$-Cγ1, FRs#		
Mutation	Frequency (x10^{-2} change/base)		Ratio	Mutation	Frequency (x10^{-2} change/base)		Ratio
/region	B-*Sharpin*$^{+/+}$	B-*Sharpin*^{cpdm}		/region	B-*Sharpin*$^{+/+}$	B-*Sharpin*^{cpdm}	
AG$_{92}$C/CDR1†	4.95	7.93	0.62	GAG$_{30}$/FR1*	11.7	5.36	2.18
TG$_{98}$G/CDR1‡	19.7	4.18	4.71	CTT$_{33}$/FR1*	22.6	8.75	2.58
CAC$_{105}$/CDR1	6.96	2.10	3.31	AA$_{38}$G/FR1	17.8	6.96	2.56
AG$_{149}$G/CDR2	3.34	2.46	1.36	G$_{46}$CT/FR1	11.6	4.60	2.52
G$_{154}$AT/CDR2	2.34	1.79	1.31	C$_{58}$TG/FR1	10.4	5.16	2.02
AAG$_{177}$/CDR2	4.96	2.81	1.77	AAG$_{114}$/FR2	4.43	2.06	2.15
G$_{184}$AG/CDR2	3.75	1.77	2.12	CG$_{128}$A/FR2	10.4	5.43	1.92
GAG$_{186}$/CDR2	3.90	5.11	0.76	C$_{208}$TG/FR3*	9.79	10.6	0.92
A$_{196}$GC/CDR2	7.43	2.96	2.51	C$_{223}$CC/FR3	16.6	16.3	1.02
AG$_{197}$C/CDR2	7.87	12.9	0.61	TAT$_{285}$/FR3*	24.8	8.11	3.06

†*The AG92C93 (Ser) codon has a high mutability and all mutations are replacement mutations except for AGT93 (36).*

‡*The TG98G (Trp) to TT98G (Leu) replacement mutation changes the affinity of Abs to NP by 10-fold (34,35). The frequency of G98 ®T98 mutation were 33.6x10–2, 11.0 x10–2, and 9.8x10–2 change/base in three B-Sharpin+/+ mice, and 7.8 x10–2, 2.9x10–2, and 0.2x10–2 change/base in three B-Sharpincpdm mice. Since only unique sequences were analyzed, the frequencies of each mutation were equivalents of the proportions of B cell clones carrying such mutations.*

#*The mutations depicted here had the highest frequencies in the CDRs and FRs, respectively, in B-Sharpin+/+ mice. Additional dominant mutations occurred at high frequencies in B-Sharpincpdm mice (6 in FR1, 4 in CDR2, and 3 in FR3).*

**The mutations are all silent mutations.*

stem cells (HSCs; **Figure 3D**). In such mice, *Cd45.2*$^+$-*Sharpin*^{cpdm} HSCs gave rise to 25-30%, instead of the expected 50% of cells in different leukocyte compartments, including IgM$^+$B220$^+$ immature B cells and IgD$^+$ mature B cells (**Figures 3E, F**), likely due to a partial defect of *Sharpin*^{cpdm} HSCs in differentiation. Upon NP-CGG immunization, the chimera mice supported the development of GC B cells, of which only 10% were *Cd45.2*$^+$-*Sharpin*^{cpdm}, significantly less than the 30% of *Cd45.2*$^+$-*Sharpin*^{cpdm} B cells within the non-GC B cell compartment (**Figure 3G**). In association with the underrepresentation of *Cd45.2*$^+$-*Sharpin*^{cpdm} GC B cells, 28% of such cells lost membrane integrity (FVD$^+$) and, among FVD$^-$ cells, 70% showed caspase 3 cleavage, both reflecting over 2-fold increases in corresponding cell frequencies in *Cd45.1*$^+$-*Sharpin*$^{+/+}$ GC B cell counterparts (**Figure 3H**). Such increases were also in line with the fold of increase in Annexin V$^+$7–AAD^{lo} apoptotic and Z-VAD-FMK$^+$ pre-apoptotic/apoptotic GC B cells in B-*Sharpin*^{cpdm} mice (**Figures 3A, B**). By contrast, non-GC *Cd45.2*$^+$-*Sharpin*^{cpdm} B cells were virtually all FVD$^-$ and showed no caspase 3 activation, confirming that the defect of *Sharpin*^{cpdm} B cells in survival was specific to GC B cells.

Overall, SHARPIN plays a B cell-intrinsic role in inhibiting apoptosis of GC B cells and mediating their survival during the T-dependent Ab response.

SHARPIN Suppresses IL-21-Induced Death in CD154-Stimulated B Cells

To understand the mechanisms underlying the increased death of *Sharpin*^{cpdm} GC B cells, we subjected purified *Sharpin*^{cpdm} B cells to stimulation by membrane-bound CD154, which mimics CD154 expressed on the plasma membrane of Tfh cells that potently engages CD40 to initiate and sustain the GC reaction (6, 38, 39). CD154-stimulated *Sharpin*^{cpdm} B cells only mildly impaired in canonical NF-κB activation, as indicated by phosphorylation of the p65 subunit at Ser333, and were largely normal in expressing p65 target genes (**Figures 4A, B**). Consequently, they showed normal proliferation and IL-4-directed CSR to IgG1 (**Figure 4C**). While neither *Sharpin*$^{+/+}$ nor *Sharpin*^{cpdm} B cells differentiated into plasma cells at a high level after 96 h of stimulation with CD154 and IL-4, they both could do so after 48 h of stimulation, and being washed to remove IL-4 and re-stimulation for 48 h with CD154 and IL-21 (**Figure 4D**). Accordingly, CD154-stimulated *Sharpin*^{cpdm} B cells were fully capable of inducing *Prdm1* (encoding BLIMP-1) and upregulating AID in the presence of IL-21 as well as undergoing IL-4- and IFNγ-directed Iγ1-Cγ1 and Iγ2a-Cγ2a germline transcription, respectively (**Figure 4E**). They also shared a similar transcriptome with their *Sharpin*$^{+/+}$ B cell counterparts,

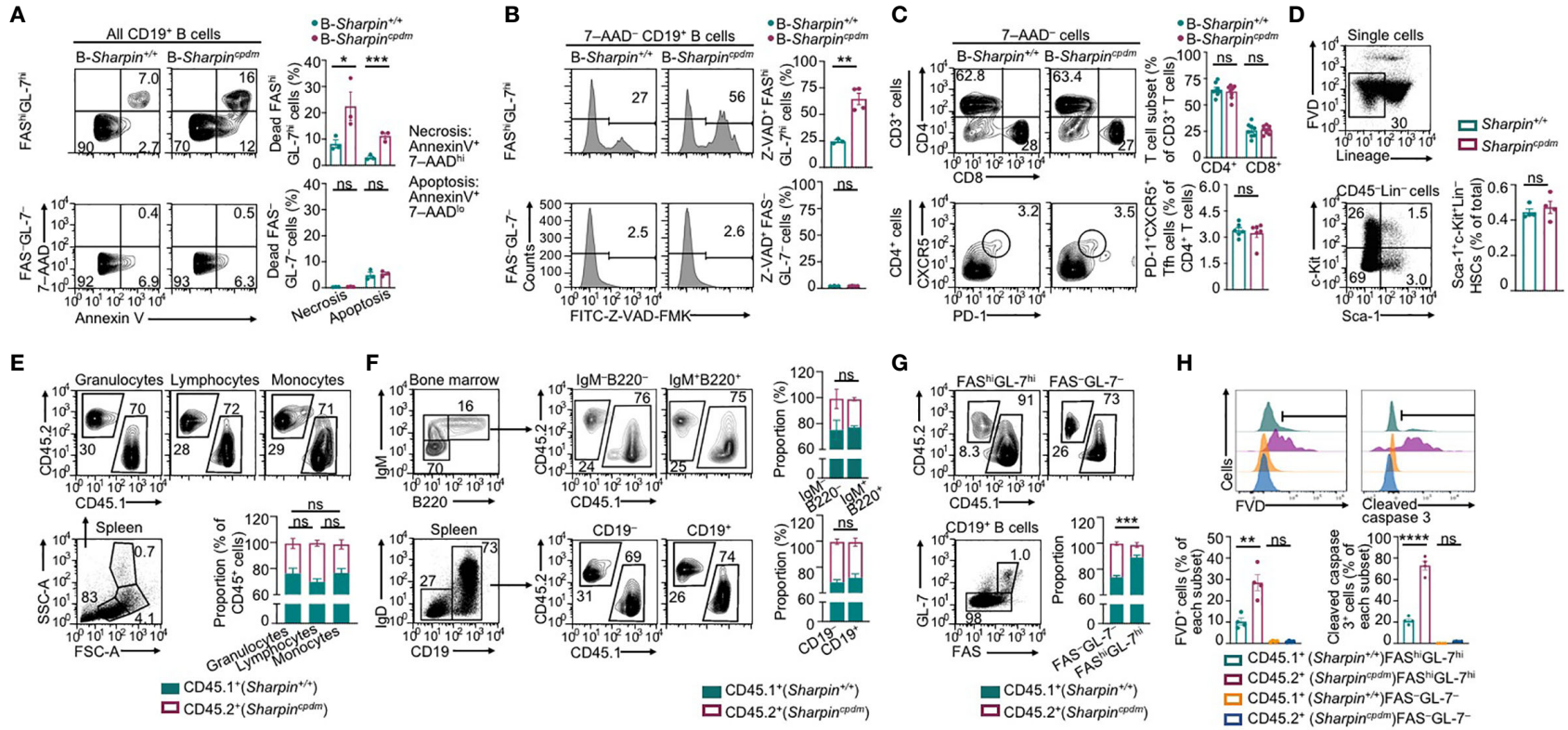

FIGURE 3 | SHARPIN is critical for germinal center B cell survival. **(A,B)** Flow cytometry analysis of apoptosis and necrosis **(A)** as well as caspase activation **(B)** in FAS^{hi}GL-7^{hi} GC B cells and FAS^{-}GL-7^{-} non-GC B cells in the spleen of B-*Sharpin*$^{+/+}$ or B-*Sharpin*^{cpdm} mice 14 d after immunization with NP-CGG/alum. **(C)** Flow cytometry analysis of CD4^{+} and CD8^{+} T cells (top panels) as well as CD4^{+}CXCR5^{+}PD-1^{+} Tfh cells (bottom) in mice, as in **(A,B)**. **(D)** Gating strategy for flow cytometry analysis of Sca-1^{+}c-Kit^{+}Lin^{-} HSCs and the proportion of such cells in the bone marrow of *Sharpin*$^{+/+}$ and *Sharpin*^{cpdm} mice. **(E)** Flow cytometry analysis of (SSC^{hi}FSC^{hi}) granulocytes, (SSC^{lo}FSC^{lo}) lymphocytes, and (SSC^{lo}FSC^{hi}) monocytes in the spleen of CD45.1^{+} *Sharpin*$^{+/+}$/CD45.2^{+} *Sharpin*^{cpdm} mixed bone marrow chimera mice (mean and s.d., n=4). **(F)** Flow cytometry analysis of the proportions of CD45.1^{+} and CD45.2^{+} cells in different B cell subsets in the bone marrow and spleen of CD45.1^{+} *Sharpin*$^{+/+}$/CD45.2^{+} *Sharpin*^{cpdm} mice (mean and s.d., n=4). **(G, H)** Flow cytometry analysis of proportions of CD45.1^{+} and CD45.2^{+} cells in FAS^{hi}GL-7^{hi} GC B cells and FAS^{-}GL-7^{-} non-GC B cells **(G)** as well as survival and caspase 3 cleavage **(H)** in such cells in CD45.1^{+} *Sharpin*$^{+/+}$/CD45.2^{+} *Sharpin*^{cpdm} mice 14 d after NP-CGG/alum immunization (mean and s.d., n=4). * p<0.05; ** p<0.01; *** p<0.001; **** p<0.0001; t-test.

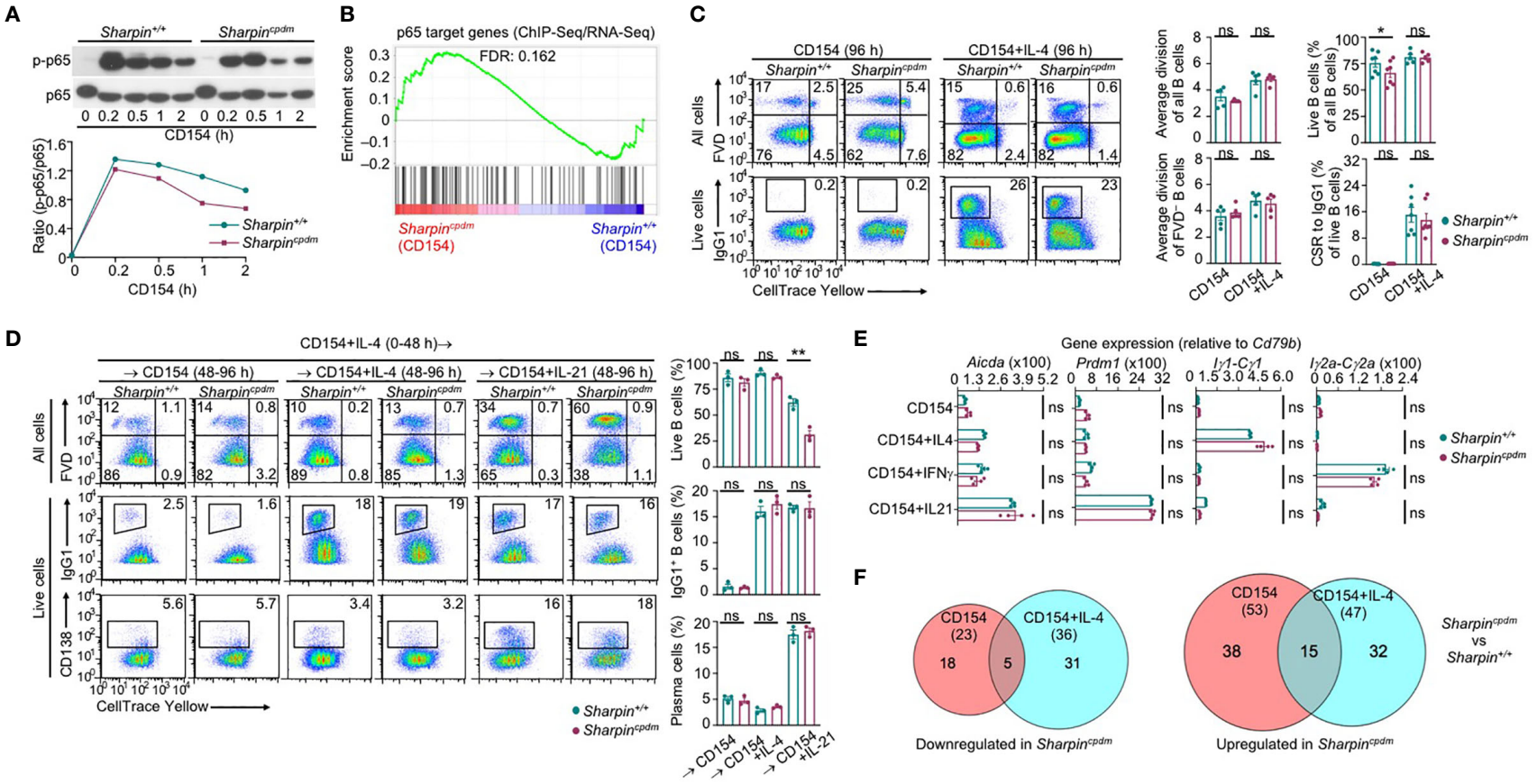

FIGURE 4 | SHARPIN is dispensable for activation, proliferation, survival, and differentiation of B cells stimulated with CD154. **(A)** Immunoblotting of phosphorylated p65 and total p65 protein levels in *Sharpin*$^{+/+}$ and *Sharpin*^{cpdm} B cells after stimulation by CD154 for the indicated time. Representative of two independent experiments. **(B)** GSEA analysis of differentially expressed genes (DEGs) in *Sharpin*$^{+/+}$ and *Sharpin*^{cpdm} B cells stimulated with CD154 for 24 h for the enrichment of p65 target genes (RNA-Seq data were pooled from two independent experiments). **(C)** Flow cytometry analysis of proliferation, survival, and CSR to IgG1 in *Sharpin*$^{+/+}$ and *Sharpin*^{cpdm} B cells stimulated with CD154 or CD154 plus IL-4 for 96 h. **(D)** Flow cytometry analysis of survival, CSR to IgG1 and plasma cell differentiation in *Sharpin*$^{+/+}$ and *Sharpin*^{cpdm} B cells after stimulation first with CD154 plus IL-4 for 48 h, washed, and then with CD154, alone or plus IL-4 or IL-21, for 48 h. **(E)** qRT-PCR analysis of gene expression, as indicated, in B cells stimulated with CD154, alone or plus IL-4, IFN-γ or IL-21, for 48 h. **(F)** The numbers of DEGs (p values < 0.01, absolute value of $\log_2$FC > 1) between *Sharpin*$^{+/+}$ and *Sharpin*^{cpdm} B cells after stimulation with CD154 or CD154 plus IL-4 for 24 h, as depicted by Venn diagram. Data were pooled from two independent RNA-Seq experiments. * p<0.05; ** p<0.01; t-test.

with only 76 (23 downregulated and 53 upregulated) and 83 (36 downregulated and 47 upregulated) differentially expressed genes upon stimulation by CD154 and CD154 plus IL-4, respectively (**Figure 4F** and **Supplementary Figure 2A**). Finally, *Sharpin*^{cpdm} B cells underwent robust proliferation, CSR, and plasma cell differentiation upon stimulation by LPS (**Supplementary Figure 2B**), showing that SHARPIN did not mediate B cell responses to T-dependent or T-independent stimuli.

IL-21 enhanced proliferation and induced plasma cell differentiation of CD154-stimulated B cells, but triggered their death, resulting in a net loss of such cells (**Figures 5A–C**). The killing effect of IL-21 was exacerbated by the *Sharpin* deficiency, leading to as few as 10% of *Sharpin*^{cpdm} B cells able to survive, virtually all of which had completed high numbers of division (**Figures 5B, C**). By contrast, *Sharpin*^{cpdm} B cells stimulated with CD154 alone or with IL-4 showed high viability, which was only marginally lower than that of *Sharpin*$^{+/+}$ B cells (**Figure 4C**). *Sharpin*^{cpdm} B cells were also normal in survival upon stimulation by αIgM plus IL-4, but defective upon stimulation IL-21 alone, LPS or LPS plus IL-4 – αIgM (alone or with IFNγ) or LPS plus IL-21 could not maintain the viability of even wildtype B cells (**Supplementary Figure 2B–D**). High doses of CD154 countered the death-inducing effect of IL-21 in *Sharpin*$^{+/+}$ B cells and more effectively in *Sharpin*^{cpdm} B cells (**Figures 5A, D, E**), showing a SHARPIN-independent pro-survival activity of strong CD40 signals.

CD40 could be engaged *in vitro* by αCD40, which activated NF-κB in wildtype B cells, albeit not as quickly or potently as CD154 (**Figures 4A**, **5F**), and require IL-21 to induce these B cells to proliferate (**Figures 5D, E**). More than half of dividing *Sharpin*$^{+/+}$ cells, however, were unable to survive, even in the presence of high doses of αCD40. αCD40-stimulated *Sharpin*^{cpdm} B cells showed much weaker NF-κB activation at early time points when B cells were particularly sensitive to the killing by IL-21 (**Figure 5F**) and failed to robustly proliferate even in the presence of IL-21, which instead triggered death in both dividing and non-dividing B cells (**Figures 5D, E**). Upon stimulation with αCD40 plus IL-4, *Sharpin*^{cpdm}, by contrast, showed comparable survival as *Sharpin*$^{+/+}$ B cells (**Figure 5G**).

To summarize, SHARPIN does not play a major role in CD154-induced B-cell NF-κB activation, gene expression, proliferation, CSR, or plasma cell differentiation. Rather, it specifically suppresses IL-21-induced B cell death through a mechanism not entirely overlapping with the one underlying the effect of CD154 in countering the killing by IL-21.

SHARPIN Inhibits Caspase 8 and Caspase 9 Activation and B Cell Apoptosis

IL-21 induced more apoptosis (AnnexinV^{+}7–AAD^{lo}) in CD154 or αCD40-stimulated *Sharpin*^{cpdm} B cells than *Sharpin*$^{+/+}$ B cells, in addition to extensive but similar degrees of necrosis (AnnexinV^{+}7–AAD^{hi}) in both – αCD40 alone triggered more necrosis than CD154 (**Figure 6A**). The heightened apoptosis in *Sharpin*^{cpdm} B cells could be alleviated by pre-treatment with CD154, BCR-crosslinking αIgD/dex or TLR9 ligand CpG, but not other TLR ligands, which instead reduced αCD40-triggered necrosis (**Figures 6A–C** and **Supplementary Figures 3A, B**). The viability of CD154 and IL-21-stimulated *Sharpin*^{cpdm} B cells could be rescued by the pan-caspase inhibitor Z-VAD-FMK in a dose-dependent manner to a level comparable to that of *Sharpin*$^{+/+}$ B cells (**Figure 6D** and **Supplementary Figure 3C**). It could also be partially restored by Z-IETD-FMK and Z-LEHD-FMK, which specifically inhibits initiator caspase 8 and caspase 9, respectively (**Figure 6D** and **Supplementary Figure 3C**), showing that *Sharpin*^{cpdm} B cell apoptosis was mediated by both the mitochondria-independent and mitochondria-dependent (intrinsic) apoptosis pathways. The integrity of mitochondria membranes was severely compromised by IL-21 in CD154-stimulated *Sharpin*^{cpdm} B cells, but much less so in *Sharpin*$^{+/+}$ B cells (**Figure 6E**). This, together with the failure of high doses of CD154 to readily improve the mitochondria membrane integrity in either cell types, indicated that IL-21 overrode CD154 to activate the intrinsic apoptosis pathway that, if not controlled by SHARPIN, led to cell death.

Like *Sharpin*$^{+/+}$ B cells, *Sharpin*^{cpdm} B cells responded to IL-21 to activate STAT3 and STAT5, downregulate the expression of BCL2 and BCL-XL to supersede the effect of CD154 in inducing these anti-apoptosis members of the BCL2 family, and upregulate BIM, a pro-apoptotic member (**Figures 7A, B**). As compared to *Sharpin*$^{+/+}$ B cells, they also expressed comparable transcript levels of anti-apoptotic (*Bcl2, Bcl2l1/Bcl2-Xl*, *Mcl2*, which were all downregulated by IL-21) and pro-apoptotic (*Bcl2l11/Bim*, *Bad* and *Bax*) genes, all of which are involved in the regulation of mitochondrial membrane permeability, but showed more cytochrome C accumulation in the cytoplasm and activation of the effector caspase 3 (**Figures 7B–D**), indicating that SHARPIN deficiency amplified IL-21-triggered intrinsic apoptosis without altering the expression of the BCL2 family factors, likely by boosting downstream caspase activation. Indeed, upon IL-21 induction, CD154-stimulated *Sharpin*$^{+/+,}$ and *Sharpin*^{cpdm} B cells underwent similar changes in the levels of BCL2, BCL-XL, BIM, BAD, and (anti-apoptotic) BAD phosphorylation, but *Sharpin*^{cpdm} B cells showed more caspase 9 activation, which depends on cytochrome C release from the mitochondria and in turn activates caspase 3 (**Figure 7E** and **Supplementary Figure 4**). The caspase 9 activation started 2 h after stimulation and continued to increase until 48 h. At this time point, caspase 8 of the mitochondria-independent apoptosis pathway was also activated in *Sharpin*^{cpdm} B cells, but not in *Sharpin*$^{+/+}$ B cells despite its activation at early time points, when caspase 9 was marginally activated (**Figure 7E** and **Supplementary Figure 4**). These, together with the rescue of the viability of *Sharpin*^{cpdm} B cells by the inhibitor of caspase 8 or caspase 9 (**Figure 6D**), showed that the SHAPRIN deficiency resulted in the synchronized activation of these two principal initiator caspases, which together triggered the irreversible apoptosis process in *Sharpin*^{cpdm} B cells.

The activation and function of caspase 8 are tightly regulated by a catalytically inactive homologous factor cFLIP, which includes the longer (cFLIP$_L$) and shorter (cFLIP$_R$) forms generated through alternative splicing of the *Cflar* transcript in mice, with cFLIP$_L$ acting as either an inhibitor or a potentiator

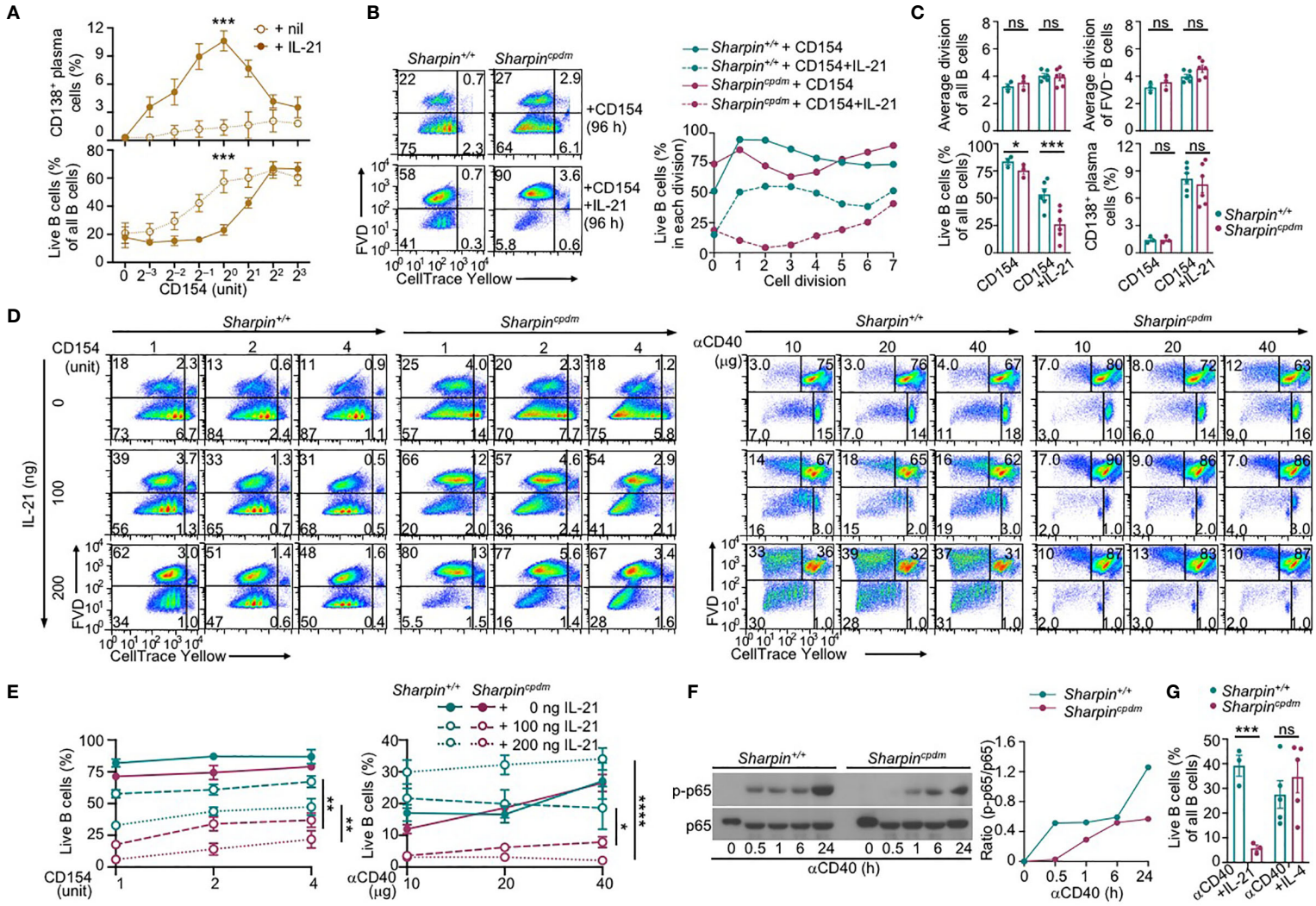

FIGURE 5 | SHARPIN deficiency exacerbates IL-21-induced death in CD154-stimulated B cells. **(A)** Flow cytometry analysis of plasma cell differentiation and B cells viability in C57 B cells stimulated with different doses of CD154, as indicated, in the absence or presence of IL-21 for 96 h (n=4, mean and s.e.m.; data at 1 unit of CD154 were analyzed for statistical differences between *Sharpin*$^{+/+}$ and *Sharpin*^{cpdm} B cells). **(B, C)** Flow cytometry analysis of proliferation, survival, and plasma cell differentiation of *Sharpin*$^{+/+}$ and *Sharpin*^{cpdm} B cells stimulated with CD154 or CD154 plus IL-21 for 96 (h) Division-linked B cell viability is depicted in **(B)**, representative of four independent experiments) and average divisions, live B cell proportions, and CD138^{+} plasma cell proportions were depicted in **(C)**. **(D, E)** Flow cytometry analysis of proliferation, survival of *Sharpin*$^{+/+}$ and *Sharpin*^{cpdm} B cells stimulated with CD154 (left panels) or αCD40 (right panels) at indicated doses in the presence of different doses of IL-21 for 96 h (n=3, mean and s.e.m.; data at 4 units of CD154 or 40 μg of αCD40 were analyzed for statistical differences between *Sharpin*$^{+/+}$ and *Sharpin*^{cpdm} B cells). **(F)** Immunoblotting of phosphorylated p65 and total p65 protein levels in *Sharpin*$^{+/+}$ and *Sharpin*^{cpdm} B cells after stimulation by αCD40 for the indicated time. Representative of two independent experiments. **(G)** Live cell proportions in *Sharpin*$^{+/+}$ and *Sharpin*^{cpdm} B cells stimulated with αCD40 plus IL-21 or IL-4 for 96 (h) $^{*}p < 0.05$; $^{**}p < 0.01$; $^{***}p < 0.001$; $^{****}p < 0.0001$; t-test.

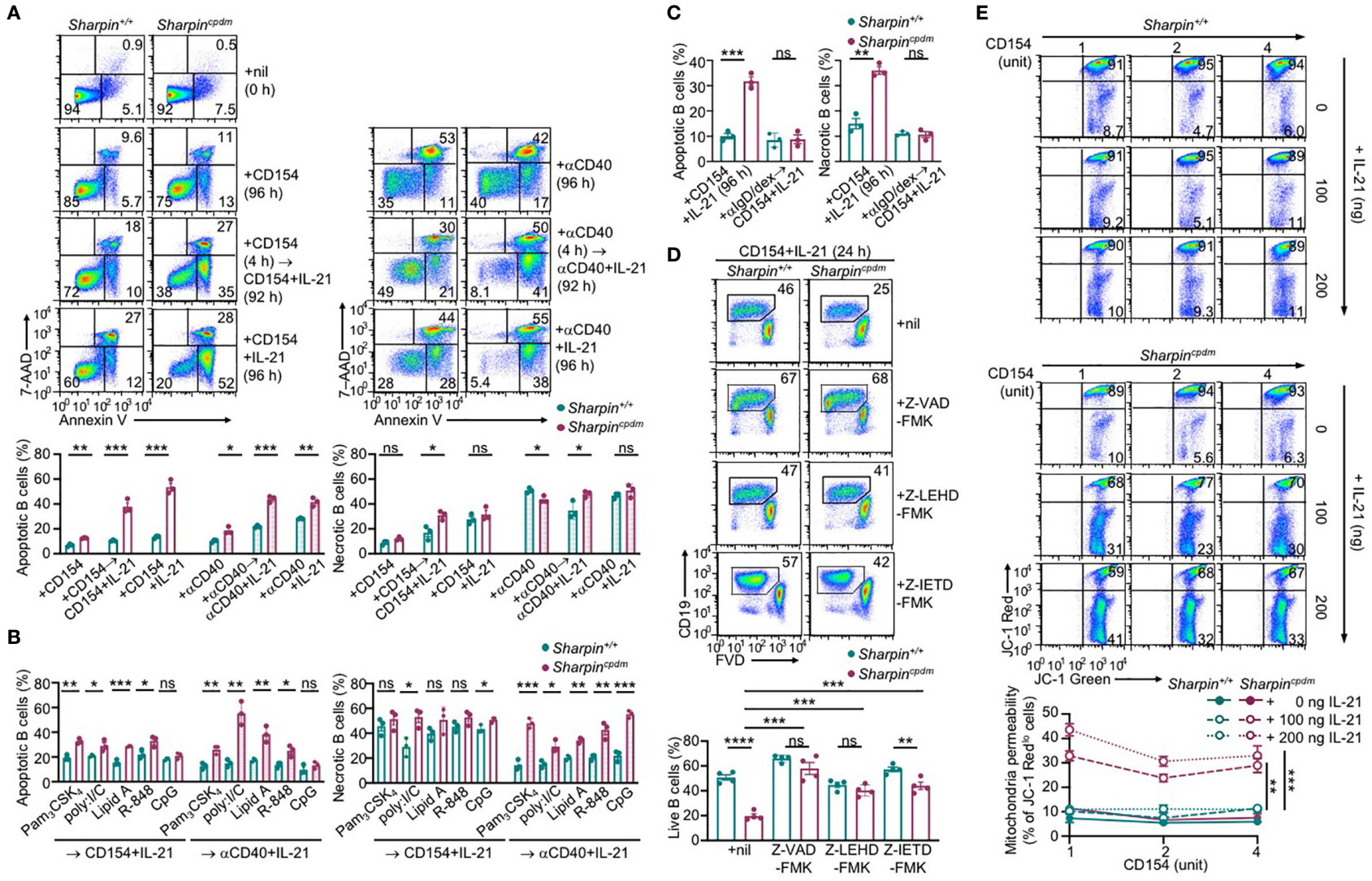

FIGURE 6 | SHARPIN inhibits IL-21-induced apoptosis in CD154-stimulated B cells. **(A)** Flow cytometry analysis of apoptosis (Annexin V^+7–AAD^{lo}) and necrosis (Annexin V^+7–AAD^{hi}) in freshly isolated *Sharpin*$^{+/+}$ and *Sharpin*^{cpdm} B cells or after stimulation with CD154 (left) or αCD40 (right) plus nil or IL-21 for 96 h, with or without priming with CD154 or αCD40 for 4 h. **(B, C)** Flow cytometry analysis of apoptosis and necrosis in *Sharpin*$^{+/+}$ and *Sharpin*^{cpdm} B cells after priming with TLR ligands (as indicated, **B**) or αIgD/dex **(C)** for 4 h and then stimulated with CD154 or αCD40 plus IL-21 for 92 h. **(D)** Flow cytometry analysis of the viability of *Sharpin*$^{+/+}$ and *Sharpin*^{cpdm} B cells stimulated with CD154 plus IL-21 in the presence of nil or pan-caspase inhibitor Z-VAD-FMK, caspase 9-specific inhibitor Z-LEHD-FMK or caspase 8-specific inhibitor Z-IETD-FMK (all 20 μM). **(E)** Mitochondrial membrane potential in B cells stimulated with CD154 and IL-21 at indicated doses for 48 h (n=4, mean and s.e.m.; data at 4 units of CD154 were analyzed for statistical differences between *Sharpin*$^{+/+}$ and *Sharpin*^{cpdm} B cells). $^*p < 0.05$; $^{**}p<0.01$; $^{***}p < 0.001$; t-test.

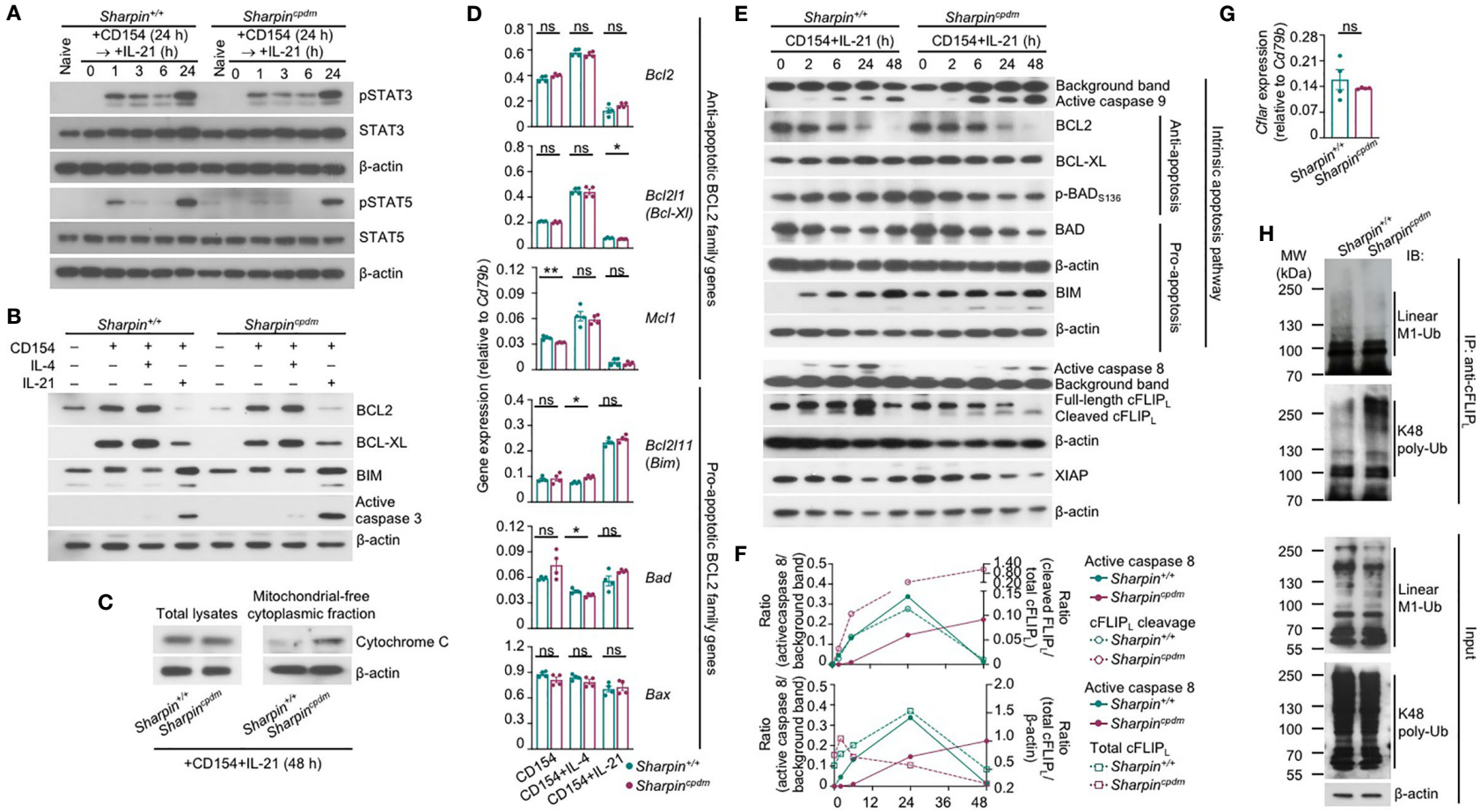

FIGURE 7 | SHARPIN inhibits caspase 8 and caspase 9 activation in B cells stimulated with CD154 and IL-21. **(A)** Immunoblotting analysis of STAT3 and STAT5 activation in *Sharpin*$^{+/+}$ and *Sharpin*^{cpdm} B cells stimulated with CD154 for 24 h and then IL-21 for different periods of time, as indicated. **(B, C)** Immunoblotting analysis of BCL2, BCL-XL and BIM expression and caspase 3 activation **(B)** and cytochrome C released into the cytosol **(C)** in *Sharpin*$^{+/+}$ and *Sharpin*^{cpdm} B cells stimulated for 48 h. **(D)** qRT-PCR analysis of gene expression, as indicated, in *Sharpin*$^{+/+}$ and *Sharpin*^{cpdm} B cells stimulated with CD154, alone or with IL-4 or IL-21, for 24 h (*p<0.05; **p < 0.01; t-test). **(E–F)** Immunoblotting analysis of caspase 8 and caspase 9 activation, expression of cFLIP$_L$, XIAP and BCL2 family members as well as BAD activation in *Sharpin*$^{+/+}$ and *Sharpin*^{cpdm} B cells stimulated with CD154 and IL-21 for different periods of time, as indicated. Quantified signals of caspase 8 activation, cFLIP$_L$ cleavage and total cFLIP$_L$ levels were depicted in **(F)**. **(G)** qRT-PCR analysis of *Cflar* expression in *Sharpin*$^{+/+}$ and *Sharpin*^{cpdm} B cells stimulated with CD154 plus IL-21 for 24 h (t-test). **(H)** Proteins in whole cell lysates (input) and immunoprecipitated by anti-cFLIP were analyzed by immunoblotting for linear M1-Ub and K48 poly-Ub levels in *Sharpin*$^{+/+}$ and *Sharpin*^{cpdm} B cells stimulated with CD154 plus IL-21 for 48 h. All immunoblotting analyses were representative of two independent experiments.

depending on its protein expression level while $cFLIP_R$ acting exclusively as an inhibitor – both isoforms are unstable proteins whose concentrations determine the sensitivity of cells to mitochondria-independent apoptosis (40). In *Sharpin*$^{+/+}$ B cells, the kinetics of the caspase 8 activation, i.e., first induced as early as 2 h after stimulation, peaking at 24 h and then decreased to the pre-stimulation level at 48 h, was mirrored by the kinetics of the cleavage of the full-length $cFLIP_L$ at Asp377 (equivalent to Asp376 of human $cFLIP_L$) to generate p43-$cFLIP_L$ and also by the kinetics of the expression of full-length or total $cFLIP_L$, likely reflecting a feedback control (**Figures 7E, F**). By contrast, full-length $cFLIP_L$ was continuously cleaved to yield p43-$cFLIP_L$ in *Sharpin*^{cpdm} B cells, with its protein level briefly induced after 2 h, starting to decrease at 6 h and diminished at 48 h, showing an inverse correlation with caspase 8 activation (**Figures 7E, F**). The reduced $cFLIP_L$ protein expression in *Sharpin*^{cpdm} B cells occurred despite normal *Cflar* gene transcription and was instead associated with decreased linear ubiquitination at the Met1 (linear M1-Ub) and increased polyubiquitination at Lys48 (K48 poly-Ub) of $cFLIP_L$ (**Figures 7G, H**), consistent with the notion that the $cFLIP_L$ protein level is controlled by proteasome degradation in a manner dependent on its K48 poly-Ub, which is catalyzed by the ITCH/AIP4 E3 ubiquitin ligase and was suggested to be hampered by linear M1-Ub of $cFLIP_L$ (41, 42). The overall linear M1-Ub was modestly reduced in *Sharpin*^{cpdm} B cells, likely reflecting the residual catalytic activities of the HOIP-HOIL sub-complex formed in the absence of SHARPIN. Finally, expression of XIAP, a potent inhibitor of the initiator caspase 7 as well as caspase 9 and caspase 3, was largely comparable in *Sharpin*$^{+/+}$ and *Sharpin*^{cpdm} B cells (**Figure 7E** and **Supplementary Figure 4**), highlighting the specificity of SHARPIN regulation of $cFLIP_L$.

Thus, SHARPIN deficiency modulates post-translational modifications of $cFLIP_L$, abolishes the expression of this caspase 8 regulator and boosts caspase 8 activation, and synchronizes the activation of caspase 8 with that of caspase 9 in the intrinsic apoptosis pathway without affecting BCL2 family factors.

SHARPIN Deficiency and HOIPIN-8 Synergize to Promote IL-21-Induced $cFLIP_L$ Loss and Apoptosis

Like the genetic ablation of *Sharpin*, LUBAC inhibitor HOIPIN-8 hampered activation of NF-κB by αCD40 in B cells, starting at 50 μM (**Supplementary Figure 5A**). At 20 μM, HOIPIN-8 did not affect NF-κB activation and had no impact on proliferation, IL-4-directed CSR to IgG1 or IL-21-triggered plasma cell differentiation in CD154-stimulated wildtype B cells (**Supplementary Figure 5B**). Neither did it adversely affect the normal proliferation or CSR in *Sharpin*^{cpdm} B cells (**Figure 8A**). Rather, HOIPIN-8 markedly increased the sensitivity of CD154-stimulated *Sharpin*^{cpdm} B cells to IL-21-induced apoptosis and cell death in a dose-dependent manner and virtually abrogated the viability of these cells after 96 h of culture, in contrast to its marginal impact on the viability of *Sharpin*$^{+/+}$ B cells (**Figures 8B, C** and **Supplementary Figure 5C**).

In *Sharpin*$^{+/+}$ B cells, total linear M1-Ub was induced upon stimulation by CD154, but returned to the basal level when IL-21 was added – IL-4 had no such dampening effect (**Figure 8D**). Treatment with HOIPIN-8 (at 20 μM) and SHARPIN deficiency each reduced linear M1-Ub, but together abrogated it in CD154 and IL-21-stimulated B cells (**Figure 8D** and **Supplementary Figure 5D**), likely due to the partial and full sensitivity of the HOIP-HOIL-SHARPIN complex and HOIP-HOIL sub-complex, respectively, to HOIPIN-8 at sub-optimal concentrations. Combining the HOIPIN-8 treatment and SHARPIN deficiency also decreased, by about 75%, linear M1-Ub induced by CD154 or CD154 plus IL-4, while each alone led to a 30-40% reduction (**Figure 8D** and **Supplementary Figure 5D**). Finally, the level of linear M1-Ub was positively correlated with the viability of B cells stimulated by CD154 or CD154 plus IL-21 (**Figure 8E** and **Supplementary Figure 5E**).

Unlike linear M1-Ub, the total K48 poly-Ub level was barely inducible; nor was it impaired by SHARPIN deficiency or the HOIPIN-8 treatment, which did not change the expression of anti-apoptotic factor BCL-XL and pro-apoptotic factor BAD – CD154 and IL-21-stimulated *Sharpin*^{cpdm} B cells did show 35% reduction of K48 poly-Ub after HOIPIN-8 treatment (**Figure 8D** and **Supplementary Figures 5D, E**). Accordingly, the levels of K48 poly-Ub level, BCL-XL, and BAD showed weak or no correlation with B cell viability (**Figure 8E**). By contrast, the expression of pro-apoptotic BIM and the level of the PARP cleavage, which is mediated by effector caspases during apoptosis, were synergistically elevated by the SHARPIN deficiency and HOIPIN-8 treatment, with both showing a strong negative correlation with the B cell viability (**Figures 8D, E** and **Supplementary Figure 5D**). Finally, the expression of the full-length $cFLIP_L$ protein closely tracked the level of linear M1-Ub, which was severely reduced in HOIPIN-8-treated CD154 and IL-21-stimulated *Sharpin*^{cpdm} B cells, and positively correlated with the B cell viability (**Figures 8D, E** and **Supplementary Figure 5D, 5E**).

In summary, the function of LUBAC in B cells is controlled by the availability of SHARPIN and the activity of HOIP. LUBAC, in turn, regulates the protein level of $cFLIP_L$ and critically promotes the survival of B cells stimulated with CD154 in the presence of IL-21.

DISCUSSION

This study has described the B cell-intrinsic role of LUBAC in promoting B cell survival from IL-21-triggered apoptosis, as relevant to the GC reaction, positive selection, and production of class-switched high-affinity Abs. Our data, as stemming from experiments involving B-*Sharpin*^{cpdm} and *Cd45.1*$^{+}$-*Sharpin*$^{+/+}$/*Cd45.2*$^{+}$-*Sharpin*^{cpdm} chimera mice, have significantly extended findings from a previous report, which showed that *mb1*$^{+/cre}$*Hoip*$^{fl/fl}$ mice displayed much reduced Ab responses, including those to T-independent Ags, but did not identify the *in vivo* defect of *mb1*$^{+/cre}$ *Hoip*$^{fl/fl}$ B cells underlying such impairment (31, 43). By contrast, our extensive analyses of B cell proliferation, survival, differentiation (CSR and plasma cell differentiation) as well as SHM and

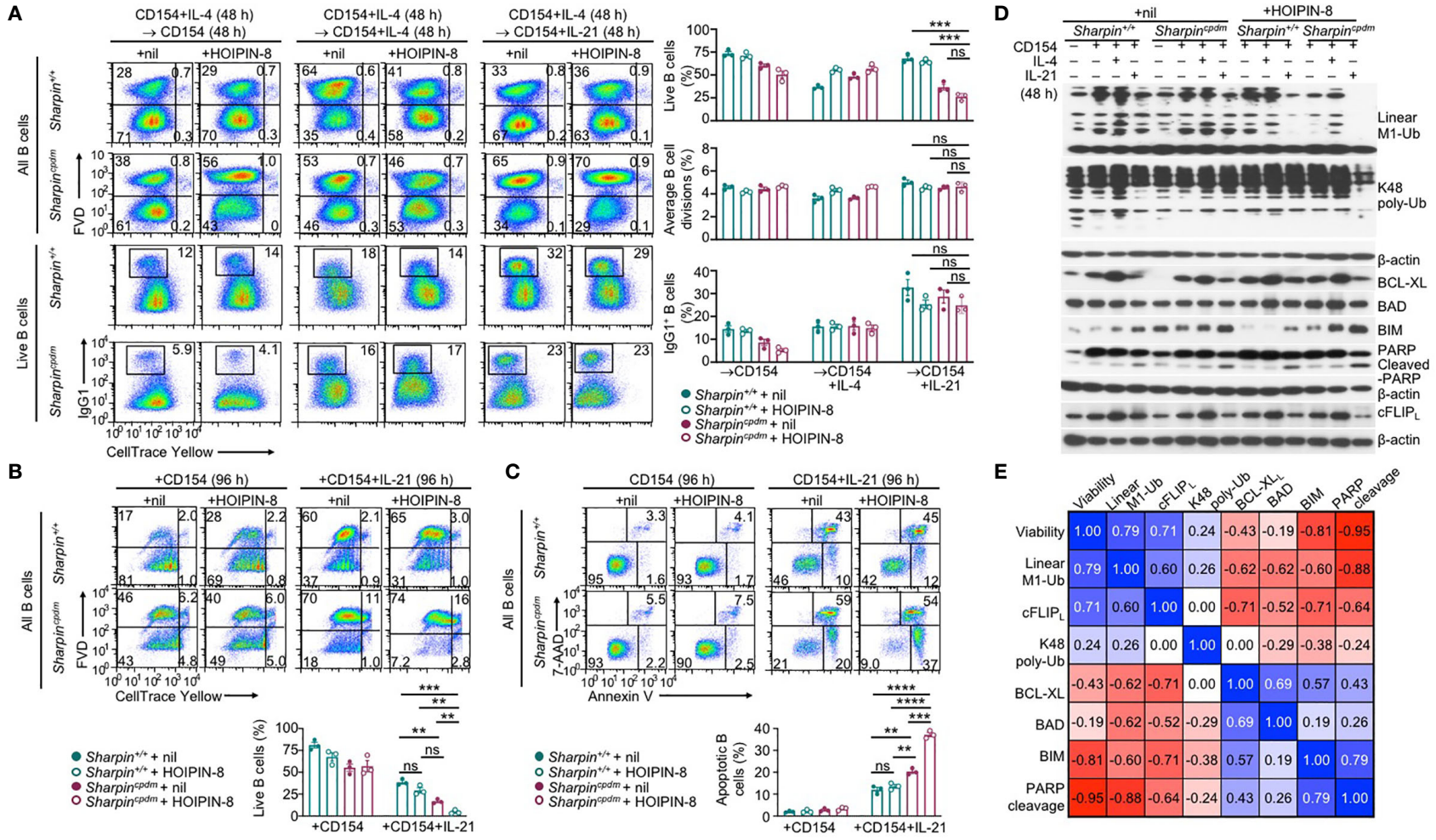

FIGURE 8 | SHARPIN deficiency and HOIPIN-8 synergize to promote IL-21-induced cFLIP$_L$ loss and apoptosis. **(A)** Flow cytometry analysis of survival, proliferation, and CSR to IgG1 in *Sharpin*$^{+/+}$ and *Sharpin*^{cpdm} B cells stimulated first with CD154 and IL-4 for 48 h, washed, and then with CD154, alone or plus IL-4 or IL-21, for 48 h in the presence of nil or HOIPIN-8 (20 μM). **(B)** Flow cytometry analysis of the viability of *Sharpin*$^{+/+}$ and *Sharpin*^{cpdm} B cells stimulated with CD154 or CD154 plus IL-21 for 96 h in the presence of nil or HOIPIN-8. **(C)** Flow cytometry analysis of apoptosis in *Sharpin*$^{+/+}$ and *Sharpin*^{cpdm} B cells stimulated with CD154 or CD154 plus IL-21 for 96 h in the presence of nil or HOIPIN-8. **(D)** Immunoblotting analysis of linear M1-Ub, K48 poly-Ub, expression of apoptosis-related factors and PARP cleavage in *Sharpin*$^{+/+}$ and *Sharpin*^{cpdm} B cells freshly isolated or stimulated, as indicated, for 24 h. Representative of two independent experiments. **(E)** Pair-wise correlation of different parameters, as indicated, in *Sharpin*$^{+/+}$ and *Sharpin*^{cpdm} B cells stimulated with CD154 or CD154 plus IL-21 in the presence of nil or HOIPIN-8 for 96 h (to determine cell viability; data from were **B**) or 24 h (other parameters; data were from **D** and **Supplementary Figure 5D**). $^{**}p < 0.01$; $^{***}p < 0.001$; $^{****}p < 0.0001$; t-test.

enrichment of a mutation that augments the affinity of BCRs have identified a key defect of SHARPIN-deficient B cells, i.e., reduced survival within GCs, that would provide a parsimonious explanation for the impaired T-dependent Ab response in mice with B cell-specific ablation of LUBAC. Confirming a causative role of the defective *Sharpin*^{cpdm} GC B cell survival in this process would require generating mice with simultaneous *Sharpin* (or *Hoip*) deletion and enforced expression of an apoptosis inhibitor, such as a dominant negative mutant of effector caspase 3 (44), specifically in GC B cells (e.g., through *Cγ1-cre* or *Aicda-cre*) – genetic alterations of a single factor in the mitochondria-dependent intrinsic pathway or the mitochondria-independent pathway would be less likely to maintain the full GC B cell viability. The viability of GC B cells in B-*Sharpin*^{cpdm} mice may also be restored by caspase 3 inhibitor Z-VAD-FMK (or possibly Z-IETD-FMK combined with Z-LEHD-FMK), but further compromised by HOIPIN-8. Finally, *Sharpin*^{cpdm} B cells were also defective in survival upon TLR ligand stimulation, likely explaining the reduced production of IgG3 and IgG2b Abs.

Shortly after the discovery of IL-21 and its crucial role in plasma cell differentiation, the potent B cell killing activity of this cytokine was recognized (10, 45, 46), although how this killing activity is circumvented in GCs and its relevance to the T-dependent Ab response remain unaddressed. This was in part due to the difficulty of untangling its effect from the important role of IL-21 in promoting the proliferation of B cells activated by sub-optimal CD40 signals (e.g., as initiated by αCD40 or low doses of CD154). As shown here, the SHARPIN deficiency decoupled the survival from the proliferation/differentiation of GC B cells *in vivo* and B cells activated by CD154 and IL-21 *in vitro*, thereby providing an opportunity to reveal the role of IL-21-triggered B cell death in the GC reaction, including the positive selection of high-affinity BCR mutants, and underlying mechanisms. CD40-activated B cells would need at least two mechanisms to survive the assault by IL-21, i.e., potent CD40 signals that induce anti-apoptotic BCL2 and BCL-XL to counter the effect of IL-21 in activating the mitochondria-dependent intrinsic apoptosis pathway (**Figure 9B**) as well as LUBAC that inhibits caspase 8, thereby preventing synchronized caspase 8 and -9 activation, full mobilization of caspase 3 and irreversible apoptosis (**Figure 9A**). The requirement for LUBAC would be important to preserve all GC B cells, irrespective of the affinity of their BCRs, particularly when such B cells are at the early phase of the iterative proliferation and selection process, i.e., completing fewer divisions. The requirement for strong CD40 signals would be consistent with the notion that GC B cell clones are differentially selected based on the quality and quantity of their contacts with Tfh cells due to their differences in BCR affinity and, therefore, the Ag uptake and presentation to Tfh cells. However, more contacts would also lead to more exposure to IL-21 produced by the same Tfh cells and, therefore, a higher threshold of B cell survival. Thus, the entwined and counteracting effects of CD154 and IL-21 would make them the prime candidate for enforcing a continuous positive selection process underpinned by the co-evolution (i.e., co-upregulation) of the death-inducing signals and the survival signal after each round of the selection. Such co-evolution would explain the stepwise improvement of the Ab affinity, a crucial aspect of the positive selection that had, however, been largely unexplored. Notably, Tfh cells were largely normal in B-*Sharpin*^{cpdm} mice despite the reduced GC reaction, a phenotype similar to that of IL-21- and IL-21R-deficient mice (11, 47), perhaps reflecting a compensatory role of CD154 plus IL-4-activated B cells in the engagement and maintenance of Tfh cells – such B cells would not be affected by the *Sharpin* deficiency in their proliferation, survival, CSR or plasma cell differentiation, as shown here. Complementing the role of Tfh cells, elevated signaling from high-affinity BCRs may also be involved in maintaining GC B cells despite being downregulated in these cells (48, 49), but unlikely to induce B cell death or involved in the stepwise affinity maturation process. Finally, the *Sharpin*^{cpdm} B cells activated *in vitro* showed normal expression of *Myc* and *mTORC1* (our RNA-Seq data, not shown), which promote the expansion of selected B cell clones (50–53), suggesting that the defective positive selection of B-*Sharpin*^{cpdm} mice was not due to reduced proliferation of high-affinity clones.

The high-throughput $V_{186.2}$-DJ_H sequences reported here could be used to construct "lineage trees". Each tree would be rooted in a distinct progenitor, acquiring a dominant branch stemming from a high-affinity founder sub-clone (e.g., that carrying the $G_{98}\rightarrow T_{98}$ mutation) and further branched with new rounds of SHM, thereby opening a window for observation into the positive selection process and its impairment in *Sharpin*^{cpdm} B cells, as lack of robust positive selection would result in overall less complex lineage trees. In addition, the exclusive occurrence of $G_{98}\rightarrow T_{98}$ in $V_{186.2}$-DJ_H-Cγ1, but not $V_{186.2}$-DJ_H-Cμ, provides additional, albeit indirect, evidence for the notion that IL-4-directed CSR to IgG1 preceded IL-21-mediated development of GCs, within which peak SHM and positive selection unfold (16). Also along this line, pre-activation of *Sharpin*$^{+/+}$ or *Sharpin*^{cpdm} B cells with CD154 plus IL-4 did not make them resistant to death induced by IL-21, the production of which lags the IL-4 production by NKT cells and Th2 cells before the GC reaction (15, 54), indicating that sensitivity to IL-21-triggered death is an important feature intrinsic to GC B cells. By contrast, pre-activation by TLR ligands promoted the survival of B cells activated by sub-optimal CD40 signaling (e.g., as initiated by αCD40) and IL-21, likely mediating their differentiation into IL-27-producing B cells (55). Finally, the ability of strong BCR crosslinking by αIgD/dex to endow *Sharpin*^{cpdm} B cells resistance to IL-21 suggests that BCR signaling partially contributed to the GC B cell survival in B-*Sharpin*^{cpdm} mice, possibly by upregulating MYC (56).

As previously shown (45, 46) and further extended here, IL-21 induced apoptosis through the intrinsic pathway by modulating the expression of the BCL2 family of pro-apoptotic and anti-apoptotic members that control the mitochondria membrane permeability and cytochrome C release for caspase 9 activation. Without a death domain (DD), the IL-21 receptor is unable to recruit DD-containing adaptors that initiate the death effector domain (DED)-dependent caspase 8 activation. CD40 has no DD either, in contrast to FAS (and other TNF receptor superfamily members, such as TNFR and TRAIL), raising the possibility that,

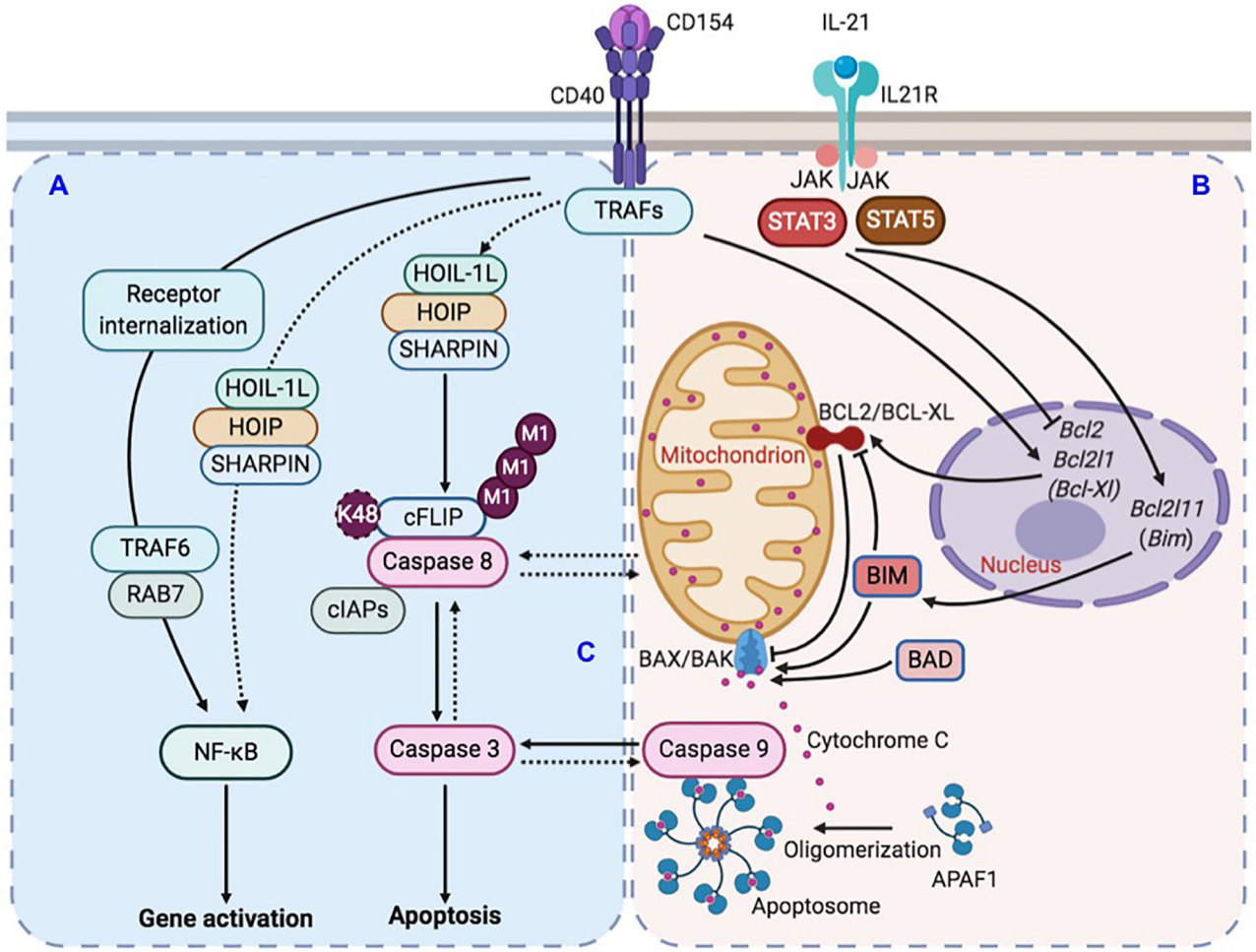

FIGURE 9 | Illustration of LUBAC-mediated suppression of IL-21-induced apoptosis in CD154-stimulated B cells. **(A)** CD40 activation in B cells upregulates LUBAC-catalyzed linear M1-Ub, including that of cFLIP, which leads to cFLIP stabilization and inhibition of caspase 8 activation. LUBAC plays a minor role to the major role of RAB7 in CD40-triggered NF-κB activation in B cells. **(B)** CD40 activation also induces the expression of anti-apoptotic factor BCL2 and BCL-XL. IL-21, however, dampens such induction and also upregulates expression of pro-apoptotic factor BIM. The combined effects of BCL2/BCL-XL downregulation and BIM upregulation would activate pro-apoptotic BAX/BAK complex to increase the mitochondria permeability and cytochrome C release into the cytoplasm to activate caspase 9. **(C)** In the absence of LUBAC, caspase 8 activation would amplify a putative caspase network, within which multiple caspases, including caspase 9 and caspase 3, would be activated in a synchronized manner due to positive-feedback loops, leading to the irreversible apoptosis process.

in CD154 and IL-21-stimulated B cells, caspase 8 was activated by a receptor-independent apoptosis process, e.g., through a macromolecular complex nucleated by the auto-aggregation of DD- and DED-containing adaptor FADD followed by pro-caspase 8 recruitment and self-activation, as occurring in cancer cells (57). Such caspase 8 activation would be subsequently suppressed in *Sharpin*$^{+/+}$ B cells due to upregulation of cFLIP, but not in *Sharpin*^{cpdm} B cells, in which cFLIP level was significantly reduced, as shown here. Nevertheless, the full and sustained activation of caspase 8 might require caspase 9 activation by IL-21 and ultimately caspase 3, perhaps within a recently suggested caspase network (58) (**Figure 9C**). Within such a network, positive feedback loops (e.g., those among the initiator caspases and between the initiator and effector caspases) would synchronize the activation of multiple caspases, as likely underpinned by caspase cleavage-mediated inactivation of anti-apoptosis factors and activation of pro-apoptotic factors, including caspase 8 activation of BID to trigger caspase 9 (59). The rescue of the viability of IL-21-stimulated B cells by enforced BCL2 overexpression or deficiency in BIM (45, 46) emphasizes the role of the intrinsic apoptosis pathway but does not rule out its collaboration with activated caspase 8 to fully activate caspase 3. Finally, IL-21 readily induced apoptosis in B cells deficient in FAS, TNFRI, or TNFRII (46), showing that IL-21 did not cause cell death indirectly by inducing these death receptors.

Although SHARPIN was originally identified as a key LUBAC component for NF-κB activation by αCD40 in Ramos B lymphoma cells (23, 24), the LUBAC pathway did not play a

major role in NF-κB activation in CD154-stimulated primary B cells, which rather use CD40 endocytosis and the RAB7-dependent endosomal pathway to activate NF-κB (39). Instead, CD154 upregulated, in addition to BCL2 and BCL-XL, and Linear M1-Ub (**Figures 9A, B**), which is exclusively catalyzed by different forms of complexes containing HOIP, HOIL-1, and/or SHARPIN and, as shown here, had a strong a positive correlation with the viability of B cells stimulated with CD154 plus different cytokine combinations. This correlation was unveiled by the partial defect of *Sharpin*^{cpdm} B cells in catalyzing Linear M1-Ub and the use of a sub-optimal dose of HOIPIN-8. Furthermore, despite the strong correlation among the B-cell viability, Linear M1-Ub, and c-FLIP$_L$ levels, a definitive role of linear ubiquitinated c-FLIP$_L$ in maintaining the B cell viability remains to be proven, possibly by the specific disruption of interaction of c-FLIP$_L$ with LUBAC and, conversely, the rescue of the viability of HOIPIN-8-treated *Sharpin*^{cpdm} B cells with enforced expression of c-FLIP$_L$, preferably a form that carries a K48 mutation and, therefore, is resistant to K48 polyubiquitination and proteasome degradation. Although it has long been recognized that cFLIP plays a role in the activation and survival of immune cells (60–65), including T cells and B cells, exactly how its level (a limiting factor in the anti-apoptosis activity) in immune cells is regulated, including by LUBAC, remains to be defined. As cFLIP also controls the pivoting between apoptosis and necroptosis, either through receptor-induced RIP kinase or receptor-independent assembly of riptosomes, whether and how cFLIP regulates necroptosis to influence the outcome of B cell viability and GC reaction needs to be explored, particularly in light of recent findings showing the unexpected role of caspase 9 in inhibiting necroptosis to promote GC B cell maintenance (66). Finally, cFLIP downregulation sensitized B lymphoma cells to TRAIL-induced apoptosis and breast cancer cells to ligand-independent but FADD-, caspase 8- and caspase 9-dependent apoptosis (65, 67), suggesting that HOIPIN-8, which downregulated cFLIP expression, could potentially be developed into therapeutics for B cell lymphoma as well as systemic lupus, particularly the disease caused by heightened apoptosis threshold due to lack of FAS.

DATA AVAILABILITY STATEMENT

The datasets presented in this study can be found in online repositories. The names of the repository/repositories and accession number(s) can be found below: NCBI SRA data PRJNA704065, BioSample accessions: SAMN18029793, SAMN18029794.

ETHICS STATEMENT

The animal study was reviewed and approved by The Institutional Animal Care and Use Committee (IACUC) of UTHSCSA.

AUTHOR CONTRIBUTIONS

Conceptualization (JW, HY, and ZX), investigation (JW, CR, HY, and ZX), visualization (JW, TL, HZ, and HY), funding acquisition (ZX), and supervision (HY and ZX). All authors contributed to the article and approved the submitted version.

FUNDING

This work was supported by NIH AI 124172, AI 131034, AI 135599, AI 153506, and DOD BC170448 grants. The UTHSCSA Flow Cytometry Core facility is supported by NIH P30 CA054174 and UL1 TR001120, and Genome Sequencing Facility supported by NIH P30 CA054174, S10 OD021805, and CPRIT Core RP160732 grants.

ACKNOWLEDGMENTS

We thank Dr. William Kaiser and Ms. Amanda Fisher for mice and reagents, Dr. Stanton McHardy and Mr. Bismarck Campos for HOIPIN-8 synthesis, and Dr. Paolo Casali for suggestions. This work was supported by NIH AI 124172, AI 131034, AI 135599, AI 153506, and DOD BC170448 grants. The UTHSCSA Flow Cytometry Core facility is supported by NIH P30 CA054174, and Genome Sequencing Facility supported by NIH P30 CA054174, S10 OD021805, and CPRIT Core RP160732 grants.

SUPPLEMENTARY MATERIAL

The Supplementary Material for this article can be found online at: https://www.frontiersin.org/articles/10.3389/fimmu.2021.658048/full#supplementary-material

Supplementary Figure 1–5 |

Supplementary Table 1 | Antibodies and reagents.

Supplementary Table 2 | Oligonucleotide sequences.

REFERENCES

1. Lund FE, Randall TD. Effector and regulatory B cells: modulators of CD4+ T cell immunity. *Nat Rev Immunol* (2010) 10:236–47. doi: 10.1038/nri2729
2. Xu Z, Zan H, Pone EJ, Mai T, Casali P. Immunoglobulin class-switch DNA recombination: induction, targeting and beyond. *Nat Rev Immunol* (2012) 12:517–31. doi: 10.1038/nri3216
3. Elsner RA, Shlomchik MJ. Germinal center and extrafollicular B cell responses in vaccination, immunity, and autoimmunity. *Immunity* (2020) 53:1136–50. doi: 10.1016/j.immuni.2020.11.006
4. Shinnakasu R, Inoue T, Kometani K, Moriyama S, Adachi Y, Nakayama M, et al. Regulated selection of germinal-center cells into the memory B cell compartment. *Nat Immunol* (2016) 17:861–9. doi: 10.1038/ni.3460
5. Barwick BG, Scharer CD, Martinez RJ, Price MJ, Wein AN, Haines RR, et al. B cell activation and plasma cell differentiation are inhibited by de novo

DNAmethylation. *Nat Commun* (2018) 9, 1900. doi: 10.1038/s41467-018-04234-4
6. Pone EJ, Zhang J, Mai T, White CA, Li G, Sakakura JK, et al. BCR-signalling synergizes with TLR-signalling for induction of AID and immunoglobulin class-switching through the non-canonical NF-kappaB pathway. *Nat Commun* (2012) 3:767. doi: 10.1038/ncomms1769
7. Craft JE. Follicular helper T cells in immunity and systemic autoimmunity. *Nat Rev Rheumatol* (2012) 8:337–47. doi: 10.1038/nrrheum.2012.58
8. Shulman Z, Gitlin AD, Weinstein JS, Lainez B, Esplugues E, Flavell RA, et al. Dynamic signaling by T follicular helper cells during germinal center B cell selection. *Science* (2014) 345:1058–62. doi: 10.1126/science.1257861
9. Ozaki K, Spolski R, Feng CG, Qi CF, Cheng J, Sher A, et al. A critical role for IL-21 in regulating immunoglobulin production. *Science* (2002) 298:1630–4. doi: 10.1126/science.1077002
10. Ozaki K, Spolski R, Ettinger R, Kim H-P, Wang G, Qi C-F, et al. Regulation of B cell differentiation and plasma cell generation by IL-21, a novel inducer of Blimp-1 and Bcl-6. *J Immunol* (2004) 173:5361–71. doi: 10.4049/jimmunol.173.9.5361
11. Zotos D, Coquet JM, Zhang Y, Light A, D'Costa K, Kallies A, et al. IL-21 regulates germinal center B cell differentiation and proliferation through a B cell-intrinsic mechanism. *J Exp Med* (2010) 207:365–78. doi: 10.1084/jem.20091777
12. Nutt SL, Hodgkin PD, Tarlinton DM, Corcoran LM. The generation of antibody-secreting plasma cells. *Nat Rev Immunol* (2015) 15:160–71. doi: 10.1038/nri3795
13. Tangye SG, Ma CS. Regulation of the germinal center and humoral immunity by interleukin-21. *J Exp Med* (2020) 217:e20191638. doi: 10.1084/jem.20191638
14. Choi MS, Brines RD, Holman MJ, Klaus GG. Induction of NF-AT in normal B lymphocytes by anti-immunoglobulin or CD40 ligand in conjunction with IL-4. *Immunity* (1994) 1:179–87. doi: 10.1016/1074-7613(94)90096-5
15. Weinstein JS, Herman EI, Lainez B, Licona-Limon P, Esplugues E, Flavell R, et al. TFH cells progressively differentiate to regulate the germinal center response. *Nat Immunol* (2016) 17:1197–205. doi: 10.1038/ni.3554
16. Roco JA, Mesin L, Binder SC, Nefzger C, Gonzalez-Figueroa P, Canete PF, et al. Class-switch recombination occurs infrequently in germinal centers. *Immunity* (2019) 51:337–350 e337. doi: 10.1016/j.immuni.2019.07.001
17. Cyster JG, Allen CDC. B cell responses: cell Interaction dynamics and decisions. *Cell* (2019) 177:524–40. doi: 10.1016/j.cell.2019.03.016
18. Rathmell JC, Cooke MP, Ho WY, Grein J, Townsend SE, Davis MM, et al. CD95 (Fas)-dependent elimination of self-reactive B cells upon interaction with CD4+ T cells. *Nature* (1995) 376:181–4. doi: 10.1038/376181a0
19. Rothstein TL, Wang JK, Panka DJ, Foote LC, Wang Z, Stanger B, et al. Protection against Fas-dependent Th1-mediated apoptosis by antigen receptor engagement in B cells. *Nature* (1995) 374:163–5. doi: 10.1038/374163a0
20. Wang J, Lenardo MJ. Essential lymphocyte function associated 1 (LFA-1): intercellular adhesion molecule interactions for T cell-mediated B cell apoptosis by Fas/APO-1/CD95. *J Exp Med* (1997) 186:1171–6. doi: 10.1084/jem.186.7.1171
21. Depoil D, Zaru R, Guiraud M, Chauveau A, Harriague J, Bismuth G, et al. Immunological synapses are versatile structures enabling selective T cell polarization. *Immunity* (2005) 22:185–94. doi: 10.1016/j.immuni.2004.12.010
22. Meyer-Hermann M, Mohr E, Pelletier N, Zhang Y, Victora GD, Toellner KM. A theory of germinal center B cell selection, division, and exit. *Cell Rep* (2012) 2:162–74. doi: 10.1016/j.celrep.2012.05.010
23. Tokunaga F, Nakagawa T, Nakahara M, Saeki Y, Taniguchi M, Sakata S, et al. SHARPIN is a component of the NF-kappaB-activating linear ubiquitin chain assembly complex. *Nature* (2011) 471:633–6. doi: 10.1038/nature09815
24. Ikeda F, Deribe YL, Skanland SS, Stieglitz B, Grabbe C, Franz-Wachtel M, et al. SHARPIN forms a linear ubiquitin ligase complex regulating NF-kappaB activity and apoptosis. *Nature* (2011) 471:637–41. doi: 10.1038/nature09814
25. Katsuya K, Oikawa D, Iio K, Obika S, Hori Y, Urashima T, et al. Small-molecule inhibitors of linear ubiquitin chain assembly complex (LUBAC), HOIPINs, suppress NF-kappaB signaling. *Biochem Biophys Res Commun* (2019) 509:700–6. doi: 10.1016/j.bbrc.2018.12.164
26. Oikawa D, Sato Y, Ohtake F, Komakura K, Hanada K, Sugawara K, et al. Molecular bases for HOIPINs-mediated inhibition of LUBAC and innate immune responses. *Commun Biol* (2020) 3:163. doi: 10.1038/s42003-020-0882-8
27. Ngo KA, Kishimoto K, Davis-Turak J, Pimplaskar A, Cheng Z, Spreafico R, et al. Dissecting the regulatory strategies of NF-kappaB RelA target genes in the inflammatory response reveals differential transactivation logics. *Cell Rep* (2020) 30:2758–2775 e2756. doi: 10.1016/j.celrep.2020.01.108
28. Sanchez HN, Moroney JB, Gan H, Shen T, Im JL, Li T, et al. B cell-intrinsic epigenetic modulation of antibody responses by dietary fiber-derived short-chain fatty acids. *Nat Commun* (2020) 11:60. doi: 10.1038/s41467-019-13603-6
29. Ye J, Ma N, Madden TL, Ostell JM. IgBLAST: an immunoglobulin variable domain sequence analysis tool. *Nucleic Acids Res* (2013) 41:W34–40. doi: 10.1093/nar/gkt382
30. Gupta NT, Vander Heiden JA, Uduman M, Gadala-Maria D, Yaari G, Kleinstein SH. Change-O: a toolkit for analyzing large-scale B cell immunoglobulin repertoire sequencing data. *Bioinformatics* (2015) 31:3356–8. doi: 10.1093/bioinformatics/btv359
31. Sasaki Y, Sano S, Nakahara M, Murata S, Kometani K, Aiba Y, et al. Defective immune responses in mice lacking LUBAC-mediated linear ubiquitination in B cells. *EMBO J* (2013) 32:2463–76. doi: 10.1038/emboj.2013.184
32. Cumano A, Rajewsky K. Structure of primary anti-(4-hydroxy-3-nitrophenyl) acetyl (NP) antibodies in normal and idiotypically suppressed C57BL/6 mice. *Eur J Immunol* (1985) 15:512–20. doi: 10.1002/eji.1830150517
33. Jacob J, Kelsoe G. In situ studies of the primary immune response to (4-hydroxy-3-nitrophenyl)acetyl. II. A common clonal origin for periarteriolar lymphoid sheath-associated foci and germinal centers. *J Exp Med* (1992) 176:679–87. doi: 10.1084/jem.176.3.679
34. Furukawa K, Akasako-Furukawa A, Shirai H, Nakamura H, Azuma T. Junctional amino acids determine the maturation pathway of an antibody. *Immunity* (1999) 11:329–38. doi: 10.1016/s1074-7613(00)80108-9
35. Allen D, Simon T, Sablitzky F, Rajewsky K, Cumano A. Antibody engineering for the analysis of affinity maturation of an anti-hapten response. *EMBO J* (1988) 7:1995–2001. doi: 10.1002/j.1460-2075.1988.tb03038.x
36. Chang B, Casali P. The CDR1 sequences of a major proportion of human germline Ig VH genes are inherently susceptible to amino acid replacement. *Immunol Today* (1994) 15:367–73. doi: 10.1016/0167-5699(94)90175-9
37. Mesin L, Ersching J, Victora GD. Germinal center B cell dynamics. *Immunity* (2016) 45:471–82. doi: 10.1016/j.immuni.2016.09.001
38. Gan H, Shen T, Chupp DP, Taylor JR, Sanchez HN, Li X, et al. B cell Sirt1 deacetylates histone and non-histone proteins for epigenetic modulation of AID expression and the antibody response. *Sci Adv* (2020) 6:eaay2793. doi: 10.1126/sciadv.aay2793
39. Yan H, Fernandez M, Wang J, Wu S, Wang R, Lou Z, et al. B cell endosomal RAB7 promotes TRAF6 K63 polyubiquitination and NF-kappaB activation for antibody class-switching. *J Immunol* (2020) 204:1146–57. doi: 10.4049/jimmunol.1901170
40. Tsuchiya Y, Nakabayashi O, Nakano H. FLIP the Switch: Regulation of Apoptosis and Necroptosis by cFLIP. *Int J Mol Sci* (2015) 16:30321–41. doi: 10.3390/ijms161226232
41. Chang L, Kamata H, Solinas G, Luo JL, Maeda S, Venuprasad K, et al. The E3 ubiquitin ligase itch couples JNK activation to TNFalpha-induced cell death by inducing c-FLIP(L) turnover. *Cell* (2006) 124:601–13. doi: 10.1016/j.cell.2006.01.021
42. Tang Y, Joo D, Liu G, Tu H, You J, Jin J, et al. Linear ubiquitination of cFLIP induced by LUBAC contributes to TNFalpha-induced apoptosis. *J Biol Chem* (2018) 293:20062–72. doi: 10.1074/jbc.RA118.005449
43. Sasaki Y, Iwai K. Crucial role of linear ubiquitin chain assembly complex-mediated inhibition of programmed cell death in TLR4-dediated B cell responses and B1b cell development. *J Immunol* (2018) 200:3438–49. doi: 10.4049/jimmunol.1701526
44. Liu X, He Y, Li F, Huang Q, Kato TA, Hall RP, et al. Caspase-3 promotes genetic instability and carcinogenesis. *Mol Cell* (2015) 58:284–96. doi: 10.1016/j.molcel.2015.03.003
45. Mehta DS, Wurster AL, Whitters MJ, Young DA, Collins M, Grusby MJ. IL-21 induces the apoptosis of resting and activated primary B cells. *J Immunol* (2003) 170:4111–8. doi: 10.4049/jimmunol.170.8.4111
46. Jin H, Carrio R, Yu A, Malek TR. Distinct activation signals determine whether IL-21 induces B cell costimulation, growth arrest, or Bim-dependent apoptosis. *J Immunol* (2004) 173:657–65. doi: 10.4049/jimmunol.173.1.657
47. Linterman MA, Beaton L, Yu D, Ramiscal RR, Srivastava M, Hogan JJ, et al. IL-21 acts directly on B cells to regulate Bcl-6 expression and germinal center responses. *J Exp Med* (2010) 207:353–63. doi: 10.1084/jem.20091738

48. Khalil AM, Cambier JC, Shlomchik MJ. B cell receptor signal transduction in the GC is short-circuited by high phosphatase activity. *Science* (2012) 336:1178–81. doi: 10.1126/science.1213368
49. Turner JS, Ke F, Grigorova IL. B cell receptor crosslinking augments germinal center B cell selection when T cell help is limiting. *Cell Rep* (2018) 25:1395–403 e1394. doi: 10.1016/j.celrep.2018.10.042
50. Dominguez-Sola D, Victora GD, Ying CY, Phan RT, Saito M, Nussenzweig MC, et al. The proto-oncogene MYC is required for selection in the germinal center and cyclic reentry. *Nat Immunol* (2012) 13:1083–91. doi: 10.1038/ni.2428
51. Calado DP, Sasaki Y, Godinho SA, Pellerin A, Kochert K, Sleckman BP, et al. The cell-cycle regulator c-Myc is essential for the formation and maintenance of germinal centers. *Nat Immunol* (2012) 13:1092–100. doi: 10.1038/ni.2418
52. Ersching J, Efeyan A, Mesin L, Jacobsen JT, Pasqual G, Grabiner BC, et al. Germinal center selection and affinity maturation require dynamic regulation of mTORC1 kinase. *Immunity* (2017) 46:1045–58 e1046. doi: 10.1016/j.immuni.2017.06.005
53. Raybuck AL, Cho SH, Li J, Rogers MC, Lee K, Williams CL, et al. B cell-intrinsic mTORC1 promotes germinal center-defining transcription factor gene expression, somatic hypermutation, and memory B cell generation in humoral immunity. *J Immunol* (2018) 200:2627–39. doi: 10.4049/jimmunol.1701321
54. Gaya M, Barral P, Burbage M, Aggarwal S, Montaner B, Warren Navia A, et al. Initiation of antiviral B cell immunity relies on innate signals from spatially positioned NKT cells. *Cell* (2018) 172:517–33 e520. doi: 10.1016/j.cell.2017.11.036
55. Yan H, Wang R, Wang J, Wu S, Fernandez M, Rivera CE, et al. BATF3-dependent induction of IL-27 by B cells bridges the innate and adaptive stages of the antibody response. *bioRxiv* (2020). doi: 10.1101/2020.06.26.117010
56. Luo W, Weisel F, Shlomchik MJ. B cell receptor and CD40 signaling are rewired for synergistic induction of the c-Myc transcription factor in germinal center B cells. *Immunity* (2018) 48:313–26 e315. doi: 10.1016/j.immuni.2018.01.008
57. Ehlken H, Krishna-Subramanian S, Ochoa-Callejero L, Kondylis V, Nadi NE, Straub BK, et al. Death receptor-independent FADD signalling triggers hepatitis and hepatocellular carcinoma in mice with liver parenchymal cell-specific NEMO knockout. *Cell Death Differ* (2014) 21:1721–32. doi: 10.1038/cdd.2014.83
58. McComb S, Chan PK, Guinot A, Hartmannsdottir H, Jenni S, Dobay MP, et al. Efficient apoptosis requires feedback amplification of upstream apoptotic signals by effector caspase-3 or -7. *Sci Adv* (2019) 5:eaau9433. doi: 10.1126/sciadv.aau9433
59. Li H, Zhu H, Xu CJ, Yuan J. Cleavage of BID by caspase 8 mediates the mitochondrial damage in the Fas pathway of apoptosis. *Cell* (1998) 94:491–501. doi: 10.1016/s0092-8674(00)81590-1
60. Zhang N, He YW. An essential role for c-FLIP in the efficient development of mature T lymphocytes. *J Exp Med* (2005) 202:395–404. doi: 10.1084/jem.20050117
61. Budd RC, Yeh WC, Tschopp J. cFLIP regulation of lymphocyte activation and development. *Nat Rev Immunol* (2006) 6:196–204. doi: 10.1038/nri1787
62. Zhang N, Hopkins K, He YW. c-FLIP protects mature T lymphocytes from TCR-mediated killing. *J Immunol* (2008) 181:5368–73. doi: 10.4049/jimmunol.181.8.5368
63. Zhang H, Rosenberg S, Coffey FJ, He YW, Manser T, Hardy RR, et al. A role for cFLIP in B cell proliferation and stress MAPK regulation. *J Immunol* (2009) 182:207–15. doi: 10.4049/jimmunol.182.1.207
64. Coffey F, Manser T. Expression of cellular FLIP by B cells is required for their participation in an immune response. *J Immunol* (2010) 184:4871–9. doi: 10.4049/jimmunol.0903506
65. Braun FK, Mathur R, Sehgal L, Wilkie-Grantham R, Chandra J, Berkova Z, et al. Inhibition of methyltransferases accelerates degradation of cFLIP and sensitizes B-cell lymphoma cells to TRAIL-induced apoptosis. *PloS One* (2015) 10:e0117994. doi: 10.1371/journal.pone.0117994
66. Zhang J, Kodali S, Chen M, Wang J. Maintenance of germinal center B cells by caspase-9 through promotion of apoptosis and inhibition of necroptosis. *J Immunol* (2020) 205:113–20. doi: 10.4049/jimmunol.2000359
67. Day TW, Huang S, Safa AR. c-FLIP knockdown induces ligand-independent DR5-, FADD-, caspase-8-, and caspase-9-dependent apoptosis in breast cancer cells. *Biochem Pharmacol* (2008) 76:1694–704. doi: 10.1016/j.bcp.2008.09.007

Conflict of Interest: The authors declare that the research was conducted in the absence of any commercial or financial relationships that could be construed as a potential conflict of interest.

frontiers in Immunology

REVIEW
published: 17 May 2021
doi: 10.3389/fimmu.2021.683710

miRNA-Mediated Control of B Cell Responses in Immunity and SLE

Stephanie L. Schell and Ziaur S. M. Rahman *

Department of Microbiology and Immunology, Pennsylvania State University College of Medicine, Hershey, PA, United States

Loss of B cell tolerance is central to autoimmune diseases such as systemic lupus erythematosus (SLE). As such, the mechanisms involved in B cell development, maturation, activation, and function that are aberrantly regulated in SLE are of interest in the design of targeted therapeutics. While many factors are involved in the generation and regulation of B cell responses, miRNAs have emerged as critical regulators of these responses within the last decade. To date, miRNA involvement in B cell responses has largely been studied in non-autoimmune, immunization-based systems. However, miRNA profiles have also been strongly associated with SLE in human patients and these molecules have proven critical in both the promotion and regulation of disease in mouse models and in the formation of autoreactive B cell responses. Functionally, miRNAs are small non-coding RNAs that bind to complementary sequences located in target mRNA transcripts to mediate transcript degradation or translational repression, invoking a post-transcriptional level of genetic regulation. Due to their capacity to target a diverse range of transcripts and pathways in different immune cell types and throughout the various stages of development and response, targeting miRNAs is an interesting potential therapeutic avenue. Herein, we focus on what is currently known about miRNA function in both normal and SLE B cell responses, primarily highlighting miRNAs with confirmed functions in mouse models. We also discuss areas that should be addressed in future studies and whether the development of miRNA-centric therapeutics may be a viable alternative for the treatment of SLE.

Keywords: miRNA, autoimmunity, B cells, germinal center, systemic lupus erythematosus

OPEN ACCESS

Edited by:
Zhenming Xu,
The University of Texas Health Science Center at San Antonio, United States

Reviewed by:
Robert A. Eisenberg,
University of Pennsylvania, United States
Nan Shen,
Shanghai JiaoTong University, China

***Correspondence:**
Ziaur S. M. Rahman
zrahman@pennstatehealth.psu.edu

Specialty section:
This article was submitted to B Cell Biology, a section of the journal Frontiers in Immunology

Received: *22 March 2021*
Accepted: *04 May 2021*
Published: *17 May 2021*

Citation:
Schell SL and Rahman ZSM (2021) miRNA-Mediated Control of B Cell Responses in Immunity and SLE. Front. Immunol. 12:683710. doi: 10.3389/fimmu.2021.683710

INTRODUCTION

B cell development and function is critical for the establishment of a B cell repertoire that can respond to a diversity of foreign antigens (1). Antigenic exposure initiates B cell responses that target invading pathogens and leads to the formation of long-lived plasma cell and memory B cell responses that protect the host against future reinfection (2). While B cells are critical for the establishment of normal immune responses against pathogens, they can become dysregulated under certain circumstances, leading to the development of autoimmunity (3). Systemic lupus erythematosus (SLE) is a complex autoimmune disease that causes multi-organ dysfunction. The onset of SLE is dependent on both the possession of susceptibility genes and the environmental triggers (e.g. infection, chemicals, retroviral elements) (4, 5). Genetic and environmental factors synergize to cause aberrantly regulated immune activation which leads to the loss of B cell tolerance

to self-antigens and high-affinity anti-nuclear antibody (ANA) production (6, 7). ANAs generated by B cells form immune complexes that enter the circulation and deposit in peripheral tissues, leading to the recruitment of myeloid cells, which promote local inflammation (8–10). Inflammation in the kidneys, termed lupus nephritis (10), and various cardiovascular disease manifestations (11) are common causes of morbidity and mortality in individuals living with SLE.

Due to the fact that much still remains unclear about the development of lupus, only one FDA approved therapy specifically developed and approved for SLE, belimumab, has emerged (12). Belimumab is a monoclonal antibody that targets B cell survival by binding to and sequestering Blys, an essential B cell survival factor. Belimumab has an encouraging efficacy in dampening disease manifestations, however it also leaves patients susceptible to infection, as it non-specifically suppresses the immune system (13, 14). A better understanding of the mechanisms involved in SLE development is required to develop novel therapeutics for SLE that may avoid some of the negative immunosuppressive effects of current therapies. The development of microRNA (miRNA) therapeutics has started to gain traction for the treatment of other diseases (15), but their implementation in autoimmunity is still lacking as more studies are required to fully elucidate the contribution of these factors to disease development and progression.

As such, efforts to understand the role of miRNA function in the development of normal B cell responses and dysregulation of these miRNAs in SLE represents a growing field. In general, miRNAs have been implicated as causative agents and biomarkers in a number of diseases (16, 17). In regard to SLE, miRNA centric studies have focused on the differences in miRNA expression between the healthy and diseased states, what cell types are altered by aberrant miRNA expression, and what genes and processes these miRNAs target to either promote or prevent autoimmunity. Many studies have focused on profiling the miRNAs that are expressed in healthy individuals versus those with SLE, with some of these studies determining the miRNAs expressed during the active versus inactive stages of disease (18–23). Cells and tissues used for miRNA profiling in SLE vary, but most studies have profiled the expression of miRNAs in peripheral blood mononuclear cells (PBMCs), B cells, T cells, and blood. Additionally, many studies have assessed miRNAs associated with lupus nephritis through the analysis of urine (24, 25). In addition to profiling miRNAs in human patients, miRNA profiling has been performed in animal models of SLE, demonstrating that there is a conserved profile between several different lupus mouse models and human patients (19, 26, 27).

Broad miRNA profiling has divulged a large amount of information about miRNA expression patterns in normal and SLE B cell responses and has opened the door for mechanistic studies. These mechanistic studies are required to determine how individual or combinations of miRNAs are specifically involved in the loss of B cell tolerance. Additionally, understanding if similar mechanisms are involved in normal protective B cell responses is important for shaping any future therapeutic pursuits. First, we will briefly outline how miRNAs function and the different stages of B cell development and response to antigen. We will then discuss key studies in non-autoimmune and autoimmune systems that frame our understanding of miRNAs in these responses and the implications for therapeutic targeting in the future.

miRNA PROCESSING AND TARGETING MECHANISMS

miRNAs are small non-coding RNAs, approximately 22 nucleotides in length, that mediate post-transcriptional gene regulation. miRNAs are transcribed from the genome by RNA Polymerase II *via* dedicated promoters or are processed from intronic or exonic sequences located in other transcription units (28–32). This generates a primary miRNA transcript (pri-miRNA). While still in the nucleus, the pri-miRNA is cleaved into the hairpin shaped pre-miRNA by the Microprocessor complex, which contains the RNAse III enzyme Drosha and RNA binding protein DGCR8 (33–36). The pre-miRNA, which is approximately 60-70 nucleotides, is exported from the nucleus into the cytosol *via* the activity of exportin-5 and ran-GTP (37). Once in the cytosol, Dicer cleaves the pre-miRNA into a duplex structure (38, 39). The mature miRNA duplex associates with Argonaute and is dissociated into the 5' guide strand, which is preferentially retained by Argonaute, and the 3' passenger (or star) strand, which is preferentially degraded (40). Binding to Argonaute and association with additional proteins that comprise the RNA Induced Silencing Complex (RISC) stabilizes the miRNA from degradation (40–42).

Once incorporated into the RISC, the miRNA has been traditionally thought to exert genetic control by base pairing with complementary sequences found in the 3' UTR of gene transcripts (43–45). However, more recently binding has also been observed within coding regions and 5' UTRs (44–46). While the 5' guide strand is typically incorporated into the RISC, the passenger strand can also be incorporated to target its own set of genes, though usually at a reduced level compared to the guide strand (47, 48). The targeting efficiency achieved by the miRNA can depend on the binding strength of the interaction, as miRNA-transcript interaction can occur through perfect or slightly imperfect complementarity with 6-8 base pair motifs located in the target transcript (49). Once the miRNA interacts with its target, negative regulation of gene expression can occur through both degradation of the transcript and translational repression (50–54). Regardless of the regulatory mechanism employed, ultimately the effect is the impediment of protein being translated from target transcripts. This process is summarized in **Figure 1**.

To date, there have been over 1000 miRNAs discovered, with each miRNA capable of targeting hundreds of genes. A significant portion of miRNAs are found in clusters in the genome, further adding to the sophistication with which they can impart genetic control (55). Importantly, miRNAs are highly

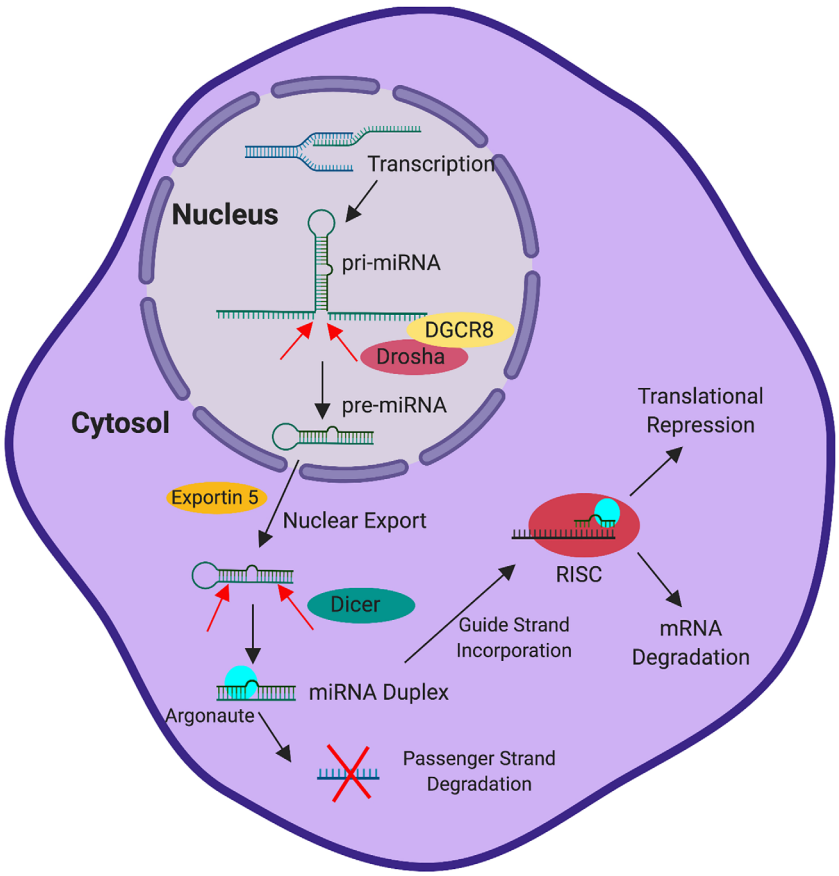

FIGURE 1 | miRNA Processing and Activity. Transcription induced in the nucleus generates a pri-miRNA transcript. The pri-miRNA is cleaved by Drosha, with the aid of co-factor DGCR8, into the pre-miRNA while still in the nucleus. Subsequently, exportin 5 exports the pre-miRNA into the cytoplasm. Following delivery into the cytoplasm, Dicer cleaves the pre-miRNA into the mature miRNA duplex. The mature miRNA duplex (associated with Argonaute) is then dissociated into two strands, the guide strand and the passenger strand. The guide strand preferentially associates with Argonaute in the RNA-induced silencing complex (RISC) and the passenger strand is preferentially degraded. Following association of the miRNA and target transcript, the RISC drives the degradation of the mRNA or mediates translational repression to control gene expression.

conserved among species, making their functional study in mouse models relevant to developing an understanding of their function in human (56, 57). In addition to binding sequence and strength of interaction, the ability of a miRNA to target complementary transcripts relies on the level of miRNA expression in the cell type of interest as well as the number and expression level of target genes in the same cell (58). Accordingly, the expression of the miRNAs and target genes vary in different tissues and cell types, and at different stages of development, making miRNA-mediated regulation a fluid process that is extremely specific to conditions and outside stimuli (59). This applies to the immune response where miRNA function is critically important at various stages (60). The profile of miRNAs among immune cell subsets and their functions in these cells confers the ability to specifically fine-tune the activity of many diverse signaling pathways associated with the activation and regulation of immune cell functions. As such, one miRNA can have vastly different gene targets and effects among different immune cell subsets (61). In this review, we focus on how this concept can be applied to miRNA function in normal B cell responses and B cell tolerance in the context of SLE.

KEY STAGES OF THE B CELL LIFE CYCLE IN DEVELOPMENT AND TOLERANCE

B cell development begins in the bone marrow with commitment of the common lymphocyte progenitor (CLP) to the B cell lineage (62), followed by further differentiation through the stages of pro B cell, pre B cell, and immature B cell (1). In the bone marrow, B cells undergo VDJ recombination to produce a diverse array of BCR specificities and processes exist to negatively select autoreactive B cells that form during this process (central tolerance) (63, 64). Functional, non-autoreactive B cells then egress to the secondary lymphoid organs where they acquire a transitional phenotype. Transitional B cells consist of three

independent fractions, the T1 fraction, the T2 fraction, and the T3 fraction (65). Transitional B cells receiving the appropriate levels of stimulation and survival signals eventually differentiate into marginal zone or follicular B cells, whereas autoreactive B cells can be regulated at the T1 and T3 stages through apoptosis or anergy (66, 67) (**Figure 2**). In SLE, defects have been observed in early stages of B cell tolerance and loss of tolerance at this stage is usually linked to the possession of certain genetic susceptibility loci (68–72).

Mature B cells enter two major pathways following antigenic challenge to generate antibody responses, the germinal center (GC) and the extrafollicular pathway. During pathogen-driven immune responses, B cell development through the GC is critical for the generation of plasma cells that secrete high-affinity,

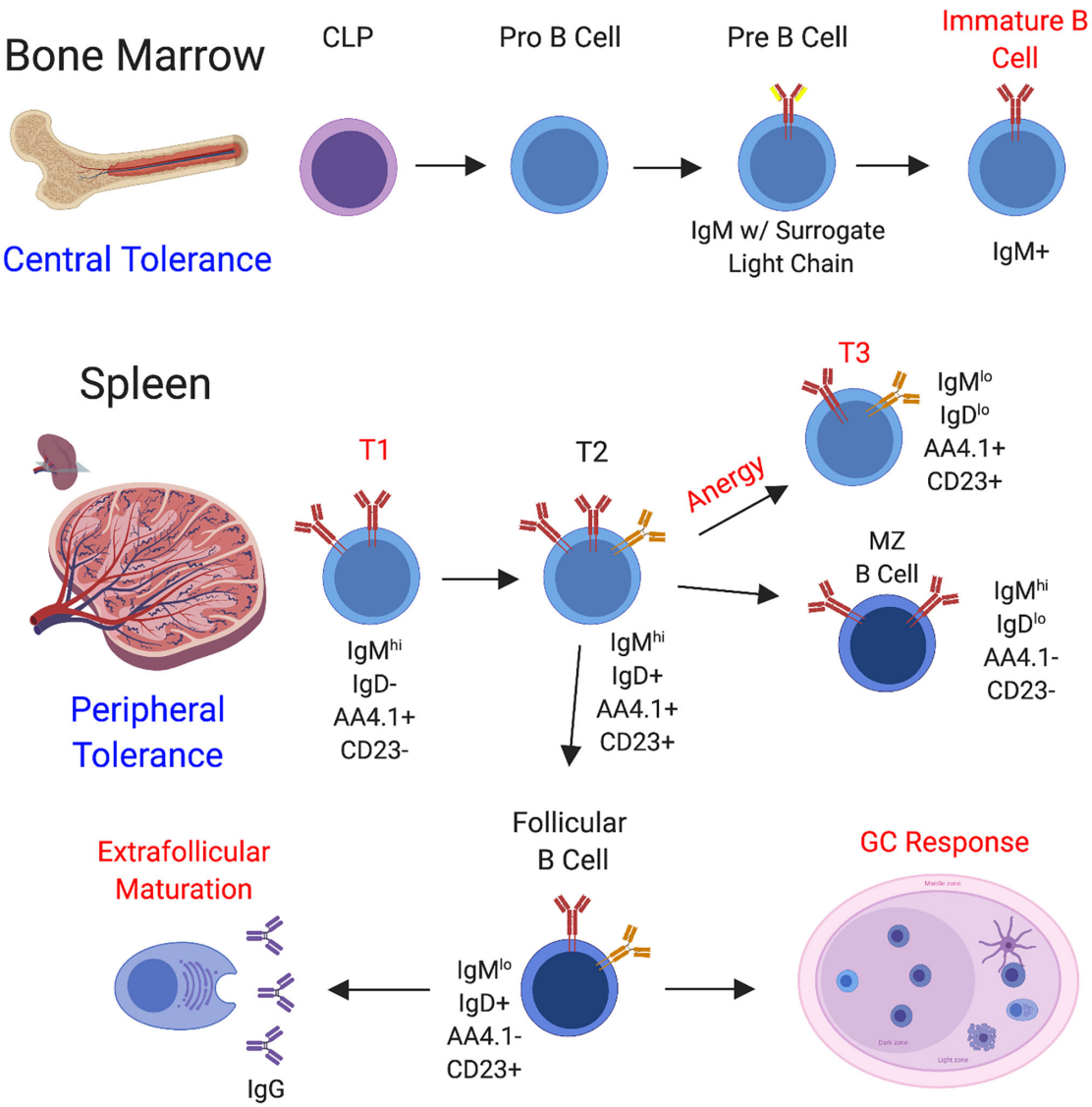

FIGURE 2 | B Cell Development and Sites of B Cell Tolerance. B cell development begins in the bone marrow through a series of steps. Hematopoietic progenitor stem cells (HPSCs) undergo a series of differentiation steps leading to the generation of the common lymphocyte progenitor (CLP), from which B cell differentiation can proceed. Throughout the stages of B cell development in the bone marrow, a functional BCR is assembled and central tolerance is employed, whereby self-reactive B cells are directed to undergo receptor editing or cell death. B cells that pass this checkpoint migrate to the secondary lymphoid organs, including the spleen (depicted here) and lymph nodes. In the spleen, B cells continue to mature and peripheral B cell tolerance is enacted at several different stages of development. B cells enter the spleen at the T1 stage and strong BCR engagement can drive apoptosis at this stage. T1 B cells can progress on to the T2 stage, and from there can be induced to seed the marginal zone and follicle. In addition to regulation at the T1 stage, transitional B cells can be directed to undergo anergy and assume the T3 phenotype, whereby the BCR is downregulated to promote hyporesponsiveness. Marginal zone B cells generally become activated to provide a source of IgM. Alternatively, the follicular B cell subset directs the generation of IgG-secreting plasmablasts through both the follicular germinal center pathway and the extrafollicular pathway. Regulation is employed through both of these pathways. To summarize, well-documented regulatory stages are highlighted in red.

class-switched antibodies and the differentiation of memory B cells (73, 74). However, GCs can become enlarged and dysregulated in SLE, leading to the production of high-affinity, class-switched autoantibodies that cause downstream pathology (74, 75). Many reviews have extensively detailed the mechanisms involved in the initiation and maintenance of GC responses driven by foreign antigen and in autoimmunity (73, 74, 76).

Alternatively, extrafollicular foci form in the red pulp and can occur rapidly in response to T-independent and T-dependent antigens (77). Activation of B cells through the extrafollicular pathway leads to rapid plasmablast formation, from which a select number of plasma cells will develop. Responses generated through the extrafollicular pathway can also undergo class-switching and somatic hypermutation independent of the GC, although at a lower frequency (77). In SLE, significant maturation of autoreactive B cells can occur outside of the GC (78–82). Ultimately, dysregulation of B cell responses at any stage of development and response to antigen can lead to autoimmunity.

miRNA FUNCTION IN PROTECTIVE B CELL RESPONSES

While the goal for therapeutic development is to ultimately understand how miRNA expression and function is dysregulated in SLE, in order to achieve this, we must also understand how miRNAs function during normal B cell responses. This is important because miRNA expression level heavily impacts its function. miRNAs may drive aberrant B cell regulation due to overexpression, underexpression, or novel expression in B cells or other cell types that affect B cell responses. Additionally, any potential therapeutic design will ideally leave miRNA function involved in normal B cell responses intact to prevent host susceptibility to infection. The studies that have shaped our current understanding of miRNA function in B cell responses are discussed below. While the focus is predominantly on the B cell and T cell intrinsic expression of these molecules, it is important to note that their expression in innate immune cell types can also shape B cell responses through the regulation of cytokines and other factors.

Technically, studies of miRNA contribution to B cell responses are comprised of multiple approaches which collectively help build a full picture of miRNA involvement. miRNA expression profiling studies establish a starting point by identifying specific miRNAs for further functional analysis. The following phenotypic studies that narrow down on individual miRNAs have implemented a combination of *in vitro* and *in vivo* approaches. While *in vitro* approaches cannot determine the absolute requirement for specific miRNAs in the generation of B cell responses that require specific signals and interactions *in vivo*, such as GC responses, they can identify and confirm mRNA targets in some cell types of interest. On the other hand, mouse models that implement overexpression (lentiviral or genetic), miRNA antagomir administration, or knockouts of individual miRNAs are valuable tools for determining the absolute and non-redundant requirements for these factors in generating specific B cell responses and highlight the function of miRNAs in the presence of stimuli that are specific to *in vivo* conditions (**Tables 1**, **2**).

Regulation of Multiple miRNAs Is Involved in Early B Cell Development

Multiple steps, outlined earlier, are involved in B cell development. miRNAs have been shown to fluctuate in expression throughout the different stages of B cell development in the bone marrow, supporting the idea that their expression is important for guiding B cells through this process (108). Broadly, deletion of DGCR8 in B cells, which inhibits miRNA processing, caused a block in B cell development from the pro-B cell to pre-B cell stage (109). This was due to increased apoptosis of pro-B cells and resulted in a severe loss of B cells in the periphery of these mice (109), indicating that global miRNA expression is indispensable for B cell development.

Specifically, multiple studies have found important roles for several miRNAs during early fate decisions that polarize progenitors to the B cell lineage, or alternatively the T cell or myeloid cell lineages (**Figure 3**). Early expression of miR-181 or miR-126 in hematopoietic progenitor cells resulted in increased commitment to the B cell lineage (88, 92). miR-126 was shown to target IRS-1 to drive this commitment decision (88). Alternatively, expression of miR-132 or miR-23a in hematopoietic progenitors or miR-128-2 in common lymphoid

TABLE 1 | Methods to Study or Therapeutically Modulate miRNAs in Mouse Models.

Objective	Methods	Purpose
Global Loss of Function	Knockout mouse models	Absolute, non-redundant function Complete loss of expression
Cell Type Specific Loss of Function	Cre-lox systems Bone marrow reconstitution	miRNA function in a specific cell type
Overexpression	miRNA mimics/agomirs (delivery by VLPs, nanoparticles, etc.) Viral vector expression	Generate autoimmunity in non-autoimmune backgrounds Prevent autoimmunity if miRNA is regulatory
Dampened Expression	Antagomirs/LNA anti-miRs Viral vector expression of sponge Heterozygous mice (if expression is reduced)	Study effects dependent on expression level More therapeutically relevant
Temporal Effects	Inducible system (e.g. Dox) Timed administration of antagomirs/viral vectors	Differentiate prophylactic versus therapeutic effects

VLP, virus like particle; LNA, locked nucleic acid; Dox, doxycycline.

TABLE 2 | miRNAs and Direct Target Genes in Protective B Cell Responses.

miRNA	Site	Confirmed or Predicted Target Gene(s)	Key Assays Performed	Ref #
miR-15	Bone Marrow	*ccne1* (cyclin E1)	LUC, GEN MOD	(83)
miR-17~92	Bone Marrow	*pten*	LUC, GEN MOD	(84)
miR-23a	Bone Marrow	*bach1*	LUC, GE	(85)
		runx1	GE	(85)
		satb1	GE	(85)
		ikzf1 (Ikaros)	GE	(85)
miR-34a	Bone Marrow	*foxp1*	LUC, GEN MOD	(86)
miR-125b	Bone Marrow	*s1pr1*	LUC, 3UTR	(87)
miR-126	Bone Marrow	*irs1*	BP, GE	(88)
miR-128-2	Bone Marrow	*adora2b* (A2B)	LUC, GE	(89)
		malt1	LUC, GE	(89)
miR-132	Bone Marrow	*sox4*	LUC, GEN MOD	(90)
miR-150	Bone Marrow	No target(s) identified	N/A	(91)
miR-181	Bone Marrow	No target(s) identified	N/A	(92)
miR-221	Bone Marrow	*pten*	LUC, GE, 3UTR	(93)
miR-17~92	Germinal Center	**B Cells** *ikzf1* (Ikaros)	LUC, GE, GEN MOD	(94)
		T Cells *rora*	LUC, GEN MOD	(95)
		T Cells *pten*	LUC, GE, GEN MOD	(96)
		T Cells *bcl2l11* (Bim)	LUC, GE, GEN MOD	(96)
miR-21	Germinal Center	No target(s) identified	N/A	(97)
miR-28	Germinal Center	Many candidates	TA	(98)
miR-146	Germinal Center	**B Cells** *chuk* (IKKα)	LUC, GE	(99)
		B Cells *rel* (c-rel)	LUC, GE	(99)
		T Cells *icos*	LUC, GE, GEN MOD	(100)
miR-155	Germinal Center	**B Cells** *aicda* (AID)	LUC, 3UTR, GEN MOD	(101, 102)
		B Cells *socs1*	GE, GEN MOD	(101)
		T Cells *peli1*	LUC, CLIP, GEN MOD	(103)
miR-217	Germinal Center	Many candidates	TA	(104)
miR-155	Extrafollicular	*spi1* (PU.1)	LUC, 3UTR	(105, 106)
miR-182	Extrafollicular	No target(s) identified	N/A	(107)

LUC, luciferase assay or equivalent assay (e.g. GFP); GEN MOD, genetic modulation of target gene/rescue; GE, gene expression analysis in miRNA KO/overexpression; 3UTR, 3' UTR binding site mutation; CLIP, CLIP assay; BP, binding Prediction; TA, transcriptomic analysis; Occurs in B cells or hematopoietic progenitors (in bone marrow) if not indicated.

progenitors (CLPs), resulted in reduced B cell lineage commitment, indicating that these miRNAs negatively regulate differentiation into the B cell lineage (85, 89, 90, 110). Mechanistically, miR-23a was able to regulate multiple transcription factors, including Ik2f1, Bach1, Satb1, and Runx1 (85), whereas miR-132 was shown to target Sox4 which was previously implicated in B cell development (90). Additionally, apoptosis modulation was responsible for a miR-128-2 dependent increase in CLPs, with A2B and Malt1 identified as candidate targets of miR-128-2 (89). The exact mechanisms of miRNA targeting involved in the activity of miR-181 in this process remains an open question.

Following lineage commitment, miR-17~92 was shown to increase PI3K activity in pro-B cells to regulate RAG expression and allow for transition to the pre-B cell stage (84). Further, miR-15 was shown to be involved in the induction of transcriptional programming required for the differentiation to the pre-B cell stage, with cyclin E1 identified a direct target gene of miR-15 and cyclin D3 identified as an indirect target of this miRNA (83). Additionally, differentiation from the pro to pre-B cell stage was revealed to be sensitive to the levels of miR-34a expression, which must be reduced to allow expression of Foxp1, a direct target of miR-34a, to occur (86).

Multiple studies also support the activity of miRNAs in later stages of B cell development in the bone marrow. miR-150 is likely involved in the transition from the pre-B cell to immature B cell stage, although aberrant premature expression can block development at earlier stages in the bone marrow (91). Downregulation of miR-125b and miR-221 have been shown to promote egress of B cells to the spleen, with S1PR1 and PI3K signaling regulation involved in this process (87, 93, 111). It is less clear which miRNAs are alternatively upregulated to promote B cell egress from the bone marrow. Ultimately, these studies indicate that there is a dynamic regulation of miRNA expression that controls the multiple stages of B cell development in the bone marrow, with a delicate balance of miRNAs providing both positive and negative regulation of these responses (**Figure 3**). Accordingly, improper miRNA expression can generate excessive B cell responses, with clinical manifestations of malignancy (112) or autoimmunity (to be discussed in detail). Mouse studies also suggest that miRNAs could play a role in clinical immunodeficiency syndromes such as severe combined immunodeficiency (SCID), since the discussed studies indicate that miRNA function is required for proper B cell development. However, the exact role of miRNAs in clinical immunodeficiency observed in human patients requires further study.

Identifying and Determining the Requirement for miRNAs in GC Response

The contributions of miRNAs to the GC response have also been extensively documented. Similar to analyses assessing the overall

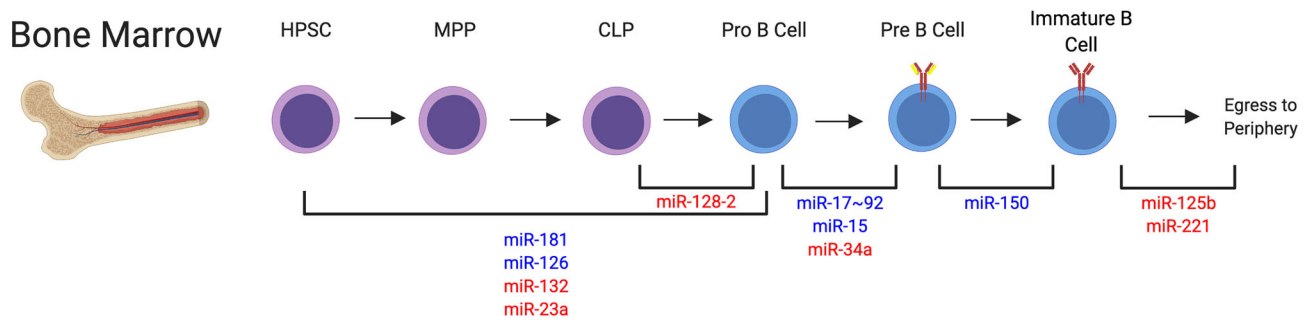

FIGURE 3 | miRNAs that Impact B Cell Development in the Bone Marrow. Many miRNAs have been identified in the regulation of B cell development through each of the individual stages. This indicates a dynamic regulation of miRNA expression is required for proper developmental programs. miRNA regulation involved at these different stages is depicted. miRNAs that positively regulate these specific steps are depicted in blue. miRNAs that negatively regulate these specific steps are depicted in red. miRNAs are indicated at their confirmed or predicted stages of activity. HPSC, hematopoietic progenitor stem cell; MPP, multipotent progenitor; CLP, common lymphocyte progenitor

importance of miRNAs in early stages of B cell development in the bone marrow, the loss of Dicer function (and thus the inability to generate mature miRNAs) in B cells undergoing class-switching *via* an AID-Cre based system effectively ablated the GC response and class-switched antibody production in mice (113). Likewise, the loss of DGCR8 function in T cells prevented the differentiation and function of follicular helper T cells (Tfh) and in turn GC B cells (95). These studies indicate that miRNA function is generally indispensable for the establishment of GC responses.

The hindrance of miRNA processing machinery represents a global loss of miRNA function. Additional studies that profile the expression of miRNAs in GC B cells and Tfh, as compared to their respective precursor cells, have identified specific miRNAs that may be absolutely crucial for mediating the differentiation and function of these specific cell types (100, 103, 114–116). We will further discuss those that have been studied in mouse models (**Figure 4**).

miR-155 Is a Positive Master Regulator of the GC Response

miR-155 has emerged as arguably the most important and well-studied miRNA during the GC response, acting as a master regulator, with both B and T cell intrinsic functions demonstrated to date. The requirement for miR-155 in GC responses and subsequent antibody production was first described in 2007 through the implementation of both overexpression and knockout systems in mice (117, 118). The absence of miR-155 resulted in reduced GC responses in both the lymph nodes and Peyer's patches, whereas overexpression enhanced these responses following immunization. A downstream effect on antigen-specific antibody production following immunization in this system was also observed (117). Subsequent studies of miR-155 function separated its B and T cell-intrinsic functions. B cell-intrinsic miR-155 expression was required for optimal GC responses and Ab production, with a primary effect on IgG1, following immunization (105). miR-155 was found to functionally target AID (*aicda*), as well as SOCS1 expression to promote cell survival *via* control of p53 (101, 102). The targeting of AID is somewhat counterintuitive as AID is required for somatic hypermutation and class-switching. However, despite AID being a verified target of miR-155, miR-155 deficiency did not overtly affect somatic hypermutation or class-switching processes when measured directly (102, 117). Therefore, the deficiency in class-switched antibody production in the absence of miR-155 is more likely associated with reduced differentiation and the survival of plasmablasts, which is further discussed later in regard to the effects of miR-155 on the extrafollicular B cell response (119). In addition to B cell-intrinsic effects of miR-155, miR-155 deficiency in T cells resulted in significantly blunted Tfh and GC B cell responses, as well as primary and memory antibody responses, demonstrating non-redundant roles for miR-155 in B and T cells that lead to similar phenotypic effects (103, 120). Mechanistically, miR-155 was found to target *peli1* in T cells to increase c-Rel expression during Tfh development, resulting phenotypically in the modulation of proliferation and CD40L expression (103). Collectively, miR-155 targets an array of genes and processes in B and T cells during the formation and activity of the GC response and can be considered a master regulatory miRNA during this process.

The miR-146 Family Negatively Regulates the GC Response

In addition to the well-described and multifaceted function of miR-155 in promoting GC responses, both miR-146a and miR-146b have emerged as negative regulators of the GC response. Further, miR-146 modulation also occurs within both B and T cells. Carola Vinuesa's group first showed that miR-146a loss in T cells through a mixed bone marrow chimeric approach resulted in the spontaneous expansion of Tfh and GC B cells, with some added effect of T cell extrinsic factors (100). As modulation of ICOS-ICOSL signaling through blockade or

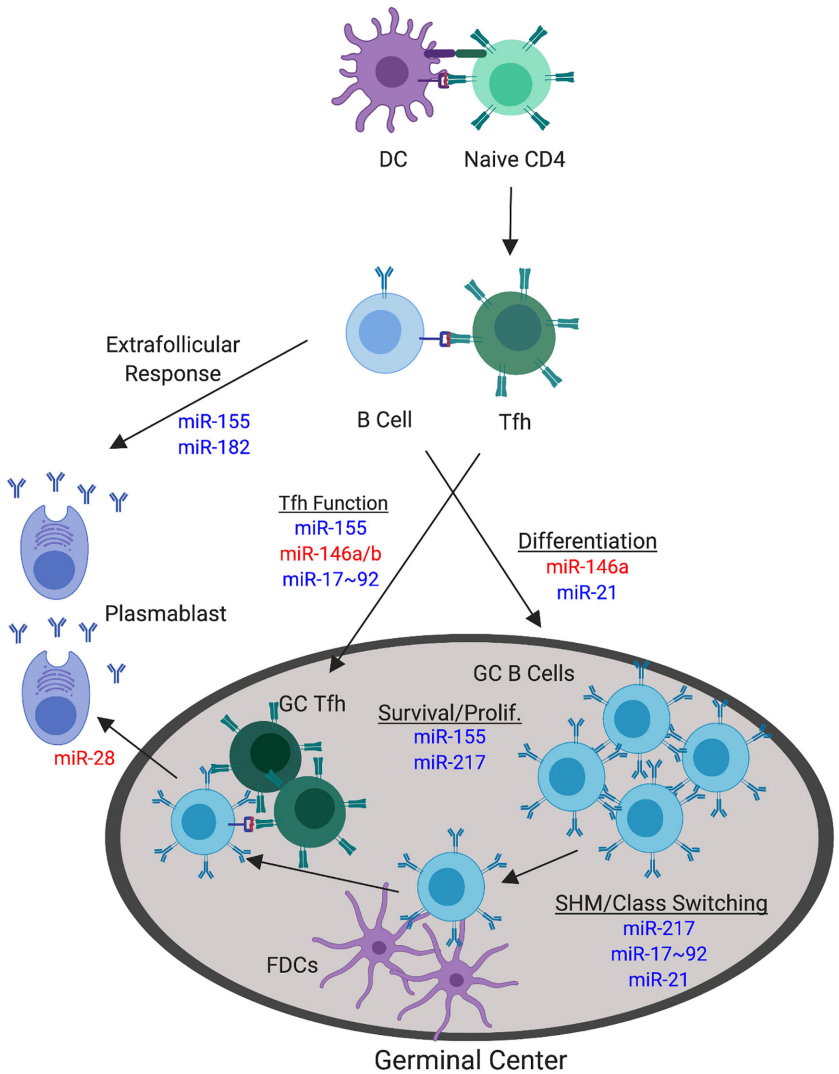

FIGURE 4 | miRNAs with Confirmed Functions in the Non-autoimmune GC Response. The germinal center (GC) response involves a number of processes that can be targeted by miRNA function. The focus herein pertains to direct modulation of GC B cell and Tfh responses during normal, non-autoimmune GC responses. Major processes involved in the GC response are underlined. miRNAs that positively regulate these specific GC processes are depicted in blue. miRNAs that negatively regulate these specific GC processes are depicted in red. miRNAs are indicated at their confirmed or predicted stages of activity.

genetic methods could rescue Tfh and GC B cell accumulation, miR-146a modulation of this signaling axis was determined as a significant form of action utilized to spontaneously control Tfh numbers (100). Another study later clarified that B cell-intrinsic miR-146a deficiency following immunization-induced response does indeed result in increased GC B cell, Tfh, and antibody responses in part due to control of CD40 signaling and control of the GC B cell differentiation process (99). However, this study did not find an effect of miR-146a alone on the modulation of Tfh responses both spontaneously and following immunization when using a Cre-flox system (99), exhibiting contrasting results to previous study. Instead, they found a cooperative T cell-intrinsic role of miR-146a and miR-146b in this process (99). While these results are slightly divergent, it is clear that the miR-146 family is collectively responsible for the negative regulation of the GC, demonstrating that miRNAs can both positively and negatively regulate GC responses.

The miR-17~92 Cluster Modulates Tfh Responses

While miR-146 is critical in negative regulation of Tfh responses, the miR-17~92 cluster has conversely emerged as a critical T cell-intrinsic positive regulator of Tfh, GC, and antibody responses as detailed by multiple studies employing immunization, viral infection, and spontaneous systems in non-autoimmune mice (95, 96, 121, 122). PTEN and Bim (*bcl2l11*) were the first

identified targets of the miR-17~92 cluster in CD4 T cells and loss of one allele each of *Pten* and Bim (*bcl2l11*) could produce a similar phenotype to the overexpression of miR-17~92 (96). More convincingly, the loss of one copy of *Pten* in mice lacking miR-17~92 in T cells could rescue the response, further suggesting that PI3K signaling is critical for miR-17~92 function (121). In addition to the promotion of Tfh function, the activity of miR-17~92 inhibits the expression of factors associated with other CD4 T cell subsets, such as the direct target of *rora* (95). A separate study tested the B cell-intrinsic requirement for miR-17~92 and did not observe a difference in GC formation, though miR-17~92 had a drastic effect specifically on the production of IgG2c (94). These data suggest that miR-17~92 primarily acts in a T cell-intrinsic manner to modulate GC responses through promoting Tfh differentiation. Conversely, its B cell intrinsic functions appear less pertinent, or may only be involved in specific types of responses.

Other miRNAs Explored in the GC Response

While the study of miR-155, miR-146, and miR-17~92 has been of primary focus in the GC field, additional studies utilizing mouse models are emerging to both support and exclude the role of other miRNAs in this process. In one study, the overexpression of miR-217 in mice resulted in enhanced GC B cell and antibody responses, including enhanced somatic hypermutation events, during primary and secondary responses following immunization (104). Conversely, dampening miR-217 function resulted in reduced GC B cell and antibody responses, indicating that miR-217 promotes these events (104). These responses were associated with the prevention of Bcl6 degradation in GC B cells (104). In a separate study, miR-28 modulation did not affect the magnitude of the GC B cell response, but the employment of a miR-28 sponge in transferred B cells resulted in enhanced memory formation and plasma cell differentiation, indicating a cell-intrinsic negative regulation during GC B cell terminal differentiation into plasmablasts (98). Lastly, we identified a role for miR-21 in driving GC responses to foreign antigen. miR-21 deficient mice exhibited a two-fold reduction in the magnitude of the GC response and reduced class-switched IgG antibody responses after immunization, indicating that miR-21 is required for optimal GC response to foreign antigen (97).

Additionally, some miRNAs are highly expressed in GC B cells or Tfh, but are dispensable for *in vivo* responses. Among these miRNAs are those contained in the miR-183 cluster (miR-182, miR-183, and miR-92) which are upregulated in GC B cells and Tfh (103, 123, 124), as well as miR-22 which is specifically upregulated in Tfh (103). However, it is worth noting that miRNA requirement may be specific to the type of ongoing B cell and GC response, so these results may not hold true for all conditions. miRNAs that have similar seed sequences may also exhibit some redundancy, meaning that loss of both miRNAs may be required to observe a phenotype *in vivo*. In summary, the miRNAs that contribute at different stages of the GC response are depicted in **Figure 4**.

miR-182 and miR-155 Are Implicated in Extrafollicular B Cell Responses

Overall, very little is currently known about the miRNAs involved in any form of extrafollicular B cell response, beyond a role for miR-182 and miR-155 (105, 107). miR-182KO mice immunized with T-dependent antigen (TD-Ag) exhibited intact GC responses, but showed reduced antibody responses at early time points following immunization, indicating an impairment in early extrafollicular B cell responses (107). This reduced early response did not affect the ability to elicit memory responses (107). Similar to miR-182KO mice, B cell intrinsic deficiency of miR-155 resulted in reduced antibody forming cell (AFC) responses at 7d post-immunization with TD-Ag, indicating impaired extrafollicular responses (105). This was shown to be dependent on miR-155 mediated regulation of PU.1 expression, which regulates the formation of plasmablasts (105, 106). Study of miR-155 indicates that some miRNA function in B cells can impact both the GC and extrafollicular B cell responses, likely because there is much crosstalk in the factors that must be activated to support both of these processes. It is likely that additional miRNAs are involved in extrafollicular B cell responses against T-dependent foreign antigens, but further study is required to identify these factors.

Considerations for Future Study of miRNAs in Protective B Cell Responses

While multiple miRNA profiling studies have been performed on B cells undergoing developmental processes and GC responses, these profiling studies are lacking to identify miRNAs which may be involved during the extrafollicular B cell response. In general, many mechanistic questions remain in regard to extrafollicular B cell function and identifying critical miRNAs and their targets can help speed up discovery of additional important pathways that mediate this response. Further, while many studies have illustrated that modulated expression of multiple B cell intrinsic miRNAs is crucial for B cell development in the bone marrow, miRNA expression in other cell types during this process such as stromal cells may also significantly impact B cell development but remain unexplored. Similarly, in addition to the B cell and T cell-intrinsic effects of miRNAs on GC responses, miRNA expression in other cell types involved in the establishment of GC responses, (i.e. follicular dendritic cells (FDCs)), Tfh-priming DCs, and T follicular regulatory cells) may significantly affect their optimal formation. Some studies have started to profile miRNA expression using FDC and FDC-like cell lines (125, 126), however further study is required to determine if this accurately represents what is observed *in vivo*. Additionally, many miRNAs modulate the cytokine microenvironment, providing a potential indirect mechanism of GC control.

The availability of mouse models and reagents for miRNAs of interest is critical in the continued study of their contribution to this process. Additionally, most of the targets identified thus far were discovered using immunization-based systems, meaning that it is unclear which miRNAs are similarly or differentially modulated in spontaneous GC and B cell responses in the

periphery. Some studies have started to address this and will be mentioned in the next section. Notably, some miRNAs such as miR-17~92 and miR-155 appear to be involved throughout multiple stages of B cell development and are critically tied to many important B cell fate decisions. Thus far, other miRNAs have only been described at one stage of B cell response. Establishing a complete picture of miRNA responses at all stages of the B cell response is an important consideration in regard to any therapeutic pursuits for autoimmune or other B cell dependent diseases.

miRNA REGULATION OF B CELL RESPONSES IN SLE

Due to the critical involvement of miRNAs at many stages of the B cell response, it is not surprising that dysregulated miRNA expression can lead to the loss of B cell tolerance at multiple stages of B cell development and effector function. As such, global miRNA expression in B cells, studied with a B cell specific knockout of Dicer, was shown to skew the B cell repertoire and result in high titers of serum autoreactive antibodies and kidney pathology (127). This study illustrated that miRNAs can collectively impact B cell tolerance. We will further discuss which individual miRNAs have been characterized in this process and what is known about the mechanisms of their activity (**Figure 5** and **Table 3**).

miR-17~92 and miR-148a Break Central B Cell Tolerance

Several miRNAs have been identified as key mediators of central B cell tolerance. The implementation of the IgM^b-macroself mouse model has recently been adopted as a mechanism to study central tolerance (141). IgM^b-macroself mice express an IgM^b superantigen and editing of the BCR in the bone marrow is unable to remedy this reactivity, resulting in deletion of nearly all B cells in the bone marrow and consequent loss of B cells in the periphery. Therefore, this model allows for the assessment of B cell tolerance by screening for B cells that have escaped this method of tolerance and entered the periphery. In one study utilizing this model, IgM^b-macroself mice reconstituted with bone marrow from CD19-Cre; miR-17~92 mice revealed that overexpression of this miRNA cluster allows developing B cells to escape central tolerance in the bone marrow (128). Most of this effect was attributed specifically to the miR-19 subfamily suppressing Pten activity (128). Further, normal levels of miR-17~92 were shown to regulate the degree of receptor editing occurring at this stage of tolerance, indicating that some level of miR-17~92 expression is important to mediate normal processes that occur during B cell development (128).

A separate study performed a functional screen of 113 miRNAs separated into 4 pools in the regulation of central B cell tolerance, also employing the IgM^b-macroself mouse model. From this screen, they identified 7 miRNAs that may be involved in escape of central tolerance. Using this model to study the effect of specific miRNAs, they determined that miR-26a, miR-26b, miR-342, miR-423, and miR-182 have modest effects on central tolerance, whereas miR-148a was identified as a key regulator of central tolerance, with increased levels promoting escape of tolerance (129). Mechanistically, miR-148a was found to regulate immature B cell apoptosis through targeting Bim, PTEN, and Gadd45α, which were also verified to regulate central tolerance in this mouse model (129). Consequently, MRL/lpr mice overexpressing miR-148a developed accelerated autoimmune manifestations and higher autoantibody titers (129).

While these studies have made significant progress toward our understanding of miRNAs that regulate central B cell tolerance, some questions still remain. Gonzalez-Martin et al. screened a subset of 113 miRNAs in hematopoietic progenitor stem cells (HPSCs). Downstream determination of miRNAs involved in loss of central B cell tolerance was dependent on their enhanced expression in B cells that seeded the spleen in their system. However, expression of these miRNAs in other cell types may indirectly impact B cell escape of central tolerance. Additionally, other miRNAs that were not screened in this study may have a significant contribution to this process. Once B cells are in the spleen, they are also regulated at the transitional stage. Little is currently known about the involvement of miRNAs in transitional B cell tolerance, but miRNAs have been identified in regulating BCR signaling induced growth and apoptosis, indicating that these may be prime candidates for the study of tolerance at the transitional stage of B cell development (142).

miRNAs in SLE-Associated GC Responses

Based on the master regulatory function of miR-155 in the GC responses, it is not surprising that miR-155 has a great importance in the onset of SLE in two different mouse models. Fas^{lpr} mice with a deficiency in miR-155 have reduced spleen size, proteinuria, and kidney pathology with age (133, 134). This was associated with reduced serum autoantibody titers and GC responses in this model (133, 134), illustrating that miR-155 is also important in promoting the formation of GCs in autoimmune-prone mice. In one of these studies, miR-155 was shown to target expression of SHIP-1 (*inpp5d*), a previously characterized miR-155 target gene (143), following BCR activation to promote B cell proliferation (134). In the other study, S1PR1 was validated as a miR-155 target. Antagonizing S1PR1 expression lead to increased Tfh responses (133), revealing another mechanism of miR-155 activity. In the pristane-induced lupus model, knockout or antagonism of miR-155 dampened diffuse alveolar hemorrhage, reduced kidney pathology, and reduced autoantibody titers, demonstrating common effects among multiple lupus models (138, 144).

Another miRNA which has been studied using multiple SLE models is miR-21. Antagonism of miR-21 was initially shown to dampen splenomegaly and autoantibody titers in the Sle1.2.3 lupus model although no detailed mechanism of action was suggested in this seminal study (145). This reduction in splenomegaly and autoantibody production was also observed in the bm12 adoptive transfer chronic graft versus host disease

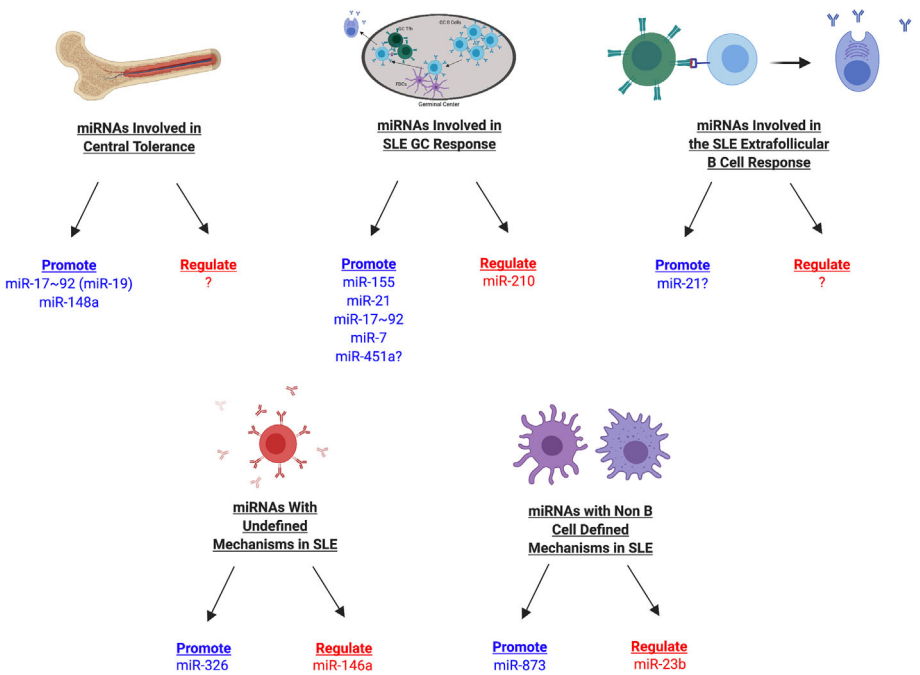

FIGURE 5 | miRNAs Involved in SLE Development in Mice. miRNAs involved in SLE development can be divided into multiple categories depending on their association with different stages of the B cell response (central tolerance, germinal center, extrafollicular response, other mechanisms), in addition to whether they promote or regulate disease manifestations. Those miRNAs that promote disease are shown in blue whereas those that regulate disease are shown in red. miRNAs with currently undefined mechanisms in SLE may later be identified during a specific stage of the B cell response or may have B cell independent mechanisms during SLE.

(cGVHD) model, which exhibits SLE-like manifestations (146). We recently addressed more concerning the mechanism of miR-21 activity and showed that miR-21 has context dependent effects in different SLE models, which is likely related to the level of miR-21 activity (97). In a TLR7 induced model where *Sle1b* mice are treated with imiquimod, miR-21 modulated plasma cell formation and autoreactive B cell selection, which was independent of the magnitude of the GC response and was

TABLE 3 | miRNAs and Direct Target Genes in SLE Responses.

miRNA	Site	Confirmed or Predicted Target Gene(s)	Key Assays Performed	Ref #
miR-17~92	Bone Marrow	*pten*	LUC, GE, GEN MOD	(128)
miR-148a	Bone Marrow	*bcl2l11* (Bim)	LUC, GE, GEN MOD	(129)
		pten	LUC, GE, GEN MOD	(129)
		gadd45a (Gadd45α)	LUC, GE, GEN MOD	(129)
miR-7	Germinal Center	*pten*	GE, LUC	(130, 131)
miR-17~92	Germinal Center	**Lymphocytes** *pten*	LUC, GE, GEN MOD	(96)
		Lymphocytes *bcl2l11*(Bim)	LUC, GE, GEN MOD	(96)
miR-21	Germinal Center	Many candidate target genes	TA	(97)
miR-145a	Germinal Center	**Whole Spleen** *irf8*	LUC, GE	(132)
miR-155	Germinal Center	**Whole Spleen** *s1pr1*	TA, LUC, GEN MOD	(133)
		inpp5d (SHIP-1)	GE	(134)
miR-210	Germinal Center	*cd23* (but likely additional targets)	LUC, TA	(135)
miR-23b	Kidney	**Non-immune cells** *tab2*	TA, LUC, GE, GEN MOD	(136)
		Non-immune cells *tab3*	TA, LUC, GE, GEN MOD	(136)
		Non-immune cells *chuk* (IKKα)	TA, LUC, GE, GEN MOD	(136)
miR-146a	Spleen	**Global** *traf6*	GEN MOD	(137)
miR-155	Lung	**Lung tissue** *ppara* (PPARα)	GE, TA, LUC, CLIP	(138)
miR-326	Plasmablast (GC/EF)?	*ets1*	GE	(139)
miR-873	Spleen	**T Cells** *foxo1*	LUC, GE	(140)

LUC, luciferase assay or equivalent assay (e.g. GFP); GEN MOD, genetic modulation of target gene/rescue; GE, gene gene expression analysis in miRNA KO/overexpression; CLIP, CLIP assay; TA, transcriptomic analysis; Occurs in B cells or hematopoietic progenitors in bone marrow if not indicated.

associated with the modulation of a number of miR-21 target genes in B cells. In addition to differences in the B cell response, myeloid cell infiltration and proinflammatory cytokine production was blunted in the absence of miR-21, suggesting that miR-21 can also control the cytokine environment (97). In contrast, in a spontaneous TLR7 overexpression model, *Sle1b*.Yaa, miR-21 was required for increased GC responses and autoimmune B cell responses (97). These data indicate that miR-21 has multifaceted effects at several different stages of the B cell response depending on the SLE model. Additional study is required to determine the cell-intrinsic contributions to these distinct responses.

While the impact of miR-17~92 on autoimmunity has not yet been tested in a standard mouse model of SLE, preliminary - study indicates that there will likely be broad effects among several SLE models. Overexpression of miR-17~92 in lymphocytes results in multiorgan autoimmune manifestations, including lymphoproliferation, kidney pathology, and the development of autoantibody titers (96), hallmarks of SLE. These mice exhibited increased GC responses (96), but the study of central tolerance suggests that miR-17~92 can affect tolerance at multiple stages of B cell development and effector function (128).

In addition to these miRNAs, multiple other studies have illustrated roles for additional miRNAs in GC responses and autoimmunity. miR-7 was studied in the MRL/lpr mouse model and was found to enhance GC responses, drive proinflammatory cytokine secretion, and impact autoantibody production and kidney pathology (130). Treatment of MRL/lpr mice with antagomir-7 for 5 weeks was able to reduce all of these responses significantly and normalized PTEN expression in B cells (130, 131). Another study addressed miR-451a deficiency in the Fas^{lpr} model and found a partial reduction in Tfh responses and a significant reduction in IL-21 production that correlated with the loss of autoantibody production and kidney pathology (132). IRF8 was verified as a gene target (132). While IRF8 is important in the GC response (147), it is unclear to what extent IRF8 modulation produces the observed effects and that what extent other mechanisms may be at play. Lastly, another study hinted that miR-210 may be involved in regulating the loss of tolerance through the GC, as the loss of miR-210 resulted in spontaneous development of autoimmunity and enhanced spontaneous GC B cell responses with age (135). The exact mechanisms of miR-451a and miR-210 in the GC responses in autoimmune-prone mice remain to be fully elucidated.

miRNAs That Modulate B Cell Tolerance *via* Other or Undefined Mechanisms

Another well studied miRNA in autoimmunity is miR-146a, which was found to prevent the development of autoimmunity, similar to its regulatory effects on the GC responses to TD-antigen immunization or spontaneous responses in non-autoimmune mouse models. This was determined by two studies employing opposite approaches. First, in the more classical BXSB model, administration of miR-146a expressing virus like particles (VLPs) reduced autoantibody production (148). Second, even in the absence of susceptibility loci, miR-146aKO mice develop a chronic inflammatory disease and autoantibody production with age (149). While it is evident that non-autoimmune spontaneous-GC responses are affected in miR-146aKO mice through a separate study previously discussed (100), analysis in autoimmune-prone mice did not directly address this mechanism and thus further study of GC responses in autoimmune-prone mice is required to determine if alteration of the GC response may be a causative factor under these conditions. However, it is difficult to directly attribute autoimmunity solely to lymphocyte dysregulation in the absence of miR-146, as these mice also exhibit a profound amount of myeloproliferation when miR-146a is globally deficient, which can be significantly reduced by attenuation of the miR-146a target gene TRAF6 (137, 149). It is likely that a combination of these factors may be involved in contributing to the overall phenotype observed, which requires further study. Additional study of human SLE genetics has revealed that the rs2431697 SNP is critically tied to miR-146a expression levels and the T/T variant at this locus correlates with disease activity, renal involvement, and autoantibody production (150). This is linked to its alterations in cell type specific enhancer activity that can control miR-146a expression by promoter interactions (151). These studies indicate that miR-146a activity has relevance in human SLE and that genetics can control miR-146a expression in SLE patients.

miR-326 is also intriguing due to its modulation of B cell responses. Enhancing miR-326 expression *via* lentiviral vector in MRL/lpr mice resulted in enhanced autoantibody production and immune complex deposition in the kidneys, which was associated with increased plasmablast responses (139). Ets-1 expression was modulated in B cells, with Ets-1 previously identified as a miR-326 target gene (152). However, the source of plasmablast generation (GC versus extrafollicular pathway) was not characterized and reverse experiments implementing lentivirus expressing miR-326 sponge showed only minimal effects on these processes, implying the need for further inquiry (139).

Two additional miRNAs have detailed roles in the development of autoimmunity but are associated with other divergent mechanisms focused on T cell and cytokine responses. miR-873 inhibition could modestly reduce autoantibody responses and proteinuria in MRL/lpr mice, but was associated with Foxo1 targeting and Th17 responses (140). MRL/lpr mice infected with a viral vector expressing a miR-23b sponge or virus engineered to overexpress miR-23b demonstrated that miR-23b has a suppressive effect on the development of kidney pathology (136). This study attributed miR-23b mediated protection from autoimmunity to its negative regulation of proinflammatory cytokine production in resident non-immune cells (136).

Considerations for Further Study

Altogether, miRNAs crucially regulate autoimmune responses, in both negative and positive manners (**Figure 5**). While these miRNAs have already been established in this context, much

study remains to identify additional miRNAs involved in autoimmunity, as well as to further determine the mechanisms involved in these processes. The list of miRNAs that modulate autoimmunity through regulation of the B cell responses is likely to grow as the tools and reagents to study these factors expand. For example, recently miR-152-3p was identified as an important miRNA in isolated human SLE B cells, which controls their activation level and production of BAFF (153). Modeling this miRNA in mouse models may reveal more information about the importance of this miRNA in driving disease progression.

Interestingly, none of the miRNAs listed above are located on the X chromosome (154). However, it would be interesting to determine if aberrant miRNA expression caused by incomplete X chromosome inactivation may contribute to the pathogenesis of SLE. Additionally, the study of miR-146a indicates that genetic susceptibility to SLE may involve mutations that lead to aberrant regulation of miRNA expression that predisposes one to SLE development (150, 151). Additional studies addressing this potential phenomenon in regard to the expression of other miRNAs will be informative.

Of further consideration for future study is the level of miRNA expression that is required to promote or restrain disease, as many of these miRNAs are expressed during normal B cell processes, but at different levels. Many of these models focus on extreme alterations in expression, either by knocking out expression entirely or significantly overexpressing the miRNA by viral vector. Approaches that fine-tune miRNA expression, such as using heterozygous mice or miRNA sponges, should be considered in future studies.

While the experimental focus on miRNA has largely pertained to their classical mechanisms of function, other mechanisms of miRNA activity are emerging that require consideration and may alter the manner in which we think about targeting them. There is evidence that miRNAs can also act as ligands by binding to and inducing pattern recognition receptor (PRR) signaling, predominately by TLR7 and TLR8, which recognize ssRNA ligands (155–157). The idea of miRNAs being able to stimulate TLRs is intriguing as this opens the door for miRNAs produced by one cell to control the genetic profile and function of surrounding cells. In fact, it has already been shown that T cells can transfer exosomes and their miRNA cargo to APCs through the immunological synapse to mediate fusion and release into the recipient cell (158). Additionally, DCs can shuttle miRNAs *via* exosomes to the cytosol of other DCs to mediate recipient gene expression (159). Interestingly, exosomes derived from SLE patients can stimulate the production of IFNα from pDCs *in vitro* through miRNA stimulation of TLRs, indicating that exosomal delivery of miRNAs can also alter the cytokine profile in disease (160). Realistically, this means that the overall phenotype observed for specific miRNAs may actually be a balance between miRNAs produced intrinsically and those internalized from surrounding cells, which may result in TLR stimulation as well as gene regulation in the recipient cell (**Figure 6**).

An initial study recently applied this concept to the T and B cell interactions required for B cell class-switching and GC formation. This study found that during *in vitro* culture, T cells can transfer multiple miRNAs, including miR-155, *via* exosomes to B cells upon formation of immune synapses. Blocking exosome release from T cells to B cells *in vivo*, and thus reducing miRNA transfer from T cells to B cells, resulted in slightly reduced B cell class-switching and GC formation. This indicates that miRNA transfer contributes to these B cell responses *in vivo*, with greater contribution from intrinsic miRNA responses (161). It is unclear if this mechanism may be amplified during autoimmune responses and which cell types may participate in this mechanism in a context dependent manner.

Lastly, while miRNAs target individual genes in the cell, they have been implicated in targeting the chromatin remodeling machinery to confer epigenetic and transcriptional changes in the genome that have broader effects on cellular function. This includes targeting factors involved in methylation, acetylation, and the SWI/SNF complex (162–168). A few studies have started to address miRNA targeting of DNA methyltransferases (DMNTs) in CD4 T cells in SLE (19, 169, 170). However, the study of miRNAs in the modulation of the chromatin remodeling machinery has not been pursued extensively. This concept is intriguing though, because SLE has been associated with epigenetic modulation, particularly hypomethylation (171). Altogether, miRNA function may not be limited to a single mode of action, but rather a combination of effects that alter the functionality of a cell and surrounding cells. This has broad implications for the mechanistic control of both non-autoimmune and autoimmune responses.

CONSIDERATIONS FOR miRNAS AS THERAPEUTIC TARGETS

miRNAs are an attractive therapeutic option for SLE and other diseases because of the ability to dampen their expression rather than completely ablate it, allowing for the ability to fine-tune gene expression to a desired level. In the context of SLE, this is an interesting concept because current therapeutics globally target B cells or employ other approaches that result in broad immunosuppression, thus ablating both anti-pathogen and autoimmune responses (172). In turn, this leaves patients on these therapies susceptible to infection. If miRNA expression can be fine-tuned to a level that allows for adequate anti-pathogen response, while significantly dampening autoimmune manifestations, miRNA targeting would be effective. Alternatively, finding miRNAs that promote autoimmunity but are not overtly involved in anti-pathogen response provides another attractive avenue of attaining specificity.

Methods for Targeting miRNAs and miRNAs in Clinical Trials for Other Diseases

In regard to the specific methods of miRNA targeting, many groups have already worked with miRNA targeting in cell culture

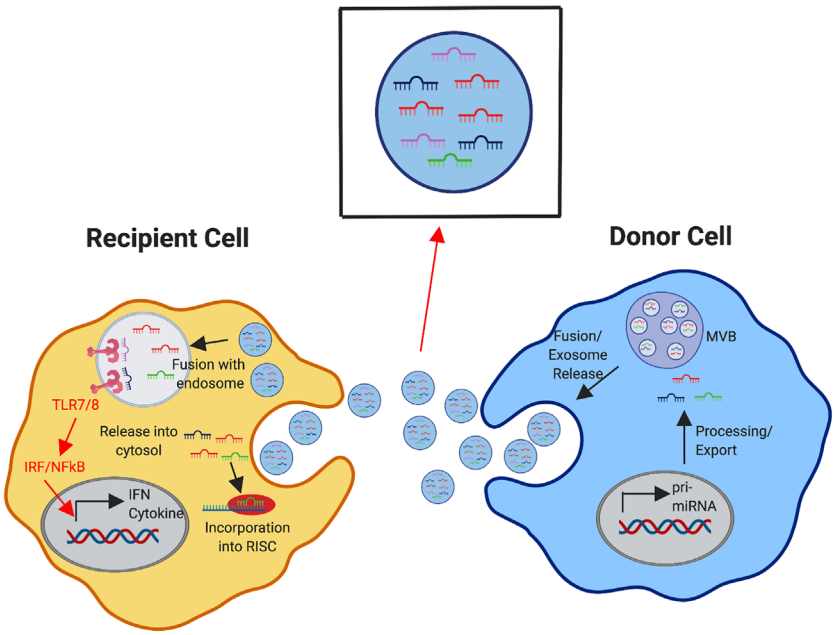

FIGURE 6 | Exosomal Delivery of miRNA to Modulate Recipient Cell Response. Donor immune cells produce and process miRNAs (as depicted in detail in **Figure 1**). The formation of multivesicular bodies (MVBs) with intraluminal vesicles containing mature miRNAs in the donor cell leads to fusion of the MVBs with the plasma membrane, releasing exosomes containing these miRNAs. Recipient immune cells can receive exosomal cargo into the cytosol by direct fusion of the exosome with the plasma membrane or exosomes can be internalized and delivered to the endosomal compartment. Within the cytosol, these received miRNAs may compete with the internally generated miRNAs for incorporation in the RNA-induced silencing complex (RISC) to mediate gene expression in the recipient cell. miRNAs that are directed into the endosomal compartment may bind to TLR7/8 to initiate downstream signaling cascades, triggering the induction of cytokines, interferons, and other interferon stimulated genes.

and in animal models through the introduction of antagomirs, which are 23 nucleotide antisense 2'-O'-methyl-modified oligonucleotide sequences bound to cholesterol (173) (**Table 1**). The cholesterol linkage allows for cellular entry while the antisense sequence promotes pairing to and neutralization of the target miRNA. Another form of anti-miRNA oligonucleotide is the locked nucleic acid (LNA) anti-miR agent. LNA anti-miRs are another form of targeted oligoribonucleotide that are stabilized due to locked nucleic acids (LNAs) (174). More recently LNA anti-miRs have been designed that are as short as 8 mer sequences (tiny LNAs) that specifically target the 5' seed region of the miRNA (175). Of note, while mature miRNA can be targeted, the pri-miRNA and pre-miRNA stages of miRNA processing can be targeted by miRNA therapies as well, preventing generation of the mature miRNA (176). While anti-miRNA oligonucleotides are intended to dampen miRNA function, some miRNAs (i.e. miR-146a) have a regulatory role in disease onset and progression. Bearing this in mind, a separate approach is to heighten the expression of these miRNAs to restore tolerance, such as through the administration of a miRNA mimic (or agomir), which is a chemically modified double stranded oligonucleotide sequence designed to mimic the miRNA of interest.

While simple injection based approaches are limited to systemic effects, targeted delivery may be achieved through viral vectors utilizing different expression promoters (177). Also advantageously, viral vector based delivery methods can promote long-term modulation of the response through forming episomes or integrating into the genome (177). Anti-miRNA sequences expressed under the control of a viral vector are referred to as miRNA sponges (178). Alternatively, viral vectors can be engineered to express miRNAs. Lastly, nanoparticles are an attractive cell-specific targeting option that continue to be studied and optimized for a variety of purposes, including as small RNA delivery vehicles (179).

Despite miRNA therapeutics being a relatively newer pursuit, some miRNA-centric therapeutics are being tested in clinical trials for the treatment of diseases. The first miRNA-centric therapeutic to advance to Phase II clinical trials was Miraversin, which dampens miR-122 expression during hepatitis C infection to prevent viral replication (176, 180). As such, many companies have emerged with the goal of designing miRNA-based therapeutics for a variety of purposes (181). miRagen has already directed a miR-155 targeting oligonucleotide (Cobomarsen) into a Phase II clinical trial in an effort to treat blood cancer (182, 183). Additionally, therapeutics targeting other miRNAs, such as miR-21, miR-29, and miR-92, have completed or are currently active for early stage trials in the treatment of fibrotic diseases, cardiovascular disease, kidney disease, and solid organ cancers (181, 184). While the implementation of miRNA-centric therapeutics is steadily increasing, to our knowledge there

are no trials to date that have focused on testing miRNA targeted therapeutics for autoimmune diseases. However, the technology exists for potential implementation.

Considerations for Implementing miRNA Therapeutics in SLE

While miRNA targeting is an interesting therapeutic option, there are some points of consideration pertaining to off-target effects and the potential stimulatory ability of miRNAs, the necessity for long-term intervention in autoimmune diseases, and miRNA redundancy. Other points of consideration will likely emerge as more groups begin testing miRNA targeting in animal models. While antagomirs/anti-miRs are, by nature, targeted therapeutics due to their base-pairing properties, design must be careful and specific to avoid off target RNA binding. Despite this concern, study suggests that off-target effects on mRNAs are minimal when using LNAs in animal models (175). In addition to the generation of sequence specific off target effects, there is evidence that miRNAs can also act as ligands by binding to and inducing PRR signaling, predominately by TLR7 and TLR8, which recognize ssRNA ligands (155–157). If miRNAs can stimulate some PRRs, we must exercise caution in therapeutically enhancing miRNA doses that could trigger downstream proinflammatory cytokine production. Conversely, some antagomirs have been shown to block TLR7 and 8 signaling in a sequence specific manner in addition to their miRNA binding effects, possibly introducing other unintended effects (185). Careful modeling, design, and testing are required to overcome these barriers to specific therapeutic design.

Another point in regard to therapeutic development is how often antagomirs would need to be introduced into the system, as miRNAs are constantly transcribed from the genome in response to immune stimuli and SLE is chronic disease. Removal of the miRNA targeting therapy will likely result in a relapse of symptoms as the original expression levels are restored following therapy discontinuation. As discussed above, the use of viral vectors that mediate long-term expression is an option but requires further study. In addition to the frequency of miRNA dosage, it is unclear which miRNAs can be targeted therapeutically or only prophylactically in regard to SLE and other autoimmune diseases. Ultimately, this likely depends on the specific miRNA of interest and whether that miRNA is dysregulated in response to genetic susceptibility gene possession or triggered by ongoing immune responses during the course of SLE progression. To determine when miRNA therapeutics would be most effective, miRNA dampening or loss of miRNAs at specific stages of disease progression in mouse models can begin to clarify therapeutic approaches and effectiveness through different stages of disease development. Lastly, while those miRNAs that produce strong effects in mouse models are of obvious consideration for targeting, miRNA redundancy does exist. Targeting multiple miRNAs, or miRNA families with conserved target sequences, may produce additive effects compared to single miRNA targeting. After weighing both the advantages and possible unintended consequences in the development of miRNA therapeutics, targeting miRNAs can be deemed as a promising option, but much proof of concept and testing remains to be addressed.

CONCLUSIONS

The studies reviewed herein demonstrate the essential roles of miRNAs in B cell responses and the development of autoimmune disease. Not only do miRNAs promote these responses, but some miRNAs also possess critical negative regulatory functions. While the studies to date have begun to elucidate the role of these factors, much work remains to fully characterize their impact during autoimmunity, as well as the capacity to effectively target them to dampen disease. Additionally, many miRNAs have yet to be studied using *in vivo* mouse systems but with increasing access to mouse models, the list of miRNAs involved in the processes discussed herein will likely expand significantly. Extensive miRNA expression profiling in cell types and specific stages of the B cell response will aid in identifying additional miRNAs worth studying in mouse models in the future. While simply identifying the miRNAs and their target genes that contribute to disease is important, further attention to the level of miRNA expression that modulates the observed effects and the stage of disease at which the miRNA of interest is involved has important therapeutic ramifications that must be addressed more heavily in future studies. Lastly, traditional miRNA mediated regulation has been of focus, but non-traditional regulation by miRNAs is an interesting avenue of research that deserves significant attention and may alter how we approach targeting miRNA function. Altogether, the further study and modeling of miRNAs in relevant animal systems will inform future therapeutic design and identify those miRNAs that may provide the most promising targets for potential miRNA-centric therapeutic development to treat SLE.

AUTHOR CONTRIBUTIONS

SS and ZR wrote the article. SS designed figures. All authors contributed to the article and approved the submitted version.

FUNDING

This work was supported by National Institutes of Health R21AI128111 to ZR.

ACKNOWLEDGMENTS

All figures were designed with Biorender software (Biorender.com).

REFERENCES

1. LeBien TW, Tedder TF. B Lymphocytes: How They Develop and Function. *Blood* (2008) 112:1570–80. doi: 10.1182/blood-2008-02-078071
2. Cyster JG, Allen CDC. B Cell Responses: Cell Interaction Dynamics and Decisions. *Cell* (2019) 177:524–40. doi: 10.1016/j.cell.2019.03.016
3. Shlomchik MJ. Sites and Stages of Autoreactive B Cell Activation and Regulation. *Immunity* (2008) 28:18–28. doi: 10.1016/j.immuni.2007.12.004
4. Gulati G, Brunner HI. Environmental Triggers in Systemic Lupus Erythematosus. *Semin Arthritis Rheum* (2018) 47:710–7. doi: 10.1016/j.semarthrit.2017.10.001
5. Balada E, Ordi-Ros J, Vilardell-Tarrés M. Molecular Mechanisms Mediated by Human Endogenous Retroviruses (HERVs) in Autoimmunity. *Rev Med Virol* (2009) 19:273–86. doi: 10.1002/rmv.622
6. Papp K, Végh P, Hóbor R, Szittner Z, Vokó Z, Podani J, et al. Immune Complex Signatures of Patients With Active and Inactive SLE Revealed by Multiplex Protein Binding Analysis on Antigen Microarrays. *PloS One* (2012) 7:e44824. doi: 10.1371/journal.pone.0044824
7. Budde P, Zucht HD, Vordenbäumen S, Goehler H, Fischer-Betz R, Gamer M, et al. Multiparametric Detection of Autoantibodies in Systemic Lupus Erythematosus. *Lupus* (2016) 25:812–22. doi: 10.1177/0961203316641770
8. Tsokos GC. Systemic Lupus Erythematosus. *N Engl J Med* (2011) 365:2110–21. doi: 10.1056/NEJMra1100359
9. Gottschalk TA, Tsantikos E, Hibbs ML. Pathogenic Inflammation and Its Therapeutic Targeting in Systemic Lupus Erythematosus. *Front Immunol* (2015) 6:550. doi: 10.3389/fimmu.2015.00550
10. Flores-Mendoza G, Sansón SP, Rodríguez-Castro S, Crispín JC, Rosetti F. Mechanisms of Tissue Injury in Lupus Nephritis. *Trends Mol Med* (2018) 24:364–78. doi: 10.1016/j.molmed.2018.02.003
11. Zeller CB, Appenzeller S. Cardiovascular Disease in Systemic Lupus Erythematosus: The Role of Traditional and Lupus Related Risk Factors. *Curr Cardiol Rev* (2008) 4:116–22. doi: 10.2174/157340308784245775
12. Dubey AK, Handu SS, Dubey S, Sharma P, Sharma KK, Ahmed QM. Belimumab: First Targeted Biological Treatment for Systemic Lupus Erythematosus. *J Pharmacol Pharmacother* (2011) 2:317–9. doi: 10.4103/0976-500X.85930
13. Pasoto SG, Ribeiro AC, Bonfa E. Update on Infections and Vaccinations in Systemic Lupus Erythematosus and Sjögren's Syndrome. *Curr Opin Rheumatol* (2014) 26:528–37. doi: 10.1097/BOR.0000000000000084
14. Leblanc-Trudeau C, Masetto A, Bocti C. Progressive Multifocal Leukoencephalopathy Associated With Belimumab in a Patient With Systemic Lupus Erythematosus. *J Rheumatol* (2015) 42:551–2. doi: 10.3899/jrheum.140577
15. Rupaimoole R, Slack FJ. MicroRNA Therapeutics: Towards a New Era for the Management of Cancer and Other Diseases. *Nat Rev Drug Discov* (2017) 16:203–22. doi: 10.1038/nrd.2016.246
16. Jin F, Hu H, Xu M, Zhan S, Wang Y, Zhang H, et al. Serum Microrna Profiles Serve as Novel Biomarkers for Autoimmune Diseases. *Front Immunol* (2018) 9:2381. doi: 10.3389/fimmu.2018.02381
17. Condrat CE, Thompson DC, Barbu MG, Bugnar OL, Boboc A, Cretoiu D, et al. miRNAs as Biomarkers in Disease: Latest Findings Regarding Their Role in Diagnosis and Prognosis. *Cells* (2020) 9(2):276. doi: 10.3390/cells9020276
18. Carlsen AL, Schetter AJ, Nielsen CT, Lood C, Knudsen S, Voss A, et al. Circulating microRNA Expression Profiles Associated With Systemic Lupus Erythematosus. *Arthritis Rheum* (2013) 65:1324–34. doi: 10.1002/art.37890
19. Pan W, Zhu S, Yuan M, Cui H, Wang L, Luo X, et al. MicroRNA-21 and microRNA-148a Contribute to DNA Hypomethylation in Lupus CD4+ T Cells by Directly and Indirectly Targeting DNA Methyltransferase 1. *J Immunol* (2010) 184:6773–81. doi: 10.4049/jimmunol.0904060
20. Stagakis E, Bertsias G, Verginis P, Nakou M, Hatziapostolou M, Kritikos H, et al. Identification of Novel microRNA Signatures Linked to Human Lupus Disease Activity and Pathogenesis: miR-21 Regulates Aberrant T Cell Responses Through Regulation of PDCD4 Expression. *Ann Rheum Dis* (2011) 70:1496–506. doi: 10.1136/ard.2010.139857
21. Guo G, Wang H, Shi X, Ye L, Wu K, Lin K, et al. NovelmiRNA-25 Inhibits AMPD2 in Peripheral Blood Mononuclear Cells of Patients With Systemic Lupus Erythematosus and Represents a Promising Novel Biomarker. *J Transl Med* (2018) 16:370. doi: 10.1186/s12967-018-1739-5
22. Zeng L, Wu JL, Liu LM, Jiang JQ, Wu HJ, Zhao M, et al. Serum miRNA-371b-5p and miRNA-5100 Act as Biomarkers for Systemic Lupus Erythematosus. *Clin Immunol* (2018) 196:103–9. doi: 10.1016/j.clim.2018.10.004
23. Duroux-Richard I, Cuenca J, Ponsolles C, Piñeiro AB, Gonzalez F, Roubert C, et al. MicroRNA Profiling of B Cell Subsets From Systemic Lupus Erythematosus Patients Reveals Promising Novel Biomarkers. *Int J Mol Sci* (2015) 16:16953–65. doi: 10.3390/ijms160816953
24. Tangtanatakul P, Klinchanhom S, Sodsai P, Sutichet T, Promjeen C, Avihingsanon Y, et al. Down-Regulation of let-7a and miR-21 in Urine Exosomes From Lupus Nephritis Patients During Disease Flare. *Asian Pac J Allergy Immunol* (2018) 37(4):189–97. doi: 10.12932/AP-130318-0280.
25. Wang G, Tam LS, Li EK, Kwan BC, Chow KM, Luk CC, et al. Serum and Urinary Free microRNA Level in Patients With Systemic Lupus Erythematosus. *Lupus* (2011) 20:493–500. doi: 10.1177/0961203310389841
26. Wang Z, Heid B, Dai R, Ahmed SA. Similar Dysregulation of Lupus-Associated miRNAs in Peripheral Blood Mononuclear Cells and Splenic Lymphocytes in MRL/lpr Mice. *Lupus Sci Med* (2018) 5:e000290. doi: 10.1136/lupus-2018-000290
27. Dai R, Zhang Y, Khan D, Heid B, Caudell D, Crasta O, et al. Identification of a Common Lupus Disease-Associated microRNA Expression Pattern in Three Different Murine Models of Lupus. *PloS One* (2010) 5:e14302. doi: 10.1371/journal.pone.0014302
28. Rodriguez A, Griffiths-Jones S, Ashurst JL, Bradley A. Identification of Mammalian microRNA Host Genes and Transcription Units. *Genome Res* (2004) 14:1902–10. doi: 10.1101/gr.2722704
29. Godnic I, Zorc M, Jevsinek Skok D, Calin GA, Horvat S, Dovc P, et al. Genome-Wide and Species-Wide in Silico Screening for Intragenic MicroRNAs in Human, Mouse and Chicken. *PloS One* (2013) 8:e65165. doi: 10.1371/journal.pone.0065165
30. Ramalingam P, Palanichamy JK, Singh A, Das P, Bhagat M, Kassab MA, et al. Biogenesis of Intronic miRNAs Located in Clusters by Independent Transcription and Alternative Splicing. *RNA* (2014) 20:76–87. doi: 10.1261/rna.041814.113
31. Saini HK, Griffiths-Jones S, Enright AJ. Genomic Analysis of Human microRNA Transcripts. *Proc Natl Acad Sci USA* (2007) 104:17719–24. doi: 10.1073/pnas.0703890104
32. Lee Y, Kim M, Han J, Yeom KH, Lee S, Baek SH, et al. MicroRNA Genes are Transcribed by RNA Polymerase II. *EMBO J* (2004) 23:4051–60. doi: 10.1038/sj.emboj.7600385
33. Han J, Lee Y, Yeom KH, Kim YK, Jin H, Kim VN. The Drosha-DGCR8 Complex in Primary microRNA Processing. *Genes Dev* (2004) 18:3016–27. doi: 10.1101/gad.1262504
34. Han J, Lee Y, Yeom KH, Nam JW, Heo I, Rhee JK, et al. Molecular Basis for the Recognition of Primary microRNAs by the Drosha-DGCR8 Complex. *Cell* (2006) 125:887–901. doi: 10.1016/j.cell.2006.03.043
35. Gregory RI, Yan KP, Amuthan G, Chendrimada T, Doratotaj B, Cooch N, et al. The Microprocessor Complex Mediates the Genesis of Microrna. *Nature* (2004) 432:235–40. doi: 10.1038/nature03120
36. Lee Y, Ahn C, Han J, Choi H, Kim J, Yim J, et al. The Nuclear RNase Iii Drosha Initiates microRNA Processing. *Nature* (2003) 425:415–9. doi: 10.1038/nature01957
37. Lund E, Güttinger S, Calado A, Dahlberg JE, Kutay U. Nuclear Export of microRNA Precursors. *Science* (2004) 303:95–8. doi: 10.1126/science.1090599
38. Ketting RF, Fischer SE, Bernstein E, Sijen T, Hannon GJ, Plasterk RH. Dicer Functions in RNA Interference and in Synthesis of Small RNA Involved in Developmental Timing in C. Elegans. *Genes Dev* (2001) 15:2654–9. doi: 10.1101/gad.927801
39. Lee Y, Jeon K, Lee JT, Kim S, Kim VN. MicroRNA Maturation: Stepwise Processing and Subcellular Localization. *EMBO J* (2002) 21:4663–70. doi: 10.1093/emboj/cdf476
40. Hammond SM, Boettcher S, Caudy AA, Kobayashi R, Hannon GJ. Argonaute2, a Link Between Genetic and Biochemical Analyses of RNAi. *Science* (2001) 293:1146–50. doi: 10.1126/science.1064023

41. Elkayam E, Kuhn CD, Tocilj A, Haase AD, Greene EM, Hannon GJ, et al. The Structure of Human Argonaute-2 in Complex With miR-20a. *Cell* (2012) 150:100–10. doi: 10.1016/j.cell.2012.05.017
42. Mourelatos Z, Dostie J, Paushkin S, Sharma A, Charroux B, Abel L, et al. miRNPs: A Novel Class of Ribonucleoproteins Containing Numerous Micrornas. *Genes Dev* (2002) 16:720–8. doi: 10.1101/gad.974702
43. Lewis BP, Burge CB, Bartel DP. Conserved Seed Pairing, Often Flanked by Adenosines, Indicates That Thousands of Human Genes are microRNA Targets. *Cell* (2005) 120:15–20. doi: 10.1016/j.cell.2004.12.035
44. Hafner M, Landthaler M, Burger L, Khorshid M, Hausser J, Berninger P, et al. Transcriptome-Wide Identification of RNA-binding Protein and microRNA Target Sites by PAR-CLIP. *Cell* (2010) 141:129–41. doi: 10.1016/j.cell.2010.03.009
45. Chi SW, Zang JB, Mele A, Darnell RB. Argonaute HITS-CLIP Decodes microRNA-mRNA Interaction Maps. *Nature* (2009) 460:479–86. doi: 10.1038/nature08170
46. Lee I, Ajay SS, Yook JI, Kim HS, Hong SH, Kim NH, et al. New Class of microRNA Targets Containing Simultaneous 5'-UTR and 3'-UTR Interaction Sites. *Genome Res* (2009) 19:1175–83. doi: 10.1101/gr.089367.108
47. Okamura K, Phillips MD, Tyler DM, Duan H, Chou YT, Lai EC. The Regulatory Activity of microRNA* Species has Substantial Influence on microRNA and 3' UTR Evolution. *Nat Struct Mol Biol* (2008) 15:354–63. doi: 10.1038/nsmb.1409
48. Guo L, Lu Z. The Fate of miRNA* Strand Through Evolutionary Analysis: Implication for Degradation as Merely Carrier Strand or Potential Regulatory Molecule? *PloS One* (2010) 5:e11387. doi: 10.1371/journal.pone.0011387
49. Lai EC. Micro RNAs are Complementary to 3' UTR Sequence Motifs That Mediate Negative Post-Transcriptional Regulation. *Nat Genet* (2002) 30:363–4. doi: 10.1038/ng865
50. Jin HY, Xiao C. MicroRNA Mechanisms of Action: What Have We Learned From Mice? *Front Genet* (2015) 6:328. doi: 10.3389/fgene.2015.00328
51. Eulalio A, Huntzinger E, Nishihara T, Rehwinkel J, Fauser M, Izaurralde E. Deadenylation is a Widespread Effect of miRNA Regulation. *RNA* (2009) 15:21–32. doi: 10.1261/rna.1399509
52. Wakiyama M, Takimoto K, Ohara O, Yokoyama S. Let-7 microRNA-mediated mRNA Deadenylation and Translational Repression in a Mammalian Cell-Free System. *Genes Dev* (2007) 21:1857–62. doi: 10.1101/gad.1566707
53. Guo H, Ingolia NT, Weissman JS, Bartel DP. Mammalian microRNAs Predominantly Act to Decrease Target mRNA Levels. *Nature* (2010) 466:835–40. doi: 10.1038/nature09267
54. Shin C, Nam JW, Farh KK, Chiang HR, Shkumatava A, Bartel DP. Expanding the microRNA Targeting Code: Functional Sites With Centered Pairing. *Mol Cell* (2010) 38:789–802. doi: 10.1016/j.molcel.2010.06.005
55. Olena AF, Patton JG. Genomic Organization of Micrornas. *J Cell Physiol* (2010) 222:540–5. doi: 10.1002/jcp.21993
56. Wheeler BM, Heimberg AM, Moy VN, Sperling EA, Holstein TW, Heber S, et al. The Deep Evolution of Metazoan Micrornas. *Evol Dev* (2009) 11:50–68. doi: 10.1111/j.1525-142X.2008.00302.x
57. Chiang HR, Schoenfeld LW, Ruby JG, Auyeung VC, Spies N, Baek D, et al. Mammalian microRNAs: Experimental Evaluation of Novel and Previously Annotated Genes. *Genes Dev* (2010) 24:992–1009. doi: 10.1101/gad.1884710
58. Denzler R, McGeary SE, Title AC, Agarwal V, Bartel DP, Stoffel M. Impact of MicroRNA Levels, Target-Site Complementarity, and Cooperativity on Competing Endogenous RNA-Regulated Gene Expression. *Mol Cell* (2016) 64:565–79. doi: 10.1016/j.molcel.2016.09.027
59. Landgraf P, Rusu M, Sheridan R, Sewer A, Iovino N, Aravin A, et al. A Mammalian microRNA Expression Atlas Based on Small RNA Library Sequencing. *Cell* (2007) 129:1401–14. doi: 10.1016/j.cell.2007.04.040
60. Mehta A, Baltimore D. MicroRNAs as Regulatory Elements in Immune System Logic. *Nat Rev Immunol* (2016) 16:279–94. doi: 10.1038/nri.2016.40
61. Hsin JP, Lu Y, Loeb GB, Leslie CS, Rudensky AY. The Effect of Cellular Context on miR-155-mediated Gene Regulation in Four Major Immune Cell Types. *Nat Immunol* (2018) 19:1137–45. doi: 10.1038/s41590-018-0208-x
62. Ramírez J, Lukin K, Hagman J. From Hematopoietic Progenitors to B Cells: Mechanisms of Lineage Restriction and Commitment. *Curr Opin Immunol* (2010) 22:177–84. doi: 10.1016/j.coi.2010.02.003
63. Bassing CH, Swat W, Alt FW. The Mechanism and Regulation of Chromosomal V(D)J Recombination. *Cell* (2002) 109 Suppl:S45–55. doi: 10.1016/S0092-8674(02)00675-X
64. Pelanda R, Torres RM. Central B-cell Tolerance: Where Selection Begins. *Cold Spring Harb Perspect Biol* (2012) 4:a007146. doi: 10.1101/cshperspect.a007146
65. Chung JB, Silverman M, Monroe JG. Transitional B Cells: Step by Step Towards Immune Competence. *Trends Immunol* (2003) 24:343–9. doi: 10.1016/S1471-4906(03)00119-4
66. Petro JB, Gerstein RM, Lowe J, Carter RS, Shinners N, Khan WN. Transitional Type 1 and 2 B Lymphocyte Subsets are Differentially Responsive to Antigen Receptor Signaling. *J Biol Chem* (2002) 277:48009–19. doi: 10.1074/jbc.M200305200
67. Merrell KT, Benschop RJ, Gauld SB, Aviszus K, Decote-Ricardo D, Wysocki LJ, et al. Identification of Anergic B Cells Within a Wild-Type Repertoire. *Immunity* (2006) 25:953–62. doi: 10.1016/j.immuni.2006.10.017
68. Yurasov S, Wardemann H, Hammersen J, Tsuiji M, Meffre E, Pascual V, et al. Defective B Cell Tolerance Checkpoints in Systemic Lupus Erythematosus. *J Exp Med* (2005) 201:703–11. doi: 10.1084/jem.20042251
69. Kanta H, Mohan C. Three Checkpoints in Lupus Development: Central Tolerance in Adaptive Immunity, Peripheral Amplification by Innate Immunity and End-Organ Inflammation. *Genes Immun* (2009) 10:390–6. doi: 10.1038/gene.2009.6
70. Dieudonné Y, Gies V, Guffroy A, Keime C, Bird AK, Liesveld J, et al. Transitional B Cells in Quiescent SLE: An Early Checkpoint Imprinted by IFN. *J Autoimmun* (2019) 102:150–8. doi: 10.1016/j.jaut.2019.05.002
71. Wang T, Marken J, Chen J, Tran VB, Li QZ, Li M, et al. High TLR7 Expression Drives the Expansion of CD19(+)CD24(hi)CD38(hi) Transitional B Cells and Autoantibody Production in SLE Patients. *Front Immunol* (2019) 10:1243. doi: 10.3389/fimmu.2019.01243
72. Giltiay NV, Chappell CP, Sun X, Kolhatkar N, Teal TH, Wiedeman AE, et al. Overexpression of TLR7 Promotes Cell-Intrinsic Expansion and Autoantibody Production by Transitional T1 B Cells. *J Exp Med* (2013) 210:2773–89. doi: 10.1084/jem.20122798
73. Victora GD, Nussenzweig MC. Germinal Centers. *Annu Rev Immunol* (2012) 30:429–57. doi: 10.1146/annurev-immunol-020711-075032
74. Domeier PP, Schell SL, Rahman ZS. Spontaneous Germinal Centers and Autoimmunity. *Autoimmunity* (2017) 50:4–18. doi: 10.1080/08916934.2017.1280671
75. Wong EB, Khan TN, Mohan C, Rahman ZS. The Lupus-Prone NZM2410/NZW Strain-Derived Sle1b Sublocus Alters the Germinal Center Checkpoint in Female Mice in a B Cell-Intrinsic Manner. *J Immunol* (2012) 189:5667–81. doi: 10.4049/jimmunol.1201661
76. Shlomchik MJ, Luo W, Weisel F. Linking Signaling and Selection in the Germinal Center. *Immunol Rev* (2019) 288:49–63. doi: 10.1111/imr.12744
77. Jenks SA, Cashman KS, Woodruff MC, Lee FE, Sanz I. Extrafollicular Responses in Humans and SLE. *Immunol Rev* (2019) 288:136–48. doi: 10.1111/imr.12741
78. William J, Euler C, Christensen S, Shlomchik MJ. Evolution of Autoantibody Responses Via Somatic Hypermutation Outside of Germinal Centers. *Science* (2002) 297:2066–70. doi: 10.1126/science.1073924
79. Luzina IG, Atamas SP, Storrer CE, daSilva LC, Kelsoe G, Papadimitriou JC, et al. Spontaneous Formation of Germinal Centers in Autoimmune Mice. *J Leukoc Biol* (2001) 70:578–84 doi: 10.1189/jlb.70.4.578
80. Mandik-Nayak L, Seo SJ, Sokol C, Potts KM, Bui A, Erikson J. MRL-Lpr/Lpr Mice Exhibit a Defect in Maintaining Developmental Arrest and Follicular Exclusion of Anti-Double-Stranded DNA B Cells. *J Exp Med* (1999) 189:1799–814. doi: 10.1084/jem.189.11.1799
81. Morel L, Blenman KR, Croker BP, Wakeland EK. The Major Murine Systemic Lupus Erythematosus Susceptibility Locus, Sle1, is a Cluster of Functionally Related Genes. *Proc Natl Acad Sci USA* (2001) 98:1787–92. doi: 10.1073/pnas.031336098
82. Jenks SA, Cashman KS, Zumaquero E, Marigorta UM, Patel AV, Wang X, et al. Distinct Effector B Cells Induced by Unregulated Toll-Like Receptor 7

Contribute to Pathogenic Responses in Systemic Lupus Erythematosus. *Immunity* (2018) 49:725–39.e726. doi: 10.1016/j.immuni.2018.08.015
83. Lindner SE, Lohmüller M, Kotkamp B, Schuler F, Knust Z, Villunger A, et al. The miR-15 Family Reinforces the Transition From Proliferation to Differentiation in Pre-B Cells. *EMBO Rep* (2017) 18:1604–17. doi: 10.15252/embr.201643735
84. Benhamou D, Labi V, Getahun A, Benchetrit E, Dowery R, Rajewsky K, et al. The C-Myc/miR17-92/PTEN Axis Tunes PI3K Activity to Control Expression of Recombination Activating Genes in Early B Cell Development. *Front Immunol* (2018) 9:2715. doi: 10.3389/fimmu.2018.02715
85. Kurkewich JL, Hansen J, Klopfenstein N, Zhang H, Wood C, Boucher A, et al. The miR-23a~27a~24-2 microRNA Cluster Buffers Transcription and Signaling Pathways During Hematopoiesis. *PloS Genet* (2017) 13:e1006887. doi: 10.1371/journal.pgen.1006887
86. Rao DS, O'Connell RM, Chaudhuri AA, Garcia-Flores Y, Geiger TL, Baltimore D. MicroRNA-34a Perturbs B Lymphocyte Development by Repressing the Forkhead Box Transcription Factor Foxp1. *Immunity* (2010) 33:48–59. doi: 10.1016/j.immuni.2010.06.013
87. Li G, So AY, Sookram R, Wong S, Wang JK, Ouyang Y, et al. Epigenetic Silencing of miR-125b is Required for Normal B-cell Development. *Blood* (2018) 131:1920–30. doi: 10.1182/blood-2018-01-824540
88. Okuyama K, Ikawa T, Gentner B, Hozumi K, Harnprasopwat R, Lu J, et al. MicroRNA-126-mediated Control of Cell Fate in B-cell Myeloid Progenitors as a Potential Alternative to Transcriptional Factors. *Proc Natl Acad Sci USA* (2013) 110:13410–5. doi: 10.1073/pnas.1220710110
89. Yang Y, Xu J, Chen H, Fei X, Tang Y, Yan Y, et al. MiR-128-2 Inhibits Common Lymphoid Progenitors From Developing Into Progenitor B Cells. *Oncotarget* (2016) 7:17520–31. doi: 10.18632/oncotarget.8161
90. Mehta A, Mann M, Zhao JL, Marinov GK, Majumdar D, Garcia-Flores Y, et al. The microRNA-212/132 Cluster Regulates B Cell Development by Targeting Sox4. *J Exp Med* (2015) 212:1679–92. doi: 10.1084/jem.20150489
91. Zhou B, Wang S, Mayr C, Bartel DP, Lodish HF. miR-150, a microRNA Expressed in Mature B and T Cells, Blocks Early B Cell Development When Expressed Prematurely. *Proc Natl Acad Sci USA* (2007) 104:7080–5. doi: 10.1073/pnas.0702409104
92. Chen CZ, Li L, Lodish HF, Bartel DP. MicroRNAs Modulate Hematopoietic Lineage Differentiation. *Science* (2004) 303:83–6. doi: 10.1126/science.1091903
93. Petkau G, Kawano Y, Wolf I, Knoll M, Melchers F. MiR221 Promotes Precursor B-cell Retention in the Bone Marrow by Amplifying the PI3K-signaling Pathway in Mice. *Eur J Immunol* (2018) 48:975–89. doi: 10.1002/eji.201747354
94. Xu S, Ou X, Huo J, Lim K, Huang Y, Chee S, et al. Mir-17-92 Regulates Bone Marrow Homing of Plasma Cells and Production of Immunoglobulin G2c. *Nat Commun* (2015) 6:6764. doi: 10.1038/ncomms7764
95. Baumjohann D, Kageyama R, Clingan JM, Morar MM, Patel S, de Kouchkovsky D, et al. The microRNA Cluster miR-17~92 Promotes TFH Cell Differentiation and Represses Subset-Inappropriate Gene Expression. *Nat Immunol* (2013) 14:840–8. doi: 10.1038/ni.2642
96. Xiao C, Srinivasan L, Calado DP, Patterson HC, Zhang B, Wang J, et al. Lymphoproliferative Disease and Autoimmunity in Mice With Increased miR-17-92 Expression in Lymphocytes. *Nat Immunol* (2008) 9:405–14. doi: 10.1038/ni1575
97. Schell SL, Bricker KN, Fike AJ, Chodisetti SB, Domeier PP, Choi NM, et al. Context-Dependent miR-21 Regulation of TLR7-mediated Autoimmune and Foreign Antigen Driven Antibody-Forming Cell and Germinal Center Responses. *bioRxiv* (2021). doi: 10.1101/2021.03.12.435182
98. Bartolomé-Izquierdo N, de Yébenes VG, Álvarez-Prado AF, Mur SM, Lopez Del Olmo JA, Roa S, et al. miR-28 Regulates the Germinal Center Reaction and Blocks Tumor Growth in Preclinical Models of non-Hodgkin Lymphoma. *Blood* (2017) 129:2408–19. doi: 10.1182/blood-2016-08-731166
99. Cho S, Lee HM, Yu IS, Choi YS, Huang HY, Hashemifar SS, et al. Differential Cell-Intrinsic Regulations of Germinal Center B and T Cells by miR-146a and miR-146b. *Nat Commun* (2018) 9:2757. doi: 10.1038/s41467-018-05196-3
100. Pratama A, Srivastava M, Williams NJ, Papa I, Lee SK, Dinh XT, et al. MicroRNA-146a Regulates ICOS-ICOSL Signalling to Limit Accumulation of T Follicular Helper Cells and Germinal Centres. *Nat Commun* (2015) 6:6436. doi: 10.1038/ncomms7436
101. Bouamar H, Jiang D, Wang L, Lin AP, Ortega M, Aguiar RC. MicroRNA 155 Control of p53 Activity is Context Dependent and Mediated by Aicda and Socs1. *Mol Cell Biol* (2015) 35:1329–40. doi: 10.1128/MCB.01446-14
102. Teng G, Hakimpour P, Landgraf P, Rice A, Tuschl T, Casellas R, et al. MicroRNA-155 is a Negative Regulator of Activation-Induced Cytidine Deaminase. *Immunity* (2008) 28:621–9. doi: 10.1016/j.immuni.2008.03.015
103. Liu WH, Kang SG, Huang Z, Wu CJ, Jin HY, Maine CJ, et al. A miR-155-Peli1-c-Rel Pathway Controls the Generation and Function of T Follicular Helper Cells. *J Exp Med* (2016) 213:1901–19. doi: 10.1084/jem.20160204
104. de Yébenes VG, Bartolomé-Izquierdo N, Nogales-Cadenas R, Pérez-Durán P, Mur SM, Martínez N, et al. miR-217 is an Oncogene That Enhances the Germinal Center Reaction. *Blood* (2014) 124:229–39. doi: 10.1182/blood-2013-12-543611
105. Vigorito E, Perks KL, Abreu-Goodger C, Bunting S, Xiang Z, Kohlhaas S, et al. microRNA-155 Regulates the Generation of Immunoglobulin Class-Switched Plasma Cells. *Immunity* (2007) 27:847–59. doi: 10.1016/j.immuni.2007.10.009
106. Lu D, Nakagawa R, Lazzaro S, Staudacher P, Abreu-Goodger C, Henley T, et al. The miR-155-PU.1 Axis Acts on Pax5 to Enable Efficient Terminal B Cell Differentiation. *J Exp Med* (2014) 211:2183–98. doi: 10.1084/jem.20140338
107. Li YF, Ou X, Xu S, Jin ZB, Iwai N, Lam KP. Loss of miR-182 Affects B-cell Extrafollicular Antibody Response. *Immunology* (2016) 148:140–9. doi: 10.1111/imm.12592
108. Jensen K, Brusletto BS, Aass HC, Olstad OK, Kierulf P, Gautvik KM. Transcriptional Profiling of mRNAs and microRNAs in Human Bone Marrow Precursor B Cells Identifies Subset- and Age-Specific Variations. *PloS One* (2013) 8:e70721. doi: 10.1371/journal.pone.0070721
109. Brandl A, Daum P, Brenner S, Schulz SR, Yap DY, Bösl MR, et al. The Microprocessor Component, DGCR8, is Essential for Early B-cell Development in Mice. *Eur J Immunol* (2016) 46:2710–8. doi: 10.1002/eji.201646348
110. Kong KY, Owens KS, Rogers JH, Mullenix J, Velu CS, Grimes HL, et al. MIR-23A microRNA Cluster Inhibits B-cell Development. *Exp Hematol* (2010) 38:629–40.e621. doi: 10.1016/j.exphem.2010.04.004
111. Knoll M, Simmons S, Bouquet C, Grün JR, Melchers F. miR-221 Redirects Precursor B Cells to the BM and Regulates Their Residence. *Eur J Immunol* (2013) 43:2497–506. doi: 10.1002/eji.201343367
112. Mazan-Mamczarz K, Gartenhaus RB. Role of microRNA Deregulation in the Pathogenesis of Diffuse Large B-cell Lymphoma (DLBCL). *Leuk Res* (2013) 37:1420–8. doi: 10.1016/j.leukres.2013.08.020
113. Xu S, Guo K, Zeng Q, Huo J, Lam KP. The RNase III Enzyme Dicer is Essential for Germinal Center B-cell Formation. *Blood* (2012) 119:767–76. doi: 10.1182/blood-2011-05-355412
114. Tan LP, Wang M, Robertus JL, Schakel RN, Gibcus JH, Diepstra A, et al. miRNA Profiling of B-cell Subsets: Specific miRNA Profile for Germinal Center B Cells With Variation Between Centroblasts and Centrocytes. *Lab Invest* (2009) 89:708–16. doi: 10.1038/labinvest.2009.26
115. Basso K, Sumazin P, Morozov P, Schneider C, Maute RL, Kitagawa Y, et al. Identification of the Human Mature B Cell Mirnome. *Immunity* (2009) 30:744–52. doi: 10.1016/j.immuni.2009.03.017
116. Ripamonti A, Provasi E, Lorenzo M, De Simone M, Ranzani V, Vangelisti S, et al. Repression of miR-31 by BCL6 Stabilizes the Helper Function of Human Follicular Helper T Cells. *Proc Natl Acad Sci USA* (2017) 114:12797–802. doi: 10.1073/pnas.1705364114
117. Thai TH, Calado DP, Casola S, Ansel KM, Xiao C, Xue Y, et al. Regulation of the Germinal Center Response by microRNA-155. *Science* (2007) 316:604–8. doi: 10.1126/science.1141229
118. Rodriguez A, Vigorito E, Clare S, Warren MV, Couttet P, Soond DR, et al. Requirement of Bic/microRNA-155 for Normal Immune Function. *Science* (2007) 316:608–11. doi: 10.1126/science.1139253
119. Arbore G, Henley T, Biggins L, Andrews S, Vigorito E, Turner M, et al. MicroRNA-155 is Essential for the Optimal Proliferation and Survival of Plasmablast B Cells. *Life Sci Alliance* (2019) 2(3):e201800244. doi: 10.26508/lsa.201800244

120. Hu R, Kagele DA, Huffaker TB, Runtsch MC, Alexander M, Liu J, et al. miR-155 Promotes T Follicular Helper Cell Accumulation During Chronic, Low-Grade Inflammation. *Immunity* (2014) 41:605–19. doi: 10.1016/j.immuni.2014.09.015
121. Kang SG, Liu WH, Lu P, Jin HY, Lim HW, Shepherd J, et al. MicroRNAs of the miR-17~92 Family are Critical Regulators of T(FH) Differentiation. *Nat Immunol* (2013) 14:849–57. doi: 10.1038/ni.2648
122. Wu T, Wieland A, Lee J, Hale JS, Han JH, Xu X, et al. Cutting Edge: miR-17-92 Is Required for Both CD4 Th1 and T Follicular Helper Cell Responses During Viral Infection. *J Immunol* (2015) 195:2515–9. doi: 10.4049/jimmunol.1500317
123. Pucella JN, Yen WF, Kim MV, van der Veeken J, Luo CT, Socci ND, et al. miR-182 is Largely Dispensable for Adaptive Immunity: Lack of Correlation Between Expression and Function. *J Immunol* (2015) 194:2635–42. doi: 10.4049/jimmunol.1402261
124. Pucella JN, Cols M, Yen WF, Xu S, Chaudhuri J. The B Cell Activation-Induced miR-183 Cluster Plays a Minimal Role in Canonical Primary Humoral Responses. *J Immunol* (2019) 202:1383–96. doi: 10.4049/jimmunol.1800071
125. Lin J, Lwin T, Zhao JJ, Tam W, Choi YS, Moscinski LC, et al. Follicular Dendritic Cell-Induced microRNA-mediated Upregulation of PRDM1 and Downregulation of BCL-6 in non-Hodgkin's B-cell Lymphomas. *Leukemia* (2011) 25:145–52. doi: 10.1038/leu.2010.230
126. Aungier SR, Ohmori H, Clinton M, Mabbott NA. MicroRNA-100-5p Indirectly Modulates the Expression of Il6, Ptgs1/2 and Tlr4 mRNA in the Mouse Follicular Dendritic Cell-Like Cell Line, FL-Y. *Immunology* (2015) 144:34–44. doi: 10.1111/imm.12342
127. Belver L, de Yébenes VG, Ramiro AR. MicroRNAs Prevent the Generation of Autoreactive Antibodies. *Immunity* (2010) 33:713–22. doi: 10.1016/j.immuni.2010.11.010
128. Lai M, Gonzalez-Martin A, Cooper AB, Oda H, Jin HY, Shepherd J, et al. Regulation of B-cell Development and Tolerance by Different Members of the miR-17~92 Family Micrornas. *Nat Commun* (2016) 7:12207. doi: 10.1038/ncomms12207
129. Gonzalez-Martin A, Adams BD, Lai M, Shepherd J, Salvador-Bernaldez M, Salvador JM, et al. The microRNA miR-148a Functions as a Critical Regulator of B Cell Tolerance and Autoimmunity. *Nat Immunol* (2016) 17:433–40. doi: 10.1038/ni.3385
130. Wang M, Chen H, Qiu J, Yang HX, Zhang CY, Fei YY, et al. Antagonizing miR-7 Suppresses B Cell Hyperresponsiveness and Inhibits Lupus Development. *J Autoimmun* (2020) 109:102440. doi: 10.1016/j.jaut.2020.102440
131. Wu XN, Ye YX, Niu JW, Li Y, Li X, You X, et al. Defective PTEN Regulation Contributes to B Cell Hyperresponsiveness in Systemic Lupus Erythematosus. *Sci Transl Med* (2014) 6:246ra299. doi: 10.1126/scitranslmed.3009131
132. Cheng J, Wu R, Long L, Su J, Liu J, Wu XD, et al. miRNA-451a Targets IFN Regulatory Factor 8 for the Progression of Systemic Lupus Erythematosus. *Inflammation* (2017) 40:676–87. doi: 10.1007/s10753-017-0514-8
133. Xin Q, Li J, Dang J, Bian X, Shan S, Yuan J, et al. miR-155 Deficiency Ameliorates Autoimmune Inflammation of Systemic Lupus Erythematosus by Targeting S1pr1 in Faslpr/lpr Mice. *J Immunol* (2015) 194:5437–45. doi: 10.4049/jimmunol.1403028
134. Thai TH, Patterson HC, Pham DH, Kis-Toth K, Kaminski DA, Tsokos GC. Deletion of microRNA-155 Reduces Autoantibody Responses and Alleviates Lupus-Like Disease in the Fas(lpr) Mouse. *Proc Natl Acad Sci USA* (2013) 110:20194–9. doi: 10.1073/pnas.1317632110
135. Mok Y, Schwierzeck V, Thomas DC, Vigorito E, Rayner TF, Jarvis LB, et al. MiR-210 is Induced by Oct-2, Regulates B Cells, and Inhibits Autoantibody Production. *J Immunol* (2013) 191:3037–48. doi: 10.4049/jimmunol.1301289
136. Zhu S, Pan W, Song X, Liu Y, Shao X, Tang Y, et al. The microRNA miR-23b Suppresses IL-17-associated Autoimmune Inflammation by Targeting TAB2, TAB3 and IKK-α. *Nat Med* (2012) 18:1077–86. doi: 10.1038/nm.2815
137. Magilnick N, Reyes EY, Wang WL, Vonderfecht SL, Gohda J, Inoue JI, et al. miR-146a-Traf6 Regulatory Axis Controls Autoimmunity and Myelopoiesis, but is Dispensable for Hematopoietic Stem Cell Homeostasis and Tumor Suppression. *Proc Natl Acad Sci USA* (2017) 114:E7140–9. doi: 10.1073/pnas.1706833114
138. Zhou S, Wang Y, Meng Y, Xiao C, Liu Z, Brohawn P, et al. In Vivo Therapeutic Success of MicroRNA-155 Antagomir in a Mouse Model of Lupus Alveolar Hemorrhage. *Arthritis Rheumatol* (2016) 68:953–64. doi: 10.1002/art.39485
139. Xia Y, Tao JH, Fang X, Xiang N, Dai XJ, Jin L, et al. MicroRNA-326 Upregulates B Cell Activity and Autoantibody Production in Lupus Disease of MRL/lpr Mice. *Mol Ther Nucleic Acids* (2018) 11:284–91. doi: 10.1016/j.omtn.2018.02.010
140. Liu L, Liu Y, Yuan M, Xu L, Sun H. Elevated Expression of microRNA-873 Facilitates Th17 Differentiation by Targeting Forkhead Box O1 (Foxo1) in the Pathogenesis of Systemic Lupus Erythematosus. *Biochem Biophys Res Commun* (2017) 492:453–60. doi: 10.1016/j.bbrc.2017.08.075
141. Duong BH, Ota T, Aoki-Ota M, Cooper AB, Ait-Azzouzene D, Vela JL, et al. Negative Selection by IgM Superantigen Defines a B Cell Central Tolerance Compartment and Reveals Mutations Allowing Escape. *J Immunol* (2011) 187:5596–605. doi: 10.4049/jimmunol.1102479
142. Kluiver JL, Chen CZ. MicroRNAs Regulate B-cell Receptor Signaling-Induced Apoptosis. *Genes Immun* (2012) 13:239–44. doi: 10.1038/gene.2012.1
143. Costinean S, Sandhu SK, Pedersen IM, Tili E, Trotta R, Perrotti D, et al. Src Homology 2 Domain-Containing inositol-5-phosphatase and CCAAT Enhancer-Binding Protein Beta are Targeted by miR-155 in B Cells of Emicro-MiR-155 Transgenic Mice. *Blood* (2009) 114:1374–82. doi: 10.1182/blood-2009-05-220814
144. Leiss H, Salzberger W, Jacobs B, Gessl I, Kozakowski N, Blüml S, et al. MicroRNA 155-Deficiency Leads to Decreased Autoantibody Levels and Reduced Severity of Nephritis and Pneumonitis in Pristane-Induced Lupus. *PloS One* (2017) 12:e0181015. doi: 10.1371/journal.pone.0181015
145. Garchow BG, Bartulos Encinas O, Leung YT, Tsao PY, Eisenberg RA, Caricchio R, et al. Silencing of microRNA-21 In Vivo Ameliorates Autoimmune Splenomegaly in Lupus Mice. *EMBO Mol Med* (2011) 3:605–15. doi: 10.1002/emmm.201100171
146. Garchow B, Kiriakidou M. MicroRNA-21 Deficiency Protects From Lupus-Like Autoimmunity in the Chronic Graft-Versus-Host Disease Model of Systemic Lupus Erythematosus. *Clin Immunol* (2016) 162:100–6. doi: 10.1016/j.clim.2015.11.010
147. Lee CH, Melchers M, Wang H, Torrey TA, Slota R, Qi CF, et al. Regulation of the Germinal Center Gene Program by Interferon (IFN) Regulatory Factor 8/IFN Consensus Sequence-Binding Protein. *J Exp Med* (2006) 203:63–72. doi: 10.1084/jem.20051450
148. Pan Y, Jia T, Zhang Y, Zhang K, Zhang R, Li J, et al. MS2 VLP-based Delivery of microRNA-146a Inhibits Autoantibody Production in Lupus-Prone Mice. *Int J Nanomedicine* (2012) 7:5957–67. doi: 10.2147/IJN.S37990
149. Boldin MP, Taganov KD, Rao DS, Yang L, Zhao JL, Kalwani M, et al. miR-146a is a Significant Brake on Autoimmunity, Myeloproliferation, and Cancer in Mice. *J Exp Med* (2011) 208:1189–201. doi: 10.1084/jem.20101823
150. Fouda ME, Nour El Din DM, Mahgoub MY, Elashkar AE, Abdel Halim WA. Genetic Variants of microRNA-146a Gene: An Indicator of Systemic Lupus Erythematosus Susceptibility, Lupus Nephritis, and Disease Activity. *Mol Biol Rep* (2020) 47:7459–66. doi: 10.1007/s11033-020-05802-y
151. Hou G, Harley ITW, Lu X, Zhou T, Xu N, Yao C, et al. SLE non-Coding Genetic Risk Variant Determines the Epigenetic Dysfunction of an Immune Cell Specific Enhancer That Controls Disease-Critical microRNA Expression. *Nat Commun* (2021) 12:135. doi: 10.1101/2020.05.13.092932
152. Du C, Liu C, Kang J, Zhao G, Ye Z, Huang S, et al. MicroRNA miR-326 Regulates TH-17 Differentiation and is Associated With the Pathogenesis of Multiple Sclerosis. *Nat Immunol* (2009) 10:1252–9. doi: 10.1038/ni.1798
153. Luo S, Ding S, Liao J, Zhang P, Liu Y, Zhao M, et al. Excessive miR-152-3p Results in Increased BAFF Expression in SLE B-Cells by Inhibiting the KLF5 Expression. *Front Immunol* (2019) 10:1127. doi: 10.3389/fimmu.2019.01127
154. Pinheiro I, Dejager L, Libert C. X-Chromosome-Located microRNAs in Immunity: Might They Explain Male/Female Differences? The X Chromosome-Genomic Context may Affect X-located miRNAs and Downstream Signaling, Thereby Contributing to the Enhanced Immune Response of Females. *Bioessays* (2011) 33:791–802. doi: 10.1002/bies.201100047

155. Zhang ZJ, Guo JS, Li SS, Wu XB, Cao DL, Jiang BC, et al. TLR8 and its Endogenous Ligand miR-21 Contribute to Neuropathic Pain in Murine DRG. *J Exp Med* (2018) 215:3019–37. doi: 10.1084/jem.20180800
156. Fabbri M, Paone A, Calore F, Galli R, Gaudio E, Santhanam R, et al. MicroRNAs Bind to Toll-like Receptors to Induce Prometastatic Inflammatory Response. *Proc Natl Acad Sci USA* (2012) 109:E2110–2116. doi: 10.1073/pnas.1209414109
157. Wang Y, Liang H, Jin F, Yan X, Xu G, Hu H, et al. Injured Liver-Released miRNA-122 Elicits Acute Pulmonary Inflammation Via Activating Alveolar Macrophage TLR7 Signaling Pathway. *Proc Natl Acad Sci USA* (2019) 116:6162–71. doi: 10.1073/pnas.1814139116
158. Mittelbrunn M, Gutiérrez-Vázquez C, Villarroya-Beltri C, González S, Sánchez-Cabo F, González M, et al. Unidirectional Transfer of microRNA-loaded Exosomes From T Cells to Antigen-Presenting Cells. *Nat Commun* (2011) 2:282. doi: 10.1038/ncomms1285
159. Montecalvo A, Larregina AT, Shufesky WJ, Stolz DB, Sullivan ML, Karlsson JM, et al. Mechanism of Transfer of Functional microRNAs Between Mouse Dendritic Cells Via Exosomes. *Blood* (2012) 119:756–66. doi: 10.1182/blood-2011-02-338004
160. Salvi V, Gianello V, Busatto S, Bergese P, Andreoli L, D'Oro U, et al. Exosome-Delivered microRNAs Promote IFN-α Secretion by Human Plasmacytoid DCs Via TLR7. *JCI Insight* (2018) 3(10):e98204. doi: 10.1172/jci.insight.98204
161. Fernández-Messina L, Rodríguez-Galán A, de Yébenes VG, Gutiérrez-Vázquez C, Tenreiro S, Seabra MC, et al. Transfer of Extracellular vesicle-microRNA Controls Germinal Center Reaction and Antibody Production. *EMBO Rep* (2020) 21:e48925. doi: 10.15252/embr.201948925
162. Seeley JJ, Baker RG, Mohamed G, Bruns T, Hayden MS, Deshmukh SD, et al. Induction of Innate Immune Memory Via microRNA Targeting of Chromatin Remodelling Factors. *Nature* (2018) 559:114–9. doi: 10.1038/s41586-018-0253-5
163. Duursma AM, Kedde M, Schrier M, le Sage C, Agami R. miR-148 Targets Human DNMT3b Protein Coding Region. *RNA* (2008) 14:872–7. doi: 10.1261/rna.972008
164. Fabbri M, Garzon R, Cimmino A, Liu Z, Zanesi N, Callegari E, et al. MicroRNA-29 Family Reverts Aberrant Methylation in Lung Cancer by Targeting DNA Methyltransferases 3A and 3B. *Proc Natl Acad Sci USA* (2007) 104:15805–10. doi: 10.1073/pnas.0707628104
165. Garzon R, Liu S, Fabbri M, Liu Z, Heaphy CE, Callegari E, et al. MicroRNA-29b Induces Global DNA Hypomethylation and Tumor Suppressor Gene Reexpression in Acute Myeloid Leukemia by Targeting Directly DNMT3A and 3B and Indirectly DNMT1. *Blood* (2009) 113:6411–8. doi: 10.1182/blood-2008-07-170589
166. Varambally S, Cao Q, Mani RS, Shankar S, Wang X, Ateeq B, et al. Genomic Loss of microRNA-101 Leads to Overexpression of Histone Methyltransferase EZH2 in Cancer. *Science* (2008) 322:1695–9. doi: 10.1126/science.1165395
167. Sander S, Bullinger L, Klapproth K, Fiedler K, Kestler HA, Barth TF, et al. MYC Stimulates EZH2 Expression by Repression of its Negative Regulator miR-26a. *Blood* (2008) 112:4202–12. doi: 10.1182/blood-2008-03-147645
168. Sakurai K, Furukawa C, Haraguchi T, Inada K, Shiogama K, Tagawa T, et al. MicroRNAs miR-199a-5p and -3p Target the Brm Subunit of SWI/SNF to Generate a Double-Negative Feedback Loop in a Variety of Human Cancers. *Cancer Res* (2011) 71:1680–9. doi: 10.1158/0008-5472.CAN-10-2345
169. Zhao S, Wang Y, Liang Y, Zhao M, Long H, Ding S, et al. MicroRNA-126 Regulates DNA Methylation in CD4+ T Cells and Contributes to Systemic Lupus Erythematosus by Targeting DNA Methyltransferase 1. *Arthritis Rheum* (2011) 63:1376–86. doi: 10.1002/art.30196
170. Qin H, Zhu X, Liang J, Wu J, Yang Y, Wang S, et al. MicroRNA-29b Contributes to DNA Hypomethylation of CD4+ T Cells in Systemic Lupus Erythematosus by Indirectly Targeting DNA Methyltransferase 1. *J Dermatol Sci* (2013) 69:61–7. doi: 10.1016/j.jdermsci.2012.10.011
171. Hedrich CM. Epigenetics in SLE. *Curr Rheumatol Rep* (2017) 19:58. doi: 10.1007/s11926-017-0685-1
172. Touma Z, Gladman DD. Current and Future Therapies for SLE: Obstacles and Recommendations for the Development of Novel Treatments. *Lupus Sci Med* (2017) 4:e000239. doi: 10.1136/lupus-2017-000239
173. Krützfeldt J, Rajewsky N, Braich R, Rajeev KG, Tuschl T, Manoharan M, et al. Silencing of microRNAs In Vivo With 'Antagomirs'. *Nature* (2005) 438:685–9. doi: 10.1038/nature04303
174. Ørom UA, Kauppinen S, Lund AH. LNA-Modified Oligonucleotides Mediate Specific Inhibition of microRNA Function. *Gene* (2006) 372:137–41. doi: 10.1016/j.gene.2005.12.031
175. Obad S, dos Santos CO, Petri A, Heidenblad M, Broom O, Ruse C, et al. Silencing of microRNA Families by Seed-Targeting Tiny LNAs. *Nat Genet* (2011) 43:371–8. doi: 10.1038/ng.786
176. Gebert LF, Rebhan MA, Crivelli SE, Denzler R, Stoffel M, Hall J. Miravirsen (SPC3649) can Inhibit the Biogenesis of miR-122. *Nucleic Acids Res* (2014) 42:609–21. doi: 10.1093/nar/gkt852
177. Herrera-Carrillo E, Liu YP, Berkhout B. Improving Mirna Delivery by Optimizing miRNA Expression Cassettes in Diverse Virus Vectors. *Hum Gene Ther Methods* (2017) 28:177–90. doi: 10.1089/hgtb.2017.036
178. Ebert MS, Sharp PA. MicroRNA Sponges: Progress and Possibilities. *RNA* (2010) 16:2043–50. doi: 10.1261/rna.2414110
179. Chaudhary V, Jangra S, Yadav NR. Nanotechnology Based Approaches for Detection and Delivery of microRNA in Healthcare and Crop Protection. *J Nanobiotechnology* (2018) 16:40. doi: 10.1186/s12951-018-0368-8
180. Ottosen S, Parsley TB, Yang L, Zeh K, van Doorn LJ, van der Veer E, et al. In Vitro Antiviral Activity and Preclinical and Clinical Resistance Profile of Miravirsen, a Novel Anti-Hepatitis C Virus Therapeutic Targeting the Human Factor miR-122. *Antimicrob Agents Chemother* (2015) 59:599–608. doi: 10.1128/AAC.04220-14
181. Chakraborty C, Sharma AR, Sharma G, Doss CGP, Lee SS. Therapeutic miRNA and Sirna: Moving From Bench to Clinic as Next Generation Medicine. *Mol Ther Nucleic Acids* (2017) 8:132–43. doi: 10.1016/j.omtn.2017.06.005
182. Seto AG, Beatty X, Lynch JM, Hermreck M, Tetzlaff M, Duvic M, et al. Cobomarsen, an Oligonucleotide Inhibitor of miR-155, Co-Ordinately Regulates Multiple Survival Pathways to Reduce Cellular Proliferation and Survival in Cutaneous T-cell Lymphoma. *Br J Haematol* (2018) 183:428–44. doi: 10.1111/bjh.15547
183. Anastasiadou E, Seto AG, Beatty X, Hermreck M, Gilles ME, Stroopinsky D, et al. Cobomarsen, an Oligonucleotide Inhibitor of miR-155, Slows DLBCL Tumor Cell Growth in Vitro and In Vivo. *Clin Cancer Res* (2021) 27:1139–49. doi: 10.1158/1078-0432.CCR-20-3139
184. Hanna J, Hossain GS, Kocerha J. The Potential for Microrna Therapeutics and Clinical Research. *Front Genet* (2019) 10:478. doi: 10.3389/fgene.2019.00478
185. Sarvestani ST, Stunden HJ, Behlke MA, Forster SC, McCoy CE, Tate MD, et al. Sequence-Dependent Off-Target Inhibition of TLR7/8 Sensing by Synthetic microRNA Inhibitors. *Nucleic Acids Res* (2015) 43:1177–88. doi: 10.1093/nar/gku1343

Conflict of Interest : The authors declare that the research was conducted in the absence of any commercial or financial relationships that could be construed as a potential conflict of interest.

frontiers in Immunology

METHODS
published: 24 May 2021
doi: 10.3389/fimmu.2021.685718

High-Throughput Detection of Autoantigen-Specific B Cells Among Distinct Functional Subsets in Autoimmune Donors

*Bryan A. Joosse[1], James H. Jackson[1,2], Alberto Cisneros, 3rd[1], Austin B. Santhin[1], Scott A. Smith[3,4,5], Daniel J. Moore[4,5,6], Leslie J. Crofford[1,4,5], Erin M. Wilfong[1,7] and Rachel H. Bonami[1,4,5]**

[1] Department of Medicine, Division of Rheumatology and Immunology, Vanderbilt University Medical Center, Nashville, TN, United States, [2] Department of Biomedical Sciences, School of Medicine Greenville, University of South Carolina, Greenville, SC, United States, [3] Department of Medicine, Division of Infectious Diseases, Vanderbilt University Medical Center, Nashville, TN, United States, [4] Department of Pathology, Microbiology and Immunology, Vanderbilt University Medical Center, Nashville, TN, United States, [5] Vanderbilt Institute for Infection, Immunology, and Inflammation (VI4), Nashville, TN, United States, [6] Department of Pediatrics, Division of Endocrinology & Diabetes, Vanderbilt University Medical Center, Nashville, TN, United States, [7] Department of Medicine, Allergy, Pulmonary, and Critical Care, Vanderbilt University Medical Center, Nashville, TN, United States

OPEN ACCESS

Edited by:
Zhenming Xu,
The University of Texas Health Science Center at San Antonio, United States

Reviewed by:
Hong Zan,
The University of Texas Health Science Center at San Antonio, United States
Ziaur S. M. Rahman,
Penn State Milton S. Hershey Medical Center, United States

***Correspondence:**
Rachel H. Bonami
rachel.h.bonami@vumc.org

Specialty section:
This article was submitted to B Cell Biology, a section of the journal Frontiers in Immunology

Received: *25 March 2021*
Accepted: *06 May 2021*
Published: *24 May 2021*

Citation:
Joosse BA, Jackson JH, Cisneros A 3rd, Santhin AB, Smith SA, Moore DJ, Crofford LJ, Wilfong EM and Bonami RH (2021) High-Throughput Detection of Autoantigen-Specific B Cells Among Distinct Functional Subsets in Autoimmune Donors. Front. Immunol. 12:685718. doi: 10.3389/fimmu.2021.685718

Antigen-specific B cells (ASBCs) can drive autoimmune disease by presenting autoantigen to cognate T cells to drive their activation, proliferation, and effector cell differentiation and/or by differentiating into autoantibody-secreting cells. Autoantibodies are frequently used to predict risk and diagnose several autoimmune diseases. ASBCs can drive type 1 diabetes even when immune tolerance mechanisms block their differentiation into antibody-secreting cells. Furthermore, anti-histidyl tRNA synthetase syndrome patients have expanded IgM^+ Jo-1-binding B cells, which clinically diagnostic IgG Jo-1 autoantibodies may not fully reflect. Given the potential disconnect between the pathologic function of ASBCs and autoantibody secretion, direct study of ASBCs is a necessary step towards developing better therapies for autoimmune diseases, which often have no available cure. We therefore developed a high-throughput screening pipeline to 1) phenotypically identify specific B cell subsets, 2) expand them *in vitro*, 3) drive them to secrete BCRs as antibody, and 4) identify wells enriched for ASBCs through ELISA detection of antibody. We tested the capacity of several B cell subset(s) to differentiate into antibody-secreting cells following this robust stimulation. IgM^+ and/or IgD^+, $CD27^-$ memory, memory, switched memory, and B_{ND} B cells secreted B cell receptor (BCR) as antibody following *in vitro* stimulation, whereas few plasmablasts responded. Bimodal responses were observed across autoimmune donors for IgM^+ $CD21^{lo}$ and IgM^- $CD21^{lo}$ B cells, consistent with documented heterogeneity within the $CD21^{lo}$ subset. Using this approach, we detected insulin-binding B cell bias towards $CD27^-$ memory and $CD27^+$ memory subsets in pre-symptomatic type 1 diabetes donors. We took advantage of routine detection of Jo-1-binding B cells in Jo-1+ anti-histidyl tRNA synthetase syndrome patients to show that Jo-1-binding B cells and total B cells expanded 20-30-fold using this culture system. Overall, these studies highlight

technology that is amenable to small numbers of cryopreserved peripheral blood mononuclear cells that enables interrogation of phenotypic and repertoire attributes of ASBCs derived from autoimmune patients.

Keywords: B cells, B cell receptor (BCR), autoimmune disease, autoantigen, myositis, Sjogren's syndrome, systemic sclerosis (scleroderma), type 1 diabetes

INTRODUCTION

B lymphocytes contribute to immune responses by presenting antigens to T cells, secreting cytokines, and differentiating into antibody-secreting cells. Autoantibodies are frequently used to predict and diagnose autoimmune diseases, highlighting the important role that B cells play in promoting autoimmunity (1–7). In some diseases, such as Sjögren's syndrome, systemic lupus erythematosus, and rheumatoid arthritis, autoantibodies have pathologic function *via* immune complex formation (8). In others, such as type 1 diabetes, autoantibodies are not directly pathogenic (9); rather, it is the antigen-presenting function of the B cell that is essential for disease (9–13). Autoimmune disease treatments such as prednisone, rituximab, or abatacept involve broad immune suppression. For example, rituximab globally depletes B cells which is effective at treating several autoimmune diseases, including rheumatoid arthritis, systemic lupus erythematosus, anti-histidyl tRNA synthetase syndrome, and systemic sclerosis (14–20). Rituximab is well-tolerated in adults, but results in diminution of vaccine responses, a key consideration for treatment of pediatric autoimmune diseases such as type 1 diabetes (21). Therapies that selectively target ASBCs would avoid the problem of broad immune suppression and should thus be safer. Selection elimination of anti-insulin B cells prevents disease in type 1 diabetes-prone mice (22); targeting ASBCs may thus offer an effective alternative to broad immunosuppression for autoimmune disease prevention and treatment. Understanding the mechanisms that govern immune tolerance breach by autoreactive B cells requires identification and study of ASBCs.

B lymphocytes express antigen-specific, membrane-bound B cell receptors but are not a major source of circulating antibody. Rather, B lymphocytes must receive the right stimulation to differentiate into plasmablasts or plasma cells that secrete BCR as circulating antibody (23). Different immune checkpoints govern whether autoreactive B cells 1) expand, 2) undergo mutation and affinity maturation, and 3) differentiate into antibody-secreting cells (23, 24). In Sjögren's syndrome, sustained Ro60 autoantibody production is due to continual generation of plasmablasts from ASBCs, rather than long-lived plasma cells, suggesting continual autoreactive B cell seeding of the peripheral repertoire is required (25). Studies in mice show that autoantigen-specific B cells (ASBCs) can retain disease-relevant autoantigen-presenting function even when immune tolerance mechanisms block their differentiation into autoantibody-secreting cells (26–28). This points to a need to identify the specific mechanisms by which ASBCs escape immune tolerance to expand and drive pathology, a process which may differ between autoimmune diseases.

Methods have been developed to track ASBCs in the broad repertoire that are as rare as 1 in 20 million cells (29). Many different B cell subsets can potentially contribute to a protective or autoimmune response that may have different responsiveness to specific stimuli. For example, whereas naïve B cells proliferate in response to BCR stimulation, anergic (B_{ND}) and $CD21^{lo}$ B cells do not (30, 31). B_{ND} and $CD21^{lo}$ subsets may serve as reservoirs for autoreactive B cells in several autoimmune diseases, including type 1 diabetes, Sjögren's syndrome, anti-histidyl tRNA synthetase syndrome, and systemic sclerosis (32–36). We sought to develop high-throughput stimulation and screening methods to identify ASBCs among total PBMCs using ELISA detection of BCRs secreted as antibody. Given the signaling differences present among autoreactive-prone B cell subsets of interest, we examined the potential of each of these subsets to respond to robust stimulation *in vitro* that includes BCR, CpG, CD40L, IL-21, and BAFF stimulation (29). We further tested the capacity of several memory B cell subsets and plasmablasts to differentiate/secrete BCR as antibody in this culture system as a mean to identify ASBCs within a polyclonal repertoire.

Abbreviations: ASBCs, Antigen-specific B cells; BCR, B cell receptor; IAA, insulin autoantibody; PBMCs, peripheral blood mononuclear cells.

MATERIALS AND METHODS

Participant Selection and Clinical Information

Systemic sclerosis and Jo-1+ anti-histidyl tRNA synthetase syndrome patients were selected from enrollees in the Vanderbilt Myositis and Scleroderma Treatment and Investigative Center (MYSTIC) cohort. A subset of systemic sclerosis patients was defined as having interstitial lung disease if a radiologist determined that fibrosis was present on a CT scan. Sjögren's syndrome patients were selected from enrollees in the B Lymphocytes in Sjögren's syndrome (BLISS) at Vanderbilt University Medical Center. Patients were eligible for the study if they were 18 years or older and had been diagnosed with systemic sclerosis by a rheumatologist or pulmonologist or Sjögren's syndrome by a rheumatologist. Clinical data were collected from the electronic medical record. One donor was obtained from the Human Immunology Discovery Initiative (HIDI) cohort. Additional autoimmune diagnoses were obtained *via* patient-reported questionnaire. These studies were approved by the Vanderbilt Institutional Review Board. Participant characteristics are outlined in **Table 1**.

Donors at risk for type 1 diabetes were recruited at Vanderbilt through their participation in Type 1 Diabetes TrialNet Pathway to Prevention (37). Type 1 Diabetes TrialNet participants were

first, second, or third-degree relatives of type 1 diabetes probands that were defined as having pre-symptomatic type 1 diabetes based on a history of positivity for two or more islet autoantibodies (IAA, GAD65, ICA, IA2, or ZNT8, defined in **Table 2**, one of which was insulin autoantibody (IAA). Participants were excluded from this cohort if they previously received insulin therapy or were diagnosed with diabetes at the time of blood draw. Participants were excluded for any of the following: fever 101°F in preceding 48hrs of clinic visit, receiving antibiotic therapy at clinic visit, weight less than 8 kg, known pregnancy, anemia at time of study initiation (Hgb <12), comorbid conditions which would render giving blood samples a risk, chronic use of immune suppressive or depleting medications, prior use of immune modulating medications, inability to meet study visit requirements, ongoing use of Accutane, age <1 year, > 60 years at the time of baseline visit. Participant characteristics are outlined in **Table 2**. This study received IRB approval by Vanderbilt and ancillary study approval by Type 1 Diabetes TrialNet. All data were managed using the REDCap software system (38).

Sample Collection and Processing

Peripheral blood mononuclear cells (PBMCs) were obtained by collecting whole blood into mononuclear cell preparation tubes with sodium heparin or sodium citrate (BD) *via* peripheral venipuncture. Cells were washed twice in PBS and red blood cells were lysed using Ack Lysis Buffer (Gibco). Cells were again washed in PBS and counted. Cells were cooled in 10% dimethyl sulfoxide (DMSO) in fetal bovine serum (FBS) at a rate of -1°C/minute until they reached a temperature of -80°C for 24-72 hours. Cells were then stored in liquid nitrogen until the time of analysis. Viability was assessed at time of sample thawing with ~ 80% average viability.

TABLE 1 | Demographics for participants included from MYSTIC, BLISS, and HIDI cohorts.

SubjectID	Cohort[a]	Gender	Age Range (years)[b]	Immunomodulatory agents at enrollment[c]	Autoimmune disease diagnosis[d]	Autoantibodies[e]
1	MYSTIC	F		MMF	SSc/ILD	Scl70
2	MYSTIC	F		None	SSc/ILD	Scl70
3	MYSTIC	M		None	SSc/ILD	Scl70
4	MYSTIC	F		None	SSc/ILD	Scl70
5	MYSTIC	F		None	SSc/ILD	None
6	MYSTIC	F		MMF/HCQ	SSc/ILD	None
7	MYSTIC	F		HCQ	SSc/ILD	Centromere
8	MYSTIC	F		None	SSc	Centromere
9	MYSTIC	M		None	SSc	RNApol3
10	MYSTIC	M		Pred/IVIG	ARS	Jo-1
11	MYSTIC	M		Pred	ARS	Jo-1
12	MYSTIC	M		None	ARS	Jo-1
13	MYSTIC	F		Pred	ARS	Jo-1
14	BLISS	F		None	SjS/ATD/T1D	SSA, SSB, ANA, RF
15	BLISS	F		HCQ	SjS/CL	SSA, SSB, ANA
16	HIDI	F		None	ATD	Unknown
			56 ± 13			

[a]*BLISS, B Lymphocytes in Sjögren's syndrome; HIDI, Human Immunology Discovery Initiative; MYSTIC, Myositis and Scleroderma Treatment and Investigative Center.*
[b]*Average ± standard deviation.*
[c]*HCQ, hydroxychloroquine; MMF, mycophenolate mofetil; Pred, prednisone.*
[d]*ATD, autoimmune thyroid disease; CL, cutaneous lupus; ILD, interstitial lung disease; ARS, anti-tRNA synthetase syndrome; SjS, Sjögren's syndrome; SSc, systemic sclerosis; T1D, type 1 diabetes.*
[e]*ANA, anti-nuclear antibodies; RF, rheumatoid factor.*

TABLE 2 | Type 1 Diabetes TrialNet participant demographics.

SubjectID	Gender	Age range (years)[a]	Oral glucose tolerance test results[b]	Autoimmune disease diagnosis[c]	Islet autoantibody positivity at blood draw[d]
17	F		Impaired	Pre-T1D	IAA, IA2, ICA, GAD65, ZNT8
18	F		Impaired	Pre-T1D	IAA, IA2, ICA, GAD65, ZNT8
19	M		Normal	Pre-T1D	IAA, IA2, ICA, GAD65, ZNT8
20	F		Impaired	Pre-T1D	IAA, IA2, ICA, GAD65, ZNT8
21	M		Impaired	Pre-T1D	IAA, GAD65
		13 ± 6			

[a]*Average ± standard deviation.*
[b]*Oral glucose tolerance test results are defined as follows based on blood glucose measurements (mg/dL): Normal: Fasting.*
<110, 1h < 200, 2h < 140, no symptoms; Impaired: Fasting ≥110, <126, 1h ≥ 200, 2h ≥ 140, <200, no symptoms.
<110, 1h < 200, 2h < 140, no symptoms; Impaired: Fasting ≥110, <126, 1h ≥ 200, 2h ≥ 140, <200, no symptoms.
[c]*Pre-T1D diagnosis based on positivity for at least two islet autoantibodies, including insulin autoantibody (IAA).*
[d]*The five islet autoantibodies screened by Type 1 Diabetes TrialNet are, GAD65, glutamic acid decarboxylase 65-kilodalton isoform; IAA, insulin autoantibody; IA2, Islet antigen 2; ICA, Islet cell antibodies; ZNT8, Zinc transporter 8.*

ELISA

384-well ELISA plates (Maxisorp) were coated with either 500 ng/ml goat anti-human Ig (Southern Biotech, 2010-01) in 1X PBS overnight at 4°C or 1 μg/mL recombinant human insulin (Sigma I2643) in borate buffered saline overnight at 37°C to assess total antibody or anti-insulin antibody, respectively. The next day, plates were washed 5X with 0.5X PBS and then blocked with 5% chicken serum in 1X PBS plus 0.5% Tween (1X PBS-T) for 1h at room temperature. Block was decanted from plates, blotted dry, and then stimulated PBMC culture supernatants (diluted 1:2 in 1X PBS-T) were added to the plates. Plates were then incubated for 1.5h at room temperature. Bound antibody was detected either by goat anti-human IgG-HRP (Southern Biotech, 2040-05) or goat anti-human IgM-HRP (Southern Biotech, 2020-05) secondary antibodies diluted in 1X PBS-T. Plates were washed 10X with 0.5% PBS. Finally, TMB Ultra ELISA substrate (Thermo Fisher, PI34029) was added, and plates were read at O.D. 370nm using a microplate reader (SpectraMax M3). Wells with fluorescence values above a cutoff of the mean + 3 standard deviations of a blank well were considered positive. Antibody concentrations were calculated using IgG/IgM standards (Sigma, I4506 and I8260, respectively).

Flow Cytometry Purification of B Cell Subsets and Analysis

Cells were stained in flow cytometry staining buffer (1X PBS containing 5% FBS, 0.02% EDTA, and 0.1% sodium azide) with the following reactive antibodies and reagents: CD19 (SJ25C1), CD21 (Bu32), CD24 (ML5), CD27 (O323), CD38 (HIT2), IgD (IA6-2), IgG (G18-145), IgM (MHM-88) (BioLegend or BD Biosciences). B cell subsets were purified using a FACSAria sorter (BD Biosciences). Data were analyzed using FlowJo software (Tree Star, Inc.). Jo-1-binding B cells were identified by flow cytometry using GST-tagged Jo-1 antigen we previously cloned and recombinantly expressed, followed by detection with anti-GST secondary antibody (Abcam), as previously described (36).

B Cell Stimulation

Cryopreserved PBMCs were rapidly thawed, washed, and resuspended in ClonaCell-HY Medium A (StemCell). PBMCs or sorted B cell subsets plated as indicated in figure legends in Medium A with 0.833 μg/ml of CpG (ZOEZOEZZZZZOEEZOEZZZT, Invitrogen) + 0.133 μg/ml each of mouse-anti-human kappa and lambda antibodies (Southern Biotech), as well as $0.033x10^6$ cells/mL viable gamma-irradiated NIH3T3 fibroblasts that were genetically engineered to express cell-surface human CD40L (CD154), secreted human B cell activating factor (BAFF), and human IL-21 (unpublished line related to (39, 40), originally provided to Dr. Smith by Dr. Deepta Bhattacharya; Washington University in St. Louis, St. Louis, MO). These stimuli drive B cells to secrete BCR as antibody to enable screening for ASBCs (29). The mixture was then plated into 96-well (300 μL total volume) or 384-well (100 μL total volume) flat bottom plates (Corning). Plates were incubated with 5% CO_2 at 37°C and screened for antibody production by ELISA after 1 wk, as described above.

Statistical Analysis

Standard statistical tests utilized for each experiment are indicated in the corresponding figure legends and significance values were calculated using Prism (GraphPad).

RESULTS

BCRs Secreted as Antibody Are Captured From Stimulated Mature Naïve and Memory B Cell Subsets

ASBCs are not always readily detectable in autoimmune individuals. A robust stimulation method allows capture of IgE ASBCs as rare as 1 in 20 million as hybridomas (29). This method relies on high-throughput ELISA screening for antigen-specific BCRs secreted as antibody following robust stimulation. One caveat with this method is that it does not provide information about the phenotypic subset from which the ASBC was derived. B cell phenotype correlates with dramatic differences in functional capacity; anergic B cells (e.g. B_{ND} cells in humans) are functionally silenced for proliferation and differentiation into antibody-secreting cells, but memory B cells are poised to rapidly contribute to protective immune responses (29). Thus, consideration of which subset(s) ASBCs are expanded in provides important information about how autoreactive B cell clones arise and function in the repertoire to promote autoimmunity. We sought to test whether this stimulation/screening method could be adapted to use flow cytometry-purified B cell subsets from autoimmune disease patient peripheral blood as inputs, as this would enable ASBCs identification coupled with phenotypic information, such as whether the ASBC had a memory phenotype *in vivo*. **Figure 1** provides an overview of the methods applied to each figure. As shown in **Figure 2A**, specific B cell subsets were purified using flow cytometry sorting. The focus of this manuscript is on B cells derived from autoimmune donors; we presented detailed immunophenotyping to compare B cell subset percentages between patients with several of the autoimmune diseases highlighted in this manuscript and healthy controls in separate manuscripts (36, 41). Purified B cell subsets (e.g. memory) were subsequently divided across wells and stimulated as in Methods to drive B cells to differentiate into antibody-secreting cells (**Figure 2B**). ELISA detects the presence of BCR secreted as antibody in $CD19^+$ IgM^+ and/or IgD^+, class-switched CD27+ memory ($CD19^+$ IgM^- IgD^- $CD27^+$), and $CD27^-$ memory ($CD19^+$ IgM^- IgD^- $CD27^-$) B cell subsets (**Figure 2C**). BCR was also detected as antibody from $CD27^+$ memory cells which included IgM^+ cells (**Figure 2F**). These data show our *in vitro* stimulation protocol can be used to screen BCRs expressed by non-class-switched and memory B cell subsets.

Autoreactive-Prone B_{ND} (Anergic) and $CD21^{low}$ B Cells Are Stimulated to Secrete BCRs as Antibody

We previously identified ASBCs using fluorescently-labeled autoantigen (36). This detection method could however miss B

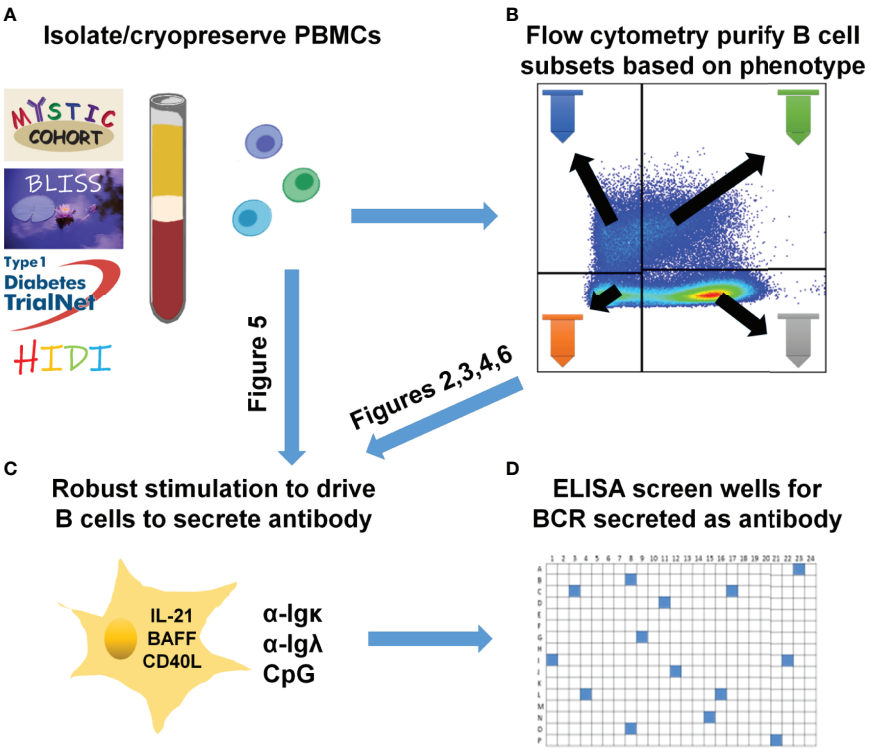

FIGURE 1 | Human B cell stimulation and high-throughput screening methods overview. **(A)** PBMCs were isolated and cryopreserved from the indicated cohorts. **(B)** Specific B cell subsets were flow cytometry-purified. **(C)** As specified for each figure, total PBMCs **(A)** were plated into 96-well plates or purified B cell subsets **(B)** were plated into 384-well plates and stimulated as in Methods to drive B cell proliferation and differentiation into antibody-secreting cells. **(D)** High-throughput ELISA screening of well supernatants identified wells containing ASBCs.

cells that downregulate surface BCR because of chronic antigen stimulation and/or immune tolerance mechanisms such as anergy. Anergy is an immune tolerance mechanism by which autoreactive B cells are functionally silenced but retained in the repertoire; they can be phenotypically identified as B_{ND} cells ($IgM^{lo/-}$ IgD^{+} $CD27^{-}$) (32). $CD21^{lo}$ B cells are an autoreactive-prone subset that is increased in the peripheral blood of patients with several autoimmune diseases (31, 33, 42). $CD21^{lo}$ B cells have been reported to be anergic, yet also to express highly mutated BCRs that are consistent with germinal center origin (31, 33, 43). Given the potential for BND and $CD21^{lo}$ B cell subsets to serve as autoreactive B cell reservoirs, we flow cytometry purified these subsets as shown in **Figure 2D** and screened wells to determine (**Figure 2E**) whether our stimulation protocol could drive B cell subsets to differentiate and secrete their BCRs as antibody (44). B_{ND} and $CD21^{lo}$ BCRs were detected as antibody following stimulation (**Figure 2F**), demonstrating that BCRs from these subsets can be evaluated using this protocol.

Plasmablast Secretion of Antibody Is Not Sustained Following *In Vitro* BCR/CD40/BAFF/Cpg/IL-21 Stimulation

B cells do not secrete antibody; rather, if they receive the right signals, they differentiate into antibody-secreting cells. Whereas plasmablasts are short-lived antibody-secreting cells that can be found in peripheral blood, plasma cells are long-lived antibody-secreting cells that can be found in the bone marrow and other tissues. Plasmablasts are enriched for ASBCs, thus we wanted to test whether this approach captures plasmablast BCRs. Flow cytometry purification identified plasmablasts as in **Figure 3A**, which were stimulated *in vitro* as in Methods (**Figure 3B**). Antibody was not detected by ELISA for plasmablast isolated from the majority of donors following this stimulation protocol (**Figure 3C**), thus other approaches are required to assay antigen-specific plasmablasts.

Limited Class-Switching Is Observed for IgM^{+}/IgD^{+} B Cells Following *In Vitro* Stimulation

Non-class-switched B cell subsets were stimulated for 6d as in Methods to test whether they undergo class-switching to IgG (**Figure 4A**). Flow cytometry analysis revealed limited class-switching away from the IgM isotype for IgM^{+} and/or IgD^{+}, B_{ND}, or IgM^{+} $CD21^{lo}$ B cells following stimulation (**Figures 4B, F, H**). Conversely, the majority of switched memory B cells were identified as IgG^{+} or IgM^{-} IgG^{-} at the end of culture (**Figure 4D**), potentially indicating IgA class switch, which was not measured in this assay. The memory B cell subset, which included both IgM^{+} and IgM^{-} B cells as input, contained both IgM^{+} and switched B cells following

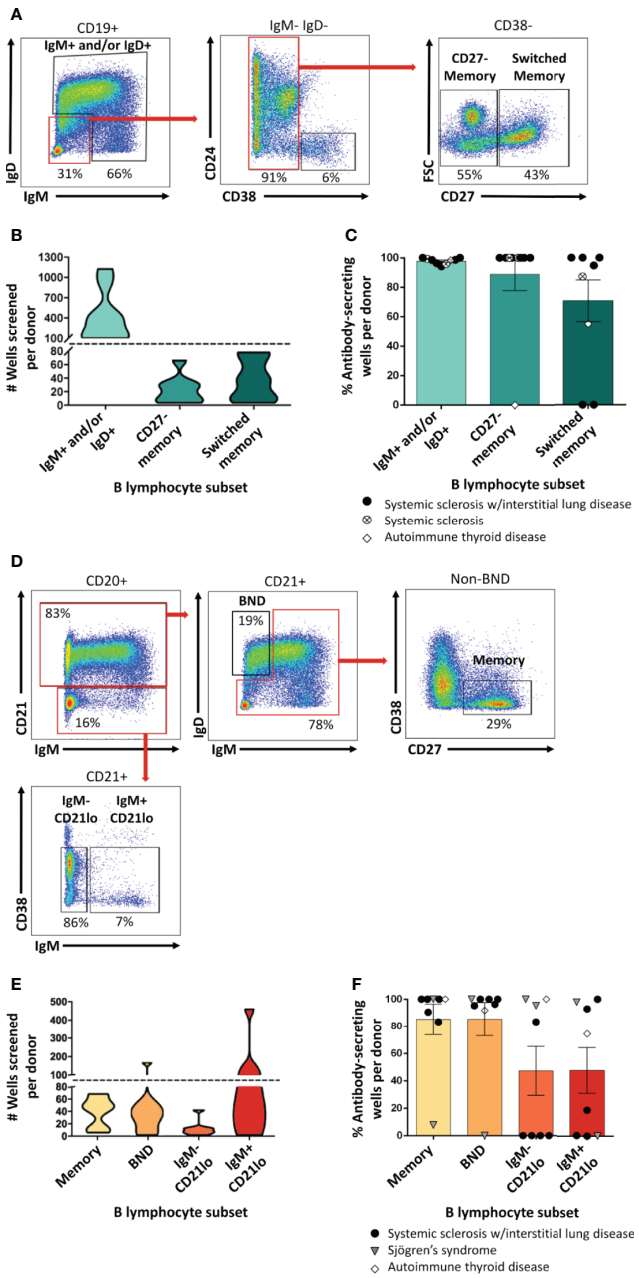

FIGURE 2 | Mature naïve, memory, and autoreactive-prone B cell subsets differentiate into antibody-secreting cells following *in vitro* stimulation. **(A)** Representative plots show flow cytometry identification of the indicated B cell subsets (gated on CD19$^+$ live singlet lymphocytes). Subsets were defined as follows: IgM$^+$ and/or IgD$^+$, CD27$^-$ memory (IgD$^+$ IgM$^+$ CD27$^-$ CD38$^-$), and CD27$^+$ switched memory (IgD$^-$ IgM$^-$ CD27$^+$ CD38$^-$). **(B)** Violin plots show the data distribution and density for the number of all wells screened for each B cell subset per donor in **(C)**, **(C)** PBMCs were isolated from systemic sclerosis/interstitial lung disease (black circle, n=6), systemic sclerosis (open circle/X, n=2), or ATD patients (open diamond, n=1) and B cell subsets were identified as in **(A)** and flow cytometry purified. Individual B cell subsets were plated in 384-well plates at ~300 B cells/well and stimulated as in Methods for 1 wk. ELISA was used to measure antibody present in culture supernatants. Wells were scored positively for antibody secretion for ELISA OD_{370nm} > 0.5. The frequency of positive wells was calculated per subset, per donor; individual points represent individual donors. **(D)** Representative plots show flow cytometry identification of the indicated B cell subsets (gated on CD19$^+$ live singlet lymphocytes). Subsets were defined as follows: memory (IgM$^-$/IgD$^-$ or IgM$^{mid/high}$ CD21$^+$ CD27$^+$ CD38$^-$), B_{ND} (IgM$^{low/neg}$/IgD$^+$ CD21$^+$), IgM$^-$ CD21^{lo} (IgM$^-$ CD27$^+$ CD38$^{mid/neg}$), or IgM$^+$ CD21^{lo} (IgM$^+$ CD21^{lo} CD38$^{mid/neg}$). **(E)** Violin plots show the data distribution and density for the number of all wells screened for each B cell subset per donor in **(F)**, **(F)** PBMCs were isolated from systemic sclerosis/interstitial lung disease (black circle, n=5), Sjögren's syndrome (filled triangle, n=2), or ATD patients (open diamond, n=1) and B cell subsets were identified as in **(D)** and flow cytometry purified. Individual B cell subsets were plated in 384-well plates at ~ 300 B cells/well and stimulated as in Methods for 1 wk. Wells were scored positively for antibody secretion for ELISA OD_{370nm} > 0.5. The frequency of positive wells was calculated per subset, per donor; individual points represent individual donors.

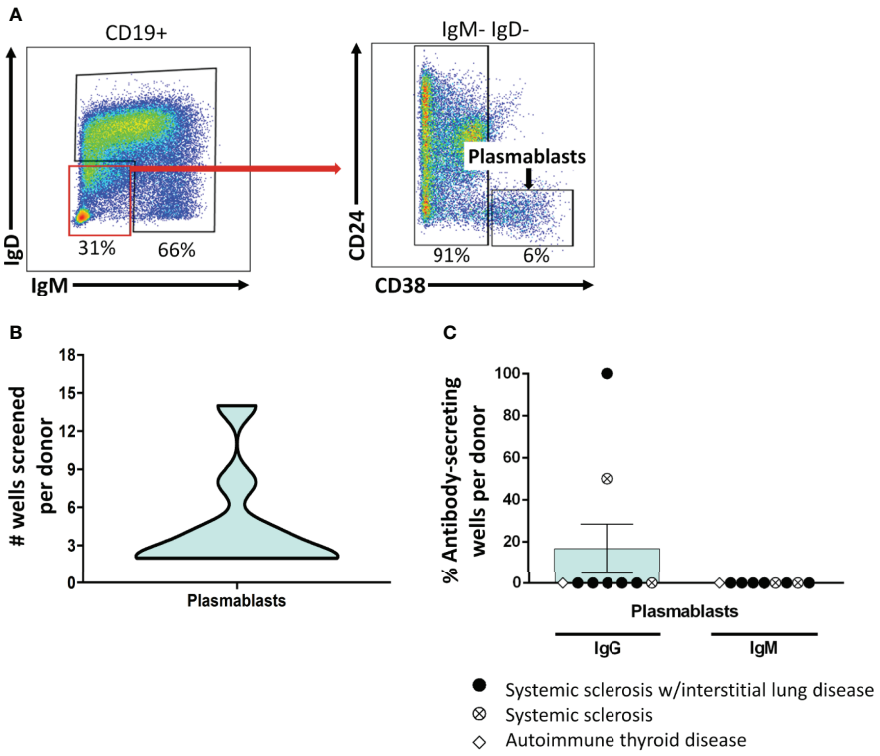

FIGURE 3 | Class-switched plasmablasts do not sustain antibody secretion following BCR/CD40/BAFF/TLR9/IL-21 stimulation. **(A)** PBMCs were isolated from autoimmune disease patients. Representative plots show flow cytometry identification of plasmablasts ($CD19^+$ IgD^- IgM^- $CD24^-$ $CD38^-$ live singlets). **(B)** B cell subsets were identified as in **(A)** and flow cytometry purified. Plasmablasts were plated in 384-well plates at ~300 plasmablasts/well and stimulated as in Methods for 1 wk. The data distribution and density of the number of plasmablast wells that were screened per donor is expressed as a violin plot. **(C)** Culture supernatants from plasmablasts plated as in **(B)** were screened for antibody production by ELISA. Wells were scored positively for antibody secretion for ELISA $OD_{370nm} > 0.5$. The frequency of positive wells was calculated per subset, per donor; individual points represent individual donors. Results from systemic sclerosis/interstitial lung disease (black circle, n=6), systemic sclerosis (open circle/X, n=2), or ATD patients (open diamond, n=1) are shown.

stimulation (**Figure 4E**), suggesting both IgM^+ and class-switched $CD27^+$ B cells survive in this culture. IgG^+ and IgM^- IgG^- B cells were observed among cultured $CD27^-$ memory and IgM^- $CD21^{lo}$ B cells as expected (**Figures 4C, G**), however the relatively high proportion of IgM^- $CD21^{lo}$ B cells that expressed IgM at the end of culture suggests class-switched B cells in these subsets may not respond as strongly as IgM^+ $CD21^{lo}$ B cells to this stimulation.

Insulin-Binding ASBCs Are Detected Among Memory B Cell Subsets From Donors at High Risk for Type 1 Diabetes

ASBCs are not always readily detectable in autoimmune individuals. For example, *ex vivo* detection of anti-insulin B cells is challenging in both humans and mice at high risk for type 1 diabetes, despite being seropositive for insulin autoantibody (22, 32). We sought to couple phenotypic information with our ASBC screening pipeline to provide methods to better understand how ASBC functional capacity changes with respect to autoimmune disease progression, or in response to immune therapy using small volumes (2-10mL) of peripheral blood. Whereas $CD27^+$ memory B cells arise through germinal center reactions, $CD27^-$ IgD^- memory B cells (increased in the autoimmune disease, SLE) do not (45, 46). Insulin is a major autoantigen in type 1 diabetes and insulin autoantibodies are one of five islet autoantibodies used by Type 1 Diabetes TrialNet to identify individuals at high risk for type 1 diabetes (3). Donors at risk for type 1 diabetes were identified as in Methods based on donor positivity for insulin autoantibody (IAA) plus at least one other islet autoantibody and PBMCs were flow cytometry sorted to identify IgM^+ and/or IgD^+, IgD^- $CD27^-$ memory, or $CD27^+$ memory B cells and stimulated as in Methods (**Figure 5A**). Wells that contained insulin-binding B cells were identified by ELISA using a secondary antibody confirmed to bind both IgM and IgG to ensure fair comparison across subsets regardless of isotype (**Figure 5B**). An increased frequency of $CD27^-$ and $CD27^+$ memory subset wells contained insulin-binding ASBCs relative to the IgM^+ and/or IgD^+ subset, suggesting insulin-binding B cells are enriched among memory B cells (**Figure 5C**). Thus, these approaches can be used to detect expanded ASBCs within specific B cell subsets.

Jo-1-Binding ASBCs Expand Following *In Vitro* Stimulation

Flow cytometry detection of ASBCs can be challenging due to low frequency of target cells. However, we recently identified a

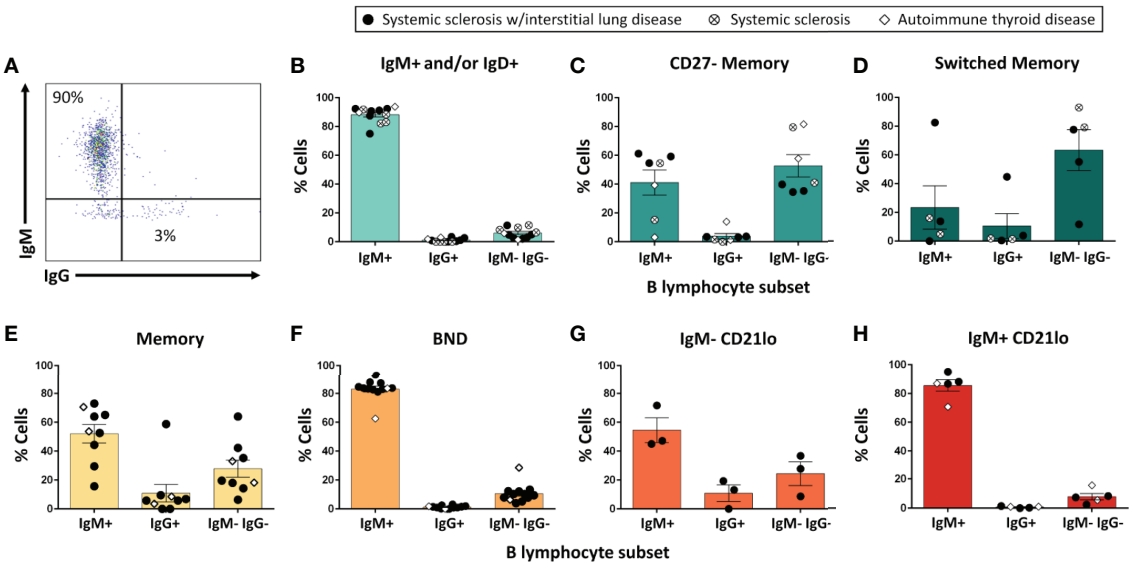

FIGURE 4 | The majority of IgM$^+$ and/or IgD+ B cells do not undergo class-switch to IgG following *in vitro* stimulation. PBMCs were isolated from systemic sclerosis/interstitial lung disease (black circle, n=6 donors; n=35 wells), systemic sclerosis (open circle/X, n=2; n=8 wells), or ATD patients (open diamond, n=1; n=11 wells). Flow cytometry-purified B cell subsets (identified as in **Figure 1**) were plated in 384-well plates at ~300 cells/well and stimulated as in Methods for 1 wk. Flowcytometry was used to measure the frequency of IgM$^+$, IgG$^+$, and IgM$^-$ IgG$^-$ cells among CD19$^+$ live singlet lymphocytes **(A)**. Flow phenotyping inclusion criteria for this analysis was > 95 lymphocyte events and > 35 CD19$^+$ events. Results for **(B)** IgM$^+$ and/or IgD$^+$, **(C)** CD27$^-$ memory, **(D)** CD27$^+$ switched memory, **(E)** memory, **(F)** BND, **(G)** IgM$^-$ CD21lo, and **(H)** IgM$^+$ CD21lo B cell subsets are shown.

readily detectable population of Jo-1-binding B cells in the peripheral blood of Jo-1 autoantibody-positive anti-histidyl tRNA synthetase syndrome patients using flow cytometry staining with labeled autoantigen (36). This created an opportunity to directly examine expansion of ASBCs following our *in vitro* stimulation protocol. The frequency of Jo-1-binding B cells was measured for n=10 Jo-1+ anti-histidyl tRNA synthetase syndrome donors; PBMCs from n=4 of these donors were stimulated for 1 wk as in Methods and cells from individual wells were flow cytometry phenotyped (**Figures 6A, E**) to determine the frequency of Jo-1-binding B cells (ASBCs), as well as total B cells following stimulation. B cells underwent an average 18-fold expansion (**Figure 6B**), whereas Jo-1-binding ASBCs expanded 32-fold on average (**Figure 6C**) following *in vitro* stimulation. These data confirm that Jo-1-binding ASBCs expand at least as well as total B cells *via* this stimulation protocol. PBMCs are divided across 384-well plates, enabling bias for particular wells towards a given antigen specificity. This is illustrated in **Figure 6D**, which shows the relative frequency of ASBCs is increased following *in vitro* stimulation as compared to the *ex vivo* frequency of ASBCs. Additionally, we showed a heterogeneity across IgM and IgG isotypes within Jo-1-binding ASBCs across different donors (**Figure 6F**). A small percentage of Jo-1-binding ASBCs were isotypes other than IgM and IgG (5-30%; IgM$^-$, IgG$^-$).

This approach could thus be applied to expand the original number of ASBCs to support downstream assays for which ASBC numbers are a limiting factor.

DISCUSSION

Specific B cell subsets function differently to coordinate protective or autoimmune responses. Hybridoma technology advancements enable capture of ASBCs as rare as 1 in 20 million cells (29), but this approach does not capture B cell subset phenotypic data. We present data to show that flow cytometry-purified B cell subsets can be stimulated using this published protocol to additionally discern the phenotypic subset of ASBCs. Knowledge about which subset (e.g. memory) ASBCs derive from and how this might change with disease progression could enhance efforts to track ASBCs as sensitive disease biomarkers to predict increasing disease severity or flares, or alternatively as barometers for immunomodulatory therapy success.

Different autoimmune diseases may arise through distinct immune tolerance checkpoint breaches. B cell differentiation into an antibody-secreting cell may be governed differently for different ASBC specificities and across different diseases; for example, whereas Ro60 autoantibodies are typically sustained and Jo-1 autoantibody levels track with IIM disease severity, insulin autoantibodies are frequently transient (25, 47–49). To encompass this potential heterogeneity, B cell subset responses were surveyed from patients with several autoimmune diseases. We find that most of the B cell subsets tested secrete BCR as antibody using this stimulation protocol. Mature naïve, B_{ND}, CD27$^+$ memory, IgM$^-$ IgD$^-$ CD27$^+$ memory, IgM$^-$ IgD$^-$ CD27$^-$ memory B cell subsets isolated from at least 70% of patients responded to this stimulation protocol by secreting antibody. This study was underpowered to uncover specific functional differences

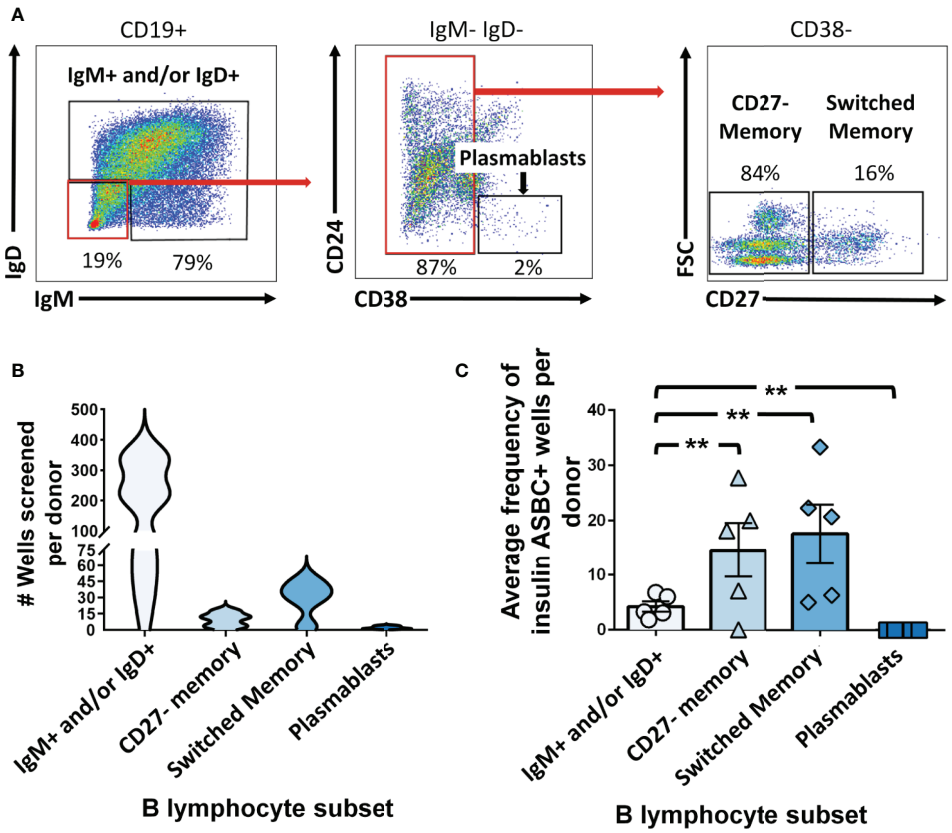

FIGURE 5 | Insulin-binding ASBCs are identified within specific B cell subsets. **(A)** Representative plots show flow cytometry identification of the indicated B cell subsets (gated on $CD19^+$ live singlet lymphocytes). Subsets were defined as follows: IgM^+ and/or IgD^+, $CD27^-$ memory (IgD^+ IgM^+ $CD27^-$ $CD38^-$), and $CD27^+$ switched memory (IgD^- IgM^- $CD27^+$ $CD38^-$). **(B)** Data distribution and density of wells screened per donor are expressed as a violin plot per subset. **(C)** PBMCs were isolated from n=5 participants at high risk for type 1 diabetes [positive for ≥ two islet autoantibodies, one of which was insulin autoantibody (IAA)]; flow cytometry-purified B cell subsets (identified as in **Figure 1**) were plated in 384-well plates at ~300 cells/well and stimulated as in Methods for 1 wk. ELISA was used to measure anti-insulin antibody in culture supernatants to identify wells containing insulin-binding ASBCs (positive wells defined as $O.D._{370nm} \geq 0.85$ which was one standard deviation above the mean and which displayed reduced insulin antibody binding when parallel supernatants were incubated with 100-fold excess soluble insulin competitor). Errors bars shown are SEM per subset. Each data point represents the average % insulin-binding ASBCs identified per donor for each B cell subset. **$p < 0.01$, Mann-Whitney U test.

present among B cells isolated from patients/participants with different autoimmune diseases. Additional studies will be required to uncover autoimmune disease-specific differences in B cell subset responses to this stimulation protocol.

Responses were more variable among IgM^- $CD21^{lo}$ and IgM^+ $CD21^{lo}$ B cell subsets; for each subset, roughly 50% of patients showed a response. Of note, an abnormal $CD19^+$ IgM^- IgD^- $CD21^{lo}$ subset has been identified in systemic sclerosis and anti-histidyl tRNA synthetase syndrome, which expresses many innate immune cell markers (unpublished observations). If these cells are not of the B lineage, that would explain their inability to secrete antibody. Alternatively, if $CD21^{lo}$ B cells have already upregulated a plasmablast/plasma cell transcriptional program, as has been suggested in the setting of infection (43), they may respond less well to stimulation, as plasmablast responses were largely absent with this stimulation protocol. Given the known functional difference identified among the broad category of $CD21^{lo}$ B cells (31, 33, 43), our data highlight the need to test this method in specific autoimmune diseases in which aberrant $CD21^{lo}$ B cell populations have been identified.

The limited antibody secretion detected from plasmablasts following this *in vitro* stimulation points to a need to apply other approaches, such as single-cell BCR sequencing, to examine the antigen-specific plasmablast repertoire. Alternatively, this stimulation protocol could be modified to include factors essential for plasmablast/plasma cell survival and differentiation, such as IL-6, IL-10, IFN-α and APRIL (50, 51). Such modifications would need to be separately tested for their impact on other B cell subsets. Innate stimulation, such as through TLR7 and TLR9, is known to drive activation of autoreactive B cells in systemic lupus erythematosus (52, 53). Studies of murine anti-insulin B cells showed that LPS (TLR4), but not ssDNA (TLR7) or CpG (TLR9) stimulation, overrode immune tolerance checkpoints to drive anti-insulin B cell proliferation (54). The innate stimuli that can drive immune tolerance breach by human anti-insulin B cells have not been investigated. The data presented here confirm insulin and

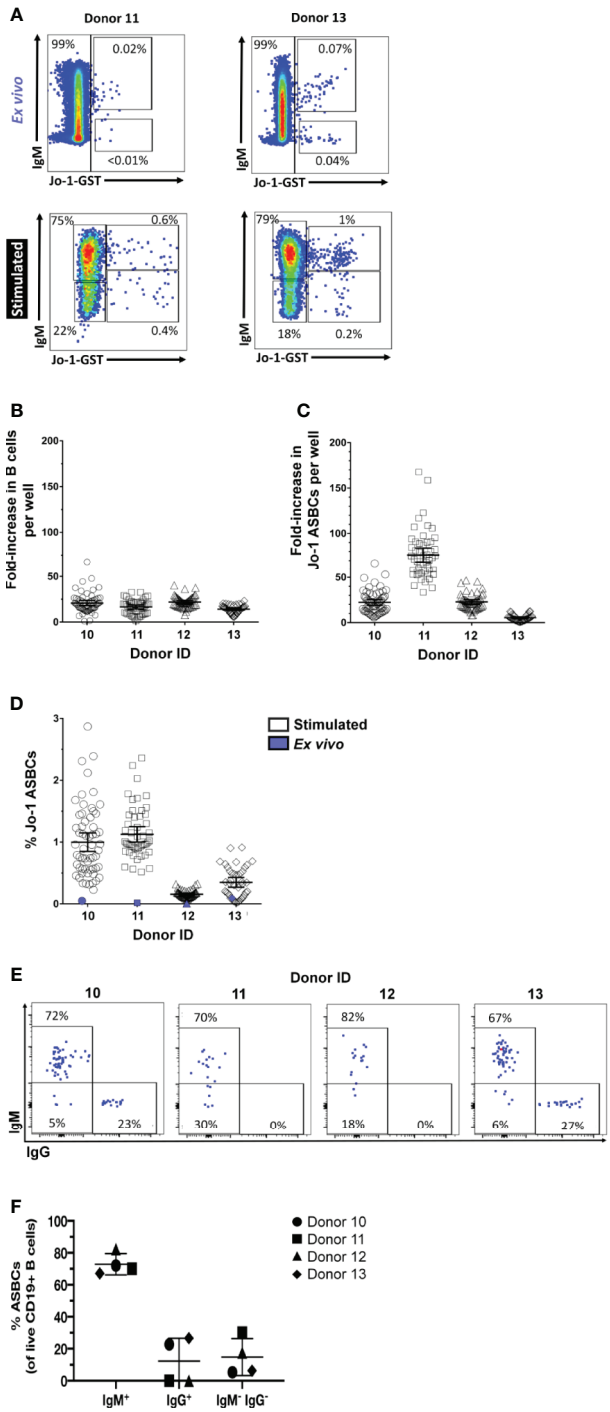

FIGURE 6 | Autoreactive Jo-1-binding ASBCs expand in response to *in vitro* stimulation. PBMCs were isolated from n = 4 Jo-1 anti-histidyl tRNA synthetase syndrome patients, and **(A)** representative plots show flow cytometry identification of total B cells as well as Jo-1-binding ASBCs *ex vivo* and following stimulation *in vitro* for 1 wk as in Methods (gated on $CD19^+$ live singlet lymphocytes). $3.3x10^4$ PBMCs were stimulated per well in 96 well plates as in Methods. An average input total B cell and Jo-1-binding B cell frequency per well was calculated based on *ex vivo* flow phenotyping data. After 1 wk of stimulation, individual wells were harvested and flow cytometry was used to determine output total B cell and Jo-1-binding ASBC frequency per well. Output frequency/input frequency was used to calculate estimated fold expansion for **(B)** total B cells or **(C)** Jo-1-binding ASBCs in each well. Individual wells are plotted. **(D)** The frequency of Jo-1-binding ASBCs *ex vivo* (purple symbol) or following *in vitro* stimulation (open symbols) is shown for each donor; individual wells are plotted. **(E)** Representative plots show flow cytometry identification of Jo-1-binding ASBCs by IgM and IgG isotypes (gated on Jo-1-GST^+ $CD19^+$ live singlet lymphocytes). **(F)** The isotype frequency of Jo-1-binding ASBCs following *in vitro* stimulation is shown for each donor; individual donors are plotted.

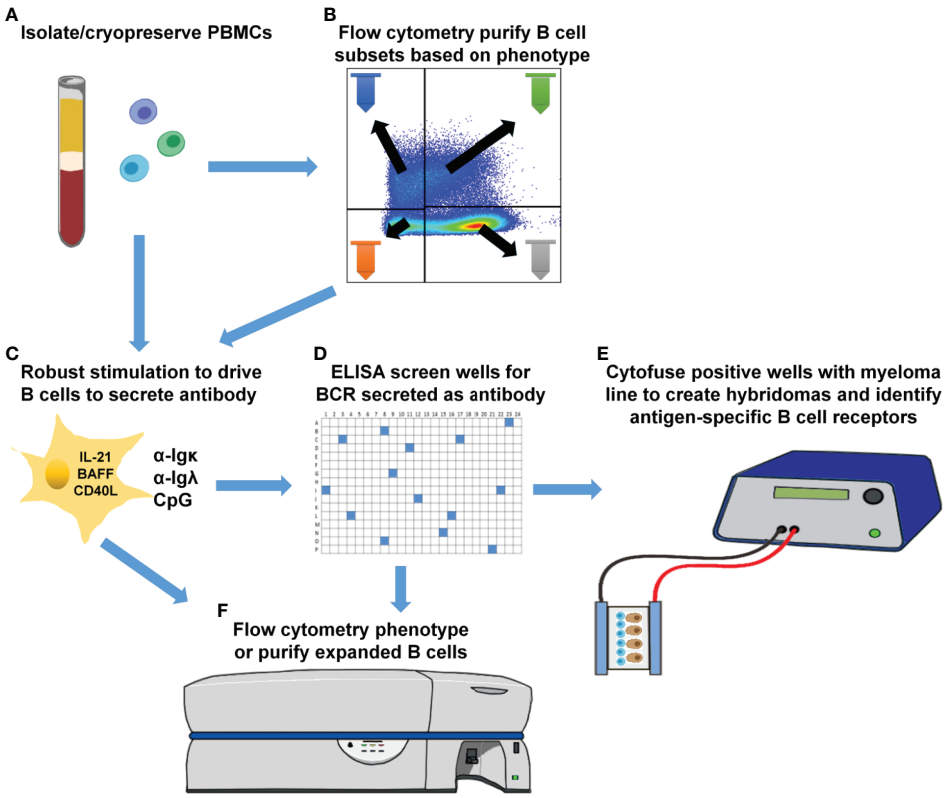

FIGURE 7 | Downstream applications for methods to phenotypically-define, expand, and identify ASBCs. **(A)** Isolate and cryopreserve PBMCs. **(B)** Optionally purify specific B cell subsets using flow cytometry cell sorting. **(C)** Plate total PBMCs (panel **A**) or purified B cell subsets (panel **B**) into 384-well plates and stimulate as in Methods to drive B cell proliferation and differentiation into antibody-secreting cells. **(D)** High-throughput ELISA screening of well supernatants to identify wells containing ASBCs. **(E)** Cytofuse candidate wells to produce human hybridoma lines or **(F)** enrich for ASBCs prior to flow cytometry phenotyping.

Jo-1-binding B cells are captured using this method; we also identify Ro-52 and Ro-60-binding B cells using this method (unpublished observations).

Purified B cells that were IgM^+ or IgD^+ underwent limited class-switching away from the IgM isotype following *in vitro* stimulation, suggesting isotype is largely preserved for non-class-switched cells. Co-expression of multiple IgH transcripts has been noted in memory B cells and is enhanced in patients with Sjögren's syndrome (55). Thus, it is possible that the limited IgG class switching among memory-phenotype B cells may reflect transcriptional programming that occurred *in vivo*, rather than in response to stimulation *in vitro*. IgG^+ B cells were detected among stimulated IgM^-/IgD^- B cell subsets, as expected, but many cells surveyed were negative for both IgM and IgG surface expression. IgM^-/IgG^- cells may be of the IgA isotype, which was not examined in this study. B cells terminally differentiated to the IgE isotype are captured by this stimulation protocol (29), but future studies are warranted to confirm whether IgA^+ B cells can be assessed using this method.

The ease with which ASBCs can be studied depends on repertoire frequency, as well as the sensitivity of the technology employed. Jo-1-binding ASBCs were detected in 50% of Jo1+ anti-histidyl tRNA synthetase syndrome patients surveyed (36), whereas magnetic sorting enrichment of insulin-binding ASBCs was used to overcome their low frequencies in at-risk/type 1 diabetic donors (32). We took advantage of the relatively high frequency of Jo-1-binding B cells *ex vivo* to measure autoreactive ASBC expansion in this culture system. Jo-1-binding ASBCs expanded 32-fold on average, suggesting this approach might be coupled with other downstream assays in which expansion of ASBCs is necessary.

In this study, we identify insulin-binding ASBCs among $CD27^+$ and $CD27^-$ memory subsets in donors at high risk for type 1 diabetes, whereas relatively fewer wells derived from IgM^+ and/or IgD^+ (presumably mature naïve) B cells from the same donors scored positive for the presence of anti-insulin ASBCs. Polyreactive B cells that bind several antigens, including insulin, have been identified in autoimmune donors among recent bone marrow emigrants and mature naïve B cells (56–58). These data suggest that if polyreactive B cells were responsible for the anti-insulin ASBCs identified, they should be skewed away from, not towards class-switched memory subsets. One limitation of this approach is that multiple B cell clones (and thus antibody specificities) are present in each well; this ELISA-based

approach limits accurate assessment of polyreactivity of ASBCs, which are not assayed separately from non-ASBCs present in the same well. Parallel ELISA screening using excess unlabeled antigen competitor is thus the most reliable method for determining antigen specificity, which we applied in this study to identify wells containing anti-insulin ASBCs. Individual B cell receptor binding attributes must be assayed directly to confirm autoantigen specificity; as such, efforts are presently underway in our laboratory to interrogate B cell receptors isolated from ASBCs present in specific B cell subsets that were immortalized as hybridomas. We demonstrate this stimulation protocol can expand ASBCs, thus it may also be amenable to combination with downstream single-cell profiling that can combine BCR repertoire (BCRseq), transcriptional profiling (RNAseq), phenotypic profiling (CITEseq), and/or antigen-reactivity profiling (LIBRAseq) (59, 60). This stimulation protocol produces B cells with sufficient viability that they can be fused to myelomas as hybridoma lines (29). We presume it will also be amenable to combination with these single-cell techniques, but this will require confirmation in future studies. **Figure 7** shows examples of downstream applications that could be coupled to B cell subset purification, stimulation, and high-throughput screening presented in this report, which include the development of human hybridoma cell lines to interrogate B cell receptor sequence and function.

DATA AVAILABILITY STATEMENT

The original contributions presented in the study are included in the article/supplementary material. Further inquiries can be directed to the corresponding author.

ETHICS STATEMENT

The studies involving human participants were reviewed and approved by Vanderbilt Institutional Review Board, Vanderbilt University Medical Center. The patients/participants provided their written informed consent to participate in this study.

AUTHOR CONTRIBUTIONS

BJ, JJ, AS, AC, and RB designed and performed experiments and analyzed resulting data. SS designed experiments and provided critical feedback. DM, LC, and EW recruited donors for these studies. BJ and RB wrote the manuscript. All authors contributed to the article and approved the submitted version.

FUNDING

National Institutes of Health Grants NIH T32AR059039, and K12HD043483, Vanderbilt Institute for Clinical and Translational Research Pilot and Feasibility Grant VR53141 (supported by Vanderbilt NIH/CTSA UL1 RR024975), Vanderbilt NIH/CTSA UL1TR000445, Juvenile Diabetes Research Foundation Strategic Research Agreement 3-SRA-2019-790-S-B, Porter Family Fund for Autoimmunity Research, the Vanderbilt Medical Research Student Research Training Program in Diabetes and Obesity [supported by the Vanderbilt Short Term Research Training Program for Medical Students (NIH grant DK007383), Vanderbilt Research Training in Diabetes and Endocrinology (NIH grant T32DK007061), and the Vanderbilt Diabetes Research and Training Center (NIH grant DK20593)], and the Vanderbilt Human Immunology Discovery Initiative supported this work, along with the Vanderbilt Medical Center Flow Cytometry Shared Resource [supported by Vanderbilt Ingram Cancer Center (P30 CA68485) and the Vanderbilt Digestive Disease Research Center (DK058404)].

ACKNOWLEDGMENTS

We would like to acknowledge the Vanderbilt Medical Center Flow Cytometry Shared Resource for performing flow cytometry sorting.

REFERENCES

1. Steck AK, Johnson K, Barriga KJ, Miao D, Yu L, Hutton JC, et al. Age of Islet Autoantibody Appearance and Mean Levels of Insulin, But Not GAD or IA-2 Autoantibodies, Predict Age of Diagnosis of Type 1 Diabetes: Diabetes Autoimmunity Study in the Young. *Diabetes Care* (2011) 34:1397–9. doi: 10.2337/dc10-2088
2. Yu L, Robles DT, Abiru N, Kaur P, Rewers M, Kelemen K, et al. Early Expression of Antiinsulin Autoantibodies of Humans and the NOD Mouse: Evidence for Early Determination of Subsequent Diabetes. *Proc Natl Acad Sci USA* (2000) 97:1701–6. doi: 10.1073/pnas.040556697
3. Sosenko JM, Skyler JS, Palmer JP, Krischer JP, Yu L, Mahon J, et al. The Prediction of Type 1 Diabetes by Multiple Autoantibody Levels and Their Incorporation Into an Autoantibody Risk Score in Relatives of Type 1 Diabetic Patients. *Diabetes Care* (2013) 36:2615–20. doi: 10.2337/dc13-0425
4. Shiboski CH, Shiboski SC, Seror R, Criswell LA, Labetoulle M, Lietman TM, et al. 2016 American College of Rheumatology/European League Against Rheumatism Classification Criteria for Primary Sjogren's Syndrome: A Consensus and Data-Driven Methodology Involving Three International Patient Cohorts. *Arthritis Rheumatol* (2017) 69:35–45. doi: 10.1002/art.39859
5. Bohan A, Peter JB. Polymyositis and Dermatomyositis (First of Two Parts). *N Engl J Med* (1975) 292:344–7. doi: 10.1056/NEJM197502132920706
6. Bohan A, Peter JB. Polymyositis and Dermatomyositis (Second of Two Parts). *N Engl J Med* (1975) 292:403–7. doi: 10.1056/NEJM197502202920807
7. McHugh NJ, Tansley SL. Autoantibodies in Myositis. *Nat Rev Rheumatol* (2018) 14:290–302. doi: 10.1038/nrrheum.2018.56
8. Elkon K, Casali P. Nature and Functions of Autoantibodies. *Nat Clin Pract Rheumatol* (2008) 4:491–8. doi: 10.1038/ncprheum0895
9. Serreze DV, Fleming SA, Chapman HD, Richard SD, Leiter EH, Tisch RM. B Lymphocytes are Critical Antigen-Presenting Cells for the Initiation of T Cell-Mediated Autoimmune Diabetes in Nonobese Diabetic Mice. *J Immunol* (1998) 161:3912–8.
10. Silveira PA, Johnson E, Chapman HD, Bui T, Tisch RM, Serreze DV. The Preferential Ability of B Lymphocytes to Act as Diabetogenic APC in NOD Mice Depends on Expression of Self-Antigen-Specific Immunoglobulin Receptors. *Eur J Immunol* (2002) 32:3657–66. doi: 10.1002/1521-4141(200212)32:12<3657::AID-IMMU3657>3.0.CO;2-E

11. Noorchashm H, Lieu YK, Noorchashm N, Rostami SY, Greeley SA, Schlachterman A, et al. I-Ag7-mediated Antigen Presentation by B Lymphocytes is Critical in Overcoming a Checkpoint in T Cell Tolerance to Islet Beta Cells of Nonobese Diabetic Mice. *J Immunol* (1999) 163:743–50.
12. Serreze DV, Chapman HD, Varnum DS, Hanson MS, Reifsnyder PC, Richard SD, et al. B Lymphocytes are Essential for the Initiation of T Cell-Mediated Autoimmune Diabetes: Analysis of a New "Speed Congenic" Stock of NOD.Ig Mu Null Mice. *J Exp Med* (1996) 184:2049–53. doi: 10.1084/jem.184.5.2049
13. Marino E, Tan B, Binge L, Mackay CR, Grey ST. B-Cell Cross-Presentation of Autologous Antigen Precipitates Diabetes. *Diabetes* (2012) 61:2893–905. doi: 10.2337/db12-0006
14. Aggarwal R, Oddis CV, Goudeau D, Koontz D, Qi Z, Reed AM, et al. Autoantibody Levels in Myositis Patients Correlate With Clinical Response During B Cell Depletion With Rituximab. *Rheumatol (Oxford)* (2016) 55:991–9. doi: 10.1093/rheumatology/kev444
15. Edwards JC, Szczepanski L, Szechinski J, Filipowicz-Sosnowska A, Emery P, Close DR, et al. Efficacy of B-cell-targeted Therapy With Rituximab in Patients With Rheumatoid Arthritis. *N Engl J Med* (2004) 350:2572–81. doi: 10.1056/NEJMoa032534
16. Smith KG, Jones RB, Burns SM, Jayne DR. Long-Term Comparison of Rituximab Treatment for Refractory Systemic Lupus Erythematosus and Vasculitis: Remission, Relapse, and Re-Treatment. *Arthritis Rheum* (2006) 54:2970–82. doi: 10.1002/art.22046
17. Jordan S, Distler JH, Maurer B, Huscher D, van Laar JM, Allanore Y, et al. Effects and Safety of Rituximab in Systemic Sclerosis: An Analysis From the European Scleroderma Trial and Research (EUSTAR) Group. *Ann Rheum Dis* (2015) 74:1188–94. doi: 10.1136/annrheumdis-2013-204522
18. Franks SE, Getahun A, Hogarth PM, Cambier JC. Targeting B Cells in Treatment of Autoimmunity. *Curr Opin Immunol* (2016) 43:39–45. doi: 10.1016/j.coi.2016.09.003
19. Vital EM, Dass S, Buch MH, Henshaw K, Pease CT, Martin MF, et al. B Cell Biomarkers of Rituximab Responses in Systemic Lupus Erythematosus. *Arthritis Rheum* (2011) 63:3038–47. doi: 10.1002/art.30466
20. Fasano S, Gordon P, Hajji R, Loyo E, Isenberg DA. Rituximab in the Treatment of Inflammatory Myopathies: A Review. *Rheumatol (Oxford)* (2017) 56:26–36. doi: 10.1093/rheumatology/kew146
21. Pescovitz MD, Torgerson TR, Ochs HD, Ocheltree E, McGee P, Krause-Steinrauf H, et al. Effect of Rituximab on Human In Vivo Antibody Immune Responses. *J Allergy Clin Immunol* (2011) 128:1295–302. doi: 10.1016/j.jaci.2011.08.008
22. Henry RA, Kendall PL, Thomas JW. Autoantigen-Specific B Cell Depletion Overcomes Failed Immune Tolerance in Type 1 Diabetes. *Diabetes* (2012) 61:2037–44. doi: 10.2337/db11-1746
23. Manjarrez-Orduno N, Quach TD, Sanz I. B Cells and Immunological Tolerance. *J Invest Dermatol* (2009) 129:278–88. doi: 10.1038/jid.2008.240
24. Meffre E, O'Connor KC. Impaired B-cell Tolerance Checkpoints Promote the Development of Autoimmune Diseases and Pathogenic Autoantibodies. *Immunol Rev* (2019) 292:90–101. doi: 10.1111/imr.12821
25. Lindop R, Arentz G, Bastian I, Whyte AF, Thurgood LA, Chataway TK, et al. Long-Term Ro60 Humoral Autoimmunity in Primary Sjogren's Syndrome is Maintained by Rapid Clonal Turnover. *Clin Immunol* (2013) 148:27–34. doi: 10.1016/j.clim.2013.03.015
26. Kendall PL, Case JB, Sullivan AM, Holderness JS, Wells KS, Liu E, et al. Tolerant Anti-Insulin B Cells are Effective Apcs. *J Immunol* (2013) 190:2519–26. doi: 10.4049/jimmunol.1202104
27. Acevedo-Suarez CA, Hulbert C, Woodward EJ, Thomas JW. Uncoupling of Anergy From Developmental Arrest in Anti-Insulin B Cells Supports the Development of Autoimmune Diabetes. *J Immunol* (2005) 174:827–33. doi: 10.4049/jimmunol.174.2.827
28. Felton JL, Maseda D, Bonami RH, Hulbert C, Thomas JW. Anti-Insulin B Cells Are Poised for Antigen Presentation in Type 1 Diabetes. *J Immunol* (2018) 201:861–73. doi: 10.4049/jimmunol.1701717
29. Wurth MA, Hadadianpour A, Horvath DJ, Daniel J, Bogdan O, Goleniewska K, et al. Human IgE mAbs Define Variability in Commercial Aspergillus Extract Allergen Composition. *JCI Insight* (2018) 3. doi: 10.1172/jci.insight.123387
30. Duty JA, Szodoray P, Zheng NY, Koelsch KA, Zhang Q, Swiatkowski M, et al. Functional Anergy in a Subpopulation of Naive B Cells From Healthy Humans That Express Autoreactive Immunoglobulin Receptors. *J Exp Med* (2009) 206:139–51. doi: 10.1084/jem.20080611
31. Isnardi I, Ng YS, Menard L, Meyers G, Saadoun D, Srdanovic I, et al. Complement Receptor 2/CD21- Human Naive B Cells Contain Mostly Autoreactive Unresponsive Clones. *Blood* (2010) 115:5026–36. doi: 10.1182/blood-2009-09-243071
32. Smith MJ, Packard TA, O'Neill SK, Henry Dunand CJ, Huang M, Fitzgerald-Miller L, et al. Loss of Anergic B Cells in Prediabetic and New-Onset Type 1 Diabetic Patients. *Diabetes* (2015) 64:1703–12. doi: 10.2337/db13-1798
33. Saadoun D, Terrier B, Bannock J, Vazquez T, Massad C, Kang I, et al. Expansion of Autoreactive Unresponsive CD21-/Low B Cells in Sjogren's Syndrome-Associated Lymphoproliferation. *Arthritis Rheum* (2013) 65:1085–96. doi: 10.1002/art.37828
34. Wehr C, Eibel H, Masilamani M, Illges H, Schlesier M, Peter HH, et al. A New CD21low B Cell Population in the Peripheral Blood of Patients With SLE. *Clin Immunol* (2004) 113:161–71. doi: 10.1016/j.clim.2004.05.010
35. Forestier A, Guerrier T, Jouvray M, Giovannelli J, Lefevre G, Sobanski V, et al. Altered B Lymphocyte Homeostasis and Functions in Systemic Sclerosis. *Autoimmun Rev* (2018) 17:244–55. doi: 10.1016/j.autrev.2017.10.015
36. Young-Glazer J, Cisneros A3rd, Wilfong EM, Smith SA, Crofford LJ, Bonami RH. Jo-1 Autoantigen-Specific B Cells are Skewed Towards Distinct Functional B Cell Subsets in Anti-Synthetase Syndrome Patients. *Arthritis Res Ther* (2021) 23:33. doi: 10.1186/s13075-020-02412-8
37. *Type 1 Diabetes Trialnet* (2021). Available at: https://www.trialnet.org/.
38. Harris PA, Taylor R, Thielke R, Payne J, Gonzalez N, Conde JG. Research Electronic Data Capture (Redcap)–a Metadata-Driven Methodology and Workflow Process for Providing Translational Research Informatics Support. *J BioMed Inform* (2009) 42:377–81. doi: 10.1016/j.jbi.2008.08.010
39. Chou C, Verbaro DJ, Tonc E, Holmgren M, Cella M, Colonna M, et al. The Transcription Factor AP4 Mediates Resolution of Chronic Viral Infection Through Amplification of Germinal Center B Cell Responses. *Immunity* (2016) 45:570–82. doi: 10.1016/j.immuni.2016.07.023
40. Nojima T, Haniuda K, Moutai T, Matsudaira M, Mizokawa S, Shiratori I, et al. In-Vitro Derived Germinal Centre B Cells Differentially Generate Memory B or Plasma Cells In Vivo. *Nat Commun* (2011) 2:465. doi: 10.1038/ncomms1475
41. Wilfong EM, Bartkowiak T, Vowell KN, Westlake CS, Irish JM, Kendall PL, et al. High-Dimensional Analysis Reveals Abnormal B Cell Subsets Associated With Specific Changes to Circulating T and Myeloid Cell Populations in Patients With Idiopathic Inflammatory Myopathies. *medRxiv* (2021) 2021:03. doi: 10.1101/2021.03.23.21253635
42. Glauzy S, Boccitto M, Bannock JM, Delmotte FR, Saadoun D, Cacoub P, et al. Accumulation of Antigen-Driven Lymphoproliferations in Complement Receptor 2/CD21(-/Low) B Cells From Patients With Sjogren's Syndrome. *Arthritis Rheumatol* (2018) 70:298–307. doi: 10.1002/art.40352
43. Lau D, Lan LY, Andrews SF, Henry C, Rojas KT, Neu KE, et al. Low CD21 Expression Defines a Population of Recent Germinal Center Graduates Primed for Plasma Cell Differentiation. *Sci Immunol* (2017) 2. doi: 10.1126/sciimmunol.aai8153
44. Townsend MJ, Monroe JG, Chan AC. B-Cell Targeted Therapies in Human Autoimmune Diseases: An Updated Perspective. *Immunol Rev* (2010) 237:264–83. doi: 10.1111/j.1600-065X.2010.00945.x
45. Fecteau JF, Cote G, Neron S. A New Memory CD27-Igg+ B Cell Population in Peripheral Blood Expressing VH Genes With Low Frequency of Somatic Mutation. *J Immunol* (2006) 177:3728–36. doi: 10.4049/jimmunol.177.6.3728
46. Wei C, Anolik J, Cappione A, Zheng B, Pugh-Bernard A, Brooks J, et al. A New Population of Cells Lacking Expression of CD27 Represents a Notable Component of the B Cell Memory Compartment in Systemic Lupus Erythematosus. *J Immunol* (2007) 178:6624–33. doi: 10.4049/jimmunol.178.10.6624
47. Krystufkova O, Hulejova H, Mann HF, Pecha O, Putova I, Ekholm L, et al. Serum Levels of B-cell Activating Factor of the TNF Family (BAFF) Correlate With anti-Jo-1 Autoantibodies Levels and Disease Activity in Patients With anti-Jo-1positive Polymyositis and Dermatomyositis. *Arthritis Res Ther* (2018) 20:158. doi: 10.1186/s13075-018-1650-8
48. Barker JM, Barriga KJ, Yu L, Miao D, Erlich HA, Norris JM, et al. Prediction of Autoantibody Positivity and Progression to Type 1 Diabetes: Diabetes Autoimmunity Study in the Young (Daisy). *J Clin Endocrinol Metab* (2004) 89:3896–902. doi: 10.1210/jc.2003-031887

49. Kulmala P, Rahko J, Savola K, Vahasalo P, Veijola R, Sjoroos M, et al. Stability of Autoantibodies and Their Relation to Genetic and Metabolic Markers of Type I Diabetes in Initially Unaffected Schoolchildren. *Diabetologia* (2000) 43:457–64. doi: 10.1007/s001250051329
50. Cocco M, Stephenson S, Care MA, Newton D, Barnes NA, Davison A, et al. In Vitro Generation of Long-Lived Human Plasma Cells. *J Immunol* (2012) 189:5773–85. doi: 10.4049/jimmunol.1103720
51. Jourdan M, de Boussac H, Viziteu E, Kassambara A, Moreaux J. In Vitro Differentiation Model of Human Normal Memory B Cells to Long-lived Plasma Cells. *J Vis Exp* (2019) (143). doi: 10.3791/58929
52. Soni C, Wong EB, Domeier PP, Khan TN, Satoh T, Akira S, et al. B Cell-Intrinsic TLR7 Signaling is Essential for the Development of Spontaneous Germinal Centers. *J Immunol* (2014) 193:4400–14. doi: 10.4049/jimmunol.1401720
53. Christensen SR, Kashgarian M, Alexopoulou L, Flavell RA, Akira S, Shlomchik MJ. Toll-Like Receptor 9 Controls anti-DNA Autoantibody Production in Murine Lupus. *J Exp Med* (2005) 202:321–31. doi: 10.1084/jem.20050338
54. Williams JM, Bonami RH, Hulbert C, Thomas JW. Reversing Tolerance in Isotype Switch-Competent Anti-Insulin B Lymphocytes. *J Immunol* (2015) 195:853–64. doi: 10.4049/jimmunol.1403114
55. Hansen A, Gosemann M, Pruss A, Reiter K, Ruzickova S, Lipsky PE, et al. Abnormalities in Peripheral B Cell Memory of Patients With Primary Sjogren's Syndrome. *Arthritis Rheum* (2004) 50:1897–908. doi: 10.1002/art.20276
56. Samuels J, Ng YS, Coupillaud C, Paget D, Meffre E. Impaired Early B Cell Tolerance in Patients With Rheumatoid Arthritis. *J Exp Med* (2005) 201:1659–67. doi: 10.1084/jem.20042321
57. Meffre E, Schaefer A, Wardemann H, Wilson P, Davis E, Nussenzweig MC. Surrogate Light Chain Expressing Human Peripheral B Cells Produce Self-Reactive Antibodies. *J Exp Med* (2004) 199:145–50. doi: 10.1084/jem.20031550
58. Wardemann H, Yurasov S, Schaefer A, Young JW, Meffre E, Nussenzweig MC. Predominant Autoantibody Production by Early Human B Cell Precursors. *Science* (2003) 301:1374–7. doi: 10.1126/science.1086907
59. Stoeckius M, Hafemeister C, Stephenson W, Houck-Loomis B, Chattopadhyay PK, Swerdlow H, et al. Simultaneous Epitope and Transcriptome Measurement in Single Cells. *Nat Methods* (2017) 14:865–8. doi: 10.1038/nmeth.4380
60. Setliff I, Shiakolas AR, Pilewski KA, Murji AA, Mapengo RE, Janowska K, et al. High-Throughput Mapping of B Cell Receptor Sequences to Antigen Specificity. *Cell* (2019) 179:1636–46.e15. doi: 10.1016/j.cell.2019.11.003

Conflict of Interest: The authors declare that the research was conducted in the absence of any commercial or financial relationships that could be construed as a potential conflict of interest.

frontiers in Immunology

ORIGINAL RESEARCH
published: 01 June 2021
doi: 10.3389/fimmu.2021.624419

Rap1 Is Essential for B-Cell Locomotion, Germinal Center Formation and Normal B-1a Cell Population

*Sayaka Ishihara[1], Tsuyoshi Sato[1], Risa Sugioka[1], Ryota Miwa[1], Haruka Saito[1], Ryota Sato[2], Hidehiro Fukuyama[2], Akihiko Nakajima[3], Satoshi Sawai[3], Ai Kotani[4] and Koko Katagiri[1]**

[1] Department of Biosciences, School of Science, Kitasato University, Sagamihara, Japan, [2] Laboratory of Lymphocyte Differentiation, RIKEN Center for Integrative Medical Sciences (IMS), Yokohama, Japan, [3] Department of Basic Science, Graduate School of Arts and Sciences, University of Tokyo, Tokyo, Japan, [4] Department of Hematological Malignancy, Institute of Medical Science, Tokai University, Isehara, Japan

OPEN ACCESS

Edited by:
Mark Robin Boothby,
Vanderbilt University Medical Center,
United States

Reviewed by:
Ziv Shulman,
Weizmann Institute of Science, Israel
Rachel Maurie Gerstein,
University of Massachusetts Medical School, United States
James Thomas,
Vanderbilt University Medical Center,
United States

***Correspondence:**
Koko Katagiri
katagirk@kitasato-u.ac.jp

Specialty section:
This article was submitted to B Cell Biology, a section of the journal Frontiers in Immunology

Received: 31 October 2020
Accepted: 17 May 2021
Published: 01 June 2021

Citation:
Ishihara S, Sato T, Sugioka R, Miwa R, Saito H, Sato R, Fukuyama H, Nakajima A, Sawai S, Kotani A and Katagiri K (2021) Rap1 Is Essential for B-Cell Locomotion, Germinal Center Formation and Normal B-1a Cell Population. Front. Immunol. 12:624419. doi: 10.3389/fimmu.2021.624419

Integrin regulation by Rap1 is indispensable for lymphocyte recirculation. In mice having B-cell-specific *Rap1a/b* double knockouts (DKO), the number of B cells in lymph nodes decreased to approximately 4% of that of control mice, and B cells were present in the spleen and blood. Upon the immunization with NP-CGG, DKO mice demonstrated the defective GC formation in the spleen, and the reduced NP-specific antibody production. *In vitro*, Rap1 deficiency impaired the movement of activated B cells along the gradients of chemoattractants known to be critical for their localization in the follicles. Furthermore, B-1a cells were almost completely absent in the peritoneal cavity, spleen and blood of adult DKO mice, and the number of B-cell progenitor/precursor (B-p) were reduced in neonatal and fetal livers. However, DKO B-ps normally proliferated, and differentiated into IgM^+ cells in the presence of IL-7. CXCL12-dependent migration of B-ps on the VCAM-1 was severely impaired by Rap1 deficiency. Immunostaining study of fetal livers revealed defects in the co-localization of DKO B-ps and IL-7-producing stromal cells. This study proposes that the profound effects of Rap1-deficiency on humoral responses and B-1a cell generation may be due to or in part caused by impairments of the chemoattractant-dependent positioning and the contact with stromal cells.

Keywords: B cells, Rap1, germinal center, B-1a, chemotactic factor

INTRODUCTION

The small GTPase Ras-related protein1(Rap1) regulates multiple functions such as cell proliferation, differentiation, and adhesion (1). Integrin-mediated regulation of lymphocyte adhesion and migration is an integral process at each step of immunosurveillance (2, 3). Rap1 is rapidly activated by chemotactic factors, induces the adhesiveness of integrins to their ligands, and

Abbreviations: GC, germinal center; NP-CGG, nitrophenyl-chicken gamma globulin; IL-7, interleukin-7; CXCL12, C-X-C motif chemokine 12; VCAM-1, vascular cell adhesion molecule-1; ALCAM, activated leukocyte cell adhesion molecule.

promotes cell polarity, which in turn facilitates the directional movement of T and B lymphocytes and their interaction with antigen presenting cells (APC) and endothelial cells (4–8). We demonstrated that Rap1-RAPL-Mst1 pathway is essential for LFA-1-dependent arrest of T and B cells on the high endothelial cells (HEV), which is critical step to home into peripheral lymph nodes (4, 9, 10).

Rap1 has 2 isoforms, Rap1a and Rap1b, which share 95% amino acid identity. Previous papers (11, 12) demonstrated the critical role of Rap1b in B-cell trafficking and differentiation using Rap1b null mice, because Rap1b is the dominant isoform of Rap1 in lymphoid cells. Rap1b-deficiency leads to reduce B-cell population in lymph nodes (LNs), and impairs the development of marginal zone B cells (11, 12), but does not affect B-1 cell development (12). There is some difference in the effects of Rap1b-deficiency on early bone marrow development and humoral responses between these papers (11, 12). It is necessary to explore the exact roles of Rap1 in B-cell development using the mice having B-cell specific double knockout of Rap1a and Rap1b.

During immune responses, B cells undergo a series of migratory events and the structure of B-cell follicles dramatically changes to facilitate the efficient production of antibodies. Epstein-Barr virus-induced molecule 2 (EBI2; also known as G-protein- coupled receptor [GPR]183) and its ligand, 7α,25-dihydroxycholesterol(7α,25-OHC), as well as C-C chemokine receptor (CCR)7, chemokine (C-C motif) ligand (CCL)21, C-X-C chemokine receptor (CXCR)5, and chemokine (C-X-C) motif ligand (CXCL)13, direct the migration of activated B cells in the follicles, and guide them to the appropriate microenvironments (13, 14). Finally, activated B cells proliferate and form germinal centers (GCs) in the center of follicles.

GCs require proper compartmentalization for an optimal immune response, and are organized into two major zones: dark and light zones (15). The dark zone contains large centroblasts that are rapidly proliferating and undergoing somatic mutation (15). It has been suggested that these cells give rise to centrocytes in the light zone that compete for antigen binding on follicular dendritic cells (FDCs) and are then dependent on receiving signals from helper T cells to survive and differentiate (16). GC organization depends on sorting of centroblasts by CXCR4 into the dark zone, because centroblasts have high CXCR4 expression and migrate toward the CXCL12, which is more abundant in the dark zone than in the light zone (17). In contrast, CXCR5 is unnecessary for the segregation of dark and light zones (17).

Two main populations of B cells, referred to as B-1 and B-2 B cells, arise from distinct progenitors that emerge at different times during development (18, 19). B-2 cells generate specific antibodies against foreign antigens. B-1 cells are subdivided into B-1a and B-1b cells, of which many B-1a cells constitutively secrete natural immunoglobulin (Ig) M antibodies and participate in the antibody response against T-independent antigens, whereas B-1b cells can undergo clonal expansion and generate specific antibody to various antigens (20–22). B-2 cells are continually replenished from hematopoietic stem cells (HSCs) in the bone marrow. Although still a subject of investigation and some debate, in general terms, B-1b cells are derived both from the fetal liver and adult bone marrow B lymphopoiesis, whereas B-1a cells can differentiate from B-1 progenitors/precursors in the fetal and neonatal livers and are maintained throughout adult life by self-renewal (23–27). Previous paper demonstrates that neonatal spleen is required for B-1a cell maintenance (24). However, as the involvement of Rap1 in B-1 cell differentiation has only been examined using adult bone marrow (BM) cells (28, 29), the precise roles of Rap1 in B-1 cell development remain to be elucidated.

B-1 progenitors arise in the embryo before B-2 progenitors, and decline by young adulthood (19). B-1 cells emerge in a distinct neonatal wave of development within 2 weeks after birth (30). On embryonic day (E) 12.5 in mice, the fetal liver becomes a major B-1 lymphopoietic and myelopoietic organ where progenitors and precursors develop progressively with time until mature B-1 cells appear between E18.5 and E19.5 (birth) (30). Vascular cell adhesion molecule (VCAM)-1-positive stromal cells support hematopoiesis, because very late antigen-4 (VLA-4), the ligand of VCAM-1, is expressed on early hematopoietic cells and plays important roles in hematopoiesis (31). Activated leukocytes cell adhesion molecule (ALCAM) is another marker expressed by these stromal cells. $ALCAM^{high}$ fetal liver cells produce IL-7 and chemokines such as CXCL12, and B-cell progenitor/precursors (B-p) including multiple stages (pro-B to pre-B) of the differentiation are chemoattracted to $ALCAM^{high}$ cells, and proliferate and differentiate when in contact with them (23, 30, 32).

In this study, using mice harboring B-cell specific knockouts of *Rap1a* and *Rap1b* (DKO mice), we demonstrate that Rap1 is not only indispensable in B-cell population of peripheral lymph nodes, but is also a key factor in B-cell locomotion and may be indirectly involved in T cell-dependent antibody production and B-1a cell generation.

MATERIALS AND METHODS

Mice

All animal experiments were carried out in accordance with Regulations for the Care and Use of Laboratory Animals in Kitasato University, and the protocols used in this study were ethically approved by the Institutional Animal Care and Use Committee for Kitasato University. *Rap*$1a^{f/f}$ mice containing floxed exons 2–3 of *Rap1a*, *Rap1b*$^{f/f}$ mice containing floxed exon 1 of *Rap1b* on C57BL/6J background were maintained under specific pathogen–free conditions (33). Those mice were crossed with mb-1-Cre mice, yielding mice with B cell–specific deletion of *Rap1a/b* (33). Fetal liver was obtained from timed mating of WT or DKO mice. The embryonic stage was designed relative to embryonic day (E) 0.5, the day of plug formation. B cells were purified from the spleens of WT and DKO mice using B cell isolation kit, mouse (Miltenyi Biotec).

Antibodies and Reagents

Fluorescence-conjugated anti-mouse CD45 allophycocyanin (APC), phycoerythrin(PE) Cy7, Brilliant Violet™ 421, CD3 FITC, B220 PE, APC, Brilliant Violet™ 711, CD19 FITC, PE, APC, IgM FITC, PECy7, APC, IgD PE, CD21 FITC, CD23 PE, CD24 PECy7, CD43 PE, CD5 PECy7, CD62L FITC, GL-7 APC, CD93 APC, LFA-1 PE, VLA-4 APC, CXCR4 APC, CXCR5 APC, CD35 FITC and IL-7R APC, CD4 FITC, CD8 FITC, CD11b FITC, Gr-1 FITC, NK1.1 FITC, TER119 FITC (e-bioscience or BioLegend), anti-ALCAM (R&D Systems), anti-Rap1 (BD Biosciences), Extracellular signal-regulated kinase (ERK), p-ERK, Akt kinase (Akt), p-Akt, β-actin and peroxidase-conjugated goat anti-mouse IgG (Cell Signaling) were used for flow cytometry, immunostaining and immunoblotting. Mouse CXCL13, CXCL12 and 7α,25-OHC were purchased from R&D Systems and Sigma. NIP-APC (4-hydroxy-3-iodo-5- nitrophenylacetate-allophycocyanin) was generated in-house (34).

Flow Cytometry and Cell Sorting

Immunofluorescence flow cytometry was performed as described previously (9). For mAbs staining, cells were washed with staining buffer (1% FBS in HBSS), resuspended in 50 µl of the same buffer, pre-incubated with purified anti-mouse CD16/32 (Biolegend) for 10 min, and incubated for 30 min at 4°C with each fluorescence-conjugated mAb or isotype control matched with primary antibody. Zombie NIR™ dye (Biolegend) was used to assess live or dead status of cells. The samples were measured using a Gallios flow cytometry or CytoFLEX (Beckman Coulter). Doublets were distinguished from single cells by plotting FSC height vs FCS area. For the isolation of B-ps, fetal liver cells of E15-15.5 mice were immunostained as above, and $CD45^+$ LIN^- ($CD3^-$, $CD4^-$, $CD8^-$, $CD11b^-$, $Gr\text{-}1^-$, $NK1.1^-$, $TER119^-$) $CD19^+B220^+CD93^+$ IgM^-cells were sorted using a Moflo XDP instrument (Beckman Coulter). The purity of the sorted populations constituted more than 95% as determined by a presorted sample run in parallel. Data were analyzed in Kaluza analysis version 2.1 (Beckman Coulter).

Immunoblot Analysis

B cells were lysed in buffer (1% Nonidet P-40, 150 mM NaCl, 25 mM Tris-HCl [pH 7.4], 10% glycerol, 2 mM $MgCl_2$, 1 mM phenylmethylsulfonylfluoride, 1 mM leupeptin, and 0.1 mM aprotinin). Cell lysates were subjected to immunoblotting (35).

Histological Examination

Preparation of frozen sections of the spleens, LNs and fetal livers from WT and DKO mice were performed as described previously (33). Sections were blocked for 1h at 20°C with PBS containing 10% goat serum and 0.1% Triton X-100 and incubated overnight at 4°C with the indicated antibodies. Nuclei were stained with SlowFade Gold antifade reagent with DAPI (invitrogen). Sections were examined on TCS SP8 (Leica).

Homing Assay

Purified B cells were labeled with 1 µM 5, 6-carboxyfluorescein diacetate (CFSE, Invitrogen) and 10 µM (5-(and-6)) ((4-chloromethyl) benzoyl) amino) tetramethylrhodamine) (CMTMR, Invitrogen). An equal number of labeled control and Rap1-deficient B cells ($1–5 \times 10^6$) was injected intravenously into a normal C57BL/6 mouse. After 1 hr, inguinal and axillary LN cells, splenocytes and peripheral blood mononuclear cells were analyzed by flow cytometry (4).

Lymphocyte Migration on ICAM-1 and VCAM-1

Migration on ICAM-1 or VCAM-1 was performed as previously described using a ΔT dish (Bioptechs Inc.) with immobilized recombinant mouse ICAM-1Fc (0.2 µg/ml) or mouse VCAM-1Fc (0.2 µg/ml) (36, 37). A total of 1×10^6 cells were loaded onto the ICAM-1 or VCAM-1-coated dish. Phase-contrast images were obtained using an Olympus Plan Fluor DL 10 ×/0.3NA objective every 15 sec for 10-15 min at 37°C using a heated stage for ΔT dishes (Bioptechs Inc.). The frame-by-frame displacements and lymphocyte velocities were calculated by automatically tracking individual cells using MetaMorph software (Molecular Devices). In each field, 30 randomly selected cells were manually tracked to measure the median velocity and displacement from the starting point.

Chamber Fabrication and Assay for Chemotaxis Towards Chemokine Gradient Using Chambers

A micro-chamber for the chemotaxis assay was fabricated following a photolithography process described earlier (38–40). In brief, polydimethylsiloxane (PDMS; Sylgard 184 Silicone Elastomer Kit, Dow Corning) solution with a mixing ratio of 10:1 (base: curing agent) was poured on a 50 µm-thick SU8-mold (SU-8 3050; MicroChem) and was cured for 1 hr at 75°C. The PDMS sheet was then peeled off from the mold. Inlets for chemoattractant and cell-loading were opened with a 1.5-mm or 2-mm diameter biopsy punch (BP-15F, BP-20F; Kai industries), respectively. The fabricated PDMS was cut using a stainless steel corer (BSV01; TKG) to form a round 10-mm diameter disc. A glass-bottom dish (P35G-0-14-C; MatTek) was treated with O_2 plasma for 10 min to clean the glass surface using a plasma etcher (FA-1; Samco). The dish and the PDMS disc were treated with an O_2 plasma for an additional 5 sec, attached together by hands and immediately heated on a hot plate for 3 min at 80°C for permanent bonding.

Custom-made migration chambers were coated with mouse VCAM-1 Fc (0.2 µg/ml), and overlaid with 30 µl of 200 nM CXCL12 or 200 nM 7α, 25-OHC with 10 µl of 0.4 µg/ml Alexa Fluor 594 dye (Thermo Fisher Scientific). The dimensions of the chamber are 500 µm wide, 50 µm high and 1mm long. B cells from the spleens of WT and DKO mice were cultured with 5µg/ml of anti-IgM $F(ab')_2$ and 2ng/ml of IL-4 for 2 days. 10 µl of activated B-cell suspension ($5x10^5$ cells) was casted into the chamber, and observed at 37°C for 180 min *via* time-lapse video microscopy. Cells were tracked using MetaMorph software.

[^{3}H]Thymidine Incorporation Assay

Purified B cells or B-ps were plated into 96-well plates in triplicates and stimulated with 2 and 10 μg/ml goat-mouse IgM F(ab́)$_2$ or 5 ng/ml IL-7 for 24-48 h. A total of 1mCi [^{3}H] thymidine (GE health Life Science) was added 6h before harvest. Labeled DNA from cells was collected on GSC filters (Whatman), and the radioactivity was measured in a scintillation counter.

Immunization With NP-CGG (Nitrophenyl-Chicken Gamma Globulin)

WT and DKO mice were intrapenitoneally injected with 100-200 μg of NP-CGG emulsified in complete Freund's adjuvant (Sigma-Aldrich). The spleens from day 14 and 20 immunized WT and DKO mice were frozen, and the crystal sections were stained with the indicated antibodies. Sera were diluted and analyzed by ELISA using microplates coated with NP_{30} or NP_{11}-BSA (4-Hydroxy-3- nitrophenylacetyl hapten conjugated to Bovine Serum Albumin) and NP-specific Ig isotypes using Clonotyping System (Southern Biotechnology Association).

Flow-Adhesion Assay

The human endothelial cell line LS12 was introduced with mouse ICAM-1 (40). They were cultured on fibronectin-coated disk and pretreated with TNFα. These disks were incubated with or without CXCL13 and placed in the flow chamber (FCS2; Bioptechs). Shear flow was generated using an automated syringe pump (Harvard Apparatus). B cells were infused in pre-warm RPMI1640 medium were infused into the flow chamber at 2 dyne cm^{-2} at 37°C. Images were recorded at 3.3-ms. Frame-by-frame displacements and velocities of B cell movements were calculated by automatically tracking individual cells using the MetaMorph software (Molecular Devices). Interaction with LS12 cell was categorized depending on dwell time: rolling; transient adhesion (0.5-10s); and stable arrest (more than 10s). the frequencies of cells exhibiting rolling, transient and stable arrest per minute are shown.

Detachment Assay

CXCL13-stimulated B cells adhesion assays were performed using a temperature-controlled parallel flow chamber (FCS2, Bioptechs Inc.), with immobilized recombinant ICAM-1Fc (36). Purified B cells were incubated with 100nM CXCL13 for 10 min and then shear stress was applied for 1min at 2 dyne/cm^2.

Pull-Down Assay

Rap1-GTP was pulled down with a GST (Glutathione S-transferase)-RBD (Ras-binding domain) of Ral guanine nucleotide dissociation inhibitor (GDS) fusion protein. Briefly, 10^7 cells were lysed in ice-cold lysis buffer [1% Triton X-100, 50 mM Tris-HCl (pH7.5), 100 mM $NaCl_2$, 10mM $MgCl_2$, 1mM phenylmethylsulfonyl fluoride, 1mM leupeptin] and incubated for 1h at 4°C with GST-fusion proteins coupled to glutathione agarose beads. The beads were washed three times with lysis buffer and subjected to western blot analysis using anti-Rap1 antibody.

Statistical Analysis

Statistical analysis was performed using two-tailed Student's t-test. *P* values less than 0.05 were considered significant.

RESULTS

The Effects of Rap1 Deficiency on B Cell Distribution

To generate *Rap1a* and *Rap1b* conditional double-knockout (DKO) mice, mice carrying floxed *Rap1a* and *Rap1b* alleles (*Rap1*$^{f/f}$) were mated with mb-1-cre transgenic mice to specifically delete Rap1 in B cells. Western blot analysis confirmed that the Rap1 protein was not expressed in B cells derived from these mice (**Figure 1A**).

The number of B cells in the peripheral lymph nodes (LNs) of DKO mice diminished to less than 4% of that of wild-type (WT) mice, and Rap1-deficient B cells were present in the blood and spleen of DKO mice at 8-10 weeks of age (**Figures 1B, C**). WT and DKO B cells were differentially labeled and adoptively transferred into normal mice. The trafficking of DKO B cells to the peripheral LNs was reduced to less than 1% of that of WT B cells (**Figure 1D**). Marginal zone (MZ) B cells were absent in the spleen of DKO mice (**Figure 1E**). As expected, Rap1-deficient B cells exhibited severe impairment in attachment to immobilized intercellular adhesion molecule (ICAM-1) in the presence of CXCL13 (**Figure S1A** in **Supplementary Material**). The interaction of B cells with the high endothelial venules (HEV) was mediated by L-selectin-mediated rolling and chemokine-triggered integrin-dependent arrest. As previously reported (33), L-selectin-dependent rolling was increased in DKO B cells, but CXCL13 and lymphocyte function-associated antigen (LFA)-1-dependent stable arrest was completely abrogated by Rap1-deficiency (**Figure S1B** in **Supplementary Material**). Although CXCL13-dependent migration of DKO B cells on the ICAM-1 was significantly reduced (**Figure S1C** in **Supplementary Material**), the splenic architecture of B-cell follicles was not disordered in DKO mice (**Figures 1E** and **S1D** in **Supplementary Material**).

In addition to the increase in mature B cells (IgM$^+$CD24^{low} CD23$^+$CD21$^+$ or IgM$^+$IgD^{high}), immature B cells (IgM$^+$CD24^{high} CD23$^-$CD21$^-$ or IgM$^+$IgD^{low}) were also significantly elevated in the blood of DKO mice (**Figure 1C**), suggesting that Rap1-deficiency impairs the retention of immature B cells in the BM, which is mediated by CXCR4 and VLA-4 (41). The proportion of mature B cells (IgM$^+$CD24^{low}CD23$^+$CD21$^+$ or IgM$^+$B220^{high}) in the BM of DKO mice was significantly reduced, compared with that of WT mice (**Figure 1F**). Taken together, these results show that Rap1 plays a central role in B-cell homing into the LNs and BM, differentiation of MZ B cells in the spleen, and retention of immature B cells in the BM.

Rap1 Is Involved in GC Formation Induced by NP-CGG Injection

To determine whether Rap1 is involved in humoral immunity by regulating the GC organization, we immunized the mice

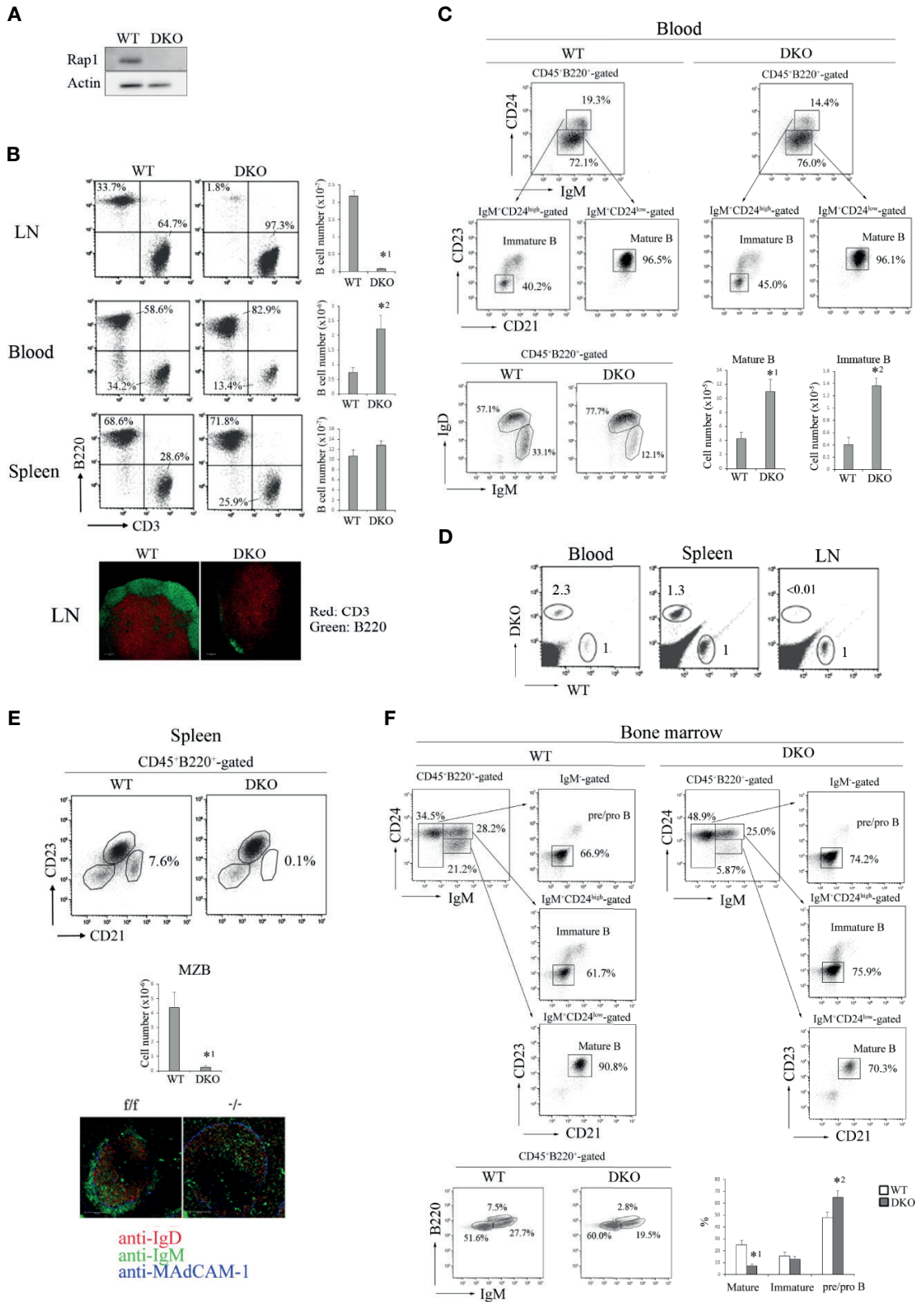

FIGURE 1 | Continued

FIGURE 1 | Effects of Rap1-deficiency on the distribution of B cells. **(A)** Expression of Rap1 in WT and DKO B cells. Actin is a loading control. **(B)** (Top, left) B220 and CD3 profiles of $CD45^+$-gated cells from the LN, blood and spleen of WT and DKO mice. The numbers indicate the percentages of $B220^+$ B cells. (Top, right) T and B cell numbers in the LN, blood and spleen. (n=5-7). The mean values and standard errors are shown. $*^1p < 0.001$, $*^2p<0.008$, compared with WT B cells. (Bottom) The sections of LNs from WT and DKO were stained with anti-CD3 (red) and B220 (green). **(C)** (Top) IgM and CD24 profiles of $CD45^+B220^+$-gated blood cells, CD23 and CD21 profiles of IgM^+CD24^{high} or IgM^+CD24^{low} cells from WT and DKO mice. Numbers indicate the percentages of IgM^+CD24^{low}, IgM^+CD24^{high}, $CD23^-CD21^-$, $CD23^+CD21^+$ B cells. (Bottom, left) IgM and IgD profiles of $CD45^+B220^+$-gated blood cells from WT and DKO mice. Numbers indicate the percentages of IgM^+ IgD^{high} and IgM^+ IgD^{low} B cells. (Bottom, right) The numbers of $IgM^+CD24^{low}CD21^+CD23^+$ mature and $IgM^+CD24^{high}CD21^-CD23^-$ immature B cells in the blood of WT and DKO mice (n=5). The mean values and standard errors are shown. $*^1p < 0.009$, $*^2p < 0.001$ compared with WT cells. **(D)** WT and DKO B cells were labeled with CFSE and CMTMR, respectively, and injected into normal mice. After 1 h, lymphocytes from the LN, spleen and blood of injected mice were analyzed. The numbers indicate the ratios of DKO cells relative to WT cells (adjusted to 1). **(E)** (Top) CD21 and CD23 profiles of $CD45^+B220^+$-gated splenocytes from WT and DKO mice. The numbers indicate the percentages of $CD21^{high}CD23^{low}$ marginal zone B cells to total $CD45^+B220^+$ cells. (Middle) The numbers of $CD21^{high}CD23^{low}$ marginal zone B cells in spleens of WT and DKO mice (n=5). The mean values and standard errors are shown. $*p < 0.005$, compared with WT cells. (Bottom) Spleen sections stained with anti-IgD (red), IgM (green) and MadCAM-1 (blue). Marginal zone B cells (IgM^+ IgD^- cells) were located outside of MadCAM-1^+ cells, and absent in the spleen of DKO mice. **(F)** (Top) IgM and CD24 profiles of $CD45^+B220^+$-gated bone marrow cells, CD23 and CD21 profiles of IgM^-CD24^{high}, IgM^+CD24^{high} and IgM^+CD24^{low} cells from WT and DKO mice. Numbers indicate the percentages of IgM^-, IgM^+CD24^{high}, IgM^+CD24^{low}, $CD23^-CD21^-$, $CD23^+CD21^+$ B cells. (Bottom, left) IgM and B220 profiles of $CD45^+B220^+$-gated bone marrow cells from WT and DKO mice. Numbers indicate the percentages of IgM^-B220^{low}, IgM^+B220^{low} and IgM^+B220^{high} B cells. (Bottom, right) The numbers of $IgM^+CD24^{low}CD21^+CD23^+$ mature B cells, $IgM^+CD24^{high}CD21^-CD23^-$ immature B cells and $IgM^-CD21^-CD23^-$ pre/pro B cells in the bone marrow of WT and DKO mice (n=6). The mean values and standard errors are shown. $*^1p < 0.002$, $*^2p < 0.03$ compared with WT cells.

intraperitoneally with NP-CGG, and analyzed splenic GCs using immunostaining and flow cytometry. The GC cells demonstrated a segmented distribution and the proportion of GL-7^+ NIP^+ GC cells was significantly reduced in the spleen of injected DKO mice (**Figures 2A, B**). NP-specific antibody titers were determined by enzyme-linked immunosorbent assay (ELISA) using 96-well plates coated with NP_{11} or NP_{30}-bovine serum antigen (BSA). Both high- and low- affinity antibodies bound to NP_{30}-BSA, whereas only high-affinity antibodies bound to NP_{11}-BSA. As shown in **Figure 2C**, injected DKO mice produced significantly lower amounts of both NP_{11}- and NP_{30}-specific IgM and IgG, compared to those of WT mice. These data indicate that Rap1 is required for the generation of GC cells.

GCs have two distinct zones, namely the dark and light zones, which are associated with important functional differences. We visualized the dark and light zones of GCs in the WT and DKO spleens by immunostaining. $CD35^+$ FDCs were enriched in the light zone, and $GL7^+$ GC cells accumulated densely in the dark zone of WT spleens (**Figure 2D**). However, $CD35^+$ FDCs did not integrate at the distal pole of the light zone, and $GL7^+$ GC cells scattered throughout the dark zone of DKO spleens (**Figure 2D**), suggesting that GC organization is also Rap1-dependent.

The proliferative response of Rap1-deficient B cells to anti-IgM $F(ab')_2$ was similar to that of WT B cells (**Figure 3A**). In addition, there were no differences in B cell antigen receptor (BCR)-mediated phosphorylation of ERK and Akt between WT and DKO B cells (**Figure 3A**). Therefore, the reduction in the number of antigen-specific GL-7^+ GC cells in injected DKO mice was not due to the impaired BCR-mediated early signaling in response to antigens.

EBI2 and 7α,25-OHC were reported to play critical roles in positioning of antigen-activated B cells within lymphoid follicles, which is important for the initial burst of B cell proliferation and GC commitment (13, 14). Since chemokines activate Rap1 through Gi-protein coupled receptors (GPCRs) in T and B lymphocytes (36, 37, 40), we examined whether 7α,25-OHC activated Rap1 in activated B cells. As shown in **Figure 3B**, 7α,25-OHC continuously activated Rap1 during 5min from 15 sec in the activated B cells. We examined the effects of Rap1 on the locomotion of activated B cells along a 7α,25-OHC gradient. The locomotion of Rap1-deficient B cells on the VCAM-1 along the 7α,25-OHC gradient was significantly decreased (**Figure 3C**).

Previous papers have reported that the segregation of light and dark zones depends on the sorting of centroblasts by CXCR4 and CXCL12 into the dark zone (17). We examined the effects of Rap1 deficiency on the directed movement of activated B cells which sense the CXCL12 gradient. As shown in **Figure 3D**, the locomotion of activated Rap1-deficient B cells on the VCAM-1 along a CXCL12-gradient was significantly diminished, compared to that of activated WT B cells. There was no difference in the expression of CXCR4 and VLA-4 between WT and Rap1-deficient activated B cells (**Figure 3E**).

These data indicate that Rap1 is important for the GC formation and involved in the positioning of activated B cells within the follicular microenvironment.

Impaired B Cell Development in the Neonatal Spleen and Liver and Fetal Liver of DKO Mice

Both B-1a ($B220^{low}CD19^{high}IgM^+CD43^+CD5^+$) and B-1b ($B220^{low}CD19^{high}IgM^+CD43^+CD5^-$) cells were almost absent in the peritoneal cavity of adult DKO mice (8-12 weeks of age) (**Figure 4A**). Although B-1b cells were present in the spleen and blood of adult DKO mice, B-1a cells were significantly decreased there (**Figures 4B, C**). These data indicated that B-1a cells were not only reduced in the peritoneal cavity, but also in the blood and spleen of DKO mice.

Since most B-1 cells are appeared at the neonatal stage (23), we examined B-1 cell development in neonatal spleens and livers. B-1a cells were clearly detected at day 10 after birth in the neonatal spleen of WT mice, but the number of B-1a cells in the neonatal spleen of 10-day-old DKO mice was only a one-tenth of that of WT mice (**Figure 5A**).

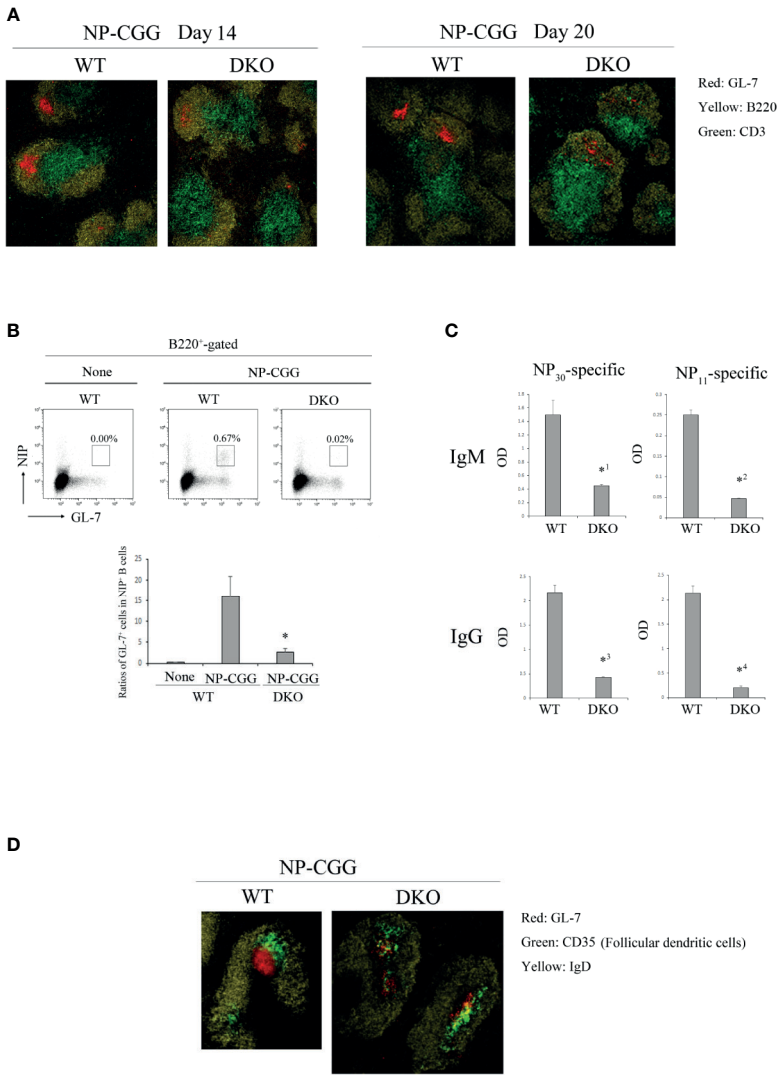

FIGURE 2 | Decreased humoral response to NP-CGG in DKO mice. **(A)** Spleen sections of WT and DKO mice injected with NP-CGG (day14 and 20) were stained with anti-GL-7 (red), anti-B220 (yellow) and anti-CD3 (green). **(B)** (Top) Antigen-specific GC B cells ($B220^+$, NIP^+, $GL\text{-}7^+$) in the spleens of WT and DKO mice uninjected or injected with NP-CGG were analyzed by flow cytometry. The numbers show the percentages of $GL\text{-}7^+$ NIP^+ cells in B cells. (Bottom) The percentages of $GL\text{-}7^+$ cells in NIP^+ B cells from the spleens of WT and DKO mice are shown (n=3). The mean values and standard errors are shown. *$p < 0.02$, compared with WT mice. **(C)** Anti-NP IgM and IgG titers in sera of WT and DKO mice injected with NP-CGG were measured by ELISA. NP_{30} and NP_{11} as hapten antigens were used for detecting low- and high-affinity anti-NP antibodies, respectively in triplicate. The mean values and standard errors are shown. $^{*1}p < 0.009$, $^{*2}p < 0.001$, $^{*3}p < 0.001$, $^{*4}p < 0.001$, compared with WT mice. **(D)** Spleen sections of WT and DKO mice injected with NP-CGG (day 20) were stained with anti-GL-7 (red), anti-IgD (yellow) and anti-CD35 (green).

There are substantial controversies about precise progenitors of B-1 cells and ontogenetic relationships between cells designated (25, 42–44) as B-1 progenitors. $B220^+CD43^+$ cells in fetal liver (42), which may overlap with $CD19^+B220^+CD93^+$ cells, and $CD19^+B220^+CD93^+$ IgM^+ transitional B cells (TrB) in neonatal spleen (23, 25) were reported to include the progenitor/precursors having the ability to differentiate into B-1 cells. Notwithstanding some disagreement, here we will refer to these reported phenotypes as those of B-ps and TrB. We examined their numbers and proportions in the livers of 1-, 5-, and 10-day-old neonatal DKO mice. B-ps ($CD45^+LIN^-CD19^+B220^+CD93^+IgM^-$) were less than 20% of those of the livers of neonatal WT mice (**Figure 5B**). The proportion of IgM^+CD93^+ transitional B cells was also significantly decreased in the neonatal liver of 1-day-old DKO mice (**Figure 5B**). IgM^+CD93^- B cells which demonstrated higher expression of B220 than that of $IgM^{-/+}$ $CD93^+$ B cells appeared in the liver of 10-day-old mice, and might be mature B cells derived from the bone marrow in DKO mice (**Figure 5B**).

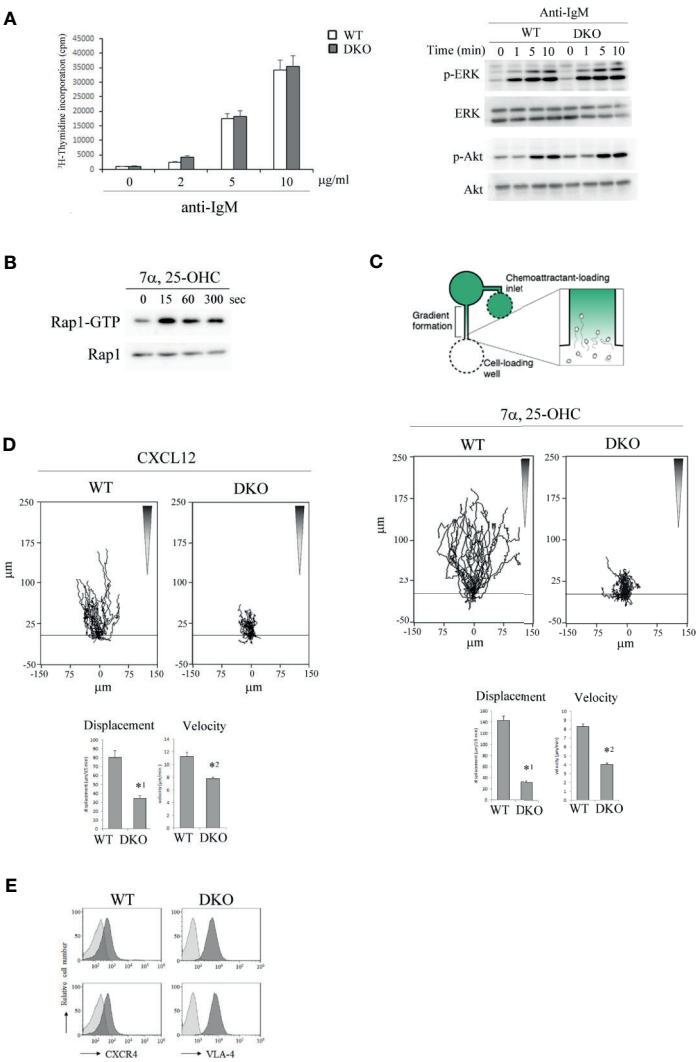

FIGURE 3 | Rap1-deficiency causes defective locomotion of activated B cells along chemotactic factors. **(A)** (Left) [^{3}H]-thymidine uptake by B cells. Primary B cells from the spleens of WT and DKO mice were unstimulated or stimulated with antigen receptor ligation by anti-IgM F(ab')$_2$ at the indicated concentrations. [^{3}H]-thymidine uptake was measured 48 hr after the stimulation in triplicate. The mean values and standard errors are shown. (Right) Phosphorylated and total ERK and Akt in stimulated WT and DKO B cells with 5μg/ml of anti-IgM F(ab')$_2$ at the indicated times are shown. **(B)** WT B cells which were cultured in the presence of anti-IgM F(ab')$_2$ and IL-4 for 2 days were stimulated with 200nM 7α,25-dihydrixycholesterol (7α,25-OHC) as indicated times. Cell lysates were pulled down with GST-Ral-GDS- RBD and immunoblotted with an anti-Rap1 antibody. **(C)** (Top) The experimental set up of scheme. B cells from the spleens of WT and DKO mice were stimulated with anti-IgM F(ab')$_2$ and IL-4 for 2 days. Time lapse sequences of those activated B cells migrating toward the source of 7α,25-OHC were recorded. (Middle) Representative tracks of the activated WT and DKO B cells on the VCAM-1 in response to 7α,25-OHC gradient are shown. Each line represents a single cell track. (Bottom) Displacement and velocity of the activated WT and DKO B cells (n=30). The mean values and standard errors are shown. $^{*1}p < 0.001$, $^{*2}p < 0.001$, compared with WT cells. **(D)** (Top) Representative tracks of the activated WT and DKO B cells on the VCAM-1 in response to CXCL12 gradient are shown. Each line represents a single cell track. (Bottom) Displacement and velocity of the activated WT and DKO B cells (n=30). The mean values and standard errors are shown. $^{*1}p < 0.001$, $^{*2}p < 0.001$, compared with WT cells. **(E)** The expression of CXCR4 and VLA-4 on the activated WT and DKO B cells.

Subsequently, we examined the number of B-ps in E15.5 fetal livers. As shown in **Figure 5C**, the number of B-ps in the livers of E15.5 fetal DKO mice was decreased by more than 40% of that of fetal WT mice. These data indicate that Rap1 is necessary for survival, proliferation or differentiation of B-ps in neonatal and fetal livers.

Rap1 Is Important for the Contact of B-ps With ALCAM^{high} Stromal Cells *via* CXCL12- and VLA-4/VCAM-1-Dependent Migration

B-cell development in the fetal liver is supported by IL-7 (31). B-ps (CD45$^+$LIN$^-$ CD19$^+$B220$^+$CD93$^+$IgM$^-$) were purified from fetal livers of E15-15.5 WT and DKO mice by cell sorting (**Figure S2A**

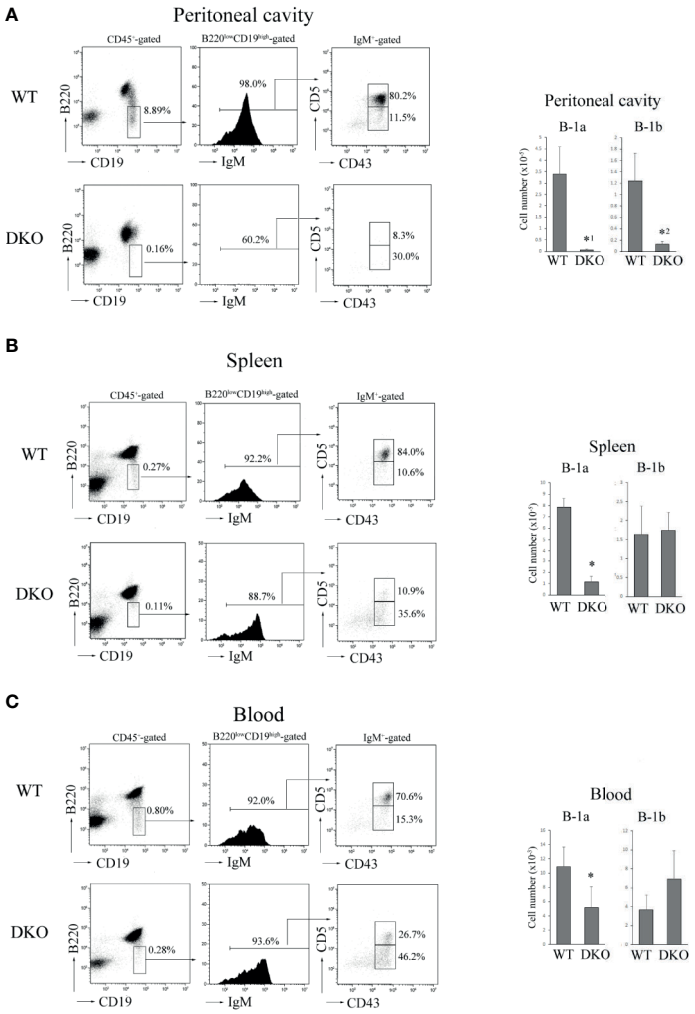

FIGURE 4 | Severe reduction of B-1a cells in the peritoneal cavity, spleen and blood of DKO mice. **(A)** (Left) B220 and CD19 profiles of $CD45^+$-gated cells (left), IgM profiles of $B220^{low}CD19^{high}$ -gated cells (center) and CD5 and CD43 profiles of IgM^+-gated cells (right) from the peritoneal cavity of adult WT or DKO mice. The numbers indicate the percentages of $B220^{low}$ $CD19^{high}$ cells, IgM^+ cells and $CD5^+CD43^+$ (B-1a) or $CD5^-CD43^+$ (B-1b) cells. (Right) The numbers of B-1a and B-1b cells from the peritoneal cavities of WT and DKO mice. The mean values and standard errors are shown (n=7). $^{*1}p < 0.02$, $^{*2}p < 0.03$, compared with WT cells. **(B)** (Left) B220 and CD19 profiles of $CD45^+$-gated cells (left), IgM profiles of $B220^{low}CD19^{high}$ -gated cells (center) and CD5 and CD43 profiles of IgM^+-gated cells (right) from the spleens of adult WT or DKO mice. The numbers indicate the percentages of $B220^{low}$ $CD19^{high}$ cells, IgM^+ cells and $CD5^+CD43^+$ (B-1a) or $CD5^-CD43^+$ (B-1b) cells. (Right) The numbers of B-1a and B-1b cells from the spleens of WT and DKO mice. The mean values and standard errors are shown (n=7). $^*p < 0.02$, compared with WT cells. **(C)** (Left) B220 and CD19 profiles of $CD45^+$-gated cells (left), IgM profiles of $B220^{low}CD19^{high}$ -gated cells (center) and CD5 and CD43 profiles of IgM^+-gated cells (right) from the blood of adult WT or DKO mice. The numbers indicate the percentages of $B220^{low}$ $CD19^{high}$ cells, IgM^+ cells and $CD5^+CD43^+$ (B-1a) or $CD5^-CD43^+$ (B-1b) cells. (Right) The numbers of B-1a and B-1b cells from the blood of WT and DKO mice. The mean values and standard errors are shown (n=5). $^*p < 0.02$, compared with WT cells.

in **Supplementary Material**) and cultured in the presence of IL-7. As shown in **Figure 6A**, the proliferative response of Rap1-deficient B-ps to IL-7 was similar to that of WT B-ps. The frequency of differentiation of Rap1-deficient B-ps into transitional B cells ($B220^+CD19^+CD93^+IgM^+$) was also similar to that of WT B-ps (**Figure 6A**). In addition, there was no difference in the expression of the IL-7 receptor between WT and DKO B-ps (**Figure S2B** in **Supplementary Material**). These data indicate that Rap1 is not involved in IL-7-dependent proliferation and differentiation of B-ps.

We explored the effects of Rap1 on VLA-4/VCAM-1-dependent migration of B-ps in the presence or absence of CXCL12. As shown in **Figure 6B**, WT B-ps, but not Rap1-deficient B-ps, actively migrated on the VCAM-1-coated plate. In particular, the displacement of Rap1-deficient B-ps was markedly impaired regardless of CXCL12. The expression of CXCR4 and VLA-4 in DKO B-ps was similar to those of WT B-ps (**Figure S2C** in **Supplementary Material**). These results indicated that the locomotion of B-ps in the fetal liver was Rap1-dependent.

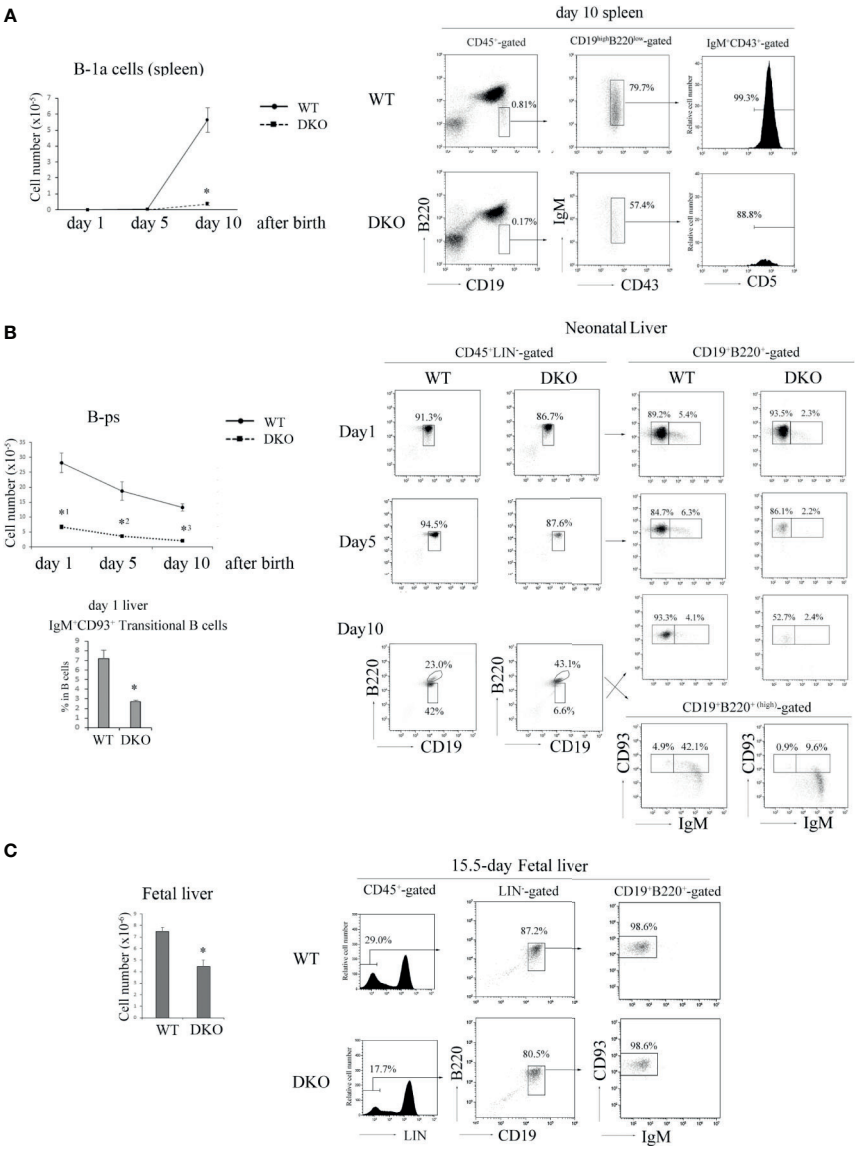

FIGURE 5 | Impaired B cell development in the neonate and fetus periods of DKO mice. **(A)** (Left) The number of B-1a ($B220^{low}$ $CD19^{high}IgM^+CD43^+CD5^+$) cells in day 1, 5 and 10 neonatal spleens of WT and DKO mice (n=5-15). *$p < 0.001$, compared with WT mice. (Right) B220 and CD19 profiles of $CD45^+$-gated cells (left), IgM and CD43 profiles of $B220^{low}CD19^{high}$-gated cells (center) and CD5 profiles of IgM^+CD43^+-gated cells (right) from day 10 neonatal spleens of WT and DKO mice. The numbers indicate the percentages of $B220^{low}$ $CD19^{high}$ cells, IgM^+CD43^+ cells and $CD5^+$ cells. **(B)** (Left upper) The number of B-ps ($CD45^+LIN^-CD19^+$ $B220^+CD93^+IgM^-$) in day 1, 5 and 10 neonatal livers of WT and DKO mice (n=5). *1$p < 0.001$, *2$p < 0.003$, *3$p<0.001$, compared with WT mice. (Left lower) Ratios of transitional B cells ($CD45^+CD19^+B220^+IgM^+$ $CD93^+$) in day 1 neonatal livers of WT and DKO mice. *$p < 0.008$, compared with WT mice. (Right) B220 and CD19 profiles of $CD45^+$ LIN^-gated cells (left), CD93 and IgM profiles of $CD19^+B220^+$ or $CD19^+B220^{+(high)}$ -gated cells from the livers of day 1, 5 and 10 neonatal WT and DKO mice (right). The numbers indicate the percentages of $CD19^+B220^+$, $CD19^+B220^{+(high)}$, IgM^- $CD93^+$ or IgM^+ $CD93^+$ B cells. **(C)** (Left) The number of B-ps in fetal livers of WT and DKO mice (n=7). *$p < 0.001$, compared with WT mice. (Right) LIN (CD3, CD4, CD8, CD11b, Gr-1, NK1.1, TER119) profiles of $CD45^+$-gated cells (left), B220 and CD19 profiles of LIN^-gated cells (center), CD93 and IgM profiles of $CD19^+B220^+$-gated cells (right) in fetal livers of WT and DKO mice. The numbers indicate the percentages of LIN^- cells, $CD19^+$ $B220^+$ cells and $CD93^+IgM^-$ cells.

$ALCAM^+$ stromal cells, which express VCAM-1 and produce CXCL12, chemoattract B-ps (31). B-ps survive and proliferate when in contact with $ALCAM^+$ stromal cells in the fetal liver (31). By immunostaining of fetal livers, we examined the contacts between B-ps and $ALCAM^+$ stromal cells. As shown in **Figures 6C** and **S2D** in **Supplementary Material**, the proportion of B-ps that demonstrated 'contact' with $ALCAM^+$ stromal cells was significantly lower in the livers of fetal DKO mice than those of fetal WT mice.

These results suggest that the reduction in the number of B-ps might be caused by the impairments in their interaction with IL-7-producing stromal cells in the fetal liver of DKO mice.

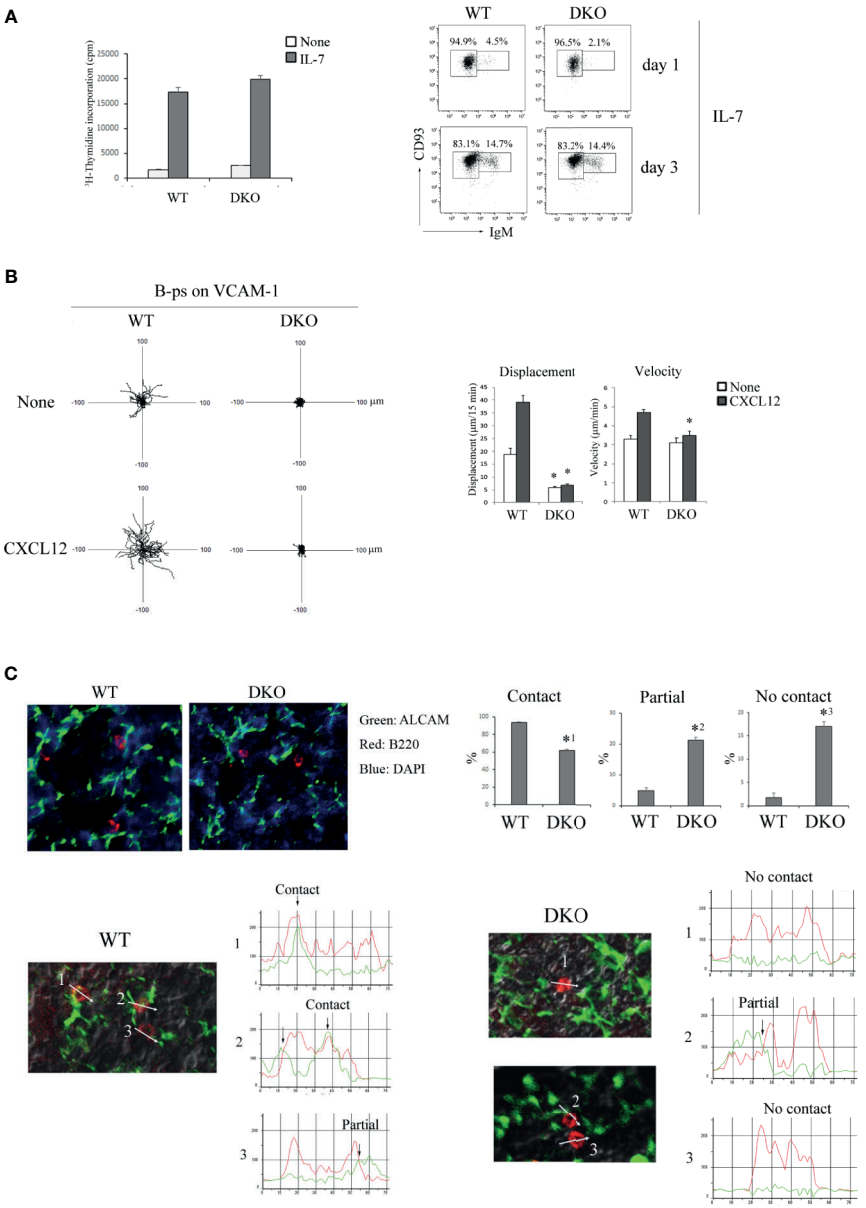

FIGURE 6 | Migration of B-ps on the VCAM-1 is dependent on Rap1. **(A)** (Left) [^{3}H]-thymidine uptake by B-ps (CD45$^+$LIN$^-$ CD19$^+$B220$^+$CD93$^+$IgM$^-$). B-ps from the fetal livers of WT and DKO mice were cultured in the absence or presence of IL-7. [^{3}H]-thymidine uptake was measured 2 days after the stimulation. The mean values and standard errors are shown. (Right) CD93 and IgM profiles of B-ps which were cultured with IL-7 for 1 and 3 days. The numbers indicate the percentages of IgM$^-$ CD93$^+$ B-ps or IgM$^+$ CD93$^+$ transitional B cells. **(B)** (Left) The tracks of WT and DKO B-ps on the VCAM-1 in the absence or presence of CXCL12 are shown. Each line represents a single cell track. (Right) Displacement and velocity of WT and DKO B-ps were measured on the VCAM-1 with or without CXCL12 (n=30). *$p < 0.001$, compared with WT B-ps. **(C)** (Top left) Fetal liver sections of WT and DKO mice were stained with anti-ALCAM (green), anti-B220 (red) and DAPI (blue). (Top right) Proportions of B-p showing contact, partial contact and no contact between B-ps and ALCAM$^+$ stromal cells (n=30). *$^1p < 0.003$, *$^2p < 0.007$, *$^3p < 0.004$, compared with WT B-ps. (Bottom) Line profiles of B220 and ALCAM intensities are generated along the direction of the arrow. The case where B220 and ALCAM overlapped in the point of more than 80% of each peak intensity, is categorized to 'contact'; the case where B220 and ALCAM overlapped in the point of more than 30% of each peak intensity, is categorized to 'partial'; the case where B220 and ALCAM overlapped in the point of less than 30% of each peak intensity, is categorized to 'no contact'.

DISCUSSION

We propose from the data presented that the absence of Rap1-deficient B cells in LN occurs as a result of defective homing or retention, leading to localization of B cells in the blood and spleen, which were consistent with the previous papers (11, 12). In contrast, B-1a cells are markedly reduced even in the spleen and blood of adult DKO mice, and the number of B-ps was

diminished in neonatal and fetal livers. Although Rap1 was reported to be directly involved in intracellular signaling to induce B-1 development using adult BM cells (28, 29), there were no defects in the proliferation and differentiation of Rap1-deficient B-ps from fetal liver in response to IL-7 *in vitro*, indicating that Rap1 is dispensable for IL-7-dependent development of B-ps. On the other hand, Rap1-deficient B-ps barely migrated on the VCAM-1 in the presence of CXCL12. Previous papers have reported that ALCAM^{high} non-hematopoietic cells were found to express VCAM-1 and support hematopoiesis by producing chemokines such as CXCL12 and cytokines, in particular, IL-7 (30–32). The contacts of B-ps with IL-7-producing stromal cells were impaired in the fetal liver of DKO mice. Defective CXCL12-dependent positioning of Rap1-deficient B-ps might have decreased their encounters and interaction with IL-7-producing stromal cells in the fetal liver. It is unproven but here is why we interpret the findings as suggesting a causal relationship between defective locomotion and reduced number of B-ps in fetal liver of DKO mice.

On the other hand, B-1b cells were absent in the peritoneal cavity, but present in the blood and spleen of adult DKO mice. These data indicate that Rap1 is necessary for the positioning of B-1b cells into the peritoneal cavity, but might be dispensable for differentiation of B-1b cells by B-cell lymphopoiesis in the bone marrow.

Previous paper (11) demonstrated that lack of Rap1b reduced the number of pro/pre-B cells and immature B cell in bone marrow. In another previous paper (12) and this study, the number of pro/pre-B cells was slightly, but not significantly reduced in bone marrow. The numbers of pro/pre-B cells were varied between individuals because Rap1-deficiency possibly might affect the differentiation of pre-B cells to immature B cells. Rap1a null mice did not show any obvious defects in the differentiation and maturation of lymphoid cells (45, 46). Taken together, Rap1b might be involved in maximal B cell development in bone marrow. Furthermore, bone marrow-derived Rap1b-deficient pro/pre-B cells normally proliferated in the presence of IL-7, but their adhesion to stromal cell line was reduced compared with WT cells (11), suggesting that Rap1b might play important roles in the interaction of pro/pre-B cells with IL-7-producing stromal cells in bone marrow. As previously reported (43), fetal pro-B cells mainly differentiated into B-1 cells, but the adult pro-B cells mainly differentiated into B-2 cells. Rap1 might be more indispensable for the interaction of B-ps with stromal cells in fetal liver than in adult bone marrow, because the steady-state of B-1a cells was severely impaired by Rap1-deficiency.

The recirculating mature B cells in bone marrow were not reduced in Rap1b null mice (11, 12), while the percentages of mature B cells in bone marrow of DKO mice were reduced to approximately one-fourth of WT mice (**Figure 1F**), suggesting that Rap1a and Rap1b have redundant roles in the repopulation of mature B cells in bone marrow. In contrast to DKO mice, B-1a and b cells normally exited in the peritoneal cavity of Rap1b null mice (12). Rap1a null mice showed normal serum level of IgM (45). These data suggest that Rap1a and Rap1b have redundant roles in B-1 development and positioning in the peritoneal cavity.

In this study, we revealed that the development of GCs in B-cell follicles during T cell-mediated immune responses was Rap1-dependent. Upon encountering antigens, activated B cells undergo multiple migratory steps, which are dependent on chemoattractants such as 7α,25-OHC and CCL21, that are expressed in distinct stromal cells (13, 14, 47). The upregulation of EBI2 and CCR7 expression on antigen-activated B cells results in their movement towards outer follicular regions and the T-cell zone to seek antigens and the help of T cells. Since antigen-activated B cells maintain CXCR5 expression, subsequent down-regulation of EBI2 and CCR7 expression induces their migration towards the central FDC-dense areas where they proliferate and form GCs (13, 47). We found that Rap1-deficiency reduced the directional locomotion of the activated B cells along the gradient of 7α,25-OHC *in vitro*, which may partly delay their proliferative responses to antigens and the formation of GCs. In addition, the movement of Rap1-deficient B-cell blasts on VCAM-1 along a CXCL12 gradient was also impaired. In the GCs, CXCL12 is expressed in more abundantly in the dark zone than in the light zone, and is required for the segregation of the dark and light zones (15, 17). Rap1 might possibly influence the locomotion of CXCR4-expressing centroblast to the dark zones.

BCR-mediated signaling and internalization of antigens are critical for the differentiation of B cells into antibody-producing cells (48, 49). B cells recognize antigens on the antigen-presenting cells (APCs) such as follicular dendritic cells, subcapsular sinus macrophages and marginal zone B cells through the B cell receptor (BCR) (49, 50). B cells capture BCR-bound antigens from APC and delivered to major histocompatibility complex (MHC) II-containing vesicles *via* actin- and microtubule-dependent processes (51–53). Peptide – MHC-II complexes are presented to T cells, which provide the signals required for B cell activation. Thus, B-cell differentiation into plasma cells is dependent on the B cell-APC interaction and BCR-dependent cytoskeletal reorganization (51–55). Rap1 plays central roles in integrin-dependent adhesion (4, 9, 10) and BCR-induced reorganization of actin and MTOC polarization (56, 57). Therefore, Rap1-deficiency might impair B-cell contact with APC and BCR-dependent antigen internalization, which also contributes to defective development of GC.

Our previous study demonstrated that Rap1 guanine nucleotide exchange factors, Ras/Rap association-guanine nucleotide exchange factor (RA-GEF)-1 and 2 play critical roles in the retention of immature B cells in the BM (40). This study confirms that Rap1 activation is required for immature B-cell retention in the BM. In contrast to T cells, immature B cells egress passively from the BM, independent of pertussis toxin (PTX)-sensitive GPCR signaling, such as that of sphingosine-1-phospohate (S1P) (41). On the other hand, the retention of these cells in the BM strictly depends on amoeboid motility mediated by CXCR4 and VLA-4 (41). In addition, RA-GEF-1 and 2 are dispensable for naïve B-cell homing into peripheral LNs (40).

However, in this study, the deficiency of Rap1 in B cells was found to be indispensable for B-cell homing into LNs. Therefore, other Rap1GEFs, such as C3G, may compensate for the chemokine-dependent integrin activation of naïve B cells required for transmigration through the HEVs.

Various aspects of B-cell development rely on chemokine- and integrin-dependent adhesion and migration, in which Rap1 plays central roles. Hence, it is important to clarify the regulatory mechanisms of Rap1 activation and downstream effector molecules is important to understand B-cell proliferation, differentiation, and function.

DATA AVAILABILITY STATEMENT

The raw data supporting the conclusions of this article will be made available by the authors.

ETHICS STATEMENT

The animal study was reviewed and approved by Regulations for the Care and Use of Laboratory Animals in Kitasato University.

AUTHOR CONTRIBUTIONS

SI and KK designed, performed experiments, and wrote the paper. TS, RiS, RM and HS performed the experiments. RyS, HF, AN, SS and AI contributed to the preparation of essential materials and commented on the experiments and paper. All authors contributed to the article and approved the submitted version.

ACKNOWLEDGMENTS

We would like to thank Ms. H. Onda for technical assistance. This work was supported by Japan Society for the Promotion of Science KAKENHI 20K16290 and 19K07612, Takeda Science Foundation, The Naito Foundation. Kitasato University Research grant for young researchers. Suzuken Memorial Foundation.

SUPPLEMENTARY MATERIAL

The Supplementary Material for this article can be found online at: https://www.frontiersin.org/articles/10.3389/fimmu.2021.624419/full#supplementary-material

REFERENCES

1. Gloerich M, Bos JL. Regulating Rap Small G-Proteins in Time and Space. *Trends Cell Biol* (2011) 21(10):615–23. doi: 10.1016/j.tcb.2011.07.001
2. Hogg N, Patzak I, Willenbrock F. The Insider's Guide to Leukocyte Integrin Signalling and Function. *Nat Rev Immunol* (2011) 11(6):416–26. doi: 10.1038/nri2986
3. Humphries JD, Chastney MR, Askari JA, Humphries MJ. Signal Transduction Via Integrin Adhesion Complexes. *Curr Opin Cell Biol* (2019) 56:14–21. doi: 10.1016/j.ceb.2018.08.004
4. Katagiri K, Ohnishi N, Kabashima K, Iyoda T, Takeda N, Shinkai Y, et al. Crucial Functions of the Rap1 Effector Molecule RAPL in Lymphocyte and Dendritic Cell Trafficking. *Nat Immunol* (2004) 5(10):1045–51. doi: 10.1038/ni1111
5. Katagiri K, Maeda A, Shimonaka M, Kinashi T. RAPL, a Rap1-Binding Molecule That Mediates Rap1-Induced Adhesion Through Spatial Regulation of LFA-1. *Nat Immunol* (2003) 4(8):741–8. doi: 10.1038/ni950
6. McLeod SJ, Li AH, Lee RL, Burgess AE, Gold MR. The Rap Gtpases Regulate B Cell Migration Toward the Chemokine Stromal Cell-Derived Factor-1 (CXCL12): Potential Role for Rap2 in Promoting B Cell Migration. *J Immunol* (2002) 169(3):1365–71. doi: 10.4049/jimmunol.169.3.1365
7. McLeod SJ, Shum AJ, Lee RL, Takei F, Gold MR. The Rap Gtpases Regulate Integrin-Mediated Adhesion, Cell Spreading, Actin Polymerization, and Pyk2 Tyrosine Phosphorylation in B Lymphocytes. *J Biol Chem* (2004) 279 (13):12009–19. doi: 10.1074/jbc.M313098200
8. Durand CA, Westendorf J, Tse KW, Gold MR. The Rap Gtpases Mediate CXCL13- and Sphingosine1-Phosphate-Induced Chemotaxis, Adhesion, and Pyk2 Tyrosine Phosphorylation in B Lymphocytes. *Eur J Immunol* (2006) 36 (8):2235–49. doi: 10.1002/eji.200535004
9. Katagiri K, Hattori M, Minato N, Irie S, Takatsu K, Kinashi T. Rap1 is a Potent Activation Signal for Leukocyte Function-Associated Antigen 1 Distinct From Protein Kinase C and Phosphatidylinositol-3-OH Kinase. *Mol Cell Biol* (2000) 20(6):1956–69. doi: 10.1128/MCB.20.6.1956-1969.2000
10. Katagiri K, Imamura M, Kinashi T. Spatiotemporal Regulation of the Kinase Mst1 by Binding Protein RAPL Is Critical for Lymphocyte Polarity and Adhesion. *Nat Immunol* (2006) 7(9):919–28. doi: 10.1038/ni1374
11. Chu H, Awasthi A, White GC2nd, Chrzanowska-Wodnicka M, Malarkannan S. Rap1b Regulates B Cell Development, Homing, and T Cell-Dependent Humoral Immunity. *J Immunol* (2008) 181(5):3373–83. doi: 10.4049/jimmunol.181.5.3373
12. Chen Y, Yu M, Podd A, Wen R, Chrzanowska-Wodnicka M, White GC, et al. A Critical Role of Rap1b in B-Cell Trafficking and Marginal Zone B-Cell Development. *Blood* (2008) 111(9):4627–36. doi: 10.1182/blood-2007-12-128140
13. Gatto D, Brink R. B Cell Localization: Regulation by EBI2 and Its Oxysterol Ligand. *Trends Immunol* (2013) 34(7):336–41. doi: 10.1016/j.it.2013.01.007
14. Yi T, Wang X, Kelly LM, An J, Xu Y, Sailer AW, et al. Oxysterol Gradient Generation by Lymphoid Stromal Cells Guides Activated B Cell Movement During Humoral Responses. *Immunity* (2012) 37(3):535–48. doi: 10.1016/j.immuni.2012.06.015
15. Allen CD, Okada T, Cyster JG. Germinal-Center Organization and Cellular Dynamics. *Immunity* (2007) 27(2):190–202. doi: 10.1016/j.immuni.2007.07.009
16. Bannard O, Horton RM, Allen CD, An J, Nagasawa T, Cyster JG. Germinal Center Centroblasts Transition to a Centrocyte Phenotype According to a Timed Program and Depend on the Dark Zone for Effective Selection. *Immunity* (2013) 39(5):912–24. doi: 10.1016/j.immuni.2013.08.038
17. Allen CD, Ansel KM, Low C, Lesley R, Tamamura H, Fujii N, et al. Germinal Center Dark and Light Zone Organization Is Mediated by CXCR4 and CXCR5. *Nat Immunol* (2004) 5(9):943–52. doi: 10.1038/ni1100
18. Hayakawa K, Hardy RR, Herzenberg LA, Herzenberg LA. Progenitors for Ly-1 B Cells Are Distinct From Progenitors for Other B Cells. *J Exp Med* (1985) 161 (6):1554–68. doi: 10.1084/jem.161.6.1554
19. Montecino-Rodriguez E, Dorshkind K. B-1 B Cell Development in the Fetus and Adult. *Immunity* (2012) 36(1):13–21. doi: 10.1016/j.immuni.2011.11.017
20. Dickinson GS, Akkoyunlu M, Bram RJ, Alugupalli KR. BAFF Receptor and TACI in B-1b Cell Maintenance and Antibacterial Responses. *Ann N Y Acad Sci* (2015) 1362:57–67. doi: 10.1111/nyas.12772
21. Pandya KD, Palomo-Caturla I, Walker JA, KS V, Zhong Z, Alugupalli KR. An Unmutated Igm Response to the Vi Polysaccharide of Salmonella Typhi Contributes to Protective Immunity in a Murine Model of Typhoid. *J Immunol* (2018) 200(12):4078–84. doi: 10.4049/jimmunol.1701348

22. Foote JB, Kearney JF. Generation of B Cell Memory to the Bacterial Polysaccharide Alpha-1,3 Dextran. *J Immunol* (2009) 183(10):6359–68. doi: 10.4049/jimmunol.0902473
23. Montecino-Rodriguez E, Dorshkind K. Formation of B-1 B Cells From Neonatal B-1 Transitional Cells Exhibits NF-Kappab Redundancy. *J Immunol* (2011) 187(11):5712–9. doi: 10.4049/jimmunol.1102416
24. Pedersen GK, Li X, Khoenkhoen S, Adori M, Beutler B, Karlsson Hedestam GB. B-1a Cell Development in Splenectomized Neonatal Mice. *Front Immunol* (2018) 9:1738. doi: 10.3389/fimmu.2018.01738
25. Pedersen GK, Adori M, Khoenkhoen S, Dosenovic P, Beutler B, Karlsson Hedestam GB. B-1a Transitional Cells Are Phenotypically Distinct and Are Lacking in Mice Deficient in Ikappabns. *Proc Natl Acad Sci USA* (2014) 111 (39):E4119–26. doi: 10.1073/pnas.1415866111
26. Ghosn EE, Sadate-Ngatchou P, Yang Y, Herzenberg LA, Herzenberg LA. Distinct Progenitors for B-1 and B-2 Cells Are Present in Adult Mouse Spleen. *Proc Natl Acad Sci USA* (2011) 108(7):2879–84. doi: 10.1073/pnas.1019764108
27. Ghosn EE, Waters J, Phillips M, Yamamoto R, Long BR, Yang Y, et al. Fetal Hematopoietic Stem Cell Transplantation Fails to Fully Regenerate the B-Lymphocyte Compartment. *Stem Cell Rep* (2016) 6(1):137–49. doi: 10.1016/j.stemcr.2015.11.011
28. Ishida D, Su L, Tamura A, Katayama Y, Kawai Y, Wang SF, et al. Rap1 Signal Controls B Cell Receptor Repertoire and Generation of Self-Reactive B1a Cells. *Immunity* (2006) 24(4):417–27. doi: 10.1016/j.immuni.2006.02.007
29. Katayama Y, Sekai M, Hattori M, Miyoshi I, Hamazaki Y, Minato N. Rap Signaling Is Crucial for the Competence of IL-7 Response and the Development of B-Lineage Cells. *Blood* (2009) 114(9):1768–75. doi: 10.1182/blood-2009-03-213371
30. Kajikhina K, Tsuneto M, Melchers F. B-Lymphopoiesis in Fetal Liver, Guided by Chemokines. *Adv Immunol* (2016) 132:71–89. doi: 10.1016/bs.ai.2016.07.002
31. Tsuneto M, Tokoyoda K, Kajikhina E, Hauser AE, Hara T, Tani-Ichi S, et al. B-Cell Progenitors and Precursors Change Their Microenvironment in Fetal Liver During Early Development. *Stem Cells* (2013) 31(12):2800–12. doi: 10.1002/stem.1421
32. Kajikhina K, Melchers F, Tsuneto M. Chemokine Polyreactivity of IL7Ralpha +CSF-1R+ Lympho-Myeloid Progenitors in the Developing Fetal Liver. *Sci Rep* (2015) 5:12817. doi: 10.1038/srep12817
33. Ishihara S, Nishikimi A, Umemoto E, Miyasaka M, Saegusa M, Katagiri K. Dual Functions of Rap1 are Crucial for T-Cell Homeostasis and Prevention of Spontaneous Colitis. *Nat Commun* (2015) 6:8982. doi: 10.1038/ncomms9982
34. Sato R, Makino-Okamura C, Lin Q, Wang M, Shoemaker JE, Kurosaki T, et al. Repurposing the Psoriasis Drug Oxarol to an Ointment Adjuvant for the Influenza Vaccine. *Int Immunol* (2020) 32(8):499–507. doi: 10.1093/intimm/dxaa012
35. Katagiri K, Hattori M, Minato N, Kinashi T. Rap1 Functions as a Key Regulator of T-Cell and Antigen-Presenting Cell Interactions and Modulates T-Cell Responses. *Mol Cell Biol* (2002) 22(4):1001–15. doi: 10.1128/MCB.22.4.1001-1015.2002
36. Katagiri K, Katakai T, Ebisuno Y, Ueda Y, Okada T, Kinashi T. Mst1 Controls Lymphocyte Trafficking and Interstitial Motility Within Lymph Nodes. *EMBO J* (2009) 28(9):1319–31. doi: 10.1038/emboj.2009.82
37. Shimonaka M, Katagiri K, Nakayama T, Fujita N, Tsuruo T, Yoshie O, et al. Rap1 Translates Chemokine Signals to Integrin Activation, Cell Polarization, and Motility Across Vascular Endothelium Under Flow. *J Cell Biol* (2003) 161 (2):417–27. doi: 10.1083/jcb.200301133
38. Fukujin F, Nakajima A, Shimada N, Sawai S. Self-Organization of Chemoattractant Waves in Dictyostelium Depends on F-Actin and Cell-Substrate Adhesion. *J R Soc Interface* (2016) 13(119):1–11. doi: 10.1098/rsif.2016.0233
39. Nakajima A, Ishida M, Fujimori T, Wakamoto Y, Sawai S. The Microfluidic Lighthouse: an Omnidirectional Gradient Generator. *Lab Chip* (2016) 16 (22):4382–94. doi: 10.1039/c6lc00898d
40. Ishihara S, Sato T, Du G, Guardavaccaro D, Nakajima A, Sawai S, et al. Phosphatidic Acid-Dependent Localization and Basal De-Phosphorylation of RA-Gefs Regulate Lymphocyte Trafficking. *BMC Biol* (2020) 18(1):75. doi: 10.1186/s12915-020-00809-0
41. Beck TC, Gomes AC, Cyster JG, Pereira JP. CXCR4 and a Cell-Extrinsic Mechanism Control Immature B Lymphocyte Egress From Bone Marrow. *J Exp Med* (2014) 211(13):2567–81. doi: 10.1084/jem.20140457
42. Hardy RR, Hayakawa K. A Developmental Switch in B Lymphopoiesis. *Proc Natl Acad Sci USA* (1991) 88(24):11550–4. doi: 10.1073/pnas.88.24.11550
43. Montecino-Rodriguez E, Leathers H, Dorshkind K. Identification of a B-1 B Cell-Specified Progenitor. *Nat Immunol* (2006) 7(3):293–301. doi: 10.1038/ni1301
44. Kobayashi M, Shelly WC, Seo W, Vemula S, Lin Y, Liu Y, et al. Functional B-1 Progenitor Cells are Present in the Hematopoietic Stem Cell-Deficient Embryo and Depend on *Cbfβ* for Their Development. *Proc Natl Acad Sci USA* (2016) 111(33):E12151–12156. doi: 10.1073/pnas.1407370111
45. Li Y, Yan J, De P, Chang H-C, Yamaguchi A, Chrisypherson IIKW, et al. Rap1a Null Mice Have Altered Myeloid Cell Functions Suggesting Distinct Roles for Closely Related Rap1a and 1b Proteins. *J Immunol* (2007) 179 (12):8322–31. doi: 10.4049/jimmunol.179.12.8322
46. Duchniewicz M, Zemojtel T, Kolanczyk M, Grossmann S, Scheele JS, Zwartkruis FJT. Rap1A-Deficeint T and B Cells Show Impaired Integrin-Mediated Cell Adhesion. *Mol Cell Biol* (2006) 26(2):643–53. doi: 10.1128/MCB.26.2.643-653.2006
47. Lu E, Cyster JG. G-Protein Coupled Receptors and Ligands That Organize Humoral Immune Responses. *Immunol Rev* (2019) 289(1):158–72. doi: 10.1111/imr.12743
48. Batista FD, Harwood NE. The Who, How and Where of Antigen Presentation to B Cells. *Nat Rev Immunol* (2009) 9(1):15–27. doi: 10.1038/nri2454
49. Phan TG, Grigorova I, Okada T, Cyster JG. Subcapsular Encounter and Complement-Dependent Transport of Immune Complexes by Lymph Node B Cells. *Nat Immunol* (2007) 8(9):992–1000. doi: 10.1038/ni1494
50. Carrasco YR, Batista FD. B Cells Acquire Particulate Antigen in a Macrophage-Rich Area At the Boundary Between the Follicle and the Subcapsular Sinus of the Lymph Node. *Immunity* (2007) 27(1):160–71. doi: 10.1016/j.immuni.2007.06.007
51. Harwood NE, Batista FD. Early Events in B Cell Activation. *Annu Rev Immunol* (2010) 28:185–210. doi: 10.1146/annurev-immunol-030409-101216
52. Song W, Liu C, Upadhyaya A. The Pivotal Position of the Actin Cytoskeleton in the Initiation and Regulation of B Cell Receptor Activation. *Biochim Biophys Acta* (2014) 1838(2):569–78. doi: 10.1016/j.bbamem.2013.07.016
53. Yuseff MI, Lennon-Dumenil AM. B Cells Use Conserved Polarity Cues to Regulate Their Antigen Processing and Presentation Functions. *Front Immunol* (2015) 6:251. doi: 10.3389/fimmu.2015.00251
54. Batista FD, Iber D, Neuberger MS. B Cells Acquire Antigen From Target Cells After Synapse Formation. *Nature* (2001) 411(6836):489–94. doi: 10.1038/35078099
55. Chen J, Li N, Yin Y, Zheng N, Min M, Lin B, et al. Methyltransferase Nsd2 Ensures Germinal Center Selection by Promoting Adhesive Interactions Between B Cells and Follicular Dendritic Cells. *Cell Rep* (2018) 25(12):3393–404.e3396. doi: 10.1016/j.celrep.2018.11.096
56. Wang JC, Lee JY, Christian S, Dang-Lawson M, Pritchard C, Freeman SA, et al. The Rap1-Cofilin-1 Pathway Coordinates Actin Reorganization and MTOC Polarization At the B Cell Immune Synapse. *J Cell Sci* (2017) 130 (6):1094–109. doi: 10.1242/jcs.191858
57. Wang JC, Lee JY, Dang-Lawson M, Pritchard C, Gold MR. The Rap2c Gtpase Facilitates B Cell Receptor-Induced Reorientation of the Microtubule-Organizing Center. *Small GTPases* (2020) 11(6):402–12. doi: 10.1080/21541248.2018.1441626

Conflict of Interest: The authors declare that the research was conducted in the absence of any commercial or financial relationships that could be construed as a potential conflict of interest.

frontiers in Immunology

ORIGINAL RESEARCH
published: 16 July 2021
doi: 10.3389/fimmu.2021.701066

Dependence on Autophagy for Autoreactive Memory B Cells in the Development of Pristane-Induced Lupus

Albert Jang[1], Robert Sharp[1], Jeffrey M. Wang[1], Yin Feng[1], Jin Wang[2,3] and Min Chen[1]**

[1] Department of Pathology and Immunology, Baylor College of Medicine, Houston, TX, United States, [2] Immunobiology and Transplant Science Center, Houston Methodist Research Institute, Houston, TX, United States, [3] Department of Surgery, Weill Cornell Medical College, Cornell University, New York, NY, United States

The production of autoantibodies by autoreactive B cells plays a major role in the pathogenesis of lupus. Increases in memory B cells have been observed in human lupus patients and autoimmune *lpr* mice. Autophagy is required for the maintenance of memory B cells against viral infections; however, whether autophagy regulates the persistence of autoantigen-specific memory B cells and the development of lupus remains to be determined. Here we show that memory B cells specific for autoantigens can be detected in autoimmune *lpr* mice and a pristane-induced lupus mouse model. Interestingly, B cell-specific deletion of Atg7 led to significant loss of autoreactive memory B cells and reduced autoantibody production in pristane-treated mice. Autophagy deficiency also attenuated the development of autoimmune glomerulonephritis and pulmonary inflammation after pristane treatment. Adoptive transfer of wild type autoreactive memory B cells restored autoantibody production in Atg7-deficient recipients. These data suggest that autophagy is important for the persistence of autoreactive memory B cells in mediating autoantibody responses. Our results suggest that autophagy could be targeted to suppress autoreactive memory B cells and ameliorate humoral autoimmunity.

Keywords: autophagy, memory B cells, autoreactive memory B cells, lupus, pristane induced lupus, autoantibody, glomerulonephritis, systemic autoimmunity

OPEN ACCESS

Edited by:
Zhenming Xu,
The University of Texas Health Science Center at San Antonio, United States

Reviewed by:
Anne Satterthwaite,
University of Texas Southwestern Medical Center, United States
Lee Ann Garrett-Sinha,
University at Buffalo, United States

****Correspondence:***
Jin Wang
jinwang@houstonmethodist.org
Min Chen
minc@bcm.edu

Specialty section:
This article was submitted to B Cell Biology, a section of the journal Frontiers in Immunology

Received: *27 April 2021*
Accepted: *30 June 2021*
Published: *16 July 2021*

Citation:
Jang A, Sharp R, Wang JM, Feng Y, Wang J and Chen M (2021) Dependence on Autophagy for Autoreactive Memory B Cells in the Development of Pristane-Induced Lupus. Front. Immunol. 12:701066. doi: 10.3389/fimmu.2021.701066

INTRODUCTION

Systemic lupus erythematosus (SLE) is characterized by profound autoantibody production and tissue destruction (1–4). Autoreactive B cells are critical for the initiation and progression of lupus (2, 5–8). Persistent autoantibody production in SLE patients suggests the involvement of humoral memory against autoantigens in disease progression (9–11). Memory B cells are long-lived cells that have lower thresholds for activation and can be rapidly activated to differentiate into antibody secreting cells (12, 13). Cellular origins of the autoantibodies in lupus have been linked to memory B cells (9–11). Dysregulation of memory B cells has been identified in SLE patients and lupus-prone *lpr* mice (14–17). Memory B cells are also associated with disease relapses in SLE patients after B

cell-directed therapies (15, 18–23). However, whether autoreactive memory B cells are critical for the pathogenesis of lupus remains to be determined.

Autophagy is a cellular digestion process during which double-membraned autophagosomes sequester cytoplasmic components, followed by fusion with lysosome and subsequent degradation of sequestered materials (24, 25). Autophagy-related genes, such as *ULK1, Atg7, Atg5/12* and *LC3*, are required for the formation of autophagosomes (26). Autophagy can help to generate energy and nutrients to protect cell viability caused by nutrient deprivation or lack of growth factors (24, 27, 28). Autophagy also contributes to quality control of cellular proteins and organelles to protect cell survival (29). We have found that autophagy is important for the long-term survival of memory B cells to maintain memory response to viral infections (30, 31). Autophagy has also been found to be critical for the protection of $CD4^+$ and $CD8^+$ memory T cells, as well as long-lived plasma cells (32–37). Using mice with Atg5 conditionally deleted in B cells, several groups have found that antibody responses are significantly reduced during T cell dependent or independent antigen immunization, parasitic infection, and mucosal inflammation (35, 36, 38). Loss of autophagy in B cells did not affect conventional B2 cell development (30, 36), class switch recombination or germinal center formation (30, 31), but impaired the maintenance of long-lived plasma cells in the bone marrow (35, 36, 38). Together these data suggest that autophagy is essential for the persistence of long-term immunological memory and antibody production. Using CD21-cre-$Atg5^{f/f}$ mice crossed with autoimmune *lpr* mice, loss of autophagy has been shown to reduce bone marrow plasma cells and autoantibodies (38). Elevated autophagy is found to be increased in B cells from lupus patients and autoimmune NZB/NZW mice (39). Deletion of Atg5 in B cells attenuates the development of autoantibody production, lymphocyte infiltration and mortality in toll-like receptor 7-transgenic mice (40). Autophagy genes, such as *ATG5*, has been reported to be associated with an increased risk of developing lupus (4, 41–45). Moreover, anti-malaria drugs chloroquine and hydroxychloroquine that have long been used to treat lupus can also suppress autophagy (46–48). Dysregulation of autophagy has been detected in SLE patients and lupus-prone mice (39–41, 43, 44, 49–51). Therefore, autophagy may play a critical role for autoimmune responses in lupus. However, memory B cells specific for autoantigens have not been formally shown in previous studies. Moreover, an essential role for autophagy in the persistence of these autoantigen-specific memory B cells has not been established.

Pristane-induced lupus is a well-established murine model of systemic lupus erythematosus (52, 53). Susceptibility to pristane-induced lupus among non-autoimmune prone mice is widespread. It has been reported that C57BL/6 or BALB/c mice can develop anti-nuclear autoantibodies and immune complex-mediated glomerulonephritis, as well as other SLE-like symptoms following a single dose injection of pristane (52, 53). In this study, we show that autoreactive memory B cells can be induced in a pristane-induced lupus mouse model. Autophagy deficiency in B cells abrogates pristane-induced autoantibody production and glomerulonephritis with B cell-specific knockout of Atg7. Moreover, adoptive transfer of wild type memory B restored autoantibody production in Atg7-deficient recipient mice. Our study suggests that autophagy is important for the persistence of autoreactive memory B cells, maintenance of autoantibody production, and sustained glomerulonephritis in pristane-induced lupus.

MATERIAL AND METHODS

Mice

$Atg7^{flox}$ mice were obtained from Dr. Masaaki Komatsu of Tokyo Metropolitan Institute of Medical Science (54) and crossed with CD19-cre knock-in mice (The Jackson Laboratory) to obtain B/$Atg7^{-/-}$ mice. *MRL* and *MRL-lpr* mice were obtained from the Jackson Laboratory. Sex and age-matched wild type or B/$Atg7^{-/-}$ mice in the C57BL/6 background at the age of 8-12 weeks were used at the start of all experiments except noted. For pristane injection, healthy sex and age-matched B/$Atg7^{-/-}$ mice and wild type controls (8-12 weeks old) were randomly separated into groups for pristane or phosphate-buffered saline (PBS) injection (as controls). A single dose of pristane (0.5 ml i.p.) was injected. Sera were collected 6 months post-injection and levels of autoantibodies were measured by ELISA. Mice were sacrificed at 6 months after pristane injection. Spleens were harvested for Fluorescence-Activated Cell Sorting (FACS) and kidneys and lungs were collected for histology analysis. At least 5 mice per group were used for each experiment. At least 10 mice per group were used for pristane injection experiments. The experiments were performed according to federal and institutional guidelines and with the approval of Institutional Animal Care and Use Committees of Baylor College of Medicine and Houston Methodist Research Institute.

Antibodies

The following antibodies from BD Biosciences were used for flow cytometry: biotinylated antibodies to CD4 (553728), CD8 (553029), IgM (553436), CD11b (553309), CD138 (553713) and GR-1 (553125); PE-conjugated antibodies to B220 (553090), CD5 (553023), CD11b (557397), IgD (558597), CD138 (553714); APC-conjugated antibodies to CD21 (558658), IgM (550676), IgD (560868), CD11b (553312), CD138 (558626) and GR-1 (553129); FITC-conjugated antibodies to GL7 (553666), IgD (553439); PE-Cy7 conjugated anti-CD11b (552820); Pacific Blue anti-CD3e (558214); PE-Cy5-anti-CD4 (553050) and APC-Cy7-anti-CD8a (557654). From Biolegend: APC-anti-mouse IgG1 (406610), PerCPCy5.5-anti-mouse IgG1(406612), Pacific Blue anti-CD38 (102720), FITC-anti-mouse IgG (405305), APC-anti-mouse IgG (405308), APC-Cy7-anti-mouse IgG (405316). From eBioscience: PerCP-Cy5.5-anti-B220 (45-0452-82), PE-anti-IgM (12-5890-83), PE-anti-CD23 (12-0232-82), Biotin-anti-mouse-IgD (13-5993-85), Streptavidin-PE (12-4317-87), PE-Cy7-streptavidin (25-4317-82). From the Jackson Immunoresearch Laboratories: normal rabbit IgG

(015-000-002) or mouse IgG (011-000-002). From Abgent: anti-LC3 (AP1802a) for immunocytochemistry. From Invitrogen: Anti-CoxIV (459600) for immunocytochemistry. From Southern Biotechnology, HRP conjugated anti-mouse IgG or IgM.

Flow Cytometry

Spleens were treated with 0.4 mg/ml liberase (Roche) at room temperature for 10 min to make single cell suspension of splenocytes, followed by lysis of red blood cells with ACK lysis buffer. After blocking with 1 μg/ml anti-CD16/CD32, 10 μg/ml rat IgG and 10 μg/ml hamster IgG, the cells were then incubated with various antibodies conjugated to FITC, PE, APC, PerCP-Cy5.5, Pacific Blue (BD Biosciences) or PE-conjugated anti-PDCA-1 (Miltenyi Biotec) and analyzed by flow cytometry. Double-stranded DNA (dsDNA) were conjugated to Alexa fluor 488 using ULYSIS Nucleic Acid Labeling Kit (U21650, Invitrogen) according to manufacturer's instructions. Autoantigen RNP/Sm (The Binding Site) was labeled with Alexa Fluor 488 using the Microscale Protein Labeling Kit (A30006, Invitrogen). To detect dsDNA-specific memory B cells and germinal center B cells, total spleen cells were stained with PE-conjugated antibodies to CD11b, IgM, IgD, GR1 and CD138 (DUMP), APC-anti-mouse IgG, PerCP-Cy5.5-anti-CD19 or B220, Pacific Blue anti-CD38 and Alexa Fluor 488-dsDNA. To detect RNP-specific memory B cells and GC B cells, total spleen cells were stained with PE-conjugated antibodies to CD11b, IgM, IgD, GR1 and CD138 (DUMP), APC-anti-mouse IgG, PerCP-Cy5.5-anti-CD19 or B220, Pacific Blue anti-CD38 and Alexa Fluor 488-RNP/Sm. $DUMP^-B220^+IgG^+dsDNA^+CD38^+$ and $DUMP^-B220^+IgG^+RNP/Sm^+CD38^+$ memory B cells, $DUMP^-B220^+IgG^+dsDNA^+CD38^-$ and $DUMP^-B220^+IgG^+RNP/Sm^+CD38^-$ germinal center B cells were analyzed by flow cytometry.

Quantitative Real Time RT-PCR (qRT-PCR)

$CD19^+IgM^{low}IgD^+CD23^+IgG^-$ naïve mature B cells, $CD19^+DUMP^-IgG^+CD38^+dsDNA^+$ and $CD19^+DUMP^-IgG^+CD38^+RNP/Sm^+$ memory B cells were sorted from 3-4 months old *lpr* mice. RNA extracted from the cells was used to prepare cDNA with the High Capacity cDNA Reverse Transcription Kit (Life Technologies). Real-time PCR was performed using Taqman Universal PCR Master Mix with specific primers for autophagy genes or 18S rRNA from the TaqMan Gene Expression Assay Kit (AB Applied Biosystem) in the ABI PRISM 7000 Sequence Detection System. The assay IDs for the primers of the analyzed genes are: Mm00504340_m1 (Atg5), Mm00512209_m1 (Atg7), Mm00437238_m1 (ULK1), Mm00458725_g1 (MAP1LC3A), Mm00782868_sH (MAP1LC3B), and Mm00553733_m1 (Atg14). Relative gene expression was normalized to 18S rRNA.

Enzyme-Linked Immunosorbent Assay (ELISA)

To detect autoantibodies against autoantigens, 96-well plates coated with Sm, or RNP (The Binding Site) were incubated with serially diluted sera at 37°C for 2h. The plates were then washed and incubated with HRP-conjugated goat anti-mouse IgG (Southern Biotechnology, Birmingham, AL) at 37°C for 1h, followed by development with TMB peroxidase EIA substrate (Bio-Rad, Hercules, CA). The reaction was stopped with 1N H_2SO_4 and the optical density at 450 nm was measured using an ELISA reader. A mixture of sera from MRL-*lpr* mice was used to establish standard curves in each plate and antibody levels were shown as relative titers.

ELISPOT

MultiScreen 96-well Filtration plates (Millipore) were coated with 2 μg/ml RNP+Sm (The Binding Site). Sorted RNP/Sm+ or nonspecific memory B cells (100, 1000, 10000/well) were activated with LPS (10ug/ml) for 3 days, then added to the plates and incubated at 37 °C for 5 h. The cells were lysed with H_2O and the wells were probed with HRP-conjugated goat anti-mouse IgG (Southern Biotechnology), followed by development with 3-amino-9-ethylcarbzole (Sigma).

Adoptive Transfer of Autoreactive Memory B Cells

Wild type mice which were injected with pristane 6 months earlier were used as donors of wild-type memory B cells. Sex and age-matched 8-12 week-old B/$Atg7^{-/-}$ and wild type mice were used as recipients of the memory B cells. $DUMP^-B220^+IgG^+CD38^+RNP/Sm^+$ memory B cells were sorted from pooled spleens of pristane injected donor mice and adoptively transferred into wild type and B/$Atg7^{-/-}$ recipient mice retrooribitally (10,000 cells/mouse). Sorted naïve cells ($2x10^5$/mouse) from untreated mice were co-injected as filler cells to minimize cell loss during injection. One day after transfer recipient mice were injected with a single dose of 0.5 ml pristane i.p. Sera were collected 2 months post-injection. For some experiments, recipient mice were immunized with 20 μg RNP/Sm precipitated with 100 μl Inject Alum (Thermo Scientific) intraperitoneally (20 μg/mice, i.p.) and sera were collected 3 days later. Levels of autoantibodies in the sera of recipients were measured by ELISA.

Histochemistry and Immunocytochemistry Staining

To detect immune complex deposits in the kidney, frozen sections of the kidneys were stained with FITC-conjugated goat anti-mouse IgG (Sigma) or FITC-conjugated goat anti-mouse complement C3 (MP Biochemical, 55500) and analyzed under a fluorescent microscope. Scores of glomerular IgG and complement C3 deposition were assigned based on the intensity of IgG/C3 deposition (range 0-3) with 0 represents no deposition and 3 representing intense depositions. Sections of kidney and lung were also stained with hematoxylin and eosin (H&E). The degree of glomerulonephritis was graded using a glomerulonephritis activity score (range 0–24) developed for the assessment of lupus nephritis in humans (55). Glomerular cells in 10 glomeruli per section were counted. We also measured anti-nuclear antibodies (ANAs) in pristane-treated mice by staining of Hep2 cells according to our described protocol (56). Hep-2 cells on slides (Medical and Biological Laboratories) were incubated with serially diluted sera followed by staining with FITC-conjugated anti-mouse IgG (Sigma). The staining was

visualized under a BX-51 fluorescence microscope (Olympus). LC3 staining were performed according to our previously described protocol (30, 31). Briefly, sorted RNP-specific memory B cells from MRL-*lpr* mice or pristane-treated wild type mice, and naïve B cells from untreated wild type mice were added to slides by cytospin. The cells were fixed, incubated with a rabbit antibody to processed LC3 (Abgent) and followed by staining with Alexa Fluor-conjugated secondary antibodies (Molecular Probes). The nucleus was counter-stained with DAPI. The cells were then analyzed using a SoftWorx Image deconvolution microscope (Applied Precision).

Statistical Analyses

Data were presented as the mean ± SEM, and *P* values were determined by two-tailed Student's *t*-test using GraphPad Prism software and are included in the figure legends. The comparison of survival curves between and WT and KO was performed by Log-rank (Mantel-Cox) test using Prism. Significant statistic differences ($P<0.05$ or $P<0.01$ or $P<0.001$ or $P<0.0001$) are indicated.

RESULTS

Increased Memory B Cells Specific for Autoantigens in Autoimmune *lpr* Mice

Autoimmune Fas-deficient *lpr* mice develop significant lymphoproliferation and increased autoantibodies against DNA and nuclear antigens (7, 57–60). These mice also exhibit nearly 10-fold increase in the percentage of IgG1$^+$ memory B cells (16, 17). We therefore determined whether memory B cells specific for autoantigens could be detected in *lpr* mice. Anti-dsDNA and anti-RNP/Sm autoantibodies are associated with lupus in both humans and mice (61, 62). We generated fluorochrome-conjugated dsDNA and RNP/Sm in order to stain B cells specific for these autoantigens. Interestingly, we detected dsDNA-specific CD19$^+$IgG$^+$IgD$^-$IgM$^-$CD38$^+$ memory B cells in MRL-*lpr* mice (**Figure 1A**). In contrast, these dsDNA-specific autoantigen-specific memory B cells were absent in age-matched control MRL mice (**Figure 1A**). We also detected RNP/Sm-specific memory B cells in MRL-*lpr* mice but not in control MRL mice (**Figure 1A**). Moreover, these

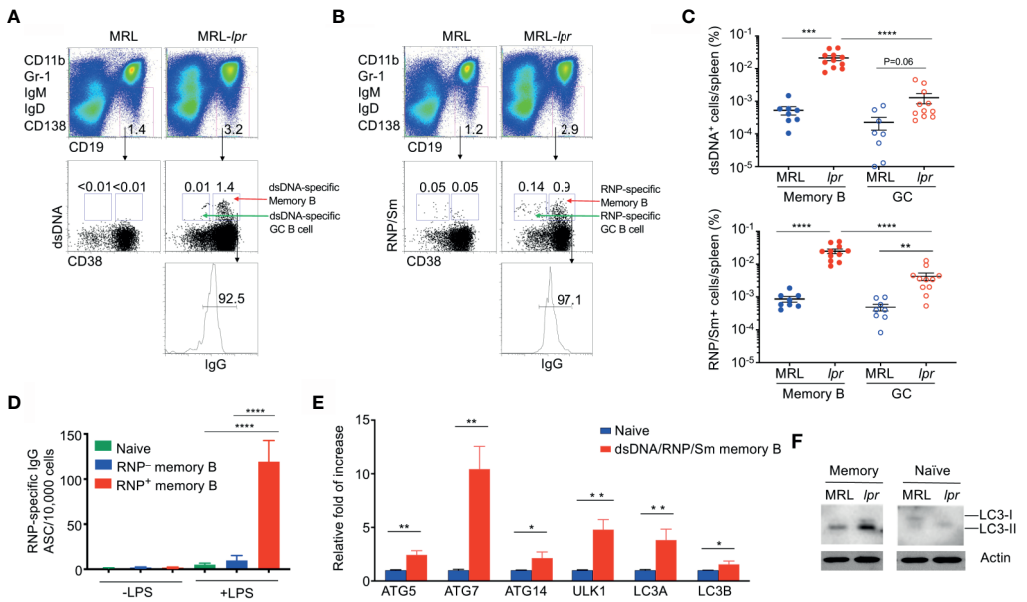

FIGURE 1 | Elevated autophagy in autoantigen-specific memory B cells. Splenocytes from MRL or MRL-*lpr* mice (4-month-old) were stained with PE-conjugated antibodies to CD11b, Gr-1, IgM, IgD and CD138, PE-Cy7-anti-CD19, Pacific Blue anti-CD38, APC-anti-IgG, and Alexa Fluor 488-conjugated dsDNA or RNP. DUMP$^-$ (IgM$^-$IgD$^-$CD11b$^-$Gr-1$^-$CD138$^-$) CD19$^+$ B cells were gated. **(A)** dsDNA-specific memory B cells (DUMP$^-$CD19$^+$CD38$^+$dsDNA$^+$IgG$^+$) or **(B)** RNP-specific memory B cells (DUMP$^-$CD19$^+$CD38$^+$RNP$^+$IgG$^+$) were analyzed by flow cytometry. **(C)** The frequency of dsDNA-specific memory B cells and RNP-specific memory B cells, as well as dsDNA-specific germinal center (GC) B cells (DUMP$^-$CD19$^+$CD38$^-$dsDNA$^+$IgG$^+$) and RNP-specific GC B cells (DUMP$^-$CD19$^+$CD38$^-$RNP$^+$IgG$^+$), in the spleen of each mouse was plotted. Data are presented as mean ± s.e.m. $^{**}P < 0.01$, $^{***}P < 0.001$, $^{****}P < 0.0001$, (n=8 for MRL and 11 for MRL-*lpr*). **(D)** RNP-specific memory B cells (DUMP$^-$CD19$^+$CD38$^+$RNP$^+$IgG$^+$) and RNP-negative memory B cells (DUMP$^-$CD19$^+$CD38$^+$RNP$^-$IgG$^+$) were sorted from MRL-*lpr* mice and stimulated with LPS in *vitro* for 3 days, the number of ASCs producing RNP-specific antibodies were measured by ELISPOT. Data are presented as mean ± s.e.m. Experiments were performed twice in triplicates using cells from a pool of 3-4 mice. $^{****}P < 0.0001$, determined by two-tailed Student's *t*-test. **(E)** Splenocytes from pooled MRL or MRL-*lpr* mice were stained as in **(A)** except that both Alexa Fluor 488-conjugated dsDNA and RNP were included for staining. Sorted dsDNA/RNP/Sm-specific memory B cells, and B220$^+$IgM^{low}IgD$^+$CD23$^+$IgG$^-$ naïve B cells were used for real-time RT-PCR analysis of indicated autophagy-related genes. Data are presented as mean ± s.e.m. Experiments were performed three times using cells from a pool of 10-15 mice. $^*P < 0.05$, $^{**}P < 0.01$, determined by two-tailed Student's *t*-test. **(F)** Western blot analysis of LC3 processing in Memory (DUMP$^-$CD19$^+$IgG$^+$CD38$^+$) and naïve B cells isolated from pooled MRL and MRL-*lpr* mice. Data are representative of two independent experiments.

$CD19^+IgG^+IgD^-IgM^-CD38^+RNP/Sm^+$ memory B cells could be activated by LPS *in vitro* to differentiate into a larger number of anti-RNP/Sm antibody secreting cells (ASCs) than RNP/Sm-negative memory B cells could, suggesting the $CD19^+IgG^+IgD^-IgM^-CD38^+RNP/Sm^+$ memory B cells identified by flow cytometry are bona fide RNP/Sm-specific memory B cells (**Figure 1D**). We found that B cells specific for dsDNA and RNP/Sm are predominantly the $CD19^+IgG^+IgD^-IgM^-CD38^+$ memory B cells, but not the $CD19^+IgG^+IgD^-IgM^-CD38^-$ germinal center (GC) B cells (**Figures 1A–C**). This indicates that *lpr* mice contain abundant memory B cells but not germinal center B cells specific for autoantigens.

Enhanced Autophagy in Memory B Cells From Lupus-Prone *lpr* Mice

We have previously observed increased autophagy in memory B cells (30). We therefore stained memory B cells with dsDNA and RNP/Sm and sorted these autoreactive memory B cells. We then examined whether these autoreactive memory B cells displayed increased autophagy gene expression. As shown by quantitative RT-PCR (qRT-PCR), autoreactive memory B cells also expressed increased levels of *Ulk1* (Atg1) and *Atg14* critical for autophagy initiation, as well as *Atg5*, *Atg7*, *Map1lc3a* and *Map1lc3b* that required for autophagosome maturation (63–65) (**Figure 1E**). These data suggest that autoreactive memory B cells from *lpr* mice display active autophagy.

The conversion from LC3-I to LC3-II isoforms is indicative of active autophagy (26, 66). We therefore performed Western blot analysis to detect LC3. In comparison with naïve B cells, memory B cells from wild type and *lpr* mice displayed increased levels of LC3-II (**Figure 1E**). Moreover, memory B cells from *lpr* mice displayed significantly increased LC3-II compared to wild type controls (**Figure 1F**). These data suggest that memory B cells from *lpr* mice display active autophagy.

Autophagy Deficiency Inhibits Pristane-Induced Autoantibody Production

It has been shown that autophagy is elevated in SLE, and may be essential for humoral autoimmune manifestations (38, 39, 49). We therefore investigated whether autophagy might be important for the protection of autoreactive memory B cells and the production of autoantibodies using a pristane-induced lupus model. We crossed CD19-cre mice with $Atg7^{flox}$ mice (54) to generate B cell-specific deletion of Atg7 ($B/Atg7^{-/-}$) on the C57BL/6 background. $B/Atg7^{-/-}$ and wild type mice were then administrated with pristane. Pulmonary hemorrhage resembling that seen in SLE has been reported to occur earlier in pristane-treated mice and causes mortality in a portion of mice on the C57BL/6 background (52, 53, 67). We observed that treatment with pristane caused 18% death in wild type mice within 4 weeks of pristane injection (**Figure 2A**). Interestingly, $B/Atg7^{-/-}$ mice were resistant to pristane-induced death (**Figure 2A**). Presumably the mortality associated with pristane-induced pulmonary vasculitis (52, 53, 67) is prevented due to the loss of autophagy in B cells (also see **Figure 3B**).

It has been reported that pristane-induced lupus induces production of a different spectrum of SLE associated autoantibodies in C57/BL6 and BALB/c mice (52, 53). C57/BL6 mice could produce anti-RNP and anti-Sm (57, 62) but not anti-dsDNA autoantibodies after pristane treatment (52, 53). We next measured lupus-associated anti-dsDNA, anti-RNP and anti-Sm autoantibody levels by ELISA in sera from these mice six months after pristane administration. Consistent with previous reports, we did not detect significant induction of anti-dsDNA autoantibodies in wild type or $B/Atg7^{-/-}$ mice on the C57/BL6 background (data not shown). We detected significant induction of anti-RNP and anti-Sm in wild type mice after pristane treatment (**Figures 2B, C**). However, the induction of anti-RNP and anti-Sm autoantibodies was dramatically reduced by 10-fold in $B/Atg7^{-/-}$ mice (**Figures 2B, C**).

We also measured anti-nuclear antibodies (ANAs) in pristane-treated mice by staining of Hep2 cells. As a positive control, we detected distinct nuclear staining with sera from B6/*lpr* mice (**Figure 2D**). We detected nuclear staining of Hep2 cells with sera from 90% pristane-treated wild type mice (**Figure 2D**). Among them, 1/10 sera gave strong nuclear staining (1:640 dilution); 4/10 sera gave medium nuclear staining (1:160 dilution); and 4/10 sera gave low nuclear staining (1:40 or 1:80 dilution). Majority of the staining pattern is speckled (**Figure 2D**), which are typically produced by elevated level of anti-RNP/Sm autoantibodies. Sera from one mouse gave strong cytoplasmic staining (data not shown). In contrast, no significant staining was observed using sera from 8 of the 10 $B/Atg7^{-/-}$ mice (**Figure 2D**). Only 1 of the 10 sera from $B/Atg7^{-/-}$ mice generated detectable but much weaker speckled nuclear staining in Hep2 cells (1:40 dilution), whereas weak cytoplasmic staining was found in sera from 1 mouse. These results indicate that pristane induces the production of ANAs in wild type mice but loss of autophagy in B cells significantly reduced ANA production in $B/Atg7^{-/-}$ mice.

Autophagy Deficiency Inhibits Pristane-Induced Glomerulonephritis and Pulmonary Vasculitis

To determine whether deficiency in autophagy affects other manifestations of autoimmunity, we examined kidneys from mice treated with pristane. Pristane treatment has been shown to induce the development of glomerulonephritis in mice (52, 53, 68). Consistently, the sizes of glomeruli in the kidney sections from pristane-treated wild type were increased compared to untreated controls (**Figure 3A**). Moreover, increased number of intraglomerular mesangial cells were found in these wild type mice treated with pristane (**Figure 3A**). In contrast, pristane treatment did not induce the increases in cellularity or sizes of glomeruli in the kidney of $B/Atg7^{-/-}$ mice. Glomerulonephritis activity score was 8.3 ± 2.8 versus 2.4 ± 1.8 for wild type and $B/Atg7^{-/-}$ mice, respectively. These results suggest that autophagy deficiency in B cells suppress pristane-induced glomerulonephritis. We also examined lungs from mice treated with pristane for signs of lupus. Pulmonary hemorrhage has been

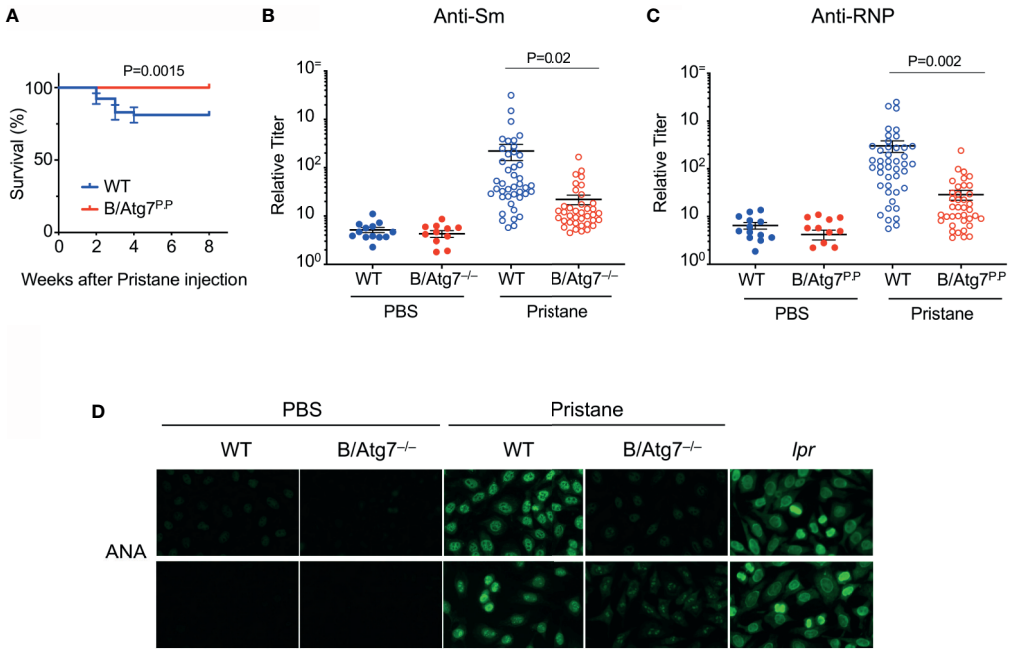

FIGURE 2 | Decreased production of autoantibodies in B/Atg7$^{-/-}$ mice injected with pristane. Sex and age-matched 8-12 weeks old B/Atg7$^{-/-}$ and wild type mice were injected with a single dose of 0.5 ml pristane or PBS (i.p.). **(A)** Mouse survival after pristane injection was plotted. Data are combined results from three experiments. (n= 53 and 48 for WT and B/Atg7$^{-/-}$ with pristane injection, respectively). The comparison of survival curves between and WT and KO was performed by Log-rank (Mantel-Cox) test using Prism. p = 0.0015. **(B, C)** Sera were collected 6 months later and levels of autoantibodies specific for Sm **(B)** or RNP **(C)** were measured by ELISA using plates coated with RNP or Sm (The Binding Site). Data are combined results from three experiments. (n=13 and 11 for WT and B/Atg7$^{-/-}$ with PBS injection, respectively; n= 43 and 38 for WT and B/Atg7$^{-/-}$ with pristane injection, respectively). **(D)** Anti-nuclear antibodies (ANAs) were detected by incubation of sera from WT (1:160 dilution) or B/Atg7$^{-/-}$ mice (1:40 dilution) injected with pristane or PBS (1:40 dilution), B6-*lpr* (1:320 dilution) with Hep2 cell slides, followed by probing with FITC-conjugated anti-mouse IgG. Sera from 9/10 of WT and 1/10 of B/Atg7$^{-/-}$ mice gave positive nuclear staining. Representative images from each group were shown (n=10 per group).

shown in SLE patients and mice induced with pristane-induced lupus (69). We observed extensive perivascular and peribronchial infiltration in wild type but not autophagy-deficient mice at 6 months after pristane injection (**Figure 3B**). These results suggest that autophagy deficiency in B cells suppress pristane-induced autoimmune manifestations of lupus.

Autoreactive B cells can lead to over-production of antibodies and the deposition of antibody-immune complexes in the kidney, which can be the cause of glomerulonephritis. We therefore examined immune complexes in the kidneys of pristane-treated mice. As expected, we observed significant IgG deposition in the glomeruli of kidneys in wild type mice treated with pristane (**Figure 3C**). In contrast, IgG deposition was significantly reduced in B/Atg7$^{-/-}$ mice (glomerulonephritis deposition score was 2.3 ± 0.5 versus 0.8 ± 0.6 for wild type and B/Atg7$^{-/-}$ mice, respectively) (**Figure 3C**). Consistent with this finding, complement C3 staining were also dramatically reduced in B/Atg7$^{-/-}$ mice when compared with wild type mice (glomerulonephritis deposition score was 2.2 ± 0.6 versus 0.7± 0.3) (**Figure 3D**), suggesting decreased complement activation in the absence of autophagy in B cells. These data support the conclusion that autophagy deficiency in B cells prevents autoimmune manifestations in the pristane-induced lupus model.

Induction of Autoreactive Memory B Cells Depends on Autophagy

We next determined whether autophagy deficiency in B cells affects the composition and activation of different cell types in the immune system. We did not detect significant changes in the numbers and composition of T cells in B/Atg7$^{-/-}$ mice compared to the wild type after the pristane treatment (**Figures 4A, B**). The number of B cells and the composition of mature B cells, as well as the transitional T1 and T2 cells, marginal zone (MZ) and follicular (FO) B cells (70) were also not significantly changed between wild type and B/Atg7$^{-/-}$ mice at six months after pristane administration (**Figures 4A, C, D**). CD11c^{+}CD11b^{+} dendritic cells and CD11c^{-}CD11b^{high} macrophages, which can phagocytose pristane, were increased after pristane injection (**Figure 4E**). However, their percentages were comparable between wild type and B/Atg7$^{-/-}$ mice (**Figure 4E**).

We next determined whether autoreactive memory B cells were present after treatment with pristane. Switched memory-like B cells (CD19^{+}CD138^{-}IgM^{-}IgD^{-}) were reported to be significantly increased in the pristane-treated BALB/c mice (71). However, whether autoantigen-specific memory B cells are expanded after pristane treatment have not been characterized. We also detected increased number of total IgG^{+} memory B cells (CD19^{+}DUMP^{-}

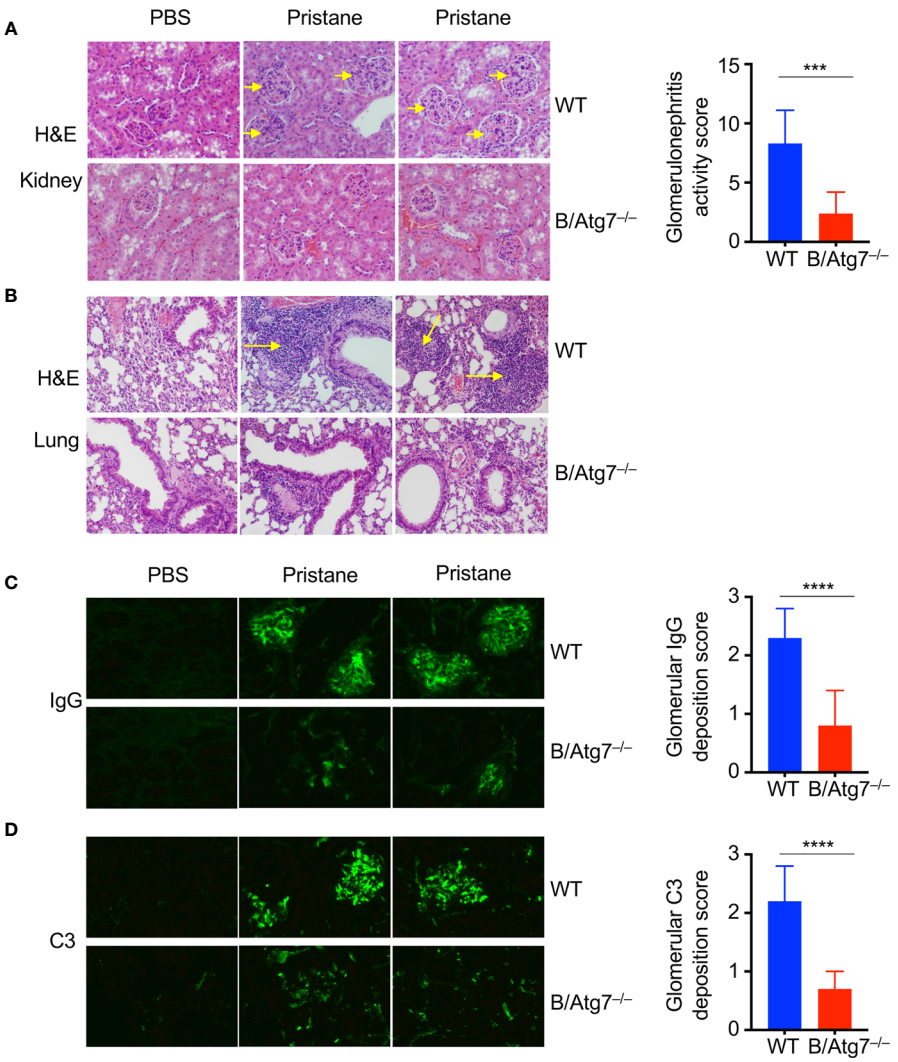

FIGURE 3 | Induction of glomerulonephritis in pristane injected-wild type but not B/Atg7$^{-/-}$ mice. H&E staining of kidney **(A)** and lung **(B)** sections of WT and B-Atg7$^{-/-}$ mice 6-month after injection with pristane or PBS. Enlarged glomeruli were marked by arrows in **(A)**. Lymphocyte infiltration was marked by arrows in **(B)**. Glomerulonephritis activity score was 8.3 ± 2.8 *versus* 2.4 ± 1.8 for wild type and B/Atg7$^{-/-}$ mice, respectively. **(C)** Kidney sections were stained with FITC-anti-mouse IgG to reveal IgG deposit. **(D)** Kidney sections were stained with FITC anti mouse-complement C3. Glomerulonephritis deposition scores for IgG and C3 were plotted and presented as mean ± SD. ***$P < 0.001$, ****$P < 0.0001$, as determined by two-tailed Student's *t*-test. Representative images from 2 mice each group were shown. (n=8 per group).

CD38^{+}IgG^{+}) in wild type mouse after pristane treatment (**Figure 4F**). Those IgG^{+} memory B cells were significantly reduced in B/Atg7$^{-/-}$ mice (**Figure 4F**). Moreover, we found that RNP/Sm-specific memory B cells (CD19^{+}DUMP^{-}CD38^{+} IgG^{+}RNP/Sm^{+}) in wild type mice could be detected by flow cytometry after injection with pristane (**Figure 4F**). These autoreactive B cells mainly display the DUMP^{-}IgG^{+}CD38^{+} memory but not the DUMP^{-}IgG^{+}CD38^{-}GC B cell phenotypes (**Figure 4F**). Moreover, such autoreactive memory B cells were significantly reduced in B/Atg7$^{-/-}$ mice (**Figure 4F**). These results suggest that autophagy is important for the development of both autoreactive memory B cells and nonautoreactive memory B cells. We also examined the IgM^{-}IgD^{-}CD19^{lo}CD138^{+} plasma cells (72) in the spleens of pristane-treated mice. We observed a slight decrease in splenic plasma cells in pristane treated B-Atg7$^{-/-}$ mice, but it did not reach statistical significance (**Figure 4G**). It is possible that a continuous replenishment of new short-lived plasma cells induced by pristane treatment compensates the loss of those cells in the absence of autophagy.

Adoptive Transfer of Autoreactive Memory B Cells Restores Autoantibody Production in B/Atg7$^{-/-}$ Mice

We found that RNP^{+} memory B cells from pristane-treated wild type mice upregulated autophagy as shown by the increased LC3 punctate staining, to a similar extent as RNP^{+} memory B cells

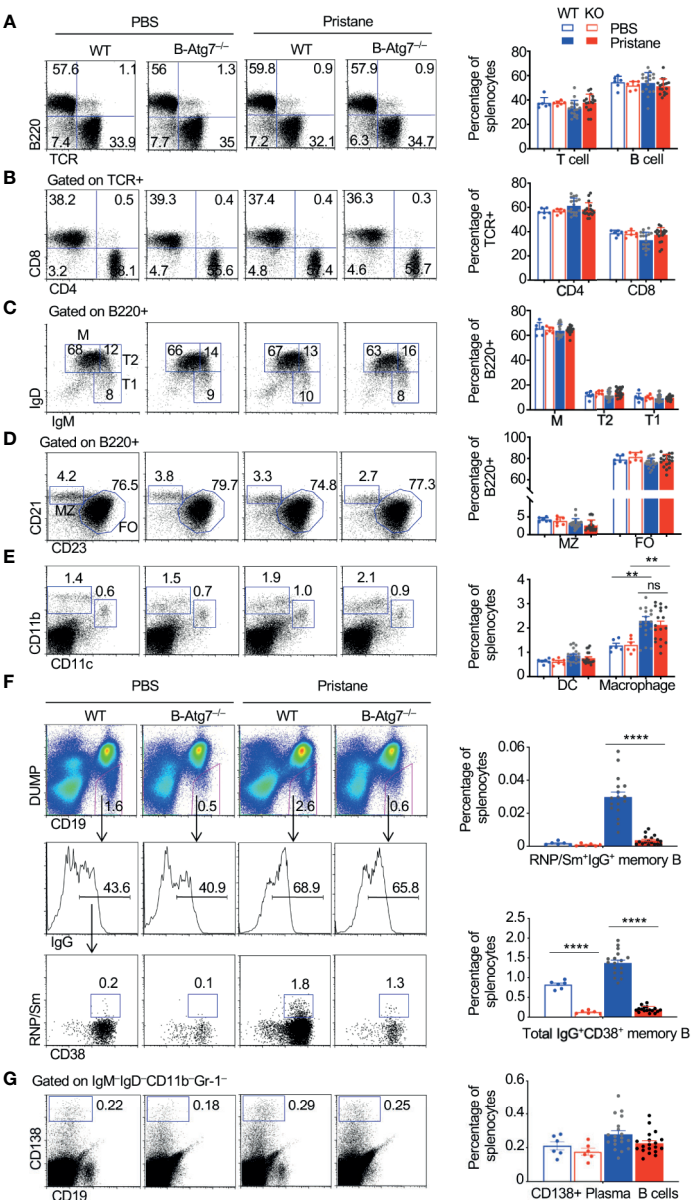

FIGURE 4 | Accumulation of autoreactive memory B cells in WT but not B-Atg7$^{-/-}$ mice injected with pristane. **(A–E)** Splenocytes from pristane or PBS injected WT or B/Atg7$^{-/-}$ mice (6-month post injection) were stained with different fluorochrome-conjugated antibodies for T, B, dendritic cells (DC), and macrophages as indicated, followed by flow cytometry analysis. **(F)** Splenocytes were also stained with PE-conjugated antibodies to CD11b, Gr-1, IgM, IgD, and CD138; PE-Cy7-anti-CD19; Pacific Blue anti-CD38; APC-anti-IgG, and Alexa Fluor 488-conjugated RNP/Sm. DUMP$^-$(IgM$^-$IgD$^-$CD11b$^-$Gr-1$^-$CD138$^-$) CD19$^+$ B cells were gated. Frequencies of RNP/Sm-specific memory B cells (DUMP$^-$CD19$^+$CD38$^+$RNP/Sm$^+$IgG$^+$) and total IgG+ memory B cells (DUMP$^-$CD19$^+$CD38$^+$IgG$^+$) were analyzed by flow cytometry. **(G)** Splenocytes were stained with biotinylated antibodies to CD11b, Gr-1, IgM, IgD followed by Streptavidin PE-Cy7 and FITC-anti-CD19. IgM$^-$IgD$^-$CD11b$^-$Gr-1$^-$ cells were gated. CD138$^+$CD19$^{lo/-}$ plasma cells were then analyzed. A representative analysis of one mice/group was shown. Percentage of each cell population in the spleen was plotted. Data are presented as mean ± s.e.m. $^{**}P < 0.01$, $^{****}P < 0.0001$, ns, not statistically significant, as determined by two-tailed Student's *t*-test.

harvested from MRL-*lpr* lupus mice did (**Figure 5A**). To confirm the RNP$^+$ memory B cells that we detected by flow cytometry (**Figure 4F**) could lead to autoantibody production, we sorted RNP/Sm-specific memory B cells from pristane-treated wild type mice and transferred them into wild type or B/Atg7$^{-/-}$ recipient mice. We then challenged recipients of memory B cells and nonrecipient controls with RNP/Sm in Alum. Three days later, sera were collected to measure the production of RNP/Sm autoantibody. We detected production of RNP/Sm autoantibody in both wild type and B/Atg7$^{-/-}$ recipient mice, suggesting CD19$^+$DUMP$^-$CD38$^+$IgG$^+$RNP/Sm$^+$ autoreactive memory B cells are functional RNP/Sm-specific memory B

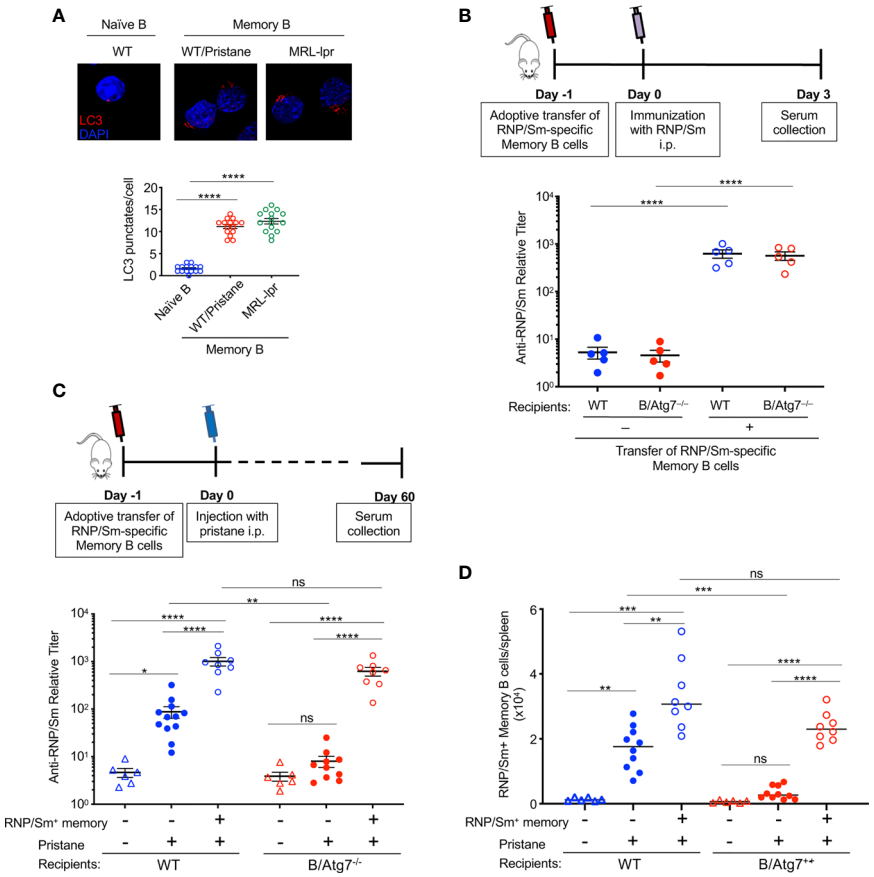

FIGURE 5 | Transfer of autoreactive memory B cells rescues autoantibody production in B-Atg7$^{-/-}$ mice. **(A)** RNP-specific memory B cells sorted from MRL-*lpr* mice or pristane-treated wild type mice, together with naïve B cells sorted from untreated wild type mice were used for immunocytochemistry staining of LC3. Data are representative of two independent experiments using cells from a pool of 3 mice each group for sorting. LC3 punctates per cell were quantitated (n=15). **(B)** RNP/Sm-specific memory B cells were sorted from pristane-treated wild type mice (5-6 mice post injection) and transferred (1x10^4 cells/mice) retroorbitally into wild type and B-Atg7$^{-/-}$ mice. Mice were injected with RNP/Sm precipitated in Alum (20μg/mice, i.p.) a day later. Sera were collected 3 days after immunization and titers of RNP/Sm-specific antibodies were determined by ELISA. **(C, D)** RNP/Sm-specific memory B cells were sorted and transferred retroorbitally into WT and B-Atg7$^{-/-}$ mice (10^4 cells/mice), followed by injection of pristane (0.5 ml, i.p.) one day later. Mice that did not receive memory cell transfer were included as controls. Sorted naïve B cells (2x10^5/mice) were co-injected as filler cells to minimize cell loss during injection. Sera were collected 2 months later, and RNP/Sm specific antibodies were measured by ELISA **(C)**. DUMP$^-$CD19$^+$CD38$^+$RNP/Sm$^+$IgG$^+$ memory B cells were also quantified **(D)**. Data are presented as mean ± s.e.m. (n=6-12). $^*P < 0.05$, $^{**}P < 0.01$, $^{***}P < 0.001$, $^{****}P < 0.0001$ (determined by two-tailed Student's *t*-test). NS, not statistically significant.

cells and can be rapidly activated to develop into autoantibody-producing cells (**Figure 5B**).

Next, we asked whether RNP/Sm-specific memory B cells could restore pristane-induced autoantibody production in B/Atg7$^{-/-}$ mice. RNP/Sm-specific memory B cells from pristane-treated wild type mice were sorted, and adoptively transferred into wild type or B/Atg7$^{-/-}$ recipient mice in parallel experiments. After 24 h, both the recipient mice and control mice without receiving cell transfer were challenged with pristane. Atg7$^{-/-}$ RNP/Sm-specific memory B cells from B/Atg7$^{-/-}$ mice were not used for transfer because not sufficient number of cells could be obtained. Two months after pristane administration, autoantibodies against RNP/Sm could be detected in some wild type mice but not B/Atg7$^{-/-}$ mice without receiving cell transfer (**Figure 5C**). However, adoptive transfer of wild type RNP/Sm-specific memory B cells resulted in significant production of RNP and Sm-specific antibodies in both wild type and B/Atg7$^{-/-}$ recipient mice two months post pristane treatment (**Figure 5C**). Flow cytometry analysis of memory B cells indicate those transferred RNP/Sm-specific memory B cells were expanded in the spleens of B/Atg7$^{-/-}$ recipient mice compared with non-recipient controls (**Figure 5D**). These results suggest that autoreactive memory B cells can restore autoantibody production in B/Atg7$^{-/-}$ mice. These results suggest that autophagy plays an important role in the protection of autoreactive memory B cells to maintain autoantibody production in lupus.

DISCUSSION

Significant expansion of memory B cells has been reported to be present in humans and mice with lupus. The contribution of the expanded memory B cell population to lupus pathogenesis is

unclear. Here we show that autoantigen-specific memory B cells can be detected in *lpr* mice, and in mice with pristane-induced lupus. Moreover, these autoreactive memory B cells increased autoantibody production after adoptive transfer. Interestingly, deficiency of autophagy led to the loss of autoreactive memory B cells and attenuated glomerulonephritis and pulmonary inflammation in a pristane-induced lupus model. These results suggest that autoreactive memory B cells are important for the maintenance of autoantibody production and autoimmune manifestations in lupus. Autophagy plays an important role in promoting autoantibody production by protecting these autoreactive memory B cells.

Previous studies have observed that switched memory B cells were increased in MRL-lpr lupus mice, however, the identity of those memory B cells has not been well characterized. Using fluorochrome-conjugated autoantigens, we detected IgG^+CD38^+ memory B cells with specificity for different autoantigens in mice with lupus by flow cytometry. We have demonstrated that autoantigen-specific memory B cells such as Sm/RNP or dsDNA specific autoreactive memory B cells are increased in MRL-lpr lupus mice. We have also found that Sm/RNP specific autoreactive memory B cells are increased in mice with pristane-induced lupus. Like memory B cells specific for foreign antigens that depend on autophagy for survival (30), these autoreactive memory B cells also upregulated expression of autophagy-related genes and display high levels of autophagy. Deletion of autophagy leads to the loss of autoreactive memory B cells and total IgG^+ memory B cells in pristane-treated mice to a similar extent, suggesting an equally critical role for autophagy in the protection of autoreactive memory B cells and normal memory B cell compartment. We have previously found that autophagy is essential for the long-term survival of memory B cells but not the generation of memory B cells after their initial formation (30, 31). We and others have also shown that autophagy is not required for GC formation and B cell activation or proliferation (30, 31, 38). It is thus possible that autoreactive memory B cells are generated in normal numbers initially but cannot persist in autophagy-deficient mice.

It has been shown that knockout of Atg5 in B cells attenuates the development of autoantibody production, lymphocyte infiltration and mortality in toll-like receptor 7-transgenic mice (40), supporting an important role for B cell autophagy in the development of lupus-like autoimmunity. In addition, autophagy is important for the survival of long-lived plasma cells and autoantibody production during autoimmune responses in *lpr* mice (38). In the current study, we show that autoreactive memory B cells specific for self-antigens can be induced in a pristane-induced mouse lupus model, but these cells are significantly reduced in autophagy-deficient mice. Adoptive transfer of autoreactive memory B cells led to autoantibody production in recipient mice. Moreover, transfer of wild type autoreactive memory B cells restored autoantibody production in autophagy-deficient mice upon pristane injection. Our data thus support an important role for autoreactive memory B cells in the development of lupus by promoting persistent autoantibody production. Although our study has demonstrated the important contribution of memory B cells to autoantibody production, we are not excluding the role of autophagy in other B cell types, particularly long-lived plasma cells in autoantibody production and immune complex deposition. Taking these data together, autophagy is likely required for the survival of both autoreactive memory B cells and autoreactive long-lived plasma cells to promote autoantibody production.

Treatment with pristane can induce glomerulonephritis with enlargements of kidney glomeruli, the accumulation of intraglomerular mesangial cells and deposits of immune complexes in the kidney. We observed that autophagy deficiency in B cells resulted in the loss of autoreactive memory B cells, reduced immune complex and complement deposition and ameliorated the development of autoimmune symptoms induced by pristane, including the glomerulonephritis and pulmonary capillaritis. These results suggest that accumulation of autoreactive memory B cells, which could lead to overproduction of autoantibodies, is potentially the main causes of kidney and lung lesions in the pristane-induced lupus model. Significant expansion of memory B cells in systemic autoimmune diseases also supports the important roles for autoreactive memory B cells in disease development.

Pristane-induced lupus can cause pulmonary hemorrhage resembling that in SLE, and cause mortality in mice on C57BL/6 background (52, 53). Our results demonstrate that loss of ATG7 in B cells reduced the susceptibility of mice to pristane-induced pulmonary hemorrhage. While treatment with pristane caused 18% death in wild type mice, $B/Atg7^{-/-}$ mice were resistant. Moreover, six months after pristane injection, $B/Atg7^{-/-}$ mice did not show significant pulmonary capillaritis or leukocyte infiltration compared to wild type controls. B cells have been reported to be required for pristane-induced pulmonary hemorrhage (52, 53, 67). Since memory B cells are potent antigen presenting cells and autophagy could regulate antigen presentation (16, 17, 73), it is possible that defective antigen presentation by autophagy-deficient memory B cells resulted in defective amplification of autoimmune responses, thus leading to the reduced susceptibility of $B/Atg7^{-/-}$ mice to pristane-induced pulmonary hemorrhage. Alternatively, reduced autoantibody production and immune complex deposits in $B/Atg7^{-/-}$ mice could significantly attenuate pristane-induced pulmonary vasculitis. These possibilities are not mutually exclusive and remain to be investigated.

Although adoptive transfer of wild type Sm/RNP specific autoreactive memory B cells restored autoantibody production in $B\text{-}Atg7^{-/-}$ mice, we did not observe significantly increased lung and kidney pathology in pristane-treated $B\text{-}Atg7^{-/-}$ mice two months after adoptive transfer (data not shown). Several mechanisms may account for this observation. First, it is possible that multiple different types of autoreactive memory B cells are needed for producing lupus pathology in kidney and lung in pristane-treated $B\text{-}Atg7^{-/-}$ mice, while transfer of Sm/RNP specific memory B cells alone is not sufficient. Second, a larger number of Sm-specific memory B cells may be required for transfer into $B\text{-}Atg7^{-/-}$ mice to produce pristane-induced lupus pathology, and it could take longer than 2 months for recipients to develop lupus pathology in kidney and lung. Third, besides

protecting memory B and plasma cell survival, autophagy may have additional roles in B cells which is also required for producing lupus pathology in pristane-treated mice. The exact mechanism leading to this phenomenon remains to be investigated.

Multiple different studies have confirmed an essential role for autophagy in the maintenance of long-lived plasma cells (35, 36, 38–40). The effect of autophagy on short-lived plasma cells has been less clear. While autophagy has been shown to be required for B cell differentiation into ASCs *in vitro*, several studies have shown that plasma cell number in the spleen is not affected by the deletion of Atg5 in B cells (36, 38). We have observed a slight decrease in the splenic $CD19^{lo}IgM^{-}IgD^{-}CD138^{+}$ plasma cells in pristane treated B-$Atg7^{-/-}$ mice, but it did not reach statistical significance (**Figure 4G**). Interestingly, it has also been shown that autophagy deficiency does not affect short-lived plasma cells in the spleen of autoimmune CD21cre$Atg5^{f/f}$ lpr/lpr mice (38). A possible explanation is that a continuous replenishment of new short-lived plasma cells induced by pristane treatment in our model compensates the loss of those cells in the absence of autophagy. Another explanation is that autophagy might be differentially required for the long-lived and short-lived plasma cell survival. Long-lived, slowly dividing plasma cells in the bone marrow might rely more on autophagy for their survival, while short-lived plasma cells rely less on autophagy for their survival.

Overall, humoral immune memory is mediated by long-lived plasma cells, as well as memory B cells which upon antigenic challenge can develop into plasma cells. We propose a model for autophagy in B cells in the regulation of pristane-induced lupus (**Figure 6**). Pristane treatment induces profound inflammation and apoptotic cell death (52, 71, 74), which led to breakdown of tolerance and activation of autoreactive B cells *via* T cell dependent or independent mechanisms. Some of the activated autoreactive B cells develop into short-lived or long-lived plasma cells which produce autoantibodies against RNP, Sm and other nuclear autoantigens, whereas some of the activated autoreactive B cells will give rise to autoreactive memory B cells. The persistent presence of autoantigens in pristane-treated mice results in continual stimulation of autoreactive memory B cells which can rapidly differentiate into long lived autoantibody-producing plasma cells. The rapid development of memory B cells into antibody-producing cells accelerates autoantibody production and sustains systemic autoimmunity in pristane-treated wild type mice. The loss of autophagy in B cells abolishes the survival of memory B cells and long-lived plasma cells, resulting in significant reduction in autoantibody production and attenuated glomerulonephritis and pulmonary inflammation in the pristane-treated B/$Atg7^{-/-}$ mice (**Figure 6**).

Memory B cells specific for autoantigens has not been demonstrated in previous studies. Whether an essential role for autophagy in the persistent of these autoantigen-specific memory B cells has not been established. Our current study shows the existence of memory B cells specific for Sm/RNP and dsDNA in *lpr* mice by flow cytometry. Moreover, Sm/RNP-specific memory B cells were reduced in the pristane-induced autoimmune lupus model. Therefore, our study demonstrates the role for autophagy in the maintenance of autoimmune memory B cells specific for defined autoantigens. In vitro differentiation and adoptive transfer experiments suggest that these memory B cells are functional autoreactive memory B cells and can develop into autoantibody-producing cells. Deficiency in autophagy reduced autoreactive memory B cells and attenuated the autoimmune manifestations in pristane-treated mice. However, transfer of wild type autoreactive memory B cells could restore autoantibody production in autophagy-deficient mice. These data suggest that autoreactive memory B cells plays an important role in the development of humoral autoimmunity. Our study, together with the previous report that autophagy is required for long-lived plasma cells in *lpr* mice (38), suggests that targeting autophagy may be effective for eliminating autoreactive memory B cells and long-lived plasma cells to control autoimmunity in lupus.

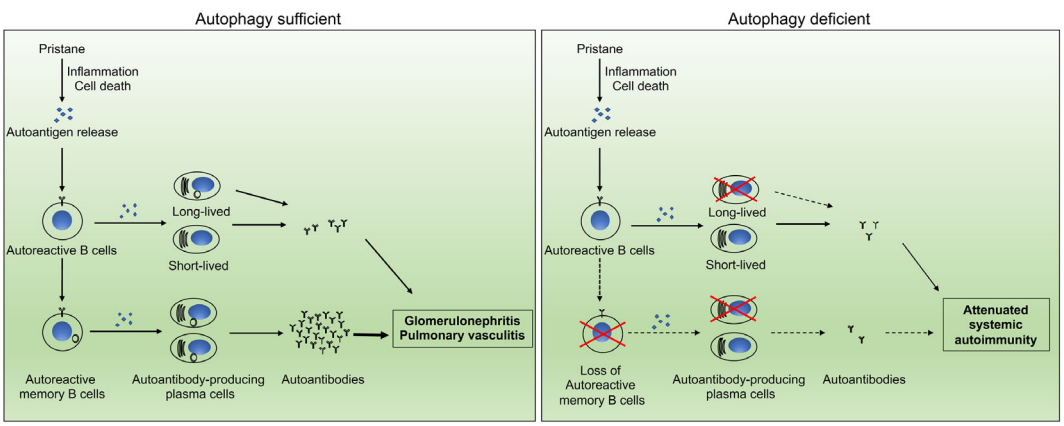

FIGURE 6 | Schematic representation of the impact of autophagy on autoantibody production. Autophagy regulates the development of systemic autoimmunity through regulation of autoreactive memory B cells and long-lived plasma cells in pristane-induced lupus model.

DATA AVAILABILITY STATEMENT

The raw data supporting the conclusions of this article will be made available by the authors, without undue reservation.

ETHICS STATEMENT

The animal study was reviewed and approved by Institutional Animal Care and Use Committees of Baylor College of Medicine and the Houston Methodist Research Institute.

AUTHOR CONTRIBUTIONS

AJ and MC designed and performed experiments and analyzed data. RS, YF, and JMW performed experiments. JW designed experiments and wrote the manuscript. MC supervised the study and wrote the manuscript. All authors contributed to the article and approved the submitted version.

FUNDING

This study was supported by funding from American Heart Association (15GRNT25700357 to MC), Lupus Research Institute (MC and JW), Department of Defense (PR140593 to MC), and the NIH (R01AI116644 and R01AI123221 to JW). Flow cytometry and cell sorting for this project was supported by the Cytometry and Cell Sorting Core at Baylor College of Medicine with funding from the NIH (P30 AI036211, P30 CA125123, and S10 RR024574).

ACKNOWLEDGMENTS

We thank Dr. Masaaki Komatsu for $Atg7^{flox}$ mice.

REFERENCES

1. Tsokos GC. Systemic Lupus Erythematosus. *N Engl J Med* (2011) 365:2110–21. doi: 10.1056/NEJMra1100359
2. Anolik JH. B Cell Biology: Implications for Treatment of Systemic Lupus Erythematosus. *Lupus* (2013) 22:342–9. doi: 10.1177/0961203312471576
3. Perl A. Pathogenic Mechanisms in Systemic Lupus Erythematosus. *Autoimmunity* (2010) 43:1–6. doi: 10.3109/08916930903374741
4. Flesher DL, Sun X, Behrens TW, Graham RR, Criswell LA. Recent Advances in the Genetics of Systemic Lupus Erythematosus. *Expert Rev Clin Immunol* (2010) 6:461–79. doi: 10.1586/eci.10.8
5. Dorner T, Jacobi AM, Lipsky PE. B Cells in Autoimmunity. *Arthritis Res Ther* (2009) 11:247. doi: 10.1186/ar2780
6. Pisetsky DS, Grammer AC, Ning TC, Lipsky PE. Are Autoantibodies the Targets of B-Cell-Directed Therapy? *Nat Rev Rheumatol* (2011) 7:551–6. doi: 10.1038/nrrheum.2011.108
7. Chan OT, Madaio MP, Shlomchik MJ. The Central and Multiple Roles of B Cells in Lupus Pathogenesis. *Immunol Rev* (1999) 169:107–21. doi: 10.1111/j.1600-065x.1999.tb01310.x
8. Nashi E, Wang Y, Diamond B. The Role of B Cells in Lupus Pathogenesis. *Int J Biochem Cell Biol* (2010) 42:543–50. doi: 10.1016/j.biocel.2009.10.011
9. Mietzner B, Tsuiji M, Scheid J, Velinzon K, Tiller T, Abraham K, et al. Autoreactive IgG Memory Antibodies in Patients With Systemic Lupus Erythematosus Arise From Nonreactive and Polyreactive Precursors. *Proc Natl Acad Sci USA* (2008) 105:9727–32. doi: 10.1073/pnas.0803644105
10. Tiller T, Tsuiji M, Yurasov S, Velinzon K, Nussenzweig MC, Wardemann H. Autoreactivity in Human IgG+ Memory B Cells. *Immunity* (2007) 26:205–13. doi: 10.1016/j.immuni.2007.01.009
11. Sweet RA, Cullen JL, Shlomchik MJ. Rheumatoid Factor B Cell Memory Leads to Rapid, Switched Antibody-Forming Cell Responses. *J Immunol* (2013) 190:1974–81. doi: 10.4049/jimmunol.1202816
12. McHeyzer-Williams LJ, McHeyzer-Williams MG. Antigen-Specific Memory B Cell Development. *Annu Rev Immunol* (2005) 23:487–513. doi: 10.1146/annurev.immunol.23.021704.115732
13. Shlomchik MJ, Weisel F. Germinal Center Selection and the Development of Memory B and Plasma Cells. *Immunol Rev* (2012) 247:52–63. doi: 10.1111/j.1600-065X.2012.01124.x
14. Mackay M, Stanevsky A, Wang T, Aranow C, Li M, Koenig S, et al. Selective Dysregulation of the FcgammaIIB Receptor on Memory B Cells in SLE. *J Exp Med* (2006) 203:2157–64. doi: 10.1084/jem.20051503
15. Dorner T, Giesecke C, Lipsky PE. Mechanisms of B Cell Autoimmunity in SLE. *Arthritis Res Ther* (2011) 13:243. doi: 10.1186/ar3433
16. Hao Z, Duncan GS, Seagal J, Su YW, Hong C, Haight J, et al. Fas Receptor Expression in Germinal-Center B Cells Is Essential for T and B Lymphocyte Homeostasis. *Immunity* (2008) 29:615–27. doi: 10.1016/j.immuni.2008.07.016
17. Takahashi Y, Ohta H, Takemori T. Fas Is Required for Clonal Selection in Germinal Centers and the Subsequent Establishment of the Memory B Cell Repertoire. *Immunity* (2001) 14:181–92. doi: 10.1016/s1074-7613(01)00100-5
18. Jacobi AM, Reiter K, Mackay M, Aranow C, Hiepe F, Radbruch A, et al. Activated Memory B Cell Subsets Correlate With Disease Activity in Systemic Lupus Erythematosus: Delineation by Expression of CD27, IgD, and CD95. *Arthritis Rheum* (2008) 58:1762–73. doi: 10.1002/art.23498
19. Edwards JC, Szczepanski L, Szechinski J, Filipowicz-Sosnowska A, Emery P, Close DR, et al. Efficacy of B-Cell-Targeted Therapy With Rituximab in Patients With Rheumatoid Arthritis. *N Engl J Med* (2004) 350:2572–81. doi: 10.1056/NEJMoa032534
20. Leandro MJ, Cambridge G, Ehrenstein MR, Edwards JC. Reconstitution of Peripheral Blood B Cells After Depletion With Rituximab in Patients With Rheumatoid Arthritis. *Arthritis Rheum* (2006) 54:613–20. doi: 10.1002/art.21617
21. Vital EM, Dass S, Buch MH, Henshaw K, Pease CT, Martin MF, et al. B Cell Biomarkers of Rituximab Responses in Systemic Lupus Erythematosus. *Arthritis Rheum* (2011) 63:3038–47. doi: 10.1002/art.30466
22. Roll P, Dorner T, Tony HP. Anti-CD20 Therapy in Patients With Rheumatoid Arthritis: Predictors of Response and B Cell Subset Regeneration After Repeated Treatment. *Arthritis Rheum* (2008) 58:1566–75. doi: 10.1002/art.23473
23. Moller B, Aeberli D, Eggli S, Fuhrer M, Vajtai I, Vogelin E, et al. Class-Switched B Cells Display Response to Therapeutic B-Cell Depletion in Rheumatoid Arthritis. *Arthritis Res Ther* (2009) 11:R62. doi: 10.1186/ar2686
24. Levine B, Klionsky DJ. Development by Self-Digestion: Molecular Mechanisms and Biological Functions of Autophagy. *Dev Cell* (2004) 6:463–77. doi: 10.1016/s1534-5807(04)00099-1
25. Yorimitsu T, Klionsky DJ. Autophagy: Molecular Machinery for Self-Eating. *Cell Death Differ* (2005) 12(Suppl 2):1542–52. doi: 10.1038/sj.cdd.4401765
26. He C, Klionsky DJ. Regulation Mechanisms and Signaling Pathways of Autophagy. *Annu Rev Genet* (2009) 43:67–93. doi: 10.1146/annurev-genet-102808-114910
27. Lum JJ, Bauer DE, Kong M, Harris MH, Li C, Lindsten T, et al. Growth Factor Regulation of Autophagy and Cell Survival in the Absence of Apoptosis. *Cell* (2005) 120:237–48. doi: 10.1016/j.cell.2004.11.046
28. Colell A, Ricci JE, Tait S, Milasta S, Maurer U, Bouchier-Hayes L, et al. GAPDH and Autophagy Preserve Survival After Apoptotic Cytochrome C Release in the Absence of Caspase Activation. *Cell* (2007) 129:983–97. doi: 10.1016/j.cell.2007.03.045

29. Green DR, Galluzzi L, Kroemer G. Mitochondria and the Autophagy-Inflammation-Cell Death Axis in Organismal Aging. *Science* (2011) 333:1109–12. doi: 10.1126/science.1201940
30. Chen M, Hong MJ, Sun H, Wang L, Shi X, Gilbert BE, et al. Essential Role for Autophagy in the Maintenance of Immunological Memory Against Influenza Infection. *Nat Med* (2014) 20:503–10. doi: 10.1038/nm.3521
31. Chen M, Kodali S, Jang A, Kuai L, Wang J. Requirement for Autophagy in the Long-Term Persistence But Not Initial Formation of Memory B Cells. *J Immunol* (2015) 194:2607–15. doi: 10.4049/jimmunol.1403001
32. Puleston DJ, Zhang H, Powell TJ, Lipina E, Sims S, Panse I, et al. Autophagy Is a Critical Regulator of Memory CD8(+) T Cell Formation. *Elife* (2014) 3. doi: 10.7554/eLife.03706
33. Xu X, Araki K, Li S, Han JH, Ye L, Tan WG, et al. Autophagy Is Essential for Effector CD8(+) T Cell Survival and Memory Formation. *Nat Immunol* (2014) 15:1152–61. doi: 10.1038/ni.3025
34. Murera D, Arbogast F, Arnold J, Bouis D, Muller S, Gros F. CD4 T Cell Autophagy Is Integral to Memory Maintenance. *Sci Rep* (2018) 8:5951. doi: 10.1038/s41598-018-23993-0
35. Pengo N, Scolari M, Oliva L, Milan E, Mainoldi F, Raimondi A, et al. Plasma Cells Require Autophagy for Sustainable Immunoglobulin Production. *Nat Immunol* (2013) 14:298–305. doi: 10.1038/ni.2524
36. Conway KL, Kuballa P, Khor B, Zhang M, Shi HN, Virgin HW, et al. ATG5 Regulates Plasma Cell Differentiation. *Autophagy* (2013) 9:528–37. doi: 10.4161/auto.23484
37. Gupta SS, Sharp R, Hofferek C, Kuai L, Dorn GW, Wang J, et al. NIX-Mediated Mitophagy Promotes Effector Memory Formation in Antigen-Specific CD8(+) T Cells. *Cell Rep* (2019) 29:1862–77.e7. doi: 10.1016/j.celrep.2019.10.032
38. Arnold J, Murera D, Arbogast F, Fauny JD, Muller S, Gros F. Autophagy Is Dispensable for B-Cell Development But Essential for Humoral Autoimmune Responses. *Cell Death Differ* (2016) 23:853–64. doi: 10.1038/cdd.2015.149
39. Clarke AJ, Ellinghaus U, Cortini A, Stranks A, Simon AK, Botto M, et al. Autophagy Is Activated in Systemic Lupus Erythematosus and Required for Plasmablast Development. *Ann Rheum Dis* (2015) 74:912–20. doi: 10.1136/annrheumdis-2013-204343
40. Weindel CG, Richey LJ, Bolland S, Mehta AJ, Kearney JF, Huber BT. B Cell Autophagy Mediates TLR7-Dependent Autoimmunity and Inflammation. *Autophagy* (2015) 11:1010–24. doi: 10.1080/15548627.2015.1052206
41. Han JW, Zheng HF, Cui Y, Sun LD, Ye DQ, Hu Z, et al. Genome-Wide Association Study in a Chinese Han Population Identifies Nine New Susceptibility Loci for Systemic Lupus Erythematosus. *Nat Genet* (2009) 41:1234–7. doi: 10.1038/ng.472
42. International Consortium for Systemic Lupus Erythematosus G, Harley JB, Alarcon-Riquelme ME, Criswell LA, Jacob CO, Kimberly RP, et al. Genome-Wide Association Scan in Women With Systemic Lupus Erythematosus Identifies Susceptibility Variants in ITGAM, PXK, KIAA1542 and Other Loci. *Nat Genet* (2008) 40:204–10. doi: 10.1038/ng.81
43. Gateva V, Sandling JK, Hom G, Taylor KE, Chung SA, Sun X, et al. **A** Large-Scale Replication Study Identifies TNIP1, PRDM1, JAZF1, UHRF1BP1 and IL10 as Risk Loci for Systemic Lupus Erythematosus. *Nat Genet* (2009) 41:1228–33. doi: 10.1038/ng.468
44. Zhou XJ, Lu XL, Lv JC, Yang HZ, Qin LX, Zhao MH, et al. Genetic Association of PRDM1-ATG5 Intergenic Region and Autophagy With Systemic Lupus Erythematosus in a Chinese Population. *Ann Rheum Dis* (2011) 70:1330–7. doi: 10.1136/ard.2010.140111
45. Dang J, Li J, Xin Q, Shan S, Bian X, Yuan Q, et al. Gene-Gene Interaction of ATG5, ATG7, BLK and BANK1 in Systemic Lupus Erythematosus. *Int J Rheum Dis* (2016) 19:1284–93. doi: 10.1111/1756-185X.12768
46. Lee SJ, Silverman E, Bargman JM. The Role of Antimalarial Agents in the Treatment of SLE and Lupus Nephritis. *Nat Rev Nephrol* (2011) 7:718–29. doi: 10.1038/nrneph.2011.150
47. Yildirim-Toruner C, Diamond B. Current and Novel Therapeutics in the Treatment of Systemic Lupus Erythematosus. *J Allergy Clin Immunol* (2011) 127:303–12. doi: 10.1016/j.jaci.2010.12.1087
48. Rubinsztein DC, Gestwicki JE, Murphy LO, Klionsky DJ. Potential Therapeutic Applications of Autophagy. *Nat Rev Drug Discovery* (2007) 6:304–12. doi: 10.1038/nrd2272
49. Gros F, Arnold J, Page N, Decossas M, Korganow AS, Martin T, et al. Macroautophagy Is Deregulated in Murine and Human Lupus T Lymphocytes. *Autophagy* (2012) 8:1113–23. doi: 10.4161/auto.20275
50. Pierdominici M, Vomero M, Barbati C, Colasanti T, Maselli A, Vacirca D, et al. Role of Autophagy in Immunity and Autoimmunity, With a Special Focus on Systemic Lupus Erythematosus. *FASEB J* (2012) 26:1400–12. doi: 10.1096/fj.11-194175
51. Bernard NJ. Connective Tissue Diseases: How do Autoreactive B Cells Survive in SLE–Autophagy? *Nat Rev Rheumatol* (2014) 10:128. doi: 10.1038/nrrheum.2014.5
52. Reeves WH, Lee PY, Weinstein JS, Satoh M, Lu L. Induction of Autoimmunity by Pristane and Other Naturally Occurring Hydrocarbons. *Trends Immunol* (2009) 30:455–64. doi: 10.1016/j.it.2009.06.003
53. Satoh M, Richards HB, Shaheen VM, Yoshida H, Shaw M, Naim JO, et al. Widespread Susceptibility Among Inbred Mouse Strains to the Induction of Lupus Autoantibodies by Pristane. *Clin Exp Immunol* (2000) 121:399–405. doi: 10.1046/j.1365-2249.2000.01276.x
54. Komatsu M, Waguri S, Ueno T, Iwata J, Murata S, Tanida I, et al. Impairment of Starvation-Induced and Constitutive Autophagy in Atg7-Deficient Mice. *J Cell Biol* (2005) 169:425–34. doi: 10.1083/jcb.200412022
55. Austin HA, LR M, KM J, TT A, Balow JE. Diffuse Proliferative Lupus Nephritis: Identification of Specific Pathologic Features Affecting Renal Outcome. *Kidney Int* (1984) 25:689–95. doi: 10.1038/ki.1984.75
56. Chen M, Wang YH, Wang Y, Huang L, Sandoval H, Liu YJ, et al. Dendritic Cell Apoptosis in the Maintenance of Immune Tolerance. *Science* (2006) 311:1160–4. doi: 10.1126/science.1122545
57. Theofilopoulos AN, Dixon FJ. Murine Models of Systemic Lupus Erythematosus. *Adv Immunol* (1985) 37:269–390. doi: 10.1016/s0065-2776(08)60342-9
58. Izui S, Kelley VE, Masuda K, Yoshida H, Roths JB, Murphy ED. Induction of Various Autoantibodies by Mutant Gene Lpr in Several Strains of Mice. *J Immunol* (1984) 133:227–33.
59. Cohen PL, Eisenberg RA. Lpr and Gld: Single Gene Models of Systemic Autoimmunity and Lymphoproliferative Disease. *Annu Rev Immunol* (1991) 9:243–69. doi: 10.1146/annurev.iy.09.040191.001331
60. Hutcheson J, Scatizzi JC, Siddiqui AM, Haines GK3rd, Wu T, Li QZ, et al. Combined Deficiency of Proapoptotic Regulators Bim and Fas Results in the Early Onset of Systemic Autoimmunity. *Immunity* (2008) 28:206–17. doi: 10.1016/j.immuni.2007.12.015
61. Frese S, Diamond B. Structural Modification of DNA–a Therapeutic Option in SLE? *Nat Rev Rheumatol* (2011) 7:733–8. doi: 10.1038/nrrheum.2011.153
62. Migliorini P, Baldini C, Rocchi V, Bombardieri S. Anti-Sm and Anti-RNP Antibodies. *Autoimmunity* (2005) 38:47–54. doi: 10.1080/08916930400022715
63. Russell RC, Tian Y, Yuan H, Park HW, Chang YY, Kim J, et al. ULK1 Induces Autophagy by Phosphorylating Beclin-1 and Activating VPS34 Lipid Kinase. *Nat Cell Biol* (2013) 15:741–50. doi: 10.1038/ncb2757
64. Hara T, Takamura A, Kishi C, Iemura S, Natsume T, Guan JL, et al. FIP200, a ULK-Interacting Protein, Is Required for Autophagosome Formation in Mammalian Cells. *J Cell Biol* (2008) 181:497–510. doi: 10.1083/jcb.200712064
65. Xie Z, Klionsky DJ. Autophagosome Formation: Core Machinery and Adaptations. *Nat Cell Biol* (2007) 9:1102–9. doi: 10.1038/ncb1007-1102
66. Kabeya Y, Mizushima N, Yamamoto A, Oshitani-Okamoto S, Ohsumi Y, Yoshimori T. LC3, GABARAP and GATE16 Localize to Autophagosomal Membrane Depending on Form-II Formation. *J Cell Sci* (2004) 117:2805–12. doi: 10.1242/jcs.01131
67. Barker TT, Lee PY, Kelly-Scumpia KM, Weinstein JS, Nacionales DC, Kumagai Y, et al. Pathogenic Role of B Cells in the Development of Diffuse Alveolar Hemorrhage Induced by Pristane. *Lab Invest* (2011) 91:1540–50. doi: 10.1038/labinvest.2011.108
68. Satoh M, Kumar A, Kanwar YS, Reeves WH. Anti-Nuclear Antibody Production and Immune-Complex Glomerulonephritis in BALB/c Mice Treated With Pristane. *Proc Natl Acad Sci USA* (1995) 92:10934–8. doi: 10.1073/pnas.92.24.10934
69. Chowdhary VR, Grande JP, Luthra HS, David CS. Characterization of Haemorrhagic Pulmonary Capillaritis: Another Manifestation of Pristane-Induced Lupus. *Rheumatol (Oxford)* (2007) 46:1405–10. doi: 10.1093/rheumatology/kem117
70. Pillai S, Cariappa A. The Follicular Versus Marginal Zone B Lymphocyte Cell Fate Decision. *Nat Rev Immunol* (2009) 9:767–77. doi: 10.1038/nri2656
71. Han S, Zhuang H, Xu Y, Lee P, Li Y, Wilson JC, et al. Maintenance of Autoantibody Production in Pristane-Induced Murine Lupus. *Arthritis Res Ther* (2015) 17:384. doi: 10.1186/s13075-015-0886-9

72. Tellier J, Nutt SL. Plasma Cells: The Programming of an Antibody-Secreting Machine. *Eur J Immunol* (2019) 49:30–7. doi: 10.1002/eji.201847517
73. Lee HK, Lund JM, Ramanathan B, Mizushima N, Iwasaki A. Autophagy-Dependent Viral Recognition by Plasmacytoid Dendritic Cells. *Science* (2007) 315:1398–401. doi: 10.1126/science.1136880
74. Weinstein JS, Delano MJ, Xu Y, Kelly-Scumpia KM, Nacionales DC, Li Y, et al. Maintenance of Anti-Sm/RNP Autoantibody Production by Plasma Cells Residing in Ectopic Lymphoid Tissue and Bone Marrow Memory B Cells. *J Immunol* (2013) 190:3916–27. doi: 10.4049/jimmunol.1201880

Conflict of Interest: The authors declare that the research was conducted in the absence of any commercial or financial relationships that could be construed as a potential conflict of interest.

frontiers in Immunology

REVIEW
published: 26 July 2021
doi: 10.3389/fimmu.2021.703918

BCR Affinity Influences T-B Interactions and B Cell Development in Secondary Lymphoid Organs

Alec J. Wishnie[1,2], *Tzippora Chwat-Edelstein*[2,3†], *Mary Attaway*[2†] *and Bao Q. Vuong*[1,2*]

[1] Biology PhD Program, Graduate Center, The City University of New York, New York, NY, United States, [2] Department of Biology, The City College of New York, New York, NY, United States, [3] Macaulay Honors College, New York, NY, United States

B cells produce high-affinity immunoglobulins (Igs), or antibodies, to eliminate foreign pathogens. Mature, naïve B cells expressing an antigen-specific cell surface Ig, or B cell receptor (BCR), are directed toward either an extrafollicular (EF) or germinal center (GC) response upon antigen binding. B cell interactions with $CD4^+$ pre-T follicular helper (pre-Tfh) cells at the T-B border and effector Tfh cells in the B cell follicle and GC control B cell development in response to antigen. Here, we review recent studies demonstrating the role of B cell receptor (BCR) affinity in modulating T-B interactions and the subsequent differentiation of B cells in the EF and GC response. Overall, these studies demonstrate that B cells expressing high affinity BCRs preferentially differentiate into antibody secreting cells (ASCs) while those expressing low affinity BCRs undergo further affinity maturation or differentiate into memory B cells (MBCs).

Keywords: BCR affinity, T follicular helper cells, germinal center, extrafollicular, B cell

OPEN ACCESS

Edited by:
Mark Robin Boothby, Vanderbilt University Medical Center, United States

Reviewed by:
Hong Zan, The University of Texas Health Science Center at San Antonio, United States
Robert W Maul, National Institute on Aging, National Institutes of Health (NIH), United States

***Correspondence:**
Bao Q. Vuong
bvuong@ccny.cuny.edu

†These authors have contributed equally to this work

Specialty section:
This article was submitted to B Cell Biology, a section of the journal Frontiers in Immunology

Received: *01 May 2021*
Accepted: *07 July 2021*
Published: *26 July 2021*

Citation:
Wishnie AJ, Chwat-Edelstein T, Attaway M and Vuong BQ (2021) BCR Affinity Influences T-B Interactions and B Cell Development in Secondary Lymphoid Organs. Front. Immunol. 12:703918. doi: 10.3389/fimmu.2021.703918

INTRODUCTION

B cells mediate the humoral immune response through the production of antigen-specific immunoglobulins (Igs) that neutralize foreign pathogens (1). After developing in the bone marrow from hematopoietic stem cells, B cells express a plasma membrane bound Ig, termed the B cell receptor (BCR), and localize to secondary lymphoid organs (SLOs), such as the spleen and lymph nodes (1, 2). B cells form B cell follicles within SLOs, where they first encounter soluble antigen or antigen presented by professional antigen presenting cells (APCs) (3, 4). In the B cell follicle, antigen and T cells stimulate B cells to alter the Ig genes. B cells change the constant region of the Ig heavy chains through class switch recombination (CSR), which alters the expressed Ig isotype from IgM to IgG, IgE, or IgA (1, 5). Unlike CSR, somatic hypermutation (SHM) generates mutations within the variable region of the Ig light and heavy chains to promote affinity maturation (5, 6). Both CSR and SHM require the enzyme activation induced cytidine deaminase (AID), as inactivating mutations in AID in mice and humans completely block both processes (5, 7). Interestingly, AID deficiency also increases the size of germinal centers and the number of germinal center B cells (5, 7).

Prior to the induction of CSR and SHM, antigen-binding to the naïve BCR induces B cell migration to the border of the T cell zone and the B cell follicle (T-B border) (8, 9). B cells migrate to the T-B border by upregulating the chemokine receptor CCR7, which responds to the T cell zone chemokines CCL19 and CCL21. These B cells also maintain expression of the chemokine receptor

CXCR5, which responds to the B cell follicle chemokine CXCL13 to prevent entry into the T cell zone (9). At the T-B border, B cells interact with pre-T follicular helper (Tfh) cells, a type of $CD4^+$ T helper (Th) cell, for the first time (8, 10). Here, BCR-antigen affinity influences the interactions between B cells and pre-Tfh cells and directs B cells toward either an extrafollicular (EF) or germinal center (GC) response (11–15). Both responses promote development and differentiation of B cells into memory B cells (MBCs); short-lived, highly proliferative plasmablasts (PBs); or terminally differentiated plasma cells (PCs) with varying lifespans (1, 16, 17). The EF response occurs earlier and results in lower affinity Igs than the GC response (18). Additionally, the EF response produces shorter lived MBCs and PCs, whereas the GC response generates longer lived MBCs and PCs (3).

The mechanisms that regulate mature B cell development in the SLOs remain unclear, specifically regarding differentiation, migration within SLOs, and the location for CSR and SHM. In this review, we discuss the signals controlling B cell progression through the EF or GC response, emphasizing the role of T-B interactions and BCR affinity in B cell fate determination. We also present emerging theories on the temporal regulation of Ig diversification within the SLO.

BCR AFFINITY AND T CELL HELP DIRECT B CELLS TO AN EF OR GC RESPONSE

After binding antigen, B cells undergo an EF or GC response, which depends in part on the BCR affinity for its antigen (3, 19) (**Figure 1**). Higher affinity BCRs preferentially induce an EF response, while lower affinity BCRs preferentially induce a GC response (11, 14, 15). BCR affinity also influences T-B cell interactions at the T-B border which, in turn, direct B cells to form a GC in the follicle or an EF response in the EF foci in the bridging channels of the spleen or medulla in the lymph nodes (20, 21).

BCR binding to antigen induces expression of B cell ligands that bind to receptors on the pre-Tfh cell surface (20). Naïve B cells exposed to high doses of α-IgM antibody, which crosslinks the BCR and mimics high affinity antigen binding to the BCR, significantly downregulate inducible T cell costimulator ligand (ICOSL) and upregulate programmed death ligand 1 (PDL1) *in vitro* (20). Ligation of ICOSL to ICOS on pre-Tfh cells promotes differentiation of the pre-Tfh cells into effector Tfh cells (22–25). Conversely, ligation of PDL1 to PD1 on pre-Tfh cells inhibits Tfh differentiation (26–29). Thus, naïve B cells expressing low affinity BCRs, which are destined for a GC response, promote differentiation of pre-Tfh cells into effector Tfh cells, whereas B cells expressing high affinity BCRs inhibit Tfh differentiation for a Tfh-independent EF response. Surprisingly, immunization of MD4 transgenic mice with high affinity hen egg lysozyme (HEL) or low affinity duck egg lysozyme (DEL) does not recapitulate the downregulation of ICOSL observed following *in vitro* stimulation of BCR with high levels of α-IgM (20). However, inhibiting ICOS-ICOSL interactions with a α-ICOSL antibody in MD4 mice immunized with DEL, but not HEL, prevents Tfh differentiation *in vivo*, suggesting that naïve B cells expressing low affinity BCRs promote Tfh differentiation *in vivo* through ICOSL (20). This result also demonstrates a role for antigen-

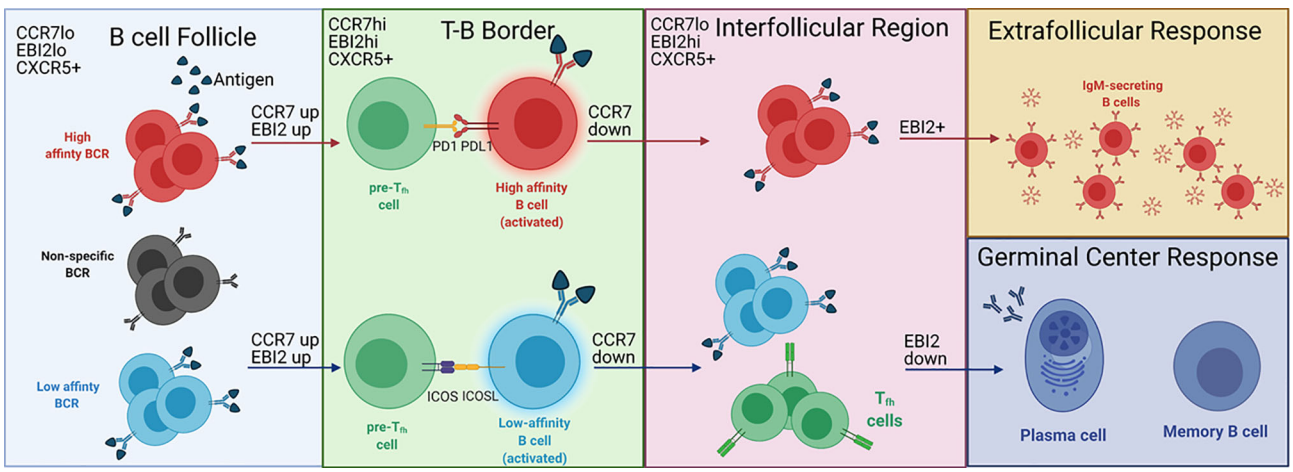

FIGURE 1 | BCR affinity controls EF versus GC B cell development at the T-B border. Antigen binding naïve B cells in the B cell follicle migrate to the T-B border after upregulating CCR7 and EBI2. B cells that do not bind antigen (black) cannot migrate to the T-B border. At the T-B border, B cells with high affinity BCRs (red cells) are $PDL1^{hi}$, allowing for PDL1-PD1 interactions with pre-Tfh cells (green cells). B cells expressing low affinity BCRs (blue cells) show stronger ICOS-ICOSL interactions with pre-Tfh cells, which induces Tfh differentiation (green cells expressing TCR in the interfollicular region). After interacting with pre-Tfh cells at the T-B border, B cells downregulate CCR7 and migrate to the interfollicular region. B cells with high affinity BCRs maintain EBI2 expression and participate in the EF response. B cells with low affinity BCRs downregulate EBI2 and enter the GC, leading to the production of long-lived plasma cells and memory B cells. The labels on the top left of each region depict the B cell expression profile of chemokine receptors that regulate localization to the respective region. This is not specified for the EF and GC responses as the expression of the chemokine receptors for each response is unclear. Adapted from reference (13).

specific B cells in the differentiation of pre-Tfh into Tfh cells, which contradicts a previous hypothesis that bystander B cells provide the only source of ICOSL involved in Tfh differentiation (20, 25). Bystander B cells are not well characterized, but do not bind antigen and constitutively express ICOSL (25). The role of bystander B cells in Tfh differentiation may explain the maintenance of ICOSL by high affinity B cells *in vivo*. Potentially, high affinity B cells express ICOSL to prevent pre-Tfh cells from interacting with bystander B cells. The upregulation of PDL1 by high affinity B cells may provide sufficient inhibitory signals to prevent ICOS-induced Tfh differentiation (20). However, PDL1 expression in relation to BCR affinity at the T-B border has not been evaluated, indicating that further studies are needed to understand the regulation of this ligand *in vivo*.

In addition to influencing the direct interactions between pre-Tfh and B cells, BCR affinity impacts B cell localization to the sites of the EF and GC responses by altering the expression of chemokine receptors on the B cell surface as demonstrated by Sacquin and colleagues (20). Within 24 hours of BCR stimulation, at which point B cells should be localized to the T-B border, B cells stimulated with α-IgM upregulate CCR7. Higher affinity B cells, as represented by increased BCR stimulation through α-IgM, upregulate CCR7 to a higher degree than lower affinity B cells. This results in a higher ratio of CCR7:CXCR5 in high affinity B cells destined for an EF response compared to low affinity B cells destined for a GC response. Because CCR7 promotes migration toward the T cell zone while CXCR5 promotes migration toward the B cell follicle, the higher CCR7:CXCR5 ratio induced by high affinity BCRs should maintain B cells near the follicular periphery, away from the center follicle where the GC develops. Thus, these data provide a mechanism by which BCR affinity controls B cell development by directing B cell localization in the follicle (9, 30).

EBI2, another chemokine receptor, also directs B cells toward an EF or GC response. The EBI2 ligand (EBI2L) is 7α,25-dihydroxycholesterol (7α,25-OHC), which is present in the interfollicular (IF) regions but absent from the GC (31, 32). Generally, EBI2 is associated with localization to the outer follicle, suggesting that it isolates B cells from the GC, possibly in conjunction with CXCR4 (33–35). Additionally, along with CXCR5 and downregulation of CCR7, EBI2 directs B cell migration from the T-B border to the IF region (**Figure 1)** (19, 32). Within the IF region, B cells destined for an EF response maintain EBI2 expression while those destined for the GC downregulate EBI2 (35). However, the signals that induce downregulation of EBI2 are unknown. ICOS-ICOSL interactions could be a signal involved in EBI2 downregulation, as EF T cell help to B cells is ICOSL independent while GC T cell help is ICOSL dependent (13, 36). Further evaluation of ICOS-ICOSL interactions in the IF region could help elucidate the regulatory signals required for B cell development in this region.

Expression of B cell lymphoma 6 protein (BCL6) is a key indicator of the GC response and another B cell intrinsic protein whose expression is influenced by BCR affinity (37, 38). Upon initial antigen encounter, B cells modulate their expression of BCL6 through the activity of interferon regulatory factor 4 (IRF4) (38, 39). High affinity B cells repress BCL6 by expressing higher levels of IRF4 (37, 40). As BCL6 expression is imperative to the GC response, the increase in IRF4 expression promotes an EF response through repression of BCL6 (37). Conversely, low affinity B cells activate lower levels of IRF4 and, in this context, IRF4 has an activating effect on BCL6, thereby promoting a GC response (37). Whether IRF4 activates or represses BCL6 depends on the region of the BCL6 locus that it binds (37). Overall, the inter-relationship between BCR affinity, IRF4, and BCL6 demonstrates how BCR affinity influences B cell development upon initial antigen encounter in SLOs.

In addition to antigen-specific BCR, which acts as a B cell intrinsic signal, Tfh-secreted cytokines function as B cell extrinsic signals that regulate B cell development within SLOs. One of the more well-studied cytokines is IL-21, which binds to the receptor IL-21R on the surface of T and B cells and induces activation of the transcriptional activator STAT3 (8, 41, 42). IL-21 can have opposing effects on B cell proliferation and differentiation depending on whether CD40 is also stimulated. Ligation of CD40 on B cells by CD40L on T cells synergizes with IL-21 to activate B cell proliferation; however, when CD40 remains unbound, IL-21 inhibits proliferation and promotes apoptosis (43). Pre-GC B cells require IL-21 to migrate from the follicular periphery to the center follicle, which is necessary for GC formation (44).

In conjunction with IL-21, IL-4 is required for proper GC development. Loss of IL-21 and/or IL-4 signaling results in small GCs *in vivo*, suggesting that these cytokines are an imperative form of Tfh cell-help for pre-GC B cells (44). Gonzalez and colleagues showed that IL-21 and IL-4 are not required to induce GC B cells, which are identified by BCL6 expression, at the T-B border. In the first three days of the adaptive immune response, loss of signaling through IL-21 and IL-4 does not alter the proliferation rate nor the population size of $BCL6^{hi}$ pre-GC B cells. However, their further survival is impaired as indicated by elevated cell death rates and increased levels of the apoptotic marker, activated caspase-3. Interestingly, loss of signaling from only one of these cytokines does not increase activated caspase-3, suggesting that IL-21 or IL-4 alone is enough to promote survival in the transition from the T-B border to the GC. Overall, these data suggest that signaling through IL-21 and IL-4 is not required to induce the GC response, but is required to maintain pre-GC B cells.

While mature B cell developmental pathways usually proceed through a combination of EF and GC pathways in response to infection, some pathogens primarily induce an EF response with a delayed GC response (18). The bacterium *Ehrlichia muris* (*E. muris*) suppresses splenic GC formation while *Borrelia burgdorferi* (B. burgdorferi) delays GC formation and promotes the production of EF, IgM expressing B cells in lymph nodes (45, 46). Additionally, *Salmonella enterica* typhimurium (*S*Tm) induces an early EF response while delaying GC formation for one month (19, 45, 47, 48). During *S*Tm infections in mice, this delay in GC formation likely results

from high levels of IL-12, which prevents Tfh differentiation by upregulating T-bet, a transcription factor that directs T cells to a helper type 1 (Th1) fate (18, 49). The resulting deficiency in Tfh development skews B cells toward an early EF response (50). Whether late GC formation occurs due to repopulation of Tfh cells remains uncertain as the numbers of Tfh cells were not analyzed past 17 days post-infection (50). Exactly why and how these bacteria induce EF responses while delaying or inhibiting GC responses remains unclear and suggests that these pathogens could be a useful infection model to evaluate the development of an EF response.

EXTRAFOLLICULAR B CELL DEVELOPMENT

The EF response provides the first wave of humoral protection by producing antibody secreting cells (ASCs) and MBCs as early as 3 days after antigen encounter (19). During the EF response, activated B cells migrate to the bridging channels of the spleen and the medullary cords of the lymph nodes, primarily due to their aforementioned expression of CXCR4 and EBI2 (20, 35, 51, 52). There, the B cells receive proliferation and survival signals such as IL-6 and a proliferation-inducing ligand (APRIL) from dendritic cells (DCs) and macrophages (51, 53). These signals cause the B cells to rapidly divide and form extrafollicular foci, where EF ASCs are generated (51, 53).

Although the majority of EF-derived Igs are IgM, activated EF B cells can undergo CSR to produce IgG and IgA (54, 55). During the EF response to certain T-independent antigens, stimulation of the BCR synergizes with toll-like receptors (TLRs) to induce CSR (56). Both BCR and TLR signaling induce NF-κB, a transcription factor required for AID expression (56, 57). The T-independent antigen lipopolysaccharide (LPS) has been proposed to stimulate both of these receptors by activating the BCR through its repetitive polysaccharide moiety as well as TLR4 through its lipid A moiety (56). Blocking CD79, a BCR co-receptor, *via* α-CD79 antibody inhibits BCR signaling and severely reduces CSR to IgG1 upon stimulation with LPS and IL-4, suggesting that signaling by BCR and TLR4 is required for CSR following LPS treatment (56, 58).

In the EF response to T-dependent antigens, activation of both the BCR and CD40 initiates strong phosphatidyinositol-3 kinase (PI3K) signaling that augments proliferation of activated B cells (59). However, strong PI3K signaling also inhibits CSR (59, 60). In T-dependent EF responses, antagonism of the PI3K signaling pathway *via* activity of PI3K interacting protein 1 (PIK3IP1) promotes CSR, which was recently demonstrated by Ottens and colleagues (61). Mice with CD19-cre mediated PIK3IP1 deletion show delayed production of IgG1 after immunization with NP conjugated to keyhole limpet hemocyanin (KLH), a T-dependent antigen. Interestingly, class switching in GC B cells remained functional, suggesting a role for PIK3IP1 in CSR specifically within the EF T cell-dependent response. However, immunization of these mice with NP-Ficoll, a T-independent antigen, did not delay IgG1 production, indicating that the T-independent EF response was not impaired by loss of PIK3IP1. These data suggest that PIK3IP1 is required to limit the high levels of PI3K signaling that results from the combination of CD40 and BCR stimulation in T-dependent EF responses, permitting CSR. Additional studies examining how PI3K regulates CSR in T-dependent EF responses will provide insight into the activation and development of mature B cells. This could be tested by overexpressing PI3K in B cells exposed to NP-Ficoll and evaluating the levels of isotype-switched B cells in the presence and absence of PI3KIP1. In the absence of CD40 stimulation, this model could reveal whether PI3K antagonizes CSR in a T-independent response.

Although they undergo CSR, EF B cells typically have not undergone SHM, which occurs in the GC dark zone (62). However, recent studies indicate that *E. muris* and *S*Tm infections, which elicit an EF response without typical GC formation, can also initiate SHM at very low levels (48, 63). High-throughput sequencing of mRNA of B cells and PBs from microdissected EF foci of mice infected with *E. muris* and *S*Tm revealed low levels of mutations in V regions, suggesting SHM occurs in these cells (48, 63). However, currently no evidence supports SHM occurring outside of the GC in humoral responses that develop classically described GC responses. If EF SHM only occurs when GC formation is delayed or does not occur, it could represent a desperate attempt by the immune system to produce high affinity antibodies, which normally form in the GC (3, 31). Investigation into the specific cytokines and chemokines secreted in response to *E. muris* and *S*Tm infections may elucidate what specific factors allow and promote EF SHM.

Regardless of SHM status, PBs produced from the EF response expand rapidly and secrete antigen-specific antibodies (64). PB differentiation during the EF response requires the same signals and transcriptional program as PB development in the GC: strong BCR signaling induces the expression of interferon regulatory factor 4 (IRF4), which in turn activates *Prdm1* whose protein product, BLIMP-1, is essential for PB development (40, 65, 66). BLIMP-1 suppresses genes involved in GC B cell and MBC formation and upregulates genes associated with the plasma cell fate (16, 67). Although the developmental program for PBs are the same in the EF response and the GC, Igs produced by EF PBs generally exhibit relatively low antigen affinity as compared to those stemming from the GC reaction, which undergo affinity maturation (68).

BCR affinity determines EF PB differentiation and fate (11, 69). Activated mature B cells with high affinity BCRs preferentially differentiate into EF PBs and among these EF PBs, those with higher affinity BCRs proliferate at a faster rate than those with lower affinity BCRs (11, 14). Interestingly, recent evidence indicates that hyperactive BCR signaling is disadvantageous to EF PB formation (69). To study the role of hyperactive BCR signaling during EF PB development, Yam-Puc and colleagues conditionally inactivated SH2 domain–containing phosphatase-1 (SHP-1), an antagonist of BCR signaling, in mice using a Cγ1-cre. Increased levels of SYK phosphorylation in SHP-1-deleted splenic B cells indicated

enhanced levels of BCR signaling. Because strong BCR signaling promotes EF PB differentiation (14), these mice with heightened BCR signaling were expected to show increased numbers of EF PBs upon immunization with sheep red blood cell (SRBC). Surprisingly, these mice had smaller EF foci and higher levels of apoptotic EF PBs than wild-type (WT) controls, suggesting a maximal limit to BCR signaling for PB development. However, as SHP-1 is a phosphatase with several targets, SHP-1 could promote EF PB survival through pathways independent of BCR signaling (70). Further studies using alternative models for BCR hyperactivity, such as constitutive activation of BCR signal transducer SYK, should be performed to confirm these findings. The exact threshold of BCR signaling needed for EF PB differentiation and expansion could also be examined, potentially by injecting α-BCR or antigens of varying affinity.

In addition to PBs, low affinity MBCs can also be produced before GC formation; however, whether these MBCs are formed within the B cell follicle before the formation of GCs or in the extrafollicular region is unclear (71). While the developmental pathways from which GC-independent MBCs arise are not yet fully understood, these MBCs develop directly from antigen-activated mature B cells and do not require BCL6 or IL-21, both of which are required for GC MBC formation (72–74). Recent evidence indicates that GC-independent MBC development relies on B-cell activating factor receptor (BAFF-R) (75). BAFF-R promotes the survival of mature, naive B cells after binding the B-cell activating factor (BAFF) ligand that is expressed by DCs, follicular DCs (FDCs), and macrophages (76). Using mice that express BCRs against HEL (SW_{HEL}) with germline deletions for BAFF-R, Lau and colleagues demonstrated that these mice had drastically reduced percentages of $IgG1^+$ MBCs with unmutated IgH variable domains and increased percentages of $IgG1^+$ MBCs with mutated IgH variable domains following immunization with HEL conjugated to SRBC (75). Conversely, overexpression of BAFF-R by retroviral transduction in SW_{HEL} B cells, which were subsequently transferred into WT mice, significantly expanded the percentage of unmutated $IgG1^+$ MBCs. The population of unmutated $IgG1^+$ MBCs was interpreted to be GC-independent due to a lack of SHM and the absence of the Y53D mutation in the Ig heavy chain variable region, which is frequently observed in SW_{HEL} GC affinity maturation, and thus implicating BAFF-R in GC-independent MBC development. In a complementary experiment, mice were administered bromodeoxyuridine (BrdU)-containing water and the B cells positive for both BrdU and the MBC marker CD38 were analyzed. Highly replicating cells, as marked by low levels of BrdU, were identified as MBCs stemming from the GC, while MBCs that differentiated before the GC reaction were identified with high levels of BrdU. WT mice treated with a BAFF-neutralizing antibody showed a large decrease in $IgM^+BrdU^+CD38^+$ and $IgG1^+BrdU^+CD38^+$ B cells, accompanied by a small but significant decrease in both affinity-maturated $BrdU^-$ MBCs and overall GC B cells 14-days post-treatment. Together, these data indicate that BAFF-R is necessary for GC-independent MBC development but dispensable for MBCs stemming from the GC. However, some of the unmutated MBCs and $BrdU^+CD38^+$ MBCs analyzed in these studies did arise from the germinal center, and additional model systems that permit accurate identification of MBC precursors both in and outside of the GC could identify GC-independent MBC populations.

GERMINAL CENTER B CELL DEVELOPMENT

Germinal Center Formation and Maintenance

The GC response provides another pathway for B cell differentiation in response to antigens. After initial activation by cognate antigens, B cells fated for the GC reaction migrate to the center of the follicle and rapidly divide, beginning the formation of the GC (77). Initiation of the GC reaction requires B cell co-stimulation by ligands expressed on the surface of T cells and APCs (78). CD40 stimulation is imperative for GC formation as CD40-deficient mice exhibit defective GC formation in both T-dependent and T-independent responses (79, 80). Within the GC, Tfh-derived cytokines and chemokines regulate mature B cell development (**Figure 2**) (31, 81). B cells in turn modify their responsiveness to these signals by modulating the expression of chemokine and cytokine receptors, which is influenced by BCR signaling and interactions with Tfh cells (12, 20, 34, 82, 83).

GC formation also requires expression of the transcriptional repressor BCL6 (25, 84, 85). BCL6 is significantly upregulated in GC B cells and Tfh cells and is considered the master regulator of the GC (10, 85, 86). Loss of BCL6 in mice impairs GC formation but permits the EF response, suggesting its function is limited to the GC response (87, 88). BCL6 suppresses transcription of p53 and p21 to inhibit apoptosis and cell-cycle arrest (89, 90). This allows for the rapid proliferation of B cells that is required for GC formation and the induction of genetically programmed DNA mutations necessary for SHM (78). BCL6 also retains B cells within the GC and prevents PC differentiation by inhibiting the expression of BLIMP-1 (78, 91). Additionally, BCL6 inhibits expression of PDL1 in GC B cells to maintain the necessary Tfh population (92).

BCL6 expression in GC B cells is both promoted and inhibited by BCR signaling and CD40 stimulation (93). Strong signaling induced by high affinity BCRs and CD40 stimulation *via* membrane-bound CD40L on the Tfh cell surface leads to mitogen activated protein kinase (MAPK)-dependent phosphorylation of BCL6 and subsequent degradation of BCL6 through the ubiquitin-proteosome pathway (93–95). Specifically, the MAPK, extracellular signal-regulated kinase 1 and 2 (ERK1/2), signals BCL6 for degradation. Conversely, p38, which is also a MAPK activated by BCR signaling and CD40 stimulation, promotes BCL6 expression. Interestingly, soluble CD40L, compared to membrane-bound, activates p38 without activating ERK1/2, permitting BCL6 expression (93). This suggests that the mode of stimulation is also an important

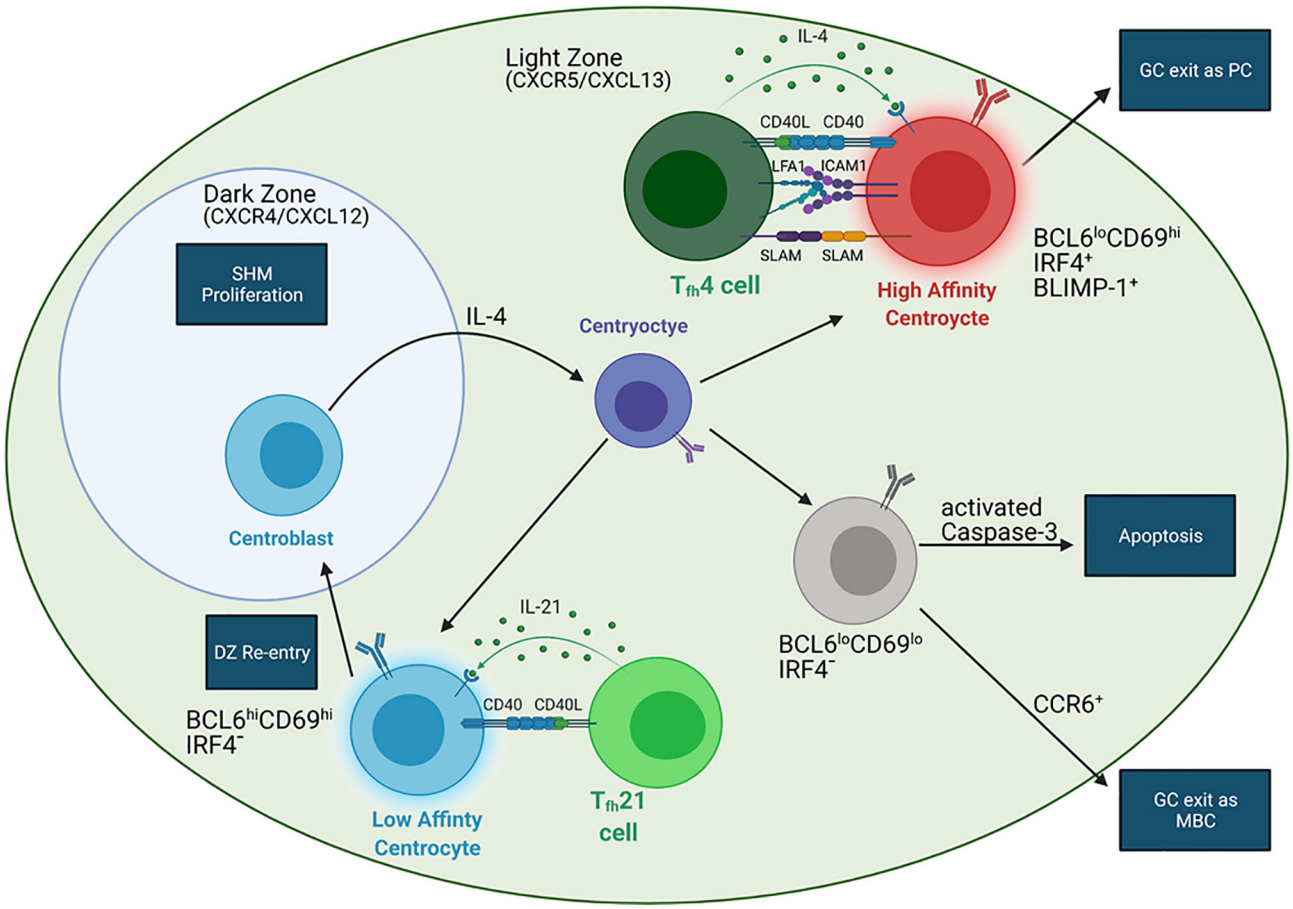

FIGURE 2 | BCR affinity controls the fate of GC B cells. In the LZ, B cells with high affinity BCRs (red) interact with IL-4 producing Tfh4 cells (dark green) distal to the DZ. IL-4 can induce BLIMP-1 expression in these B cells, leading to GC exit and formation of long-lived plasma cells (LLPCs). These B cells have stronger interactions with Tfh B cells than B cells expressing low affinity BCRs due to upregulation of ICAM1 and SLAM. LZ B cells with low affinity BCRs (blue) interact with IL-21 secreting Tfh21 cells (light green) more proximal to the DZ. These B cells do not upregulate BLIMP-1 but are converted into centroblasts (blue cell in DZ) *via* IL-21, allowing for DZ entry and GC recycling. Centroblasts do not express a functional BCR. Migration into the DZ is dependent on CXCR4, which responds to the DZ chemokine CXCL12. When the centroblasts exit the DZ, they convert into centrocytes with varying BCR affinities (purple) *via* IL-4 signaling. The affinity of the newly mutated BCR (purple) may or may be increased, which will influence the next step in B cell development. Migration into the LZ depends on CXCR5, which responds to the LZ chemokine CXCL13. Another population of LZ B cells (gray) are relatively quiescent and may be either MBC precursors or an apoptotic population. CCR6 expression indicates MBC precursors while activated caspase-3 expression indicates apoptotic B cells. Additionally, CD40-CD40L interactions are required in all Tfh-B interactions.

factor in mediating the GC response through BCL6. Furthermore, while strong BCR signaling leads to BCL6 degradation, basal or tonic BCR signaling permits BCL6 expression to retain B cells in the GC. In this context, BCL6 inhibits expression of the apoptosis-promoting phosphatase PTPROt and permits survival of low-affinity B cells in the GC (94).

While BCL6 is considered the master regulator of the GC reaction, other proteins control GC B cell development. Like BCL6, BACH2 inhibits expression of BLIMP-1 and p21, thereby preventing premature PC differentiation and apoptosis, respectively (96–99). Furthermore, the inhibition of BLIMP-1 by BACH2 increases class-switched PCs, as mouse splenic B cells more readily become IgM-expressing PCs in the absence of BACH2 (98). Loss of BLIMP-1 on a BACH2$^{-/-}$ background rescues the CSR deficiency of BACH2 single mutants, suggesting that inhibition of BLIMP-1 by BACH2 promotes CSR (98). Complete ablation of BACH2 following GC formation collapses the GC B cell population *in vivo* and increases the rate of B cell apoptosis *in vitro*, suggesting that BACH2 maintains GC B cell survival (96, 97). The loss of GC B cells in BACH2$^{-/-}$ mice may also be due to the role of BACH2 in BCR-induced B cell proliferation, which is significantly reduced in response to α-IgM stimulation because BACH2$^{-/-}$ B cells are unable to transition into S phase (97). Interestingly, BACH2$^{-/-}$ B cell proliferation in response to LPS is comparable to WT B cells, suggesting that BACH2 regulates a BCR-specific proliferation pathway (97). Thus, in GC B cells BACH2 promotes progression

through the cell cycle and inhibition of apoptosis upon BCR stimulation (97). Additional experiments evaluating the temporal regulation of BACH2 expression could improve our understanding of its role in GC B cell maintenance and clonal expansion.

Inhibition of p21 transcription by BACH2 and BCL6 is imperative to the GC reaction; however, repression of p21 can also be carried out *via* epigenetic modifications (90, 97, 100). The methyltransferase EZH2 binds to the *CDKN1A* locus, which encodes for p21, and induces H3K27me3 to repress transcription. Similar to BCL6 and BACH2, EZH2 is required for GC formation (100). To repress *CDKN1A* transcription, EZH2 directly binds the *CDKN1A* promoter while BCL6 interacts with the transcriptional activator MIZ-1, which also binds to the *CDKN1A* promoter, indicating complementary modes of repressing p21 expression by BCL6 and EZH2 (90, 100). On the other hand, BACH2 binds upstream of the *CDKN1A* promoter, suggesting it may work in tandem with EZH2 and/or BCL6 (97). Similar to BACH2 deficiency, loss of EZH2 suppresses the G1/S transition, providing further support for their synergistic activity in the regulation of p21 expression and cell cycle progression (100). Whether these proteins bind directly or indirectly to one another at the *CDKN1A* locus or whether they function in tandem or complementary genetic pathways requires further evaluation.

Germinal Center Light and Dark Zones

Formation of the GC from the rapidly dividing B cells polarizes it into two zones, the dark zone (DZ) and light zone (LZ), which appear histologically distinct due to differing lymphocyte densities (62). Devoid of Tfh cells, the DZ contains B cells and FDCs and is the site of SHM (62). In contrast, the LZ contains Tfh cells, B cells, and FDCs and is the location of T-dependent selection of antigen-specific B cells (34, 62). DZ B cells, also called centroblasts, are highly proliferative and generally larger than LZ B cells, termed centrocytes (62). Centrocytes express mutated, functional BCRs whereas centroblasts only express non-functional BCRs, reflecting the aforementioned selection that occurs in the LZ and affinity maturation within the DZ **(Figure 2)** (34, 62).

The original model for GC entry proposed that B cells first enter the DZ, due to their expression of CXCR4, which is attracted to CXCL12 that is more abundant in the DZ than the LZ (101). Within the DZ, the cells undergo SHM and proliferate, and then downregulate CXCR4, while maintaining CXCR5 expression, permitting migration to the LZ where the ligand CXCL13 is expressed by FDCs (77, 101). Once in the LZ, the B cells stop dividing and undergo selection (62, 78). However, recent studies suggest a more dynamic model in which the DZ and LZ are less discrete compartments that allow GC B cells to cycle between the two zones (34). Two-photon laser microscopy studies in mice have revealed bidirectional trafficking of antigen-specific B cells between the DZ and LZ (102, 103). Additionally, dividing cells are detected in both the LZ and DZ, contradicting the idea that GC B cells exclusively proliferate within the DZ (102, 104). However, another study, using multiphoton microscopy and flow cytometry, shows that B cells only divide within the DZ (105). Victora and colleagues revealed a net movement of B cells from the DZ to the LZ and that Tfh cell help dictates whether a B cell will return to the DZ, largely supporting earlier models of B cell dynamics. Accordingly, the exact developmental and migratory paths of a GC B cell remain debatable, though they are most likely more dynamic than the original model.

The LZ is classically thought to be the site of CSR. This was first postulated by a study showing that centrocytes only express limited Ig isotypes, suggesting that isotype switching is initiated within GCs and after SHM (106). Additionally, 5′Sγ–Sμ3′ excision circles are detectable within GCs in human tonsils, suggesting that their deletion during CSR occurred in GC B cells (106). However, a recent study by Roco and colleagues refutes this assumption and postulates that CSR occurs before GC formation (107). Germline transcripts (GLTs), an indicator for the onset of CSR, and class-switched antibodies emerge 1.5-2.5 days post-immunization, whereas EFPBs and nascent GCs do not appear until 3.5 days post-immunization, suggesting that CSR occurs before GC formation. Additionally, expression of transcription factors and enzymes that regulate CSR, such as Foxo1, c-Myc and APE1, are downregulated in GC B cells. Moreover, both LZ and DZ B cells have markedly reduced GLTs, as compared to EFPBs and pre-GC B cells. However, this new model remains controversial, in part because a mechanistic understanding of the distinct factors that regulate, and consequently mark, AID activity specifically at V genes for SHM in GC B cells versus S regions during CSR in EFPBs remains elusive (18). In addition, as previously mentioned, CSR occurs in the EF response which raises the question of whether CSR is a GC-independent process or whether two distinct, CSR pathways exist: one specific to the EF response and one specific to the GC (54, 55).

In support of the hypothesis that CSR is a GC-independent process, Sundling et al. recently proposed that the increase in IgG^+ B cells compared to IgM^+ B cells in the GC results from stronger positive selection of IgG^+ B cells and counter-selection of IgM^+ cells (108). To eliminate ongoing CSR as the explanation for the increase in IgG^+ and decrease in IgM^+ GC B cells over time, Sundling and colleagues co-transferred MD4 and SW_{HEL} B cells into WT recipient mice. While both cell types are high affinity for HEL, MD4 cannot undergo CSR. After immunization with HEL, both MD4 and SW_{HEL} B cells expressing IgM in the GC decrease over time with the same kinetics, suggesting that the decrease in IgM^+ GC B cells is not due to ongoing CSR. Similarly, co-transfer of SW_{HEL} B cells deleted for Sμ (ΔSμ), which cannot complete CSR, along with SW_{HEL} B cells WT for Sμ, yielded the same result. Furthermore, $IgG1^+$ B cells spend more time in the cell cycle, more frequently enter the DZ, and are more likely to differentiate into PCs than their IgM+ counterparts, indicating stronger positive selection for IgG+ GC B cells (82, 108, 109). Along with the study by Roco et. al., these recent data support a model in which B cells undergo CSR at low levels prior to entering the GC, wherein high-affinity IgG^+ GC B cells are

positively selected over IgM^+ and low-affinity GC B cells to undergo proliferation and differentiation into PCs (107, 108). Thus, the role of the GC is not to induce CSR, rather it is to expand the population of high affinity, class-switched B cells by inducing high rates of proliferation and differentiation into IgG^+ PCs. However, this model for the role of the GC is not definitively accurate and requires further evaluation. Transfer of IgG^+ SW_{HEL} B cells into SW_{HEL} AID knockout and WT mice could test this hypothesis by revealing if the IgG^+ B cell population expands in comparison to the IgM^+ population. Because AID-deficient B cells cannot undergo CSR, expansion of the IgG^+ B cell population can be attributed to clonal expansion rather than ongoing CSR. If the model suggested by Sundling and colleagues is correct, then the transferred IgG^+ SW_{HEL} B cells should outcompete the AID knockout B cells and unswitched WT B cells. If CSR does indeed occur in the GC, then in the WT mice, the endogenous (i.e. not transferred) B cells should switch and expand at a similar rate to the transferred, IgG^+ B cells.

Role of BCR Affinity in the Germinal Center

The GC reaction is heavily influenced by BCR affinity and T-B interactions **(Figure 2)** (12, 13). High affinity LZ B cells have stronger interactions with GC Tfh cells as compared to low affinity LZ B cells because BCR signaling affects an ICOSL-dependent feed-forward mechanism of serial entanglement **(Figure 3)** (13). In this model, antigen presentation from MHCII on the B cell surface to Tfh cells activates the release of intracellular Ca^{2+} in Tfh cells, which induces CD40L localization to the Tfh cell surface (13, 110). B cells expressing higher affinity BCRs present more antigen than those expressing lower affinity BCRs, leading to more CD40L on the Tfh cell surface (13). Thus, higher affinity BCRs indirectly lead to stronger CD40 stimulation on the B cell through increased CD40L on the Tfh cell surface. CD40 stimulation leads to ICOSL expression on the B cell surface, which stimulates ICOS on the Tfh cell and increases intracellular Tfh Ca^{2+} signaling (13). Because Ca^{2+} signaling also induces the release of cytokines, such as IL-21 and IL-4, by Tfh cells, this model provides a mechanism by which higher affinity B cells receive more help from Tfh cells in the LZ (10, 111). This relationship between BCR affinity and ICOSL activity differs from interactions at the T-B border, where high affinity BCRs prevent ICOS-ICOSL interactions from inducing Tfh differentiation, as would be expected (20). Conversely, in the GC LZ, B cells expressing high affinity BCRs receive more help signals, through CD40 and cytokine signaling, by increasing Tfh activity through ICOS-ICOSL ligation (10, 13, 111).

Tfh-secreted cytokines IL-21 and IL-4 are critical for proper GC B cell development and migration within the GC **(Figure 2)** (10, 44, 111). In mice, inhibition of IL-4-signaling through the deletion of STAT6 results in an increased ratio of centroblasts: centrocytes (44). Conversely, deletion of the IL-21R results in a higher percentage of centrocytes (44). This suggests that IL-4 promotes conversion of centroblasts to centrocytes and IL-21 regulates development of centrocytes into centroblasts, which are localized to the DZ. Additionally, IL-21 maintains expression of BCL6 in GC B cells, while IL-4 plays a role in preventing apoptosis and, along with CD40 signaling, promotes isotype switching to IgG1 (10, 111).

While both IL-21 and IL-4 are secreted by Tfh cells in the GC LZ, an individual Tfh cell can only secrete one of these cytokines – Tfh4 cells produce IL-4, whereas Tfh21 cells produce IL-21 (83). Compared to Tfh21 cells, Tfh4 cells localize further from the DZ, closer to the periphery of the GC, and induce BLIMP-1 expression, suggesting they could be more involved in controlling PC differentiation and B cell exit from the GC (83). Conversely, Tfh21 cells induce BCL6 expression, which antagonizes BLIMP-1 and retains B cells in the GC (10, 83). Interestingly, a larger percentage of Tfh21 cells than Tfh4 cells

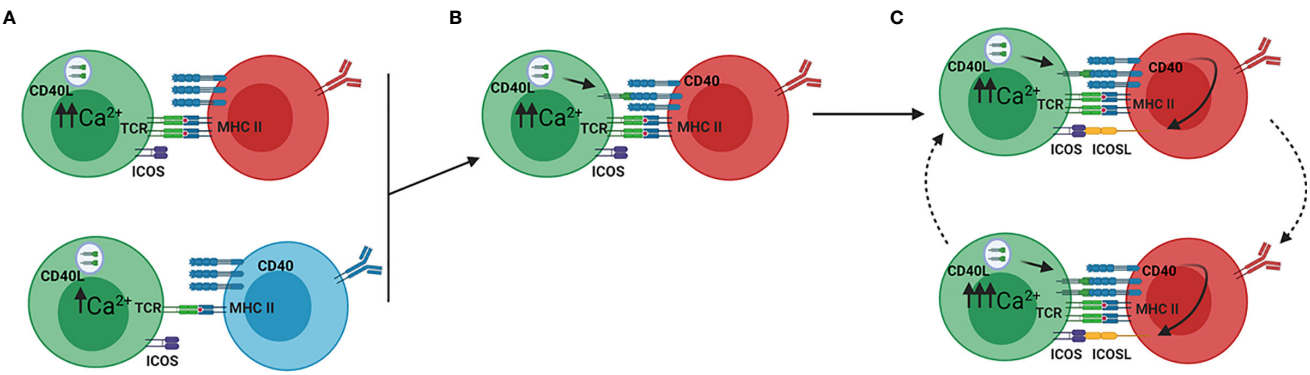

FIGURE 3 | ICOSL driven feed forward model of serial entanglement. **(A)** Antigen specific B cells present antigen to Tfh cells *via* MHCII on the B cell surface. Tfh cells (green) bind the MHCII-antigen complex *via* the T cell receptor (TCR), which activates calcium signaling within the Tfh cell. B cells expressing high affinity BCRs (red) present more antigen than those expressing low affinity BCRs (blue), thereby inducing a more Ca^{2+} release. **(B)** Ca^{2+} signaling in the Tfh cells induces translocation of CD40L to the Tfh cell surface, which binds CD40 on the B cell surface. **(C)** Stimulation of CD40 on B cells induces the expression of ICOSL on the B cell. ICOSL binding to ICOS on the Tfh cell surface induces increased $Ca2^+$ signaling, which again leads to translocation of CD40L to the Tfh cell surface. In this model, B cells increase their expression of ICOSL, which prepares them for stronger entanglement with Tfh cells. Adapted from reference (13).

appears within the first 8 days of the GC response, but between days 8 and 15 Tfh4 cells become the dominant population, suggesting that the role of IL-21 diminishes while the role of IL-4 increases as the GC reaction progresses (83). Based on the roles of Tfh21 and Tfh4 cells in the LZ, this could represent a change from affinity maturation to PC differentiation (83).

Along with these two populations of GC Tfh cells, the model of serial entanglement described earlier could provide a clearer understanding of LZ B cell development. Through increased ICOSL expression and antigen presentation on MHCII, B cells with high affinity BCRs induce increased Ca^{2+} signaling in Tfh cells, which will in turn secrete higher levels of IL-21 or IL-4 (**Figures 2**, **3**) (13).This suggests that these cytokines act as B cell extrinsic signals that direct B cell development based on BCR affinity, a B cell intrinsic characteristic (13). B cells that interact with Tfh4 cells at the LZ periphery may be induced to differentiate into IgG1-secreting PCs, if IL-4 signaling is strong enough (13, 83). If the BCR affinity is too low, then IL-4 signaling would not be sufficient to induce differentiation and these B cells will migrate toward the DZ, where they may interact with Tfh21 cells, transition into centroblasts, and enter the DZ to undergo affinity maturation (13, 44, 83).

Though Tfh cells are localized to the LZ, the strength of their interactions with LZ B cells influences the events in the DZ (82, 109). B cells that present higher amounts of antigen to Tfh cells in the LZ upregulate metabolism genes and drivers of cell cycle progression, such as c-Myc and E2F transcription factors, in the DZ (82). These B cells also show faster progression through S phase, faster replication fork progression, prolonged DZ retention, and increased rounds of replication (82, 109). These data suggest that increased Tfh cell help in the LZ influences the transcriptome of B cells that, in turn, controls their progression through and replication in the DZ. The data also suggest that events in the LZ can directly influence the events in the DZ and supports the idea that the DZ and LZ are not discrete compartments that act independently of each other (34). How Tfh cells communicate with B cells in the LZ to direct B cell development in the DZ remains to be determined. IL-21 could be an important LZ factor involved in controlling the transcriptome of DZ B cells as it activates c-Myc through the transcriptional regulator STAT3, promotes the centrocyte to centroblasts conversation, and is secreted by Tfh21 cells interacting with B cells proximal to the DZ (41, 42, 44, 83). However, IL-21 has a diverse range of effects on the B cell transcriptome, as represented by its ability to induce BLIMP-1 and BCL6, suggesting other signals are required (10, 41, 42, 111).

B cells expressing high affinity BCRs in the LZ preferentially differentiate into PCs while those expressing lower affinity BCRs preferentially remain in the GC for further affinity maturation (12). These subsets of LZ B cells can be identified by three LZ B cell markers: BCL6, CD69, and IRF4 **(Figure 2)** (12). CD69 marks positively selected LZ B cells after BCR or CD40 stimulation, IRF4 antagonizes BCL6 to promote BLIMP-1 expression and PC differentiation, and BCL6, as discussed previously, retains B cells in the GC (112–114). $BCL6^{lo}CD69^{hi}IRF4^{+}$ LZ B cells are PC precursors that have stronger interactions with Tfh cells, as indicated by upregulation of ICAM1 and SLAM, in comparison to $BCL6^{hi}CD69^{hi}IRF4^{-}$ LZ B cells that recycle through the GC for further affinity maturation (12). Consistent with this hypothesis, CD40 haploinsufficiency, which reduces Tfh-B cell interaction strength, significantly reduces the population size of PC precursors without affecting the overall GC B cell population or the GC recycling population (12). Future studies evaluating Tfh interactions with LZ B cells based on these three markers could provide insight into how Tfh cells regulate B cell development in the GC and improve our ability to track B cells through the GC. Because Tfh4 cells induce BLIMP-1 expression, the $BCL6^{lo}CD69^{hi}IRF4^{+}$ PC precursors may be interacting with Tfh4 cells (12, 83). Conversely, the $BCL6^{hi}CD69^{hi}IRF4^{-}$ GC recycling population may be interacting with Tfh21 cells near the DZ, as Tfh21 cells promote BCL6 expression (12, 83).

In addition to the two LZ B cell populations discussed, a third population has been identified as $BCL6^{lo}CD69^{lo}IRF4^{-}$ (12). This gene expression profile reflects a quiescent population that is exiting the GC, suggesting it could be an MBC precursor population or an apoptotic population (12). Further studies examining CCR6, a GC marker for MBC precursors, and activated caspase-3 expression could help distinguish between these hypotheses **(Figure 2)** (115). Additionally, studies that identify the fate of the $BCL6^{lo}CD69^{lo}IRF4^{-}$ LZ B cell population can be used to characterize PC precursors, GC recycling B cells, and MBC precursors. Interestingly, BACH2 haploinsufficiency inhibits MBC development and promotes PC differentiation (96, 98, 116). However, the role of BACH2 in MBC differentiation is independent of its effect on BLIMP-1 because deletion of both does not improve MBC differentiation relative to deletion of BACH2 alone (96). The mechanism by which BACH2 induces MBC differentiation in the GC remains unknown. Interestingly, BACH2 expression in GC B cells correlates inversely with the strength of T cell help and BCR affinity, which is consistent with the idea that GC-derived MBCs arise from lower affinity B cells (96, 117). This result emphasizes the inter-relationship between BCR affinity, T cell help, and terminal B cell differentiation (96).

DISCUSSION

The humoral immune response is a dynamic, complex process that is regulated by many signals and interactions between B cells and other cell types, especially $CD4^{+}$ Tfh cells. Even though B cell development has been extensively studied, the regulatory mechanisms that control this process are still being explored with new models and genetic engineering tools such as CRISPR. Recent studies have elucidated a role for BCR affinity in controlling B cell development through EF and GC responses (12, 13, 20, 69, 82, 109). At the T-B border and within the GC, high affinity BCRs direct B cells to differentiate into ASCs, while low affinity BCRs direct B cells to enter or remain in the GC for affinity maturation (11, 12, 14, 15). While the processes governing the choice between affinity maturation and differentiation into ASCs have become clearer, the processes that control B cell differentiation into MBCs remain unclear. While MBCs seem to mainly arise from lower affinity B cells,

some high affinity LZ B cells become MBCs, suggesting that BCR affinity is not the only signal determining MBC fate (115, 117). However, these signals are unknown and further exploration of MBC differentiation could promote the production of vaccines that confer effective long-term immunity.

Additionally, the processes that guide B cells to complete Ig maturation (SHM and CSR) in SLOs remain under investigation. The presence of class-switched EF Igs and recent molecular analysis of early CSR events suggests that CSR occurs outside of the GC, which challenges earlier models positing that CSR occurs within the GC (54, 55, 107). Similarly, SHM, which was previously thought to occur in the GC DZ, may also occur at low levels in EF B cells, particularly when GC formation is delayed or inhibited (48, 63). However, why EF SHM may occur during specific immune responses remains unknown. Improving our understanding of these processes and the locations in which they occur will provide us insight into Ig maturation and B cell development in SLOs and new model systems to produce effective therapeutic antibodies or vaccines.

AUTHOR CONTRIBUTIONS

AJW, TC-E, and MA wrote the manuscript. BQV edited the manuscript. All authors contributed to the article and approved the submitted version.

FUNDING

This work was supported by The National Institute on Minority Health and Health Disparities (5G12MD007603), The National Cancer Institute (2U54CA132378), and The National Institute of General Medical Sciences (1SC1GM132035).

ACKNOWLEDGMENTS

All figures were created at BioRender.com.

REFERENCES

1. Murphy KM, Weaver C. *Janeway's Immunobiology. 9 ed.* New York, NY: Garland Science/Taylor & Francis (2017).
2. Gutzeit C, Chen K, Cerutti A. The Enigmatic Function of IgD: Some Answers at Last. *Eur J Immunol* (2018) 48(7):1101–13. doi: 10.1002/eji.201646547
3. Cyster JG, Allen CDC. B Cell Responses: Cell Interaction Dynamics and Decisions. *Cell* (2019) 177(3):524–40. doi: 10.1016/j.cell.2019.03.016
4. Vazquez MI, Catalan-Dibene J, Zlotnik A. B Cells Responses and Cytokine Production are Regulated by Their Immune Microenvironment. *Cytokine* (2015) 74(2):318–26. doi: 10.1016/j.cyto.2015.02.007
5. Muramatsu M, Kinoshita K, Fagarasan S, Yamada S, Shinkai Y, Honjo T. Class Switch Recombination and Hypermutation Require Activation-Induced Cytidine Deaminase (AID), a Potential RNA Editing Enzyme. *Cell* (2000) 102(5):553–63. doi: 10.1016/S0092-8674(00)00078-7
6. Di Noia JM, Neuberger MS. Molecular Mechanisms of Antibody Somatic Hypermutation. *Annu Rev Biochem* (2007) 76:1–22. doi: 10.1146/annurev.biochem.76.061705.090740
7. Revy P, Muto T, Levy Y, Geissmann F, Plebani A, Sanal O, et al. Activation-Induced Cytidine Deaminase (AID) Deficiency Causes the Autosomal Recessive Form of the Hyper-IgM Syndrome (Higm2). *Cell* (2000) 102(5):565–75. doi: 10.1016/S0092-8674(00)00079-9
8. Ma CS, Deenick EK, Batten M, Tangye SG. The Origins, Function, and Regulation of T Follicular Helper Cells. *J Exp Med* (2012) 209(7):1241–53. doi: 10.1084/jem.20120994
9. Reif K, Ekland EH, Ohl L, Nakano H, Lipp M, Förster R, et al. Balanced Responsiveness to Chemoattractants From Adjacent Zones Determines B-Cell Position. *Nature* (2002) 416(6876):94–9. doi: 10.1038/416094a
10. Song W, Craft J. T Follicular Helper Cell Heterogeneity: Time, Space, and Function. *Immunol Rev* (2019) 288(1):85–96. doi: 10.1111/imr.12740
11. Chan TD, Gatto D, Wood K, Camidge T, Basten A, Brink R. Antigen Affinity Controls Rapid T-Dependent Antibody Production by Driving the Expansion Rather Than the Differentiation or Extrafollicular Migration of Early Plasmablasts. *J Immunol* (2009) 183(5):3139–49. doi: 10.4049/jimmunol.0901690
12. Ise W, Fujii K, Shiroguchi K, Ito A, Kometani K, Takeda K, et al. T Follicular Helper Cell-Germinal Center B Cell Interaction Strength Regulates Entry Into Plasma Cell or Recycling Germinal Center Cell Fate. *Immunity* (2018) 48(4):702–15.e4. doi: 10.1016/j.immuni.2018.03.027
13. Liu D, Xu H, Shih C, Wan Z, Ma X, Ma W, et al. T-B-Cell Entanglement and ICOSL-Driven Feed-Forward Regulation of Germinal Centre Reaction. *Nature* (2015) 517(7533):214–8. doi: 10.1038/nature13803
14. Paus D, Phan TG, Chan TD, Gardam S, Basten A, Brink R. Antigen Recognition Strength Regulates the Choice Between Extrafollicular Plasma Cell and Germinal Center B Cell Differentiation. *J Exp Med* (2006) 203(4):1081–91. doi: 10.1084/jem.20060087
15. Taylor JJ, Pape KA, Steach HR, Jenkins MK. Apoptosis and Antigen Affinity Limit Effector Cell Differentiation of a Single Naïve B Cell. *Science* (2015) 347(6223):784. doi: 10.1126/science.aaa1342
16. Tellier J, Shi W, Minnich M, Liao Y, Crawford S, Smyth GK, et al. Blimp-1 Controls Plasma Cell Function Through the Regulation of Immunoglobulin Secretion and the Unfolded Protein Response. *Nat Immunol* (2016) 17(3):323–30. doi: 10.1038/ni.3348
17. Malkiel S, Barlev AN, Atisha-Fregoso Y, Suurmond J, Diamond B. Plasma Cell Differentiation Pathways in Systemic Lupus Erythematosus. *Front Immunol* (2018) 9(427). doi: 10.3389/fimmu.2018.00427
18. Elsner RA, Shlomchik MJ. Germinal Center and Extrafollicular B Cell Responses in Vaccination, Immunity, and Autoimmunity. *Immunity* (2020) 53(6):1136–50. doi: 10.1016/j.immuni.2020.11.006
19. Jenks SA, Cashman KS, Woodruff MC, Lee FE, Sanz I. Extrafollicular Responses in Humans and SLE. *Immunol Rev* (2019) 288(1):136–48. doi: 10.1111/imr.12741
20. Sacquin A, Gador M, Fazilleau N. The Strength of BCR Signaling Shapes Terminal Development of Follicular Helper T Cells in Mice. *Eur J Immunol* (2017) 47(8):1295–304. doi: 10.1002/eji.201746952
21. MacLennan ICM, Toellner K-M, Cunningham AF, Serre K, Sze DMY, Zúñiga E, et al. Extrafollicular Antibody Responses. *Immunol Rev* (2003) 194(1):8–18. doi: 10.1034/j.1600-065X.2003.00058.x
22. Akiba H, Takeda K, Kojima Y, Usui Y, Harada N, Yamazaki T, et al. The Role of ICOS in the CXCR5<sup<+</sup< Follicular B Helper T Cell Maintenance In Vivo. *J Immunol* (2005) 175(4):2340. doi: 10.4049/jimmunol.175.4.2340
23. Choi YS, Kageyama R, Eto D, Escobar TC, Johnston RJ, Monticelli L, et al. ICOS Receptor Instructs T Follicular Helper Cell Versus Effector Cell Differentiation *via* Induction of the Transcriptional Repressor Bcl6. *Immunity* (2011) 34(6):932–46. doi: 10.1016/j.immuni.2011.03.023
24. Nurieva RI, Chung Y, Hwang D, Yang XO, Kang HS, Ma L, et al. Generation of T Follicular Helper Cells is Mediated by Interleukin-21 But Independent of T Helper 1, 2, or 17 Cell Lineages. *Immunity* (2008) 29(1):138–49. doi: 10.1016/j.immuni.2008.05.009
25. Xu H, Li X, Liu D, Li J, Zhang X, Chen X, et al. Follicular T-Helper Cell Recruitment Governed by Bystander B Cells and ICOS-Driven Motility. *Nature* (2013) 496(7446):523–7. doi: 10.1038/nature12058
26. Good-Jacobson KL, Szumilas CG, Chen L, Sharpe AH, Tomayko MM, Shlomchik MJ. PD-1 Regulates Germinal Center B Cell Survival and the

Formation and Affinity of Long-Lived Plasma Cells. *Nat Immunol* (2010) 11 (6):535–42. doi: 10.1038/ni.1877
27. Hams E, McCarron MJ, Amu S, Yagita H, Azuma M, Chen L, et al. Blockade of B7-H1 (Programmed Death Ligand 1) Enhances Humoral Immunity by Positively Regulating the Generation of T Follicular Helper Cells. *J Immunol* (2011) 186(10):5648. doi: 10.4049/jimmunol.1003161
28. Khan AR, Hams E, Floudas A, Sparwasser T, Weaver CT, Fallon PG. PD-L1hi B Cells are Critical Regulators of Humoral Immunity. *Nat Commun* (2015) 6:5997. doi: 10.1038/ncomms6997
29. Zuccarino-Catania GV, Sadanand S, Weisel FJ, Tomayko MM, Meng H, Kleinstein SH, et al. CD80 and PD-L2 Define Functionally Distinct Memory B Cell Subsets That are Independent of Antibody Isotype. *Nat Immunol* (2014) 15(7):631–7. doi: 10.1038/ni.2914
30. Allen CDC, Okada T, Cyster JG. Germinal-Center Organization and Cellular Dynamics. *Immunity* (2007) 27(2):190–202. doi: 10.1016/j.immuni.2007.07.009
31. Gatto D, Brink R. The Germinal Center Reaction. *J Allergy Clin Immunol* (2010) 126(5):898–907. doi: 10.1016/j.jaci.2010.09.007
32. Yi T, Wang X, Kelly LM, An J, Xu Y, Sailer AW, et al. Oxysterol Gradient Generation by Lymphoid Stromal Cells Guides Activated B Cell Movement During Humoral Responses. *Immunity* (2012) 37(3):535–48. doi: 10.1016/j.immuni.2012.06.015
33. Crotty S. T Follicular Helper Cell Differentiation, Function, and Roles in Disease. *Immunity* (2014) 41(4):529–42. doi: 10.1016/j.immuni.2014.10.004
34. Mesin L, Ersching J, Victora GD. Germinal Center B Cell Dynamics. *Immunity* (2016) 45(3):471–82. doi: 10.1016/j.immuni.2016.09.001
35. Pereira JP, Kelly LM, Xu Y, Cyster JG. EBI2 Mediates B Cell Segregation Between the Outer and Centre Follicle. *Nature* (2009) 460(7259):1122–6. doi: 10.1038/nature08226
36. Sweet RA, Ols ML, Cullen JL, Milam AV, Yagita H, Shlomchik MJ. Facultative Role for T Cells in Extrafollicular Toll-Like Receptor-Dependent Autoreactive B-Cell Responses In Vivo. *Proc Natl Acad Sci* (2011) 108(19):7932. doi: 10.1073/pnas.1018571108
37. Ochiai K, Maienschein-Cline M, Simonetti G, Chen J, Rosenthal R, Brink R, et al. Transcriptional Regulation of Germinal Center B and Plasma Cell Fates by Dynamical Control of IRF4. *Immunity* (2013) 38(5):918–29. doi: 10.1016/j.immuni.2013.04.009
38. Shinnakasu R, Kurosaki T. Regulation of Memory B and Plasma Cell Differentiation. *Curr Opin Immunol* (2017) 45:126–31. doi: 10.1016/j.coi.2017.03.003
39. Robinson MJ, Ding Z, Pitt C, Brodie EJ, Quast I, Tarlinton DM, et al. The Amount of BCL6 in B Cells Shortly After Antigen Engagement Determines Their Representation in Subsequent Germinal Centers. *Cell Rep* (2020) 30 (5):1530–41.e4. doi: 10.1016/j.celrep.2020.01.009
40. Sciammas R, Li Y, Warmflash A, Song Y, Dinner AR, Singh H. An Incoherent Regulatory Network Architecture That Orchestrates B Cell Diversification in Response to Antigen Signaling. *Mol Syst Biol* (2011) 7 (1):495. doi: 10.1038/msb.2011.25
41. Konforte D, Simard N, Paige CJ. IL-21: An Executor of B Cell Fate. *J Immunol* (2009) 182(4):1781. doi: 10.4049/jimmunol.0803009
42. Wu Y, van Besouw NM, Shi Y, Hoogduijn MJ, Wang L, Baan CC. The Biological Effects of IL-21 Signaling on B-Cell-Mediated Responses in Organ Transplantation. *Front Immunol* (2016) 7:319. doi: 10.3389/fimmu.2016.00319
43. Jin H, Carrio R, Yu A, Malek TR. Distinct Activation Signals Determine Whether IL-21 Induces B Cell Costimulation, Growth Arrest, or Bim-Dependent Apoptosis. *J Immunol* (2004) 173(1):657–65. doi: 10.4049/jimmunol.173.1.657
44. Gonzalez DG, Cote CM, Patel JR, Smith CB, Zhang Y, Nickerson KM, et al. Nonredundant Roles of IL-21 and IL-4 in the Phased Initiation of Germinal Center B Cells and Subsequent Self-Renewal Transitions. *J Immunol* (2018) 201(12):3569. doi: 10.4049/jimmunol.1500497
45. Racine R, Jones DD, Chatterjee M, McLaughlin M, MacNamara KC, Winslow GM. Impaired Germinal Center Responses and Suppression of Local IgG Production During Intracellular Bacterial Infection. *J Immunol* (2010) 184(9):5085. doi: 10.4049/jimmunol.0902710
46. Hastey CJ, Elsner RA, Barthold SW, Baumgarth N. Delays and Diversions Mark the Development of B Cell Responses to Borrelia Burgdorferi Infection. *J Immunol* (2012) 188(11):5612. doi: 10.4049/jimmunol.1103735
47. Cunningham AF, Gaspal F, Serre K, Mohr E, Henderson IR, Scott-Tucker A, et al. Salmonella Induces a Switched Antibody Response Without Germinal Centers That Impedes the Extracellular Spread of Infection. *J Immunol* (2007) 178(10):6200. doi: 10.4049/jimmunol.178.10.6200
48. Di Niro R, Lee S-J, Vander Heiden JA, Elsner RA, Trivedi N, Bannock JM, et al. Salmonella Infection Drives Promiscuous B Cell Activation Followed by Extrafollicular Affinity Maturation. *Immunity* (2015) 43(1):120–31. doi: 10.1016/j.immuni.2015.06.013
49. Kallies A, Good-Jacobson KL. Transcription Factor T-Bet Orchestrates Lineage Development and Function in the Immune System. *Trends Immunol* (2017) 38(4):287–97. doi: 10.1016/j.it.2017.02.003
50. Elsner RA, Shlomchik MJ. IL-12 Blocks Tfh Cell Differentiation During Salmonella Infection, Thereby Contributing to Germinal Center Suppression. *Cell Rep* (2019) 29(9):2796–809.e5. doi: 10.1016/j.celrep.2019.10.069
51. Chappell CP, Draves KE, Giltiay NV, Clark EA. Extrafollicular B Cell Activation by Marginal Zone Dendritic Cells Drives T Cell–Dependent Antibody Responses. *J Exp Med* (2012) 209(10):1825–40. doi: 10.1084/jem.20120774
52. Hargreaves DC, Hyman PL, Lu TT, Ngo VN, Bidgol A, Suzuki G, et al. A Coordinated Change in Chemokine Responsiveness Guides Plasma Cell Movements. *J Exp Med* (2001) 194(1):45–56. doi: 10.1084/jem.194.1.45
53. Mohr E, Serre K, Manz RA, Cunningham AF, Khan M, Hardie DL, et al. Dendritic Cells and Monocyte/Macrophages That Create the IL-6/APRIL-Rich Lymph Node Microenvironments Where Plasmablasts Mature. *J Immunol* (2009) 182(4):2113–23. doi: 10.4049/jimmunol.0802771
54. Marshall JL, Zhang Y, Pallan L, Hsu M-C, Khan M, Cunningham AF, et al. Early B Blasts Acquire a Capacity for Ig Class Switch Recombination That is Lost as They Become Plasmablasts. *Eur J Immunol* (2011) 41(12):3506–12. doi: 10.1002/eji.201141762
55. Bergqvist P, Gärdby E, Stensson A, Bemark M, Lycke NY. Gut IgA Class Switch Recombination in the Absence of CD40 Does Not Occur in the Lamina Propria and Is Independent of Germinal Centers. *J Immunol* (2006) 177(11):7772. doi: 10.4049/jimmunol.177.11.7772
56. Pone EJ, Zhang J, Mai T, White CA, Li G, Sakakura JK, et al. BCR-Signalling Synergizes With TLR-Signalling for Induction of AID and Immunoglobulin Class-Switching Through the non-Canonical NF-κb Pathway. *Nat Commun* (2012) 3(1):767. doi: 10.1038/ncomms1769
57. Tran TH, Nakata M, Suzuki K, Begum NA, Shinkura R, Fagarasan S, et al. B Cell–Specific and Stimulation-Responsive Enhancers Derepress Aicda by Overcoming the Effects of Silencers. *Nat Immunol* (2010) 11(2):148–54. doi: 10.1038/ni.1829
58. Cerutti A, Zan H, Schaffer A, Bergsagel L, Harindranath N, Max EE, et al. CD40 Ligand and Appropriate Cytokines Induce Switching to IgG, IgA, and IgE and Coordinated Germinal Center and Plasmacytoid Phenotypic Differentiation in a Human Monoclonal IgM<sup<+</sup<IgD<sup< +</sup< B Cell Line. *J Immunol* (1998) 160(5):2145.
59. Clayton E, Bardi G, Bell SE, Chantry D, Downes CP, Gray A, et al. A Crucial Role for the P110δ Subunit of Phosphatidylinositol 3-Kinase in B Cell Development and Activation. *J Exp Med* (2002) 196(6):753–63. doi: 10.1084/jem.20020805
60. Omori SA, Cato MH, Anzelon-Mills A, Puri KD, Shapiro-Shelef M, Calame K, et al. Regulation of Class-Switch Recombination and Plasma Cell Differentiation by Phosphatidylinositol 3-Kinase Signaling. *Immunity* (2006) 25(4):545–57. doi: 10.1016/j.immuni.2006.08.015
61. Ottens K, Schneider J, Kane LP, Satterthwaite AB. PIK3IP1 Promotes Extrafollicular Class Switching in T-Dependent Immune Responses. *J Immunol* (2020) 205(8):2100. doi: 10.4049/jimmunol.2000584
62. Victora GD, Nussenzweig MC. Germinal Centers. *Annu Rev Immunol* (2012) 30(1):429–57. doi: 10.1146/annurev-immunol-020711-075032
63. Trivedi N, Weisel F, Smita S, Joachim S, Kader M, Radhakrishnan A, et al. Liver Is a Generative Site for the B Cell Response to Ehrlichia Muris. *Immunity* (2019) 51(6):1088–101.e5. doi: 10.1016/j.immuni.2019.10.004
64. Tellier J, Nutt SL. Plasma Cells: The Programming of an Antibody-Secreting Machine. *Eur J Immunol* (2019) 49(1):30–7. doi: 10.1002/eji.201847517

65. Sciammas R, Shaffer AL, Schatz JH, Zhao H, Staudt LM, Singh H. Graded Expression of Interferon Regulatory Factor-4 Coordinates Isotype Switching With Plasma Cell Differentiation. *Immunity* (2006) 25(2):225–36. doi: 10.1016/j.immuni.2006.07.009
66. Klein U, Casola S, Cattoretti G, Shen Q, Lia M, Mo T, et al. Transcription Factor IRF4 Controls Plasma Cell Differentiation and Class-Switch Recombination. *Nat Immunol* (2006) 7(7):773–82. doi: 10.1038/ni1357
67. Minnich M, Tagoh H, Bönelt P, Axelsson E, Fischer M, Cebolla B, et al. Multifunctional Role of the Transcription Factor Blimp-1 in Coordinating Plasma Cell Differentiation. *Nat Immunol* (2016) 17(3):331–43. doi: 10.1038/ni.3349
68. Shlomchik MJ, Weisel F. Germinal Center Selection and the Development of Memory B and Plasma Cells. *Immunol Rev* (2012) 247(1):52–63. doi: 10.1111/j.1600-065X.2012.01124.x
69. Yam-Puc JC, Zhang L, Maqueda-Alfaro RA, Garcia-Ibanez L, Zhang Y, Davies J, et al. Enhanced BCR Signaling Inflicts Early Plasmablast and Germinal Center B Cell Death. *iScience* (2021) 24(2):102038–. doi: 10.1016/j.isci.2021.102038
70. Garg M, Wahid M, Khan F. Regulation of Peripheral and Central Immunity: Understanding the Role of Src Homology 2 Domain-Containing Tyrosine Phosphatases, SHP-1 & SHP-2. *Immunobiology* (2020) 225(1):151847. doi: 10.1016/j.imbio.2019.09.006
71. Inoue T, Moran I, Shinnakasu R, Phan TG, Kurosaki T. Generation of Memory B Cells and Their Reactivation. *Immunol Rev* (2018) 283(1):138–49. doi: 10.1111/imr.12640
72. Kaji T, Ishige A, Hikida M, Taka J, Hijikata A, Kubo M, et al. Distinct Cellular Pathways Select Germline-Encoded and Somatically Mutated Antibodies Into Immunological Memory. *J Exp Med* (2012) 209(11):2079–97. doi: 10.1084/jem.20120127
73. Taylor JJ, Pape KA, Jenkins MK. A Germinal Center–Independent Pathway Generates Unswitched Memory B Cells Early in the Primary Response. *J Exp Med* (2012) 209(3):597–606. doi: 10.1084/jem.20111696
74. Zotos D, Coquet JM, Zhang Y, Light A, D'Costa K, Kallies A, et al. IL-21 Regulates Germinal Center B Cell Differentiation and Proliferation Through a B Cell–Intrinsic Mechanism. *J Exp Med* (2010) 207(2):365–78. doi: 10.1084/jem.20091777
75. Lau AWY, Turner VM, Bourne K, Hermes JR, Chan TD, Brink R. BAFFR Controls Early Memory B Cell Responses But is Dispensable for Germinal Center Function. *J Exp Med* (2020) 218(2). doi: 10.1084/jem.20191167
76. Mackay F, Schneider P. Cracking the BAFF Code. *Nat Rev Immunol* (2009) 9(7):491–502. doi: 10.1038/nri2572
77. Stebegg M, Kumar SD, Silva-Cayetano A, Fonseca VR, Linterman MA, Graca L. Regulation of the Germinal Center Response. *Front Immunol* (2018) 9:2469–. doi: 10.3389/fimmu.2018.02469
78. Klein U, Dalla-Favera R. Germinal Centres: Role in B-Cell Physiology and Malignancy. *Nat Rev Immunol* (2008) 8(1):22–33. doi: 10.1038/nri2217
79. Kawabe T, Naka T, Yoshida K, Tanaka T, Fujiwara H, Suematsu S, et al. The Immune Responses in CD40-Deficient Mice: Impaired Immunoglobulin Class Switching and Germinal Center Formation. *Immunity* (1994) 1(3):167–78. doi: 10.1016/1074-7613(94)90095-7
80. Gaspal FM, McConnell FM, Kim MY, Gray D, Kosco-Vilbois MH, Raykundalia CR, et al. The Generation of Thymus-Independent Germinal Centers Depends on CD40 But Not on CD154, the T Cell-Derived CD40-Ligand. *Eur J Immunol* (2006) 36(7):1665–73. doi: 10.1002/eji.200535339
81. Havenar-Daughton C, Lindqvist M, Heit A, Wu JE, Reiss SM, Kendric K, et al. CXCL13 is a Plasma Biomarker of Germinal Center Activity. *Proc Natl Acad Sci USA* (2016) 113(10):2702–7. doi: 10.1073/pnas.1520112113
82. Gitlin AD, Mayer CT, Oliveira TY, Shulman Z, Jones MJK, Koren A, et al. T Cell Help Controls the Speed of the Cell Cycle in Germinal Center B Cells. *Science* (2015) 349(6248):643. doi: 10.1126/science.aac4919
83. Weinstein JS, Herman EI, Lainez B, Licona-Limón P, Esplugues E, Flavell R, et al. TFH Cells Progressively Differentiate to Regulate the Germinal Center Response. *Nat Immunol* (2016) 17(10):1197–205. doi: 10.1038/ni.3554
84. Ding BB, Bi E, Chen H, Yu JJ, Ye BH. IL-21 and CD40L Synergistically Promote Plasma Cell Differentiation Through Upregulation of Blimp-1 in Human B Cells. *J Immunol* (2013) 190(4):1827–36. doi: 10.4049/jimmunol.1201678
85. Allman D, Jain A, Dent A, Maile RR, Selvaggi T, Kehry MR, et al. BCL-6 Expression During B-Cell Activation. *Blood* (1996) 87(12):5257–68. doi: 10.1182/blood.V87.12.5257.bloodjournal87125257
86. Basso K, Dalla-Favera R. Chapter 7 - BCL6: Master Regulator of the Germinal Center Reaction and Key Oncogene in B Cell Lymphomagenesis. In: Alt FW, Editor. *Adv Immunol* (2010) 105:193–210. Academic Press. doi: 10.1016/S0065-2776(10)05007-8
87. Ye BH, Cattoretti G, Shen Q, Zhang J, Hawe N, Rd W, et al. The BCL-6 Proto-Oncogene Controls Germinal-Centre Formation and Th2-Type Inflammation. *Nat Genet* (1997) 16(2):161–70. doi: 10.1038/ng0697-161
88. Fukuda T, Yoshida T, Okada S, Hatano M, Miki T, Ishibashi K, et al. Disruption of the Bcl6 Gene Results in an Impaired Germinal Center Formation. *J Exp Med* (1997) 186(3):439–48. doi: 10.1084/jem.186.3.439
89. Phan RT, Dalla-Favera R. The BCL6 Proto-Oncogene Suppresses P53 Expression in Germinal-Centre B Cells. *Nature* (2004) 432(7017):635–9. doi: 10.1038/nature03147
90. Phan RT, Saito M, Basso K, Niu H, Dalla-Favera R. BCL6 Interacts With the Transcription Factor Miz-1 to Suppress the Cyclin-Dependent Kinase Inhibitor P21 and Cell Cycle Arrest in Germinal Center B Cells. *Nat Immunol* (2005) 6(10):1054–60. doi: 10.1038/ni1245
91. Shapiro-Shelef M, Lin K-I, McHeyzer-Williams LJ, Liao J, McHeyzer-Williams MG, Calame K. Blimp-1 Is Required for the Formation of Immunoglobulin Secreting Plasma Cells and Pre-Plasma Memory B Cells. *Immunity* (2003) 19(4):607–20. doi: 10.1016/S1074-7613(03)00267-X
92. Peng C, Hu Q, Yang F, Zhang H, Li F, Huang C. BCL6-Mediated Silencing of PD-1 Ligands in Germinal Center B Cells Maintains Follicular T Cell Population. *J Immunol* (2019) 202(3):704. doi: 10.4049/jimmunol.1800876
93. Batlle A, Papadopoulou V, Gomes AR, Willimott S, Melo JV, Naresh K, et al. CD40 and B-Cell Receptor Signalling Induce MAPK Family Members That can Either Induce or Repress Bcl-6 Expression. *Mol Immunol* (2009) 46(8):1727–35. doi: 10.1016/j.molimm.2009.02.003
94. Juszczynski P, Chen L, O'Donnell E, Polo JM, Ranuncolo SM, Dalla-Favera R, et al. BCL6 Modulates Tonic BCR Signaling in Diffuse Large B-Cell Lymphomas by Repressing the SYK Phosphatase, PTPROt. *Blood* (2009) 114(26):5315–21. doi: 10.1182/blood-2009-02-204362
95. Niu H, Ye BH, Dalla-Favera R. Antigen Receptor Signaling Induces MAP Kinase-Mediated Phosphorylation and Degradation of the BCL-6 Transcription Factor. *Genes Dev* (1998) 12(13):1953–61. doi: 10.1101/gad.12.13.1953
96. Shinnakasu R, Inoue T, Kometani K, Moriyama S, Adachi Y, Nakayama M, et al. Regulated Selection of Germinal-Center Cells Into the Memory B Cell Compartment. *Nat Immunol* (2016) 17(7):861–9. doi: 10.1038/ni.3460
97. Miura Y, Morooka M, Sax N, Roychoudhuri R, Itoh-Nakadai A, Brydun A, et al. Bach2 Promotes B Cell Receptor–Induced Proliferation of B Lymphocytes and Represses Cyclin-Dependent Kinase Inhibitors. *J Immunol* (2018) 200(8):2882. doi: 10.4049/jimmunol.1601863
98. Muto A, Ochiai K, Kimura Y, Itoh-Nakadai A, Calame KL, Ikebe D, et al. Bach2 Represses Plasma Cell Gene Regulatory Network in B Cells to Promote Antibody Class Switch. *EMBO J* (2010) 29(23):4048–61. doi: 10.1038/emboj.2010.257
99. Ochiai K, Katoh Y, Ikura T, Hoshikawa Y, Noda T, Karasuyama H, et al. Plasmacytic Transcription Factor Blimp-1 Is Repressed by Bach2 in B Cells*. *J Biol Chem* (2006) 281(50):38226–34. doi: 10.1074/jbc.M607592200
100. Béguelin W, Rivas MA, Calvo Fernández MT, Teater M, Purwada A, Redmond D, et al. EZH2 Enables Germinal Centre Formation Through Epigenetic Silencing of CDKN1A and an Rb-E2F1 Feedback Loop. *Nat Commun* (2017) 8(1):877. doi: 10.1038/s41467-017-01029-x
101. Allen CDC, Ansel KM, Low C, Lesley R, Tamamura H, Fujii N, et al. Germinal Center Dark and Light Zone Organization is Mediated by CXCR4 and CXCR5. *Nat Immunol* (2004) 5(9):943–52. doi: 10.1038/ni1100
102. Allen CDC, Okada T, Tang HL, Cyster JG. Imaging of Germinal Center Selection Events During Affinity Maturation. *Science* (2007) 315(5811):528. doi: 10.1126/science.1136736
103. Schwickert TA, Lindquist RL, Shakhar G, Livshits G, Skokos D, Kosco-Vilbois MH, et al. In Vivo Imaging of Germinal Centres Reveals a Dynamic Open Structure. *Nature* (2007) 446(7131):83–7. doi: 10.1038/nature05573
104. MacLennan ICM. Germinal Centers. *Annu Rev Immunol* (1994) 12(1):117–39. doi: 10.1146/annurev.iy.12.040194.001001

105. Victora GD, Schwickert TA, Fooksman DR, Kamphorst AO, Meyer-Hermann M, Dustin ML, et al. Germinal Center Dynamics Revealed by Multiphoton Microscopy With a Photoactivatable Fluorescent Reporter. *Cell* (2010) 143(4):592–605. doi: 10.1016/j.cell.2010.10.032
106. Liu YJ, Malisan F, de Bouteiller O, Guret C, Lebecque S, Banchereau J, et al. Within Germinal Centers, Isotype Switching of Immunoglobulin Genes Occurs After the Onset of Somatic Mutation. *Immunity* (1996) 4(3):241–50. doi: 10.1016/S1074-7613(00)80432-X
107. Roco JA, Mesin L, Binder SC, Nefzger C, Gonzalez-Figueroa P, Canete PF, et al. Class-Switch Recombination Occurs Infrequently in Germinal Centers. *Immunity* (2019) 51(2):337–50.e7. doi: 10.1016/j.immuni.2019.07.001
108. Sundling C, Lau AWY, Bourne K, Young C, Laurianto C, Hermes JR, et al. Positive Selection of IgG+ Over IgM+ B Cells in the Germinal Center Reaction. *Immunity* (2021) 54(5):988–1001.e5. doi: 10.1016/j.immuni.2021.03.013
109. Gitlin AD, Shulman Z, Nussenzweig MC. Clonal Selection in the Germinal Centre by Regulated Proliferation and Hypermutation. *Nature* (2014) 509 (7502):637–40. doi: 10.1038/nature13300
110. Nüsslein HG, Frosch KH, Woith W, Lane P, Kalden JR, Manger B. Increase of Intracellular Calcium is the Essential Signal for the Expression of CD40 Ligand. *Eur J Immunol* (1996) 26(4):846–50. doi: 10.1002/eji.1830260418
111. Gong F, Zheng T, Zhou P. T Follicular Helper Cell Subsets and the Associated Cytokine IL-21 in the Pathogenesis and Therapy of Asthma. *Front Immunol* (2019) 10:2918–. doi: 10.3389/fimmu.2019.02918
112. Calado DP, Sasaki Y, Godinho SA, Pellerin A, Köchert K, Sleckman BP, et al. The Cell-Cycle Regulator C-Myc is Essential for the Formation and Maintenance of Germinal Centers. *Nat Immunol* (2012) 13(11):1092–100. doi: 10.1038/ni.2418
113. Huang C, Gonzalez DG, Cote CM, Jiang Y, Hatzi K, Teater M, et al. The BCL6 RD2 Domain Governs Commitment of Activated B Cells to Form Germinal Centers. *Cell Rep* (2014) 8(5):1497–508. doi: 10.1016/j.celrep.2014.07.059
114. Saito M, Gao J, Basso K, Kitagawa Y, Smith PM, Bhagat G, et al. A Signaling Pathway Mediating Downregulation of BCL6 in Germinal Center B Cells Is Blocked by BCL6 Gene Alterations in B Cell Lymphoma. *Cancer Cell* (2007) 12(3):280–92. doi: 10.1016/j.ccr.2007.08.011
115. Suan D, Kräutler NJ, Maag JLV, Butt D, Bourne K, Hermes JR, et al. CCR6 Defines Memory B Cell Precursors in Mouse and Human Germinal Centers, Revealing Light-Zone Location and Predominant Low Antigen Affinity. *Immunity* (2017) 47(6):1142–53.e4. doi: 10.1016/j.immuni.2017.11.022
116. Kometani K, Nakagawa R, Shinnakasu R, Kaji T, Rybouchkin A, Moriyama S, et al. Repression of the Transcription Factor Bach2 Contributes to Predisposition of IgG1 Memory B Cells Toward Plasma Cell Differentiation. *Immunity* (2013) 39(1):136–47. doi: 10.1016/j.immuni.2013.06.011
117. Wong R, Belk JA, Govero J, Uhrlaub JL, Reinartz D, Zhao H, et al. Affinity-Restricted Memory B Cells Dominate Recall Responses to Heterologous Flaviviruses. *Immunity* (2020) 53(5):1078–94.e7. doi: 10.1016/j.immuni.2020.09.001

Conflict of Interest: The authors declare that the research was conducted in the absence of any commercial or financial relationships that could be construed as a potential conflict of interest.

Publisher's Note: All claims expressed in this article are solely those of the authors and do not necessarily represent those of their affiliated organizations, or those of the publisher, the editors and the reviewers. Any product that may be evaluated in this article, or claim that may be made by its manufacturer, is not guaranteed or endorsed by the publisher.

frontiers in Immunology

ORIGINAL RESEARCH
published: 26 August 2021
doi: 10.3389/fimmu.2021.705307

Impaired B Cell Apoptosis Results in Autoimmunity That Is Alleviated by Ablation of Btk

Jacqueline A. Wright[1†], Cassandra Bazile[1†], Emily S. Clark[1], Gianluca Carlesso[2], Justin Boucher[1], Eden Kleiman[1], Tamer Mahmoud[2], Lily I. Cheng[3], Darlah M. López-Rodríguez[1], Anne B. Satterthwaite[4], Norman H. Altman[5], Eric L. Greidinger[6] and Wasif N. Khan[1]*

[1] Department of Microbiology and Immunology, Miller School of Medicine, University of Miami, Miami, FL, United States, [2] Early Oncology Discovery, Early Oncology R&D, AstraZeneca, Gaithersburg, MD, United States, [3] Oncology Safety/Pathology, Clinical Pharmacology and Safety Sciences, AstraZeneca, Gaithersburg, MD, United States, [4] Department of Immunology, University of Texas Southwestern Medical Center, Dallas, TX, United States, [5] Department of Pathology, Miller School of Medicine, University of Miami, Miami, FL, United States, [6] Department of Medicine, Miller School of Medicine, University of Miami, Miami, FL, United States

OPEN ACCESS

Edited by:
Jayanta Chaudhuri,
Memorial Sloan Kettering Cancer Center, United States

Reviewed by:
Keishi Fujio,
The University of Tokyo, Japan
David A. Fruman,
University of California, Irvine, United States

***Correspondence:**
Wasif N. Khan
wnkhan@miami.edu

[†]These authors share first authorship

Specialty section:
This article was submitted to B Cell Biology, a section of the journal Frontiers in Immunology

Received: 05 May 2021
Accepted: 30 July 2021
Published: 26 August 2021

Citation:
Wright JA, Bazile C, Clark ES, Carlesso G, Boucher J, Kleiman E, Mahmoud T, Cheng LI, López-Rodríguez DM, Satterthwaite AB, Altman NH, Greidinger EL and Khan WN (2021) Impaired B Cell Apoptosis Results in Autoimmunity That Is Alleviated by Ablation of Btk. Front. Immunol. 12:705307. doi: 10.3389/fimmu.2021.705307

While apoptosis plays a role in B-cell self-tolerance, its significance in preventing autoimmunity remains unclear. Here, we report that dysregulated B cell apoptosis leads to delayed onset autoimmune phenotype in mice. Our longitudinal studies revealed that mice with B cell-specific deletion of pro-apoptotic Bim (*BBim*$^{fl/fl}$) have an expanded B cell compartment with a notable increase in transitional, antibody secreting and recently described double negative (DN) B cells. They develop greater hypergammaglobulinemia than mice lacking Bim in all cells and accumulate several autoantibodies characteristic of Systemic Lupus Erythematosus (SLE) and related Sjögren's Syndrome (SS) including anti-nuclear, anti-Ro/SSA and anti-La/SSB at a level comparable to NODH2h4 autoimmune mouse model. Furthermore, lymphocytes infiltrated the tissues including submandibular glands and formed follicle-like structures populated with B cells, plasma cells and T follicular helper cells indicative of ongoing immune reaction. This autoimmunity was ameliorated upon deletion of Bruton's tyrosine kinase (Btk) gene, which encodes a key B cell signaling protein. These studies suggest that Bim-mediated apoptosis suppresses and B cell tyrosine kinase signaling promotes B cell-mediated autoimmunity.

Keywords: autoimmunity, apoptosis, Bcl-2-like 11 (Bim), B cell tolerance, systemic lupus - erythematosus, autoantibodies, Sjogren's syndrome, Bruton's tyrosine kinase (Bkt)

INTRODUCTION

A vast B cell repertoire is generated by a random recombination of exons that are assembled to encode a diverse set of B cell receptors (BCRs) necessary to mount antigen-specific immune responses against a large variety of pathogen-derived antigens as well as potential neoantigens. The process called V(D)J recombination inherently produces a large number of self-reactive B cell clones. Therefore, exquisitely controlled mechanisms of immune tolerance operate during development in the bone marrow (BM)

to eliminate autoreactive clones (1, 2). The primary mechanisms of tolerance in the BM include receptor editing, clonal deletion by apoptosis and anergy. Central tolerance eliminates most of the autoreactive B cells immediately after completing and displaying their assembled BCRs. Additional tolerance checkpoints purge the autoreactive B cell clones that variably escape these controls in the BM or are generated in the germinal centers during an immune response (3, 4).

While relatively strong BCR signaling results in the immature B cell negative selection, tonic or low level BCR signaling is continuously required for the survival and maturation of newly formed immature B cells in the BM as well as after their emigration to the spleen as transitional 1 (T1) B cells (5–9). We and others have shown that B cells at the T1 stage remain sensitive to apoptosis to serve as a second tolerance check point allowing deletion of autoreactive B cells in the periphery (7–9). These studies also showed that the window of opportunity for self-tolerance is limited as progression into transitional 2 (T2) B cells allows BCR engagement to promote positive selection (7, 10–13). BCR signaling in T2 cells induces sustained NF-kB activation, upregulation of BAFFR (TNFRSF13c) and more robust synergy between BCR and BAFFR. Excess availability of BAFF and increased BAFFR signaling can sway BCR-engaged autoreactive transitional B cell clones to undergo maturation into follicular (Fo) and marginal zone (MZ) B cells and can promote autoimmunity (6, 7, 14–17). BAFF function becomes particularly important when other B cell coreceptors positively influence autoreactive B cell activation (5, 6, 14, 16, 18). For example, self RNA and DNA reactive B cell clones receive the first antigen specific signal *via* the BCRs, which endocytose nucleic acids and deliver them to endosomal TLR7 or TLR9. TLRs can then provide the second signal to activate autoreactive B cells (19–23). Availability of BAFF can enhance positive selection of BCR and TLR activated autoreactive B cells and promote their maturation. Thus, TLR and BAFFR can synergize to dysregulate autoreactive BCR signaling towards B cell survival and maturation (18). Recent studies with systemic lupus erythematosus (SLE) patients have identified polymorphisms in genes that dysregulate signaling downstream of BCR, BAFFR and TLRs, supporting synergy between these receptors can promote positive selection of autoreactive B cells leading to autoimmunity (18, 24–26).

Importantly, autoimmune diseases associated with autoAbs are highly common in humans. In fact, both SLE and SS involve B cell hyperactivity that contributes to the development of autoimmune disease manifestation (27). However, whether or not apoptosis-mediated B cell immune tolerance prevents autoimmune disease is an active area of research (16, 28, 29). Clonal deletion of autoreactive B cells by apoptosis can be mediated by cell-extrinsic Fas/FasL – dependent pathway and cell intrinsic mechanisms controlled by pro-apoptotic members of the Bcl-2 family (30, 31). In fact, both pathways may eventually converge on the executioner caspases to induce cell death. Therefore, dysregulated apoptosis is a contributing factor to the escape of autoreactive B cells. However, the physiological role for cell intrinsic pathways, including BH3-only proapoptotic members of the Bcl-2 family, such as Bcl-2-like 11 (Bim) remains elusive (32, 33). Bim is particularly critical in facilitating apoptosis when autoreactive B cells are destined to die (34). Although genetic alterations have been made in apoptosis pathways that variably promote SLE-like disease including *Bim*$^{-/-}$ (C57BL/6 X 129Ssv) (35), B6.Fas$^{lpr/lpr}$ and B6.Bim$^{-/-}$.Fas$^{lpr/lpr}$ (31, 36), the contributions of specific immune cells lacking Bim to autoimmune pathology are not yet fully elucidated. Global deletion of Bim (*Bim*$^{-/-}$) results in SLE-like autoimmune disease in mice with splenomegaly and lymphadenopathy accompanied with lymphocyte infiltration and autoantibody production on a mixed C57BL/6x129Sv genetic background (35). Because Bim is also required for negative selection of T cells at multiple checkpoints and in myeloid cells, the contribution of apoptosis regulation in specific cell types to autoimmune pathology in Bim$^{-/-}$ mice remained unknown. Subsequent adaptive transfer experiments demonstrated that Bim-deficient dendritic cells (DCs) can drive autoimmune pathology (37, 38). More recently, conditional gene deletion approach was used to demonstrate that myeloid cell-specific deletion of Bim led to a severe SLE disease whereas they noted CD4 T cell- or B cell-specific Bim gene deletion did not result in significant manifestation of autoimmunity (39). Another excellent study interrogating Bim function in B cells, did not observe autoimmune phenotype and focused on B cell lymphoma genesis (39, 40). However detailed B cell analysis, particularly relating to autoimmunity was not shown in either study (39, 40). Cumulatively, prior studies implicate Bim in suppressing autoimmunity mediated by myeloid and dendritic cells whereas its role in restraining T and B cells in promoting autoimmune disease remains work in progress.

Here we report detailed longitudinal studies in mice with CD19-Cre mediated B cell-specific Bim deletion the revealing a delayed onset SLE/SS-like autoimmune disease in C57BL/6 background. The *BBim*$^{fl/fl}$ mice had more exaggerated B cell expansion than the Bim null mice, which display a mild autoimmunity in the C57BL/6 background, whereas the increase in T cell numbers was comparable. Autoantibody production included Anti-dsDNA, Anti-SSA, anti-SSB autoantibodies (autoAbs) characteristic of SLE and SS, and their levels were comparable or exceeded autoantibody levels in age-matched NODH2h4 mice. These autoimmune phenotypes were accompanied with lymphocyte infiltration of salivary submandibular glands (SG) which were populated by B cell, Tfh and plasma cells. Thus, Bim-mediated B cell apoptosis suppresses a wide range of autoAbs production and dysregulated apoptosis in B cells promotes T cell activation and participation in autoimmunity. The autoimmunity in *BBim*$^{fl/fl}$ mice was remediated by deletion of Btk, a key B cell signaling tyrosine kinase, suggesting contribution of altered B cell signaling to autoimmune pathology supporting utility of Btk and tyrosine kinase inhibitors in autoimmunity (41, 42).

METHODS

Mice

Adult B57BL/6 (B6) mice were originally obtained from Jackson Laboratory, Bar Harbor, ME and were subsequently bred in

house. $Bim^{fl/fl}$ mice were generated by Korsmeyer group (43) and were obtained from S. Zinkel, Vanderbilt University. B lineage specific Bim-deficient mice were generated by intercrossing $Bim^{fl/fl}$ mice with $CD19^{cre}$ mice (44). All B$Bim^{fl/fl}$ used were heterozygous for $CD19^{cre}$. It has been shown that mice expressing $CD19^{cre}$ have no discernable effect on B cell development (44). The original *Bim-/-* mice in *B6.129S1-Bcl2l11tm1.1Ast/J*[56] had been backcrossed into C57BL/6J (Jackson Laboratory). Spleens from the Bim-deficient mice were kindly provided by Richard T Libby, Flaum Eye Institute, University of Rochester Medical Center, referred here as *Bim-/-*. The generation of $Btk^{-/-}$ mice have been previously described (45). Mice were treated humanely in accordance with federal, state, and institutional guidelines.

Cell Isolation and *In Vitro* Culture Conditions

Spleens were removed and mechanically disrupted, generating a single cell suspension. Red blood cells were then lysed using RBC lysis buffer (Biolegend) according to manufacturer's instructions. Splenic B cells were enriched by negative selection to avoid inadvertent activation, either by autoMACS depletion using anti-CD43 microbeads (Miltenyi Biotec) or using anti-CD43 microbeads B cell enrichment kit (BD Biosciences). B cell purity was determined to be between 92-98% as determined by flow cytometric analysis using antibodies directed against CD19 and IgM (**Table 1**). For B cell proliferation assays, purified B cells were cultured in RPMI (Hyclone laboratories) supplemented with 10% fetal calf serum, 55nM β-mercaptoethanol, 2nM L-glutamine and 100IU penicillin/streptomycin in a 37°C humidified incubator. *In vitro* cultures were left nonstimulated or treated with $F(ab')_2$ goat anti-mouse IgM (10μg/ml; Jackson ImmunoResearch Laboratories), recombinant human BAFF purified from Chinese Hamster ovary cells (46) (100ng/ml), anti-CD40 (2.5μg/ml; BD Bioscience), LPS (2.5μg/ml Sigma- Aldrich), or CpG (1.0μg/ml) at the times indicated. To measure cell death, purified B cells were stimulated with LPS (1μg/ml), CPG (ODN-1826 1μg/ml; InvivoGen), CL097 (1μg/ml; InvivoGen), or $Fa(b')_2$ goat anti-mouse IgM (1μg/ml) in the absence or in the presence of IL-21 (25ng/ml; RnD System) for 48 hours at 37°C. To assess cytokine production, total splenocytes were stimulated with CPG or CL097 for 24 hours and PMA (50ng/ml) and ionomycin (500ng/ml) were added to the culture for the last 4 hours.

TABLE 1 | Antibodies used in this study.

Ab	Conjugate	Clone	Manufacturer	Catalog No.	Dilution
B cell antibodies					
AA4	PE-Cy7	AA4.1	Biolegend	136506	100x
B220	V500	RA3-6B2	BD Bioscience	561226	200x
CD19	PE-CF594	ID3	BD Bioscience	562291	200x
CD21	PE	7g6	BD Bioscience	552957	200x
CD23	PerCP-CY5.5	3B4	Biolegend	101618	200x
CD138	APC	281-2	Biolegend	142506	100x
IgD	Pac Blue	11-26c.2a	Biolegend	405711	400x
IgM	BV711	II/41	BD Bioscience	743327	400x
T cell antibodies					
CD3	BV605	ucht1	Biolegend	300459	100x
CD4	BV711	GK1.5	BD Bioscience	563050	100x
CD8	BV605	53-6.7	BD Bioscience	563152	100x
CD44	PE	im7	eBioscience	12-0441-83	200x
CD62L	Alexa Fluor 700	mel-14	eBioscience	56-0621-82	200x
Cytokine, proliferation and viability antibodies					
Annexin V	FITC	–	Biolegend	640922	–
7AAD	–	–	Biolegend	640922	–
IFNα	FITC	RMMA-1	PBL assay science	22100-3	100x
IFNβ	FITC	MMHB-3	PBL assay science	21400-3	100x
IFNγ	BV786	Q31-378	BD Bioscience	564723	100x
IL-6	PE	MP5-20F3	MP5-20F3	504504	100x
L-10	BV605	JES5-16E3	BD Bioscience	564082	100x
Ki-67	PE-Cy7	B56	BD Bioscience	561283	100x
Immunohistochemistry Antibodies					
Goat anti-mouse CD3	–	M20	Santa Cruz Biotechnology	SC-1127	100x
CD19	Biotin	ID3	BD Bioscience	553784	100x
Anti-goat	Alexa Fluor 647	–	Life Technologies	A-21447	1000x
Streptavidin	Alexa Fluor 488	–	Biolegend	405235	100x

Flow Cytometry

For phenotypic analysis, single-cell suspensions were prepared from spleens, inguinal lymph nodes, submandibular lymph nodes, tertiary lymphoid structures (TLS) and the blood of WT, B*Bim*$^{fl/fl}$, Bim$^{-/-}$, Btk$^{-/-}$ and B*Bim*$^{fl/fl}$ × Btk$^{-/-}$ mice. Cells were stained with fluorescently labelled antibodies in various combinations to identify; B cells and subpopulations including T1, MZ, pMZ, An1, CD21lo and, CD4 and CD8 T cells and their subpopulations including T follicular cells, as defined below. Antibodies, fluorochrome labelling and sources are detailed in **Table 1** and indicated in figure legends.

Intracellular cytokine staining was carried out by first staining cell surface markers in PBS with 2% serum after incubation with FcR-block (CD16), washed and stained with antibodies to various cytokines (IFN-γ, IFN-α, IL-6, IL-10 and TNF-α) using the BD Biosciences fix/perm kit. Dead cells and doublets were excluded from the FCM analysis by Live/Dead dye (BD Biosciences) and SSC-W/SCC-H and FCS-W/FSC-H gating protocols. Dead cells and cells undergoing apoptosis were detected by staining with AnnexinV and 7AAD. All flow cytometry data was acquired on a BD LSR II flow cytometer and analyzed using the FlowJo software package (Tree Star).

Definition of Cell Types by Flow Cytometry

Cell types were defined by the following markers: T1 B cells (CD19+, IgMhi, IgDlo, CD21-, CD23-) MB B cells (CD19^{+}, IgM^{hi}, IgD^{lo}, CD21^{hi}, CD23^{lo}) FoB1 cells (CD19+, IgMlo, IgDhi CD21int CD23+), FoB2 cells (CD19+, IgMhi, IgDhi CD21int CD23+) Plasma cells (B220^{+}CD138^{+}) and Anergic B cells (B220+ AA4+ IgD+ IgMlo). T cells (CD19- CD3+ CD5+), CD4+ T cells (CD19- CD3+ CD4+ CD8-), CD8+ T cells (CD19- CD3+ CD4- CD8+), Tfh cells (CD4+ PD1+ CXCR5+), effector memory T cells (CD44+ CD62L-), Central memory T cells (CD44+CD62L+), Naïve T cells (CD44- CD62L-).

^{3}H-Thymidine Incorporation Cell Proliferation Assay

Cell proliferation was measured by ^{3}H-Thymidine (Perkin Elmer) incorporation into replicative strands of DNA. Cells were cultured in U bottom microplates and stimulated with the indicated agonists for the specified times either in the continuous presence of 1 microcurie per well of ^{3}H-Thymidine for 48 hours or ^{3}H-Thymidine was added in the last 16 hours of the 72 hours incubation period at 37°C in humidified. The ^{3}H-Thymidine labeled DNA was captured on fiber filter disks, which were then placed in a liquid scintillation counting vials before counting on a scintillation beta-counter.

Quantitative PCR

RNA was extracted from freshly isolated cells (*ex vivo*) or after culture *in vitro* with agonists using the RNeasy Mini Kit (Qiagen) and used to synthesize cDNA. RNA was quantified on a NanoDrop 1000 prior to use in the RT-PCR reactions. Reverse Transcription was carried out using equivalent amounts of RNA, dNTP, M-MLV reverse transcriptase, RNase inhibitor, nuclease free water, Random Hexamer, 10xPCR buffer and $MgCl_2$ (All from Applied Biosystems). Taqman Real time reactions used TaqmanUniversal Master Mix or Taqman Fast Advanced Master Mix (Applied Biosystems) and changes in gene expression were determined by running samples on the Stratagene Max 3000p Detection Systems or Step One Real Time System (Applied Biosystems). Primer/Probe combinations were obtained from applied biosystems; (Mm00477631_m1), Bmf (Mm00506773_m1), Btk (Mm00442712_m1), IFNa1 (Mm03030145_gH), IFNb (Mm00439552_s1), IFNg (Mm00801778_m1), IL-6 (MM00446190), IL12p10 (Mm00434169_m1), Mcl-1 (Mm01257351_g1) MCP-1 (Mm00441242_m1), TNFa (Mm00443258_m1), TLR7 (Mm00446590), and TLR9 (Mm00446193_m1). The relative mRNA fold induction for each gene was calculated relative to 18S ribosomal RNA or GAPDH expression.

Autoantibody Array

Sera from mice of indicated ages were hybridized to an array containing approximately 75 autoantigens as described (47). Briefly, IgM and IgG antibodies were detected with Cy3 and Cy5 coupled secondary antibodies. Data were normalized to total Ig levels and clustered by antigen. Red indicates greater reactivity than the average for each antigen, green indicates lower reactivity than the average for each antigen.

ELISA Detection of Antibody Isotypes

Blood samples were obtained by retro-orbital bleeding of mice using heparin containing microcentrifuge tubes. Samples were centrifuged to pellet the RBC before the serum was drawn off and stored at -80 until analysis. For the determination of Igs (total Ig, IgM, IgG1, IgG2a, IgG2c, and IgG3) in the serum/plasma using SBA clonotyping system according to the manufacturer's instructions (Southern Biotechnology Associates). Briefly, plates were coated with 5 μg/ml of capture Ab, and serum (diluted 1/1,000) was incubated and bound Igs were revealed by HRP-labeled secondary Abs. Results are plotted as the concentration of each Ig isotype.

Serum autoAbs against ANAs, nRNP, SSA, and SSB were measured using ELISA kits (Alpha Diagnostics, San Antonio, TX, USA). Sera were diluted 20-fold before the assay and the manufacturer protocol was followed. Positive values for autoreactive antibodies were determined by the manufacturers cut off value. Soluble BAFF was measured using a mouse BAFF quantikine ELISA respectively (R&D systems). Serum was diluted 50-fold and the manufacturer protocol was followed and ELISA plates were developed and absorbance (absorbance 450nm) using microplate ELISA reader.

ELISpot for Mouse IgM and IgG

Detection and enumeration of B cells secreting IgM and IgG was determined by ELISpot according to the manufacturer's instructions. Briefly, antigen was coated onto the ELIspot plate and B cells from the indicated genotypes were incubated on the plate for 16-24 hours before spots were detected. After the incubation time, the plate was washed and biotinylated antigen was added. The plate was washed again prior to the addition diluted Streptavidin-ALP which was incubated for 1 hour. At the completion of the incubation time, the plate was washed and the

substrate solution (BCIP/NBT-plus) was added and incubated until distinct spots emerged. The color development was then stopped by washing the plate with tap water and allowed to dry before reading on a ELISpot reader.

Cytokine Bead Array

Serum cytokine levels were determined by cytokine bead array in accordance with the manufacturer's guidelines (551287 BD Biosciences). Briefly, serum samples were mixed cytokine labeled capture beads. Each capture bead mixture has a distinct fluorescence when acquired by FCM. The intensity of brightness in the PE channel reveals the cytokine concentration. FCAP Array software (BD Biosciences) was used to calculate results.

Immunohistochemistry

Spleens, LN, intestines, liver, kidney, salivary glands and other tissues from WT and B$Bim^{fl/fl}$ mice were formalin (10%) fixed immediately upon harvest, paraffin embedded for H&E staining or frozen in for immunofluorescence staining. Sections were stained with anti- mouse CD19 biotinylated (revealed by streptavidin Alexa Fluor 488) and anti-mouse CD3 (revealed by Alexa Fluor 647 conjugated goat anti-mouse Ab) to visualize B and T cells. Slides were analyzed using a Zeiss Axiovert 200M fluorescence microscope and the Axiovision 4.6 data analysis software program. For H&E staining spleen, kidneys, Pancreas, salivary glands, liver, lungs, and intestines were harvested from control and mutant mice. Tissues were reviewed and scored by a board-certified veterinary pathologist. Scores of inflammation and glomerulonephritis were determined and scored as (0, none; 1, mild; 2, moderate; 3, severe; and 4 extensive). Slides were analyzed and imaged using the Olympus VS120 slide scanner.

Statistical Analyses

Data collected were compared by two-tailed Students t test. Values of $^*p \leq 0.05$ were considered statistically significant.

RESULTS

B Cell-Specific Deletion of Bcl2l11 ($BBim^{fl/fl}$) Leads to Expansion of B and T Cells

To address the significance of B cell-intrinsic regulation of apoptosis in establishing tolerance in the wild type B cell repertoire, we crossed a CD19-cre mouse to a mouse carrying Loxp flanked Bim gene (Bcl2l11) alleles in C57BL/6 background, previously described by Korsmeyer group (43). The mouse produced by this intercross was confirmed for Bim deletion in the B lineage, termed $BBim^{fl/fl}$ (**Supplementary Figure 1A**). We found that $BBim^{fl/fl}$ mice developed splenomegaly and lymphadenopathy at a relatively early age with a corresponding increase in splenic weight, size and cellularity (**Figures 1A, B** and **Supplementary Figure 2A**). Splenic lymphoid follicles appeared normal in young $BBim^{fl/fl}$ mice (**Figure 1C**), but with age the lymphoid follicles in the $BBim^{fl/fl}$ mice were enlarged and fused due to enlarged B cell zones and became disorganized in one year and older mice (**Supplementary Figure 2D**). The overall splenic B cell numbers were increased 2-3 fold in young adult $BBim^{fl/fl}$ mice relative to littermate control mice (**Figure 1D**), consistent with recent reports of B cell-specific Bim deletion (39, 48). In contrast to the previous reports, the increase in B cell numbers and ratios was maintained into relatively old age (**Figure 1D**).

The overall T cells were also variably increased in the $BBim^{fl/fl}$ relative to control mice but to a lesser extent relative to the expansion of B cells (**Figure 1E**). Like B cells, the increases in T cells did not wane with age (**Figure 1E**).

Prior studies have reported that the SLE-like phenotype observed in systemically Bim-deficient mice ($Bim^{-/-}$) in a mixed genetic background (SV129 x C57BL/6) was much milder in pure C57BL/6 background (35, 36, 49). Therefore, we compared overall B and T cell proportions and numbers in the $BBim^{fl/fl}$ mice with $Bim^{-/-}$ mice, both in C57BL/6 background. In agreement with the prior reports, we found that the numbers of B cells were increased (1.5-2-fold) in $Bim^{-/-}$ mice relative to WT. However, the expansion of B cells in the $BBim^{fl/fl}$ mice was greater (3-fold) relative to $Bim^{-/-}$ mice (**Figure 1F**), whereas T cells were increased comparably (1.5-2-fold) between the two genotypes (**Figure 1G**). These data suggest a critical B cell-autonomous role for Bim in B cell homeostasis, which is more apparent in the Bim-sufficient milieu in the $BBim^{fl/fl}$ mice. In addition, Bim-sufficient T cell compartment also appears to be influenced by dysregulated B cells directly and/or indirectly including an increase in T cells.

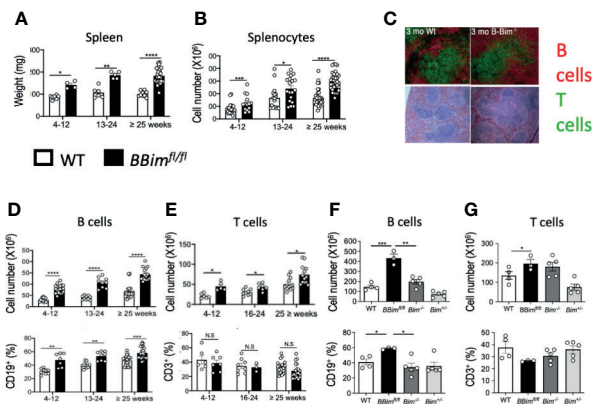

FIGURE 1 | B cell lineage-specific deletion of Bim resulted in expansion of splenic B and T cells. Spleen weights and splenocyte numbers, B cells and T cells were identified by FCM using established cell surface markers as described in materials and methods. **(A)** Spleen weights at different ages from $BBim^{fl/fl}$ *and* WT mice. **(B)** Total splenocyte numbers. **(C)** Immunofluorescence image showing splenic follicles (top panel) stained for B220+ B cells (red) and CD3+ T cells (green) and H&E images (bottom panel) showing follicular structure and lymphocyte organization (top panel) of spleens from 3 month old mice. **(D)** Numbers (top panel) and proportions (bottom panel) of splenic **(D)** B cells and **(E)** T cells. **(F, G)** Quantification of splenic B and T cells in $BBim^{fl/fl}$ relative to $Bim^{-/-}$ mice. Numbers (top panel) and proportions (bottom panel) of **(F)** B cells and **(G)** T cells. Data is representative of >3 independent experiments. Not significant (N.S) $P > 0.05$, $^*P \leq 0.05$, $^{**}P \leq 0.01$, $^{***}P \leq 0.001$, $^{****}P \leq 0.0001$, calculated by Students T- test and Mann-Whitney non-parametric test.

In young *BBim$^{fl/fl}$ mice* (4-12 wk old) the numbers of all mature FoB1 and FoB2 and T1 B cell subsets were increased 2-4 fold, except B1 B cells (**Figures 2A–C** and data not shown). In contrast, the proportions of MZ and precursor (pMZ) B cells were significantly decreased in *BBim$^{fl/fl}$* mice with age relative to WT mice, which also reflected in a modest decrease in their numbers (**Figures 2D, E**). In what may be a related finding, the reduction in CD21 expression was greater in *BBim$^{fl/fl}$* than WT B cells (**Figure 2E**, bottom panels). We noted that CD21$^-$ and CD23$^-$ double negative (DN) B cells were significantly increased in *BBim$^{fl/fl}$* spleens and progressively further increased with age relative to WT (**Figure 2F**). Given increased numbers of T1 B cells escape deletion in the *BBim$^{fl/f}$*, we wondered whether anergic (An1/T3) B cells that have a shorter life span and are hypersensitive to apoptosis may live longer and accumulate, consistent with previous findings (34). Indeed. the anergic An1/T3 B cells increased in the *BBim$^{fl/fl}$* mice (**Figure 2G**). The abnormal increases in T1 and An1/T3 B cells may be consequential for autoAb production as plasma B cells were also increased (**Figure 2H**). An increase in T1 B cells, which serves as a first peripheral tolerance checkpoint suggests that this otherwise apoptosis-sensitive population survives negative selection. Likewise, An1 B cells also acquire resistance to apoptosis and may contribute to break in tolerance in *BBim$^{fl/fl}$* mice. The potential for T-B interaction was investigated by evaluating CD40 on B cell and helper T cells. The cell surface CD40 expression is reduced in lupus patient B cells that resemble ABC B cells (50), but there was no difference in the CD40 levels in WT and in *BBim$^{fl/fl}$* B cells (**Figure 2I**). The CD4 and CD8 T cell numbers were increased with age but proportions were not significantly altered (**Figures 2J–M**). The T cell subset analysis revealed that effector CD4 T cells were increased (**Figures 2N, O**), but CD8 T cells were not (**Figures 2P, Q**). These data suggest that dysregulated apoptosis in B cells by loss of Bim promotes accumulation of autoreactive B cell populations and CD21^{lo}CD23^{lo} B cells, which may be related to SLE-associated Tbet$^+$ B cells (51), along with an increase in CD4 T effector and Tfh cells (**Figures 2R, S**) raise the possibility of autoimmune pathogenesis in *BBim$^{fl/fl}$* mice. This potential is also supported by the findings that *BBim$^{fl/fl}$* mice die earlier than their WT counterparts (**Supplementary Figure 2E**).

BBim$^{fl/fl}$ Mice Display Systemic Autoimmunity

Our data suggests that Bim mediated apoptosis is critical for B cell homeostasis and loss of this regulatory function may lead to autoimmune pathogenesis, which is not consistent with previous reports (39, 40, 52). We therefore, aimed to better define the pathophysiological effects of B cell specific loss of Bim, we analyzed various tissues for immune cell infiltration and damage in cohorts of *BBim$^{fl/fl}$* and WT mice at different ages. We found that with age (6 months and older), the *BBim$^{fl/fl}$* mice displayed lymphocytic infiltration in the liver and the lungs (**Supplementary Figure 2B**), as previously described for *Bim$^{-/-}$* mice (35, 43). In addition, the majority of the *BBim$^{fl/fl}$* mice had immune cell infiltration in the SGs, and kidneys (**Figures 3A–C** and **Supplementary Figure 2C**). Given these tissues are affected in SLE and SS they were further analyzed by immunohistochemistry. We found that glomeruli in *BBim$^{fl/fl}$* mice were disorganized and damaged (**Figure 3C** upper panels) with evidence of T cell infiltration and to a lesser extent B cell infiltration, (**Figure 3C** lower panels). Consistently, *BBim$^{fl/fl}$* mice also showed an increase in Bun/Crea ratio in the blood (**Figure 3D**). The glomerular damage was present in 40% of *BBim$^{fl/fl}$* mice but not observed in the WT controls (**Figures 3E, F**).

Enlarged SGs are among the characteristic features of SS, therefore, *BBim$^{fl/fl}$* SGs were more closely examined by histology and expanded to immune cell phenotype by FCM. Histological examination of the SGs revealed significant lymphoid hyperplasia, consisting of small lymphocytes (**Figure 4A**). Furthermore, immune cell infiltrates in the SGs formed follicle-like structures populated with B cells and plasma cells (PCs) (**Figures 4B, C**). These data suggest chronic inflammation, which may result in the loss of SG acini and impaired SG function. To uncover any T cell contribution to the PC formation FCM analysis of submandibular LNs was performed. The results revealed a two-fold increase in the T follicular helper cells (PD1$^+$CXCR5$^+$Bcl6$^+$) in *BBim$^{fl/fl}$* relative to WT mice (**Figures 4D, E** and **Supplementary Figures 3A–D**). Tertiary lymphoid structures (TLSs) are often formed at the site of inflammation and are associated with autoimmune inflammation (8, 53). We found that *BBim$^{fl/fl}$* mice had TLSs in the proximity of SGs as well as in the abdomen as a network of strings of lymph node-like structures (**Supplementary Figure 4A**). The TLS in the *BBim$^{fl/fl}$* mice were composed of different proportions of B cells, T cells and dendritic cells in different mice. B cell phenotype was also distinct containing different ratios of CD23$^-$CD21$^+$ MZ-like and CD21$^+$CD23$^+$ FoB like B cells (**Supplementary Figure 4B**). The extent of infiltration and neogenesis of TLS varied between mice. Taken together, these data support the notion that apoptosis-resistant B cells escape self-tolerance mechanisms in *BBim$^{fl/fl}$* mice and can mediate SS- and SLE-like autoimmune pathology. Our findings differ with recent studies reporting no obvious autoimmune pathology in mice with B cell-specific Bim deletion, perhaps due to analysis limited to relatively young mice (39, 48).

SLE and Sjögen's Signature autoAbs in *BBim$^{fl/fl}$* Mice

To extend our findings of systemic autoimmunity in *BBim$^{fl/fl}$* mice, serum immunoglobulins were measured by ELISA. While both young and old *BBim$^{fl/fl}$* mice displayed increased circulating IgG2a/c (**Figures 5A, B**, right panels). The IgM levels were low in young mice but increased in older mice (**Figures 5A, B**, left panels), whereas IgG1 increased only in the young mice and IgG3 was not changed (**Supplementary Figures 5A, B**). Consistently, IgG2a/c antibody secreting cells (ASCs) were also increased in the older *BBim$^{fl/fl}$* mice (**Figure 5C**).

For a comprehensive analysis of autoAb breadth and specificity, we used an autoantigen (autoAg) array representing more than 90 of the most common autoantigens in serum from mice grouped by ages; 2-3, 6-9 months, one-year and over one-

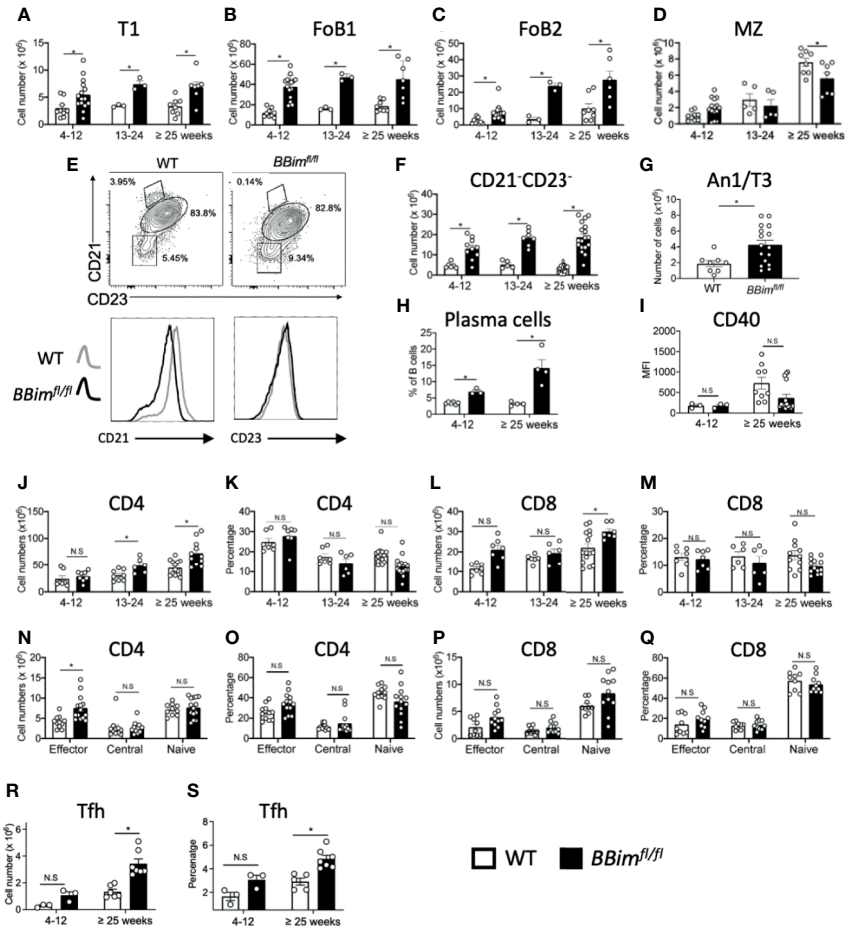

FIGURE 2 | *BBim*$^{fl/fl}$ mice have expanded effector B and T cell populations in the spleen. Splenic B and T cell subpopulations were identified by FCM using established cell surface markers described in materials and methods. **(A–D)** Numbers of T1, FoB1, FoB2 and MZ plus pre-MZ B cells subsets in *BBim*$^{fl/fl}$ and WT mice in the indicated age groups. **(E)** Representative FCM plots showing gating strategy to quantify CD21 and CD23 double negative (DN) B cells within total B cells (top panels) and histograms displaying CD21 and CD23 expression showing reduced CD21 expression in B cells from *BBim*$^{fl/fl}$ relative to WT mice (bottom panels). **(F)** Numbers of CD21$^-$ CD23$^-$ DN B cells in *BBim*$^{fl/fl}$ and WT mice. **(G)** Numbers of anergic (An1/T3) B cells. **(H)** Numbers of plasma cells. **(I)** MFI values of CD40 in B cells **(J–Q)** Quantification of splenic CD4 and CD8 T cell populations on CD3+ gated cells in the ≥ 25 week old *BBim*$^{fl/fl}$ and WT mice. Representative graphs displaying **(J)** CD4 T cell numbers and **(K)** proportions and **(L)** CD8 T cell numbers and **(M)** proportions. **(N)** Cell numbers and **(O)** proportions of CD4 effector, central memory and naïve CD4 subsets. **(P)** CD8 T cell numbers and **(Q)** proportions of CD8 effector, central memory and naïve T cells. **(R)** Cell numbers and **(S)** percentages of Tfh cells. Data is representative of >3 independent experiments. Not significant (N.S) $P > 0.05$, *$P \leq 0.05$, calculated by Students T- test and Mann-Whitney non-parametric test.

year. IgM and/or IgG autoAbs to several known autoantigens particularly those characteristic of SLE and SS were present in the serum from mice of the indicated genotypes and ages (**Figures 6A, B**). Each serum specimen was taken from a different mouse so each time point would be independent. Many autoAbs showed overexpression in the majority of *BBim*$^{fl/fl}$ mice, whereas this pattern was not seen with any autoantibodies at any time points for the WT or NODH2h4 mice. Among the earliest autoAbs to emerge were all of the tested SS-associated antibodies (Ro52/SS-A, Ro60/SS-A, La/SS-B, CENP-B), and a variety of lupus-associated autoantibodies targeting DNA complexes, ribonucleoproteins, and connective tissue/structural antigens, collectively including nuclear, cytoplasmic, membrane-bound, and extracellular targets. Over time, many additional lupus-associated autoantibodies emerged. All the SS and SLE autoantibodies showed persistence over time, and showed progression from IgM to also IgG expression (**Figures 6A, B**).

The presence of autoAbs to autoantigens characteristic of SS and SLE including anti-dsDNA, -sm/RNP, -La/SSB, -Ro/SSA were confirmed by ELISA (**Figures 6C–G**). Some of older *BBim*$^{fl/fl}$ mice had a tendency of increased autoreactive ASCs in the LNs associated with the sSGs relative to WT controls, although only anti-SSA IgM was statistically significant (**Supplementary Figure 6**). Together, autoAb array, ELISA and ELISpot data demonstrate that SLE/SS characteristic autoAbs were elevated much more frequently among *BBim*$^{fl/fl}$ mice relative to WT controls.

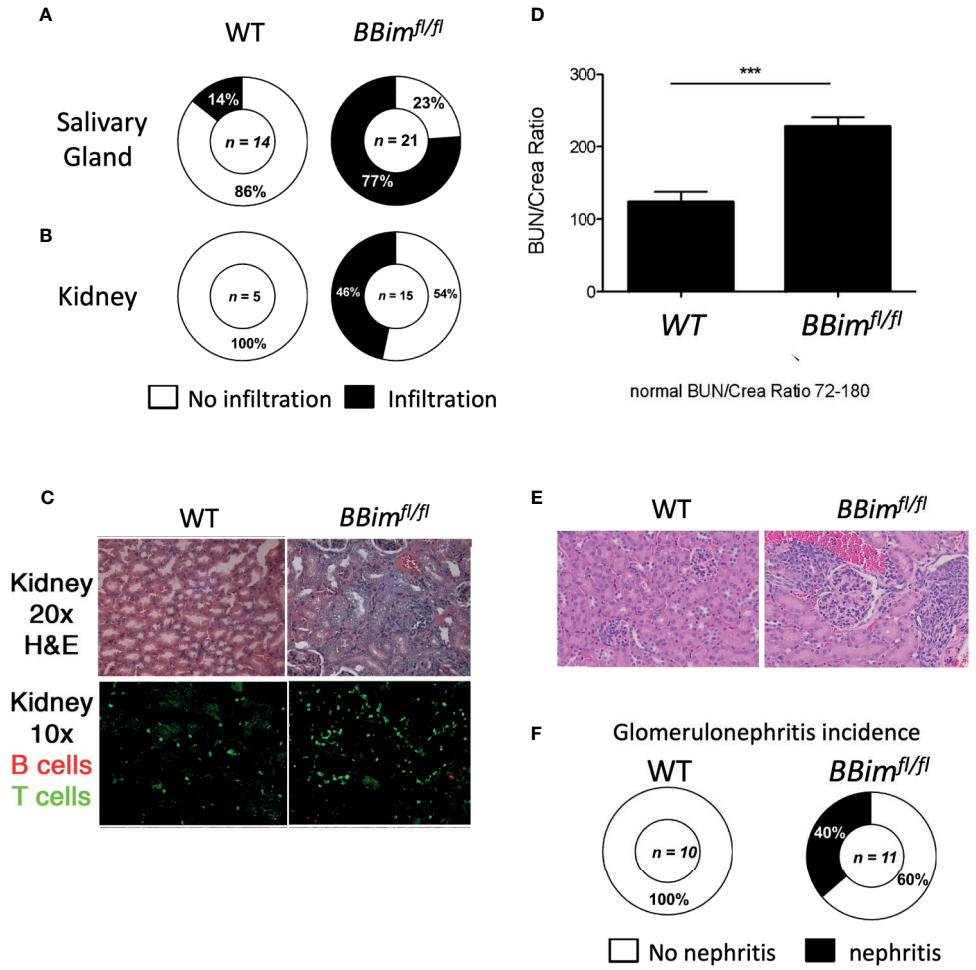

FIGURE 3 | *BBim*$^{fl/fl}$ mice exhibit multiorgan lymphocyte infiltration and kidney damage. Tissues from ≥ 6 month old WT (n ≥3) and *BBim*$^{fl/fl}$ (n ≥8) mice were assessed for tissue damage. Representative pie charts show incidence of inflammation in the **(A)** salivary glands, and **(B)** kidneys. **(C)** Representative H&E images showing glomeruli in kidney sections (top panels) and immunofluorescence images of kidney sections (bottom panels) showing infiltrated T cells (green) and B cells (red) **(D)** Blood urea nitrogen and plasma creatine levels (BUN/crea) in the blood (age ≥ 6 month old) **(E)** H&E stained images of kidney sections showing enlarged glomeruli (glomerulonephritis) in *BBim*$^{fl/fl}$ relative to WT mice. **(F)** Incidence of kidney damage in the *BBim*$^{fl/fl}$ and WT mice. ***P ≤0.001, calculated by Students T-test.

Dysregulation of B cells and autoAb production in SLE-like autoimmune disease are influenced by both innate (TLR) and adaptive (CD40) pathways and Tfh secreted IL-21 which regulates B cell differentiation into plasma cells, memory B cells and CD11c^{hi} ABC B cells (50, 54, 55). IL-21 can regulate B cell proliferation, differentiation or apoptosis in a context-dependent manner (56, 57). For example, IL-21 can promote both proliferation and differentiation as well as apoptosis in B cells costimulated with anti-CD40, whereas this combination can rescue BCR and TLR9 induced cell death (23, 55–57). Mechanistically, IL-21 inhibits TLR4 and TLR9 induced proliferation by downregulating anti-apoptosis members of the Bcl-2 family and inducing Bim-dependent apoptosis (23, 55–57). Due to relevance of both adaptive and innate pathways in autoAb production (58, 59), we determined whether B cells in the *BBim*$^{fl/fl}$ mouse model are protected from IL-21 induced apoptosis under TLR or CD40 costimulatory conditions (**Figures 7A–D** and **Supplementary Figures 7A–C**). The *BBim*$^{fl/fl}$ B cells were more resistant to IL-21-induced apoptosis relative to WT controls in response to stimulation *via* TLR4 (LPS), TLR9 (CpG),TLR7 (CL097), and anti-CD40 Abs (**Figures 7A–D** and **Supplementary Figure 7A**). Although, the anti-CD40 Abs enhanced B cell viability similarly in both WT and *BBim*$^{fl/fl}$ B cells, IL-21 induced significant apoptosis in WT B cells but not *BBim*$^{fl/fl}$ B cells (**Figure 7D** and **Supplementary Figure 7A**), as previously shown (56). Similar results were obtained with costimulation of peripheral blood B cells with IL-21 plus CL097 and IL-21 plus anti-CD40 (**Supplementary Figure 7B, C**). The rescue of IL-21 induced apoptosis by CD40 may require use of optimal dose and presentation of CD40L (e.g., membrane bound

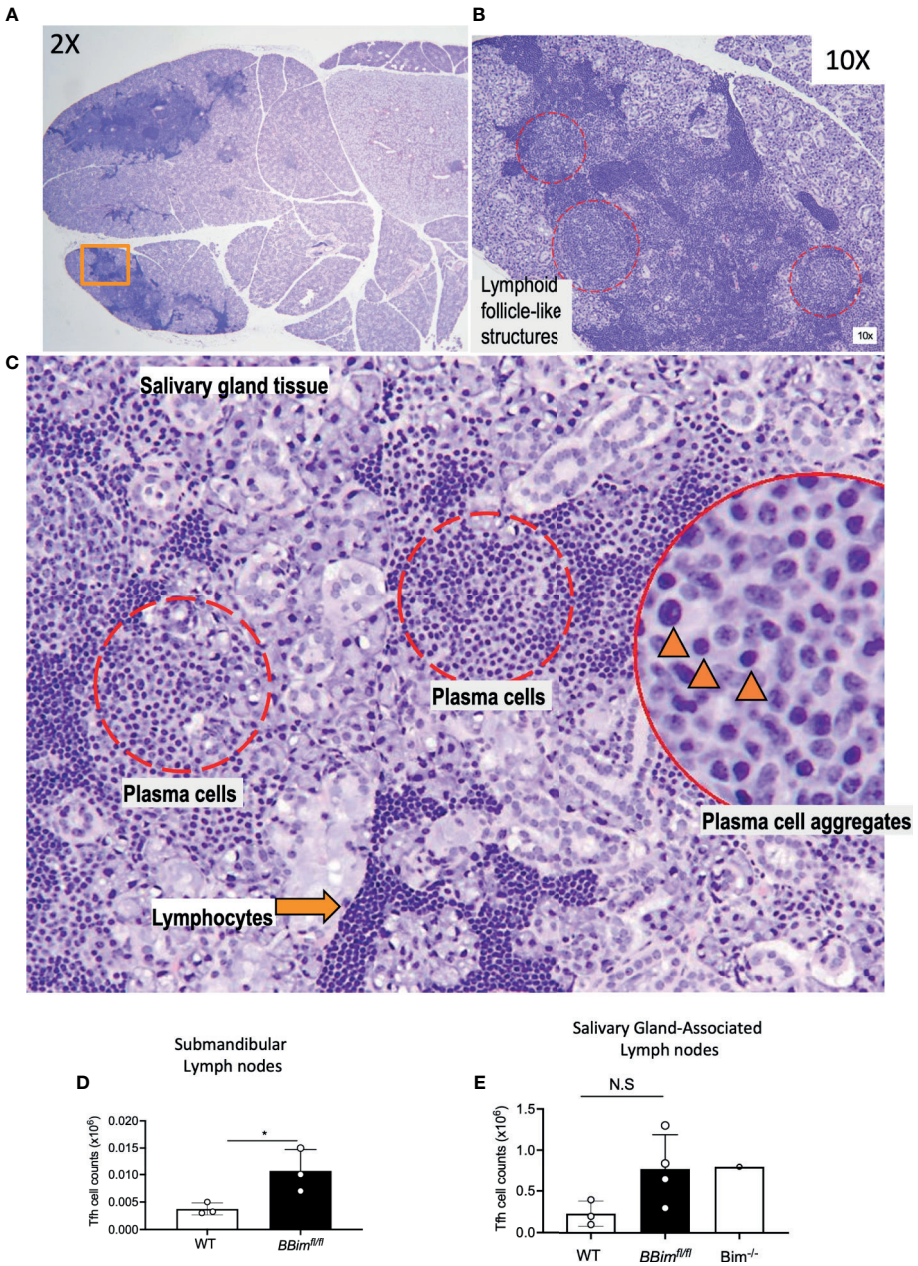

FIGURE 4 | Salivary glands in *BBim*$^{fl/fl}$ mice display ongoing immune reaction. **(A)** Salivary gland from an 8.5 month old *BBim*$^{fl/fl}$ mouse showing aggregates of lymphoid infiltrates (H&E, 2x magnification). **(B)** Region of salivary gland indicated by an orange rectangle in **(A)**, showing pale areas with of lymphoid follicle-like structures (red dotted circles, 10x). **(C)** Higher magnification (20x) of one of these areas demonstrates plasma cell aggregates (red dotted circles); plasma cells are identified by ovoid cells with abundant pale basophilic cytoplasm and eccentric nucleus (inset, black arrowheads, 40x), adjacent to lymphocytic infiltrates identified by smaller cells with scant cytoplasm and prominent dark round nucleus (orange arrow). **(D)** Numbers of Tfh cells in the submandibular lymph nodes and **(E)** salivary gland associated lymph nodes. Not significant (N.S) $P > 0.05$, *$P \leq 0.05$, calculated by Students T- test.

CD40L) as was recently reported (55). These data suggest that B cells from *BBim*$^{fl/fl}$ mice are significantly protected from IL-21 induced apoptosis under both innate and adaptive costimulatory conditions and that innate, adaptive or both mechanisms may contribute to autoAb production targeting autoantigens associated SS and SLE in *BBim*$^{fl/fl}$ mice.

BBim$^{fl/fl}$ B Cells Can Proliferate Upon BCR and TLR Stimulation

To understand the underpinnings of autoimmunity in *BBim*$^{fl/fl}$ mice, B cells were analyzed for spontaneous and induced survival and proliferation. Comparable expression of Ki67 in B cells isolated from WT and *BBim*$^{fl/fl}$ mice indicated that Bim-

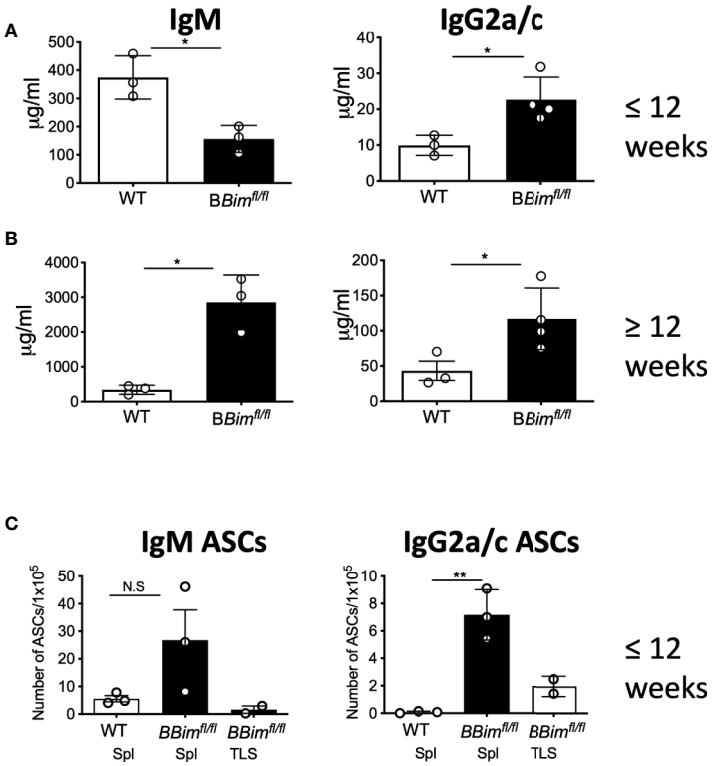

FIGURE 5 | *BBim*$^{fl/fl}$ mice exhibit hypergammaglobulinemia and increased ASCs. Quantification of serum immunoglobulins and ASCs in WT and *BBim*$^{fl/fl}$mice. **(A)** IgM and IgG2a/c levels in serum from mice ≤ 12 weeks old **(B)** IgM and IgG2a/c levels in mice ≥ 12 weeks old mice. Numbers of **(C)** IgM and IgG2a/c ASCs in splenocytes in mice ≥ 12 weeks old. Data is representative of >3 independent experiments. Not significant (N.S) P > 0.05, *P ≤ 0.05, **P ≤ 0.01, calculated by Students T-test.

deficiency does not impair B cell proliferation *in vivo* (**Figure 8E**). To assess BCR induced proliferation *in vivo*, we immunized mice with TNP-Ficoll, a prototypical T cell-independent type-2 antigen that induces clonal B cell expansion and production of antibody response without T cell help (**Figures 8A, B**). The data demonstrated that the numbers of IgM and IgG3 ASCs were greater in the *BBim*$^{fl/fl}$ than in the WT control mice. These results demonstrate that B cells in *BBim*$^{fl/fl}$ mice are capable of proliferation *in vivo* and can do so upon engagement of the BCR with antigen.

Because altered homeostasis of the B cell compartment is likely the driving force in the development of autoimmunity in *BBim*$^{fl/fl}$ mice, we sought to determine mechanisms of B cell expansion. Therefore, the ability of *BBim*$^{fl/fl}$ B cells to proliferate *in vitro* was assessed in response to stimulation *via* TLR4, TLR9 and the BCR with or without combination with BAFF. Purified B cells were cultured in the presence or absence of anti-IgM (Fab_2), BAFF, LPS, and CpG individually or in the indicated combinations for 72 hrs or for a shorter duration (48h) and B cell proliferation measured by DNA synthesis by ^{3}H-Thymidine incorporation (**Figures 8C, D**). The results showed that *BBim*$^{fl/fl}$ B cells proliferated more than the WT controls and BAFF enhanced BCR stimulatory effect, suggesting that *BBim*$^{fl/fl}$ B cells can respond to stimulation *via* key receptors that regulate B cell survival and proliferation. A greater effect of BAFF on BCR induced proliferation of the mutant compared to WT cells could result from *in vivo* BAFF deprivation as indicated by reduced circulating BAFF in *BBim*$^{fl/fl}$ mice (**Figure 8F**). Overall, our data shows that Bim-deficient B cells isolated from *BBim*$^{fl/fl}$ mice can proliferate *in vivo* and can be induced to proliferate *in vitro*. These results are consistent with prior studies showing that Bim-deficient B cells can proliferate normally (43), whereas they differ with another study reporting defective proliferation (60). The reasons for these differences are not clear as both prior studies used *Bim-/-* mice generated in the Korsmeyer laboratory (43). In fact, our data indicates that B cells isolated from *BBim*$^{fl/fl}$ mice can proliferate better under certain conditions, possibly due to the differences in the *in vivo* milieu in mice with B cell-specific deletion compared to the mice lacking Bim in all cells, as indicated by gene expression differences in B cells from the two strains (**Supplementary Figure 8**). An alternative possibility is that the proportion of *BBim*$^{fl/fl}$ B cells that undergo cell division is reduced relative to WT, but their numbers are increased due to resistance to BCR and TLR activation induced cell death in cultures (61, 62). These *BBim*$^{fl/fl}$ B cells undergo DNA synthesis and incorporate ^{3}H-Thymidine independent of the history of cell cycle and number of cell divisions. Consistent with this interpretation, prior studies have shown that while there are substantial numbers of non-dividing cells in Bim-deleted B cell cultures, the number of B cells that had

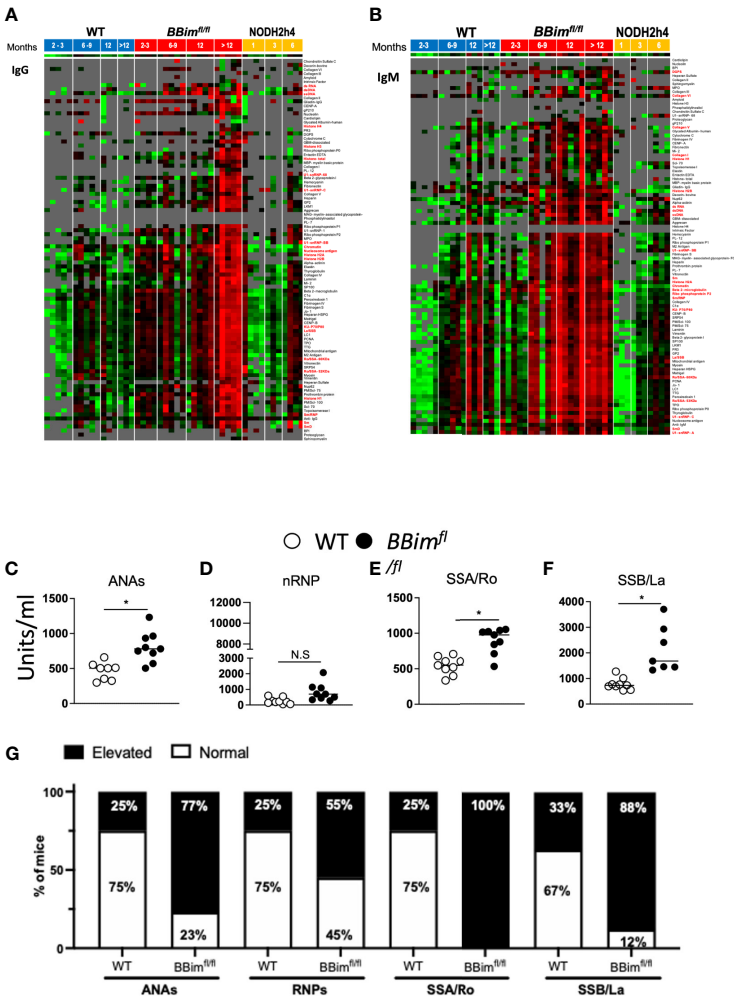

FIGURE 6 | *BBim*$^{fl/fl}$ mice exhibit elevated titers of SLE/SS signature autoAbs. Serum from mice of indicated age groups were screened for autoAbs by hybridizing to an array containing over 90 autoantigens. Each serum specimen was taken from a different mouse so each time point would be independent. Red boxes indicate greater reactivity than the average for each antigen and green boxes indicate lower reactivity than the average for each antigen. Reactivities close to the mean are displayed in black/gray. Some of the SS and SLE-associated autoAb names are highlighted in red. **(A, B)** Heat maps with clustering of WT (left), *BBim*$^{fl/fl}$ (middle) and NODH2h4 (right). Supervised clustering of autoAbs was performed with normalized signal intensities for baseline IgG and IgM autoAbs. **(A)** IgG and **(B)** IgM autoAbs showing higher reactivity (red) appeared in serum of *BBim*$^{fl/fl}$ mice by 6-9 months. At 12 months, additional IgM antibodies emerged and persisted, which were again followed by the subsequent development of IgG antibodies in most instances. In each case tested (with the exception of PR3 antibodies (vasculitis-associated) which remained persistently IgM only), IgM antibodies appeared at time points either concurrent with or prior to the emergence of IgG antibodies, and both IgM and IgG persisted through all subsequent time points. The autoantibodies that emerged included all of the tested SS-associated antibodies (Ro52/SS-A, Ro60/SS-A, La/SS-B, CENP-B), and a variety of lupus-associated autoantibodies (chromatin, ssDNA, alpha-actinin, vitronectin, snRNP, Beta2-GPI, PCNA, nucleosome Ag, Sm-D, Histone H2B, peroxiredoxin 1, ribophosphoprotein P0, myosin, Heparan HSPG, Matrigel, Vitronectin, Heparin, collagen IV). Additional autoantibodies emerging in the same time frame included those targeting some autoimmune hepatitis antigens (LKM1, mitochondrial Ag, LC-1), some myositis-associated antigens (SRP54, Jo-1, Nup6.2), celiac disease –associated targets (DGPS, TTG), as well as the following antigens: C1alpha, the Crohn's-associated antigen GP2, and the thyroiditis-associated antigen TPO. At 12 months, additional IgM antibodies emerged and persisted, followed by the development of IgG in most instances includingU1-snRNP-BB, U1-RNP-C, laminin, hemocyanin, aggrecan, fibrinogen s, autoimmune hepatitis antigens (M2 antigen, SP100), and a scleroderma/myositis-associated target (PM-Scl75). However, some of IgM autoAbs were not accompanied/followed by IgG autoAbs, exemplified by the myositis –associated antigen PL12 and neuropathy-associated myelin associated glycoprotein-Fc (MAG) and collagen V (in older mice).In addition, aged BBimfl/fl mice developed some additional IgM autoAbs to lupus-associated autoantigens in the majority of tested mice including GBM-associated, and prothrombin protein, which were associated with concurrent emergence of IgG against the same targets. Several autoAbs were upregulated only in aged mice and only as IgG, including additional lupus-associated specificities (U1-snRNP68, U1-snRNP1, Sm, total histone, histone H2A, Histone H1, Heparan Sulfate, Entactin-EDTA, collagen II, fibronectin, elastin, fibrinogen IV, ribophosphoprotein P1, ribophosphoprotein p2), a myositis-associated target (Mi-2), some scleroderma-associated specificities (CENP A, Ku P70-p80, Scl-70, Topoisomerase I, PM-Scl100), an autoimmune hepatitis-associated target (gp210), a thyroiditis-associated antigen (thyroglobulin), and the vasculitis-associated target MPO. **(C–F)** Serum from*BBim*$^{fl/fl}$ *and WT* mice (age ≥ 24 weeks old) were assessed for autoAbs distinctive for SS and SLE by ELISA. **(G)** Representative bar graphs show the frequency of elevated (filled bar) and normal (open bar) autoantigens titers in WT and *BBim*$^{fl/fl}$ mice. Elevated titers were determined by calculating the positive index as stated in the ELISA kit protocol (alpha diagnostic international). Data is representative of >3 independent experiments. Not significant (N.S) $P > 0.05$, *$P \leq 0.05$, calculated by Students T-test and non-parametric Mann-Whitney test.

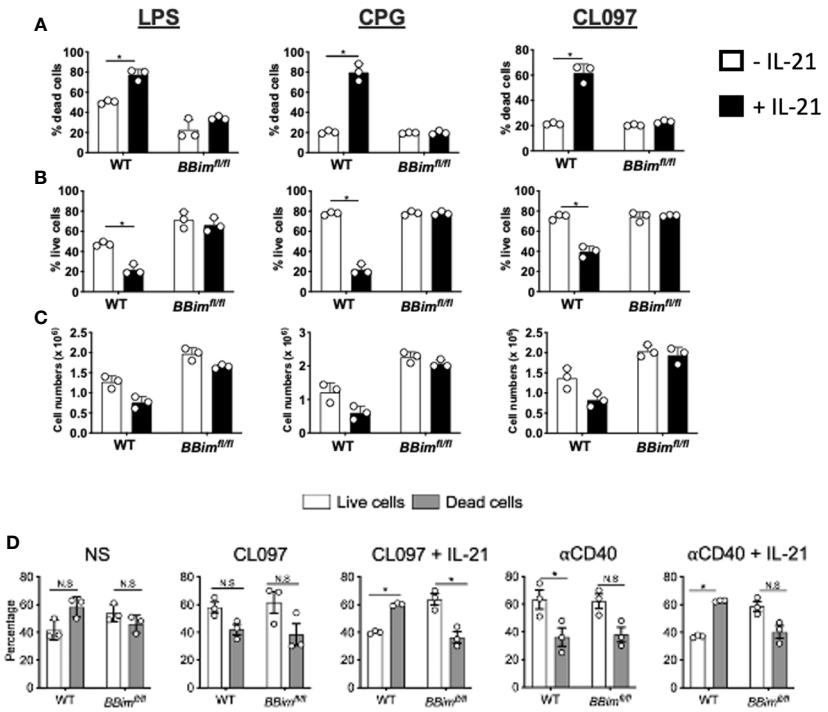

FIGURE 7 | *BBim*$^{fl/fl}$ B cells are resistant apoptosis costimulated with IL-21 and *via* TLR4, TLR7, TLR9 or CD40. Purified B cells from WT and *BBim*$^{fl/fl}$ mice were incubated for 48 hours with the indicated TLR agonists or anti-CD40 in the absence or in the presence of IL-21 (25ng/ml) and then analyzed for **(A)** dead cells and **(B)** live cells distinguished using a fixable viability dye (Invitrogen). **(C)** Numbers of live B cells in the cultures (trypan blue-) **(D)** Splenocytes from *BBim*$^{fl/fl}$ and WT mice were treated with TLR7 agonist (CL097) or anti-CD40 Abs in the absence or in the presence of IL-21 (25ng/ml), stained with annexin V and 7AAD and analyzed by FCM. Bar graphs showing percentages of B cells that are live (white; 7AAD- Annexin V-) and dead (gray; 7AAD+/- Annexin V+) after culture for 48 hours. Not significant (N.S) $P > 0.05$, $^*P \leq 0.05$, calculated by Students T-test.

undergone cell division was not significantly different relative to the WT B cells (40). Together, these results suggest that at least a proportion of B cells from *BBim*$^{fl/fl}$ mice undergo cell division and BAFF may also contribute to B cell expansion in addition to prolonged survival.

To further dissect the underlying reasons for the differences in proliferation of B cells in *BBim*$^{fl/fl}$ mice and those isolated from *Bim*$^{-/-}$ mice previously reported, we compared gene expression profiles between the two genotypes. This analysis included genes that may display compensatory expression such as Bim-related genes encoding BH-3 only pro-apoptotic, along with the anti-apoptotic genes of the Bcl-2 family as well as TLRs and the TLR and BCR signal mediator, Btk, which has been implicated in B cell mediated autoimmunity in mice (63). RNA from purified B cells isolated from *Bim*$^{-/-}$, *Bim*$^{-/+}$, *BBim*$^{fl/fl}$ and WT mice was subjected to qRT-PCR. We found that Bmf mRNA was increased in *BBim*$^{fl/fl}$ B cells (3-4 fold) relative to those isolated from Bim$^{-/-}$, Bim$^{-/+}$ and WT mice (**Supplementary Figure 8A**). The expression of Blcl2 or Mcl1 was reduced in *Bim*$^{-/-}$ B cells relative to WT and *B-Bim*$^{fl/fl}$ B cells (**Supplementary Figures 8C, D**). These results suggest differences in gene expression profiles in B cells lacking Bim based on whether they developed in a Bim-deficient *versus* Bim-sufficient milieu. Increased BH-3 only pro-apoptotic Bmf, which functions in a similar manner to Bim in B cells as deletion of both genes compounds the increase in B cell phenotype (52), suggest some functional compensation of loss of Bim in the *BBim*$^{fl/fl}$ B cells. Interestingly, Btk mRNA was also modestly increased in the *BBim*$^{fl/fl}$ B cells relative to *Bim*$^{-/-}$ B cells (**Supplementary Figure 8B**). In contrast, TLR7 and TLR9 mRNA were largely comparable among the genotypes (**Supplementary Figures 8E, F**), suggesting altered TLR expression is not responsible for increased proliferation *via* TLR7 or TLR9 (**Figures 8C, D**). In this context, both Btk and BH3 only proteins are involved in regulating intracellular $Ca2^+$ flux that is important for B cell proliferation. Thus, an increase in Bmf and Btk may contribute to restoring *BBim*$^{fl/fl}$ B cell proliferation relative to B cells from Bim$^{-/-}$ mice. The nature of this compensation and the inductive signals that drive Bmf and Btk expression remain to be elucidated by careful comparative studies.

Deletion of Btk in *BBim*$^{fl/fl}$ Mice Reduced Symptoms of Autoimmunity

BCR and TLR signaling control B cell selection, growth, activation and differentiation into antibody secreting cells (ASCs). There is a modest increase in Btk gene expression in *BBim*$^{fl/fl}$ mice (**Supplementary Figure 8**) and B cells from *BBim*$^{fl/fl}$ mice express increased levels of certain cytokines (IL-6, IL-10 and IFNa) in response to stimulation *via* TLR7 and

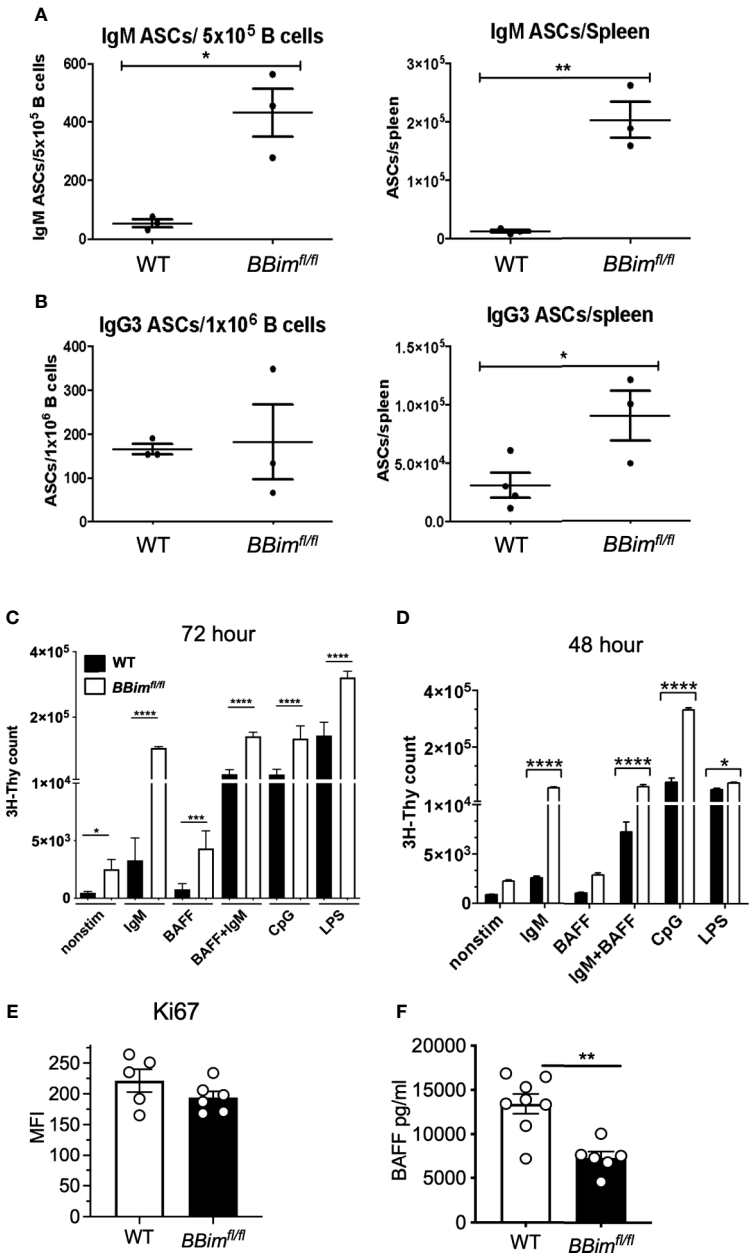

FIGURE 8 | BCR and TLR induced *BBim*$^{fl/fl}$ B cell proliferation is enhanced by BAFF. B cells from WT and *BBim*$^{fl/fl}$ mice were analyzed for differences in activation and proliferation. WT and *BBim*$^{fl/fl}$ mice were immunized with TNP-Ficoll, before measuring B cell and antibody response by ELISpot. Quantification of **(A)** IgM and **(B)** IgG3 antibody secreting B cells from *BBim*$^{fl/fl}$ and WT mice. **(C)** ^{3}H-Thymidine incorporation assay after treatment with indicated agonist for72 hours. **(D)** ^{3}H-Thymidine incorporation of B cells treated with the indicated agonist for 48 hours. **(E)** MFI of Ki67 in B cells from *BBim*$^{fl/fl}$ and WT mice. **(F)** Circulating BAFF levels in serum from *BBim*$^{fl/fl}$ and WT mice. *P ≤ 0.05, **P ≤ 0.01, ****P ≤ 0.0001, calculated by Students T-test.

TLR9 (**Supplementary Figure 9**), both of which utilize Btk for signaling. To test Btk function in the observed autoimmunity, *Btk*$^{-/-}$ (45) and *BBim*$^{fl/fl}$ mice were intercrossed (DKO). Deletion of Btk did not alter overall proportion of splenic B cells in the DKO mice (**Figure 9A**), however, B cell subpopulation distribution was altered and reduced some characteristic features of autoimmune pathology in the *BBim*$^{fl/fl}$ mice (**Figure 9**). Specifically the proportion of mature splenic FoB1 cells (IgM^{lo}IgD^{hi}) was decreased, but not of mature FoB2 cells (IgM^{hi}IgD^{hi}, **Figures 9B, C**), the proportion of immature transitional (T1, IgM^{hi}IgD$^{lo/-}$) B cells was increased (**Figure 9D**), whereas MZ (**Figure 9E**) and anergic B cells (An1 or T3, **Figure 9F**) was decreased in the DKO mice compared to *BBim*$^{fl/fl}$ or WT mice. These outcomes are consistent with our and others

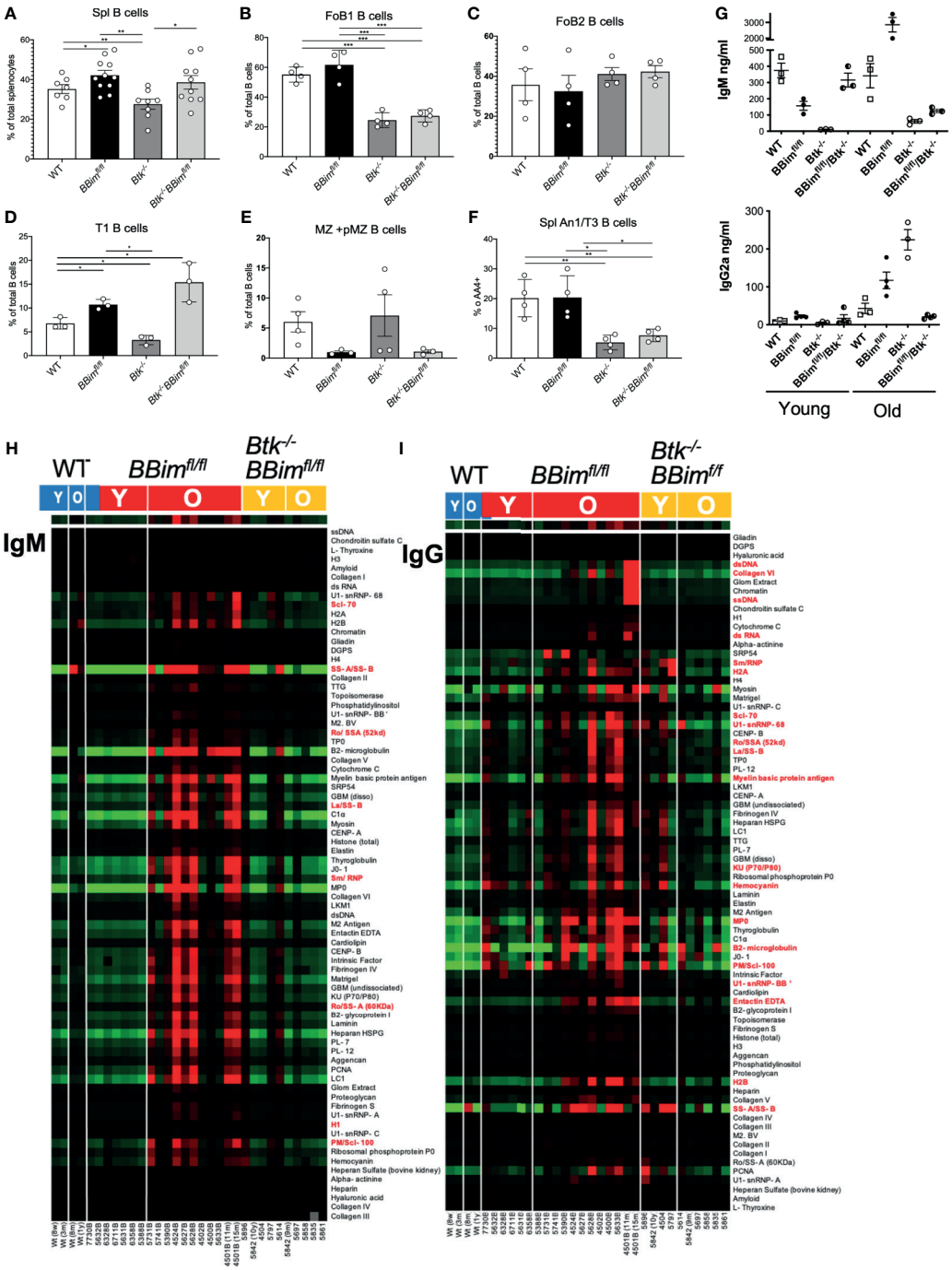

FIGURE 9 | Deletion of Btk in *BBim*$^{fl/fl}$ mice reduced symptoms of autoimmunity. **(A)** Graph displaying splenic B cell percentages in WT, *BBim*$^{fl/fl}$, *Btk*$^{-/-}$ and *Btk*$^{-/-}$*BBim*$^{fl/fl}$ mice. **(B–F)** Representative graphs comparing percentages of the listed B cells subpopulations in WT, *BBim*$^{fl/fl}$, Btk$^{-/-}$, and *Btk*$^{-/-}$ *BBim*$^{fl/fl}$ mice. **(G)** Basal IgM and switched IgG2a antibodies in the serum of young (≤ 12 weeks old) and old (≥ 12 weeks old) mice. **(H, I)** Heat map with clustering of autoAbs in the serum from WT (left), *BBim*$^{fl/fl}$ (middle) and *Btk*$^{-/-}$*BBim*$^{fl/fl}$ (right) mice of indicated ages **(H)** IgM and **(I)** IgG autoAbs. *P ≤ 0.05, **P ≤ 0.01, ***P ≤ 0.001, calculated by Students T-test.

previous findings that loss of Btk selectively reduces FoB1 cells and affects An1 B cell survival (64). These cellular alterations was accompanied with reduced lymphocytic tissue infiltration in the DKO mice (**Supplementary Figure 2B**, right panels). There was a modest increase in the proportions of IL-6^{+} and IFNα^{+} B cells in the *BBim*$^{fl/fl}$ relative to control B cells

(**Supplementary Figures 9A, C**). However, Btk deletion had no significant effect on the circulating cytokines tested including (**Supplementary Figure 10**).

We also noticed that Btk deletion decreased overall basal serum IgM and IgG2a (**Figure 9G**). To determine if overall reduction in the immunoglobulin levels in the DKO mice had an effect on the accumulation of autoAbs, we analyzed serum using autoantigen arrays. Results show that both IgM and IgG autoAbs were decreased in the DKO mice (**Figures 9H, I**). However, IgM autoAbs were reduced in both young and old (**Figure 9H**), IgG autoAbs were decreased only in the old *DKO* mice (**Figure 9H**). Taken together, these results indicate that Btk-dependent signaling likely contributes to aberrant B cell activation and autoimmune pathology in the *BBim*$^{fl/fl}$ mice. This interpretation is consistent with previous reports that overexpression of Btk transgene led to SLE-like autoimmune disease and expression of SYK, another B cell kinase is increased in B cells from lupus patients (63, 65, 66).

DISCUSSION

Self-reactive B cells arise routinely during BCR diversification and are purged to avoid autoimmunity by receptor editing, anergy and apoptosis. Failure of any of these mechanisms could cause autoimmune disease, however, the precise contribution of each of these tolerance mechanisms in eliminating autoreactive B cells and preventing autoimmunity is unclear. To examine the contribution of B cell apoptosis in preventing autoAb production and autoimmune disease, we rendered B cells tolerance-compromised by B cell-specific deletion of proapoptotic Bcl-2 family member Bim, a known regulator of immune tolerance in B and T cells (34, 37). Our longitudinal analysis of *BBim*$^{fl/fl}$ mice indicates that apoptosis contributes to the elimination of autoreactive B cells significantly enough that dysregulation of apoptosis leads to the development of autoimmunity. However, the manifestation of autoimmune disease becomes apparent only with age; although autoAbs and tissue damage can be detected at a relatively young age (< 6 months), the pathogenesis is clearly evident after six months. Nonetheless, our data shows that autoAbs against several prototypical autoantigens associated with SLE and SS are present in *BBim*$^{fl/fl}$ mice at elevated level compared to NODH2h4, a widely used autoimmune mouse model (**Figure 6**). One possible explanation of the delayed onset of autoimmunity in *BBim*$^{fl/fl}$ mice is that the events that trigger autoreactive B cell activation such as inflammation, innate and/or T cell mediated signals take a while to accumulate and manifest in older mice. Furthermore, *BBim*$^{fl/fl}$ B cells are not entirely resistant to apoptosis as they may employ other proapoptotic pathways including Noxa, Puma and Bmf as shown in BAK and BAX double knockout mice (43). These data are consistent with prior findings that autoreactive B cell hyperactivity and autoantibody production in autoimmune diseases involves B cell intrinsic innate TLR signals and adaptive T helper cell signals (*via* CD40) as well as homeostatic regulation by BAFF (23, 67–69) and that depletion of B cells is beneficial for patients with several autoimmune diseases including SLE, RA, SS and MS (70).

Bim is expressed in all tissues including hematopoietic cells and it is a key physiological facilitator of apoptosis in lymphocytes purging autoreactive B and T cells (37, 71). Prior gene targeting experiments have demonstrated that systemic deletion of the gene encoding Bim leads to a systemic SLE-like autoimmune condition in a mixed 129SV x C57BL/6 genetic background. Subsequent reports indicated that SLE-like autoimmunity in Bim-deficient mice gets much milder when bred to pure C57BL/6 background. One explanation for a milder autoimmune response and pathology in Bim-deficient mice is reduced functionality of immune cells. For example, T cells in Bim-deficient mice are defective in TCR-induced activation and IL-2 production due to impaired calcium signaling (72). Additionally, T cell development is impaired at the DN to DP stages in the thymus altering T cellular composition and repertoire in the Bim-deficient mice (73). Alternatively, global loss of Bim in the whole body reduces release of self-antigens from dead and dying host cells that trigger autoimmune response. The data presented here demonstrates that B cell-specific deletion of Bim in C57BL/6 background can lead to SLE and SS-like autoimmune disease with age. We hypothesize that Bim-sufficient T cells and other immunocytes are more potent in promoting B cell activation in *BBim*$^{fl/fl}$ mice contributing to progression of autoimmunity. Our data showing expanded B cell compartment is consistent with prior studies using mb-cre or CD23-cre mediated B cell specific Bim deletion (40). The B cell expansion does not appear to be entirely due to extended survival as *BBim*$^{fl/fl}$ B cells could proliferate *in vitro* and during an immune response *in vivo*. The delayed appearance and mild autoimmune disease in the *BBim*$^{fl/fl}$ mice may explain why autoimmunity escaped detection particularly in younger mice (39, 74).

The immune cell expansion in the *BBim*$^{fl/fl}$ mice was not limited to B cells; an increase in T cells also contributed to the splenomegaly and lymphadenopathy. In this regard, autoimmune disease observed in mice lacking Bim selectively in the myeloid cell-lineage was accompanied with B cell expansion (39). However, mice with a B lineage specific deletion of Bim, described here provide an opportunity to investigate B cell subset-specific role in the development of autoimmunity. While FoB cells were markedly increased, B1 and MZ B cells which are often associated with the development of autoimmunity (75), were not increased suggesting B cell subtype-specific function of Bim in autoimmune pathogenesis. It is possible that the B1 and MZ B cell subsets are changed phenotypically in *BBim*$^{fl/fl}$ mice and contribute to autoimmunity in the *BBim*$^{fl/fl}$ mice. Future experiments will determine the effector functions and localization of B1 and MZ present in *BBim*$^{fl/fl}$ mice. In addition to mature FoB cells, we observed an increase in immature T1 and anergic T3 (An1) B cells. Like immature B cells in the bone marrow, T1 B cells are targeted for negative selection in the periphery to remove autoreactive B cells (7, 11, 18). Furthermore, T3 anergic B cell population is a rich source of autoreactive B cells (76). An

increase in these B cell populations may contribute to break in B cell tolerance in *BBim*$^{fl/fl}$ mice.

SS has been long thought to be a T cell mediated disease especially in the initiation of the autoimmune process within the submandibular SG, however, there is growing evidence that B cells play multiple pathophysiological roles and may be important in the development of SS (77, 78). We found that *BBim*$^{fl/fl}$ mice displayed particularly strong SS phenotype with lymphocytic infiltration of SG, consisting of B cells, plasma cells and Tfh cells (**Figures 2**, **4**). The *BBim*$^{fl/fl}$ mice displayed hypergammaglobulinemia and had elevated autoAbs, including anti-SSB and anti-SSA autoAbs that are characteristic of SS (**Figures 5**, **6**). These data suggest that break in B cell self-tolerance can initiate the autoimmune process that lead to SS-like autoimmunity. However, whether anti-SSB and anti-SSA specific B cell expansion and activation occurs with the help of T cells and/or depends on the second signal *via* the TLRs and BAFFR remains to be determined. Thus, our data reveal a novel role for B cells in the initiation and progression of SS. It is unclear how B cells initiate autoimmune reaction. One possibility is that this role is associated with *BBim*$^{fl/fl}$ B cell function as autoantigen presenting cells, as suggested by their ability to produce inflammatory cytokines like myeloid cells to initiate adaptive immune response (39). Further comparative studies may reveal distinct and overlapping functions of apoptosis resistant B and myeloid cells in autoimmunity.

We found that deletion of Btk reduced autoimmune pathology and autoantibody accumulation in *BBim*$^{fl/fl}$ mice (**Figure 9**). These data suggest that Btk contributes to the hyperresponsiveness of *BBim*$^{fl/fl}$ B cells to BCR and TLR signaling and differentiation into antibody producing cells. These data are consistent with appearance of SLE-like autoimmune disease in mice overexpressing Btk (65, 79), whereas pharmacological inhibition of Btk kinase by PCI-32765 decreased the disease symptoms in several autoimmune models (80). It is possible that loss of Btk function in myeloid cells contributed to the reduction in autoimmune pathology in the *Btk*$^{-/-}$*BBim*$^{fl/fl}$ mice. Future myeloid-specific Btk deletion experiments will address this possibility.

We have demonstrated here that loss of Bim in B cells alone is sufficient to cause SLE/SS-like autoimmunity in C57BL/6 background, notwithstanding, delayed onset. We propose a model in which B cell-specific loss of Bim promotes autoimmunity in several ways. First, by allowing the survival of autoreactive T1 B cells that can go through maturation, damage host tissues by promoting activation of the innate and T cells leading to tissue immune cell infiltration, notably of the SGs and secrete autoAbs that possibly form immune complexes leading to kidney damage. Although, the B cells in *BBim*$^{fl/fl}$ mice primarily display prolonged survival, they may accumulate sufficient activation signals by self-nucleic acids over time and may present RNA/DNA complexed protein autoantigens to activate autoreactive T cells. This T and B cell interaction likely further promotes proliferation of immune cells and the release of inflammatory cytokines which reinforce the innate and humoral immune response to self-antigens as has been previously proposed (20). In support of this we observed an increase in mature FoB and tolerance susceptible T1 and anergic T3 B cells and the ability of *BBim*$^{fl/fl}$ B cells to undergo cell division *in vitro* in response to key immune response regulatory receptors, anti-IgM, BAFF-R and TLR, suggesting *in vivo* priming. Primed B cells in this model would be more responsive to unmethylated CpGs and RNA/protein complexes found in serum or apoptotic bodies from neighboring cells undergoing normal apoptotic processes in the Bim-sufficient mileue in the *BBim*$^{fl/fl}$ mice, fueling a feedback loop whereby B cell activation regulates the immune response to react against self-antigens. In support of this idea, genetic models have shown that impairment of effector cell apoptosis participates in the breakdown of tolerance through chronic signaling caused by repeated exposures to self-antigen resulting in autoimmunity (81). With the predisposition to autoimmunity, *BBim*$^{fl/fl}$ mice can serve as a model for interrogation of genetic and environmental factors that trigger B cell mediated autoimmune disease. Amelioration of autoimmune pathology by Btk deletion in our studies is consistent with our and others' prior studies indicating contribution of altered B cell signaling to autoimmunity and support the therapeutic use of Btk inhibitors in autoimmune diseases (41, 42, 79).

DATA AVAILABILITY STATEMENT

The original contributions presented in the study are included in the article/**Supplementary Material**. Further inquiries can be directed to the corresponding author.

ETHICS STATEMENT

The animal study was reviewed and approved by Office of the Vice Provost for Research Institutional Animal Care & Use Committee Office (IACUC) University of Miami FL 33136.

AUTHOR CONTRIBUTIONS

JAW, CB, ESC, DL-R, GC, and WNK designed research; JAW, ESC, CB, DL-R, GC, LIC, and TM, performed research; JAW, ESC, CB, DL-R, GC ELG and WNK analyzed data; NHA and LIC performed pathology and JAW, CB, ESC, GC, ELG and WNK wrote the paper. All authors contributed to the article and approved the submitted version.

FUNDING

This work was funded by National Institutes of Health grant R21AI088511-01 and Intramural Funding Program, Sylvester Comprehensive Cancer Center, University of Miami to (WK).

ACKNOWLEDGMENTS

We would like to thank, Dr. Oliver Umland (Diabetes Research Institute, University of Miami) for his expertise and help with flow cytometry and sorting experiments and Sylvester Comprehensive

Cancer Center, Flow Cytometry Shared Resource. We thank Ms. Daniela Rocca for technical assistance. We would also like to thank Dr. Richard T Libby Flaum Eye Institute, University of Rochester Medical Center, Rochester, NY for providing spleens from Bim-deficient mice.

SUPPLEMENTARY MATERIAL

The Supplementary Material for this article can be found online at: https://www.frontiersin.org/articles/10.3389/fimmu.2021.705307/full#supplementary-material

REFERENCES

1. Pelanda R, Schwers S, Sonoda E, Torres RM, Nemazee D, Rajewsky K. Receptor Editing in a Transgenic Mouse Model: Site, Efficiency, and Role in B Cell Tolerance and Antibody Diversification. *Immunity* (1997) 7:765–75. doi: 10.1016/S1074-7613(00)80395-7
2. Pelanda R, Torres RM. Central B-Cell Tolerance: Where Selection Begins. *Cold Spring Harb Perspect Biol* (2012) 4:a007146. doi: 10.1101/cshperspect.a007146
3. Meffre E, Casellas R, Nussenzweig MC. Antibody Regulation of B Cell Development. *Nat Immunol* (2000) 1:379–85. doi: 10.1038/80816
4. Mayer CT, Nieke JP, Gazumyan A, Cipolla M, Wang Q, Oliveira TY, et al. An Apoptosis-Dependent Checkpoint for Autoimmunity in Memory B and Plasma Cells. *Proc Natl Acad Sci USA* (2020) 117:24957–63. doi: 10.1073/pnas.2015372117
5. Meyer-Bahlburg A, Rawlings DJ. B Cell Autonomous TLR Signaling and Autoimmunity. *Autoimmun Rev* (2008) 7:313–6. doi: 10.1016/j.autrev.2007.11.027
6. Stadanlick JE, Kaileh M, Karnell FG, Scholz JL, Miller JP, Quinn WJ3rd, et al. Tonic B Cell Antigen Receptor Signals Supply an NF-kappaB Substrate for Prosurvival BLyS Signaling. *Nat Immunol* (2008) 9:1379–87. doi: 10.1038/ni.1666
7. Castro I, Wright JA, Damdinsuren B, Hoek KL, Carlesso G, Shinners NP, et al. B Cell Receptor-Mediated Sustained C-Rel Activation Facilitates Late Transitional B Cell Survival Through Control of B Cell Activating Factor Receptor and NF-κb2. *J Immunol* (2009) 182:7729–37. doi: 10.4049/jimmunol.0803281
8. Khan WN, Wright JA, Kleiman E, Boucher JC, Castro I, Clark ES. B-Lymphocyte Tolerance and Effector Function in Immunity and Autoimmunity. *Immunol Res* (2013) 57:335–53. doi: 10.1007/s12026-013-8466-z
9. Meyer-Bahlburg A, Andrews SF, Yu KO, Porcelli SA, Rawlings DJ. Characterization of a Late Transitional B Cell Population Highly Sensitive to BAFF-Mediated Homeostatic Proliferation. *J Exp Med* (2008) 205:155–68. doi: 10.1084/jem.20071088
10. Petro JB, Castro I, Lowe J, Khan WN. Bruton's Tyrosine Kinase Targets NF-kappaB to the Bcl-X Promoter *via* a Mechanism Involving Phospholipase C-Gamma2 Following B Cell Antigen Receptor Engagement. *FEBS Lett* (2002) 532:57–60. doi: 10.1016/S0014-5793(02)03623-2
11. Hoek KL, Antony P, Lowe J, Shinners N, Sarmah B, Wente SR, et al. Transitional B Cell Fate is Associated With Developmental Stage-Specific Regulation of Diacylglycerol and Calcium Signaling Upon B Cell Receptor Engagement. *J Immunol* (2006) 177:5405–13. doi: 10.4049/jimmunol.177.8.5405
12. Andrews SF, Dai X, Ryu BY, Gulick T, Ramachandran B, Rawlings DJ. Developmentally Regulated Expression of MEF2C Limits the Response to BCR Engagement in Transitional B Cells. *Eur J Immunol* (2012) 42:1327–36. doi: 10.1002/eji.201142226
13. Kleiman E, Salyakina D, De Heusch M, Hoek KL, Llanes JM, Castro I, et al. Distinct Transcriptomic Features Are Associated With Transitional and Mature B-Cell Populations in the Mouse Spleen. *Front Immunol* (2015) 6. doi: 10.3389/fimmu.2015.00030
14. Cancro MP. Signalling Crosstalk in B Cells: Managing Worth and Need. *Nat Rev Immunol* (2009) 9:657–61. doi: 10.1038/nri2621
15. Mackay F, Schneider P, Rennert P, Browning J. BAFF AND APRIL: A Tutorial on B Cell Survival. *Annu Rev Immunol* (2003) 21:231–64. doi: 10.1146/annurev.immunol.21.120601.141152
16. Mackay F, Silveira PA, Brink R. B Cells and the BAFF/APRIL Axis: Fast-Forward on Autoimmunity and Signaling. *Curr Opin Immunol* (2007) 19:327–36. doi: 10.1016/j.coi.2007.04.008
17. Mackay F, Woodcock SA, Lawton P, Ambrose C, Baetscher M, Schneider P, et al. Mice Transgenic for BAFF Develop Lymphocytic Disorders Along With Autoimmune Manifestations. *J Exp Med* (1999) 190:1697–710. doi: 10.1084/jem.190.11.1697
18. Rawlings DJ, Metzler G, Wray-Dutra M, Jackson SW. Altered B Cell Signalling in Autoimmunity. *Nat Rev Immunol* (2017) 17:421–36. doi: 10.1038/nri.2017.24
19. Fillatreau S, Manfroi B, Dorner T. Toll-Like Receptor Signalling in B Cells During Systemic Lupus Erythematosus. *Nat Rev Rheumatol* (2021) 17:98–108. doi: 10.1038/s41584-020-00544-4
20. Christensen SR, Shupe J, Nickerson K, Kashgarian M, Flavell RA, Shlomchik MJ. Toll-Like Receptor 7 and TLR9 Dictate Autoantibody Specificity and Have Opposing Inflammatory and Regulatory Roles in a Murine Model of Lupus. *Immunity* (2006) 25:417–28. doi: 10.1016/j.immuni.2006.07.013
21. Green NM, Laws A, Kiefer K, Busconi L, Kim YM, Brinkmann MM, et al. Murine B Cell Response to TLR7 Ligands Depends on an IFN-Beta Feedback Loop. *J Immunol* (2009) 183:1569–76. doi: 10.4049/jimmunol.0803899
22. Leadbetter EA, Rifkin IR, Hohlbaum AM, Beaudette BC, Shlomchik MJ, Marshak-Rothstein A. Chromatin-IgG Complexes Activate B Cells by Dual Engagement of IgM and Toll-Like Receptors. *Nature* (2002) 416:603–7. doi: 10.1038/416603a
23. Sindhava VJ, Oropallo MA, Moody K, Naradikian M, Higdon LE, Zhou L, et al. A TLR9-Dependent Checkpoint Governs B Cell Responses to DNA-Containing Antigens. *J Clin Invest* (2017) 127:1651–63. doi: 10.1172/JCI89931
24. Braley-Mullen H, Sharp GC, Medling B, Tang H. Spontaneous Autoimmune Thyroiditis in NOD.H-2h4 Mice. *J Autoimmun* (1999) 12:157–65. doi: 10.1006/jaut.1999.0272
25. Saeed M. Lupus Pathobiology Based on Genomics. *Immunogenetics* (2017) 69:1–12. doi: 10.1007/s00251-016-0961-7
26. Manjarrez-Orduno N, Marasco E, Chung SA, Katz MS, Kiridly JF, Simpfendorfer KR, et al. CSK Regulatory Polymorphism Is Associated With Systemic Lupus Erythematosus and Influences B-Cell Signaling and Activation. *Nat Genet* (2012) 44:1227–30. doi: 10.1038/ng.2439
27. Theodorou E, Nezos A, Antypa E, Ioakeimidis D, Koutsilieris M, Tektonidou M, et al. B-Cell Activating Factor and Related Genetic Variants in Lupus Related Atherosclerosis. *J Autoimmun* (2018) 92:87–92. doi: 10.1016/j.jaut.2018.05.002
28. Goodnow CC, Vinuesa CG, Randall KL, Mackay F, Brink R. Control Systems and Decision Making for Antibody Production. *Nat Immunol* (2010) 11:681–8. doi: 10.1038/ni.1900
29. Tischner D, Woess C, Ottina E, Villunger A. Bcl-2-Regulated Cell Death Signalling in the Prevention of Autoimmunity. *Cell Death Dis* (2010) 1:e48. doi: 10.1038/cddis.2010.27
30. Hughes P, Bouillet P, Strasser A. Role of Bim and Other Bcl-2 Family Members in Autoimmune and Degenerative Diseases. *Curr Dir Autoimmunity KARGER* (2005), 74–94. doi: 10.1159/000090773
31. Hutcheson J, Scatizzi JC, Siddiqui AM, Haines GK3rd, Wu T, Li QZ, et al. Combined Deficiency of Proapoptotic Regulators Bim and Fas Results in the Early Onset of Systemic Autoimmunity. *Immunity* (2008) 28:206–17. doi: 10.1016/j.immuni.2007.12.015
32. Tsubata T. B-Cell Tolerance and Autoimmunity. *F1000Res* (2017) 6:391. doi: 10.12688/f1000research.10583.1
33. Huang DC, Strasser A. BH3-Only Proteins-Essential Initiators of Apoptotic Cell Death. *Cell* (2000) 103:839–42. doi: 10.1016/S0092-8674(00)00187-2
34. Oliver PM, Vass T, Kappler J, Marrack P. Loss of the Proapoptotic Protein, Bim, Breaks B Cell Anergy. *J Exp Med* (2006) 203:731–41. doi: 10.1084/jem.20051407
35. Bouillet P, Metcalf D, Huang DC, Tarlinton DM, Kay TW, Kontgen F, et al. Proapoptotic Bcl-2 Relative Bim Required for Certain Apoptotic Responses, Leukocyte Homeostasis, and to Preclude Autoimmunity. *Science* (1999) 286:1735–8. doi: 10.1126/science.286.5445.1735
36. Hughes PD, Belz GT, Fortner KA, Budd RC, Strasser A, Bouillet P. Apoptosis Regulators Fas and Bim Cooperate in Shutdown of Chronic Immune Responses and Prevention of Autoimmunity. *Immunity* (2008) 28:197–205. doi: 10.1016/j.immuni.2007.12.017

37. Bouillet P, Purton JF, Godfrey DI, Zhang LC, Coultas L, Puthalakath H, et al. BH3-Only Bcl-2 Family Member Bim Is Required for Apoptosis of Autoreactive Thymocytes. *Nature* (2002) 415:922–6. doi: 10.1038/415922a
38. Chen M, Huang L, Wang J. Deficiency of Bim in Dendritic Cells Contributes to Overactivation of Lymphocytes and Autoimmunity. *Blood* (2007) 109:4360–7. doi: 10.1182/blood-2006-11-056424
39. Tsai F, Homan PJ, Agrawal H, Misharin AV, Abdala-Valencia H, Haines GK3rd, et al. Bim Suppresses the Development of SLE by Limiting Myeloid Inflammatory Responses. *J Exp Med* (2017) 214:3753–73. doi: 10.1084/jem.20170479
40. Liu R, King A, Bouillet P, Tarlinton DM, Strasser A, Heierhorst J. Proapoptotic BIM Impacts B Lymphoid Homeostasis by Limiting the Survival of Mature B Cells in a Cell-Autonomous Manner. *Front Immunol* (2018) 9:592. doi: 10.3389/fimmu.2018.00592
41. Kendall PL, Moore DJ, Hulbert C, Hoek KL, Khan WN, Thomas JW. Reduced Diabetes in Btk-Deficient Nonobese Diabetic Mice and Restoration of Diabetes With Provision of an Anti-Insulin IgH Chain Transgene. *J Immunol* (2009) 183:6403–12. doi: 10.4049/jimmunol.0900367
42. Zarrin AA-O, Bao KA-O, Lupardus P, Vucic D. Kinase Inhibition in Autoimmunity and Inflammation. *Nat Rev Drug Discov* (2021) 20:39–63. doi: 10.1038/s41573-020-0082-8
43. Takeuchi O, Fisher J, Suh H, Harada H, Malynn BA, Korsmeyer SJ. Essential Role of BAX,BAK in B Cell Homeostasis and Prevention of Autoimmune Disease. *Proc Natl Acad Sci USA* (2005) 102:11272–7. doi: 10.1073/pnas.0504783102
44. Rickert RC, Roes J, Rajewsky K, lymphocyte-specific B. Cre-Mediated Mutagenesis in Mice. *Nucleic Acids Res* (1997) 25:1317–8. doi: 10.1093/nar/25.6.1317
45. Khan WN, Alt FW, Gerstein RM, Malynn BA, Larsson I, Rathbun G, et al. Defective B Cell Development and Function in Btk-Deficient Mice. *Immunity* (1995) 3:283–99. doi: 10.1016/1074-7613(95)90114-0
46. Thompson JS, Bixler SA, Qian F, Vora K, Scott ML, Cachero TG, et al. BAFF-R, a Newly Identified TNF Receptor That Specifically Interacts With BAFF. *Science* (2001) 293:2108–11. doi: 10.1126/science.1061965
47. Li QZ, Zhou J Fau - Wandstrat AE, Wandstrat Ae Fau - Carr-Johnson F, Carr-Johnson F Fau - Branch V, Branch V Fau - Karp DR, Karp Dr Fau - Mohan C, et al. Protein Array Autoantibody Profiles for Insights Into Systemic Lupus Erythematosus and Incomplete Lupus Syndromes. *Immunity* (2018) 49 (4):725–39.e6. doi: 10.1016/j.immuni.2018.08.015
48. Liu L, Allman WR, Coleman AS, Takeda K, Lin TL, Akkoyunlu M. Delayed Onset of Autoreactive Antibody Production and M2-Skewed Macrophages Contribute to Improved Survival of TACI Deficient MRL-Fas/Lpr Mouse. *Sci Rep* (2018) 8:1308. doi: 10.1038/s41598-018-19827-8
49. Egle A, Harris AW, Bouillet P, Cory S. Bim is a Suppressor of Myc-Induced Mouse B Cell Leukemia. *Proc Natl Acad Sci USA* (2004) 101:6164–9. doi: 10.1073/pnas.0401471101
50. Hao Y, O'Neill P, Naradikian MS, Scholz JL, Cancro MP. A B-Cell Subset Uniquely Responsive to Innate Stimuli Accumulates in Aged Mice. *Blood* (2011) 118:1294–304. doi: 10.1182/blood-2011-01-330530
51. Jenks SA, Cashman KS, Zumaquero E, Marigorta UM, Patel AV, Wang X, et al. Distinct Effector B Cells Induced by Unregulated Toll-Like Receptor 7 Contribute to Pathogenic Responses in Systemic Lupus Erythematosus. *Front Immunol* (2021). doi: 10.3389/fimmu.2021.658048
52. Hübner A, Cavanagh-Kyros J, Rincon M, Flavell RA, Davis RJ. Functional Cooperation of the Proapoptotic Bcl2 Family Proteins Bmf and Bim In Vivo. *Mol Cell Biol* (2009) 30:98–105. doi: 10.1128/MCB.01155-09
53. Corsiero E, Delvecchio FR, Bombardieri M, Pitzalis C. B Cells in the Formation of Tertiary Lymphoid Organs in Autoimmunity, Transplantation and Tumorigenesis. *Curr Opin Immunol* (2019) 57:46-52. doi: 10.1016/j.coi.2019.01.004
54. Wei C, Anolik J, Cappione A, Zheng B, Pugh-Bernard A, Brooks J, et al. A New Population of Cells Lacking Expression of CD27 Represents a Notable Component of the B Cell Memory Compartment in Systemic Lupus Erythematosus. *J Immunol* (2007) 178:6624–33. doi: 10.4049/jimmunol.178.10.6624
55. Wang J, Li T, Zan H, Rivera CE, Yan H, Xu Z. LUBAC Suppresses IL-21-Induced Apoptosis in CD40-Activated Murine B Cells and Promotes Germinal Center B Cell Survival and the T-Dependent Antibody Response. *Front Immunol* (2021) 12:658048. doi: 10.3389/fimmu.2021.658048
56. Jin H, Carrio R, Yu A, Malek TR. Distinct Activation Signals Determine Whether IL-21 Induces B Cell Costimulation, Growth Arrest, or Bim-Dependent Apoptosis. *J Immunol* (2004) 173:657–65. doi: 10.4049/jimmunol.173.1.657
57. Mehta DS, Wurster AL, Whitters MJ, Young DA, Collins M, Grusby MJ. IL-21 Induces the Apoptosis of Resting and Activated Primary B Cells. *J Immunol* (2003) 170:4111–8. doi: 10.4049/jimmunol.170.8.4111
58. Johnson JL, Scholz JL, Marshak-Rothstein A, Cancro MP. Molecular Pattern Recognition in Peripheral B Cell Tolerance: Lessons From Age-Associated B Cells. *Curr Opin Immunol* (2019) 61:33–8. doi: 10.1016/j.coi.2019.07.008
59. Naradikian MS, Myles A, Beiting DP, Roberts KJ, Dawson L, Herati RS, et al. Cutting Edge: IL-4, IL-21, and IFN-Gamma Interact To Govern T-Bet and CD11c Expression in TLR-Activated B Cells. *J Immunol* (2016) 197:1023–8. doi: 10.4049/jimmunol.1600522
60. Craxton A, Draves KE, Clark EA. Bim Regulates BCR-Induced Entry of B Cells Into the Cell Cycle. *Eur J Immunol* (2007) 37:2715–22. doi: 10.1002/eji.200737327
61. Banerjee A, Grumont R, Gugasyan R, White C, Strasser A, Gerondakis S. NF-kappaB1 and c-Rel cooperate to promote the survival of TLR4-activated B cells by neutralizing Bim via distinct mechanisms. *Blood* (2008) 112(13):5063–73. doi: 10.1182/blood-2007-10-120832
62. Gerondakis S, Grumont Rj Fau - Banerjee A, Banerjee A. Regulating B-Cell Activation and Survival in Response to TLR Signals. *Blood* (2012) 119 (16):3744–56. doi: 10.1182/blood-2011-12-397919
63. Rip J, de Bruijn MJW, Appelman MK, Pal Singh S, Hendriks RW, Corneth OBJ. Toll-Like Receptor Signaling Drives Btk-Mediated Autoimmune Disease. *Front Immunol* (2019) 10:95. doi: 10.3389/fimmu.2019.00095
64. Nyhoff LE, Clark ES, Barron BL, Bonami RH, Khan WN, Kendall PL. Bruton's Tyrosine Kinase Is Not Essential for B Cell Survival Beyond Early Developmental Stages. *J Immunol* (2018) 200:2352–61. doi: 10.4049/jimmunol.1701489
65. Kil LP, de Bruijn MJ, van Nimwegen M, Corneth OB, van Hamburg JP, Dingjan GM, et al. Btk Levels Set the Threshold for B-Cell Activation and Negative Selection of Autoreactive B Cells in Mice. *Blood* (2012) 119:3744–56. doi: 10.1182/blood-2011-12-397919
66. Fleischer SJ, Giesecke C, Mei HE, Lipsky PE, Daridon C, Dorner T. Increased Frequency of a Unique Spleen Tyrosine Kinase Bright Memory B Cell Population in Systemic Lupus Erythematosus. *Arthritis Rheumatol* (2014) 66:3424–35. doi: 10.1002/art.38854
67. Ettinger R, Kuchen S, Lipsky PE. The Role of IL-21 in Regulating B-Cell Function in Health and Disease. *Immunol Rev* (2008) 223:60–86. doi: 10.1111/j.1600-065X.2008.00631.x
68. Green NM, Marshak-Rothstein A. Toll-Like Receptor Driven B Cell Activation in the Induction of Systemic Autoimmunity. *Semin Immunol* (2011) 23:106–12. doi: 10.1016/j.smim.2011.01.016
69. Groom JR, Fletcher CA, Walters SN, Grey ST, Watt SV, Sweet MJ, et al. BAFF and MyD88 Signals Promote a Lupuslike Disease Independent of T Cells. *J Exp Med* (2007) 204:1959–71. doi: 10.1084/jem.20062567
70. Lee DSW, Rojas OL, Gommerman JL. B Cell Depletion Therapies in Autoimmune Disease: Advances and Mechanistic Insights. *Nat Rev Drug Discov* (2021) 20:179–99. doi: 10.1038/s41573-020-00092-2
71. Enders A, Bouillet P, Puthalakath H, Xu Y, Tarlinton DM, Strasser A. Loss of the Pro-Apoptotic BH3-Only Bcl-2 Family Member Bim Inhibits BCR Stimulation-Induced Apoptosis and Deletion of Autoreactive B Cells. *J Exp Med* (2003) 198:1119–26. doi: 10.1084/jem.20030411
72. Ludwinski MW, Sun J, Hilliard B, Gong S, Xue F, Carmody RJ, et al. Critical Roles of Bim in T Cell Activation and T Cell-Mediated Autoimmune Inflammation in Mice. *J Clin Invest* (2009) 119:1706–13. doi: 10.1172/JCI37619
73. Li YF, Xu S, Huang Y, Ou X, Lam KP. Tyrosine Kinase C-Abl Regulates the Survival of Plasma Cells. *Sci Rep* (2017) 7:40133. doi: 10.1038/srep40133
74. Ludwig LM, Roach LE, Katz SG, LaBelle JL. Loss of BIM in T Cells Results in BCL-2 Family BH3-Member Compensation But Incomplete Cell Death Sensitivity Normalization. *Apoptosis* (2020) 25:247–60. doi: 10.1007/s10495-020-01593-6

75. Amezcua Vesely MC, Schwartz M, Bermejo DA, Montes CL, Cautivo KM, Kalergis AM, et al. FcgammaRIIb and BAFF Differentially Regulate Peritoneal B1 Cell Survival. *J Immunol* (2012) 188:4792–800. doi: 10.4049/jimmunol.1102070
76. Nojima T, Reynolds AE, Kitamura D, Kelsoe G, Kuraoka M. Tracing Self-Reactive B Cells in Normal Mice. *J Immunol* (2020) 205(1):90–101. doi: 10.4049/jimmunol.1901015
77. Nguyen CQ, Hu MH, Li Y, Stewart C, Peck AB. Salivary Gland Tissue Expression of Interleukin-23 and Interleukin-17 in Sjogren's Syndrome: Findings in Humans and Mice. *Arthritis Rheum* (2008) 58:734–43. doi: 10.1002/art.23214
78. Cornec D, Devauchelle-Pensec V, Tobon GJ, Pers JO, Jousse-Joulin S, Saraux A. B Cells in Sjogren's Syndrome: From Pathophysiology to Diagnosis and Treatment. *J Autoimmun* (2012) 39:161–7. doi: 10.1016/j.jaut.2012.05.014
79. Hutcheson J, Vanarsa K, Bashmakov A, Grewal S, Sajitharan D, Chang BY, et al. Modulating Proximal Cell Signaling by Targeting Btk Ameliorates Humoral Autoimmunity and End-Organ Disease in Murine Lupus. *Arthritis Res Ther* (2012) 14:R243. doi: 10.1186/ar4086
80. Honigberg LA, Smith AM, Sirisawad M, Verner E, Loury D, Chang B, et al. The Bruton Tyrosine Kinase Inhibitor PCI-32765 Blocks B-Cell Activation and Is Efficacious in Models of Autoimmune Disease and B-Cell Malignancy. *Proc Natl Acad Sci USA* (2010) 107:13075–80. doi: 10.1073/pnas.1004594107
81. Pollard KM, Cauvi DM, Mayeux JM, Toomey CB, Peiss AK, Hultman P, et al. Mechanisms of Environment-Induced Autoimmunity. *Annu Rev Pharmacol Toxicol* (2021) 61:135–57. doi: 10.1146/annurev-pharmtox-031320-111453

Conflict of Interest: Authors GC, LC, and TM are employed by AstraZeneca.

The remaining authors declare that the research was conducted in the absence of any commercial or financial relationships that could be construed as a potential conflict of interest.

Publisher's Note: All claims expressed in this article are solely those of the authors and do not necessarily represent those of their affiliated organizations, or those of the publisher, the editors and the reviewers. Any product that may be evaluated in this article, or claim that may be made by its manufacturer, is not guaranteed or endorsed by the publisher.

Advantages of publishing in Frontiers

OPEN ACCESS
Articles are free to read for greatest visibility and readership

FAST PUBLICATION
Around 90 days from submission to decision

HIGH QUALITY PEER-REVIEW
Rigorous, collaborative, and constructive peer-review

TRANSPARENT PEER-REVIEW
Editors and reviewers acknowledged by name on published articles

Frontiers
Avenue du Tribunal-Fédéral 34
1005 Lausanne | Switzerland

Visit us: www.frontiersin.org
Contact us: frontiersin.org/about/contact

REPRODUCIBILITY OF RESEARCH
Support open data and methods to enhance research reproducibility

DIGITAL PUBLISHING
Articles designed for optimal readership across devices

FOLLOW US
@frontiersin

IMPACT METRICS
Advanced article metrics track visibility across digital media

EXTENSIVE PROMOTION
Marketing and promotion of impactful research

LOOP RESEARCH NETWORK
Our network increases your article's readership